EMPA AKADEMIE
Zentrum für Wissenstransfer

INRETS
The french national institute for transport and safety research

TU Graz

JRC
EUROPEAN COMMISSION

18th International Symposium

Transport and Air Pollution

Proceedings

May 18 – 19, 2010

Dübendorf, Switzerland

www.empa.ch/TAP2010

Editor

Dr Martin Weilenmann / Rosemarie Lacher

Impressum

Empa – Materials Science and Technology
Überlandstrasse 129
CH-8600 Dübendorf / Switzerland

Publisher

Empa

Organisation

Dr Martin Weilenmann
Rosemarie Lacher
Phone: +41 823 46 79
Fax: +41 823 40 44
e-mail: tap@empa.ch
www.empa.ch/TAP2010

ISBN 978-3-905594-57-7

EMPA

Materials Science & Technology

Preface

Ladies and Gentlemen, Dear Participants,

Traffic emissions and air quality have been topics for several decades already. Many improvements were achieved by a better control of combustion and appropriate aftertreatment systems. These achievements however were beaten out to a certain extent by the grow of traffic and of vehicle size and weight, such that in many “hot spots” local air quality is not satisfactory and mostly these hot spots are close to urban areas, where people live and work.

In parallel the global warming became a central environmental problem and traffic as a major contributor of CO_2 and other greenhouse gases is in focus in this discussion. On the side of impact this means that air quality research today shows two dimensions, the global one dealing with global warming, and the local one of polluting humans, animals, plants and soil. On the side of technology the researchers and car manufacturers are challenged by a variety of technologies and fuels all promising reduced greenhouse gas potential, for which engines and aftertreatment systems need to be developed to improve or at least keep the low unit emissions of the actual models.

All these open questions ask for new tools in measurement and simulation for two aspects: to understand the mechanisms that are not well known yet, as well as to develop the necessary technology on time. Thus, this field of traffic related air pollution will keep its actuality for the future.

The Transport and Air Pollution symposium provides a forum for a broad interdisciplinary research community for knowledge exchange at a scientific level. The French National Institute for Transport and Safety Research (INRETS), the Institute of Internal Combustion Engines and Thermodynamics at the University of Technology of Graz and formerly the National Centre of Air Pollution (NCAR) jointly organized the TAP conferences. Newly from this year on also Empa the Swiss research institute for Material Science & Technology and the EU Joint Research Centre (JRC) of Ispra are in this team of organisers.

This conference is the 18th in this Transport and Air Pollution series and we hope you will enjoy your visit to Zurich and Duebendorf. We hope that the conference will meet your expectations in promoting the scientific exchange, extending and strengthening of contacts.

The work of all contributing authors and the scientific committee is gratefully acknowledged. We also want to express special thanks to the staff organising this conference.

Christian Bach Martin Weilenmann

Dübendorf, May 2010

Content

Session 1: Roadside and Tunnel Studies

Real-Time Vehicle Emission Monitoring Along Roadsides

U. Stelwagen[1], R. De Lange[1], N.E. Ligterink[1], G.A. Klunder[2], A. Bigazzi[3], J.H. Duyzer[2], J. Van Baalen[1], R.T. Van Katwijk[2], M.C. Kruithof[1], S. van Ratingen[2], J.H. Weststrate[2], I.R. Wilmink[2]*

[1] TNO Science and Industry, P.O. Box 155, NL-2600 AD, Delft, The Netherlands, uilke.stelwagen@tno.nl
[2] TNO Building and Construction, P.O. Box 49, NL-2600 AA, Delft, The Netherlands
[3] Portland State University, P.O. Box 751, Portland, OR 97207, USA

Abstract

In the worldwide efforts to reduce the emissions of greenhouse gasses in general and those emitted by vehicles in particular, vehicle emission monitoring is important. It provides accurate knowledge of real-world emissions of vehicles as input for vehicle emission models. Real-time emission monitoring along roadsides can be used in dedicated monitoring to eliminate air-quality hotspots, by assessing and optimizing local emission reducing measures like traffic light schemes. Also, it can be used to identify high-emitter vehicles.

The main focus of this paper is the roadside emission measurement experiment performed in 2009. In this experiment simultaneous concentration measurements of CO_2, NO_x, NO and NO_2 were carried out with simultaneous measurements of particulate matter and TSP. This information was enhanced with vehicle speed and acceleration from radar measurements together with vehicle class information derived from video identified license plates. In total over 8000 vehicles were measured. The experiment showed that a combination of a limited number of measurements combined with emission and dispersion modelling may provide a reliable real-time estimation of air quality in complex situations.

Introduction

Road traffic produces emissions and therefore contributes to higher concentrations of harmful pollutants such as nitrogen dioxide (NO_2) and particular matter (PM_{10}). In addition, worldwide road traffic produces considerable amounts of the greenhouse gas emissions, of which carbon dioxide (CO_2) is the most important. The obvious link between road traffic activity and local air pollution often results in a strong focus on traffic when air-quality hotspots have to be eliminated. This is even more the case since influencing the traffic activity is one of the few possibilities to reduce the air pollution near busy streets. Although the link between traffic activity and air-pollution is well known, it appears to be rather difficult to accurately determine the exact emissions and resulting concentration levels at all places of interest around a traffic situation because many different parameters influence air quality.

Traffic management can contribute to decreased vehicle emissions, by favorably influencing flows, speeds, speed dynamics and composition of traffic. Examples are (dynamic) speed limits, optimization of traffic signal control, or closure of routes for all or part of the vehicle fleet. To reduce adverse impacts, the deployment of these measures should be limited to only those situations where the air quality limit values are about to be exceeded. In order to determine this, it has to be possible to assess the air quality and the expected traffic emissions reasonably accurately.

This paper provides a view on how emissions can be reduced using emissions monitoring and management techniques that combine both measurements and modelling. In addition, a measurement experiment is described and results are given.

Vehicle Emissions, the Broader Picture

The concentrations of air pollutants are determined by their existing background concentrations, by the actual emissions from road traffic, but also by time and situation specific parameters such as wind speed and direction, sun or rain, building density and the presence of trees. Hence,

direct measurement to get insight in the actual local air quality is complex and requires many measurement locations to get an accurate view on the hourly, daily or yearly averaged concentrations. Therefore, there is a strong wish to (be able to) use only measurements from a very limited number of measurement points and, together with information on vehicle intensities, feed these into high level (micro-)traffic, emission and air quality estimation models, which in turn provide the realistic and detailed wide area information necessary for intelligent traffic management (Figure *1*).

This estimation model approach can be enhanced using a video and radar based emission monitoring (VRBEM) concept to indirectly measure, or rather estimate, actual vehicle emissions in real-time. With a detailed instantaneous emission model like VERSIT+ (Ligterink and De Lange, 2009), accurate emissions can be estimated, given that vehicle characteristics and velocity and acceleration for the passing vehicles are known. The latter information can be acquired in real-time with a combined video-radar system. The video system provides license plate info from which vehicle characteristics follow and the radar system provides speed and acceleration trajectories. The estimated emissions can then be fed into a detailed emission dispersion model like HEAVEN (Klunder et al., 2009) to calculate concentrations of pollutants.

Emission and dispersion estimation models are relatively quick and can be used (semi-)real-time. Together with microscopic traffic simulations, this may provide a realistic prediction of the air quality situation to come (minutes to hours time scale) and thus could facilitate emission driven traffic management systems. Based on the estimations and predictions of the current wider area situation, traffic measures could be applied to limit the air pollution, as shown in Figure *1*. Model studies, using microscopic traffic simulations and emission models have shown the potential of such an approach (e.g. Van Den Elshout et al., 2009).

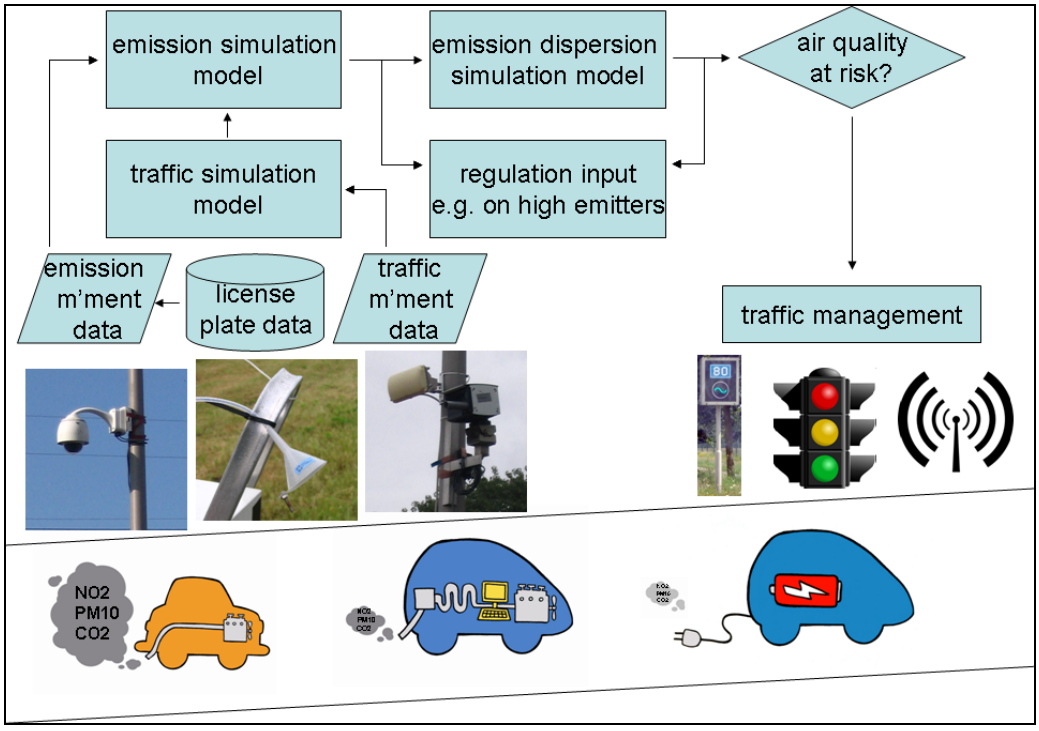

Figure 1 *Emission measurement for air quality management and input to emission regulation.*

It should be noted that one of the critical issues in the described methodology is an accurate estimation of the real-world emissions based on the vehicle characteristics and the velocity and acceleration time history. The instantaneous emissions are highly determined by type of vehicle. Trucks, busses, light commercial and passenger vehicles each have their own emission characteristics. However, within each vehicle category also the fuel type, year of manufacture, technology and state of maintenance have a significant influence. Furthermore the traffic situation and driving style affect the emissions. Therefore an extended and solid measurement base for the emission model is required. In previous years, the possibilities of capturing the real-world emissions were limited. In the Dutch In-Service Testing program (Vermeulen et al., 2010), real-world emissions were measured in a laboratory on a roller bench. A more recently

developed technique, such as portable measurement systems (PEMS) allows an accurate characterization of the emissions in various real-world situations. However, this technique is less suitable for measurement of large numbers of vehicles, i.e. for fleet level info. In addition, other recent techniques such as optical remote emission sensing (RES) and the VRBEM concept provide the possibility to measure emissions along road-sides. These methods provide the possibility of measuring huge numbers of vehicles in a short time and with limited resources. Examples of RES have been demonstrated earlier (e.g. Sjödin et al., 2008). Although the measured emissions are not necessarily representative for emission prediction of longer trips, the technique is still considered valuable due to the high numbers of vehicles that can be measured. The representativeness of RES could be enhanced by combining it with the VRBEM concept.

Emission Measurement Experiment 2009

In 2009 TNO performed an emission measurement experiment alongside a Dutch four-lane motorway in the city of Delft. Main goals of this experiment were to test whether single-point, simultaneous concentration measurements of CO_2, NO_x, NO, NO_2 and particulate matter could be measured accurately enough to provide,

- in combination with video and radar measurements on the passing vehicles, useful information on the emissions of vehicles both on individual level as on fleet level;
- in combination with emissions and dispersion modelling, useful information on air quality in a wider area around the measurement point.

The measurement location is schematically presented in Figure 2. The four-lane motorway consists of two lane pairs separated by a grass strip of about 8 meters wide. About 25 meters to the left (in the figure) of camera 2 is a T-junction with traffic lights (see Figure 5 for overview). Hence, vehicles passing the measurement location had just come around one of the two turns and were usually accelerating at a speed between 35 and 55 km/h.

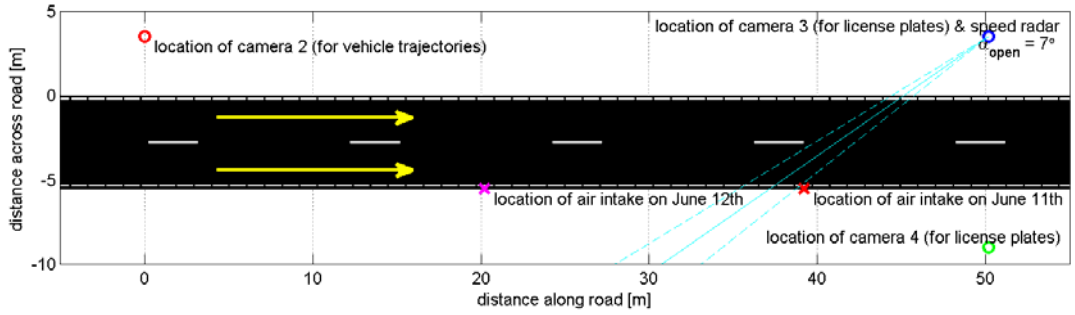

Figure 2 Schematic map of the measurement location. A T-junction with thru-going road and traffic lights lies about 25 m left of the sketched location. See Figure 5 for a more detailed map.

During the two measurement days, the following signals were simultaneously and continuously measured all day:

- concentrations of CO_2, NO_x, NO and NO_2 at 4 Hz;
- wind speed and direction, air temperature, pressure and relative humidity at 1 Hz;
- particulate matter, TSP, condensation nuclei, PM_{10}, $PM_{2.5}$ and PM1.0 at 0.2 Hz;
- license plate video images at 25 Hz;
- radar vehicle position and speed info at 5 Hz;
- video images at 25 Hz.

As an example for the gas concentration measurements, a 5 minute CO_2 signal is depicted in Figure 3. From the recorded license plates, detailed vehicle information – e.g. vehicle brand,

type, fuel, build year etc. – was obtained from the Dutch national vehicle authority RDW for (nearly) all passing vehicles. Using this detailed information, the vehicles were classified into emission relevant vehicle classes, e.g. LPADEUR4 indicates a light duty passenger vehicle using diesel fuel and of European vehicle emission class Euro 4. Hence, the individual peaks or groups of peaks, can be attributed to individually classified vehicles or groups of vehicles and can be labeled accordingly. Due to the nearby traffic lights, vehicles tended to pass in small groups of closely spaced vehicles. This, together with the relatively slow response (seconds to tens of seconds per individual emission peak) of the gas analyzer instruments, made it usually difficult or even impossible to separately identify the emission peaks of each individual vehicle. A faster and preferably remote emission measurement system, directly measuring the emissions very near each vehicle tailpipe, seems an absolute must for that level of precision.

The dispersion of the different emission components, dispersion mainly due to the wind and the turbulence from passing vehicles, is very likely equal. Hence, meaningful concentration ratios relative to the CO_2 concentration can be calculated. An example of this approach is given in Figure 3. Such concentration ratios were compared to calculated emission ratios for vehicles of known vehicle class using realistic vehicle emission models like VERSIT+ (Ligterink and De Lange, 2009) and EnViVer (based on VERSIT+). Although a comprehensive statistical evaluation for all measured vehicles was not performed, realistic average emission ratios were calculated for all cases where individual vehicle peaks were well separated from each other. Also note that Figure 3 reveals a high NO_x emitter, as the very high NO_x peak in the center of the graph appeared to be from a heavy truck.

Though the particulate matter measurement systems were rather slow compared to the other instruments, the PM measurements clearly showed that only very few vehicles were emitting very much above average levels. Hence, also high emitters of fine particles can be detected from roadside concentration measurements, even though individual identification was hindered by the relative slowness of the PM monitors.

Assuming an average CO_2 emission per vehicle class, emission factors in g/km were estimated from the experiment. A first comparison showed that these emissions were reasonably in line with the standard emission factors from VERSIT+ for urban situations. For a more dedicated comparison more detailed speed/acceleration data of individual vehicles is needed. Although both the radar and video measurements were very instructive for analyzing the emission data, they proved not yet accurate enough to provide speed/acceleration trajectories that could be used for emission prediction using VERSIT+. This needs improvement in future measurement campaigns.

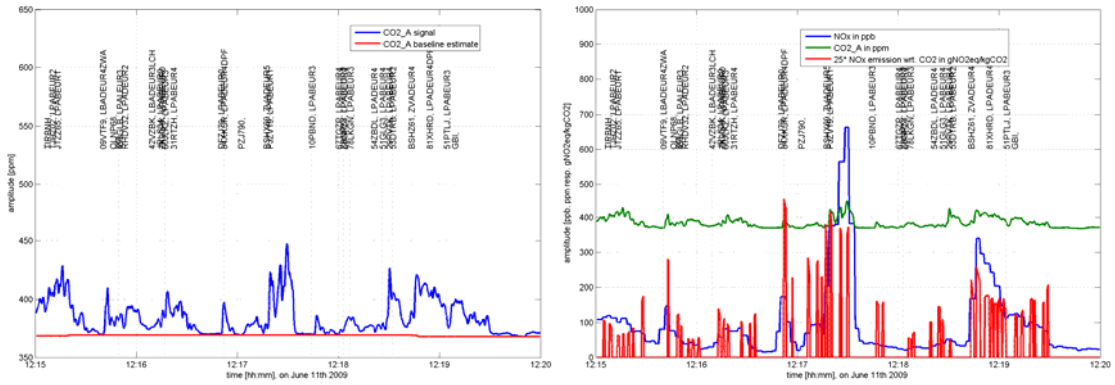

Figure 3 Example of measured CO_2 concentration signal with vehicle class information labeling (left). Example of calculated NO_x/CO_2 concentration ratio (in red on the right). Note that because of the NO_x measurement system being considerably slower than the CO_2 measurement system, the ratio was only calculated around clear CO_2 peaks after low-pass filtering of the CO_2 signal.

Using traffic flow information from the T-junction traffic system detectors (vehicle counting) in combination with the measured fleet composition (from the license plate info), the traffic/emission simulation program EnViVer (a combination of traffic simulation program VISSIM (Wilmink et al., 2009) and emission simulation program VERSIT+) the emissions around the entire junction were simulated. An example result of such emission modelling is given in Figure 4. Next, using the simulated emissions from EnViVer as input, the emission dispersion modelling program HEAVEN can be used to estimate pollutant concentrations in a wide area

around the motorway in order to get an idea of the air quality. An example result of such emission dispersion modelling is given in Figure 5.

Figure 4 Total NO_x emissions from all traffic on June 11th 2009 between 8 AM and 9 AM around the T-junction as calculated with EnViVer.

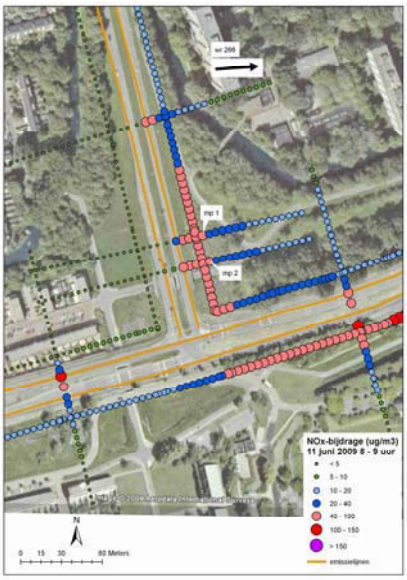

Figure 5 Concentration simulations with emission dispersion model HEAVEN of the hourly averaged NO_x contribution (µg/m3) in receptors around the T-junction on June 11th 2009 between 8 AM and 9 AM, using the EnViVer simulated NO_x emissions as input.

Discussion and Future Plans

From the data of over 8000 vehicles gathered in the two day experiment together with emission and dispersion modelling, it followed that:

- realistic values for individual vehicle emission factors could be derived;
- high-emitter vehicles could be detected;
- with 38 %, the share of NO_2 in NO_x was higher than assumed hitherto;
- large emission differences were observed for individual vehicles depending on vehicle type and vehicle speed dynamics;
- around intersections about 50 % higher emissions (than average urban) were observed.

Finally, the experiment showed that a combination of a limited number of measurements and detailed modelling may provide a reliable real-time estimation of air quality in complex situations such as near crossings.

New measurements are planned for 2010 and these will be extended with a system for simultaneous remote emission measurements taking snapshots from emissions in the direct vicinity of the exhaust tailpipe of individually passing vehicles. This should provide a better view on actual emissions on both individual vehicle and vehicle fleet level. Enhanced with the VRBEM emission monitoring concept, this combination of emission- and air-quality measurement and modelling is believed to provide a solid base for more dedicated road traffic related air-quality monitoring and management programs.

Acknowledgement

This work has been conducted as part of the TRANSUMO project, Advanced Traffic Monitoring (ATMO). The TRANSUMO (TRANsition SUstainable MObility) program is a Dutch platform for companies, government and knowledge institutes cooperating in the development of knowledge with regard to sustainable mobility.

References

Bigazzi A., H. Van Lint, G.A. Klunder, N.E. Ligterink, U. Stelwagen (t.b.p. 2010), Comparing Traffic Data Sources for Local Emissions and Roadside Air Quality Estimates at a Signalized Intersection, *To be published in 2010*.

Van Den Elshout S., M. Mahmod, I. Arts, B. van Arem (2009), Decision making on short term traffic measures to influence traffic related air pollution, *ETTAP2009, Toulouse, France*.

Klunder G.A., I.R. Wilmink (2009), Real-time monitoring of emissions with traffic data, simulation and air quality measurements, *ITS Stockholm 2009.*

Klunder G.A., I.R. Wilmink, N.E. Ligterink, U. Stelwagen, E. Meijer, J.H. Weststrate, J.H. Duyzer, S. Van Ratingen, J. Baan, R. Van Katwijk, H. Van Lint (2009), Transumo ATMO - Monitoren van Emissies, *TNO report (in Dutch) TNO-034-DTM-2009-03811, November 10th 2009, pp. 54.*

Ligterink, N.E., J. van Baalen, A.R.A. Eijk, W.J. Mak, W. Broeders, P. Vortisch, (2008) Predicting local vehicle emissions using VERSIT+ and VISSIM, *ITS 2008.*

Ligterink N.E., R. De Lange (2009), Refined vehicle and driving-behaviour dependencies in the VERSIT+ emission model, *17th International Transport and Air Pollution Conference, Toulouse, France.*

North R., J. Van Baalen, J. Cohen, N. Hoose, J. Polak (2009), On-demand evaluation of alternative strategies for environmental traffic management, *ITS Stockholm 2009*.

Sjödin, A., Jerkson, M., (2008), Evaluation of European Road Transport Emission Models against On-Road Emission Data as Measured by Optical Remote Sensing, *16th international Transport and Air Pollution Conference, Graz, 2008.*

Vermeulen, R., A.R.A. Eijk, N.E. Ligterink, H. Baarbé, (2010), Netherlands In-Service Testing Programme for Emissions of Heavy Duty Engines and Vehicles; developments from on-cycle to real world emissions, *To be published at the 18th International Transport and Air Pollution Conference, TAP 2010.*

Wilmink I.R., F. Viti, J. Van Baalen, M. Li (2009), Emission modelling at signalised intersections using microscopic models, *ITS Stockholm 2009*.

Speed Dependence of NO_2/NOx Emission Ratio?

J. Thudium[*1], *R. Alvarez*[2], *M. Weilenmann*[2]

[1] Oekoscience, Werkstrasse 2, CH-7001 Chur, Switzerland. Thudium@oekoscience.ch

[2] Empa, Swiss Federal Laboratories for Materials Testing and Research, Laboratory for Internal Combustion Engines. Ueberlandstrasse 129, CH-8600 Duebendorf, Switzerland

1. Introduction

Although levels of emitted nitrogen oxides (NOx) have fallen sharply, roadside measurements indicate that ambient concentrations of nitrogen dioxide (NO_2) appear to be stabilizing or even to be rising.

This rise in the ratio of NO_2 to NOx parallels the implementation of oxidation catalytic converters in diesel vehicles. These converters oxidize carbon monoxide and hydrocarbons originating from imperfect combustion in the engine, but may also convert NO to NO_2 in certain temperature conditions. In addition, more and more diesel cars are equipped with original equipment manufacturer (OEM) particle filter (PF) systems that employ NO_2 to oxidize trapped soot at lower temperatures. This NO_2 is intentionally generated from engine-out NO in the catalytic converter preceding the trap, but not controlled. Excess NO_2 may thus escape from the system as tailpipe emissions. Consequently, precise measurement of vehicle emissions of NO and NO_2 were performed (Alvarez et al., 2008).

Since NO_2 formation in diesel engines depends on temperature conditions, the NO_2/NOx ratio could depend on engine power and therefore on vehicles speed. Emission values from a measuring campaign with 20 diesel vehicles (Alvarez et al., 2008) with real-world highway cycles were reinvestigated with respect to speed dependency of the NO_2/NOx ratio. The results are compared with the corresponding guidelines if the handbook of emission factors (HBEFA 3.1, 2010).

On different highway sections in Austria, two different speed limits (100 km/h and 130 km/h) are applied depending on air pollution level. Different NO_2/NOx emission ratios of passenger cars and light duty vans due to different speeds should be detected in roadside ambient NOx and NO_2 measurements; this is presented in the last section of this paper.

2. NO_2/NOx emission ratios for diesel vehicles in real-world highway conditions

Emission ratios of NO_2/NOx of current car fleets are presented for real-world highway driving situations, concretely the BAB cycle (Bundesautobahn Deutschland) and the Common Artemis Driving Cycle (CADC) (André, 2004). The 20 vehicles are grouped according to their combustion principle and certification category: 5 diesel Euro-3 (PD3) and 9 Euro-4 (PD4). Diesel cars with OEM PFs are discussed as a separate group (6 PD4 PF), since NO_2 is intentionally formed in the precatalytic converter of some of these systems to oxidize particles in the trap.

The speed range for the different highway conditions was from 100 km/h to 140 km/h. For each speed level, the average of total NOx and NO_2 emission was calculated for all vehicles in the same group (PD3, PD4 and PD4 PF) together with the respective mean NO_2/NOx ratio. At a speed of 140 km/h, the NOx emission factors are 2-3 times higher than at 100 km/h. For our purposes the emission ratio of NO_2/NOx is of interest.

There is no evidence for a speed dependency of the NO_2/NOx emission ratio for the vehicle sample PD3, see Figure 1. For vehicle sample PD4, the NO_2/NOx ratio of the emission factor decreases by about -0.002/ (km/h) and for sample PD4 PF by about -0.004/ (km/h). Thus, the NO2/NOx emission ratio of Euro-4 diesel vehicles features a speed dependency.

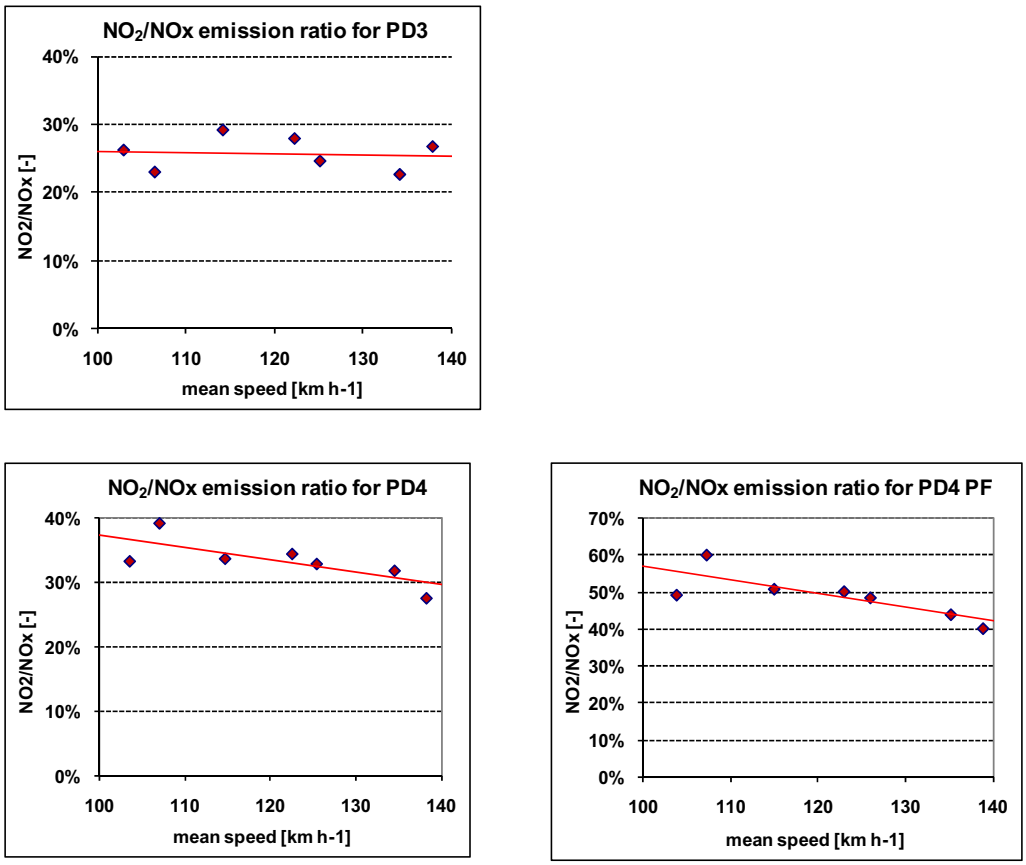

Figure 1: Mean NO_2/NOx emission ratios for diesel vehicle samples Euro-3 (PD3), Euro-4 (PD4) and Euro-4 with particle filter (PD4 PF) in dependency on mean vehicle speed.

3. NOx and NO_2 emissions of passenger cars on Austrian rural highways according to HBEFA 3.1

Emission factors of NOx and NO_2 for an average fleet of passenger cars on e.g. rural Austrian highways are derivable from the handbook of emission factors (HBEFA 3.1, 2010) for different mean speeds. They show a strong dependence on vehicles speed in good agreement with the emission above-mentioned measurements. Although the absolute emission factors are expected to decrease strongly in the next years, the relative speed dependence shall remain stable (fig. 2). In accordance to HBEFA 3.1 however, the NO_2/NOx emission ratio should not be dependent on vehicles speed (fig. 3).

The NO_2/NOx emission ratios for passenger cars presented in fig. 3 coming from HBEFA 3.1 are rather smaller than those presented in fig. 1. The HBEFA 3.1 gives average values for all Euro classes and also gasoline vehicles corresponding to the mean fleet, in that example of Austrian highways, whereas the diesel Euro-4 vehicles (fig. 1) show comparatively high NO_2/NOx ratios.

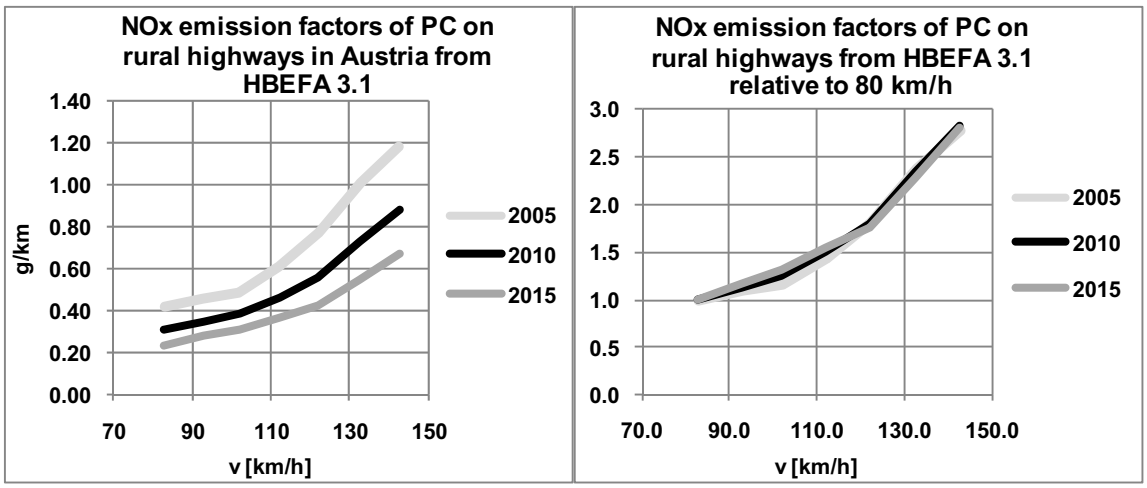

Figure 2: NOx emission factors of passenger cars (PC) on rural Austrian highways as derived from HBEFA 3.1, for 2005, 2010 and 2015; absolute values (left-hand) and relative to emission factors at 80 km/h (right-hand).

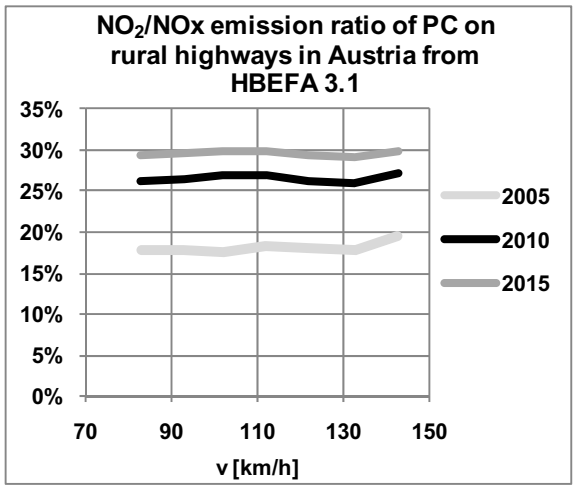

Figure 3: NO_2/NOx emission ratios of passenger cars (PC) on rural Austrian highways as derived from HBEFA 3.1, for 2005, 2010 and 2015.

4. Effect on mean vehicles speed on NO_2/NOx ratio of roadside ambient air pollution

The data base of 20 diesel vehicles is rather small for a generalized statement concerning speed dependence of the NO_2/NOx emission ratio. In addition, roadside ambient air pollution measurements of NOx and NO_2 at Austrian highways with varying speed limits have been investigated regarding speed effects on NO_2/NOx ratios.

On several highway sections in Austria, temporary speed limits alternate between 100 km/h and 130 km/h to improve air quality (Thudium et al., 2009). If NO_2/NOx emission ratios depend on

vehicles' speed, a shift of the NO_2/NOx-ratio of measured air concentrations between these two speed phases should be derivable from roadside measurements.

A comparison between the two speed limit phases of 130 km/h and 100 km/h demands building of a really comparable database, since the NO_2/NOx ratio in ambient air depends on different parameters: the portion of light vehicles at total NOx emissions of the highway, the atmospheric mixing conditions, the amount of NOx concentration and the day time.

For explanation, roadside measurements at Kundl in Tyrol, Austria, performed in 2007 before installing variable speed limits are shown in figure 4 (Thudium, 2007): vertical transports in the atmosphere are very essential for diluting air pollutants, especially in valleys. In thermal inversions, these transports are reduced, leading to enhanced NOx concentrations. NO_2 concentrations are only slightly enhanced because of limited availability of ozone (fig. 4). The portion of NO_2 within NOx concentration depends on the amount of NOx for chemical reasons, what can be seen from the monthly averages of NOx and NO_2/NOx (fig. 4).

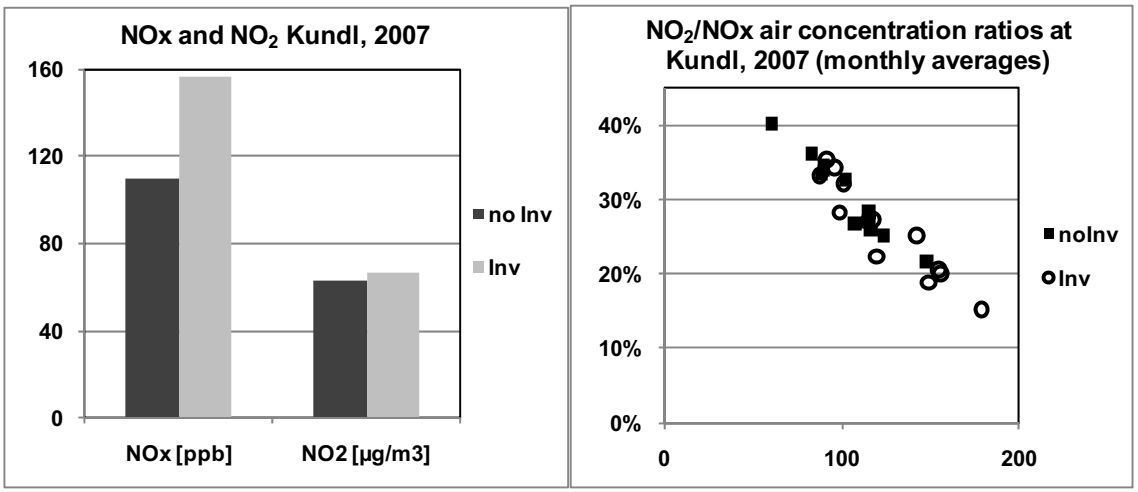

Figure 4: Mean NOx and NO_2 air concentrations at Kundl, roadside station in Tyrol, Austria, 2007 with and without thermal inversion, respectively (left-hand) and monthly averages of NO_2/NOx ratios (right-hand).

Typical NO_2/NOx ratios at a certain NOx level don't differ when there is inversion or not, but there are higher NOx values with inversion than without inversion, leading to lower NO_2/NOx ratios. The NO_2/NOx ratio shows a typical diurnal variation with a minimum in the morning and with lower values over the whole day in case of inversion (fig. 5).

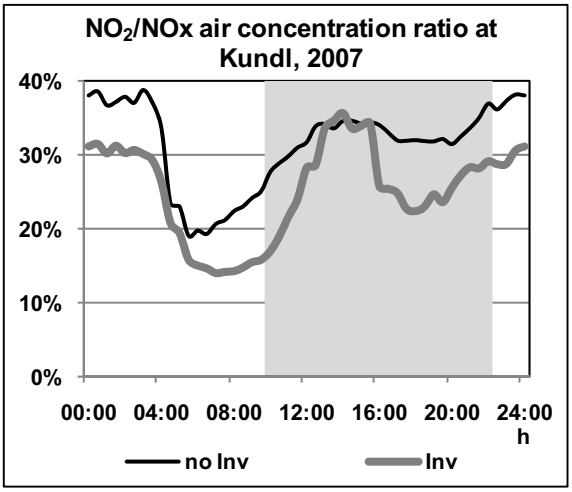

Figure 5: Diurnal variation of NO_2/NOx air concentration at Kundl, 2007, with and without thermal inversion, respectively.

In consequence, an evaluation of the influence of vehicles speed on NO_2/NOx ratio of roadside air concentration has to be investigated in speed limit intervals where other variables essentially determining the NO_2/NOx ratio are similar. So a division in inversion and 'no inversion' situations had to be made. Only workdays on day time between 10 and 22 h were considered, so that the frequencies of speed limit of 100 km/h and 130 km/h were about 50% each. Furthermore only periods were considered where the portion of light vehicles NOx emissions at total highway emission were within certain limits, so that the average of that portion was equal for both speed limits at about 40%. Thus, the influence of heavy duty trucks emitting only small portions of NO_2 (HBEFA 3.1) on ambient air NO_2/NOx ratio was kept constant.

Finally the comparison of NO_2/NOx ratios between situations with speed limit of 100 km/h and 130 km/h, respectively, has to be performed per interval of NOx, as shown in fig. 6:

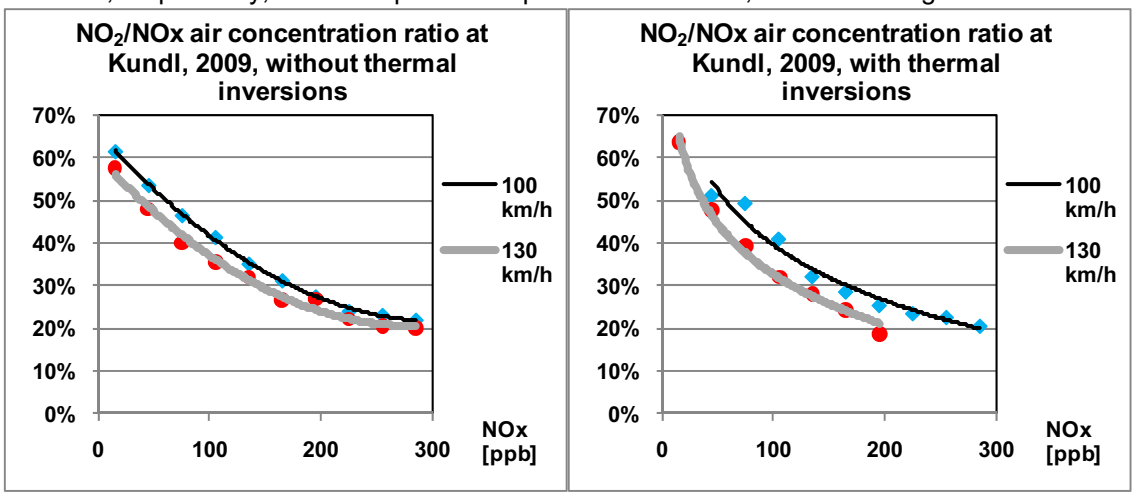

Figure 6: Roadside NO_2/NOx air concentration ratio at Kundl (Tyrol, Austria), 2009, for speed limits of 100 km/h and 130 km/h, respectively, in situations without (left-hand) and with (right-hand) thermal inversions.

The NO_2/NOx ratio in air concentration was larger with a speed limit of 100 km/h than with a speed limit of 130 km/h; the difference amounts to 3-4% in absence of thermal inversions. In the presence of thermal inversions, the difference of NO_2/NOx ratio in air concentration between the speed limits of 100 km/h and 130 km/h amounts to 4-8%, but there residual NO_2 from former times may also play a role.

With a speed limit of 130 km/h, it's not only the faster speeds of passenger cars and light duty vehicles which lead to smaller portions of NO_2 in the NOx emissions (the absolute amounts of emissions are always increasing with speed!). Then the style of driving becomes more aggressive, the speeds are more varying, both leading to lower NO_2/NOx emission ratios intentionally. In October 2006, with permanent speed limit of 130 km/h on this highway, the amount of passenger cars with more than 150 km/h was 15 times more frequent (0.7% of all passenger cars) than in November 2006 with a permanent speed limit of 100 km/h. Speeds with more than 160 km/h were in October 10 times more frequent than in November 2006. Such very fast vehicles oblige all the others to evade on the right-hand lane which is rather occupied by trucks.

5. Conclusions

Emission measurements of NOx and NO_2 with 20 diesel vehicles of certification category Euro-3 and 4 show a speed dependence of the NO_2/NOx ratio for Euro-4 vehicles, where higher vehicle speeds lead to lower ratios. Although the handbook of emission factors HBEFA 3.1 does not contain such dependence, roadside air concentration measurements with different speed limits indicate lower NO_2/NOx ratios at increased vehicle speeds. It has to be emphasized that with higher speeds the absolute emissions both of NOx and NO_2 increase essentially; only the ratio of the two compounds decreases.

References

Alvarez R., M. Weilenmann and J. Favez (2008), Evidence of increased mass fraction of NO_2 within real-world NOx emissions of modern light vehicles — derived from a reliable online measuring method, *Atmos. Environ.,* 42, 4699–4707.

André M. (2004), The ARTEMIS European driving cycles for measuring car pollutant emissions, *Science of the Total Environment 334–335*, 73–84.

Handbook of Emission Factors, HBEFA 3.1 (2010), Infras.

Thudium J., C. Chélala and T. Greiner (2009), Air Pollution Abatement by flexible Speed Regulation on Austrian Highways - Pollution controlled Traffic Management, Actes INRETS no. 122 (paper no. 46).

Thudium J. (2007), Evaluation von Tempo 100 auf der Unterinntalautobahn im Winter 2006/07, Bericht im Auftrag des Amtes der Tiroler Landesregierung.

Emission factors for paved and unpaved roads - validation by tunnel and field measurements

P. J. Sturm, M. Henn and G. Bachler

Graz, University of Technology, Institute for Internal Combustion Engines and Thermodynamics, A-8010 Graz, Austria, sturm@tugraz.at

Abstract

Emission estimates are the basis of assessments of air pollution scenarios, regardless if they have to be done for current situations or projections. Today simulation is a common tool to estimate the emissions of emitters like road traffic. The emission factors for vehicles are based on tests of single vehicles or engines. Although there is already a big amount of data available, compared to the traffic on the roads, this is still a quite small number. To validate the emission factors, real world measurements are required. Tunnel measurements are predestined to such validations because boundary conditions in tunnels are rather easy to consider and the emission behaviour of a huge amount of vehicles can be monitored.

A very weak point in emission estimations are the so called non exhaust emissions. They depend strongly on parameters related to road surface, driving situation and ambient conditions. Road tunnel measurements can in this certain case cover only a small segment of driving and surface conditions. However, at least for this situations a reliably emission factor can be determined. Another big uncertainty in the emission estimation is the non exhaust emission on unpaved roads. This paper aims at validating emission factors for exhaust emissions and developing emission factors for paved and unpaved roads.

Keywords

Vehicle emissions
Emission factor validation
Non exhaust PM emissions paved roads
Non exhaust PM emissions unpaved roads
Tunnel measurements
Field measurements

Definitions

NO_X nitrogen oxides
Delta NO_x difference of nitrogen oxides pollution levels between kerb side and background (measurement) stations
PM_{10} particulate matter with an aerodynamic diameter below 10 µm
Delta PM_{10} difference of particulate matter (<10 µm) pollution levels between kerb side and background (measurement) stations
$PM_{2.5}$ particulate matter with an aerodynamic diameter below 2.5 µm
CO carbon monoxide
CMA Calcium magnesium acetate
HDV heavy duty vehicle (> 3.5 to)
LDV light duty commercial vehicle (< 3.5 to)
PC passenger car (< 3.5 to)

Validation of emission factors by tunnel measurements

Current state of the art for emission estimations is the usage of emission models like HBEFA (INFRAS 2010), Mobile (US-EPA 2009) or network based models like NEMO (Rexeis and Hausberger 2005). All of these models rely on emission factors derived from tests on chassis dynamometers (passenger cars and light duty commercial vehicles) or engine tests (heavy duty vehicles). Although great emphasis is put on the usage of real world cycles for the tests in order to derive reliable emission factors for real world driving, validation of these data is required.

Validation by tunnel measurements

Tunnel measurements are an appropriate tool to validate and in some cases even to develop vehicle emission factors (e.g. Sturm et al. 2001, Hausberger et al. 2003. Imhof et al. 2006, Henn et al. 2009). Road tunnels act like a big laboratory. Boundary conditions like air volume flow, vehicles in the tunnel, etc. are well known. A measurement of the concentrations of the in-tunnel air quality allows for a quantification of traffic emissions inside the tunnel. In order to validate emission factors for NO_X, PM_{10}, $PM_{2.5}$, as well as for CO, measurements in several tunnels were made. The longer a tunnel, the better the results for validation measurements, as the influence of ambient factors are getting smaller: Measurements were performed in the Plabutsch tunnel, a 10 km long city tunnel with a transverse ventilation system and the Kalcherkogel tunnel, a 2 km long tunnel, equipped with a longitudinal ventilation system. Both tunnels are situated on motorways and have two bores with unidirectional traffic.

For longitudinal ventilated tunnels the standard approach to derive emission factors out of measurements is shown in Equation 1. The difference in volume flows (concentrations times air volume flow) between in-tunnel air quality and outside air quality (or between two measurement locations inside the tunnel) divided by the length of the tunnel and the averaging time of the measurements results in the emission quantity.

Equation 1: basic equation for the calculation of emissions in tunnels

$$emissions = \frac{\left(concentration_{measured} - concentration_{outside}\right) \cdot \dot{V}}{length \cdot time}$$

$\dot{V}$	flow rate through the tunnel
Length	distance of the set-up from the entrance portal
Time	time resolution of the measurement values

The evaluation of the emissions bases on the fact that all emissions are accumulated between the two measurement locations. A measurement set up in the middle of the tunnel will be able to detect the sum of the emissions between portal and measurement point. Different to ambient dilution, dilution in a tunnel can be clearly determined via air flow inside the tunnel. For longitudinal ventilation mass conservation is a stringent criterion that must be achieved.

A simple comparison between calculated emissions from traffic times emission factor and measurement gives already information about the accuracy of the factors. The situation is different for PM_{10} and $PM_{2.5}$ as the simulated emissions take into consideration the exhaust emissions only, whereas the measured emissions in the tunnel include the non exhaust particle emissions originating from abrasion and resuspension as well. Assuming that the exhaust emissions can be simulated with sufficient accuracy, the difference between simulated and measured PM emissions can be assigned to non-exhaust emissions. Remark: applying this assumption results in the fact that a validation of exhaust PM emission factors is not possible.

The simulation of the emissions inside the tunnel was performed using the emission network model NEMO (Rexeis et al., 2005), a special software tool, developed at the Institute for Internal Combustion Engines and Thermodynamics at Graz University of Technology, which is able to consider the traffic composition, traffic situation and road gradient to simulate vehicle emissions.

For transverse ventilated systems the calculation would be different, as such systems have a permanent air exchange at each location of the tunnel. To overcome this problem during the measurements in the Plabutsch tunnel, for the concerned ventilation section both fans (supply and exhaust air) were stopped. This leads to a longitudinal behaviour of the flow inside the tunnel and the analyses could be made similar to longitudinal ventilated tunnels. The measurements lasted in general over a couple of weeks in both tunnels and took place in 2008 and 2209 in the Plabutsch and in 2009 in the Kalcherkogel tunnel.

Validation of nitrogen oxides (NOx) emission factors

Figure 7 to Figure 8 show the comparison between measured and simulated NO_X emissions. All correlations show a very good congruence for simulation and measurement. The determination coefficient R^2 deviates between 0.75 for the Kalcherkogel and 0.9 for the Plabutsch tunnel. As the measured path in the Plabutsch tunnel is longer than in the Kalcherkogel (5 km versus 1

km), the uncertainties of the results in the Plabutsch are smaller. In all three cases the NOx simulated vs. measured are within +/-10%. Taking into consideration the uncertainties in the description of the vehicle fleet and the vehicle weight (especially HDV) the fit can be considered as very good, the emission factors can be considered as validated.

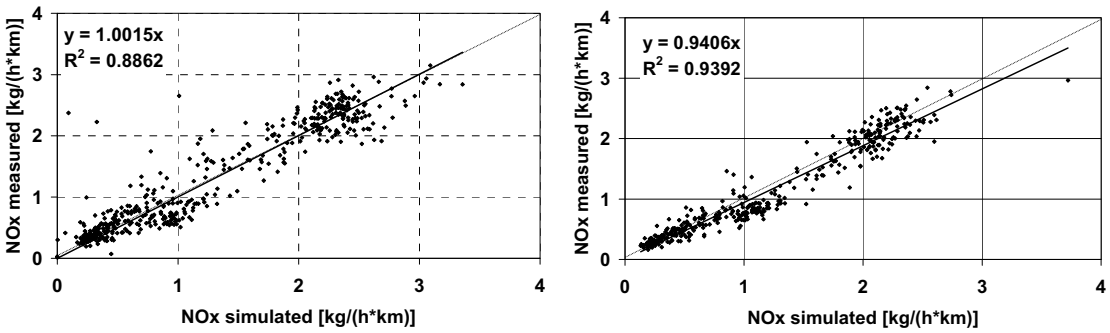

Figure 7: Comparison of measured and simulated NO_X emissions in the Plabutsch tunnel 2008 (left), 2009 (right)

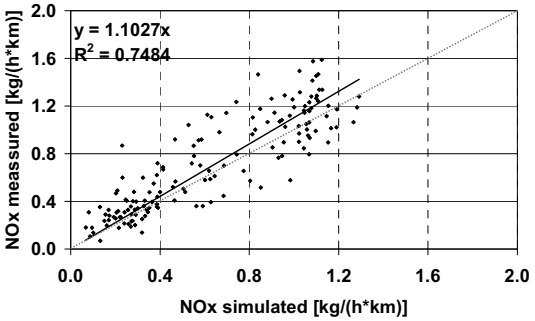

Figure 8: Comparison of measured and simulated NO_X emissions in the Kalcherkogel tunnel 2009)

Validation of carbon monoxide (CO) emission factors

For carbon monoxide the simulating situation is different to PM and NOX. This pollutant does not have much importance for Diesel cars, as by the lean-burn-combustion concept most of the produced CO is oxidised before leaving the tailpipe. On the other side, gasoline cars don't emit very much CO after a three-way catalytic converter. Nevertheless, because of its high toxicology, CO is a limited pollutant, especially for tunnel air quality. As mentioned above, pollutants in a tunnel are accumulating between the entrance and the exit portal. Therefore critical CO concentrations must be avoided to guarantee a sufficient air quality in the tunnel.

Figure 9 shows the comparison of measured and simulated CO emissions in the Plabutsch and the Kalcherkogel tunnel. The correlation for the Plabutsch shows a R² of 0.78 which is rather high, whereas the gradient of the regression line is only 0.43.

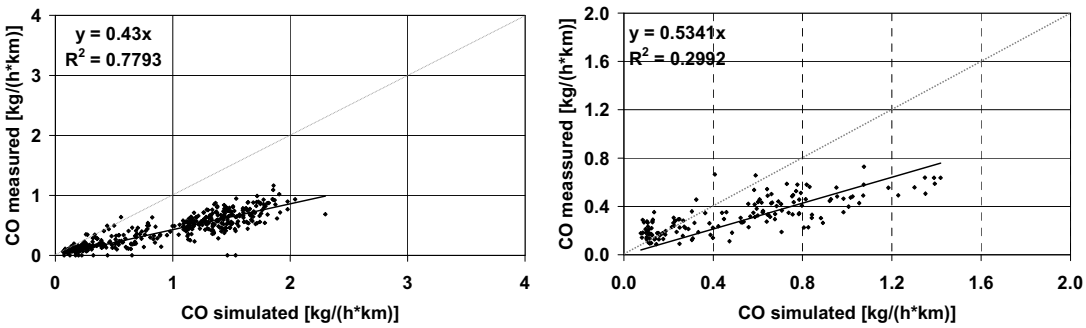

Figure 9: Comparison of measured and simulated CO emissions in the Plabutsch tunnel (left) and the Klacherkogel tunnel (right)

For the Kalcherkogeltunnel the R^2 of 0.3 is lower, whereas the gradient of the regression line is a little bit higher than in the Plabutschtunnel (0.53).

For both tunnels the simulated CO emissons are about the double of the mesaured ones. There seems to be a need for a more detailed investigation in this topic.

Derivation of $PM_{2.5}$ emission factors

As emission standards and legislation are getting more stringent, and $PM_{2.5}$ is now also included in the air quality acts, this pollutant becomes more and more important. Exhaust PM can be allocated 100% to $PM_{2.5}$. The difference between measured and simulated $PM_{2.5}$ emissions (exhaust part only) can be allocated to abrasion and resuspension.

Figure 10 shows the comparison of simulated and measured $PM_{2.5}$ emission factors. The correlation factor R^2 is about 0.8, the gradient is 0.5, which means, that approximately half of the $PM_{2.5}$ emissions in a tunnel is caused by abrasion and resuspension.

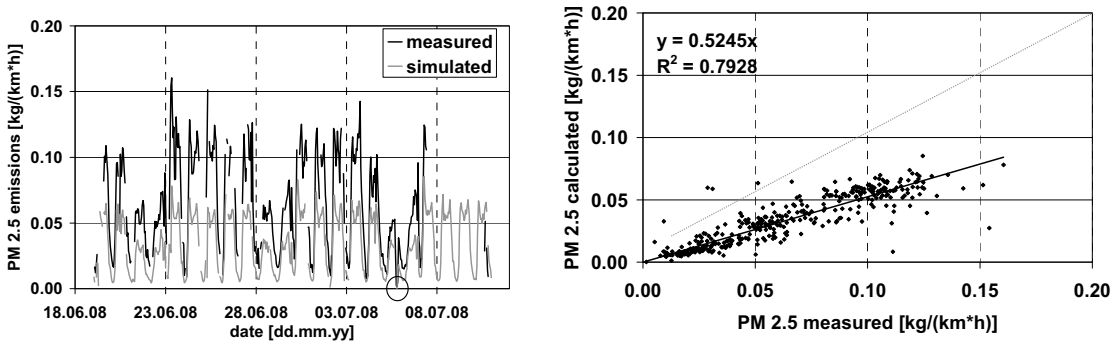

Figure 10: Comparison of measured and simulated $PM_{2.5}$ emissions in the Plabutsch tunnel (2009)

Using a multiple regression, emission factors for PC as well as for HDV can be derived from these results as shown in Figure 11.

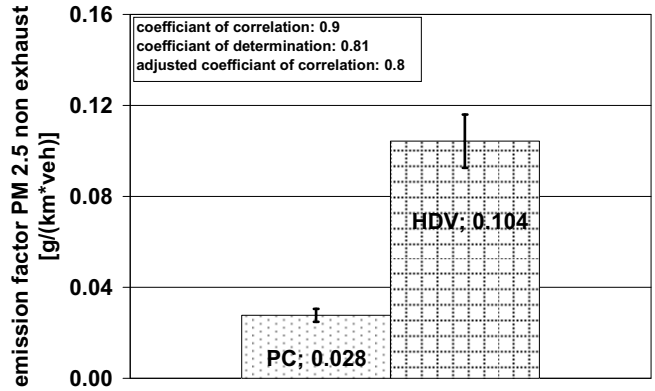

Figure 11: $PM_{2.5}$ non exhaust emission factors for PC and HDV

In Table 1 statistical values for the $PM_{2.5}$ emission factors are shown. The coefficient of multiple correlation is about 0.9, which is rather high. The standard deviation is about 0.0029 g/(km*veh) for PC and 0.0117 g/(km*veh) for HDV.

Table 1: statistical values for $PM_{2.5}$ non exhaust emission factors

coefficiant of multiple correlation	0.90
coefficiant of determination	0.81
coefficiant of adjusted determination	0.80
standard deviaton PC[g/(km*veh)]	±0.0029
standard deviaton HDV[g/(km*veh)]	±0.0117
non-exhaust emission factor PC [g/(km*veh)]	0.028
non-exhaust emission factor HDV [g/(km*veh)]	0.104

Derivation of PM_{10} emission factors on unpaved roads by field measurements

Air quality measurements on an unpaved road in Klagenfurt (Austria) were carried out from 30th of July to the 25th of August 2009 to derive emission factors for PM_{10} and NO_x. The measurement setup consisted of two kerb side measurement points at a distance of 300 m between them and a local background station 150 m away from the unpaved road. The two kerb side locations were necessary because of diverging road surface (northern section-unpaved, southern section-unpaved and partly asphalted). The measurement setup is listed below.

Table 2: measurement setup

nr	site	component	method	device
MP1	kerb north	PM_{10}	nephalometer with ß-radiation	Sharp 5030 (Thermo Scientific)
		wind direction	ultrasonic anemometer	USA-1 (Metek)
		wind speed	Doppler radar	SDR
		traffic		
MP2	kerb south	PM_{10}	nephalometer with ß-radiation	Sharp 5030 (Thermo Scientific)
		NO_x	chemiluminescence	Thermo 42i (Thermo Instruments)
MP3	150m background	PM_{10}, $PM_{2.5}$, PM_1	optical	Grimm
		NO_x	chemiluminescence	Horriba
		wind direction	ultrasonic anemometer	USA (Metek)
		wind speed		

The calculation of the emission factors is based on the windward-leeward principle in order to get the differences in PM_{10} and NO_x concentrations (delta PM_{10} and delta NO_x) caused by traffic. These traffic induced concentration levels serve together with traffic data (split into PC, LDV and HDV) as a basis for the next calculation step. NO_x emission factors were calculated with the network model NEMO (Rexeis et al., 2005). The assumption that the NOx emission calculation is accurate is proven by the validation experiment described above. The fleet averaged NO_x emission factor was calculated and then multiplied with the ratio of delta PM_{10} to delta NO_x. This approach leads to a fleet averaged PM_{10} emission factor derived from field measurements as shown in equation 2.

Equation 2: calculation of fleet averaged PM_{10} emission factor

$$efPM10[g/km*veh.] = efNOx[g/km*veh.] * \frac{deltaPM10}{deltaNOx}$$

$\dot{efPM10}[g/km*veh.]$ fleet averaged PM_{10} emission factor

$\dot{efNOx}[g/km*veh.]$ fleet averaged NO_x emission factor

deltaPM₁₀ difference in PM_{10} concentrations

delta NOₓ difference in NO_x concentrations

Vehicle fleet data (number of vehicles, category, and speed) was recorded by a radar device. Based on this information the specified PM_{10} (total) emission factors per vehicle category were calculated. In the next step the PM_{10} exhaust emissions per vehicle category were calculated with NEMO. This assumes that the PM exhaust emission can be calculated with sufficient accuracy. The difference between PM_{10} (total) and PM_{10} exhaust emissions can than be allocated to PM_{10} non exhaust emissions per vehicle category.

The course of PM_{10} and NO_x daily mean values during the measurement campaign are shown in Figure 12. MP1 and MP2 reflect the concentration levels at kerb side. Rain events resulted in reduced emissions. However, this has to be taken carefully as the concentration events are average values for 24 hours while the rain event is just an indication that it rained on that specific day. It can be the case that e.g. on a day with rain in the late evening the PM emission is still high, as the reducing effect was too late to remarkably influence the PM non-exhaust emission. On 24th of August a chemical dust suppressant (CMA) was applied at a distance of 150 m along the southern section (MP2) within the framework of the Life-Project CMA+ (CMA 2010). The amount used was 90 g/m². As the stretch close to MP1 was kept untreated a dust binding effect should be visible in the readings of the PM monitors.

The comparison between the PM_{10} daily mean values of both kerb side stations in Figure 13 shows an averaged 28% higher PM_{10} level at MP1 than at MP2. The day after CMA application showed a 47% higher PM_{10} level at MP1 compared to MP2. The correlation between both delta PM_{10} levels shows an averaged 42% higher delta PM_{10} level at MP1 than at MP2, whereas the day after CMA application a 65% higher delta PM_{10} level at MP1 has been measured. This shows clearly a positive effect of CMA.

Figure 14 shows the PM_{10} exhaust emission factors per vehicle category, which were calculated with NEMO. Variations of PM_{10} exhaust emission factors are results of different average driving speeds. The PM_{10} non exhaust emission factors have been calculated for both sections. The results in Figure 15 show that, besides diverging road surfaces and driving speeds, many other factors e.g. vehicle induced turbulence or weather conditions lead to daily variations.

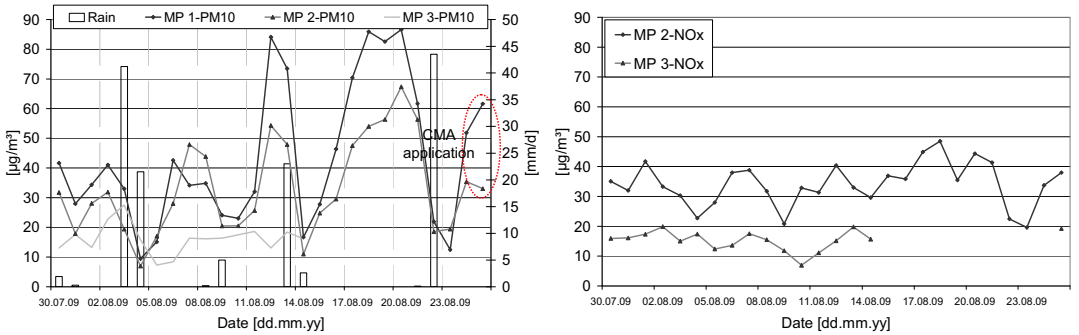

Figure 12: Trend of PM_{10} (left) and NO_X (right) daily mean values (30.07.-25.08.2009)

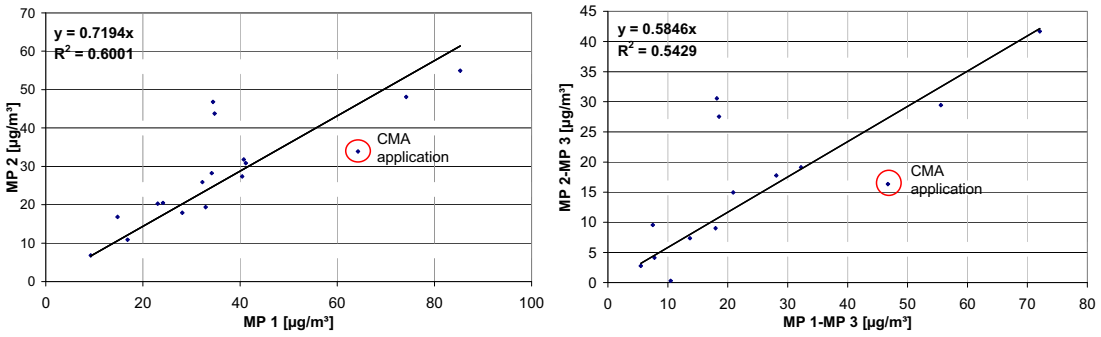

Figure 13: Correlation of PM_{10} (left) and deltaPM_{10} (right) daily mean values (30.07.-25.08.2009)

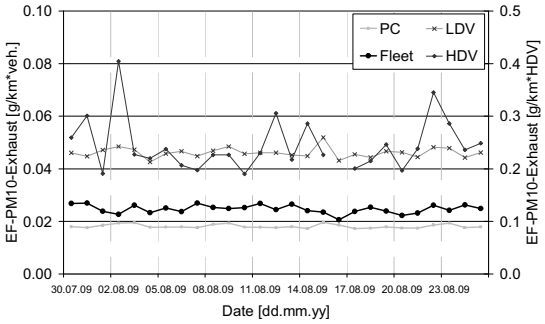

*Figure 14: Simulated PM_{10} exhaust emission factors [g/km*veh.]*

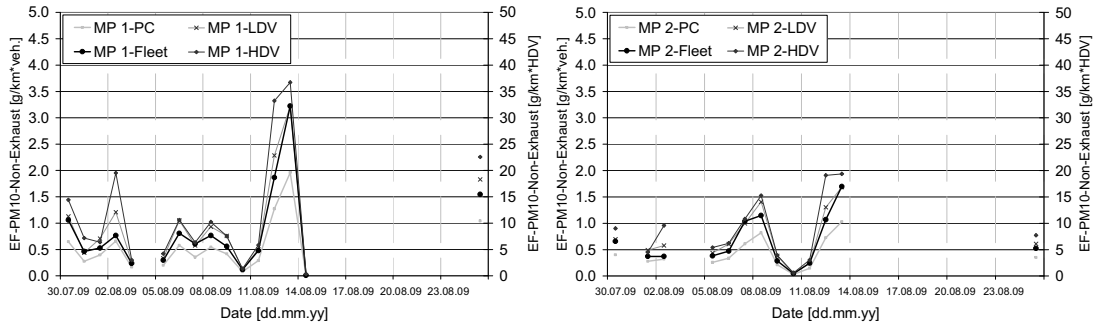

*Figure 15: Calculated PM10 non exhaust emission factors [g/km*veh.] at MP1 and MP2*

Using multiple regression analyses PM10 non exhaust emission factors could be derived for that specific stretch. Table 3 shows the results for PM exhaust (calculated via NEMO) and PM non-exhaust (derived from the measurements). The high values of the standard deviations result form the varying meteorological conditions as well as from different moisture content of the surface.

*Table 3: PM10 exhaust and non exhaust emission factors [g/km*veh.] for unpaved roads per vehicle category with standard deviation.*

vehicle category	Efa [g/km*veh.] PM_{10} exhaust	Efa [g/km*veh.] PM_{10} non exhaust (MP1)	Efa [g/km*veh.] PM_{10} non exhaust (MP2)
PC	0.018±0.0007	0.556±0.4861	0.426±0.2771
LDV	0.046±0.0018	0.960±0.8277	0.730±0.4639
HDV	0.245±0.0500	11.846±10.5372	8.818±5.7263
Fleet	0.025±0.0016	0.833±0.7768	0.640±0.4471

*Table 4: Several published PM_{10} non exhaust emission factors [g/km*veh.] for paved and unpaved roads*

	paved road urban	paved road rural	unpaved road	Reference
Fleet			1.45+/-0.37	Kantamaneni et al (1996)
Fleet			31.14 – 2047.94	U.S.EPA, AP-42 (2006)
PC	0.090 – 0.022	0.022		Düring et al. (2004)
HDV	0.8 – 0.2	0.2		Düring et al. (2004)

Table 4 lists several published PM_{10} non exhaust emission factors for paved and unpaved roads. Compared to the fleet averaged PM_{10} non exhaust emission factors in Table 3 these factors are remarkably higher. The factors according to U.S.EPA are based on a surface silt content of 35%, a surface moisture content of 0.03%, a vehicle speed of 30 km/h and a vehicle weight < 3.5 t. This shows, that the values from US EPA (2006) as well as from Kantamaneni et al. (1996) are overestimation the real situation.

Conclusion

Several measurement campaigns were performed in order to validate vehicle emission factors for NO_X, CO as well as to derive emission factors for $PM_{2.5}$ on paved and PM_{10} on unpaved roads. For NO_X a very good congruence between simulated and measured emissions could be found. The determination factor varies between R^2=0.75 and R^2=0.94. The gradient of the regression line is for every experiment around 1 ± 10%. The results for CO show that there is a rather big gap between simulation and measurement. The correlation factor varies very strongly between 0.3 (Kalcherkogel tunnel) and 0.8 (Plabutsch tunnel). The gradient of the correlation line is about 0.53 (Kalcherkogel tunnel) and 0.43 (Plabutsch tunnel). As there are no other sources of CO in a tunnel, the results for simulation and measurement should be congruent. For the examined tunnels there seem to be a big uncertainty in the CO simulation.

The $PM_{2.5}$ non exhaust emission factors for paved roads (tunnel measurements) amount to 0.028 ± 0.0029 g/(km*veh) for PC and 0.104 ± 0.0117 g/(km*veh) for HDV. Additionally half of the $PM_{2.5}$ particle emissions in a tunnel can be related to abrasion and resuspension.

PM_{10} non exhaust emission factors were derived for unpaved roads. The results came up with values around 0.426 – 0.556 g/(km*veh) for PC, 0.730 – 0.960 g/(km*veh) for LDV an 8.818 – 11.846 g/(km*veh) for HDV, but all of them having a high value of the standard deviation. The high values for the standard deviations reflect the varying conditions in terms of surface humidity and meteorology.

References

CMA (2010), www.feinstaubfrei.at; www.life-cma.at

Düring I,. Lohmeyer A., Moldenhauer A., Nitzsche E., Stockhause M. (2004), Projektbericht zum Forschungsvorhaben "Berechnung der Kfz-bedingten Feinstaubemissionen infolge Aufwirbelung und Abrieb für das Emissionskataster Sachsen".

Hausberger S., Rodler J., Sturm P.J., Rexeis M. (2003), Emission factors for heavy-duty vehicles and validation by tunnel measurements, Atmospheric environment, pp 5237-5245

Henn M., Rodler J., Sturm P.J. (2009), PM10 non-exhaust particle emissions – determination and quantification, in: ETTAP 2009 Transport and Air Pollution Symposium, Environment and Transport Symposium, Toulouse, France

Imhof D., Weingartner E., Prevot A.S.H., Ordonez C., Kurtenbach R., Rodler J., Sturm P.J., McCrae I., Eckström M., Baltensberger U. (2006), Aerosol and NOx emission factors and submicron particle number

size distributions in two road tunnels with different traffic regimes; Atmospheric chemistry and physics, Vol 6/2006 pp 1-16

INFRAS (2010) Emission Factor Handbook, Version 3.1, http://www.hbefa.net/e/index.html

Katamaneni R., Adams G., Bamesberger L., Allwine E., Westberg H., Lamb B., Claiborn C. (1996), The Measurement of Roadway PM10 Emission Rates using Atmospheric Tracer Ratio Techniques. Atmospheric Environment Vol. 30, No. 24.

Rexeis M., Hausberger S. (2005), Calculation of Vehicle Emissions in Road Networks with the model "NEMO", Transport & Airpollution Conference; ISBN: 3-902465-16-6, Graz.

Rodler J., Sturm P.J., Bacher M., Sjödin A., Eckström M., Kurtenbach R., McCrae I., Boulter P., Staehelin J., Imhof D., (2006), Quality of emission factors - improvements and validation in road tunnel experiments, Transport and Air Pollution Symposium, Environment and Transport Symposium, Reims, France

Sturm P.J., Rodler J., Lechner B., Almbauer R.A, (2001), Validation of emission factors for road vehicles based on street tunnel measurements, International International Journal of Vehicle Design Vol 27, Nos 1-4, pp65-75

US-EPA (2009) MOBILE 6 Vehicle Emission Modelling Software (http://www.epa.gov/otaq/m6.htm#m60)

US-EPA (2006), Recommendations for Emission Factor Equations in AP-42, 5th Edition, Compilation of Air Pollutant Emission Factors, Volume 1, Chapter 13: Miscellaneous Sources. November 2006.

Interaction between Road Pavement and Tyre Studs Cause Emission of Nanoparticles

M. Gustafsson[1], G. Blomqvist[1], A. Gudmundsson[2]

1 VTI – Swedish National Road and Transport Research Institute, SE-581 95 Linköping, Sweden, mats.gustafsson@vti.se
2 Division of Ergonomics and Aerosol Technology, Department of Design Sciences, Lund University, P.O. Box 118, SE-221 00 Lund, Sweden

Background

Studded tyres are the most common winter tyre type in the Nordic countries. Their main advantage is a superior grip on icy roads (Scheibe and Kirkland, 2002). It has been shown, though, that they are also able to produce high concentrations of inhalable particles (PM_{10}) through road surface wear (Hussein et al., 2008, Gustafsson et al., 2009a). In many city and street environments they strongly contribute to violations of the air quality standard for PM_{10}. The studs wear road surface stone material into small fragments, which are emitted to the air, either directly or through suspension after storage on humid road surfaces. Since these mechanically generated particles are mainly in the coarse inhalable fraction ($PM_{10-2,5}$) they play an important role for the mass based PM_{10} air quality standards.

At VTI (Swedish National Road and Transport Research Institute) a road simulator is used for studying formation processes and properties of wear particles from the interaction between road surface and tyres (Gustafsson et al., 2008). The main focus is to investigate how pavement and tyre properties can be adjusted to produce less wear related PM_{10}, but particle properties and their connection to health effects is of growing interest.

Already in the first tests at the road simulator, back in 2003, particle number size distributions revealed a particle mode around 20-40 nm. This mode was first suggested to originate in road simulator electrical motors, but this could be ruled out by measuring in the motor ventilation air. The particles were described and hypothesized to originate in thermal degradation of carbon reinforcing filler material (soot agglomerates) and volatilisation of softening oils originating in the tyre rubber in Dahl et al. (2006) and Blomqvist et al.(2007). To further study the origin of these wear related nanoparticles a research project called NanoWear was initiated in 2005 and finished in 2009. This paper describes some findings from NanoWear and following research.

Methods

The road simulator at VTI is used to produce wear particles from pavement and tyres (Figure 1). Particle sampling in the simulator hall (13.5 x 11.3 x 5.3 m = 808.5 m3) makes it possible to sample wear particles with very low contamination from surrounding sources and no influence from tail-pipe emissions. The road simulator consists of four wheels that run along a circular track with a diameter of 5.3 m. A separate DC motor is driving each wheel and the speed can be varied up to 70 km h^{-1}. At 50 km h^{-1} a radial movement of the vertical centre axis is started to force the tyres to wear evenly on the pavement. Any type of pavement can be applied to the simulator track and any type of tyre can be mounted on the axles. During measurements the simulator hall is not ventilated although pressure gradients might cause minor self-ventilation. An internal air cooling system is used to temperate the simulator hall down to sub-zero temperatures. The hall is also equipped with a large filter fan, acting as a sink to simulate outdoor mixing for more natural sampling conditions.

Before testing with a new pavement, the pavement is worn according to a standardised cycle in order to achieve a wearing course of a certain age.

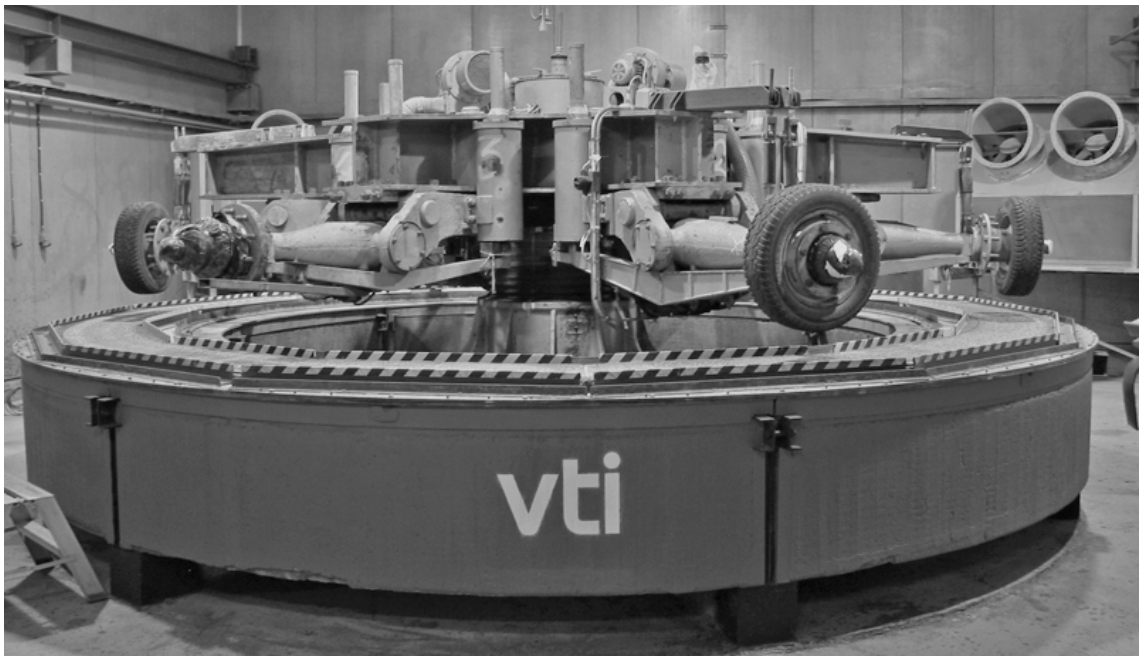

Figure 1. The road simulator at VTI

The road simulator test cycle that is normally used is described as:

1. 1.5 h 30 km h^{-1}

2. 1.5 h 50 km h^{-1} with radial movement

3. 2 h 70 km h^{-1} with radial movement

If particle sampling at high concentrations are to be performed, the above cycle is completed with

4. 1 h 70 km h^{-1} with radial movement and filter fan sink.

By using a standardised test cycle, measurements using different combinations can easily be compared.

In the tests presented in this paper, a stone mastic asphalt (SMA) pavement was used with a maximum stone size of 16 mm. The matrix stone material was quartzite from the Dalbo quarry in Sweden. Tyres were run on this pavement using the above mentioned test cycle. The tyres presented were two new standard studded winter tyres and two summer tyres from well known brands. Also, to investigate the influence of tyre rubber as opposed to tyre studs on particle generation, studded tyres taken out of the production before mounting the studs were used in one experiment. To simulate realistic temperature condition for the two tyre types, winter tyres were tested with an initial pavement temperature at around 0°C, while summer tyres were tested at around 15°C.

The particle size distribution measurements were performed at the road simulator using an Aerodynamic Particle Sizer (APS, model 3321, TSI Inc., USA) and a Scanning Mobility Particle Sizer (SMPS, TSI Inc., USA). The APS was equipped with an omni-directional PM_{10} inlet (Ruprecht & Patachnik) and the sampling time was set to 60 s. The APS was placed about 2 m from the edge of the pavement and the height of the inlet was about 2 m from the floor (1 m above the pavement). The SMPS system consisted of a Differential Mobility Analyzer (DMA, model 3071, TSI Inc., USA) and a Condensation Particle Counter (CPC,model 3010, TSI Inc., USA). The aerosol and the sheath air flow rates were set to 0.3 l min^{-1} and 3 l min^{-1} respectively, giving a detectable size range of 10-500 nm with up and down scan timings of 60 s and 30 s respectively. The SMPS system was placed outside the closed room housing the road simulator and the aerosol was sampled through a 2.0 m ¼" copper tube. During the testing sessions, the background aerosol was measured before starting the road simulator. For calculated mass

concentrations a density of 2.8 and 1.0 was used for the APS and SMPS measurements respectively.

Results

Total particle number concentrations during the test cycle reveal that studded tyres generate high concentrations, while summer tyre generate low concentrations and only sometimes react at the speed changes during the cycle. Particle number concentrations are similar for all three tested studded tyres (Figure 2).

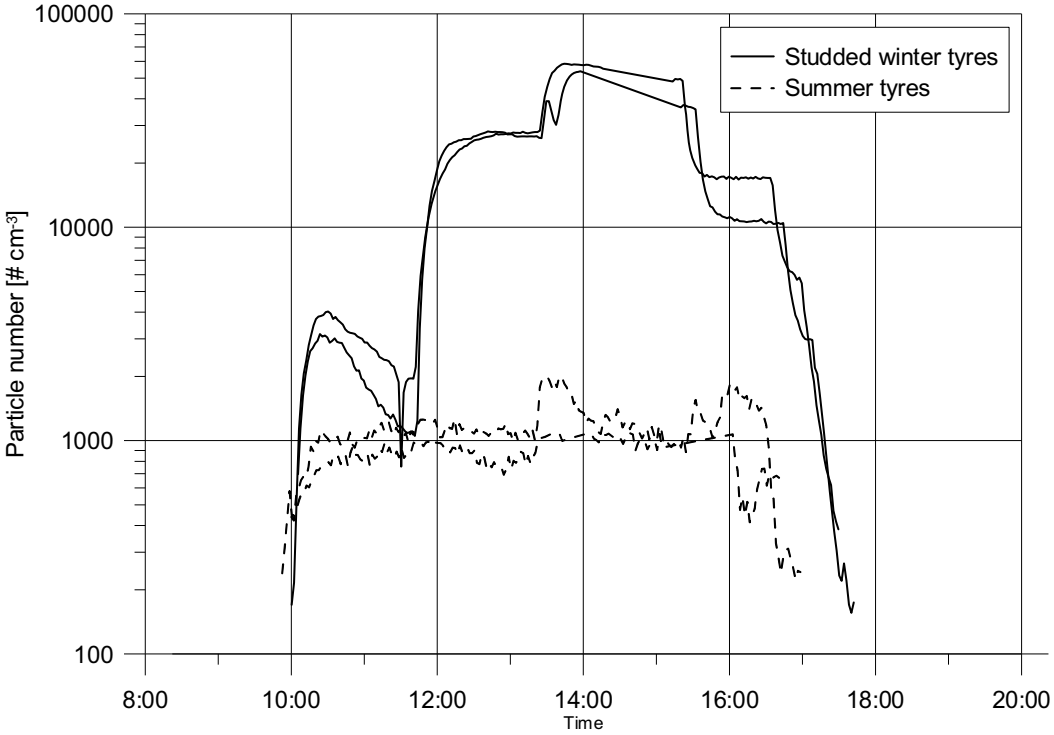

Figure 2: Particle number concentrations for studded winter tyres and summer tyres.

Particle size distributions show that the particles generated during the studded tyre tests have a number concentration with a wide maximum at about 30-40 nm, while the two summer tyres have a concentration minimum at about the same sizes (Figure 3). Studying single tyre types at different speeds shows that the studded tyre particle mode grows as speed increases indicating a speed related source (Figure 4). For a summer tyre a mode between 40-200 nm declines with increasing speed while a mode below 40 nm seems to increase on increased speed, but the concentrations over the whole size spectrum is very low.

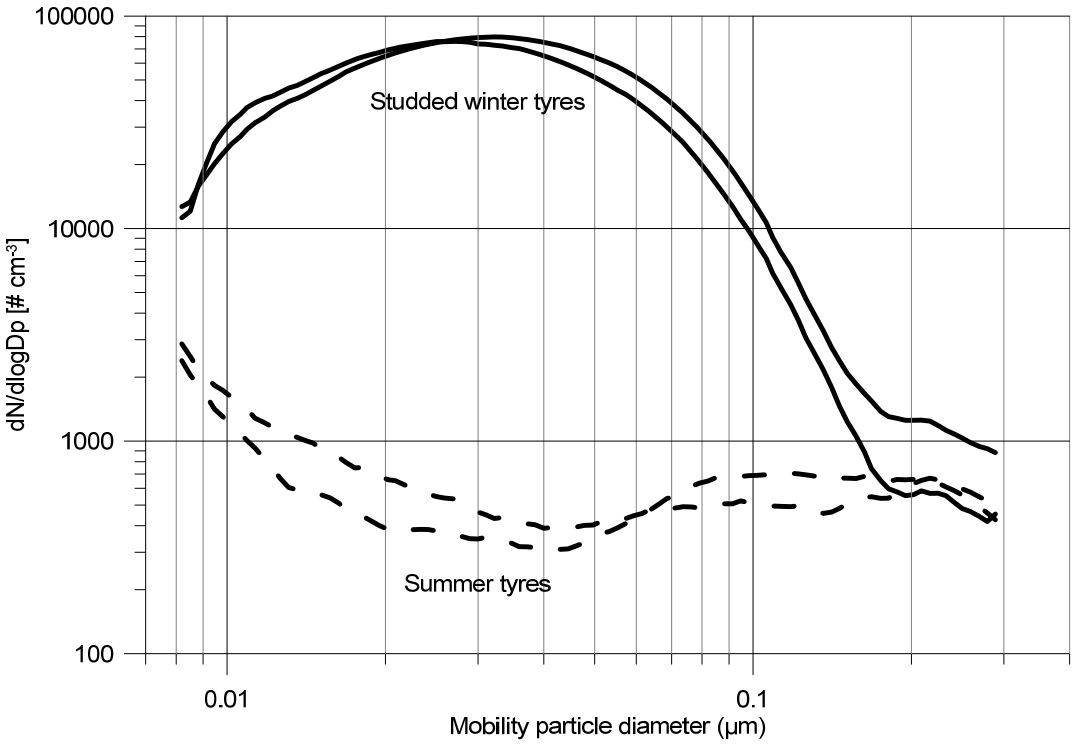

Figure 3: Particle number distributions at 70 km/h when running two different studded tyre brands and two different summer tyre brands in the road simulator.

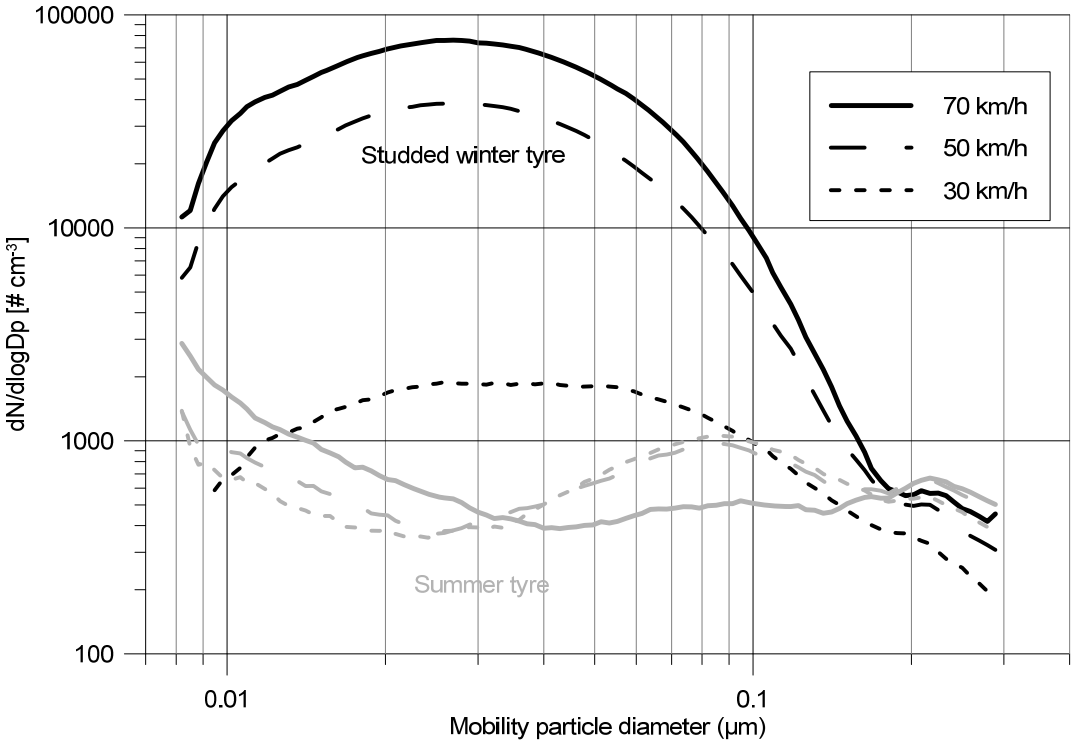

Figure 4: Particle number distributions at different speeds for one studded and one summer tyre brand.

In the experiment using studded tyres with and without the studs (same tyre brand and model), the tyre with studs generates the typical nanoparticle mode, while the tyre which never got its studs mounted in the thread generates a size distribution resembling the distribution of a

summer tyre (Figure 5). This result implies that the particle mode that forms when using studded tyres is related to the tyre studs rather than the tyre rubber.

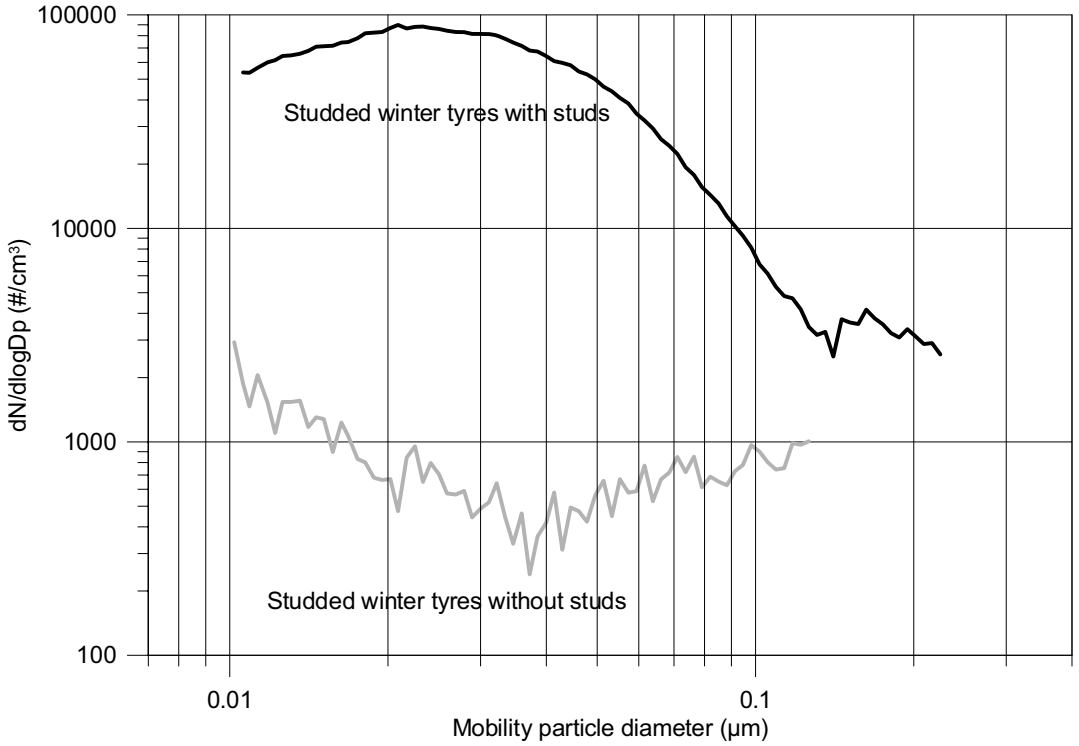

Figure 5: Particle number distributions at 70 km/h when running the same studded tyre brand with and without studs in the road simulator.

Conclusions and Discussion

Studded tyres are well known to produce mechanically generated coarse particles in the PM_{10} size fraction and thereby contributing to surpassing the environmental quality standard in street and road environments (Hussein et al, 2008). Ultrafine particles (<100 nm) on the other hand, are normally related to combustion exhaust (e.g. Zhu et al., 2002). This paper shows that, in laboratory conditions, ultrafine particles form in the wear process between studded tyres and road pavement. The test with studded tyres without studs shows that our previous theory that the ultrafines originate in softening oils from the tyre rubber (Dahl et al., 2006) is likely to be wrong. Rather, the particles form in the contact between the studs and pavement stone or between the studs and pavement bitumen.

Nevertheless, nanoparticles even smaller than the particle mode in focus in this investigation appear during tests with all kinds of tyres, as for example the mode below about 30 nm increasing with speed in Figure 4. Occasional unstudded winter tyres seem to emit rather high amounts of this nanoparticle mode. The mode is much more sporadic and the source and formation process unknown. The previously suggested (Dahl et al., 2006; Blomqvist et al, 2007) sources carbon reinforcing filler material and volatilisation of softening oils might be an explanation.

The emission factors of the stud related particle mode have been calculated to be 0,1-1 % of emission factors observed for tail-pipe exhaust (Dahl et al., 2006) and their implication from a public health perspective depends on their composition and occurrence in real traffic which remains to investigate. A chemical tracer is probably needed to identify the particles occurrence, since they are in the same size range as exhaust particles and are likely to quickly interact with the ambient aerosol.

Ongoing research aims at sampling and analysing the ultrafine particles to identify the source and process that emits these particles, as well as finding a suitable tracer and investigating potential health effects.

References

Blomqvist, G., Gustafsson, M., Gudmundsson, A., Dahl, A. and Swietlicki, E. (2007) Ultra-fine particles from tyre and pavement interaction, In: Sokhi, R. and Neophytou, M. (Eds.) Urban Air Quality, Proceedings of short papers presented at the *6th International Conference on Urban Air Quality*, Cyprus 27–29 March 2007. Digital CD Proceedings, ISBN 978-1-905313-46-4.

Dahl, A., A. Gharibi, E. Swietlicki, A. Gudmundsson, M. Bohgard, A. Ljungman, G. Blomqvist, M. Gustafsson (2006), Traffic-generated emissions of ultrafine particles from pavement tire interface, *Atmospheric Environment*, 40 (7), 1314-1323.

Gustafsson M., G. Blomqvist, A. Gudmundsson, A. Dahl, E. Swietlicki, M. Bohgard, Bohgard, J. Lindbom, A. Ljungman (2008), Properties and toxicological effects of particles from the interaction between tyres, road pavement and winter traction material, *Science of The Total Environment,* 393: 226-240.

Gustafsson M., G. Blomqvist, A. Gudmundsson, A. Dahl, P. Jonsson, E. Swietlicki (2009a), Factors influencing PM10 emissions from road pavement wear, *Atmospheric Environment,* 43: 4699-4702.

Hussein, T., C. Johansson, H. Karlsson and H. Hansson (2008), Factors affecting non-tailpipe aerosol particle emissions from paved roads: On-road measurements in Stockholm, Sweden, *Atmospheric Environment*, 42(4), 688-702.

Scheibe, R. R., K. C. Kirkland (2002), An overview of studded and studless tire traction and safety, Research Report, Research Project Agreement T2695, Task 21, Washington State Transportation Commission, Department of Transportation and U.S. Department of Transportation, Federal Highway Administration.

Zhu Y., W.C. Hinds, S. Kim, C. Sioutas (2002). Concentration and size distribution of ultrafine particles near a major highway, *Journal of the Air and Waste Management Association*, 52 (9), 1032-1042.

ALSTOM Hybrid shunter locomotive

Authors : R. Hesnard[1] & J. Oostra[2]

1 Alstom Transport, Renovation engineering manager for Train Life Service activities. 93482 St Ouen, France, renaud.hesnard@transport.alstom.com

2 Alstom Transport, Project Manager for Train Life Service activities. Ringdijk 390C, Ridderkerk, The Netherlands, jolt.oostra@transport.alstom.com

1. Abstract

ALSTOM, leader in traction drive system, developed a modernisation hybrid pack for shunter loco to allow industrial yards and terminal station to enter into the era of environmentally friendly traction. The 4 years development achieved by ALSTOM results in a locomotive with fuel consumption reduction of 40%. The high efficiency and the better use of the diesel engine result in a CO2 reduction of 100tons per year and per loco, and a particle emission reduction of 70%.

2. Conventional shunter locomotives

Hauling is a core activity of railways operations. It consists, for example, in collecting cars or wagons for construction of a train or distribution of wagons in an industrial area. Rail shunters are required in depots, in freight yards, in passengers' terminal stations, in industrial plants connected to rail network, in harbours and in multimodal terminals. Railways operators dedicate specific hauling locomotives fleets for those duties. Industrial sites connected to the rail network own hauling locomotives for freight wagons shunting on their sites. In order to be able to operate without collecting energy from the overhead line, or on non-electrified tracks, the energy source of those locomotives is a diesel engine leading to the consumption of huge quantity of fuel.

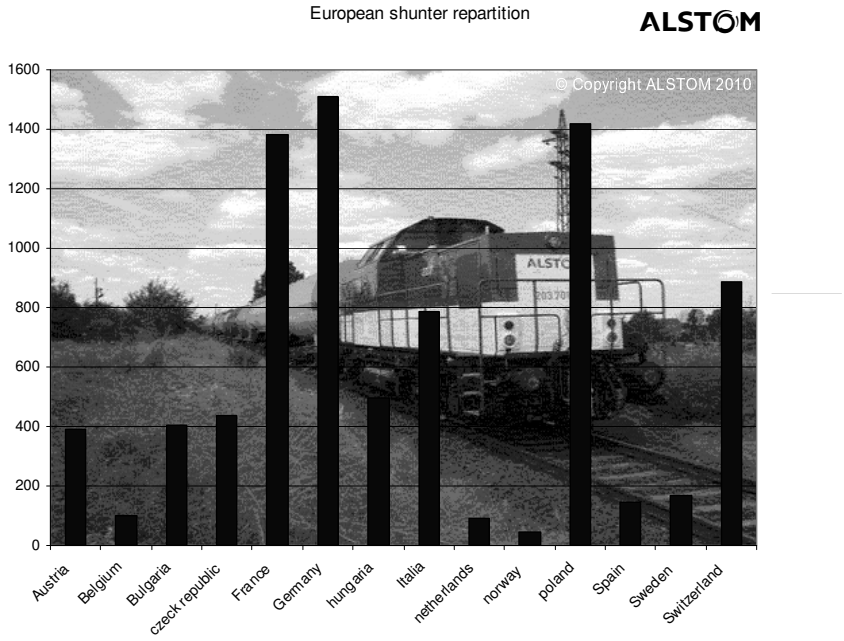

Figure 1 : European shunter repartition

Classical diesel electric or diesel hydraulic traction drives within a power range from 500 kW to 1000 kW can fulfil most shunting mission profiles. The locomotive power pack is sized to fit with the maximum traction effort required for an application. For, instance, in heavy industry,

hauling locomotives shall be able to pull a heavy train, and the traction effort required is around 150 KN.

A conventional shunter consumes on average a total of around 140.000 litres of fuel per year. The European shunting fleet consumes about 1 million m3 of fuel per year corresponding to an estimated emission of 3Mtons of CO_2. Because the engine is always running, noise emission is another issue.

The conventional power train of a hauling locomotive, called shunter, consists in a diesel engine, connected to a torque converter that transmits the power to the bogies thanks to shafts. This type of shunter is called diesel hydraulic locomotive. The torque converter consists of a variable speed transmission, increasing the torque of the engine at low speed thanks to oil turbines. The power losses of such equipment are rather inconvenient and generated due to the oil viscosity. As shown on figure 2, the global efficiency (grey) at low speed is under 50%, so the wasted energy pass over 50% of the engine power. The losses are even higher when locomotive trail very heavy trains.

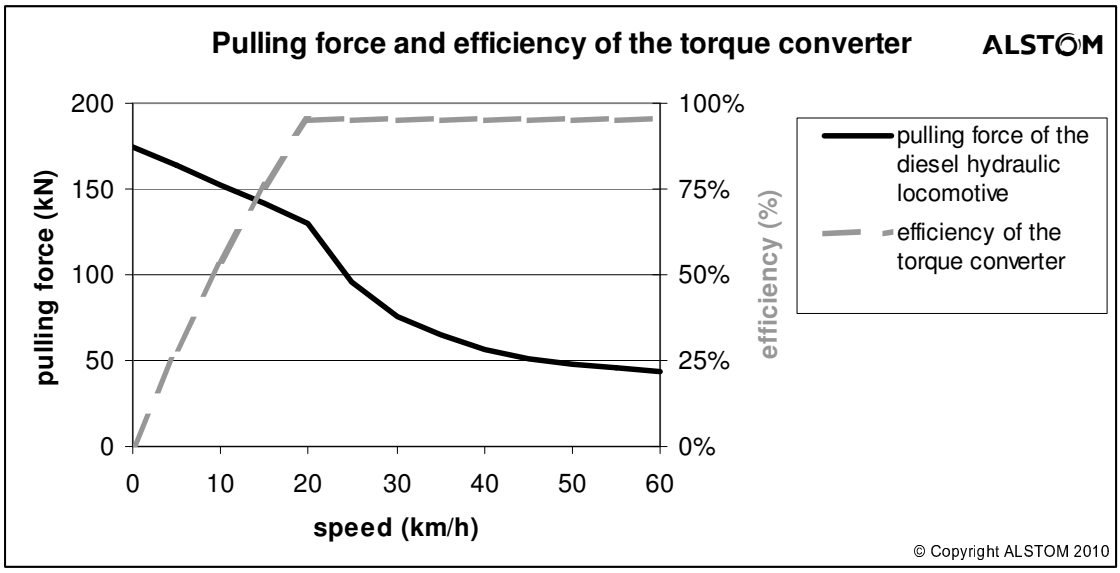

Figure 2 : Torque converter efficiency curve

The torque converter component permits to reach very high torque value and pulling force at low speed, but decreases the general efficiency of the power train.

The power pack is sized to match the expected performance on the heaviest train that the locomotive will have to pull. However, the hauling locomotive will hardly be used at maximum power, since it is most of the time used to pull individual trailer, light train, or even only auxiliaries at standstill.
The result of this dimensioning of the power pack is a heavy cost of maintenance, strong fuel consumption and a high level of pollution since the engine is not used at its best efficiency running point. The Figure 3 represents the running point of the diesel engine on a standard graph of specific fuel consumption. Most of the lifetime of the engine, it is running at idle speed, generating power only for auxiliaries (the group of running point at the bottom left of the graph). At this running point, the specific fuel consumption is above 300g/KWh that is a very low efficiency performance of the engine. Indeed, the engine is able to consume less than 200g/KWh when it is used at higher loads. However, as for automotive application, full load is hardly reached in the lifetime of the engine. As shown in the graph, there is only a few running points at heavy load of the engine. It results in a maintenance and consumption cost corresponding to a powerful engine, but very hardly used at its best efficiency point.

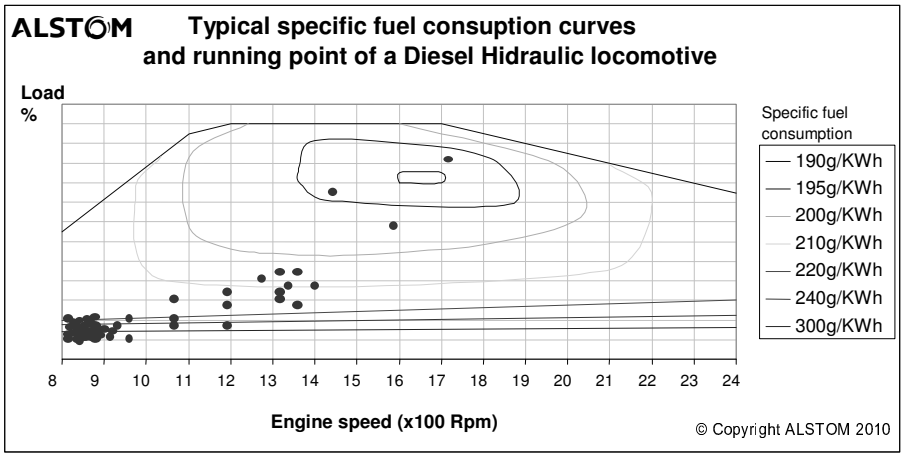

Figure 3 : running points of a Diesel Hydraulic hauling locomotive.

The engine is used most of the time at idle speed. This idling operation of the diesel engine is generating “non productive” fuel consumption, noise, emissions and engine life duration reduction.

3. Hybrid diesel electric traction: a good solution for shunter locomotives

Growing awareness of the limitations of the classical diesel hauling locomotives has pushed to investigate the feasibility of alternative solutions. Given the considerable impact of long idling time and variable power requirements during hauling activities, a hybrid technology combining electrical traction drive, accumulators’ batteries and a diesel generator have been investigated.
In the automotive industry, hybrid technology has successfully entered the market, demonstrating clear benefits in urban traffic, having close similarities with hauling operation. Hybrid technology can be proposed as a renovation package for existing locomotives, limiting the capital expenditures and extending the expected life duration of the existing fleets. It can also be offered for new locomotives as an alternative hybrid power pack.

By its leadership position in traction drive system, ALSTOM is prospecting all the alternative traction drive systems. For shunting activities, ALSTOM launched a research and development program on the hybrid traction.
Main target of hybridizing locomotives is to optimize the power generation on the average need of the locomotive. Thanks to an energy buffer (the batteries), the diesel generator shall not be sized on the peak value of power needed, but on the average value.
In this way, generator is used to fill the buffer, which implies a downsizing of the diesel generator and an optimization of its running point.
Moreover, the power generation is not needed for little applications, as for the auxiliary supplies. Theses functions can be powered thanks to the buffer, and the diesel generator is launched only when batteries need to be loaded, or when the driver need to get the full performance of the shunter.

As presented in the figure 4, a diesel generator providing power to batteries is used most of the time close to the optimum set point in term of efficiency.

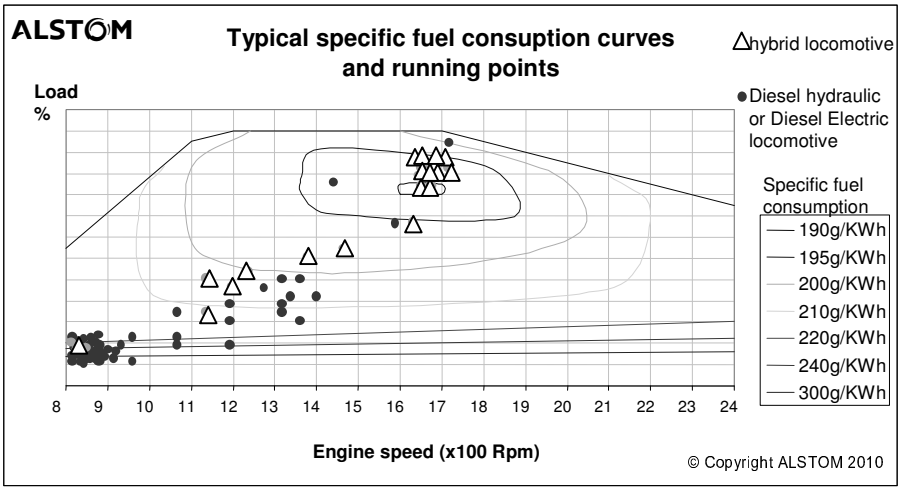

Figure 4 : comparison of the running point repartition of the diesel hydraulic vs hybrid loco

This figure clearly compares the running points of a diesel hydraulic locomotive (round shape), to a hybrid locomotive. At the opposite to the common locomotive, the diesel engine is used most of the time at full load, close to the optimum running point, under 200g/KWh. This is implied by the power management of the locomotive, launching the diesel engine when power demand exceed the battery power, or when batteries need to be charged. As soon as the power demand is low, the diesel engine shuts down and the battery supplies the locomotive. In this way, the fuel is most of the time consumed with a good efficiency, bringing important fuel savings and pollution reduction.

4. Electrical architecture

The basic features of this hybrid solution designed by ALSTOM are (figure 5):

1. A combination of batteries and a diesel generator as power supply, connected to an electrical “power bus”
2. A traction power converter supplying power to the electrical traction motors.
3. An auxiliary converter supplying 3 phase AC currents for Air compressor, air conditioning and other auxiliary system
4. A battery charger and auxiliary batteries supply DC low voltage for the control functions of the locomotive.
5. An Energy Management System, based upon continuous monitoring of the requested power and of the state of charge of the batteries.

The traction power converter, the auxiliary power converter and the battery charger receive primary energy from the “power bus”.

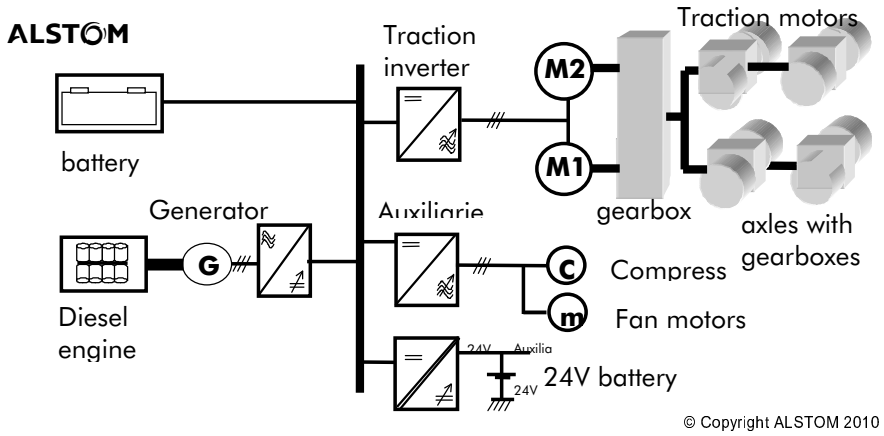

Figure 5: electrical architecture

If the total power requested by the loads connected to the “power bus” is lower than the maximum power output from the batteries, the locomotive is operated on the batteries only. If the total requested power exceeds the maximum output of the batteries, then the diesel generator is operated in parallel with the batteries. Reaching the threshold for low state of charge of the batteries will trigger the diesel generator, which will operate as a batteries charger. This is illustrated in the figure 6. In figure 6 the locomotive is performing 13 trips, with idling intervals in between.
The maximum power output of the batteries and the diesel generator set is constantly monitored during operation of the locomotive. The Energy management System will automatically manage the traction power, the diesel generator power and the battery load to optimize performance of the locomotive, the fuel consumption, the gas emissions and the global life cycle cost of the locomotive.
Depending of the customer requirements and the specificities of each mission profile, the hybrid solution must be customized in terms of dimensioning for each application.

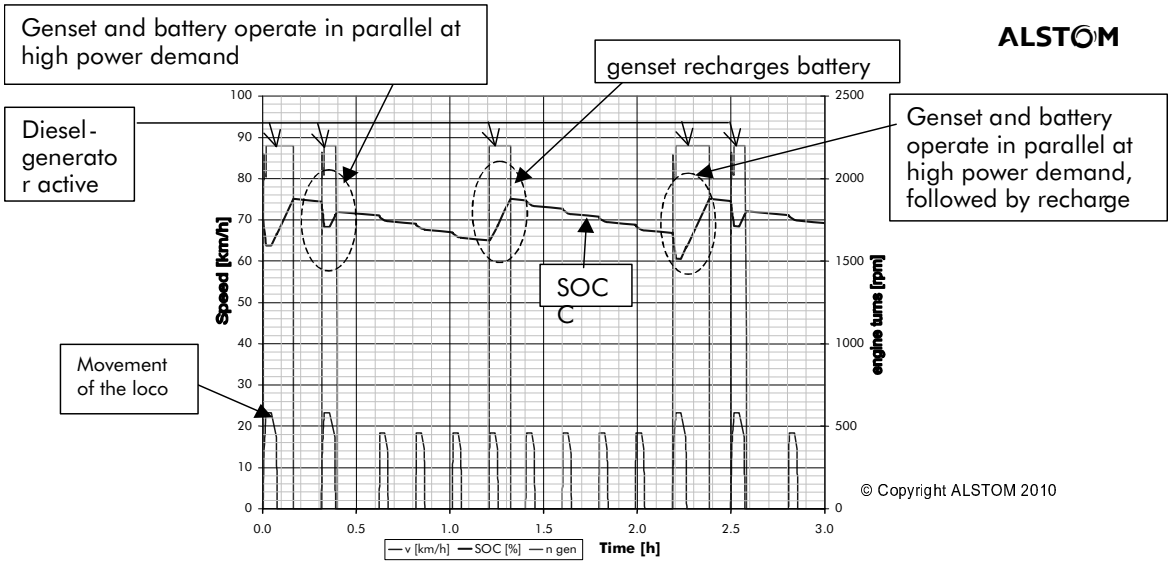

Fig 6 : mission profile and State Of Charge (SOC) of the batteries

The previous graph illustrates that during a 3 hours operating time of a shunter, a hybrid locomotive designed according to the electrical architecture here above could turn off the diesel engine for 80% of the time.

5. Gas emissions and savings

Fuel consumption savings
First results of tests and measurements performed by ALSTOM show a fuel saving of around 40%. This fuel saving ensures a payback of the additional cost of batteries of 3 – 5 years. After this first period, the hybrid technology ensures a profitable investment, generating huge saving thanks to the fuel consumption and the reduced maintenance of the small diesel engine.

The fuel savings are generated by:

- The good efficiency of the diesel engine of the generator set. When the Generator set is on, the engine will nearly always be running very close to its optimum set point, and its efficiency will be at its best. The volume of fuel consumed per kWh will be constant, with no dependencies from the mission profile. At the opposite, a conventional Diesel hydraulic shunting locomotive will adjust the engine running point to the current need. It results in a variation of the specific fuel consumption, and so a decrease of the general efficiency of the engine.
- The fact that the generator set will not be operated for most of the duration of the idling time. In this case the generator set with its constant level of efficiency produces

the energy needed by the locomotives to sustain the standstill periods. On the contrary, on a classical diesel shunter locomotive, this energy will be supplied by the diesel engine in idling mode, with a poor efficiency. Large engines idling consumption is not depending from the power output (provided it is relatively small; less than 10 % of nominal power), but from the duration of the operation.

- No hydraulic torque converter, which generate poor efficiency in the lower speed range.

A comparison of the real use of the fuel consumption is presented on figure 7, and presents a fuel saving according to the technology.

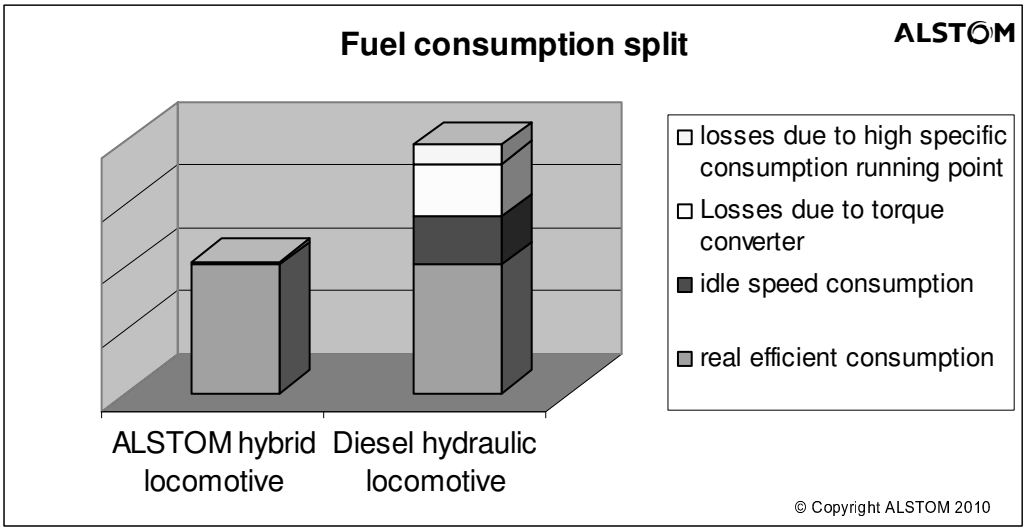

Figure 7 : fuel consumption comparison

Depending of the type of mission that vary from a customer to another, the fuel consumption savings are around 40% and the lifetime of the battery is between 5 and 10 years. So the global life cycle cost of the locomotive is significantly cheaper than a conventional locomotive.

Pollution limitation :
Pollutant emission will be reduced automatically by the fact that the global system efficiency is increased. Furthermore, as the engine will be operating closed to its optimum point, the gas treatments runs better than at low (idle mode) speed and the particles emissions are, according to engine manufacturer data sheets, reduced by 70% compared to a conventionally used-diesel engine. For the residents, pollutant is perceived through characteristic smell of a diesel engine. Pollutant reduction will drastically reduce the impact on the environment.

Noise reduction :
Noise generated by the Railway Transport is a real issue. There many complaints from residents about noise level, especially near the depots where shunting locos are operating. Typically, in railway terminal station, shunter are used to collect and built a train. These stations are often located in the city centre, and generates noise disturbance to the inhabitants. It is obvious that a hybrid loco “silent” during 80% of its operational time will bring a real relief to residents living near depots.

Remote Measurements of Ship Emissions: The SIRENAS-R Campaign

J. M. Balzani Lööv[1], B. Alfody[1], F. Lagler[1], J. Hjorth[1] and A. Borowiak[1].*

[1] Joint Research Centre, Institute for Environment and Sustainability, 21027 Ispra (Va), Italy.
jacob.balzani@jrc.ec.europa.eu

Introduction

Atmospheric emissions from ships have not been focus of regulations until recent years. While shipping remains an efficient way to transport goods, at the same time, the lack in regulations allowed the use of the heavy fuel oil, the residue remaining after refining crude oil, characterised by high sulphur content. Also the emissions of nitrogen oxides have been unregulated until 2000. The resulting pollution from nitrogen oxides (NO_X) and sulphur dioxide (SO_2), which has negative effect on human health and the environment (eg. Eyring et al., 2005, Galloway et. al., 2005; Corbett, 2007), will overcome the diminished pollution on land where emissions have been effectively controlled. The International Maritime Organization (IMO) filled this void by establishing MARPOL Annex VI which was adopted in 1997 and entered into effect in 2005. In the EU, Directive 1999/32/EC as amended by 2005/33/EC sets limits for the sulphur content in fuels. Currently, the Annex specifies that in the North Sea and Baltic Sea Sulphur Emission Control Areas (SECAs) no fuel can be burned if its sulphur content exceeds 1.5% by mass. Outside of SECAs, the limit is 4.5%. In addition from 1 January 2010 the EU Directive stipulates that ships at berth in EU ports must burn fuels with less than 0.1% sulphur. For NO_X the emission, limits are relative to power output (g NO_X/KWh) depending on the speed of the engine. According to the year of construction of the ship different three different tiers exists for ships built after 2000, 2011, and 2016. This regulation should reduce NO_X emissions by 15-22% (relatively to the actual limits) for new ships built after 2011 and by 80% for ships built after 2016.

The effective measure of the ship emissions and their control is not an easy task because the use of higher sulphur fuel is likely to happen outside the harbours. In addition the production of NO_X during real operating conditions might differ from the standard certification procedure of the engines.

In order to overcome the difficulties to perform on-board inspections the Joint Research Centre (JRC) of the European Commission, on behalf of DG Environment, is currently carrying out a study (2009 - 2010) to evaluate potential remote sensing techniques for the detection of SO_2 and NO_X in exhaust gas plumes of ships. The main aim is to develop an assessment system that can be employed routinely by regulatory authorities in the Member States as a means of identifying gross polluting vessels so as to increase the effectiveness of port state controls and improve compliance with legally binding fuel sulphur limits.

For the purpose of the study a comparison measurement campaign has been carried out at the entrance of the Port of Rotterdam (The Netherlands) during autumn 2009 under the name SIRENAS-R (Ships Investigation REmotely about NO_X And Sulphur - Rotterdam). Several European research institutes measured from different platforms (land, sea and air) emissions ratios and total emissions of passing ships.

SIRENAS-R Overview

The main goal of the campaign was to inter-compare different remote sensing methods for measuring ship emissions. Those methods are aimed at giving sufficiently robust and reliable indication of non-compliance with sulphur limits for used fuels, and to provide reliable information on the actual emission of a vessel (as well with a view to an emission trading scheme).

In Table 1 are summarized the different institutes involved in the measurement campaign. The evaluated measurement methods were Differential Optical Absorption Spectrometry (DOAS) as described in Mellqvist et al. (2007) , Light Detection and Ranging (LIDAR, Swart et al., 2007), UV-Imaging (Prata et al., 2008) and classical gaseous air pollutant instrumentation (hereinafter referred as “Sniffing”, eg. Segers and Duyzer, 2007) based on chemiluminescence (NOx), UV-fluorescence (SO_2) and non-dispersive IR (CO_2). Additionally, to complement the

measurements, CO_2 emissions have been modeled, using Automated Identification System (AIS) data (Jalkanen et al., 2009).

Table 1: Contribution and type of measurements of different Institutes to the SIRENAS-R campaign.

Technique	Measured Compounds	Institute
"Sniffing"	NO-NO_X-CO_2-SO_2 [ppb]	JRC (European Commission - Joint Research Centre)
"Sniffing"	NO-NO_X-CO_2-SO_2 [ppb]	TNO (Netherlands Organization for Applied Scientific Research)
"Sniffing"/DOAS	NO-NO_X-CO_2-SO_2 [ppb]//[Kg/s]	Chalmers University of Technology
LIDAR	SO_2[Kg/s]	RIVM (National Institute for Public Health and the Environment)
UV-Imaging	SO_2[Kg/s]	NILU (Norwegian Institute fo Air Research)
AIS Modelling	-	FMI (Finnish Metereological Institute)

The campaign lasted about 3 weeks during the month of September 2009. In order to maximize the number of sampled ship the location was chosen at the entrance of the Port of Rotterdam along the Neue Waterweg, being the busiest port of Europe. Land-based measurements have been performed in three different sites. The use of several sites was important to assure the right wind direction for the "Sniffing" and LIDAR measurements. In addition, on selected days, it has been possible to test the feasibility for ship- and helicopter-based measurements. This allowed investigating if a different behavior existed for certain ships before arrival to the harbor or while transiting in territorial waters. Also in order to provide a measured standard, stacks emissions were measured during 10 consecutive days on board a commercial RoPax (Roll-On-Roll-Off-Passenger-ship) ferry which could be monitored by the involved institutes several times during the campaign.

The combined use of different methods, measurement locations and platforms allowed us to design different experiments, in particular:

- Estimate accuracy and precision for the measurement of the sulphur content of fuels and NO_X emissions factors using "Sniffers".
- Estimate accuracy and precision for the measurement of SO_2 total emissions performed by optical measurements.
- Evaluate accuracy and precision for the use of modeled CO_2 and measured SO_2 emissions to retrieve the sulphur content of the fuel.
- Improving the accuracy for modeling of CO_2 and NO_X emissions.
- Evaluate the global operability of each system and the effectiveness of performing measurements from ship and helicopter.

At present the large amount of data collected during the campaign is still under evaluation and presents many interesting features worth further investigation.

First Results: JRC-IES measurement data

The mobile laboratory of IES was equipped with the following measurement instruments: 2 LI-COR CO_2 analyzers, 2 Thermo SO_2 analyzers, 2 Environment NO_x analyzers, 2 Grimm aerosol spectrometer, 1 TSI condensation particle counter and meteorological sensors (air pressure, temperature, relative humidity, wind). The duplicated equipment allowed for simultaneous measurements at two different heights (5 and 15 meters).

The weather conditions were satisfactory during the whole measurement campaign. Only 3 days from the total 15 days were inadequate for the sniffing measurement. During the measurement days altogether 626 ships were registered manually. In the 32% of the ship passages the plume catch was successful, providing appropriate concentration values for the further calculations. (Calculation of sulphur content of the fuel and the NO_x emission rate

normalized by fuel consumption.) In the 68% of the cases the plum catch was inefficient due to inadequate wind direction or plume overlapping that made the source identification difficult or impossible. In the case of low emitters such as tug boats and local boat transportation, calculation of the S/C ratio was difficult because of high background concentration of CO_2.

Table 2 summarizes the distribution of the types of the measured ships. Port services and inland vessel, used mainly in harbour and rivers, generally use distillate fuel with low sulphur content (Marine Gas Oil, MGO). Service ships of the port are generally small boats with low emission rates (low signal of the CO_2 measurement), so in their cases the calculation of sulphur content of the fuel was difficult. The inland vessels have higher emission rates; however, the efficient measurement of SO_2 concentration requires ideal wind conditions because of the low sulphur content of the fuel. The land based sniffing technique is suitable for monitoring the emissions of big ocean-going ships that were 55% of the total (cargo, container, tanker, RoRo, and ferry). In these cases calculation of the sulphur content of the fuel was possible with high certainty, if the wind direction favored for the measurement and plumes did not overlap. The low percentage of the successful measurements (32%) should be evaluated with the consideration of the above discussion.

Table 2: Distribution of the measurement ships among the main ship types.

Type of ship	%
Port service	22
Cargo	21
Tanker	18
Inland vessel	17
Container	8
Coaster	6
RoRo	4
Ferry	3

Sulphur content of the fuel can be calculated based on its sulphur-carbon ratio. This ratio was derived from the SO_2/CO_2 ratio of the exhaust gas (plume). Considering the molecular weight of carbon (12 g/mol) and sulphur (32 g/mol); and the carbon mass percent in the fuel (87 ± 0.4%; Cooper, 2005), sulphur mass percent of the fuel can be calculated by the following formula:

$$S[\%] = \frac{c(SO_2)[ppb]}{c(CO_2)[ppm]} \cdot \frac{1}{1000} \cdot \frac{32}{12} \cdot 0.87 \cdot 100 = \frac{c(SO_2)[ppb]}{c(CO_2)[ppm]} \cdot 0.232$$

The concentration ratio was calculated as the ratio of the net peak areas of the measured SO_2 and CO_2 concentrations. Figure 1 illustrates measurement results of an optimal plume catch. It is shown in the figure that the starting and ending time of the SO_2 and CO_2 peaks are different. By calculating the ratio of the net peak areas the effect of this difference can be avoided.

The calculated sulphur content varied within a wide interval for the measured ships; from 0.01% up to 1.5%. The fuel sulphur content was lower than 0.06% in the case of 18% of the measured ships. Tug boats and other boats being on duty in the harbor belong to this group that use generally sulphur depleted fuel (e.g. diesel). In addition a few container ships and tankers are members of this group as well. The mean sulphur content of this group is 0.03%, while the normalized standard deviation is 50%. The sulphur contents of the remaining 82% of the measured ships lie between 0.06% and 1.5%, following a normal distribution. This wide range was divided into 5 intervals with equal range. This bimodal sulphur content distribution is

illustrated in Figure 2. It can be concluded from the results that all measured ships complied with the SECA limit for fuel sulphur.

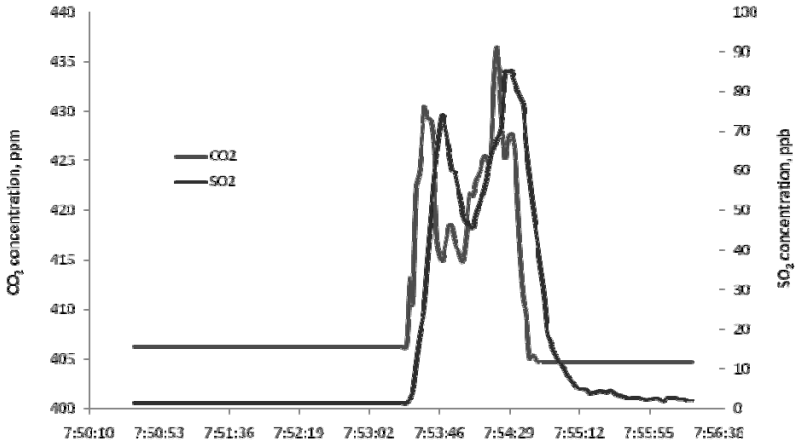

Figure 1: Variation of SO_2 and CO_2 concentrations during plume passage.

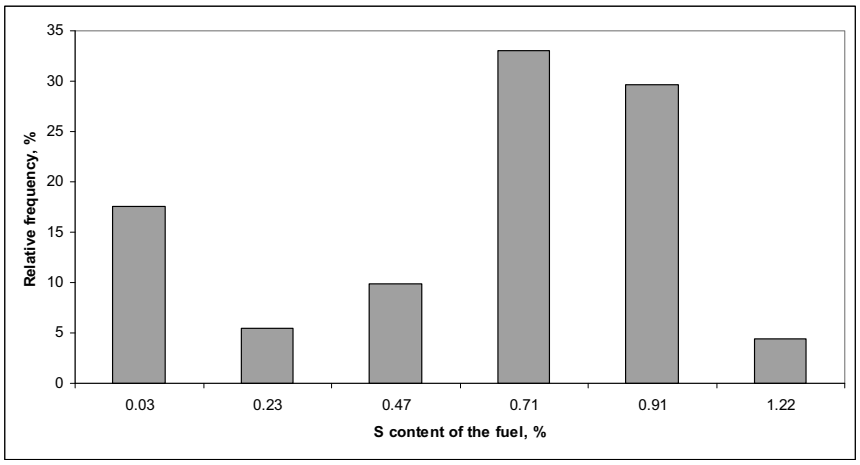

Figure 2: Sulphur content distribution of the measured ships.

Regarding NO_x, the engine power weighted emission is regulated by IMO. As displayed in Figure 3, the limit value is a function of the rated engine.

Composing the NO_x/CO_2 ratio, fuel mass weighted NO_x emission factor can be calculated. Considering the molecular weight of carbon (12 g/mol) and oxygen (16 g/mol); and the carbon mass percent in the fuel (87%), the fuel mass weighted NO_x emission can be calculated (in g/kg). This value can be converted to engine power weighted NO_x emission applying the typical specific fuel efficiency (210 g/kWh ± 10%; Cooper, 2005; Dalsoren et al., 2009). The engine power weighted NO_x emission of the measured ships varied between 0.87 g/kWh and 14.7 g/kWh following normal distribution as it can be seen in Figure 4. The weighted NO_x emission in the 70% of the ships (sum of the first 3 intervals) are lower than the lowest IMO limit (9.8 g/kWh). The weighted emissions of the last 2 intervals are lower than the IMO limit for 400 rpm and lower engine speeds. However, we in order to comment on the compliance with the IMO limit by the ships within these two intervals, the rated engine speed has to be known.

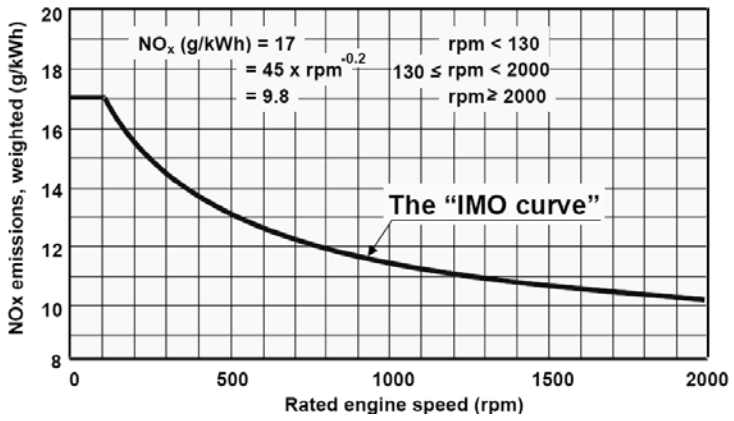

Figure 3: Engine power weighted NO_x emission limit (Tier I, described in IMO, Marpol annex VI) as a function of the rated engine speed.

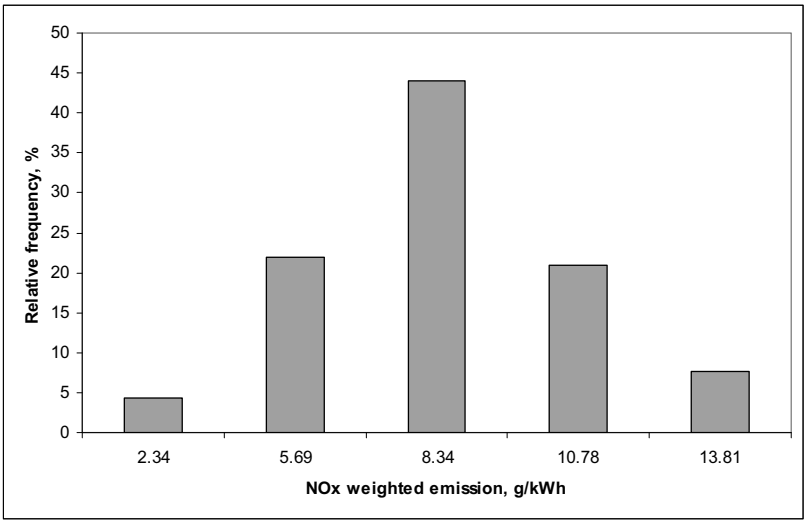

Figure 4: Distribution of the engine power weighted NO_x emission of the measured ships.

References

Cooper, DA. (2005), HCB, PCB, PCDD and PCDF emissions from ships. Atmos. Environ., 39, 4901-4912.

Dalsoren, SB., Eide, MS., Endresen, O., Mjelde, A., Gravir, G. and Isaksen, ISA. (2009), Update on emissions and environmental impacts from the international fleet of ships: the contribution from major ship types and ports. Atmos. Chem. Phys., 9, 2171-2194.

Corbett, J. J., Wang, C., Winebrake, J. J., & Green, E. (2007), Allocation and forecasting of global ship emissions. Clean Air Task Force Report .

Eyring, V., Köhler, H., Van Aardenne, J., & Lauer, A. (2005), Emissions from international shipping: 1. The last 50 years. Journal of Geophysical Research-Atmospheres, 110, D17305.

Galloway, J. N., Aber, J. D., Erisman, J. W., Seitzinger, S. P., Howarth, R. W., Cowling, E. B., & Cosby, B. J. (2003), The nitrogen cascade. BioScience, 53, 341--356.

Jalkanen, J.-P., Brink, A., Kalli, J., Pettersson, H., Kukkonen, J. & Stipa, T. (2009), A modelling system for the exhaust emissions of marine traffic and its application in the Baltic Sea area. Atmos. Chem. Phys, 9, 9209-9223.

Mellqvist, J., Berg, N., & Ohlsson, D. (2007), Remote surveillance of Fluegas Emissions from Ships - annual report to Vinnova 2007. Chalmers Istitute of Technology internal report.

Prata, F., Knudsen, S., & Shongwe, B. (2008), Ground-based UV Imaging Cameras for Industrial Gas and Particle Measurements. NILU internal report.

Segers, A. and Duyzer, J. H. (2007), Ratio of SO2/CO2 from Ships emission. TNO internal report.

Swart, D., Berkhout, A., Bergwerff, J., & Broekman, M. (2007), Zwaveldioxide-uitstoot van zeeschepen op afstand gemeten met lidar. RIVM technical report.

PARALLEL MONITORING CAMPAINES IN AN INTERNATIONAL ROMANIAN AIRPORT

F. Popescu[1], I. Ionel[1], C. Talianu[2], I. Belegante[2]*

[1] University „Politehnica" of Timisoara, Bv. Mihai Viteazu nr.1, Chair TMTAR, 300222, Timisoara, Romania, E-mail: ionel_monica@hotmail.com,

[2] National Institute of R&D for Optoelectronics, Laser Remote Sensing Department, 1 Atomistilor Street, P.O. Box MG-5, RO-77125, Magurele, Ilfov, Romania

Background and scope of the research

Aviation is a growth sector worldwide. The growth of air traffic operations in the EC has resulted in an increase in traffic at the nation's major airports, accompanied by a corresponding increase in emissions. Increased travel air, thanks to low-cost airlines, is growing in geometric progression air pollution, as well. According to a study by the European Environment Agency (EEA), during 1995-2004, EU air space increased by 49 percent. Even if EU environmental policies have managed to cause a 7.9 % reduction in emissions of greenhouse gases, was not a satisfactory result because if there was this massive increase in air transport, emissions would have been reduced by 14 %. European Environment Agency conducted a survey after which it was found that European policies to reduce greenhouse emissions are powerless in the face of continued growth in the volume of global travel. Airport-related activities result in the emission of a host of air pollutants that adversely affect public health and the environment, including nitrogen oxides (NO_x), hydrocarbons (HC), particulate (PM), carbon monoxide (CO), and other toxics. NOx and HC are precursor emissions of ground-level ozone, which causes lung irritation and aggravates diseases such as asthma, chronic bronchitis, and emphysema. PM have adverse cardiopulmonary effects and contribute to regional environmental problems such as haze and acid rain. Toxics such as benzene and formaldehyde are known or probable human carcinogens. While emissions from most source sectors are declining due to the implementation of more stringent control programs and EC & national legislation, the growth in air travel and the continued lack or weakness of concrete implementation control programs for aircraft engines and correlated other combustion devices from the airport's ground service equipments is resulting in increased pollution from airport considered superficial sources [15]. Presently, the regulations and standards, affecting aircraft and other airport sources of emissions typically, fall worldwide into two distinct categories: (1) Measures that set limits on particular sources of emissions. These include both aircraft engine emission standards and road vehicles, and (2) National regulations establishing ambient pollutant concentrations for local air quality conditions (e.g. local air quality limit values).This distinction is important because, whilst all the individual emission sources operating at, or in the vicinity of, a particular airport may meet limits pertaining to that type of source (including standards for aircraft engines), the local pollutant concentrations thresholds still may not be met.

Directive 2003/87/CE is giving advice concerning the introduction of airport activities in the green certification commerce fro emitted GHG. Recently, more than 30 airports have promised to reduce emissions of greenhouse gases, which is the most important of its kind in the history of the aviation industry. Approximately 11 companies (representing a quarter of Europe's air traffic) that own airports representing one fourth of air traffic in Europe, have signed a plan to eliminate or reduce emissions of greenhouse gases from activities carried out on the ground, including passenger's journeys to and from airports. The EC already has a plan to reduce emissions from the airlines, which will start in 2012, but there is a similar program for airports, as well. A responsible cut for approximately 5 % of total emissions is expected. Important airports announced already intentions to become neutral in terms of carbon dioxide emissions by 2015 in the industry's biggest commitment yet to fighting climate change. In March 2010, both airports and airlines have agreed to implement a new landing system that would reduce emissions by 500,000 tons of carbon dioxide and would save 100 million pounds of fuel cost up in late 2013. The new system involves landing the descent continues, what will replace landings by lowering done in several stages, which is practiced at this time in 100 European airports. EU proposed naval and air industries to reduce emissions of greenhouse gases by 20 percent over the next ten years (by 2020), and a concrete United Nations program to fight global warming. Moreover, the European Union is urging the United States, China and India to accept the UN treaty to end the heat waves, storms and flooding linked to global warming. UN hopes to organize a further summit in to sign a new treaty to replace the one in Kyoto after it expires in

2012. Kyoto Treaty excludes these two industries, but the EU intends to introduce legislation in the new rules for air operators, which will impose limits on emissions of carbon dioxide and will surpass those which require a special permit to buy from companies with lower emissions. According to EU experts, aviation and marine industry is, to each 3 % of global CO_2 emissions [15].

On national area, in respect to airport traffic and related activities, in addition to general air quality legislation, three legal documents were released: Order NB 152/558/1119/532 – 13.02.2008, Order NB 678/1344/915/1397 – 30.06.2006, Order NB 720 – 03.08.2007 mainly for pollutant control, air quality in the airport area and noise control. With EU accession, Romania came into force and that low-cost airline has increased the number of flights and passengers. Nationally, the number of aircraft operations (defined as one takeoff *or* one landing) has grown substantially Presently in Romania the fleet consists of 375 Aircraft, 91 aircraft models, 50 air operators [16]. Airport activities have in Romania measurable impacts on local air quality, although data were insufficient to quantify these impacts. Studies showed that while the airport contributes to air quality issues in the area, its impact cannot be differentiated from the preponderance of other emissions, specifically mobile sources [4]. Notably, significant improvements have been made over the past two decades regarding aircraft fuel efficiency and quality and other technical improvements to reduce emissions. However, these advancements may be offset in the future by the forecasted growth of airport operations and other aviation activities. Because aircraft are only one of several sources of emissions at an airport, it is also considered essential to effectively manage emissions from terminal, maintenance and heating facilities, airport ground service equipments (GSE), and various ground transport travelling around, to and from airports. Optimizing airport design, layout and infrastructure, modifying operating practices for greater efficiencies, retrofitting the GSE fleet to “no-“ or “low-” emitting technologies, and promoting other environmentally-friendly modes of ground transport are some of the current opportunities airports and the rest of the aviation industry can adopt or apply to help meet these goals and encourage sustainable development in commercial air transportation.

Airport studies confirm that aircraft continue to be a relatively small contributor to regional pollution although aircraft-related NO_x contributions could increase as air traffic increases and other non-aircraft emission sources become progressively cleaner [9] [10]. Under these circumstances, regular check, for purpose of the science but also to verify the levels according the environmental protection regulations have been carried out. For ex. in the East midlands airport a study focusing on the compounds known to be emitted by mobile sources (e.g., cars, trucks, and aircraft), with particular attention to compounds associated with aircraft operations (e.g., takeoff, landing, refuelling, idling, and maintenance) was performed [13], [14]. The general goals of some studies were to assess long-term ambient concentrations of selected air toxics in the immediate vicinity of the airport and to determine whether contributions from airport operations can be distinguished from the contributions of other background sources [14], [15]. A combination of real-time monitoring and discrete sampling equipment was used to quantify pollutants, meteorological data, and traffic of airplanes. Thus benzene is attested from continuous measurements not to be over the limits, also NO_2 and PM10 [11] and insignificant contribution of other sources was confirmed. In [12] one demonstrates that whilst the operation of aircraft is the most obvious source of emissions to air other key sources include the operation of cars, vans and buses to service the aircraft and those journeys, primarily by car, to and from the airport site made by passengers and staff. Still the levels of monitored concentrations for NO_x, PM 10, PM 2.5, benzene were relatively modest. [13] reveals the fact that in several airports the air quality is determined by three sources: specific to the airport, vicinity road and other sources, forming a background, of important contributions, all.

As no regular check through direct on line measurement are usual organized in Romania, one planned a parallel monitoring campaign, accomplished by two independent laboratories, thus the scope of the research is not only to detect the level of pollution caused by local sources in the airport, but also the extension of the possible polynomial correlation between the results, for same specie. From a Romanian perspective it is one of the first monitoring campaigns in time, on line, research in this area has been accomplished. The impact of Romanian airports on the air quality is basically not best known; the Romanian National Air Quality Monitoring Network is still in a development phase and is not covering airports’ vicinity [2]. The only available data on environmental impact of Romanian airports are given by environmental impact studies based on estimation from emission factors and rarely on direct measurements [9]. The scope of the research undertaken and reported in the present article is (i) to *measure the concentrations of*

air pollutants in a regional Romanian airport in order to minimize the exposure of the passengers and the health risk involved, as well (ii) to *determine comparative values*, achieved by two independent laboratories, in order to correlate the values, not only for attesting measurement accuracy, but also for observing the standard deviation between them. The measurements have been accomplished in a large regional airport, located in the west side of Romania.

Experimental

Figure 1: Location and relative position of the two laboratories.

Figure 1 indicates the location and relative position of both laboratories. The experimental setup consists in two mobile air quality monitoring laboratories, one from University *Politehnica* of Timisoara (UPT) and one from National Institute of R&D for Optoelectronics (INOE) [4], [5], [6], [7], [8]. Each laboratory is equipped with reference point instruments for major pollutants. Meteorological sensors (wind speed and direction, air temperature, pressure and humidity) were mounted in standard conditions, near the mobile laboratories. Following pollutants have been continuously measured, with 3 min resolution, over the entire measuring episode (4 days, approx. 1500 comparative data sampling values/specie), with high precision equipment [3]: (1) CO measured with Non Dispersive Infrared, reference method EN 14626:2005, uncertainty U = 4 % for recorded values; (2) SO2 measured with UV fluorescence, reference method: EN 14212:2005, U = 1.76 %; (3) NO, NO_2 and NO_x measured with chemiluminescences, reference method: EN 14211:2005, U = 2.06 %. The detailed flights schedule was obtained and all international and national flights were counted. Meteorological data were on line recorded. All in-the-field and laboratory measurements adhered to the standard quality assurance/quality control procedures, typically associated with equipment setup and calibration, duplicate/blank samples, and data recording/reporting. Quality assurance was achieved in the field by trained and qualified technicians that visited each monitoring station on an average of twice a day to check on the operation of the continuous instruments, the shelters in which they are housed and to set up or collect the time-integrated samplers. Other tasks were related also to include zero, span and precision calibration checks on the continuous instruments as well as beginning and ending flow rate and time clock checks on the 24-hour samplers.

The experimental results are presented in figures 2 to 4.

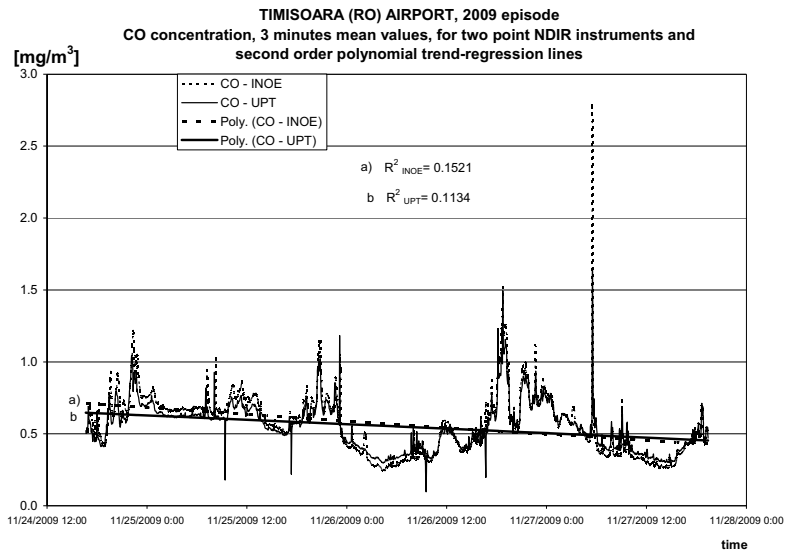

Figure 2: CO comparative recorded values, during the November 2009 episode, Timisoara airport.

Figure 2 shows the carbon monoxide CO recorded values, measured with reference NDIR point measurement instruments. A very good correlation of the measured values can be observed for the CO-UPT and CO-INOE instruments. The different instruments determined result in good agreement. The measurements respect the same trend but the values are (especially for UPT lab) registering peaks (positive and negative). This could be caused by an error in span gas calibration, but much more realistic is the correlation with the departures and arrivals of national/regional, international and charters responsible for an intensive carbon monoxide emission. The higher values for CO have only been recorded during the departure or landing of the aircrafts. This result demonstrates that the selected placement of the mobile air laboratories near the airport facilities and apron is ideal for depicting the air quality and that the measured values can be considered representatives for the airport facilities surroundings. The measured values for carbon monoxide are much lower than the 10 mg/m^3 limit value, regulated by 2000/69/EC Directive. They are considered as normal and specific to the analyzed airport conditions, because the airport location is far-off from the city or any main road and the only CO source is represented by the aircrafts.

Figure 3 shows the mean measured values of sulphur dioxide SO_2, from two instruments. The SO_2 concentration in air is continuously measured and recorded (one value every second) and mediated. The correlation between the instruments is acceptable, differences that can be considered equivalent within the measurement uncertainty. The recorded values for SO_2 are not higher then the 350 µg/m^3 limit value regulated by 1999/30/EC Directive but they are higher then the background values (7 µg/m^3). The 3 minutes mean value have been used for an easy observation of the influence of airplanes traffic on pollutants concentration, that is the main purpose of this study. The SO_2 concentrations below 150 µg/m^3 have only moderate (and reversible) irritant effect on human respiratory system, but in synergy with NO_x and high air humidity can cause permanent pulmonary impairment [10], [11], [15]. The only possible source responsible for the SO_2 high values is the airplane fuel because there are no other possible emission sources of SO_2 in the airport vicinity (no main road traffic or industrial areas in the vicinity). The ground support vehicles are limited in number (5 busses and 2 passenger cars) and their contribution to airport emissions is insignificant [1].

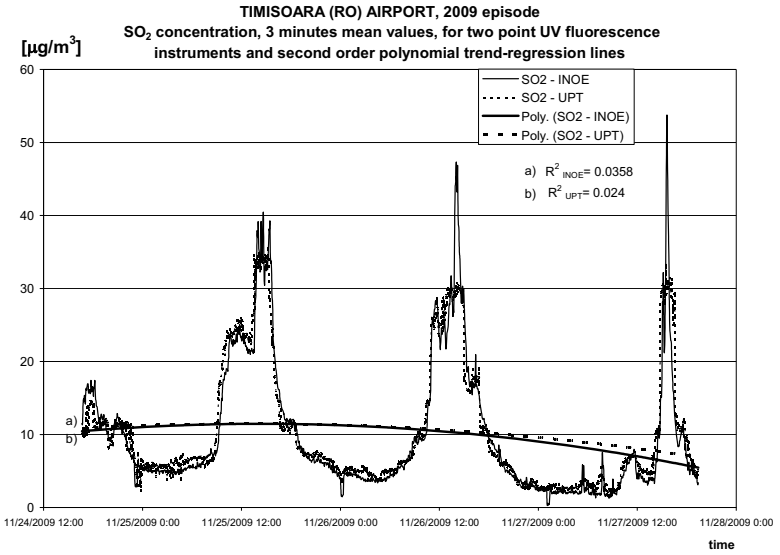

Figure 3: SO_2 measurements and polynomial trend regression lines.

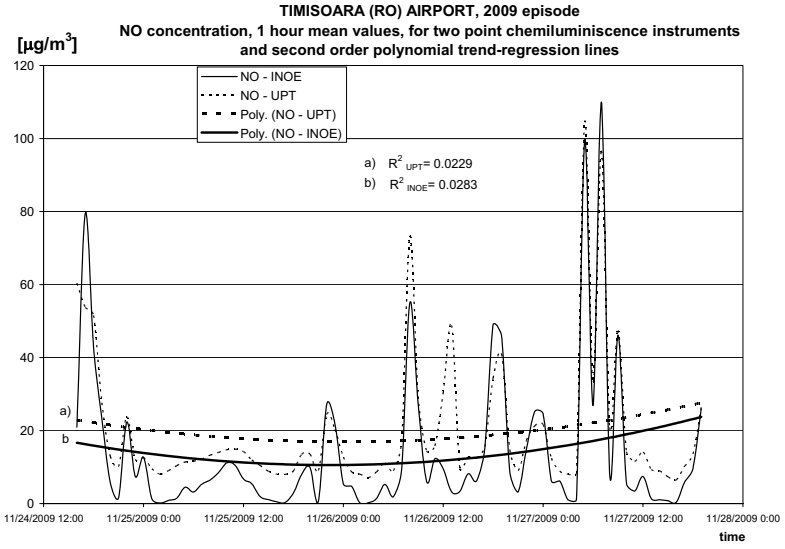

Figure 4: NO_2 measurements and polynomial trend regression lines.

Figure 4 shows the measured values for NO_2, with two identical instruments. The correlation between the instruments is good, polynomial trend lines have been added for better resolution. Because the highest measured values are overlapping airplane traffic on apron, it is clear that the only possibility to reduce NO_2 concentration is to manage more efficient airplane taxiing procedures.

Table 1 is indicating the average values for the main pollutants and also the correlation factor, considered to be a good one.

Table 1: Average values and correlation coefficient between the measurements.

Pollutant	UPT, in μg/m^3	INOE in μg/m^3	Correlation factor between data sets INOE - UPT)
NO	19.907	14.089	0.911
CO	0.551	0.566	0.992
SO2	10.285	9.935	0.976

CONCLUSIONS

An episode of on line continuously measurements of the concentrations of relevant pollutants in a large international Romanian airport, for 4 consecutive days, in November 2009 were reported and analyzed. The higher values have been recorded mostly when the airplanes are fuelling. A matter of concern is the fact that the airplane parking - fuelling area is near (~ 80 meters) the airport facilities, and that between “check in“ location and departure by the special cars the passengers might be thus exposed to high pollutant occasional levels. A very simple solution for this potential risk is to move the airplanes taxing area in the opposite side of the airport or more far away as presently. This solution is an advantage also regarding the NO_2 and SO_2 exposure. The aircrafts should be stationed and maintained as far as possible from the passengers’ platforms and the airplanes should taxi near the airport passenger facilities only before departures. The period of measurements conducted is relevant but still not sufficient large to be considered as representative for air quality in the area, thus extended measurements should continue The novelty of the accomplished research still consists in the fact that it reveals primarily in-situ measurement campaigns in a Romanian airport. Also the fact that, main pollutants have been measured in parallel by different instruments, with good correlation, is to be outlined. It is concluded that the airport activities have measurable impacts on local air quality, although the data were insufficient to quantify these impacts. The study showed that while the airport contributes to air quality issues in the area, its impact cannot be differentiated from the preponderance of other emissions, specifically mobile sources.

References

[1] Wang YW., Yang J., Jiang WM., (2009), Impact of large cities’ expansion on air pollution, *International workshop on Geoscience and Remote Sensing,* Vol. 1, 393-396.

[2] Nicolae D., Talianu C., Carstea, E., Radu C., (2007), Using classification to derive aerosol number density from lidar measurements, *Journal for Optoelectronics and Advanced Materials*, Vol 9 (11), 3518-3521.

[3] Nicolae D., Cristescu, C.P., (2006), Laser remote sensing of tropospheric aerosol, *Journal for Optoelectronics and Advanced Materials*, Vol 8 (5), 1781-1795.

[4] Ionel, I., Ionel S., Popescu F., Padure G., Dungan L.I., Bisorca D., (2008), Method for determination of an emission factor for a surface source, *Optoelectronics and Advance Materials – Rapid Communication Journal*, Vol 2 (12), 851 – 854.

[5] Ionel I., Ionel S., Nicolae D., (2007), Correlative comparison of two optoelectronic carbon monoxide measuring instruments, *Journal for Optoelectronics and Advanced Materials*, Vol 9 (11), 3541-3545.

[6] Ionel I., Apostol G., Popescu F., Apascaritei M., (2009), Air quality monitoring in an international airport, BENA Conference, Alba Iulia, May 6-7, accepted *Journal of Environmental Protection and Ecology* with NB 1573B/07.07.09, under print 2010.

[7] Belegante L., Zisu D., Ionel I., et al., (2007), Air pollution monitoring using the open path technique - art. No. 674520, *Conference on remote Sensing of Clouds and the Atmosphere XII, Remote Sensing of Clouds and the Atmosphere XII*, Florence, Italy, 17 - 19 September, 74520.

[8] Apascaritei, M., Popescu, F. Ionel, I., (2009), Air pollution level in urban region of Bucharest and in rural region, *SSE'09 Proceedings of the 11th WSEAS International Conference on Sustainability in Science Engineering*, 330 – 335.

[9] ***, http://www.hochtief-airport.com/airport_en/22.jhtml HOCHTIEF Airport GmbH,

[10] ***, Airport air quality guidance manual, International Civil Aviation Organization, Preliminary edition, 2007.

[11] **** http://www.omega.mmu.ac.uk/Air-Quality-Conference/BernardFisher.pdf.

[12] **** http://www.epa.gov/iaq/schools/tfs/guidem.html

[13] **** http://www.environcorp.com/projects/article.php.

[14] **** http://www.eastmidlandsairport.com/emaweb.nsf/Content/AirQuality.

[15] **** (2003), Controlling Airport-Related Air Pollution - Prepared *by* Northeast States for Coordinated Air Use Management and Centre for Clean Air Policy.

[16] *** http://aeronave.22web.net/index.php.

Ship Emissions Estimates based on AIS data

M. Winther[1], M.S. Plejdrup[1], J. Christensen[2], H.R. Olesen[2], T. Ellermann[2]*

[1] Aarhus University, NERI, Department of Policy Analysis, 4000 Roskilde, Denmark, mwi@dmu.dk

[2] Aarhus University, NERI, Department of Atmospheric Environment, 4000 Roskilde, Denmark

Abstract

A new and detailed emission inventory for ships based on AIS data has been set up for the marine waters around Denmark, in a spatial resolution of 1x1 km. The model has been used to assess the impact of the IMO (International Maritime Organisation) NO_x emission requirements and the sulphur reductions for marine fuels in the SECA (Sulphur Emission Control Area) areas around Denmark. For SO_2 and $PM_{2.5}$, the sulphur reductions lead to significant emission reductions. From 2007 to 2020, the SO_2 and $PM_{2.5}$ emissions are expected to reduce by 91 % and 54 %, respectively. For NO_x a small increase in total emissions of 2% is expected from 2007 to 2020. Without stricter IMO emission standards the emission increase would have corresponded to the increase in fuel consumption, i.e. 15 %. Thus, calculated on average the effect of IMO regulations is a decrease in the NO_x emissions of 11 % per unit of fuel. The reductions in the average NO_X emission factor will continue after 2020.

1. Introduction

Since 2006 the ship activities in the marine waters around Denmark have been registered by the so-called AIS (Automatic Information System) system. All ships larger than 300 GT (Gross Tonnage) are required to carry a transponder, which transmits information on the ship's identity and position to land-based receiving stations. The availability of AIS data has enabled the construction of more detailed and precise emission inventories for ships than previously made.

In 2009, the project "Contribution from ships to air pollution in Denmark" was carried out by the National Environmental Research Institute (NERI), which is part of Aarhus University (AU), on behalf of the Danish Environmental Agency (Danish EPA).The project examines the SO_2, NO_x and particulate emission contribution from ships to the overall air quality in Denmark for the years 2007, 2011 and 2020.

An important outcome of the project is a new AIS (Automatic Information System) based emission inventory for ships, with a spatial resolution of 1x1 km. Another important project goal is to assess the impact of the IMO (International Maritime Organisation) NO_x emission requirements and the sulphur reductions for marine fuels in the SECA (Sulphur Emission Control Area) areas around Denmark agreed by the EU and IMO.

This paper describes the AIS emission inventory and the calculated emission results. A short summary of the methodology will be given including the descriptions of AIS data, vessel data, engine load functions, fuel consumption and emission factors, and assumptions relevant for ship engines. In the results part, focus will be on fuel consumption and SO_2, NO_x and particulate emissions for 2007 and the achieved emission reductions for the years 2011 and 2020. Emission results will be presented on GIS maps as well.

2. Methodology

AIS data are requested from the Danish Maritime Safety Administration (DaMSA). In order to calculate fuel consumption and emissions for ships in the area these data are used together with vessel technical information from Lloyd's Register, engine load functions provided by DTU (Technical University of Denmark) and general fuel consumption and emission factors provided by NERI. In order to facilitate the inventory calculations, assumptions are also made regarding fuel type, engine types and average engine life times.

For each single vessel in the AIS dataset, ship category, engine type, fuel type, main engine and auxiliary engine size are determined using the technical data from Lloyds Register and supplementary information from DTU and MAN Diesel. The vessel sailing speed is found between each AIS signal and the instantaneous engine load is calculated from basis functions (five representative ship classes) using main engine size and vessel sailing speed as input.

The fuel consumption and emissions from each vessel during the time between two consecutive AIS signals are calculated by combining engine size, engine load, time duration between the AIS signals and fuel consumption and emission factors corresponding to the vessel's engine and fuel type. The baseline results are calculated for the year 2007 and results for the prognosis years 2011 and 2020 are obtained by using forecasted fuel consumption and emission factors from NERI and expectations for sea traffic growth from Danish Ship-owners' Association.

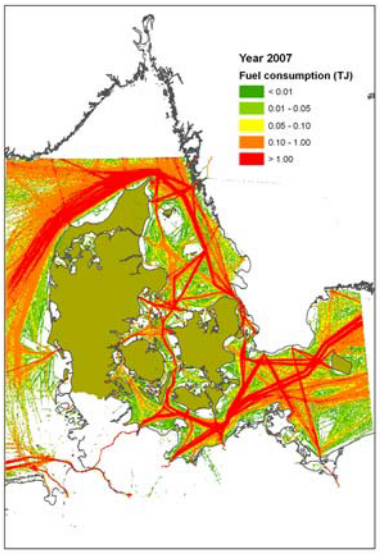

Figure 1 AIS inventory area used in the present project

AIS data

AIS signals represent a huge amount of data. In order to restrict the volume of data, a limited marine area around Denmark was appointed as being of primary interest (c.f. Figure 1) and only data from that area were requested from DaMSA. Furthermore, in order to represent the year 2007, not all data for the entire year was considered. The present project uses 12 two-days periods, one period for each month, representing both weekend days and normal working days. The following AIS data are used: Vessel IMO and MMSI codes, call sign, time of AIS signal, and latitude-longitude coordinates. For each ship, the sailing speed between two AIS signals is found from the time between the signals and the corresponding latitude-longitude registrations.

Vessel data

Relevant technical data for each ship is found by linking the vessel's IMO and MMSI codes and call sign from AIS data to the technical registrations from Lloyd's Register's database. The latter data consists of main engine size, engine stroke type (2-stroke/4-stroke), vessel flag and general ship category. The information on general ship category is used to group the vessels into five ship classes (representative types) from which engine load functions can be established.

Engine types, fuel types and average engine life times

From Lloyds' database a distinction between 2-stroke and 4-stroke engines as well as gas turbine engines is given. It is necessary to further allocate these data into the general engine types: Gas turbine, slow speed, medium speed and high speed engines for which fuel consumption and emission data are available. The following table shows the applied classification, which is based on information from MAN Diesel (pers. comm., Flemming Bak, 2009) and Winther (2008).

Table 1: Estimated main engine size and fuel type for ship engines in the present study

Engine type (Lloyd's)	Engine size (kW)	Engine type (estimated)	Fuel type (estimated)	Engine life time (years, estimated)
Gas turbine		Gas turbine	Diesel	30
2-stroke		Slow speed (2-stroke)	HFO	30
4-stroke	<= 1000	High speed (4-stroke)	Diesel	10
	1000-4000	Medium speed (4-stroke)	Diesel	30
	> 4000	Medium speed (4-stroke)	HFO	30

Traffic forecast

The Danish Ship-owners' Association was requested to provide a forecast for the development in ship traffic for the present study. The Association expects that in 2011 the amount of traffic will be back at the 2007 level after a decrease related to the current financial crisis (pers. comm. Jacob Clasen, Danish Ship-owners' Association, 2009). In recent years there has been a large annual growth in traffic of around 5 %. However, in the second part of 2008 the traffic began to decrease due to the global financial crisis and the expectation is that this drop in sea transport activity will not become outbalanced until 2011.

From 2011 to 2020 the Danish Ship-owners expect an annual traffic growth of between 3-4 % for goods carrying vessels and hence 3.5 % is used in the present survey. The traffic levels for passenger ships are expected to be the same as for 2007.

Engine load functions

An extensive database with ship data maintained by DTU has been used to produce the basic equations for service speed (V_s) as a function of main engine (ME) service power (P_s) shown in Table 2 (H. O. Kristensen, 2009). Technical data from a large number of vessels (in brackets) form the base for the equations for the five most common ship categories: Container ships (240), Tankers (199), Bulk Carriers (74), Ro-Ro cargo (59) and Ro-Ro passenger ships (91). The direct data source is the Royal Institution of Naval Architects. Since 1990 they have annually published technical details for around 50 ships of all classes and types in their publication series "Significant Ships" (http://www.rina.org.uk). The latter source of information is regarded throughout the maritime community as the most reliable source of technical data directly linked to individual vessels (pers. comm. Hans Otto Kristensen, DTU, 2009).

Table 2: Speed–power relations in the model

Ship category	V_s as a function of P_s
Container ships	$V_s = 3.7 \cdot Ln(P_s) - 14.8$
Tankers	$V_s = 1.12 \cdot Ln(P_s) + 4.6$
Bulk carriers	$V_s = 1.31 \cdot Ln(P_s) + 2.8$
Ro-Ro Cargo ships	$V_s = 3.82 \cdot Ln(P_s) - 15.9$
Ro-Ro Passenger ships	$V_s = 0.00037 \cdot P_s + 14.5$

Based on experience, the necessary engine power (P_{cal}) for ship propulsion at an observed sailing speed (V_s) is found by adjusting the engine service power (P_S) with the observed:service speed ratio to the 3rd power:

$$P_{cal} = P_s \cdot \left(\frac{V_{obs}}{V_S} \right)^3 \quad (1)$$

Finally, the engine load percentage, %MCR, is expressed as:

$$\%MCR = \frac{P_{cal}}{P_{ME}} \cdot 100 = P_s \cdot \left(\frac{V_{obs}}{V_S} \right)^3 / P_{ME} \cdot 100 \quad (2)$$

For the ship categories: Container ships, Tankers, Bulk Carriers, Ro-Ro cargo the installed auxiliary engine (AE) power is expressed as a function of main engine size in the state of the art AE-ME functions agreed by IMO MEPC (Marine Environment Protection Committee) at its 59th meeting (IMO MEPC, 17 August 2009). The AE-ME equations have been developed by DTU and the underlying data base is fuel consumption data reported by large shipping companies:

AE = 5 % ME, ME < 10000 kW (3)

AE = 250 kW + 2.5 % ME, ME > 10000 kW (4)

For Ro-Ro passenger ships the installed AE power is estimated to be 20 % of the ships ME size, based on queries from the database kept by DTU. For all ship categories, the average auxiliary engine load is assumed to be 50 % (pers. comm. H.O. Kristensen, DTU, 2009).

Fuel consumption and emission factors

The specific fuel consumption (sfc) and NO_x emission factors used in the model are calculated as average factors of g/kWh for each inventory year using curve fitted factors per engine production year (Figure 2) and the average engine life times shown in Table 1.

NO_x emissions from ships are regulated by IMO (International Maritime Organisation) in a three tiered approach (Marpol 73/78 Annex VI, and further amendments). The curve fitted factors for engines in compliance with the Tier I (2000) and older engines are provided by MAN Diesel. For engines in compliance with Tier II (2011) and Tier III (2016) emission standards, emission factors are estimated by adjusting the Tier I emission factors in two steps, relative to the Tier II:Tier I and Tier III:Tier I ratios. For sfc, no improvements are assumed for engines produced after 2000.

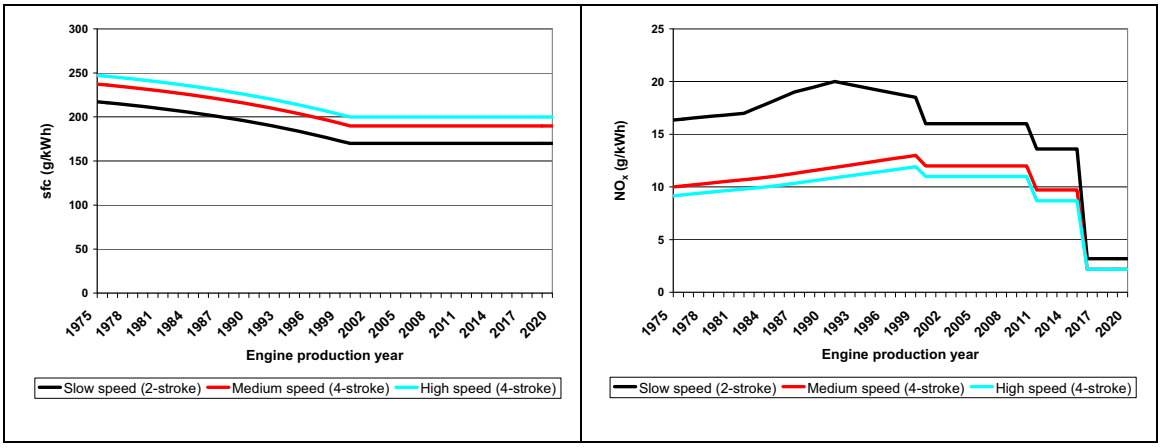

Figure 2: Sfc and NO_x emission factors per engine production year

For SO_2, the emission factors are calculated from sfc and sulphur percentage (S %), by using 2.0 kg SO_2/kg S, the chemical relation between burned sulphur and generated SO_2 (e.g. Winther, 2008). The S % for heavy fuel oil (HFO) and marine diesel (MD) follow the current EU and IMO legislation for SECA areas, and the S % (in brackets) are for 2007 (HFO: 1.5 %; MD: 0.2 %), 2011 (HFO: 1 %; MD: 0.1 %) and 2020 (HFO: 0.1 %; MD: 0.1 %).

The particulate emission factors are calculated as a function of S % by using an emission factor equation for total TSP expressed by the Ministry of Transport (2000) derived from

measurements made by Lloyd's (1995). The $PM_{2.5}$ fraction of total TSP is taken as 98.5 %, based on information from MAN Diesel.

Please refer to Olesen et al. (2009) for a detailed overview of the current IMO emission legislation for NO_x and the current EU and IMO legislation for the SECA areas in relation to S % for marine fuels.

Calculation procedure

For each ship, the fuel consumption and emissions are found by summarising the product of engine load (%MCR), main/auxiliary engine size (kW), AIS signal time interval (s) and fuel consumption/emission factor (g/kWh):

$$E(X) = \sum_i \%MCR \cdot P_E \cdot EF_{k,l,X} \cdot \Delta t_i / 3600 \quad (5)$$

Where E = fuel consumption/emissions (g), %MCR = engine load (%), Δt = sailing time between AIS signal (s), P_E = main/auxiliary engine size (kW), EF = fuel consumption/emission factor in g/kWh, i = AIS signal interval, k = fuel type, l = engine type, X = calculation year.

3. Results

Figure 3 shows the fuel consumption and emission totals from ship traffic in the AIS inventory area for the three scenario years 2007, 2011 and 2020, also broken down per ship category.

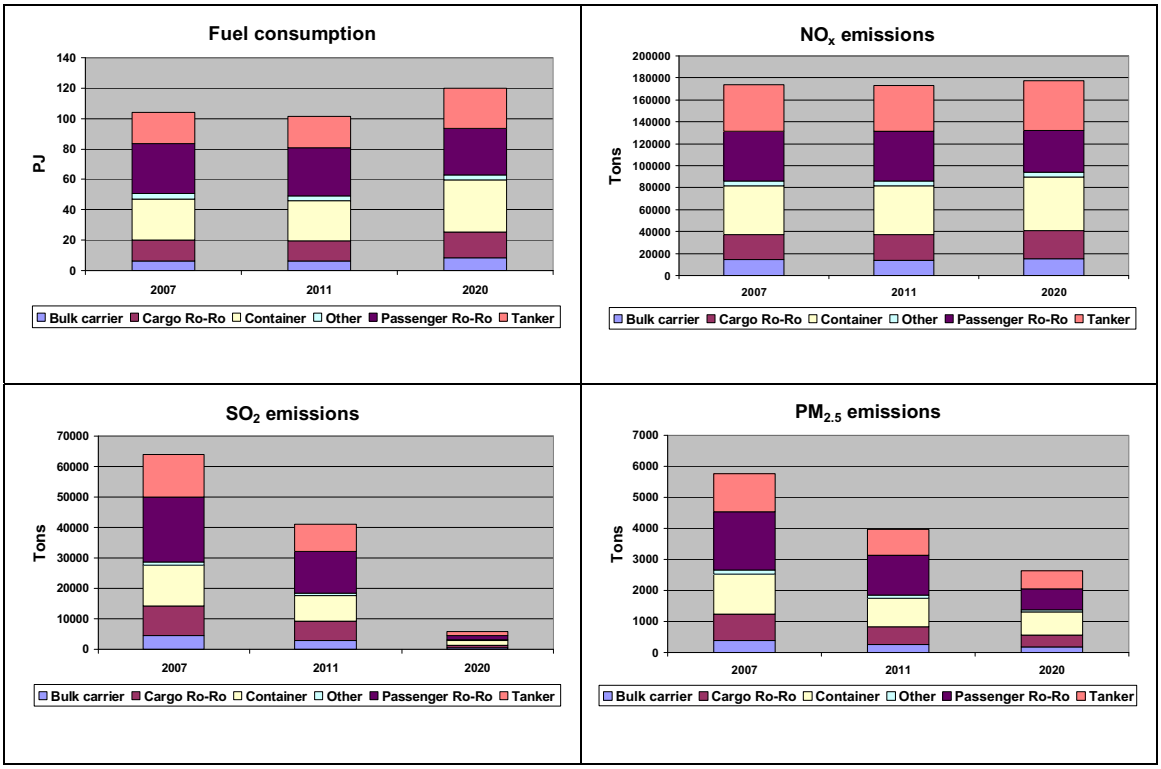

Figure 3: Fuel consumption and emissions from ship traffic in the waters around Denmark for the three scenario years 2007, 2011 and 2020.

The 15 % increase in fuel consumption from 2007 to 2020 is a product of the envisaged growth in sea traffic and the gradually improved fuel efficiency for newer engines in historical years. The expected traffic growth for goods carrying vessels is around 36 % from 2007 to 2020, whereas sailing activities with passenger ships is expected to remain on the same level for the same period.

For SO_2 and $PM_{2.5}$, the reductions of the sulphur content lead to significant emission reductions. From 2007 to 2020[2011], the SO_2 emission reductions are 91 % [36 %] whereas the $PM_{2.5}$ reductions are 54 % [31 %].

For NO_x a marginal increase in total emissions of 2 % is expected from 2007 to 2020. Without stricter emission standards the increase would have corresponded to the increase in fuel consumption, i.e. 15 %. Thus, calculated on average the effect of IMO regulations is a reduction in the NO_x emissions of 11 % *per unit of fuel*. The reductions in the average NO_X emission factor will continue after 2020.

Today passenger ships are the largest source of fuel consumption and emissions of SO_2 and $PM_{2.5}$ with shares of around one third of the calculated totals. However, from 2007/2011 these shares drop to one fourth in 2020 due to the underlying traffic composition in these years. As an end result, container ships become the largest source of fuel consumption and emissions in 2020.

Passenger ships, containers and tankers have almost the same NO_x emission shares in 2007 and 2011. However, due to the increase in traffic for goods transportation vessels from 2007/2011 to 2020, the relative fuel consumption and emission importance for container and tanker ships become larger than for passenger ships in 2020.

In 2007 (and 2011) the calculated heavy fuel oil share of the total fuel consumption is 82 %. The corresponding emission shares are even higher being mostly pronounced for SO_2 (97 %) and $PM_{2.5}$ (92 %) due to the higher S % for heavy fuel oil. In 2020 the heavy fuel oil share has marginally changed to 81 % but due to the significant reduction of the sulphur content for this fuel type the emission shares of SO_2 and $PM_{2.5}$ become similar to those of fuel consumption.

The most pronounced reductions in ship emissions take place for SO_2 and these reductions are illustrated in Figure 4. The maps yield an overview of sea traffic around Denmark. Clearly visible are the main shipping lanes from the inner Baltic Sea (Bothnian Bay) to the North Sea, the major Danish domestic ferry routes and the ferry routes connecting Denmark, Sweden, Germany and Poland.

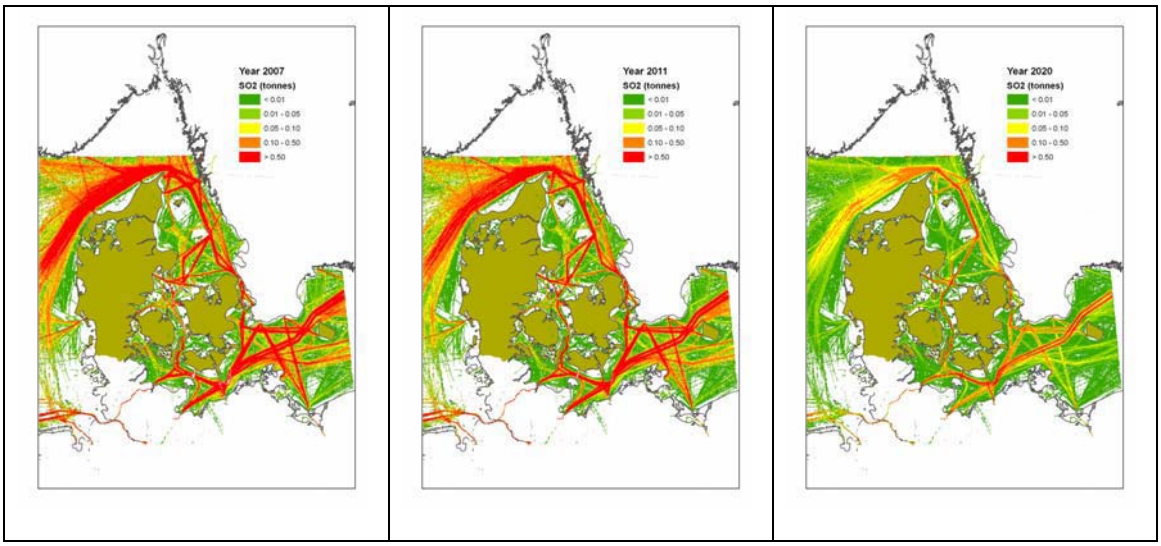

Figure 4: Maps of yearly emissions of SO_2 per km^2 for the years of 2007, 2011 and 2020

4. Conclusion

A new and detailed emission inventory for ships based on AIS data has been set up for the marine waters around Denmark, in a spatial resolution of 1x1 km. The model results clearly show the main shipping lanes from the inner Baltic Sea (Bothnian Bay) to the North Sea, the major Danish domestic ferry routes and the ferry routes connecting Denmark, Sweden, Germany and Poland.

The fuel consumption increases by 15 % from 2007 to 2020 being a product of the envisaged growth in sea traffic and the gradually improved engine fuel efficiency in historical years. The expected traffic growth for goods carrying vessels is around 36 % from 2007 to 2020 whereas passenger ship traffic is expected to remain on the same level for the same period.

The S % reductions for marine fuels used in the North Sea and Baltic Sea, being appointed SECA areas, lead to significant emission reductions for SO_2 and $PM_{2.5}$. From 2007 to 2020, the SO_2 emission reductions are 91 %, whereas the $PM_{2.5}$ reductions are 54 %. For NO_x a marginal increase in total emissions of 2 % is expected from 2007 to 2020. Without stricter IMO emission standards the increase would have corresponded to the increase in fuel consumption, i.e. 15 %. Thus, calculated on average the effect of IMO regulations is a reduction in the NO_x emissions of 11% per unit of fuel. The reductions in the average NO_X emission factor will continue after 2020.

5. References

DTU (2009), Unpublished data material provided by Senior researcher Hans Otto Kristensen, Dep. of mechanical engineering, Section of coastal, maritime and structural engineering, DTU.

Lloyd's Register of Shipping (1995), Marine Exhaust Emissions Research Programme. Lloyd's Register Engineering Services, United Kingdom, London.

Olesen, H.R., Winther, M., Ellermann, T., Christensen, J.H. & Plejdrup, M.S. (2009), Ship emissions and air pollution in Denmark: Present situation and future scenarios, *Environmental Project 1307.* Available at http://www2.mst.dk/udgiv/publikationer/2009/978-87-92548-77-1/pdf/978-87-92548-78-8.pdf

Ministry of Transport (2000), TEMA2000 - et værktøj til at beregne transporters energiforbrug og emissioner i Danmark (TEMA2000 - a calculation tool for transport related fuel use and emissions in Denmark). Technical report. Available at http://www.trm.dk/sw664.asp

Winther (2008), Fuel consumption and emissions from navigation in Denmark from 1990-2005 - and projections from 2006-2030. *Technical Report from NERI no. 650*. 109 pp. Available at: http://www2.dmu.dk/Pub/FR650.pdf

Session 2: Emission Measurement

Real-time Analysis of Aromatic Compounds in Vehicle Emissions by Resonance-enhanced Multiphoton Ionisation – Time-of-flight Mass Spectrometry (REMPI-TOFMS)

*T. Adam *[1], C. Astorga [1], G. Martini [1], A. Perujo[1], U. Manfredi [1], A. Krasenbrink [1], M. Sklorz [2], M. Elsasser [3], R. Zimmermann [2,3]*

[1] EC Joint Research Centre Ispra, Institute for Environment and Sustainability, Transport and Air Quality Unit, 21027 Ispra (VA), Italy
[2] Analytical Chemistry, Institute of Chemistry, University of Rostock, 18051 Rostock, Germany
[3] Institute of Ecological Chemistry, Helmholtz Zentrum München, 85764 Neuherberg, Germany
* corresponding author: thomas.adam@jrc.ec.europa.eu

Introduction

Vehicle exhaust is a complex matrix consisting of a large number of different species. Characterization of non-regulated compounds is of growing interest due to their possible impact on environment and human health. In this context, mono-aromatic species (e.g. benzene) and polycyclic aromatic hydrocarbons (PAH) play a key role due to their known or suspected carcinogenic and/or toxic potential. Chemical analysis is usually carried out by conventional off-line techniques like GC-MS or GC-FID. Results are usually given as total amount per test or as emission factors in yield per distance. However, variations in concentration or short time fluctuations of the constituents are not resolved, which might be essential in order to understand the complex formation and decomposition reactions in exhaust. In addition, sampling, storage, dilution, ageing, and contact with other chemicals like solvents might lead to modifications or the formation of artifacts. The ideal situation would be to measure fresh, undiluted, and non-aged exhaust by analyzing many compounds at the same time. But this analytical task is very difficult to achieve. Time-of-flight mass spectrometry (TOFMS) is one possibility. However, compound ionisation is often done by conventional electron impact (EI) ionisation. Thereby, target analytes are ionized by bombardment with electrons having a kinetic energy of ca. 70 eV. This ionisation process leads to massive fragmentation of the generated ions. Thus, interpretation of TOF mass spectra of complex matrices might be difficult or even impossible due to the superposition of numerous fragments and mother ions. As a consequence, soft ionisation techniques are required, which inhibit fragmentation. Resonance-enhanced multi-photon ionisation (REMPI) is known to be a highly sensitive and selective soft ionisation method, in particular for aromatic species. Instead of electrons, laser generated UV photons are used for photoionisation. The soft character is given by the low excess energy transferred onto the ions i.e. the little energy difference between the required ionisation energy and the applied photon energy. In 2009, a campaign was carried out at the EC-JRC Vehicle Emission Laboratory (VELA), which dealt with the application of REMPI-TOFMS for the time-resolved investigation of gaseous aromatic compounds in the exhaust of different vehicle types. In the framework of this paper, first results of this project are presented.

Experimental Section

The investigated vehicle fleet ranged from a heavy duty truck, various light duty vehicles powered by gasoline, diesel, biodiesel, ethanol, and liquefied petroleum gas (LPG) as well as two stroke scooters and a hand-held utility machine. Test cycles performed were official cycles like the New European Driving Cycle (NEDC) for light duty, European Transient Cycle (ETC) for heavy duty, ECE47 and the World-Harmonized Motorcycle Test Cycle (WMTC) for the two-wheelers as well as self-developed steady state and speed ramp cycles. Therefore, the REMPI-TOFMS was set up at different test facilities i.e. chassis dynamometers for various vehicle types and fuels as well as a test bench for small engines.

A sketch of the experimental set-up is illustrated in Figure 1. The mobile REMPI-TOFMS was placed inside the test cell and connected to the exhaust pipe of the vehicles. Thereby, a heated

sampling system (200°C, 4L/min) was connected to the tail pipe to which, in turn, the heated transfer line of the REMPI-TOFMS was orthogonally attached. Latter consisted of a deactivated silica capillary (length 1.5 m; i.d. 0.32 mm; T = 220 °C) by which a constant volume of exhaust was continuously drawn into the instrument (flow 8 mL/min; residence time < 1 s). This enabled to analyze undiluted and non-aged exhaust. The principle of REMPI-TOFMS is described in detail in the literature e.g. (Mühlberger et al. 2001, Zimmermann et al. 1999), therefore, only a brief description is given here. Fundamental Nd:YAG laser pulses (1064 nm) are used for non-linear generation of UV light (266 nm) by a two-fold frequency-doubling (SHG: second harmonic generator). The UV pulses are directed into the ionisation chamber straight underneath the inlet needle of the transfer line. Soft photoionisation of the aromatics in the exhaust is induced by a sequential two-photon absorption process via an electronic transition state (see Figure 1).

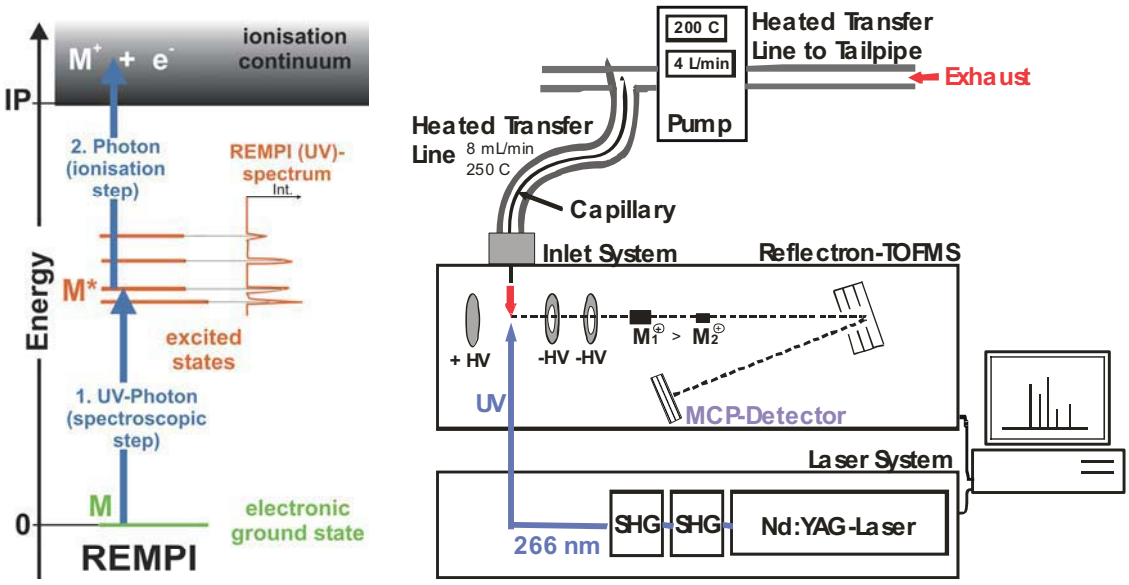

Figures 1: Sketch of the Instrumental Set-up and REMPI Ionisation Scheme

The generated molecular ions are extracted into the flight tube of the reflectron TOFMS. Mass spectra are recorded via a transient recorder PC card whereby data processing is done by a custom-made software. Calibration is carried out by applying external gas standards, which was done for a variety of mono-aromatics. Compounds, where no calibration gases are available, were semi-quantified by taking into account the ratios of the photoionisation cross-section of the target compound and a calibrated species. The photoionisation cross-section is a property, which accounts for the compound's probability of being ionized under certain conditions and is constant for a fixed UV wavelength and photon density. As a consequence, the ratio of two photoionisation cross-sections is constant, too. These ratios were determined beforehand under lab-conditions for a great number of compounds. In principle, 20 complete mass spectra per second can be recorded since a 20 Hz laser was used. In the framework of this paper, on-line data with a time-resolution of 1 Hz is presented. Figure 1 illustrates the instrumental set-up and the REMPI ionisation scheme.

Results and Discussion

Figure 2 shows a REMPI-TOF mass spectrum of heavy duty (HD) diesel exhaust recorded at a steady state test. The steady state HD test consisted of five phases (idle, 40 km/h, 60 km/h, 90 km/h, idle) of five minutes each. The graph illustrates an average of all recorded spectra during the top speed phase (90 km/h) excluding the acceleration events (60 km/h – 90 km/h and 90 km/h – 0 km/h). It can be seen that the accessible species range from mono-aromatics like benzene, styrene and phenol and higher homologues, to naphthalenes, indanes, phenanthrenes, and pyrenes.

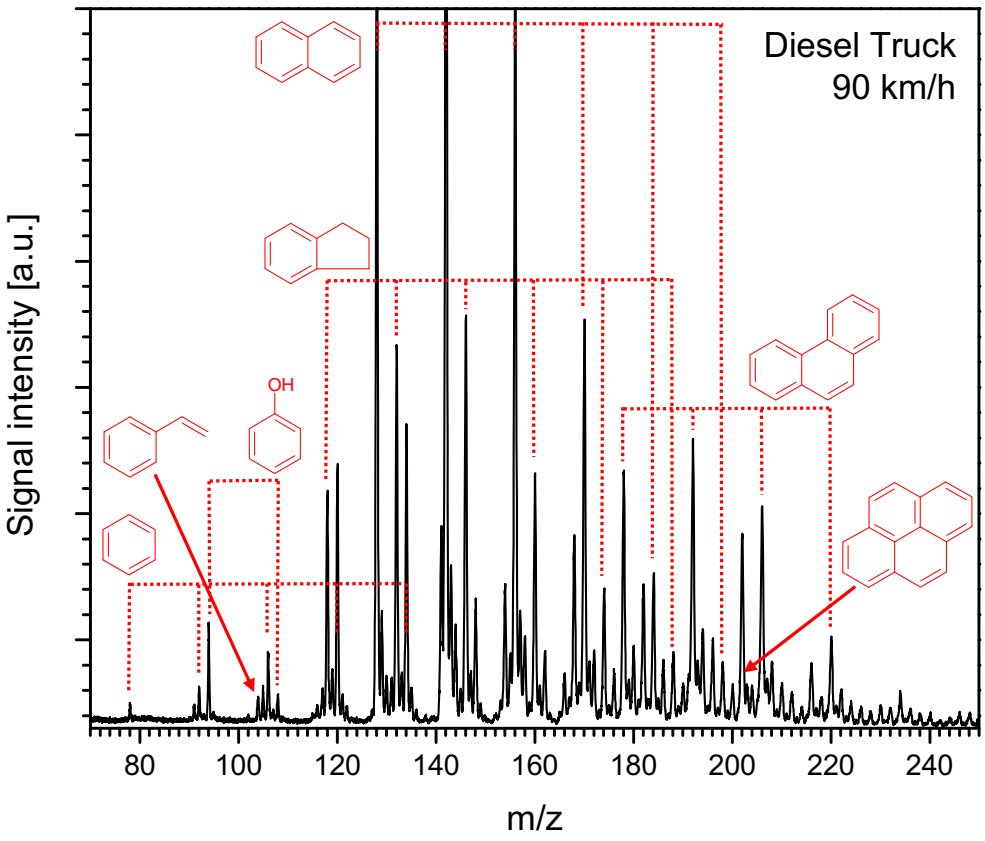

Fig. 2: REMPI-Spectrum of a Diesel Truck (EURO III) at 90 km/h (averaged over 5 minutes)

Figure 3 depicts the concentrations of toluene, naphthalene, and phenanthrene in the exhaust of a speed ramp test of a diesel van (Euro 3). Y-axes are adjusted to allow a comparison of the time-profiles. The speed ramp test comprised nine stages (idle, 50 km/h, 90 km/h, 120 km/h, 140 km/h, 120 km/h, 90 km/h, 50 km/h, and idle) of two minutes each. For the speed ramp tests, the engine was warmed up by a previous test. In contrast, cold-start tests (not shown here) revealed strong signals for various components during the first seconds of the test. It can be seen that toluene (similar to benzene) strongly emerged during the first acceleration from idle to 50 km/h. After the acceleration event the concentration of toluene decreased but was still detectable and, in turn, increased sharply again during the second acceleration event from 50 km/h to 90 km/h. For the rest of the cycle only little concentrations could be detected. Naphthalene followed partly the behaviour of toluene but also resulted in elevated yields during the following steady speeds, in particular the top speed of 140 km/h. Furthermore, yields emitted during the second acceleration were much more pronounced than for the first event. A possible reason is that toluene is stronger influenced by unburned fuel and decomposition reactions in the catalytic converter, whereas naphthalene is more formed by pyrosynthetic reactions at high levels of fuel and moderate temperatures. Phenanthrene, in contrast, featured elevated levels for 120 km/h and a very strong increase at the acceleration from 120 km/h to 140 km/h. However, this behaviour was not consistent for all runs throughout the test series. Phenanthrene always featured the highest signal during the top speed event of 140 km/h but of different measures. Therefore, yields and chemical compositions varied, especially for the highest speed. Results showed that velocities beyond the highest speed of the legislative test cycles (120 km/h for NEDC) can result in a strong increase in emission for a some compounds. This effect has been confirmed by speed ramp cycles with other vehicles.

In general, this example demonstrates that various aromatic compounds can behave differently during combustion. The fuel content but also pyrosynthetic formation and decomposition reactions during combustion are responsible for this. Consequently, emission factors or total yields of whole tests are not sufficient to study the complex mechanisms during combustion. If

the presence of aromatic compounds in exhaust wants to be fully understood, they must be measured on a real-time basis.

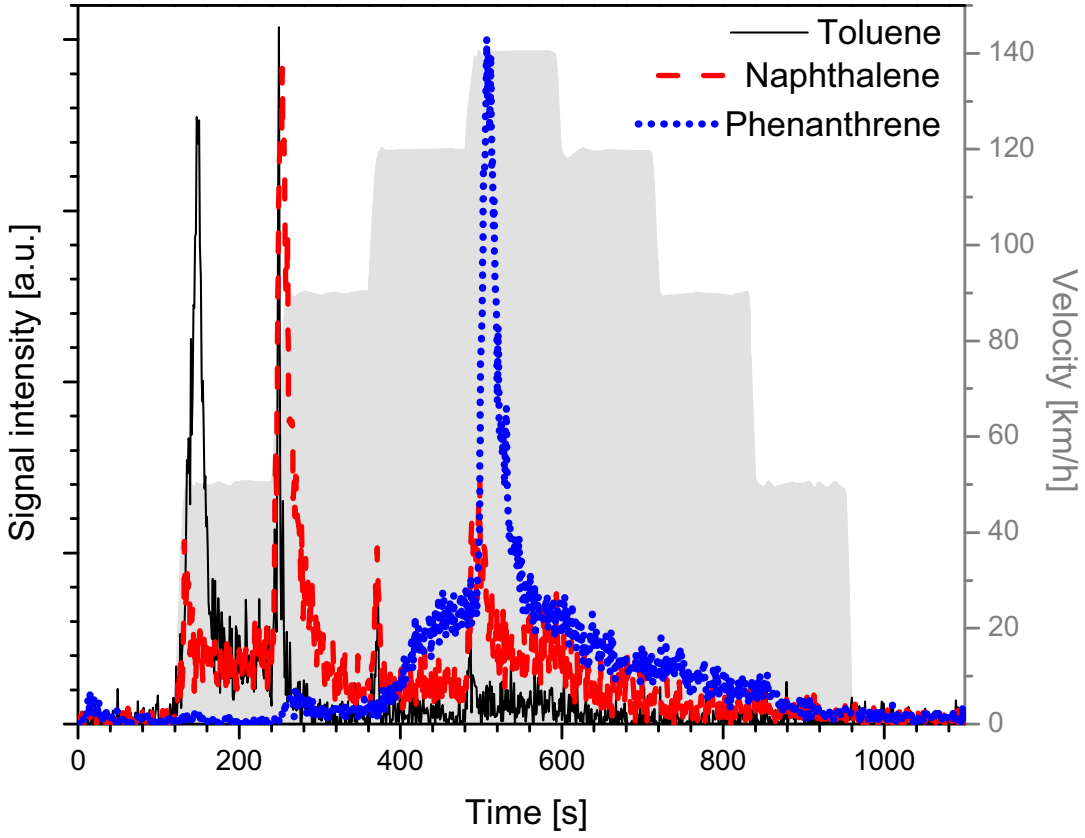

Fig. 3: Time-resolved concentrations of toluene, naphthalene, and phenanthrene of a diesel passenger car (Euro 3) of a speed ramp test cycle.

Time-resolved concentrations of the analytes during cold-start tests demonstrated the high influence of unburned fuel during the first seconds of the cycles. By comparing cycles with the engine cold and the engine hot, the approximation of the signals and the gradual warm-up of the engine and the catalytic converter system could be studied. In this regard, it could be shown that the environmental benefits of dual fuel vehicles running on liquefied petroleum gas (LPG) and gasoline are minimized due to the fact that the engines always start on gasoline, even when LPG is selected as fuel. This short cold-start period on gasoline leads to tremendous yields and, as a consequence, influences negatively the emission factor of the complete test cycle.

Furthermore, the time-profiles of aromatic exhaust constituents were used to compare their concentrations for different vehicles. Focus was on health-relevant species e.g. benzene. Increased yields were determined for two-stroke engines. In particular, tests with a hand-held utility machine revealed that potential users might be exposed to high concentrations.

References

Mühlberger F., Zimmermann R., Kettrup A (2001), A mobile mass spectrometer for comprehensive on-Line analysis of trace and bulk components of complex gas mixtures: parallel application of the laser-based ionisation methods VUV single-photon ionisation, resonant multiphoton ionisation, and laser-induced electron impact ionisation, *Analytical Chemistry*, 49, 257-266

Zimmermann R., Dorfner R., Kettrup A (1999), Direct analysis of products form plant material pyrolysis, *Journal of Analytical and Applied Pyrolysis*, 73, 3590-3604

Particles emitted by 2- and 4-stroke engines: Aspects from chasing and test bench experiments

S. Weimer[1,2], R. Richter[2], C. Mohr[2], D. Schreiber[1], A.S.H. Prevot[2], M. Mohr[1], P. Dimopoulos Eggenschwiler[1]

[1] Empa, Laboratory for internal combustion engines, 8600 Dübendorf, Switzerland

[2] PSI, Laboratory for Atmospheric Chemistry, 5232 Villigen, Switzerland

Abstract

The behavior of particles emitted by scooters and diesel vehicles were investigated in test bench as well on-road by chasing experiments. Particle characterization techniques included particle number, size distribution, soot concentration, and chemical composition of the non-refractory particle components, measured by a quadrupole Aerosol Mass Spectrometer (Q-AMS). This instrument provides on-line quantitative measurements of the chemical composition and size distribution of the volatile and semi-volatile fraction of sub-micron aerosol particles (approximately particle matter smaller than 1.0µm). Particle number was measured by a Condensation Particle Counter (CPC), size distributions were monitored by a Scanning Mobility Particle Sizer (SMPS), and the soot concentrations were quantified by the Micro Soot Sensor (MSS). Additionally, an evaporation tube was used to evaporate volatile particle components to study the volatility of the particles.

Scooter emissions were characterized by very high volatile particle numbers at low exhaust temperatures. Specifically, the organic species measured by the AMS were completely removed after several minutes of warm–up leading to particle mass concentrations below the detection limit. Our results comply with findings from other publications. They underline the observations that these particles consist almost entirely of unburned lubrication oil and volatile organic hydrocarbons. In contrast, particles emitted by a diesel vehicle exhibited low organic carbon fraction being only a small part of the total carbon. In general solid diesel particles consist mainly of agglomerated carbonaceous primary particles, which are often referred to as soot. Our measurements were carried out for three velocities. The observations revealed enhanced particle concentrations when the vehicle speed was increased.

Chasing experiments, where the identical measurements techniques have been applied in the wake of the respective vehicle using a mobile laboratory, confirmed the test bench results.

Introduction

Road traffic is one of the most important emission sources of primary air pollutants in the industrialized world. Regarding particle emissions there is a current public debate how to reduce particulate matter (PM) which is driven by the results of epidemiological studies (Dockery et al. 2009).

Particle mass emitted by vehicles is already limited since Euro 1. Yet, particle number (PN) limit will be introduced in Euro 6. PN is of importance specifically because small particles (< 30 nm) contribute mainly to this parameter. Moreover, the smaller the particles are the higher the impact on human health. However, the impact of particles on human health depends as well on the chemical properties of the particulates.One of the objectives of this study was to investigate the chemical and physical particle properties of 2-and 4- stroke engines by using state-of-the-art instrumentation. In addition, differences of the results from chasing experiments and test bench measurements were analyzed.

Experimental Set Up

Engine Specification

A scooter model Kymco Super 90 LC (2001) was utilized which exhibit a displacement of 49 cm3 and a power of 3.94 kW. The 2-stroke engine was equipped with an oxidation catalyst. The 4-stroke engine was a BMW 530d EURO3 with a displacement of 2926 cm^3 and 142 kW engine power as well equipped with an oxidation catalyst

Test bench and Chasing Experiment

The test bench experiments were performed at the Empa test facility. The tailpipe emissions passed three dilution stages (see Figure 1 (A)). An evaporation tube (ET) was optionally installed to evaporate volatile particle components at 300°C. The dilution was controlled by pressure and temperature sensors and by CO_2 instruments upstream and downstream of the dilution stages. The instruments were installed inside the mobile laboratory for the test bench experiments. Additional particle number measurements were performed parallel using the CVS (constant volume sampler) tunnel (B).

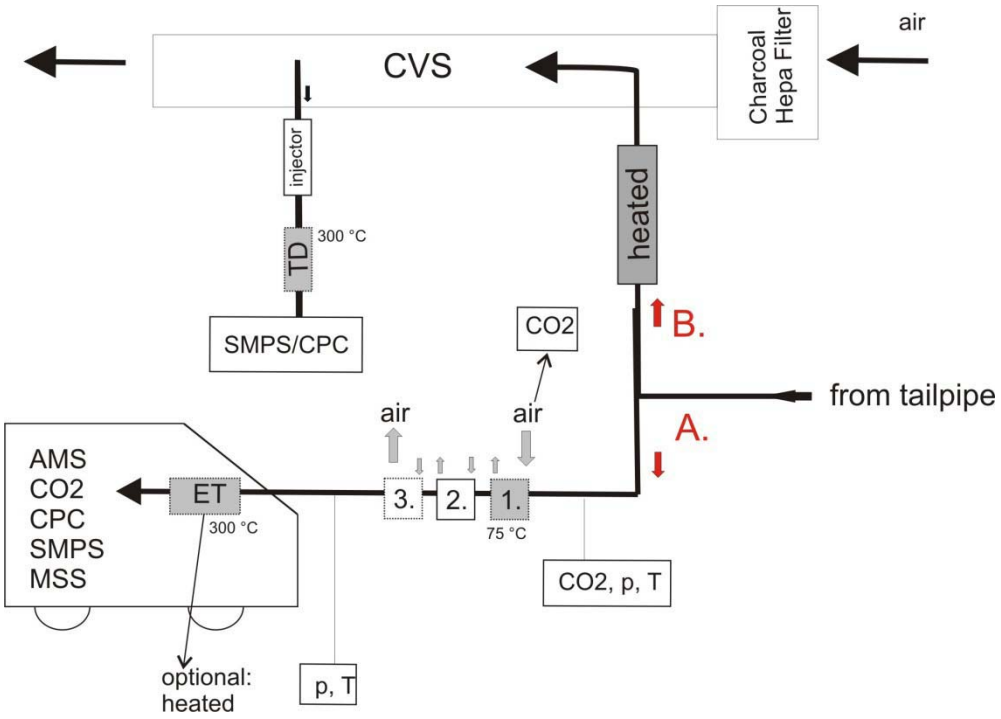

Figure 1: Sketch of the test bench measurements. (A) The instruments were set up in the mobile laboratory with which as well chasing experiments were performed. (B) Additional test bench measurements for the diesel vehicle were carried out using the CVS (Constant Volume Sampler) tunnel (AMS = Aerosol Mass Spectrometer, CPC = Condensation Particle Counter, MSS = Micro Soot Sensor, SMPS = Scanning Mobility Particle Sizer, ET = Evaporation Tube, p = pressure, T = temperature).

The physical properties were measured by a CPC and SMPS whereas the chemical properties such as organic matter (OM) were measured by an AMS. The refractory components were detected by a MSS. Chasing experiments were performed at the military airport in Dübendorf. A test track was used of around 1000 m where we chased the tested vehicle with the PSI mobile laboratory in a distance of 10 m. Further description about the mobile laboratory can be found in Weimer et al. 2009. Due to the limited length the experiments were carried out at velocities at

30, 50 and 80 km/h for the 4-stroke engine. The velocities driven for the scooter were 30, 50 and 60 km/h. Since the SMPS took 3 minutes for one scan, a bag sampler was installed on the roof of the mobile laboratory for the chasing experiments. Two valves (in front and back of the vehicle) of the bag could be closed to catch the plume when the mobile laboratory was inside an emission plume indicated by enhanced CO_2 concentrations.

Results

Particles emitted by a 2-stroke engine

In Figure 2 particle number size distributions are presented for the scooter measurements. Results yielded that the mode was situated at 50 nm for the test bench experiments whereas varied between 30 to 40 nm for the chasing experiments. When the evaporation tube was applied the particle number concentration decreased to ambient concentrations values. This hints to the fact that the particle components were volatile. Several publications suggested that the particles are supposed to be small droplets that consist entirely of unburned lubrication oil and volatile organic hydrocarbons (Murillo et al., 2005, Etissa et al. 2008).

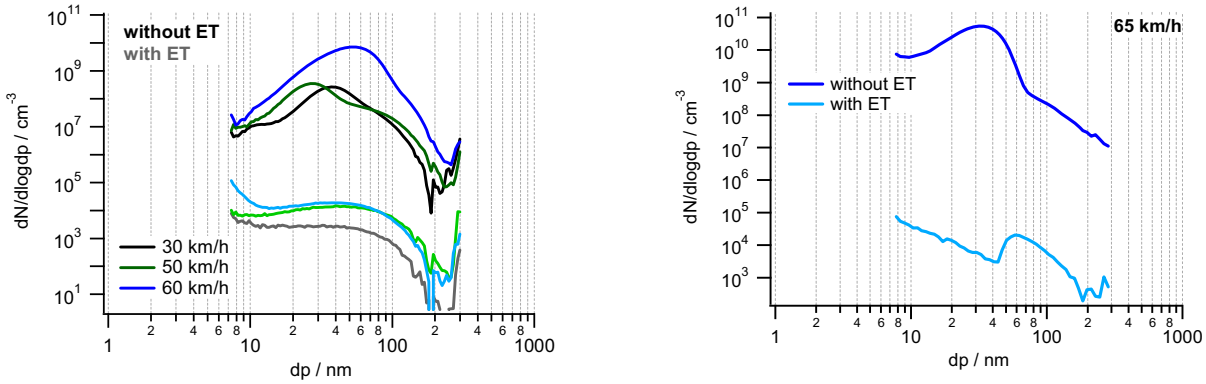

Figure 2: Particle number size distribution of scooter measurements at the test bench (a) and for chasing experiments (one bag sample) (b) for different velocities with and without ET.

Chemical composition of the particulates from the 2-stroke engine was studied using the Aerosol Mass Spectrometer. In Figure 3 the time series of exhaust gas temperature, mode of the SMPS, and organic species of one cold start are presented. The mode of the number size distribution changed from 100 to 30 nm with increasing exhaust gas temperature. The mass concentration of the organic species decreases as well. The oxidation catalyst becomes more efficient with exhaust temperature increase and reduces volatile particle components. It should be mentioned that the AMS detection limit was reached for these low concentrations and especially for particle diameter size lower than 30 nm.

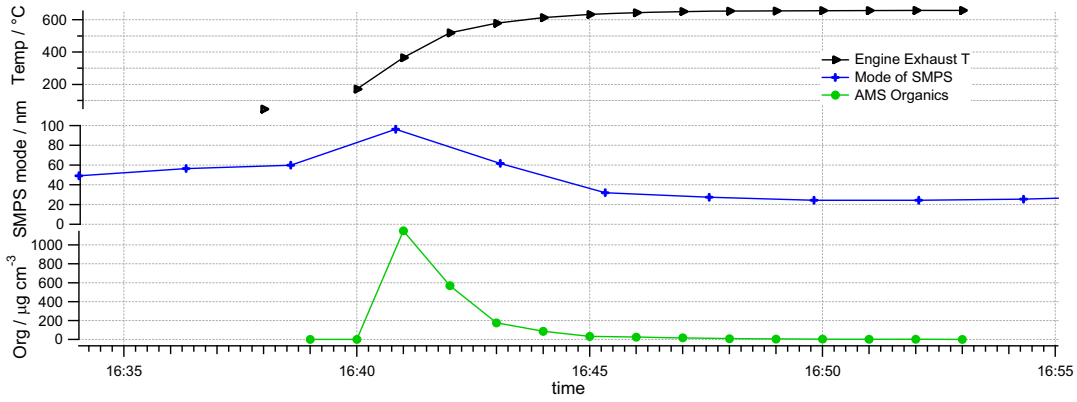

Figure 3: Time series of one cold start. Engine exhaust temperature (black), mode of the SMPS particle number size distribution (blue), and organics (OM) measured with the AMS (green) are presented.

Particles emitted by a 4-stroke engine

Results of test bench and chasing experiments for the 4-stroke engine used are depicted in Figure 4. Note that we used fuel with low sulfur content. Two bag sampler measurements are presented as well as measurements using sampling line (A) and (B). The particle concentrations exhibited lower values for the measurements with 4-stroke than with the 2-stroke engine. The particle mode varied between 50-55 nm for 30 km/h and 50 km/h while it was shifted to larger particle diameters for 80 km/h (64-70 nm).

The results revealed that the laboratory measurements can mimic the particle emissions for ambient conditions quite well especially when the non-volatile fraction dominates the particle components. In this respect, Table 1 presents mass concentration of organic matter (OM) and black carbon (BC) for test bench measurements at 120 km/h indicating that the amount of BC is larger than the OM concentration.

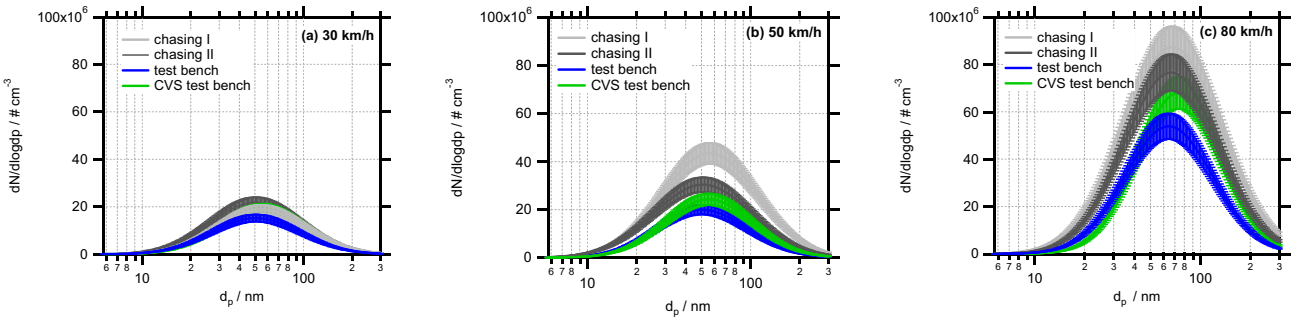

Figure 4: Number size distribution of pathway (A) (blue), of pathway (B) (green) and of two chasing bag samplers (gray and black) are presented for (a) 30, (b) 50 and (c) 80 km/h. The error bars were estimated to be 10 % of the concentration.

Table 1: Concentrations for organic matter (OM) in mg/m^3, black carbon (BC) in mg/m^3 measured with the MSS and number concentration in 1/cm^3 with the CPC are presented for three experiments (Exp I-III) with and without evaporation tube for 120 km/h.

	OM		BC		Number	
	without	with	without	with	without	with
Exp I	1.6±0.04	1.4±0.04	8.7±0.9	8.9±0.9	1.2e8±1.2e7	1.1e8±1.1e7
Exp II	1.5±0.03	1.4±0.04	9.5±1.0	9.5±1.0	1.e28±1.2e7	1.0e8±1.0e7
Exp III	2.0±0.04	1.7±0.04	10.0±1.0	10.0±1.0	1.2e8±1.2e7	1.1e8±1.1e7

As we have shown the chasing experiments confirm the test bench results. However for the diesel vehicle we only observed an accumulation mode situated at around 70 nm. This mode is often called soot mode. Recent studies have shown the occurrence of a nucleation mode at particle diameters of smaller 30 nm. The measurements of these highly volatile particles are difficult to detect since the nucleation mode depends on various parameters such as temperature, dilution rate, relative humidity, and sulfur content of the fuel (Kittelson et al. 1998, Giechaskiel et al. 2005, Scheer et al. 2005). For engines equipped with a DPF the results look differently (Schreiber et al. 2007). The volatile components will not be able to condensate on the soot particles which are removed from the DPF. They exit the exhaust pipe and may form a nucleation mode.

Conclusions

Two different kinds of particles could be analyzed using a 2-stroke and a 4-stroke engine. The particles emitted by scooters are of volatile components and disappear when an evaporation tube is used. Furthermore, the mass concentration decreases substantially to values below the AMS detection limit when the exhaust temperature increases. A Euro 3 4-stroke engine was used to study the physical and chemical properties of particles. The particles are mostly of refractory material for this diesel engine which was not equipped with a DPF. Further investigations should be performed for test bench accompanied by chasing experiments for future generation vehicles. Specifically volatile particle components will play a more dominant role in particle number concentrations with the removal of soot particulates.

References

Dockery, D.W. (2009): Health effects of particulate air pollution. *Ann Epidemiol., 19, 257-263.*

Etissa, D., M. Mohr, D. Schreiber, P.A. Buffat (2008): Investigation of particles emitted from modern 2-stroke scooters. *Atmospheric Environment 42, 183-195.*

Giechaskiel, B., L. Ntziachristos, Z. Samaras, V. Scheer, R. Casati, R. Vogt (2005): Formation potential of vehicle exhaust nucleation mode particles on-road and in the laboratory. *Atmospheric Environment, 39, 3191-3198.*

Murillo, S., J.L. Miguez, J. Porteiro, L.M. Gonzalez, E. Granada, J.C. Moran (2005): LPG: pollutant emission and performance enhancement for spark-ignition four strokes outboard engines. *Applied Thermal Engineering 25 (13), 1882-1893.*

Kittelson, D.B., W.F. Watts, J.P. Johnson (2004): Nanoparticle emissions on Minnesota highways. *Atmospheric Environment, 38, 9-19.*

Scheer, V., U. Kirchner, R. Casati, R. Vogt, B. Wehner, S. Philippin, A. Wiedensohler, N. Hock, J. Schneider, S. Weimer, S. Borrmann (2005): Composition of semi-volatile particles from diesel exhaust. *SAE Technical Paper Series 2005-01-0197.*

Schreiber, D., A.-M. Forss, M. Mohr, P. Dimopoulos (2007): Particle characterization of modern CNG, gasoline and diesel passenger cars. *SAE Technical Paper Series 2007-24-0123.*

Weimer, S., C. Mohr, R. Richter, J. Keller, M. Mohr, A.S.H. Prevot, U. Baltensperger (2009): Mobile measurements of aerosol number and volume size distributions in an Alpine valley: Influence of traffic versus wood burning. *Atmospheric Environment 43, 624-630.*

Investigations of Diesel Emissions with DPF+SCR in VERTdePN

J. Czerwinski [1], Y. Zimmerli [1],N. Heeb [2], A. Mayer [3], G. D'Urbano [4]*

[1] *AFHB, Berne University of Applied Sciences, CH-2500 Biel, jan.czerwinski@bfh.ch*

[2] *EMPA, Swiss Federal Laboratories for Materials Testing and Research, CH-8600 Duebendorf*

[3] *TTM, Technik Thermische Maschine, Fohrhölzlistrasse 14b, CH-5443 Niederrohrdorf*

[4] *FOEN, Federal Office of Environment, CH-3000 Bern*

ABSTRACT

The most efficient way and the best available technology (BAT) [*)] to radically reduce the critical Diesel emission components particles (PM&NP) and nitric oxides (NO_x) are the combined exhaust gas aftertreatment systems (DPF+SCR). SCR (selective catalytic reduction) is regarded as the most efficient deNO_x-system. The combined systems are already offered today by several suppliers for retrofitting of HD vehicles.
The presented results are a part of the work in the international network project VERT [*)] dePN (de-activation, de-contamination, disposal of particles and NO_x), which has the objectives to establish the test procedures and quality standards and to introduce the SCR-, or combined DPF+SCR-systems in the VERT verification procedure.

Examples of results for some of the investigated systems are given.
The most important findings are:

- the average NO_x conversion rate at transient operation strongly depends on the operation load profile, on the exhaust gas temperature profile and the resulting urea dosing control,
- the particle number filtration efficiency, which is verified at stationary engine operation, is valid also at the transient operation,
- secondary nanoparticles are produced due to urea injection, they nevertheless do not impact significantly the overall filtration efficiency of the system (here: DPF upstream & SCR downstream, differences of PCFE in the range of 0.1%),
- the OEM NO_x-sensors of the investigated systems are appropriate tool for the in-use control,
- the system with catalyzed DPF (upstream) attains higher overall deNO_x-efficiencies due to NO_2-production in the DPF,
- for the investigated systems there are no critical emissions of unregulated components, NH_3 & N_2O.

INTRODUCTION & OBJECTIVES

Laboratories for IC-Engines and Exhaust Emission Control of the University of Applied Sciences Biel, Switzerland (AFHB) participate since 1992 at the Swiss activities about nanoparticle analytics and DPF verification.

The Swiss Federal Office of Environment BAFU and the Swiss Federal Roads Office ASTRA decided to support further activities of VERT to develop appropriate testing procedures and to define the quality criteria of dePN systems for retroffiting.

The application of combined systems (DPF+SCR) as retrofitting raises different technical and commercial problems. In general opinion, this retofitting will be possible mostly through the incentives, or restrictions with respect to low emission zones LEZ, [1] and decisions of several authorities.

*) Abbreviations see at the end of paper

The present paper shows some results of further research on different combined systems (DPF+SCR) in the VERTdePN project. This is a continuation of information given in [2].
The objectives are to show new findings about:

- results in different dynamic test cycles,
- secondary nanoparticles,
- comparisons of different investigated systems.

2. TEST-ENGINE

Test engine

There are following engine data:

Manufacturer:	Iveco, Torino Italy
Type:	F1C Euro 3
Displacement:	3.00 Liters
RPM:	max. 4200 rpm
Rated power:	100 kW@3500rpm
Model:	4 cylinder in-line
Combustion process:	direct injection
Injection system:	Bosch Common Rail / 1600 bar
Supercharging:	turbocharger with intercooling
Emission control:	none
Development period:	until 2000 (Euro 3)

3. MEASURING SET-UP AND INSTRUMENTATION

Engine dynamometer and standard test equipment

Fig. 1 represents the special systems installed on the engine, or in its periphery for analysis of the regulated and unregulated emissions.

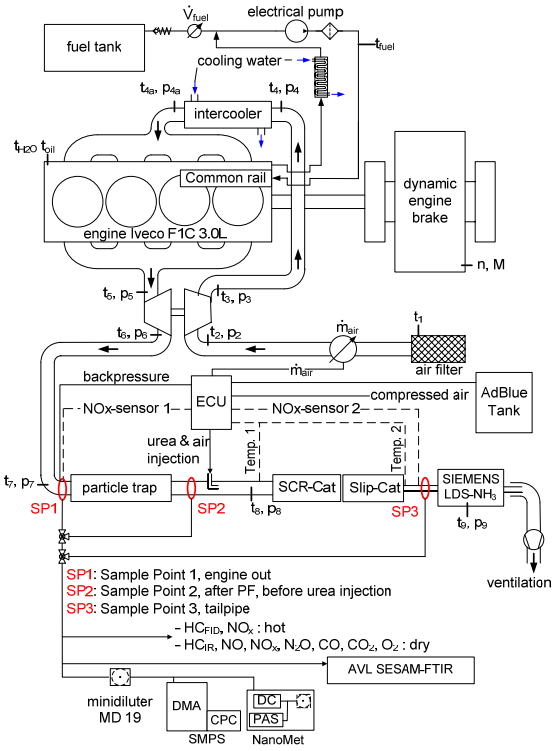

Fig. 1: Measuring set-up

Particle size analysis

To estimate the filtration efficiency of the DPF, as well as to detect the possible production of secondary nanoparticles, the particle size and number distributions were analysed with following apparatus:

- SMPS – Scanning Mobility Particle Sizer, TSI (DMA TSI 3071, CPC TSI 3025 A)
- NanoMet – System consisting of:
  - PAS – Photoelectric Aerosol Sensor (Eco Chem PAS 2000) indicates the carbonaceous total surface of the aerosol
  - DC – Diffusion Charging Sensor (Matter Eng. LQ1-DC) indicates the totale surface of the aerosol independently of the chemical properties

The nanoparticulate measurements were performed at constant engine speed (warm) with SMPS and NanoMet. During the dynamic engine operation NanoMet and CPC were used.

4. TEST PROCEDURES

The dynamic testing was started with the European Transient Cycle ETC and continued with the WHTC (worldwide heavy duty transient cycle). Also two city-bus cycles: NYCC (New York City Cycle) and Braunschweig Bus Cycle were prepared for the engine dynamometer and investigated. All these cycles were defined on the basis of full (non limited) engine map. They cause very different operating collectives of the engine, which is depicted with different traces of exhaust gas temperature at tailpipe, Fig. 2.

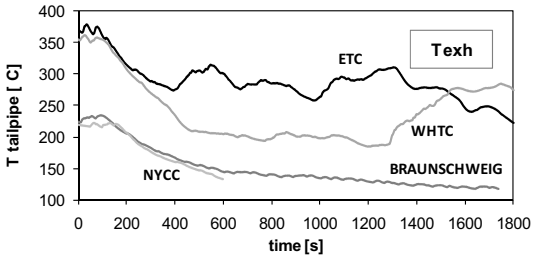

Fig. 2: Exhaust temperature in the investigated dynamic test cycles

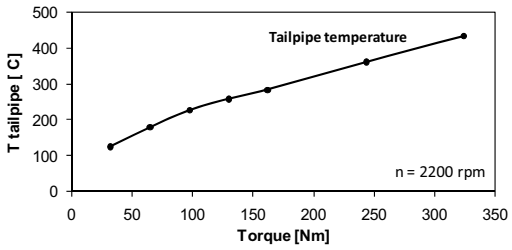

Fig.3: Torque & exhaust temperature in the steps-test

Before the start of each dynamic cycle the same procedure of conditioning was used to stabilize the thermal conditions of the exhaust gas aftertreatment system. This conditioning was: 5 min at point 1 (2200 rpm/FL) and 0.5 min of idling.
For the low-load cycles (NYCC and Braunschweig) the conditioning was: 5 min 1600 rpm / 165 Nm and 0,5 min idling.
For a more detailed investigations different sampling positions (SP, see Fig. 1) were used in the 4-points test:

SP 0 sampling engine out w/o aftertreatment system
SP 1 sampling engine out with aftertreatment system
SP 2 sampling after DPF (before urea dosing) with aftertreatment system
SP 3 sampling at tailpipe with aftertreatmentsystem.

For testing emission results in function of exhaust gas temperature at 2200 rpm with increasing engine load a steps-test, Fig. 3, was used: 10%, 20% 30%, 40% 50%, 75% and 100%.

5. (DPF+SCR) SYSTEMS

The results were obtained from combined systems consisting of a DPF upstream the urea dosing and a Vanadium based SCR catalyst downstream (as in Fig. 1).
Between DPF and SCR there was a mixing tube of 1.0m, without mixer.
Sometimes an ammonia slip catalyst was used as a modulus at the end of the system. These (DPF+SCR) systems are designed for transient application. They have an electronic control unit, which uses the signals of: air flow, NO_x before/after system and temperatures before/after SCR modulus.
Following three variants were investigated:

PF1 + SCR; PF1 + SCR + slip cat.; PF3 + SCR.

PF1 is a catalytically coated Cordierite DPF, PF3 is a uncoated SiC DPF with FBC (40 ppm Fe, double dosing for testing purposes).
Both DPF's have a VERT-conform filtration quality, in average for NP filtration efficiency FE > 99%.
The used feed factor was generally α = 0.9 (during the investigation of secondary nanoparticles, Fig. 6 & 7 the feed factor was α = 1.0).

6. RESULTS

Different test cycles

Tests were performed with different driving cycles with non limited engine map (NEM). The timeplots of tailpipe temperature over the cycle duration for all investigated test cycles are represented in Fig. 2. Fig. 4 summarizes the most important results: integral average emissions measured with different methods and Fig. 5 shows the conversion rates in different driving cycles.

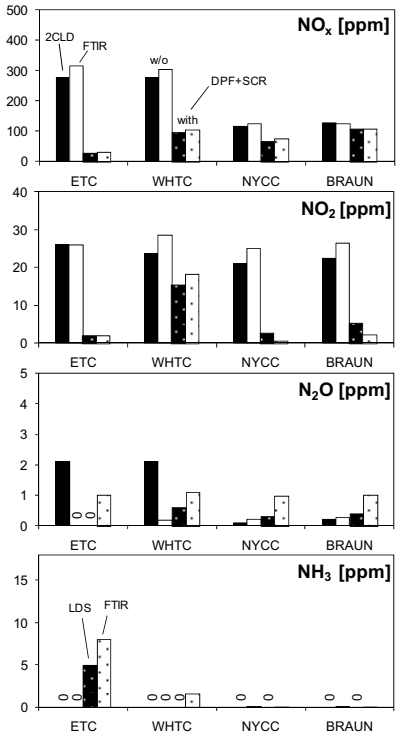

Fig.4: Integral average emission values in dynamic cycles.

The New York City Cycle (NYCC) and the Braunschweig-Cycle are low-load cycles, which were developed in those cities and represent the city bus driving.
The exhaust temperatures in the low load cycles are too low (< 200°C) to enable the full working potential of the SCR-system. The urea injection is usually cut off at t_{exh} 190-200°C to prevent the danger of deposition of solid urea crystals in the system.
In the low load cycles there is a lower average emission of NO_x, but there is also a poor NO_x-conversion rate, due to the urea dosing strategy.
There are generally very low emission values of N_2O (< 2 ppm) and for NH3 (present only in ETC with SCR NH_3 < 8 ppm).

For the comparisons of different measuring technics in Figures 4 & 5 it can be said:

- very good correspondence of NO_x & NO_2 measured with FTIR and with 2CLD,
- good correspondence of NH_3 measured with FTIR and with LDS,
- a weak agreement of N_2O measured with FTIR and with ULTRAMAT; this is the case, since the measured N_2O-values are very low – mostly at the detection limit,
- the relative values, like conversion rates K_x are well estimated with all measuring methods.

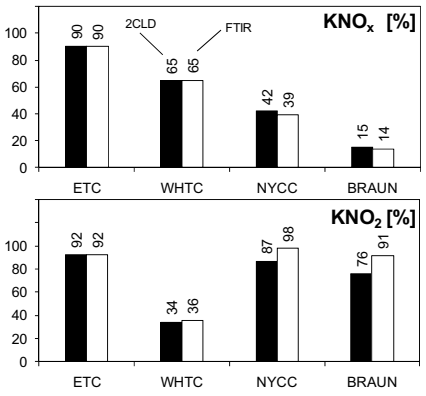

Fig.5: Comparison of reduction efficiencies in dynamic cycles, PF1+SCR, α=0.9

Finally it must be followed, that the investigated SCR-system in the present configuration is a little efficient NO_x reduction measure in the low-load city driving. This was already found in [2], by comparing the results of high-load-ETC (nonlimited engine map NEM) with low-load-ETC (limited engine map LEM).

Secondary nanoparticles

The production of secondary nanoparticles downstream the urea dosing point was found and reported in [2]. These nanoparticles can be produced as secondary pollutants during the deNOx process. They can consist of unreacted urea, cyanuric acid, ammonium nitrate, sulfates and others.
In the present part of investigations there were 2 objectives:

- to systematically indicate the secondary NP by means of PM, SMPS and NanoMet at sampling positions SP2 & SP3, (SP2 ... after DPF & before urea dosing, SP3 ... after SCR),
- to provide samples of particle mass for elemental analytics at the EMPA Analytical Laboratory for estimate of the particle composition.

The SMPS nanoparticles measurements after DPF (SP2) and after SCR (SP3) could confirm the presence of secondary nanoparticles in all operating points of the 4 points test.
Fig. 6 shows an example of the SMPS size distributions and the integrated particle counts in different size spectra at 2200 rpm / 50%. The increase of particle mass between SP2 and SP3 as a result of secondary particles production is visible.
Fig. 7 represents the particle mass PM, the mass-related filtration-efficiency PMFE and the particle counts related filtration efficiency PCFE in all operating points and at all sampling positions SP0, SP2 & SP3. At two OP's there is a little, but well pronounced increase of PM between SP2 and SP3. This causes a significant reduction of PMFE, but no significant reduction of PCFE. This means that the secondary NP's are mostly of bigger sizes.
It can be summarized that the presence of secondary nanoparticles after the SCR-system was confirmed. In some cases the secondary NP can offer a measurable contribution to the increase of particle mass.

Comparisons of different aftertreatment systems

Fig. 8 represents the reduction rates of regulated gaseous components with the investigated aftertreatment systems in the 4 points test.

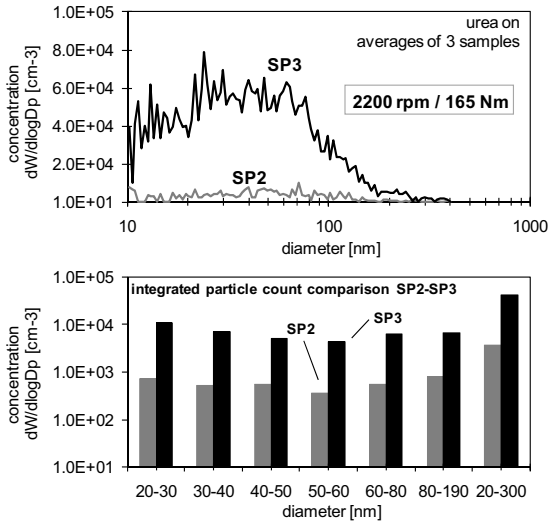

Fig.6: SMPS-size spectra at SP2 & SP3, PF1+SCR, α=1.0

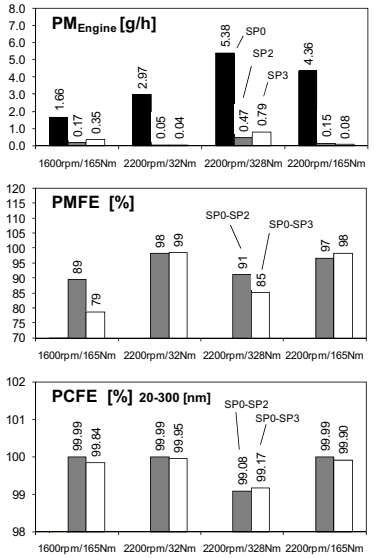

Fig.7: Particle mass and counts reduction in the **4** points test, PF1+SCR, α=1.0

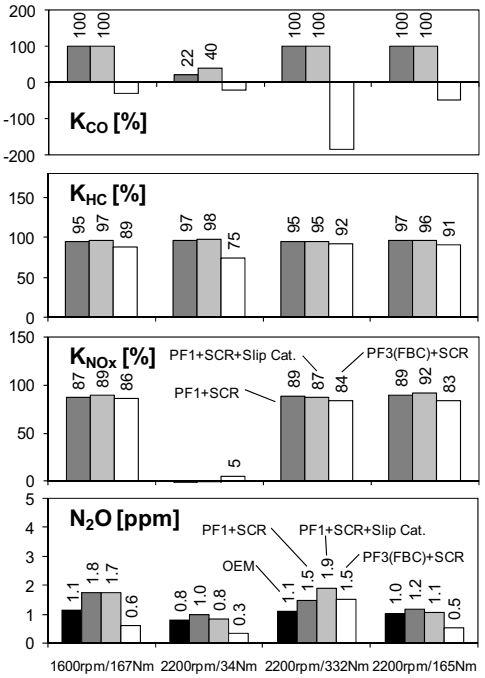

Fig.8: Reduction rates of regulated emissions components and N_2O in the 4 points test with different DPF+SCR systems

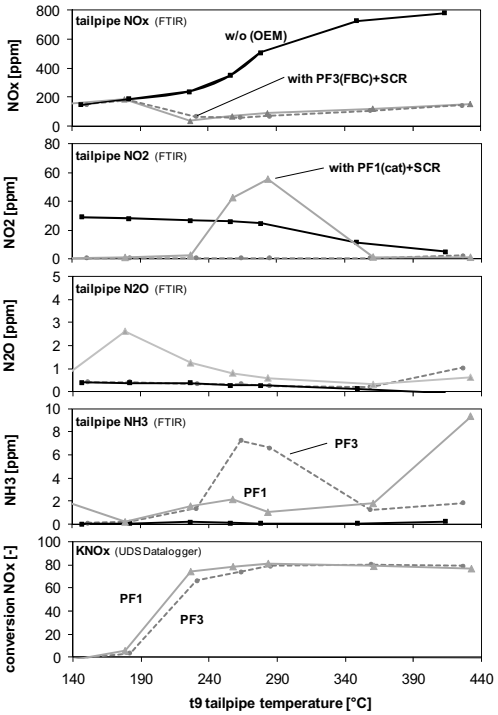

Fig.9: Comparison of different systems in steps-test at 2200 rpm:
Reference - PF1(cat.)+SCR-PF3(FBC)+SCR, 60s average values of stationary operating

With uncatalysed PF3 there is an increase of CO-negative values of K_{CO}-mostly at the highest OP with the highest backpressure.
HC is also converted in a Vanadium based SCR-catalyst, so there are still significant conversion rates K_{HC} with the system PF3 (FBC).

NO_x is not reduced at the lowest OP due to the switched off urea. With a working SCR at higher OP's there is a tendency of slightly lower K_{NOX}-values with the uncatalysed PF3 (FBC). The principal reason is the lower NO_2 availability after this PF3.
Emissions of nitrous oxide N_2O are very low (< 2 ppm) and deviate less than 1 ppm from the original values without aftertreatment (OEM).
Emissions of ammonia NH_3 are not represented, since they are generally at zero level, except of one value (10 ppm) for the PF1 (cat.) + SCR at the highest OP (2200 rpm / 332 Nm).
Fig. 9 compares the different exhaust aftertreatment systems in the steps-test at 2200 rpm.
Following effects can be remarked:

- reduction of NO_x by $t_{exh} \geq 190°C$,
- emission of NO_2 with PF1 (cat) in the t_{exh} range 240-340 °C
- emission of NH_3 (up to 8 ppm) with PF3 in the t_{exh} range 240-340°C
- emission of NH_3 (up to 10 ppm) with PF1 in the t_{exh} range < 390°C
- with PF1 (cat) start of NOx conversion at slightly lower t_{exh}, ($\Delta t \approx 10$-15°C), than for uncatalysed PF3,
- same values of maximum K_{NOX} for all systems.

7. CONCLUSIONS

The most important results from the investigated combined DPF+SCR systems can be summarized as follows:

Different test cycles

- in the low-load transient cycles (NYCC & Braunschweig) there are very low NO_x conversion efficiencies due to low exhaust gas temperatures and limited urea dosing,
- the investigated SCR-system in the present configuration is a little efficient NO_x reduction measure in the low-load city driving.

Measuring technics

- there are generally good correlations of NO_x, NO & NO_2 values measured with CLD & with FTIR; for very low absolute values (after SCR) the correlations of some parameters become weaker,
- there is a good correlation between NH3 / FTIR and NH3 / LDS, nevertheless with a clear tendency of higher readings with FTIR; this difference is negligible below $NH_3 = 10$ ppm,
- there is a weak agreement of N_2O measured with FTIR and with ULTRAMAT; this is the case, since the measured N_2O-values are very low – mostly at the detection limit,
- the differences are caused partly by different sampling positions and partly by different conditions for the possible intermediary reactions in the sampling line,
- the relative values, like conversion rates K_x are well estimated with all measuring methods.

Secondary nanoparticles

- the production of secondary nanoparticles (NP) in the SCR-system was confirmed; in certain cases they are also visible as a slight increase of particle mass (PM).

Comparisons of different systems

- the system with FBC has a slightly lower K_{NOX}-values due to lower NO_2-availibility from uncatalysed PF3,
- the systems with catalysed PF1 have an efficient elimination of CO and HC, but in spite of the SCR (downstream) they can produce a higher NO_2/NO_x-ratio at certain operating conditions,
- for both systems there are no critical emissions of unregulated components, like ammonia, nitrous oxide, hydrocyanic acid, isocyanic acid and formaldehydes (not represented in this report).

8. LITERATURE

[1] www.lowemissionzones.eu
[2] Czerwinski, J.; Zimmerli, Y.; Mayer, A.; Heeb, N.; Lemaire, J.; D'Urbano, G.; Bunge, R.; Testing of Combined DPF+SCR Systems for HD-retrofitting VERTdePN. SAE Techn. Paper 2009-01-0284.

Tailpipe emissions from garbage trucks in the metropolitan area of Milan, Italy and their evolution by 2010

P. Dilara, C. Pastorello, G. Martini, P. Bonnel, U. Manfredi*
European Commission, Joint Research Centre, Ispra, (VA) 21027, Italy

Introduction

Air pollution still remains a problem in Europe and throughout the world, especially for urban agglomerations, with high density of traffic and industrial activities (EEAa, 2009). However, only few studies focus on the contribution of transport from public waste collection and cleaning activities in a large urban centre. Milan is one of the biggest cities in Europe, with a population of 1.3 million people and 8 thousand commuters per day, and one of the most densely populated area in Italy. The combination of high traffic volumes and high industrial activities with unfavourable weather conditions makes air pollution a high priority problem in the metropolitan area of Milan, where both the short-term (24-h average) and the long-term (annual average) PM10 standard of 40 μg/m3 are largely exceeded (Lonati et al, 2005). Similar to the majority of the European large metropolitan areas, the contribution of road transport is very high for all the important pollutants. More than 55% of NOx and PM and more than 30% of VOC emissions come from the transport sector in the municipality of Milan (ARPA Lombardia and Regione Lombardia, 2009; AMA, 2007). Despite the many studies on the subject, the contribution of the waste collection agency was never calculated in detail, although its large fleet has an inevitable contribution to urban traffic emissions.

AMSA is the Milan Environmental Services Agency that takes care of the waste collection and of the street's cleaning of the entire Milan metropolitan area. In order to accomplish its mission and to satisfy the need of one of the most populated areas of Italy, AMSA owns around 1200 vehicles used primarily in the services of waste collection and street cleaning services in the Milan area. In an effort to minimize its environmental impact, AMSA has announced the adoption of different measures aiming at mitigating the effects on air quality associated with their activity, such as fast renewal of vehicle fleet and increased use of compressed natural gas (CNG) instead of diesel. This paper will focus on the potential environmental benefits of these strategic measures between the years 2005-2010. The effects of the planned measures are estimated both in terms of emissions and of average emission factors.

Experimental Campaign

An experimental campaign of emission measurements was designed and executed using PEMS (Portable Emission Measurement System) on two compactor garbage trucks, with the aim to obtain some initial real-world emission data. A EURO V compactor garbage truck fuelled with natural gas (CNG) and a EURO V compactor garbage truck fuelled with diesel fuel + 25% biodiesel (B25) were tested on their normal driving pattern during two normal working days each. Wednesday and Thursday were selected for the experiments because the load of garbage collected and thus length of stops made are similar on the two days (see table1).

Table 1: Experimental data on the on-road collection of PEMS data.

		CNG 1 Day_1	Diesel 1 Day_1	CNG 2 Day_1	Diesel 2 Day_1	CNG 1 Day_2	Diesel 1 Day_2	CNG 2 Day_2	Diesel 2 Day_2
Trip duration	[s]	8679	8033	8291	8730	9519	9439	6896	7586
Trip distance	[km]	19.66	17.11	17.52	18.82	15.29	14.47	13.09	12.45
Average speed	[km/h]	8.16	7.67	7.61	7.76	5.78	5.52	6.83	5.91
Aver. air temp.	[degC]	24.11	18.18	27.90	19.13	20.88	20.13	22.37	21.24

From the data regarding the runs, which are seen in Table 1, it is confirmed that the average speed of these trucks is extremely low (i.e. below 10km/h).

PEMS results

The mean emissions over the 4 trips for the two vehicles are shown in Figure 1. As expected, the NOx and PM emissions of the Diesel garbage truck are significantly higher than the same emissions of the CNG fuelled vehicle. CO2, CO and HC of the CNG vehicle are instead higher. It has to be mentioned that these data are limited but still support the general conclusions of the paper.

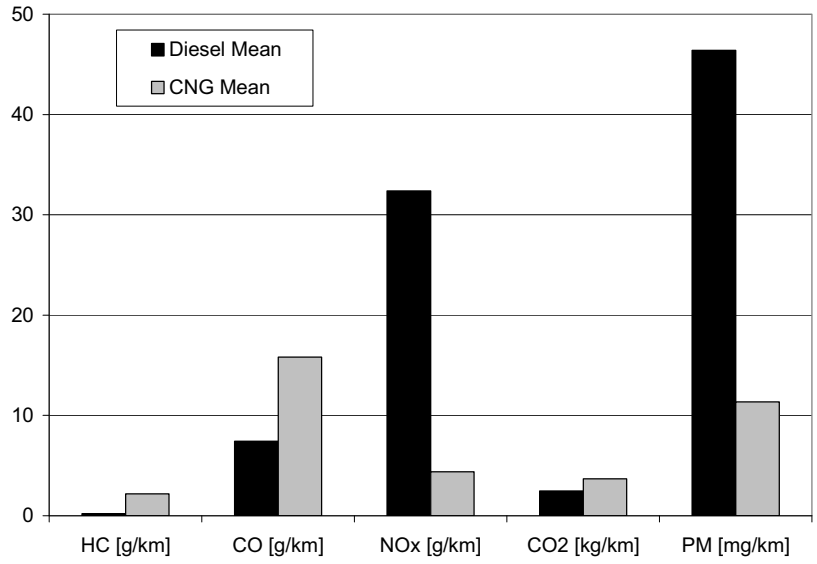

Figure 1 Mean emissions of Diesel and CNG compactor garbage trucks over 4 trips as measured by PEMS

Fleet Characteristics

For this study AMSA provided the complete fleet composition from the years 2005 until 2010 (for 2010 the fleet composition is forecasted), with details on: vehicle class (passenger cars, light trucks and heavy duty vehicles), vehicle weight, registration according to emission limits (conventional, euro 0, euro 1, etc…), fuel, registration year, engine power and mileage. For the

evolution of the vehicle fleet composition the following were taken into account: a decrease in older (i.e. pre-euro 3) vehicle categories is balanced by an increase in newer ones (Figure 2).

In the AMSA plan, pre-Euro 1 vehicles will not be used after the year 2008, Euro 1 vehicle categories are expected to disappear in 2010 and the euro 2 vehicles are expected to decrease from 37% to 13% in the same period.

Non road mobile machineries (NRMM) also are included in the AMSA fleet. These vehicles are registered as agricultural machinery in Italian vehicle register and they are used for sweeping and cleaning the roads. The CNG vehicles are heavy duty vehicles used for the collection of the waste.

AMSA also provided the actual mileage for all vehicle categories and for all years for the period 2005-2008. Total mileage of the fleet for the years 2009 and 2010 was provided by AMSA: the mileage for each vehicle categories and for each vehicle legislation class was extrapolated following the trends. Over the period 2005-2010 an increase of the mileage driven times the fleet of about 18% can be observed, while a steep increase of CNG vehicles total annual mileage (more than 500%) is expected due to the increase in the CNG fleet.

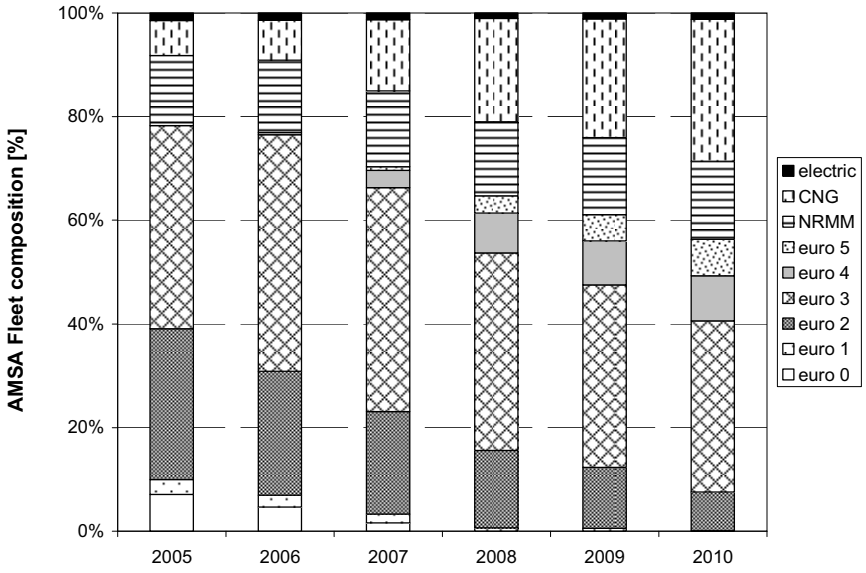

Figure 2: The AMSA fleet composition projected up to 2010, according to the AMSA plans.

Emission Factors

The COPERT model (EEAb, 2009) was used to calculate emission factors for the AMSA standard vehicle fleet (i.e. except for the CNG vehicles where the emission factors contained in COPERT are of low quality). An average speed value of 15 km/h and 10 km/h for light duty vehicles and heavy duty vehicles, respectively, was derived by dividing the total kilometers driven by the total hours the vehicles were operational. The speed range between 5 and 15 km/h is typical of a waste collector in real operating conditions, driving on routes classified as urban and suburban (Martini, 2009, Caserini et al, 2005) and was used for running the COPERT model

with the AMSA standard vehicle fleet. Similar speeds were observed also during the PEMS runs within this study.

For the CNG fuelled waste collection vehicles, a set of emission factors were estimated on the basis of a review of available emission factors for CNG urban buses. Considering that buses driving is similar to the waste collection one, characterized by stop and go traffic situation and low mean speeds, and that their weight is comparable, the CNG urban buses data were used for estimating emission of CNG waste collection vehicles.

For the NRMM the emission factors are taken from the relevant chapter in the EMEP/EEA Air Pollutant Emission Inventory Guidebook (Chapter 1.A.4 in EEAb, 2009).

Results and Discussion

The total emissions of the AMSA fleet in the period 2005-2010 are shown in Figure 3. Even if the fleet mileage is expected to increase in 2010, the plot shows a decrease of emissions for all the pollutants due to the high renewal rate of the fleet. In particular, the emissions of PM, NOx and VOC are projected to decrease 32%, 22% and 15%, respectively. The general picture is very similar to the one for the emissions of both Diesel and Gasoline fuelled PC+LDV+HDV, as well as for the NRMM emissions. In fact the sum of these two emission sources account for more than 95% of the emissions in year 2005, while this percentage drops to a varying degree for the different pollutants by the year 2010, mostly due to the substitution of the fleet with CNG fuelled vehicles.

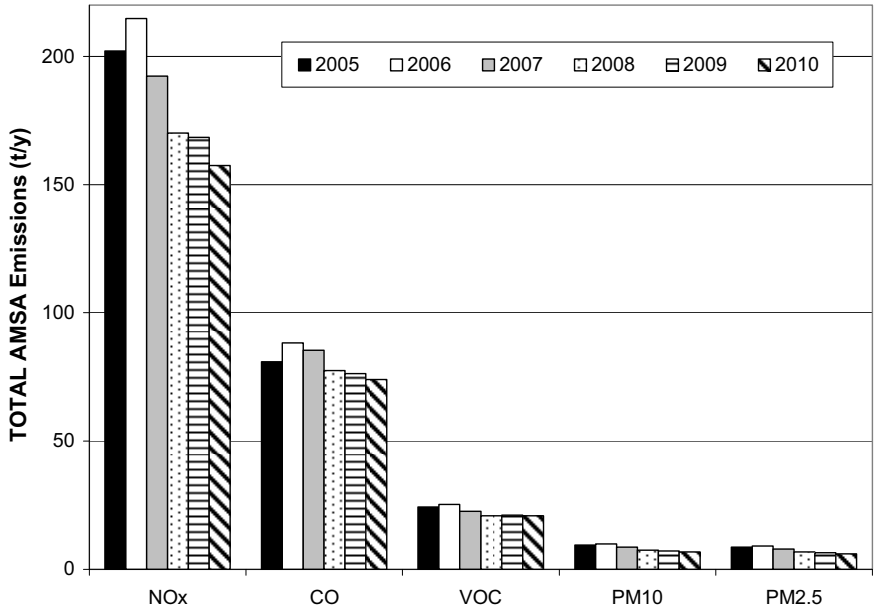

Figure 3: Evolution of total AMSA fleet emissions (in tons per year).

The general effect of fleet renewal and substitution by CNG vehicles can better be seen in Figure 4, where a mean emission factor for the whole AMSA fleet was calculated by dividing the total emissions by the total km run per year. Compared to 2005, we see a reduction due to improved technologies of almost 40% for PM10 and 20% for CO, while the other pollutants fall between these two extremes.

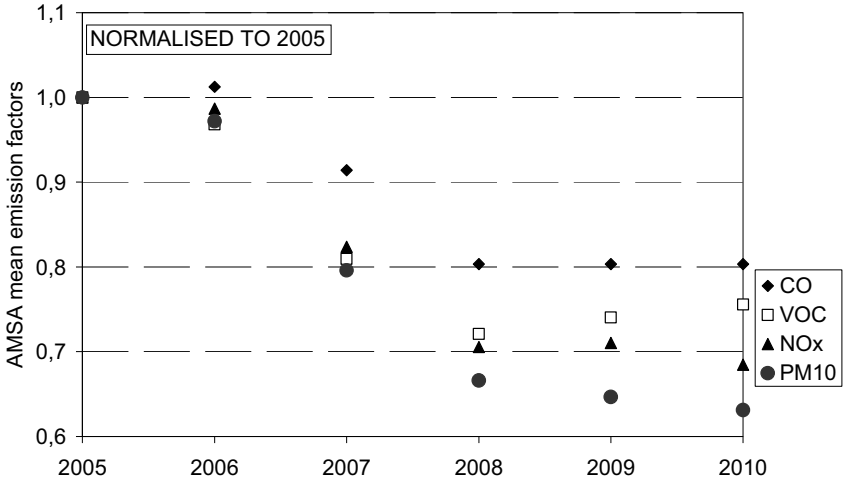

Figure 4: Evolution of mean emission factors for the AMSA fleet

Finally, in order to put the emissions of AMSA in perspective to the total emissions from the same sectors in the province of Milan, it was calculated that for the year 2005, the total AMSA emissions accounted for 0.6% of NOx, 0.3% of PM and 0.2% of CO_2 emissions from the road and non-road transport sector in Milan (see Table 2). These percentages are rather high considering that the fleet of AMSA comprises of only 1000 vehicles, i.e. only 0.014% when compared to 7 million vehicles for the Milan province, but expected, since due to the particular driving mode of these vehicles, they are expected to pollute more than the normal fleet.

Table 2 – Contribution of AMSA emissions to Milan total road transport and NRMM emissions for the year 2005

	NOx	**VOC**	**CO**	**PM10**	**PM2.5**	**CO2**
	t/year	t/year	t/year	t/year	t/year	kt/year
Milan Road Transport	30418	24049	76451	2409	2024	6164
Milan NRMM	4594	1238	3338	530	521	463
Milan Total (RD+NRMM)	35012	25287	79789	2939	2544	6627
AMSA Total	202	24	81	9	9	12
% AMSA	0.58	0.10	0.10	0.32	0.34	0.19

Conclusions

The benefits in terms of emissions reduction resulting from measures taken by the Milan Environmental Services Agency (AMSA), like the renewal of the fleet and the partial switch to CNG vehicles, in order to reduce the impact of waste collection and street cleaning on air quality, have been estimated.

In the period 2005-2010 the reduction of the total AMSA fleet emissions was estimated to be 32%, 22% and 15% for PM, NOx and VOC respectively. VOCs decrease to a lesser extend due to the fleet change to CNG vehicles, which in average have higher VOC emission factors than conventional vehicles, while most of the benefit of this introduction of CNG vehicles can be seen in the decrease of primary PM.

However the scarcity and thus uncertainty of CNG emission factors has to be kept in mind. More work is needed in order to improve the quality of the CNG emission factors. In fact the quality of emission factors can be one of the most important contributors to the total uncertainty of emissions, especially in cases where the fleet and fuel usage is know with high accuracy (Kouridis, 2010), like in the present case.

Acknowledgements: The authors would like to thank the Milan Environmental Services Agency (AMSA-AZIENDA MILANESE SERVIZI AMBIENTALI) for the availability of their fleet data for this work.

References

ARPA Lombardia and Regione Lombardia. INEMAR, Inventario emissioni in atmosfera. Emissioni in Lombardia nel 2005 - dati finali. (in Italian). 2009 (In Italian). Internet website: http://www.ambiente.regione.lombardia.it/inemar/webdata/main.seam

AMA – Agenzia Mobilita' e Ambiente Milano. Rapporto Qualita' dell'aria, Energia e Aspetti fisici. 2007 (In Italian). Internet website: http://www.ama-mi.it/.

Caserini S, Seminati P.. Valutazione ambientale ed economica del passaggio a gas naturale dei mezzi di trasporto pubblico e per la raccolta di RSU: il caso di Brescia. Economia delle fonti d'energia e dell'ambiente 2007, n.1, 65-80. Franco Angeli ed. ISSN 1125-1263 (in Italian).

EEAa. Ensuring quality of life in Europe's cities and towns. EEA Report No 5/2009. Internet website: http://www.eea.europa.eu

EEAb. EMEP/EEA Air Pollutant Emission Inventory Guidebook 2009. Internet website: http://www.eea.europa.eu/themes/air/emep-eea-air-pollutant-emission-inventory-guidebook

Kouridis C. Gkatsoflias D, Kioutsoukis I, Ntziachristos L, Pastorello C, Dilara P., in Uncertainty Estimates and Guidance for Road Transport Emission Calculations, EUR Report, JRC, 2010.

Lonati G, Giugliano M, Butelli P, Romele L, Tardivo R. (). Major chemical components of PM2.5 in Milan (Italy). *Atmos Environ* 2005; 39, 10: 1925-1934.

Martini G. Measuring heavy duty CO2 emissions in real world driving conditions. Diesel Emission Conference, 23-25 June 2009, Brussels, Belgium.

Session 2: Air Quality Measurement and Modelling

Size resolved ultra fine particle model for a traffic tunnel

B. De Maerschalck[1], I. Nikolova[1], S. Jannssen[1], P. Vos[1]*

[1] VITO, Dep. Of Atmospheric Modelling , Boeretang 200, 2400 Mol, Belgium, bart.demaerschalck@vito.be

Introduction

When investigating traffic related ultra fine particles (UFP) and their behaviour in the atmosphere on a local scale, road tunnels form an interesting environment, both in the perspective of measurement campaigns and model development and testing. In a traffic tunnel, external factors that influence local air quality are limited or relatively easy to monitor compared to urbanized environments: uniform quasi one-dimensional wind flow, well mixed concentrations, generally quasi continuous traffic flows, high traffic contribution, limited inflow of fresh air. These limitations in environmental complexity together with the simple geometry makes it also feasible to model traffic emitted pollutants accurately and fast. In principle the full 3D dispersion model can be reduced to a one-dimensional quasi-steady-state problem. This makes the model not only suitable for testing emission models or back-calculating traffic emissions from measurements, but it also makes the model attractive as a test platform for developing and testing different chemical and physical transformation models. One can not only test and validate the performance of sub models, but can also investigate the effects of different transformation processes on the local air quality before implementing the transformation processes into complex fully 3D air quality models

Proposed is a one-dimensional quasi steady state UFP model for a road tunnel with naturally ventilation. The model is coupled with a size resolved ultra fine particle emission model for different traffic conditions. The model returns at every location inside the tunnel a continuous size distribution of ultra fine particles. The model has been compared with measurement data taken in the Antwerp Craeybeckxtunnel.

1D Tunnel model

Considering the general dispersion model for a number concentration *c* ($[\#/m^3]$) in the atmosphere (Seinfeld and Pandis 2006):

$$\frac{\partial c}{\partial t} + u\frac{\partial c}{\partial x} + v\frac{\partial c}{\partial y} + w\frac{\partial c}{\partial z} = \frac{\partial}{\partial x}\left(K_{xx}\frac{\partial c}{\partial x}\right) + \frac{\partial}{\partial y}\left(K_{yy}\frac{\partial c}{\partial y}\right) + \frac{\partial}{\partial z}\left(K_{zz}\frac{\partial c}{\partial z}\right) + R + E - S\,, \quad (1)$$

with $[u,v,w,]^{\mathrm{T}}$ the velocity vector, K_{ii} the turbulent flux coefficients, R the chemical and physical reaction terms, E the emissions ($[\#/m^3 s]$) and S the sink terms. For a simple traffic tunnel one can significantly simplify this equation by considering the following assumptions:

- Assume a uniform mean flow inside the tunnel: $[u, v, w] = [u_t, 0, 0]$ with u_t the wind speed inside the tunnel, also called the ventilation speed.
- Concentration is homogeneous along the cross section of the tunnel and the dilution in the direction perpendicular to the driving direction is instantaneous: $\frac{\partial c}{\partial y} = \frac{\partial c}{\partial z} = 0$.

- Emission is considered as a constant line source: $E = E_T/A_t$ with A_t the cross sectional area of the tunnel ($[m^2]$) and E_T the traffic emission per meter road ($\#/m\,s$),
- If the variation in time of the line-source and the ventilation speed is low, a quasi steady state solution can be obtained. Therefore assume: $\frac{\partial c}{\partial t} = 0$
- Assume that the ventilation speed inside the tunnel is high enough so that the lateral transport of particles and gases is mainly advection driven, therefore : $\frac{\partial}{\partial x}\left(K_{xx}\frac{\partial c}{\partial x}\right) \ll u\frac{\partial c}{\partial x}$.

These simplifications lead to the following one-dimensional steady state dispersion model:

$$u\frac{\partial c}{\partial x} = \frac{E_T}{A_t} + R - S\ . \tag{2}$$

In a first approach the reaction terms, R, will be neglected and the only sink term considered is due to deposition on the pavement, walls and tunnel ceiling. As such, the sink term per meter roadway tunnel is defined as:

$$S = \frac{v_d\,P_t\,c}{A_t}\ , \tag{3}$$

where the deposition speed v_d, is a function of the particle size, but also of the surface type. Therefore, the deposition velocity, v_d, in (3) is the effective deposition velocity:

$$v_d = \frac{1}{P_t}\sum_{i=1}^{4} v_{d,i}\,P_i\ , \tag{4}$$

with i referring to the surface. The modelling of the deposition velocity is based on a resistance scheme as in Seinfeld and Pandis (Seinfeld and Pandis 2006). Figure 1 shows de deposition speed as a function of the particle size for different ventilation speeds (De Maerschalck, Janssen et al. 2010).

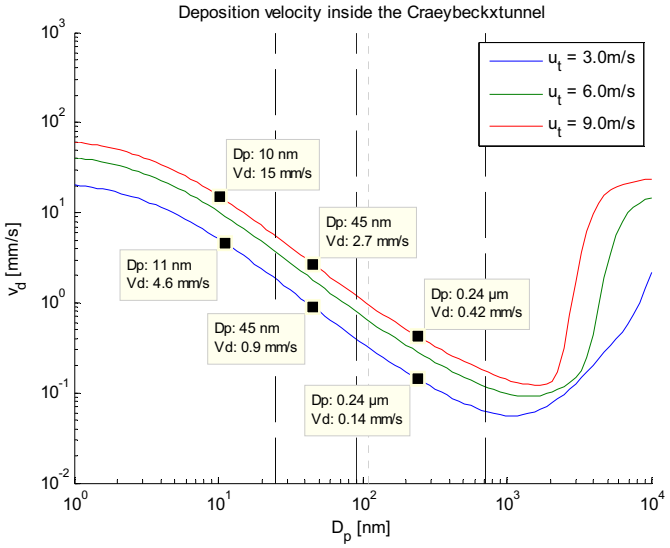

Figure 1: Deposition speed for different wind speeds as a function of the particle size.

If one solves (1) exactly, the following analytic solution can be obtained:

$$c(x) = \frac{E_T}{v_d P_t} - \left(\frac{E_T}{v_d P_t} - c_0\right) e^{-v_d P_t x/u_t A_t}\ , \tag{5}$$

with c_0 the inlet concentration at the entrance of the tunnel. This is in general the summation of the background concentration and the local contribution of the traffic activity in front of the tunnel entrance. Notice that when the deposition velocity goes to zero in the limit the concentrations inside the tunnel will become a linear function in x:

$$\lim_{v_d \to 0} c(x) = \frac{E_T}{u_t A_t} x + c_0 \ , \tag{6}$$

This clearly expresses that due to accumulation effects the concentrations inside the tunnel increase with increasing tunnel length. The rate of increase is dependent on the traffic activity, the tunnel size and the ventilation speed. The ventilation inside a roadway tunnel can be naturally driven or forced by ventilation fans. In traffic tunnels with separated pipes, often the momentum created by the traffic flow is high enough to drive the ventilation speed.

Continuous size distribution

Equation (5) gives the exact solution for a simplified scalar advection equation. In general UFP is characterized by a wide distribution of particle diameters. Therefore the tunnel model is coupled with a UFP emission model which provides a continuous size distribution of emitted particles (Nikolova, Janssen et al. 2010).

The UFP-emission model gives the emissions as a size distribution of ultra-fine particles emitted per meter and per second. As input it needs the traffic activity of passenger cars and heavy duty vehicles. The size distributions are modelled by a summation of log-normal probability density functions:

$$\frac{\mathrm{d}E}{\mathrm{d}\log D_p} = \sum_i \sum_j \frac{E_{ij}}{\sqrt{2\pi}\log\sigma_{ij}} e^{-\frac{(\log D_p - \log D_{pg_{ij}})^2}{2\log^2 \sigma_{ij}}} \ . \tag{7}$$

Here i is referring to the vehicle class (type, engine, fuel, 15 in total) and j is referring to the size mode. For most vehicle classes the model gives two size modes: nucleation mode ($D_p \leq 30nm$) and Aitken mode ($30nm < D_p \leq 0.1\mu m$). D_p is the particle diameter, $D_{pg_{ij}}$ the mean particle diameter per mode and vehicle class, σ_{ij} the standard deviation and E_{ij} the total emission per mode an vehicle class. Notice that the total number of emitted particles per meter and per second is equal to:

$$E_{tot} = \int_{-\infty}^{\infty} \frac{\mathrm{d}E}{\mathrm{d}\log D_p} \, \mathrm{d}\log D_p = \sum_i \sum_j E_{ij} \ , \tag{8}$$

and for the total emission per vehicle class:

$$E_i = \sum_j E_{ij} \ . \tag{9}$$

Figure 2 shows a typical output of the UFP emission model for two different driving conditions: highway driving conditions on the left and rural driving conditions in the right plot. The traffic activity is based on an in situ measurement campaign the Antwerp Craeybeckxtunnel with 3600 passenger cars and 560 heavy duty vehicles per hour.

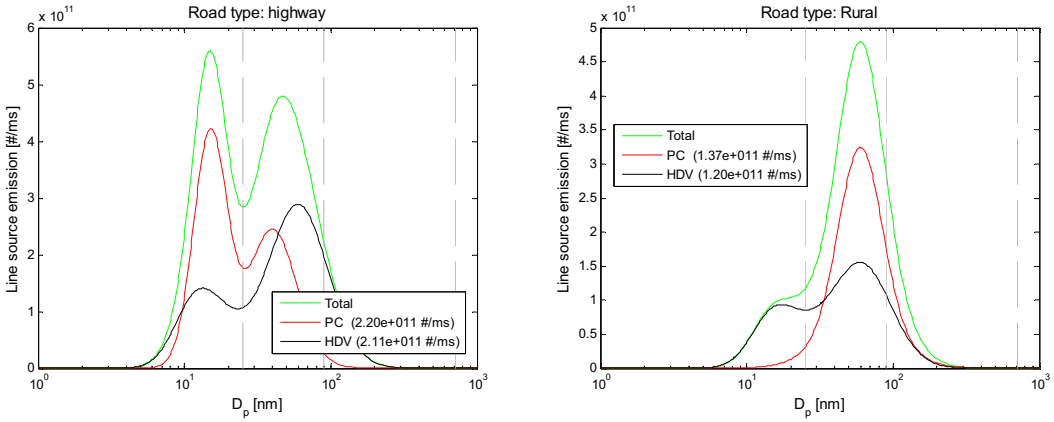

Figure 2: UFP emission [#/ms] for different driving conditions, Left: Highway, Right: Rural

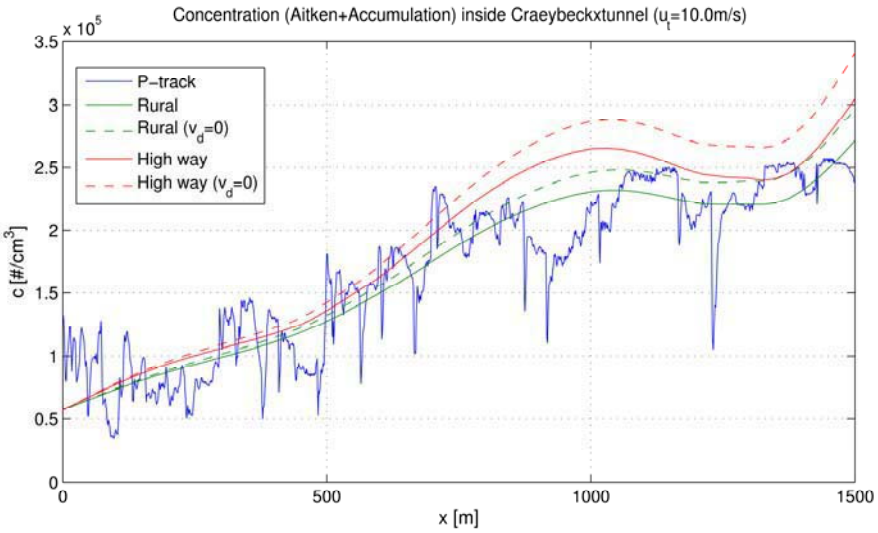

Figure 3 : Modelled and measured total number concentrations (Aitken + Accumulation mode) in the Antwerp Craeybeckxtunnel. (modelled driving conditions: Highway and Rural, continuous lines : with size dependent deposition, dashed lines : linear model without deposition modelled).

Comparison to tunnel measurements

The Antwerp Craeybeckxtunnel consist of two separate tubes of about 1.6 km long, with in each tube four driving lanes. The tunnel connects the ring of Antwerp with the E19 highway towards Brussels. The tunnel is about 20.75 meters wide and 6.5 meters high. Speed limit inside the tunnel is 100 km/h, average speed is 80 km/h. It is one of the roads with the highest traffic activity in Flanders with on a normal working day more than 50.000 vehicles per tube. Traffic activity is continuously monitored by double inductive loops at the end of the tunnel. Ventilation is mainly traffic induced. Only when very high CO concentrations are monitored an active ventilation system is automatically switched on. This happens very rarely.

Total number concentration (Aitken + Accumulation mode, $20nm \leq D_p \leq 1\mu m$) has been measured during a short measurement campaign by walking through the tunnel with a mobile Ptrack measurement device (Mishra, Berghmans et al. 2009). The ventilation speed during the measurement was about 10m/s.

Figure 4 shows the modelled and measured total number concentrations (Aitken + accumulation mode):

$$N_{Aitk.+Acc.}(x) = \int_{\log 20}^{\log 1000} \left.\frac{\mathrm{d}\,N}{\mathrm{d}\log D_p}\right|_x \mathrm{d}\log D_p \ . \tag{10}$$

The green lines are the modelled concentrations under rural driving conditions, while the red lines are with highway driving conditions, which are more realistic for the time of the measurements. The dashed lines are without any deposition modelled as in (6), while the continuous lines are with the size dependent deposition speed like in equation (5). Notice that the dashed lines do not show a linear increase along the tunnel length, like one would expect from equation (6). This is due to the variation in traffic activity during the measurement, which took about half an hour to go through the tunnel. At each location a quasi steady state has been modelled with the emission based on the actual traffic activity.

Effect of size dependent deposition on the particle size distribution

Figure 4 shows the evolution of the size distribution inside the tunnel for a constant line source emission as in Figure 2. The graphs show the modelled size distributions at different locations inside the tunnel. The blue line is the linear model without taken any deposition into account, while the red line is the full model with size dependent deposition velocity. In case of the zero deposition model, the concentrations are only increasing due to the accumulation effect, but the shape of the distribution remains unchanged. When deposition is taken into account the number of particles is not growing as fast for all particle sizes. Due to more efficient deposition for the very small particles, the size distribution inside the tunnel is changing, although the size distribution of the emission is the same along the tunnel length. Therefore the effect of the deposition on UFP-concentrations strongly depends on the shape of the size distribution itself.

So far only size dependent deposition has been taken into account. It is expected that due to the high concentrations inside the tunnel, coagulation will have a significant effect as well (Gidhagen, Johansson et al. 2003). Therefore, at the moment of writing efforts are taken to implement a size dependent coagulation rate as well. However, since coagulation is a highly nonlinear process the model will no longer have an analytic solution and will have to be solved numerically.

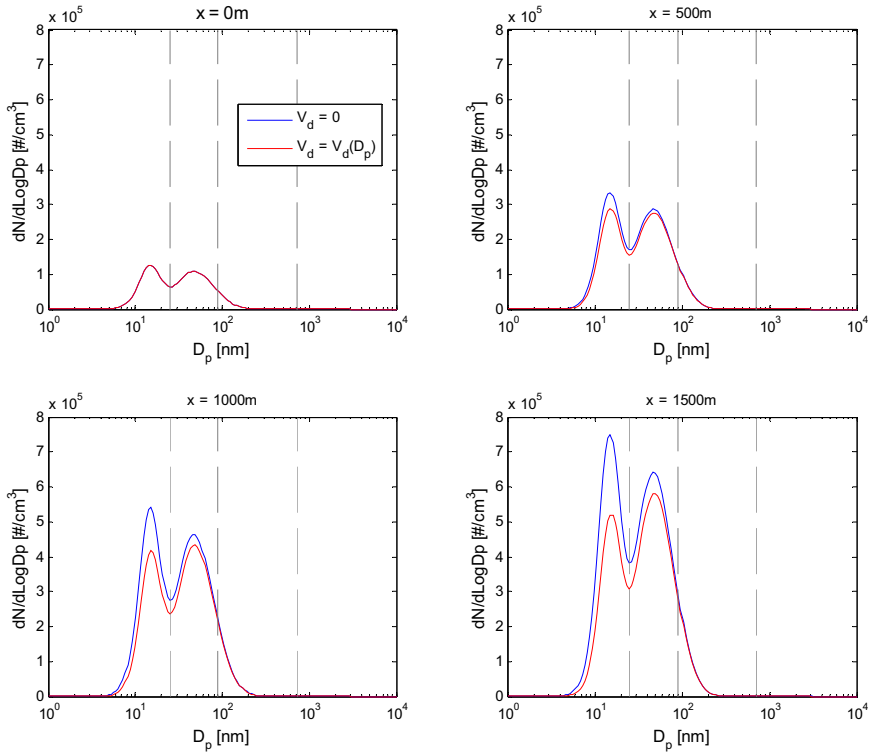

Figure 4: Modelled size distribution along the Antwerp Craeybeckxtunnel at different locations (entrance, 500m, 1000m, 1500m) inside the tunnel with (red) and without deposition (blue) modelled. (Highway driving conditions, Passenger cars: 3600/h, Heavy duty: 560/h, tunnel ventilation speed: 10m/s)

References

De Maerschalck, B., S. Janssen, et al. (2010), Size Resolved Ultra Fine Particles Modeling inside a Roadway Tunnel: Emissions, Dispersion and Deposition Processes. *In preparation*.

Gidhagen, L., C. Johansson, et al. (2003), Model simulation of ultrafine particles inside a road tunnel. *Atmospheric Environment* 37, 2023–2036.

Mishra, V., P. Berghmans, et al. (2009), Size resolved ultrafine particulate concentration levels in Craeybeckx tunnel, Antwerp. *In preparation*.

Nikolova, I., S. Janssen, et al. (2010), An emission model for traffic induced ultrafine particles – a continues size distribution approach. *Atmospheric Environment* Submitted.

Seinfeld, J. H. and S. N. Pandis (2006), *Atmospheric chemistry and physics*, New Jersey, John Wiley.

Impact of roadside noise barriers on particle size distributions and pollutants concentrations near freeways

*Zhi Ning[1], Neelakshi Hudda[1], Nancy Daher[1], Winnie Kam[1], Jorn Herner[2], Kathleen Kozawa[2], Steven Mara[2], Constantinos Sioutas[1]**

* Corresponding author: Constantinos Sioutas, Sc.D, email: sioutas@usc.edu;
[1] Civil and Environmental Engineering Department, University of Southern California, 3620 South Vermont Avenue, Los Angeles, CA 90089, USA
[2] California Air Resources Board, Research Division, 1001 ''I'' Street, P.O. Box 2815, Sacramento, CA 95812, USA

Abstract

Increasing epidemiological evidence has established an association between a host of adverse health effects and exposure to ambient particulate matter (PM) and co-pollutants, especially those emitted from motor vehicles Although PM and their co-pollutants dispersion profiles near the open freeway have been extensively characterized by means of both experimental measurements and numerical simulations in recent years, such investigations near freeways with roadside barriers have not been well documented in the literature. A few previous studies suggested that the presence of roadside structures, such as noise barriers and vegetation, may impact the decay of pollutant concentrations downwind of the freeway by limiting the initial dispersion of traffic emissions and increasing their vertical mixing due to the upward deflection of airflow. Since the noise barriers are now common roadside features of the freeways, particularly those running through populated urban areas, it is pertinent to investigate the impact of their presence on the particles and co-pollutants concentrations in areas adjacent to busy roadways. This study investigated two highly trafficked freeways (I-710 and I-5) in Southern California, with two sampling sites for each freeway, one with and the other without the roadside noise barriers. Particle size distributions and co-pollutants concentrations were measured in the immediate proximity of freeways and at different distances downwind of the freeways. The results showed the formation of a "concentration deficit" zone in the immediate vicinity of the freeway with the presence of roadside noise barrier, followed by a surge of pollutant concentrations further downwind at 80-100m away from freeway. The particle and co-pollutants concentrations reach background levels at farther distances of 250-400m compared to 150-200m at the sites without roadside noise barriers.

Introduction

In recent years, several toxicological studies have reported the ability of particulate matter (PM) to generate reactive oxygen species in biological systems (Sagai et al., 2000; Donaldson et al., 2002; Xia et al., 2004). In urban areas, the primary source of ambient PM and co-pollutants come from motor vehicles (Ning and Sioutas, 2010), which raises serious health concerns for the part of the population who live and/or work in the communities nearby busy roadways. Several epidemiological studies have reported a strong and positive association between a community's proximity to highly trafficked roadways and the risk of adverse health effects among population in the community (Delfino, 2002; McConnell et al., 2006)

Particle and gaseous pollutants dispersion profiles near open freeways have been well documented by means of both experimental measurements (Zhu et al., 2002a; Zhu et al., 2002b) and numerical simulations (Zhang et al., 2004; Jacobson et al., 2005) in recent years. Although these studies have characterized the roadside particle and co-pollutants dispersion profiles quite extensively, the roadways under investigation were often open -field without considering any roadside obstacles. These roadside structures may affect the characterization of pollutants decay profiles downwind of roadway by limiting or blocking the initial dispersion of traffic-induced emissions from roadway and increasing their vertical mixing due to the upward deflection of airflow caused by the obstacles (Holscher et al., 1993; Heist et al., 2009). Given that the noise barriers, built to reduce noise levels in areas nearby roadways, are common roadside features of highly trafficked freeways, particularly those running through densely populated areas, it is pertinent to investigate the effect of their roadside presence on particles and co-pollutants concentration levels in areas adjacent to the busy roadways.

Experimental methodology

Figure 1Location of the sampling sites: (a) I-710 without roadside barrier; (b) I-710 with roadside barrier; (c) I-5 without roadside barrier; (d) I-5 with roadside barrier.

An intensive summer sampling campaign has been carried out in the present study during June-July, 2009 to investigate the impact of roadside noise barrier on the dispersion profile of particles and co-pollutants emitted from freeways. Two highly trafficked freeways in greater Los Angeles area (I-710 and I-5) were selected, with two sampling sites (one with roadside noise barrier and the other without) located along the span of each freeway. At each of the four sites, a stationary sampling Station was set up located in the immediate proximity of the freeways to characterize the freeway emissions, while a mobile platform was deployed along the trajectories downwind of the traffic emissions from freeway to collect ambient data at varying distances. Figure 1 (a, b, c & d) shows the location of the four sampling sites and the route of the mobile platform at the downwind area of the selected freeways. Two sampling instrument sets were deployed simultaneously, one at the stationary sampling station and the other in the mobile platform. The concentration ratios of NO_2, CO, and BC at different downwind distances of the freeway were determined by normalizing the downwind data from mobile platform with their corresponding data collected from the stationary sampling station.

Results and discussion

1. Overview of the sampling campaign

Sampling sites		I-710		I-5	
		Non-noise barrier	Noise barrier	Non-noise barrier	Noise barrier
Samping dates and time		06/08/09 (2PM-5PM); 06/09/09 (3PM- 7PM)	06/02/09 (1PM - 4PM); 06/05/09 (1PM - 5PM)	07/06/09 (1PM - 4PM); 07/02/09 (12PM-4PM)	06/25/09 (1PM - 5PM); 06/29/09 (1PM - 5PM)
Total Vehicle Flow[1] (vehicles/hour)	Average	12170	12212	8460	8677
	Stdev	563	599	405	300
Truck Flow[1] (vehicles/hour)	Average	490	516	673	610
	Stdev	124	101	136	138
T (°C)	Average	21.7	23.7	28.4	25.0
	Stdev	0.9	2.3	1.0	4.5
RH (%)	Average	57.0	43.3	48.6	51.0
	Stdev	4.4	2.5	8.8	3.5
Wind speed (m/s)	Average	2.0	3.1	1.9	0.9
	Stdev	0.3	0.5	0.4	0.2
Wind Direction[2] (deg true N)	Average	233	229	225	225
	Stdev	16	10	42	25
CO (ppm)	Average	1.5	1.4	N/A	
	Stdev	0.4	0.1		
BC (ug/m3)	Average	11.0	11.6	10.6	9.5
	Stdev	6.3	1.4	4.2	1.5
NO2 (ppb)	Average	152.2	87.3	93.9	79.3
	Stdev	38.0	8.2	31.2	4.9
SMPS Number Concentration (#/cm^3)	Average	1.2e5	1.1e5	8.0e4	7.5e4
	Stdev	5.0e4	2.3e4	3.4e4	2.4e4
SMPS Mass Concentration (µg/m^3) (10-225nm)	Average	6.4	6.7	7.5	7.2
	Stdev	2.4	1.5	3.1	1.7

Table 1 Summary of the meteorological parameters and pollutant concentrations measured in the immediate proximity of freeways

Table 1 shows the summary of the meteorological conditions, traffic volumes and average freeway pollutants concentrations measured in the immediate proximity of the freeways during the sampling campaign. The average CO concentrations were 1.5±0.4 and 1.4±0.1 ppm at the two sites in the immediate proximity of I-170 freeway. The BC concentrations measured in the two sites at I-710 freeway were 11.0±6.3 and 11.6±1.4 μg/m^3, comparable to 10.6±4.2 and 9.5±1.5 μg/m^3 measured at I-5. The average particle number concentrations measured by SMPS (10-225 nm) at both I-710 sites (1.2±0.5e5 and 1.1±0.2e5 particles cm^{-3}) are higher than those at I-5 sites (8.0±3.4e4 and 7.5±2.4e4 particles cm^{-3}), due to higher traffic volume on I-710.

2. Evolution of particle size distributions downwind of freeway

Figures 2a and 2b show the average particle size distributions at various distances downwind of I-710 (20, 40, 80, 200 and 450m) and I-5 (20, 40, 90, 120, 400m) freeways without roadside noise barriers as measured by FMPS (6-523nm).The particle size distributions in the immediate proximity of both freeways displayed a mono-modal shape, with a distinct peak at approximately 10 nanometers (~ 10 nm), indicating new particle formation by nucleation of supersaturated semi-volatile organic vapors in the exhaust (Alam et al., 2003). As particles were transported away from the freeway, the particle size distributions changed markedly, with a dramatic decrease in the number concentrations. In Figure 2a, the particle number concentrations at ~10nm were 1.7e5, 1.3e5 and 7.9e4 particles cm^{-3}, at 20m, 40m, and 80m, respectively, which accounted for only 63%, 48%, and 29% of that measured in the immediate proximity of freeway. Several atmospheric processes may contribute to this significant change in size distribution and concentration, including particle evaporation and diffusion (Hinds, 1999) and semi-volatile vapor condensation (Zhang et al., 2004). At 200m, the particle size distribution displays a broad shoulder between 20-50nm, similar to that measured at 450m, a clear indication that the particle concentrations have reached background levels at 200m where the size distributions no longer change significantly with distance. On the other hand, Figure 2b shows the particle size distributions at various distances downwind of the I-5 freeway.

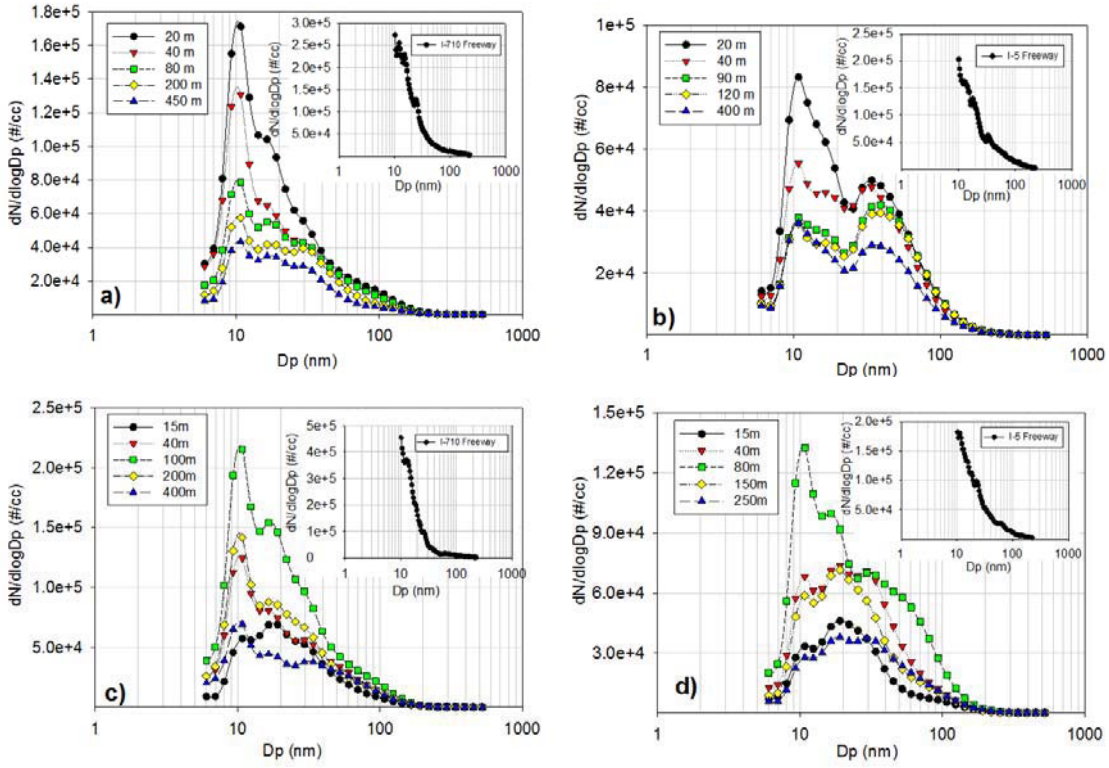

Figure 2: Particle size distributions measured at various distances downwind of freeway (a) I-710 without roadside barrier; (b) I-5 without roadside barrier; (c) I-710 with roadside barrier; (d) I-5 with roadside barrier.

In contrast to the observations near I-710, the particle size distributions displayed a consistent bimodal trend. At 20m, the modal concentration at ~10nm was 8.3e4 particles cm^{-3}, nearly half of that measured in the immediate proximity of the freeway, indicating rapid dilution and the associated particle evaporation and diffusional loss. As the particles are further transported away from the freeway, particle number concentrations gradually decrease at both modes, and the second mode is shifted from 34nm (at 20m) to about 40 nm (at 120m), indicating the possibility of small particle evaporation vapor condensation onto pre-existing particles (Shi et al., 1999; Zhang et al., 2004) as well as possible coagulation at different dilution conditions (Hinds, 1999; Zhu et al., 2002b). At 120 m, the nucleation mode particles at ~10nm reached a concentration of 3.6e4particles cm^{-3}, similar to the background level at 450 m; however, number concentration of particles at the larger size mode of 39 nm continued to drop after 120m until it reached background levels at 400m. Nucleation mode particles have a shorter residence time in the atmosphere, so they decay much faster and reach background levels at a shorter distance than larger particles (Raes et al., 2000). Figures 2c and 2d show the average particle size distributions at various distances downwind of the sections of I-710 (15, 40, 100, 200, 400 m) and I-5 (15, 40, 80, 150, 250m) freeways with roadside noise barriers. As shown in Figure 2c, at 15m downwind of I-710 freeway, particle size distributions displayed a mono-modal trend, with a slight peak at 10 nm and a broad shoulder at 16-19 nm. The 10 nm modal concentration is 5.7e4 particles cm^{-3}, i.e. significantly lower than that (1.7e5 particles cm^{-3}) measured at a similar downwind distance (20m) without roadside noise barriers, as shown in Figure 2a. With increasing downwind distance from freeways, particle number concentrations gradually increased and the nucleation mode at ~10nm became more pronounced, indicating the diminishing of the recirculation cavity and the increasing influence of freeway emissions. At 40 m, the modal concentration at ~10nm was 1.2e5 and 6.8e4 particles cm^{-3} for I-710 and I-5 freeway, respectively, about two times higher than those measured at 10-15m. As the particles are further transported away from the recirculation cavity, the elevated source follows its trajectory and the plume gradually reattaches to the ground (Bowker et al., 2007). The peak size distribution and number concentration were observed at 100 m and 80 m for the I-710 and I-5 freeway, respectively. At 200m downwind of I-710 with roadside barriers, particle size distribution still displays a sharp mono-modal shape, with peak concentrations of 1.4e5 particles cm^{-3} at 10nm, which is 2.5 times the background level measured at 200m for the I-710 site without roadside barrier. As the particles traveled further downwind at 400m near I-710, the particle size distribution and number concentration reached the background level as shown in Figure 2c. The much longer downwind distance (400m vs. 200m) needed to reach background levels indicates a larger impact zone from traffic emission sources for freeway sections featured with roadside noise barriers.

3. Co-pollutants concentrations at different downwind distances

Figure 3 shows the normalized concentrations of carbon monoxide (CO), nitrogen dioxide (NO2) and black carbon (BC) at distance downwind of the freeways and exponential decay curves were used to fit the decreasing ratios with increasing downwind distances. The best fitting decay equations and corresponding R^2 values are listed in Table 2. As shown in Figure 3a and 3b, all pollutants concentration ratios decreased exponentially with increasing downwind distances of the freeway. Within 150 m, all pollutants concentrations reach asymptotically background levels. Similar observations have been reported extensively in the recent literature (Zhu et al., 2002b; Baldauf et al., 2008; Clements et al., 2009). In contrast, the concentration ratios downwind of the freeway sections with roadside noise barriers displayed a different trend, as shown in Figure 3c and 3d. At downwind distance of 15m, the closest location downwind of the I-710, the pollutants concentration ratios were 0.36, 0.28 and 0.22 for CO, NO_2 and BC, respectively, comparable to the background levels measured at 400m (0.33, 0.26, and 0.28 for CO, NO_2 and BC, respectively). The low concentration ratios are consistent with the observations of particle number and mass concentrations, due to the strong turbulence that exists in the recirculation cavity of the roadside noise barrier (Finn et al., 2010). At 80-100m, where the concentrations have dropped to background levels for the non-barrier sites (Figure 3a), the pollutants displayed a peak ratio of 0.57, 0.59, and 0.67 for CO, NO_2, and BC, respectively, as shown in Figure 3c for the I-710 with barrier. The dramatic difference of the pollutant concentration profiles downwind of the freeway underscores the impact of roadside noise barrier on pollutant dispersion. As the pollutants are transported further away from freeways, their concentrations gradually decrease and reach background concentrations at 400 m and 250m for I-710 and I-5, respectively. The results suggest that the freeway roadside features, such as noise barriers,

should also be taken into consideration in assessing public exposure to ambient pollutants from traffic emissions in the community nearby busy freeways.

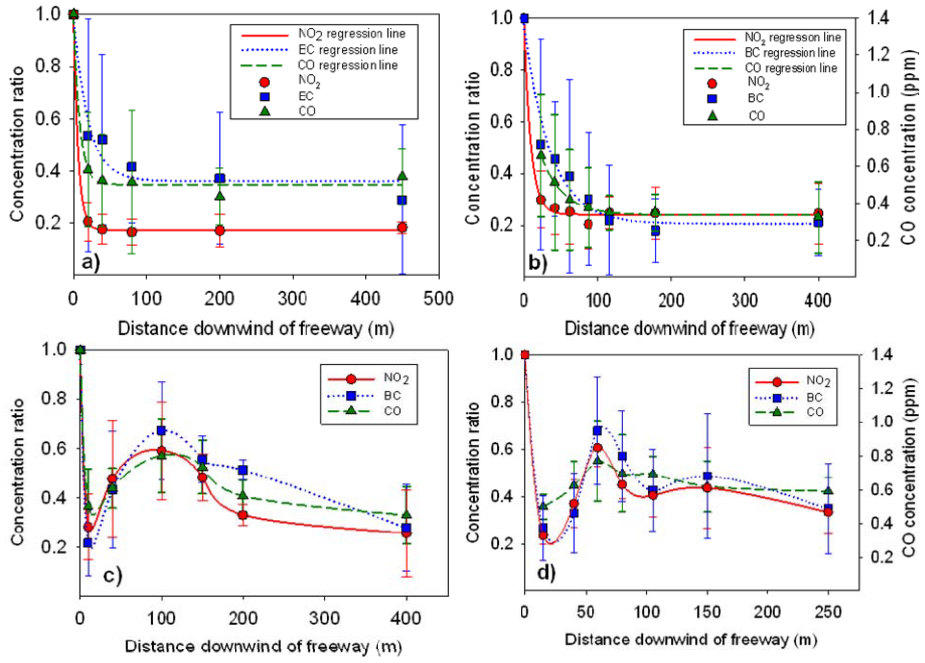

Figure 3 BC and pollutants normalized concentrations at different distance (a) I-710 no noise barrier (b) I-5 no noise barrier; (c) I-710 with noise barrier; (d) I-5 with noise barrier

	NO_2	BC	CO
I-710	$y=0.17+0.83\ e^{(-0.16\ x)}$ $R^2=0.99$	$y=0.36+0.63\ e^{(-0.05\ x)}$ $R^2=0.97$	$y=0.35+0.65\ e^{(-0.12x)}$ $R^2=0.99$
I-5	$y=0.24+0.76\ e^{(-0.11\ x);}$ $R^2=0.99$	$y=0.21+0.77\ e^{(-0.03\ x)}$ $R^2=0.98$	-

Table 2 Concentration decay curve equation and coefficients ("x" is the distance downwind of the freeway from the stationary sampling station; "y" is the normalized concentration ratio).

Summary and Conclusions

The present study investigated the evolution of particle size distributions and pollutants concentrations downwind of two major freeways (I-710 and I-5) sections in Southern California, both featured with and without roadside noise barriers. The results corroborate those of earlier studies by showing that the particle number and pollutants concentrations decay exponentially near freeways without the roadside noise barriers. The background pollutant concentrations are reached within 150 m downwind of freeway without roadside barriers. With the presence of roadside barrier, the dynamics of particle and co-pollutants dispersion change dramatically. A recirculation cavity is formed in the close vicinity downwind of the barrier, as observed at 15 m in the present study, resulting in a concentration deficit zone in the lee of the barrier. The particle size distributions and co-pollutants concentrations were comparable to background levels. With the increasing downwind distance, particles and gaseous co-pollutant concentrations increase and peak at 80-100m, where the plume of elevated traffic emissions sources reattaches to the ground. The background particle and co-pollutants concentrations were reached at distances of 250-450m, farther than the sites near non-barrier freeways. The much longer downwind distance needed to reach background levels indicates a larger impact zone of traffic emission sources near the freeways with roadside noise barriers. Our results suggest that freeway roadside features, such as noise barriers and plantation, should also be

taken into consideration in assessing population exposure to ambient particles and co-pollutants from traffic emissions.

Acknowledgements

We would like to acknowledge Dr. Katharine Moore for her significant contributions in the implementation of experiment. Also, we would like to thank Ali Attar, Kalam Cheung, for their assistance in the field and data work, and the support of University of Southern California Provost's Ph.D. fellowship. This study was funded by EPA under the STAR program through grant RD-8324-1301-0 and by California Air Resources Board through ARB Contact 05-317 to the University of Southern California.

References

Alam, A., J. P. Shi and R. M. Harrison, (2003). Observations of new particle formation in urban air. *Journal of Geophysical Research-Atmospheres* 108(D3): .

Baldauf, R., E. Thoma, M. Hays, R. Shores, J. Kinsey, B. Gullett, S. Kimbrough, V. Isakov, T. Long, R. Snow, A. Khlystov, J. Weinstein, F. L. Chen, R. Seila, D. Olson, I. Gilmour, S. H. Cho, N. Watkins, P. Rowley and J. Bang, (2008). Traffic and meteorological impacts on near-road air quality: Summary of methods and trends from the Raleigh near-road study. *Journal of the Air & Waste Management Association* 58(7): 865-878.

Bowker, G. E., R. Baldauf, V. Isakov, A. Khlystov and W. Petersen, (2007). The effects of roadside structures on the transport and dispersion of ultrafine particles from highways. *Atmospheric Environment* 41(37): 8128-8139.

Clements, A. L., Y. L. Jia, A. Denbleyker, E. McDonald-Buller, M. P. Fraser, D. T. Allen, D. R. Collins, E. Michel, J. Pudota, D. Sullivan and Y. F. Zhu, (2009). Air pollutant concentrations near three Texas roadways, part II: Chemical characterization and transformation of pollutants. *Atmospheric Environment* 43(30): 4523-4534.

Delfino, R. J., (2002). Epidemiologic evidence for asthma and exposure to air toxics: Linkages between occupational, indoor, and community air pollution research. *Environmental Health Perspectives* 110: 573-589.

Donaldson, K., D. Brown, A. Clouter, R. Duffin, W. MacNee, L. Renwick, L. Tran and V. Stone, (2002). The pulmonary toxicology of ultrafine particles. *Journal of Aerosol Medicine-Deposition Clearance and Effects in the Lung* 15(2): 213-220.

Finn, D., K. L. Clawson, R. G. Carter, J. D. Rich, R. M. Eckman, S. G. Perry, V. Isakov and D. K. Heist, (2010). Tracer studies to characterize the effects of roadside noise barriers on near-road pollutant dispersion under varying atmospheric stability conditions. *Atmospheric Environment* 44: 204-214.

Heist, D. K., S. G. Perry and L. A. Brixey, (2009). A wind tunnel study of the effect of roadway configurations on the dispersion of traffic-related pollution. *Atmospheric Environment* 43(32): 5101-5111.

Hinds, W. C., 1999. Aerosol technology : properties, behavior, and measurement of airborne particles (2nd Edition). New York, J. Wiley.

Holscher, N., R. Hoffer, H. J. Niemann, W. Brilon and E. Romberg, (1993). Wind-Tunnel Experiments on Microscale Dispersion of Exhausts from Motorways. *Science of the Total Environment* 134(1-3): 71-79.

Jacobson, M. Z., D. B. Kittelson and W. F. Watts, (2005). Enhanced coagulation due to evaporation and its effect on nanoparticle evolution. *Environmental Science & Technology* 39(24): 9486-9492.

McConnell, R., K. Berhane, L. Yao, M. Jerrett, F. Lurmann, F. Gilliland, N. Kunzli, J. Gauderman, E. Avol, D. Thomas and J. Peters, (2006). Traffic, susceptibility, and childhood asthma. *Environmental Health Perspectives* 114(5): 766-772.

Ning, Z. and C. Sioutas, (2010). Atmospheric Processes Influencing Aerosols Generated by Combustion and the Inference of Their Impact on Public Exposure: A Review. *Aerosol and Air Quality Research* 10(1): 43-58.

Raes, F., R. Van Dingenen, E. Vignati, J. Wilson, J. P. Putaud, J. H. Seinfeld and P. Adams, (2000). Formation and cycling of aerosols in the global troposphere. *Atmospheric Environment* 34(25): 4215-4240.

Sagai, M., H. B. Lim and T. Ichinose, (2000). Lung carcinogenesis by diesel exhaust particles and the carcinogenic mechanism via active oxygens. *Inhalation Toxicology* 12: 215-223.

Shi, J. P., A. A. Khan and R. M. Harrison, (1999). Measurements of ultrafine particle concentration and size distribution in the urban atmosphere. *Science of the Total Environment* 235(1-3): 51-64.

Xia, T., P. Korge, J. N. Weiss, N. Li, M. I. Venkatesen, C. Sioutas and A. Nel, (2004). Quinones and aromatic chemical compounds in particulate matter induce mitochondrial dysfunction: Implications for ultrafine particle toxicity. *Environmental Health Perspectives* 112(14): 1347-1358.

Zhang, K. M., A. S. Wexler, Y. F. Zhu, W. C. Hinds and C. Sioutas, (2004). Evolution of particle number distribution near roadways. Part II: the 'road-to-ambient' process. *Atmospheric Environment* 38(38): 6655-6665.

Zhu, Y. F., W. C. Hinds, S. Kim, S. Shen and C. Sioutas, (2002a). Study of ultrafine particles near a major highway with heavy-duty diesel traffic. *Atmospheric Environment* 36(27): 4323-4335.

Zhu, Y. F., W. C. Hinds, S. Kim and C. Sioutas, (2002b). Concentration and size distribution of ultrafine particles near a major highway. *Journal of the Air & Waste Management Association* 52(9): 1032-1042.

CO_2 Distribution and Transport in Urban Areas - A Task for High Resolution Urban CFD

*A. Gartmann*1, M.D. Müller1, R. Vogt1, E. Parlow1*

[1] Institute of Meteorology, Climatology and Remote Sensing, University of Basel, Klingelbergstrasse 27, CH-4056 Basel, Switzerland, Andres.Gartmann@unibas.ch

Summary

The pressure on urban areas due to a high population density leads to problematic air quality in urban areas, which in turn influences the quality of life and health of lot of people. It is a key issue to understand the mechanisms and properties of airborne pollution transport in urban areas to be able to assess the impact of the pollution and to improve the air quality. Flow patterns in urban areas are heterogeneous and complex due to the variable topology and the variety of influencing parameters, such as meteorological properties, as well as potential emission sources. Long-term measurement campaigns are time and cost intensive and the results are mostly point measurements with a small spatial significance (Grimmond et al., 2002; Li et al., 2006). CO2 is one of the important gaseous exhausts in cities and has various anthropogenic sources. Different measurement campaigns show strong variances in CO2 concentrations on the neighbourhood scale both in time and space in urban areas (Vogt et al., 2006; Weber and Weber, 2008). Computational Fluid Dynamics (CFD) methods provide the necessary means to simulate the spatial and temporal distribution of CO_2 in urban areas and to improve the understanding of the key air pollution transport mechanisms (Li et al., 2006). The validation of the CFD simulations should be based on existing high resolution measurements (Murena et al., 2009). For this reason, a parametrical study was carried out to define the numerical parameters, such as mesh resolution and boundary conditions, and the results compared to the data set of the *Basel Urban Boundary Layer Experiment* (BUBBLE) (Rotach et al., 2005). In a measurement campaign in the city of Basel, Switzerland, a strong dependency of the CO_2 concentration difference between two sides of a building on the approaching wind directions could be found (Vogt et al., 2006). The phenomenon was modelled using fully three dimensional *Reynolds-Averaged-Navier-Stokes* (RANS) computations around the city block and the reasons for the strong dependency could be identified with the three dimensional numerical results and the analysis of the flow patterns.

Parametrical Study

CFD calculations in urban areas are influenced by: (1) physical, e.g. meteorological conditions, as well as (2) numerical parameters, such as applied turbulence model, mesh resolution and element shapes, as well as boundary conditions. Based on the guidelines for CFD in urban areas (Franke et al., 2004; Yoshihide et al., 2008), a parameter study was conducted within a street canyon and compared to BUBBLE data, (Rotach et al., 2005). A measurement tower was located within a deep street canyon in a densely built-up area of the city of Basel. During the one year campaign, wind fields were measured on six levels using Sonic Anemometers with a time resolution of 20 Hz. For the parametrical case study, RANS models with both k-ε and RNG k- ε turbulence models were used with different meshing methods, resolution and boundary conditions for the mean velocity and the turbulent properties of the model: the turbulent kinetic energy (TKE) and dissipation.

Meshing: Four meshing methods were tested using cell size resolutions between 4 m and 0.8 m: A) plain tetrahedral B) tetrahedral with prism layers around walls C) tetrahedral with prism layers around walls and hexacore in the free stream regions D) Cartesian. The plain tetrahedral meshes show poor results near walls, as the changing distances of the tetrahedrons to the wall resulting in changing y+ value (distance to the wall), which is a key value for the necessary wall functions (ANSYS, 2006). The strongest correlation with the measured profiles was achieved using a minimum of three prism cell layers around walls. The additional hexacore in the free stream regions had a minor influence on the results and only small on the divergence properties of the computations. The advantage of tetrahedral meshes is their ability to represent the geometrical data more or less independently of the resolution. Although dependent on mesh resolution, using Cartesian meshes results in a simplification of the geometrical data. In direct comparison to the tetrahedral meshes, the Cartesian meshes render poor results for the wind

patterns within the street canyon. The best results were found using tetrahedral meshes with approximate 1 m resolution and minimum three prismatic layers around walls, as can be seen in Figure 1.

Stability / Equations: Due to the strong heterogeneity of the topology in urban areas, stability has a minor influence within the lower urban boundary layer (Lundquist and Chan, 2006). This allows the simplification of neglecting buoyancy and thermal effects, which is applicable for flow with dominant advection.

Turbulence Models: The widely applied k-ε-turbulence closure for RANS calculation has limitations, due to the overproduction of kinetic energy in regions with stagnation flow situations (Franke et al., 2004). The comparison of computations with the RNG k- ε approach showed no significant changes in the test cases.

Boundary conditions – Mean Velocity: The three most frequent wind directions and magnitudes at top of the tower (32 m above ground) within the one year for the measurement site were selected and used to define the boundary conditions of the test cases. For the logarithmic inlet profiles of the mean velocity equation (1) (Richards and Hoxey, 1993) was applied in combination with the friction velocity U_{fric} (2)

$$U(z) = \frac{U^*_{fric}}{\kappa} \cdot \ln\left(\frac{z + z_0}{z}\right) \qquad (1) \qquad U^*_{fric} = \frac{\kappa \cdot U_h}{\ln\left(\frac{h + z_0}{z}\right)} \qquad (2)$$

The subscript h denotes a reference altitude over ground for the mean velocity, z_0 is the roughness length and κ the von Karman constant. The comparison between simple uniform inlet conditions and logarithmic profiles are only apparent at street level, where higher magnitudes for the uniform inlet conditions can be found. Nevertheless, the logarithmic profiles are recommended.

Boundary conditions – TKE and dissipation: Two approaches were tested: (A) using a constant TKE value k, suggested by Richards and Hoxey (1993), where Cμ is the model constant for the k-ε model (Cμ = 0.09) and the dissipation ε equation (4).

$$k = \frac{U^{*2}_{fric}}{\sqrt{C_\mu}} \qquad (3) \qquad \varepsilon = \frac{U^{*2}_{fric}}{\kappa \cdot (z + z_0)} \qquad (4)$$

and (B) a simple relation between the turbulence intensity I and the mean velocity U equation (5) with a constant dissipation based on a length scale L_t, equation (6), (ANSYS, 2006).

$$k = \frac{3}{2} \cdot U^2(z) \cdot I^2(z) \qquad (5$$

$$\varepsilon = \frac{k^{3/2}}{L_t} \qquad (6)$$

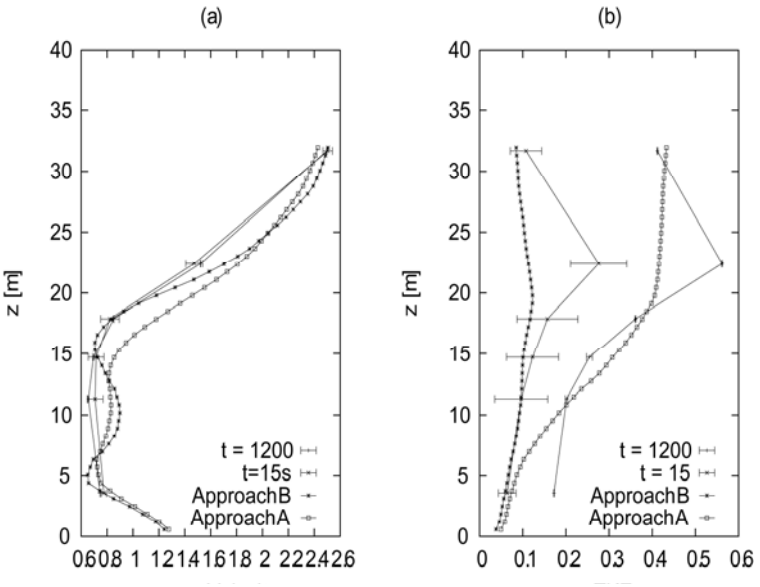

Figure 1: Comparison between modelled data (Approach A and B) and measured data (time average interval for Reynolds decomposition 1200s and 30s): (a) mean velocity, (b)

For the mean velocity, a good correlation between the modelled values and the measurements was found, as can be seen in Figure 1 (a). Using approach (A) leads to TKE profiles with higher TKE, than with approach (B). On roof level (approx. 20 m above ground) the significant

change is not recognisable with constant inlet values (A) and a minor correlation could be found in the mean velocity profiles, Figure 1 (b).

Comparison of modelled and measured TKE: Figure 2 (a) shows the correlation between the mean velocity and the TKE values for a time average interval of 1200s, (b) for 30s intervals.

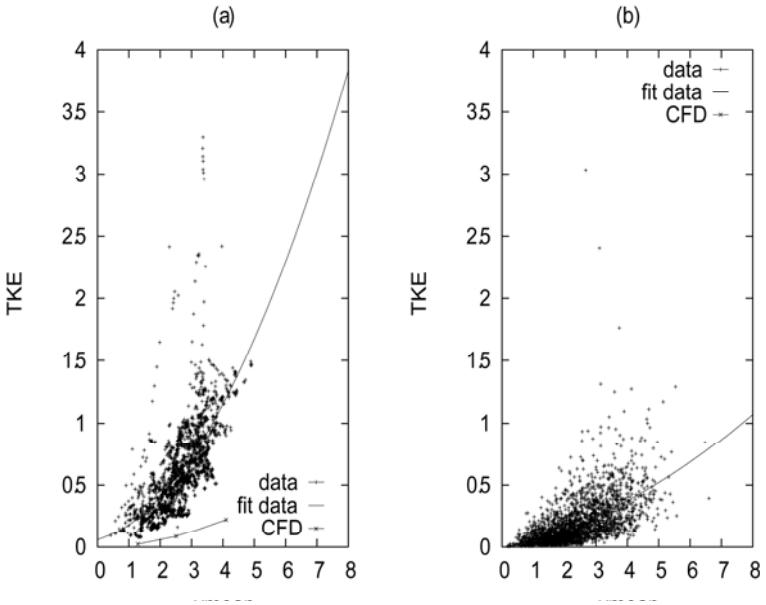

Figure 2: TKE magnitude top tower (32 m above ground and above roof level) data points (+), fit and CFD results, average time interval (a) 1200s, (b) 30s

There is a strong dependency between time average intervals used for the Reynolds decomposition and the TKE values in a street canyon. The mean velocity values are only weakly influenced by the time average intervals, as can be seen in Figure 1 (a). Figure 1 (b) shows the influence of the average time intervals on the TKE distribution within the street canyon and the mean deviation. Constant boundary conditions for TKE lead to comparable results for average time intervals of > 600s, but then to weaker correlations with mean velocity values, see Figure 1. The best results were found with the boundary conditions (B) for the TKE (I = 5%-10%) together with average time range of 15 - 60s for all studied conditions and over all levels in the street canyon. The true TKE values in cities are difficult to determine due to problems in models and observations: 1) observed TKE values are strongly dependent on averaging time scales, which can not be properly determined 2) turbulence models are semi-empiric not completely physically based.

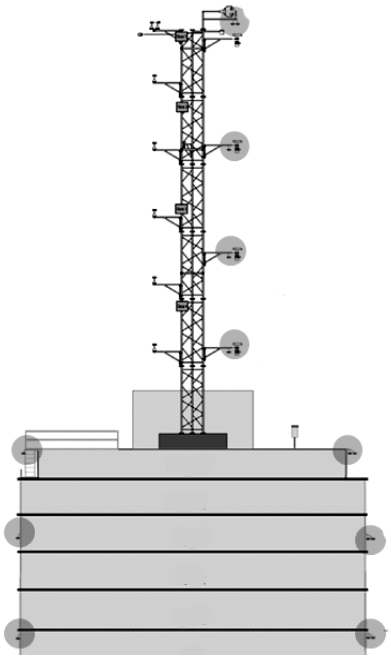

Figure 3: Cross section through the measurement setup. Circles indicate inlet points for the CO2 measurement (adapted from Eitel, 2006)

Conclusion: Using the discussed parameters for element shapes, mesh resolution and boundary conditions, comparable results between measured data and CFD models were found. For the comparison with experimental data, the average interval for the Reynolds decomposition must be chosen in dependency of the modelled situations and conditions.

CO_2 case study - Experimental Results

The measurements were carried out around a 20 m high building in Basel, Switzerland. In front of the building, a main street is located with NS orientation and heavy traffic. At the rear of the building a large backyard is surrounded by smaller buildings. Between September 2004 and August 2005, a closed-path gas analyzer (Li6262, LiCOR) and a multiplexer system with 10 inlets were used to measure the CO_2 concentration at 21, 15 and 4m above ground on each side and at 25, 28.5, 34 and 40m over the top of the building. The detailed

configuration can be seen in Figure 3. The temporal measurement resolution was 30min. The CO_2 profiles show large differences between the concentrations of street and backyard values, with a strong dependency on wind direction. During dominant West wind flow situations, the CO_2 concentration on the street side is much higher in comparison to the concentration profile on the rear side of the building. In cases of East wind, the differences between both sides of the building are negligible. There is practically no dependency on stability conditions and only a weak dependency on traffic frequency.

CO_2 case study - CFD Setup

The setup is an ideal case for using CFD methods to analyse the cause of the dependency on dominant wind directions. For this study the commercial CFD Code ANSYS CFX 11.0 was used, for the meshing of the *Computer Aided Design* (CAD) data the corresponding package ANSYS ICEM CFD. The dispersion of pollutants is dominated by micro scale wind patterns within the urban boundary layer, (Li et al., 2006). For the geometrical representation of the buildings, a high resolution CAD model was used (Figure 4). The buildings within 150 m of the measurement location were resolved in the CFD computations. As found by Yoshihide et al. (2006), and based on the results from the parametrical study, the tetrahedral element shapes with three prism layers around walls were used. The k-ε turbulence model was used for turbulence closure, and a coupled Eulerian model to simulate dispersion (ANSYS, 2006). As the method is based on multi-component flow, the simulated fluid was given the gaseous fluid properties of air, CO_2 and N_2 as a constraint. The influence of the CO_2 traffic source is modelled as a surface source term with constant fluxes from the streets. Due to the irregular traffic frequency on the main street compared to the smaller streets, different source strengths had to be defined. For the weekend situations (Table 1), the source strengths on the streets were reduced by half, due to lower traffic density. For the comparison and the analysis of the experimentally determined CO_2 characteristics, six conditions were modelled: three West and three East with advection dominated wind situations. As discussed above, the average time interval has a strong influence on the TKE distribution in urban areas. As the averaging interval of the concentration profiles was 30 min, the approach (A) (constant TKE) was used. Both for the TKE level, and the background CO_2 concentrations, the data from the top of the measurement tower was used (40m above ground).

Figure 4: CAD Model showing buildings, the location of the main street and a dominating wind direction (West wind)

CFD Results

The measured and the simulated CO_2 concentration differences were calculated based on equation (7), where c_i expresses the concentration at 4, 15 and 21 m above street level. The relative error is computed using equation (8).

$$\lambda_{meas/num} = \sum_{i=0}^{3} c_{front,i} - \sum_{i=0}^{3} c_{back,i} \qquad (7) \qquad \eta = \left| \frac{\lambda_{num} - \lambda_{meas}}{\lambda_{meas}} \right| \qquad (8)$$

Table 1 summarizes the measured CO_2 concentrations based on equation (7) and the simulated concentration profiles.

Table 1: Six modelled situations showing differences between days of the week and wind directions

Nr.	day	date	WA	λ_{meas}	λ_{num}	η
1	Sunday	03.07.05	East	5.4	6.7	0.24
2		17.07.05	West	32.2	66.7	1.07
3	Saturday	23.07.05	East	13.3	16.1	0.21
4		23.07.05	West	51.3	49.3	0.04
5	Weekday	28.07.05	East	6.9	4.5	0.34
6		21.07.05	West	52.7	66.9	0.27

As can be seen in Table 1, a good correlation could be found between the numerical results and the experimental data (relative error < 30%). The reason for the outlier on the Sunday West wind situation could not be definitely evaluated.

Discussion

Using the cross section of the concentration fields, the levels of the CO_2 layers could be visualized and analyzed based on the two dominating wind directions W and E (Figure 5).

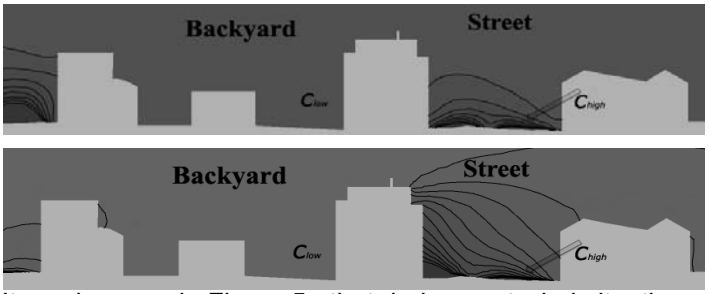

Figure 5 (a) CO_2 mass part for the multi-component fluid during E wind situation on Saturday. The contour lines are from CO_2 mass part 2E04 – 6.2E-04

(b) during W wind situation indicated high and low concentration levels

It can be seen in Figure 5a that during east wind situations, the CO_2 concentration is high in the lower levels of the street canyon, but low in the higher regions. During West wind situations (Figure 5b) the street canyon flow patterns created by the dominating wind result in elevated CO_2 concentrations on the left side of the street canyon to the top of the building. A three dimensional analysis of the flow pattern shows that the main flow direction is parallel to the building wall. During West wind situations the flow creates a large eddy (Figure 6b), rotating clockwise, in the street canyon. The large eddy transports the CO_2 emitted in the street to the measurement inlets. The separation line of the flow is defined by the altitude of the larger

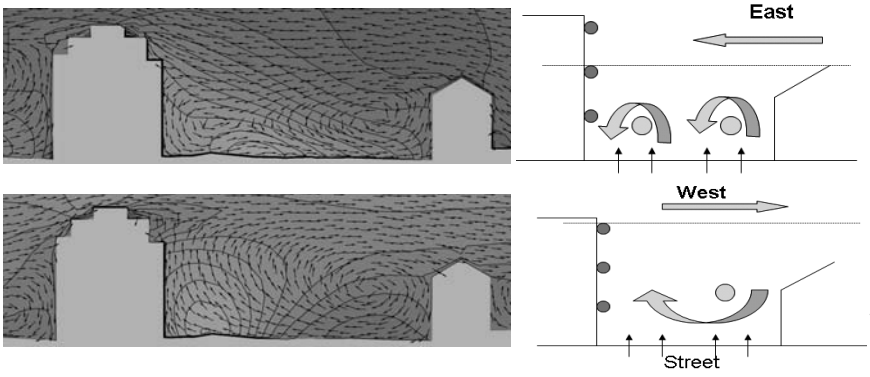

Figure 6: (a) Vector plot west wind with contour lines for velocity magnitude along main street. Contour line from -3.7 – 2 m s^-1

(b) during west and corresponding schematic flow patterns

building (left side of the street canyon). During East wind situations, Figures 5a and 6a, two smaller vortices are developed rotating counter-clockwise. The separation line between the two flow patterns is defined by the level of the lower building. The analysis of the three dimensional expansion of the flow shows a strong gradient in mean velocity along the main street (see magnitude contour in Figure 6b) and the described clockwise eddy during West wind situations. In this case, the CO_2 is gathered along the street and transported by the vertex towards the measurement inlet points. In case of East wind, the CO_2 from the street is captured by the flow patterns in the low levels above the street and transported by the counter-clockwise rotating eddies away from the measurement inlets.

Conclusion and outlook

The results from the parametric study are in accordance with the recommendations for CFD calculations in urban areas. The results show the ability of CFD to model complex flow patterns with highly heterogeneous geometry in very good agreement with high resolution temporal measurements in street canyons, where complex flow patterns can evolve. The validation with measurement data, especially for turbulent kinetic energy values, which are highly sensitive to average time, also lead to good results, except in the detached flow regions at roof level. There was found a strong dependency on the time average interval of the Reynolds decomposition between the TKE values in a street canyon. A recommendation for the choice of the boundary conditions is made dependent on the time intervals required. This case study demonstrates the usefulness of CFD methods in analyzing and simulating realistic flow patterns in urban areas based on a comparison with a dependent quantity, a proxy for air pollution, CO_2 concentration. In five of six cases the measured concentration differences along two profiles could be modelled and a clear explanation for the phenomenon provided based on process understanding derived from the CFD model. One of the larger problems dealing with urban CAD data, is their lack of volumetric consistency. Modern meshing methods, require CAD volume-consistent geometries. Volume consistency, in this context, signifies the inclusion of all simple surface information with no errors, such as holes or double surface entries. For larger spatial extensions, a Cartesian meshing method has to be applied, which can deal with CAD data lacking volume consistence, as most of the urban CAD models are (Krischok and Döllner, 2006).

References

ANSYS Inc. (2006), ANSYS CFX, Version 11.0, Reference Manual

Eitel J. (2006), CO_2-Flüsse und –Konzentrationen über einer urbanen Fläche im Jahreszyklus, *Diploma Thesis*, University of Basel

Franke J., C. Hirsch, A.G. Jensen, H.W. Krüs, M. Schatzmann, P.S. Westbury, S.D. Miles, J.A. Wisse, N.G. Wright (2004), Recommendations on the use of CFD in predicting pedestrian wind environment, *COST Action C14 "Impact of Wind and Storms on City Life and Built Environment" Working group 2 – CFD techniques*

Grimmond C.S.B., T.S. King, F.D. Cropley, D.J. Nowak, C. Souch (2002), Local-scale fluxes of carbon dioxide in urban environments: methodological challenges and results from Chicago, *Environmental Pollution*, 116, 243–254

Krischok D, J. Döllner (2006), Kopplung eines 3D-Stadtmodell-Visualisierungssystems mit einem Finite-Elemente-Simulationssystem, Universitaet Potsdam Mathematisch-Naturwissenschaftliche Fakultät Hasso-Plattner-Institut für Softwaresystemtechnik

Li X., C. Liu, D. Leung, K.E. Lam (2006), Recent progress in CFD modelling of wind field and pollutant transport in street canyons, *Atmospheric Environment*, 40, 5640–5658

Lundquist J.K., S.T. Chan (2006), Consequences of Urban Stability Conditions for Computational Fluid Dynamics Simulations of Urban Dispersion, *Journal of applied Meteorology and Climatology*, 46, 1080 - 1097

Murena F., G. Favale, S. Vardoulakis, E. Solazzo (2009), Modelling dispersion of traffic pollution in a deep street canyon: Application of CFD and operational models, *Atmospheric Environment*, 43, 2303–2311

Richards P.J., R.P. Hoxey (1993), Appropriate boundary conditions for computational wind engineering models using the k-E turbulence model, *Journal of Wind Engineering and Industrial Aerodynamics*, 46 & 47, 145-153

Rotach M.W., R. Vogt, C. Bernhofer, E. Batchvarova, A. Christen, A. Clappier., B. Feddersen, S.-E. Gryning, G. Martucci, H. Mayer, V. Mitev, T.R. Oke, E. Parlow, H. Richner, M. Roth, Y.A. Roulet, D. Ruffieux, J. Salmond, M. Schatzmann & J. Voogt (2005), BUBBLE - an Urban Boundary Layer Meteorology Project, *Theoretical and Applied Climatology*, 81 (3-4), 231-261

Vogt R., J. Eitel, E. Parlow (2006): 'Coupling of backyard to street canyon CO2 concentrations', *6th International Conference on Urban Climate ICUC-6*, Göteborg, Sweden, June 12-16

Weber S., K. Weber (2008), Coupling of urban street canyon and backyard particle concentrations, *Meteorologische Zeitschrift*, 17, 3, 251-261

Tominaga Y., A. Mochida, R. Yoshie, H. Kataoka, T. Nozu, M. Yoshikawa, T. Shirasawa (2008), AIJ guidelines for practical applications of CFD to pedestrian wind environment around buildings, *Journal of Wind Engineering and Industrial Aerodynamics*, 96, pp. 1749–1761

Modelling Estimation of the Contribution of the Road Transport to the Particulate Matter Concentration over Italy

A Balzarini[1], G. Pirovano[1], G.M. Riva[1], A.M. Toppetti[1]*

[1] ERSE, Via rubattino, 54, 20134 Milano, Italy, maurizio.riva@erse-web.it

Abstract

A modelling study, aiming at evaluating the contribution of road transport and other important sources to particulate matter concentration over Italy, has been performed by means of the CAMx chemical and transport model. CAMx implements the PSAT algorithm, an advanced source apportionment tool, able to discriminate the contribution of different sources both to the primary and secondary fraction of particulate matter concentration. The model has been applied for the whole 2005. CAMx has been driven by the WRF meteorological model; emissions have been derived from the Italian official inventory and the EMEP database and arranged in a model ready form by means of the SMOKE processor; finally, the initial and boundary conditions have been obtained by a CHIMERE model run at European scale. The PSAT tool has been applied to evaluate the contribution to PM concentrations of road transport, split into passengers cars and other vehicles, as well as other main emission sectors, such as energy production, and domestic heating. On a national basis, vehicle emissions yield the 5%-15% of the PM2.5 annual mean concentration and this contribution is highest near densely populated and highly industrialized urban areas. It represents a remarkable result because produced by a single emission category. Light/heavy duties and motorcycles have a similar pattern to vehicle emissions, showing highest contributions near the most polluted areas the major transit routes. Moreover, they could be very relevant in areas characterized by low circulation conditions such as the Po Valley, where their contribution range between 1 and 5 $\mu g/m^3$, corresponding to 10%-20% of the total PM2.5 concentration. Energy production proved to be less important, while biomass burning for domestic heating can provide significant contribution in residential areas.

Introduction

The presence of particulate matter in atmosphere derives from several transformation processes, involving emissions produced by most of the anthropogenic activities as well as some natural processes. Italy is often subject to high concentrations of particulate matter, mainly during winter time, when severe stagnant conditions lead to frequent exceedances of the air quality standards (Lonati et al., 2005; Vecchi et al., 2008). Urban areas usually suffer the worst conditions, driven by the contribution of transport and heating emissions (Bedogni et al., 2008). Particularly road transport contributes to the primary fraction (i.e. directly emitted) of particulate matter, but provides a relevant contribution to the secondary fraction (i.e. produced in the atmosphere) too, being among the most emitting sources of both organic and inorganic PM precursors.

By means of chemical transport models is possible to describe the main phenomena driving the pollution processes as well as to discriminate the role played by the different sources. To this aim, the CAMx model (ENVIRON, 2008) implements the PSAT algorithm (Wangstrom et al., 2008), an advanced source apportionment tool, able to discriminate the contribution of different sources both to the primary and secondary fraction of particulate matter concentration. Source apportionment for primary aerosols is relatively simple to simulate because their source-receptor relationships are essentially linear. Whereas for secondary aerosols, PSAT handles the non-linear chemical system using reactive tracers to apportion primary PM, secondary PM and gaseous precursors to secondary PM among different source categories and source regions. Such a numerical approach can represent a very powerful tool because it allows not only to detect the role played by the different emission sources, but also to investigate, source by source, the influence of non linearity on the evolution of the particulate matter concentration.

Modelling configuration

Air quality simulations have been performed by means of the CAMx (Comprehensive Air quality Model with eXtensions, version 4.51) chemical transport model (ENVIRON, 2008). CAMx is an

Eulerian model that allows to simulate emission, dispersion, chemical reaction and removal processes of pollutants in the troposphere. The model employed the Carbon Bond 05 (CB05) gas-phase mechanism (Yarwood et al., 2005), the RADM-AQ aqueous chemistry mechanism (Chang et al., 1987), the SOAP algorithm for the organic species partitioning (Strader et al., 1999) and the ISORROPIA scheme to simulate the thermodynamic equilibrium of the inorganic particles (Nenes et al., 1999).

The meteorological fields have been reconstructed by means of the Weather Research and Forecast modelling system (WRF version 3.1.1, Skamarock et al., 2008). The meteorological simulations have been conducted over two different domains: a master domain (3870x3555 km^2) with 45 km spatial resolution that covers the whole Europe and it is intended to capture synoptic features and general circulation patterns, and a nested domain (1350x1530 km^2) that covers the whole Italian Peninsula, with a grid step of 15 km. The domain's vertical grid contains 27 layers extending from the surface up to 20 km. Land use and topography dataset were interpolated from the USGS global cover, while temperature and soil moisture were provided from the ECMWF global analysis with 0.5 deg spatial resolution and temporal resolution of 6 hours (http://www.ecmwf.int). The WRF model reproduces all meteorological fields required by the chemical and transport model, such as wind direction and speed, temperature, pressure, relative humidity, cloud water content and rain.

Anthropogenic gridded emissions have been compiled with the Sparse Matrix Operator Kernel Emission processor (SMOKE version 2.6). This processor is able to convert emission inventory data into a model ready form (http://www.smoke-model.org/). The Italian input emission's dataset was derived from the Italian official inventory while the input emission values of neighbouring countries were taken from the EMEP database. Emission data for gaseous pollutants (SO_2, CO, NO_X, VOC, NH_3) and particulate matter (PM10 and PM2.5) have been estimated for all main anthropogenic emission sectors such as transport, heating, agriculture, energy production and industrial processes. Otherwise natural emissions were calculated with a sea salt processor based on Gong (Gong et al., 2002) and the biogenic emissions model (MEGAN version 2.03, Guenther et al., 2006). All emissions are injected in the CAMx model implemented with the PSAT algorithm. CAMx simulation covers the whole Italian domain (1290x1470 km^2), with horizontal resolution of 15 km and 13 growing levels in vertical direction. This domain is smaller than the meteorological one to reduce the effect of the meteorological border cells. Initial and boundary conditions were obtained by a CHIMERE model run at European scale (Bessagnet et al., 2004). The CAMx model has been applied for the whole 2005 and the PSAT algorithm has been set up in order to account for the contribution to gas and PM concentration of the following categories of the Italian emissions: passengers cars, other road transports, domestic heating from biomass burning, energy production.

Table 1: Contribution of different emission sources to the annual 2005 emission.

Contribution of different emission sources to the annual 2005 emission over Italy [Mg]						
PSAT categories	NH3	VOCs	SO_X	NO_X	PM10	PM2.5
Power plant	204	4101	112224	83715	3505	3330
residential heating - biomass	0	34932	0	4658	18141	17334
road transport - passenger cars	14980	175622	1306	226766	21844	17713
Other road transport	467	191206	1080	272195	26323	23129
other sources	395944	807006	2748561	470219	101339	74658
total	411595	1212868	2863170	1057554	171152	136164

Table 1 shows the contribution of the main emission sources to the total emission over Italy. Emissions from other road transports and passenger cars represent the major contribution to total NO_X, VOCs, PM10 and PM2.5 emissions. Anthropogenic NO_X emissions amount to 1057554 Mg, due to passenger cars (21.44%) and light/heavy duties and motorcycles (25.74%). NO_X emissions from power plants and residential heating account for 7.92% and 0.44%, respectively. PM10 emissions from other road transport yield the 15% of the total PM10 emissions, while passenger cars contribute to 13%. PM10 can also be emitted from residential heating (10.60%). A similar pattern can be shown in PM2.5 and VOCs emissions, while emissions from power plants add up to 112224 Mg of total SO_X. NH_3 derives from other sources, but passenger cars can generate a small fraction of the total emission (3.64%).

Results and comparison to observations

CAMx model calculates the average hourly concentration of different pollutions at each grid cell. Figure 1 illustrates the average yearly concentration of NO_X and PM2.5 over the Italian domain.

Nitrogen Oxides are emitted predominantly by fossil fuel combustion processes, as road transport, domestic heating and energy production. Therefore, these compounds can be considered as primary emitted and their concentrations are directly connected to their emissions distribution. The highest concentrations of Nitrogen Oxides have been found in Milan, Turin, Naples and Rome, showing annual average concentrations higher than 40 ppb. Such high concentrations are also observed near the major cities and along the Po Valley major transit route, where computed values range between 25 and 30 ppb. Conversely in the remaining rural areas CAMx simulated up to 15 ppb. The navigation provides an important contribution only in the South-West Mediterranean Sea, beyond Sicily region.

The spatial distribution of PM2.5 concentration is clearly connected with the different sources that influence its air concentration. Higher concentrations have been found near urbanised regions. Particularly, Po Valley area is densely populated, highly industrialized and known to have a relatively high level of anthropogenic pollution. In this site the concentration ranges from 20 to 30 $\mu g/m^3$, exceeding the threshold of 20 $\mu g/m^3$ fixed by the European Directive 2008/50/CE. Notably the area of Milan shows concentration values of 40 $\mu g/m^3$. However the concentrations decrease sharply as one moves from urban and suburban to rural site and then to remote sites. In different rural sites the simulated average concentration is quite similar and ranges between 10 to 18 $\mu g/m^3$. The striking difference between urban-suburban areas and remote locations evidences the dominant role of anthropogenic emissions to PM2.5 concentrations. The PM is produced mainly by vehicles and domestic heating emissions; as a result the average distribution of particular matter has a similar pattern to NO_X. But the difference in average concentration of PM2.5 between urban and rural sites is fewer than in the NO_X one. This is caused by the aerosol secondary fraction, usually stemming from gas-to-particle partitioning of semivolatile inorganic and organic vapours, which have a more homogeneous distribution over the Italian domain then primary species.

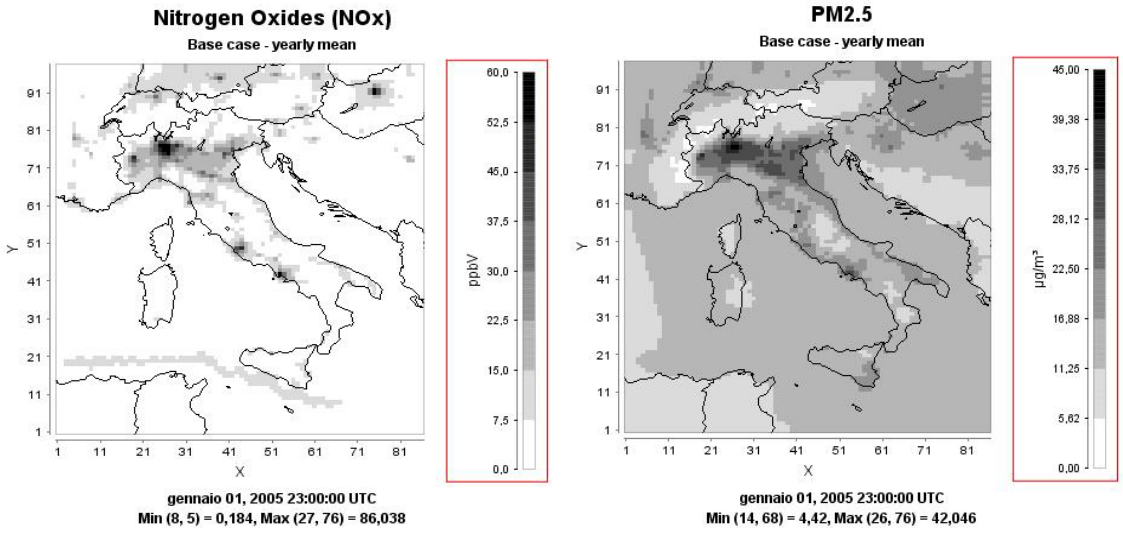

Figure 1: Yearly average concentration of NO_X and PM2.5.

CAMx results have been compared to a set of 215 measurements stations located in Italy. Stations have been grouped according their position and representativeness: RUBG= Rural background; SUBG= Suburban background; URBG=Urban background; TRAF= Traffic; INDS= Industrial. CAMx performances have been evaluated considering the yearly time series of observed and computed daily mean values at each station. Performance evaluation has been focused on NO_X, an important precursor of both O_3 and PM, and PM10, because not enough PM2.5 observations were available over Italy for 2005 (Table 2).

Observed NO_X (NO_X = NO+NO_2) concentrations show an increasing trend from rural (18.5 ppb) to traffic (59.4 ppb) stations, due to the influence of emission sources. CAMx performances are rather good only at rural stations (FB=0.05 and RMSE=16.66), confirming that adopted

resolution is adequate in reproducing the concentration of primary compounds only far from emission sources. Indeed, at suburban and urban background stations model puts in evidence a growing distance from the observed mean (FB=-0.16 and -0.39) and a reduced standard deviation. At urban stations the sigma ratio is around 0.4 with a corresponding RMSE of 34.4 ppb.

Observed PM10 values ranges from 27.0 and 39.3 $\mu g/m^3$. Background stations show increasing concentrations from rural to urban, the latter being even higher than traffic sites. CAMx reproduces rather well the different behaviour of the 5 groups, but underestimates the observed mean concentrations showing a FB ranging from 6% to 35% and a corresponding RMSE ranging between 16.7 and 27.7 $\mu g/m^3$. Standard deviation is underestimated too, varying between 0.65 and 0.8. Discrepancies between observed and computed values are in agreement with literature (De Meij et al., 2009; Lonati et al., 2010), confirming that the model reconstruction of PM10 over Italy is still a critical issue.

Table 2: Yearly values of the performance indicators averaged over each subset of stations. See text for details.

		Yearly mean		Standard Deviation(σ)		Corr	FB	RMSE
	Group	Observed	Computed	Observed	Computed			
NO_X	RUBG	18.5	16.1	14.8	8.0	0.45	0.05	16.66
	SUBG	30.7	19.2	22.4	9.5	0.47	-0.16	26.04
	URBG	43.2	26.4	33.6	12.4	0.55	-0.39	34.43
	TRAF	59.4	14.8	29.9	5.9	0.45	-1.09	51.23
	INDS	47.7	9.1	38.9	3.9	0.37	-0.84	57.57
PM10	RUBG	31.3	23.5	18.5	13.1	0.33	-0.06	22.80
	SUBG	35.2	25.1	21.1	12.8	0.28	-0.25	24.76
	URBG	39.3	26.6	23.4	15.3	0.34	-0.37	27.66
	TRAF	36.2	23.8	16.6	9.7	0.24	-0.34	22.35
	INDS	27.0	22.9	13.5	9.4	0.25	-0.11	16.75

Source apportionment analysis

The source apportionment analysis has been focused on four different emission groups: energy production, biomass burning from domestic heating, vehicles emissions and other road transports. In this section are presented only the contributions of passenger cars and other road transports to the total PM2.5 concentration (Figure 2).

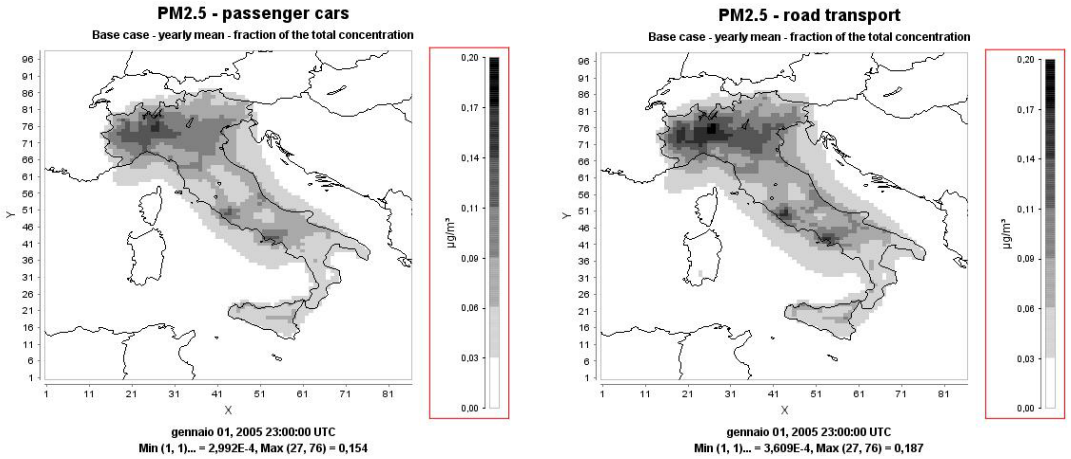

Figure 2: Contribution of passenger cars and other road transports to the total concentration of PM2.5. The data are represented as a fraction of the total concentration (We considered only PM2.5 total concentrations > 3 $\mu g/m^3$).

The highest contributions from vehicles have been observed in the most polluted cities, especially in Milan, Turin, Naples and Rome and along the main motorways. High levels of PM2.5 from vehicles are reported for the Po Valley region. Here the model simulates particulate matter concentrations higher than 3 $\mu g/m^3$, while in the remaining rural sites the passenger cars contribution achieves only 1 $\mu g/m^3$ (not shown). On a national basis vehicle emissions yield the 5%-15% of the annual mean concentration of PM2.5 and this contribution is highest near densely populated and highly industrialized urban areas. It represents a remarkable result because produced by a single emission category.

Light/heavy duties and motorcycles, namely other road transports, have a similar pattern to vehicle emissions. They exhibit the highest contributions near the most polluted areas, such as Milan, Rome and Naples and near the major transit routes. In particular, they could be very relevant in areas characterized by low circulation conditions such as the Po Valley, where a contribution ranging between 1-5 $\mu g/m^3$ (not shown) and corresponding to 10%-20% of the total PM2.5 concentration is observed.

The PSAT algorithm can be applied also to specific receptors. In this work we extended the evaluation at two different receptors, located near Milan and Rome urban cities. The figure below presents the contribution of the main sources to the total PM2.5 concentration for Rome and Milan. As discussed before, the passenger cars provide the highest contribution to total PM2.5 concentrations over Italy, while energy production proved to be less important. Particularly vehicle emissions yield the 14% of the total annual mean both in Milan and Rome as well as the light/heavy duties and motorcycles. The energy production contributes to 2% in Milan and 1% in Rome. The biomass burning for domestic heating provides up to 5% of the total concentration registered in Milan and to 10% in Rome. The PM2.5 concentrations are also influenced by long-range air mass transports, represented by boundary conditions (BC). This contribution can achieve the 20% of the total PM2.5 concentration in Rome.

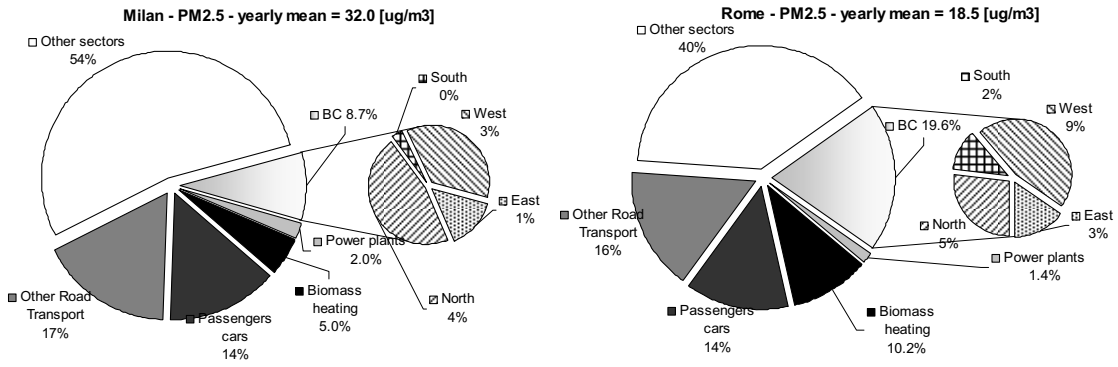

Figure 3: Contribution of different emission sources and boundary conditions to the total concentration of PM2.5.

Conclusions

The effect of the road transport and the energy production on the particulate matter concentration is computed for the Italian Peninsula. To this aim the CAMx model has been applied for the entire 2005. The meteorological fields have been processed using the WRF model and the anthropogenic emissions have been obtained by the SMOKE processor. Natural emissions of sea salts and biogenic VOCs have been estimated too. The CAMx model has been implemented invoking the embedded source apportionment algorithm (PSAT) able to discriminate the contribution of different sources to the primary and secondary PM concentrations.

The simulation results show the highest concentrations of PM2.5 and NO_X near the major polluted areas such as Milan, Turin, Naples and Rome. In these sites NO_X concentration can achieve 40 ppb, while PM2.5 generally exceeds the threshold of 20 $\mu g/m^3$ fixed by the European Directive 2008/50/CE. CAMx provided rather good performance in reproducing primary compounds concentrations only at rural sites, due to the grid resolution. PM10 concentrations are reproduced fairly well over the whole domain, though an underestimation of the yearly mean values ranging from 6% to 35% has been observed.

At the same time, PSAT algorithm has allowed to trace the contribution of transport, domestic heating by biomass burning and energy production to the annual concentration of PM2.5. On national basis vehicle emissions yield the 5-15% of the total PM2.5 emission and the other road transports contribute to 10-20% of the total PM2.5 emission. The source apportionment analysis has been focused also on Milan and Rome urban cities. Passenger cars yield the 14% of the annual PM2.5 mean both in Milan and Rome as well as the light/heavy duties and motorcycles. The contribution of power plants emissions is 2% in Milan and 1% in Rome. In this city an important role is played by long-range air mass transports, with values of 20% of the total PM2.5.

Acknowledgements

This work has been financed by the Research Fund for the Italian Electrical System under the Contract Agreement between ERSE and the Ministry of Economic Development - General Directorate for Energy and Mining Resources stipulated on July 29, 2009 in compliance with the Decree of March 19, 2009.

References

Bedogni M., S. Casadei and G. Pirovano (2008), Assessing the contribution of the main emission sources to particulate matter concentrations in the Milan area, *12th Int. Conf. on Harmonisation within Atmospheric Dispersion Modelling for Regulatory Purposes*, Cavtat, Croatia, 6-9 October 2008.

Bessagnet B., A. Hodzic, R. Vautard, M. Beekmann, S. Cheinet, C. Honore, C. Liousse and L. Rouil (2004), Aerosol modeling with CHIMERE-preliminary evaluation at the continental scale, *Atmospheric Environment*, 38, 2803-2817.

Chang J.S., R.A. Brost, I.S.A. Isaksen, S. Madronich, P. Middleton, W.R. Stockwell and C.J Walcek (1987), A Three-dimensional Eulerian Acid Deposition Model: Physical Concepts and Formulation, *Journal of Geophysical Research*, 92, 14,681-14,700.

De Meij A., A. Gzella, C. Cuvelier, P. Thunis, B. Bessagnet, J.F. Vinuesa, L. Menut, H.M. Kelder (2009), The impact of MM5 and WRF meteorology over complex terrain on CHIMERE model calculations, *Atmos. Chem. Phys*., 9, 6611–6632.

ENVIRON (2008), CAMx User's Guide.

Gong S.L., L.A. Barrie and M. Lazare (2002), Canadian Aerosol Module (CAM): A size-segregated simulation of atmospheric aerosol processes for climate and air quality models 2. Global sea-salt aerosol and its budgets, *Journal of Geophysical Research*, 107(D24), 4779.

Guenther A., T. Karl, P. Harley, C. Wiedinmyer, P.I. Palmer and C. Geron (2006), Estimates of global terrestrial isoprene emissions using MEGAN (Model of Emissions of Gases and Aerosols from Nature), *Atmospheric Chemistry and Physics*, 6, 3181–3210.

Lonati G., M. Giugliano, P. Butelli, L. Romele, and R. Tardivo (2005), Major chemical components of PM2.5 in Milan (Italy), *Atmospheric Environment*, 39, 1925–1934.

Lonati G., G. Pirovano, G.A. Sghirlanzoni, A. Zanoni (2010), Speciated fine particulate matter in Northern Italy: A whole year chemical and transport modelling reconstruction, *Atmospheric Research* 95, 496–514.

Nenes A, C. Pilinis and S.N. Pandis (1999), Continued Development and Testing of a New Thermodynamic Aerosol Module for Urban and Regional Air Quality Models, *Atmospheric Environment*, 33, 1553-1560.

Skamarock W.C., J.B. Klemp, J. Dudhia, D.O. Gill, D.M. Barker, M.G. Duda, X. Huang, W. Wang, J.G. Powers (2008), A Description of the Advanced Research WRF Version 3, *NCAR Technical Note* NCAR/TN-475+STR, Boulder, Colorado.

Strader R., F. Lurmann and S.N. Pandis (1999), Evaluation of secondary organic aerosol formation in winter, *Atmospheric Environment*, 33, 4849-4863.

Vecchi R., M. Chiari, A. D'Alessandro, P. Fermo, F. Lucarelli, F. Mazzei, S. Nava, A. Piazzalunga, P. Prati, F. Silvani, and G. Valli (2008), A mass closure and PMF source apportionment study on the sub-micron sized aerosol fraction at urban sites in Italy, *Atmospheric Environment*, 42, 2240-2253.

Wagstrom K.M., S.N. Pandis, G. Yarwood, G.M. Wilson and R.E. Morris (2008), Development and application of a computationally efficient particulate matter apportionment algorithm in a three-dimensional chemical transport model, *Atmospheric Environment*, 42, 5650– 5659.

Session 3: Electro and Hybrid Vehicles

Foresight of Electric transport in France: an opportunity with a smart demand side management

Eric Vidalenc – ADEME - Economy and Foresight Department - Economist

Abstract

In France, the new green policy "Grenelle de l'environnement" planned to build a lot of infrastructures of public transportation, particularly railways. Besides, some decisions are taken to promote electric vehicles.
Electric transports are seen as "ecologically friendly", actually, it can be a good mean of transportation for environment (energy consumption and CO2 emissions are only evaluated in this study). But, if electricity production is too much "carboned", it can be a worst solution in a *well*-to-*wheel analysis* compared to conventional fuel vehicles.
With a low carbon dioxide emission average factor for electricity production, France is seen as the good place to introduce electric vehicles. But mass penetration of electric transports can be more problematic in long term, especially if considering new electrical uses.
This paper demonstrates how the environmental performance can be really different according to the electricity production (considering average and marginal factor of emission, g CO2 / kWh), the load of battery and the level of consumption for light vehicles.
Smart grid and smart metering must bring solutions to these stakes in the next years.

Results

Electric transport offers many environmental advantages and can help to free the transport sector from its dependency on oil. In terms of greenhouse gas emissions, the large-scale development of electric transport, combined with measures for the reduction in transport demand, modal transfer and improvements to vehicle efficiency, is essential for putting private personal transport on the right track to achieve ambitious objectives such as "factor 4" in France and "factor 2" on a global scale. The following main points emerge from this analysis:

- The main development objectives announced must however be analyzed in terms of their impact on the electrical power generation system, in order to assess their consequences in respect of energy and CO_2 emissions. The development of electric rail transport is still an interesting alternative to other modes of transport for reducing CO_2 emissions. This form of transport should therefore be preferred.
- The integration of a million electric vehicles into the fleet by 2020 should not pose any major problems provided that an intelligent charging management system is implemented and consumption levels are low. This development must take place in conditions leading to lower emissions than those of internal combustion engine vehicles within this timeframe.
- In the longer term, over 4 million electric vehicles could be put in place, subject to compliance with Grenelle plan commitments, in view of the average non-carbon capacities envisaged at present (8 GW in power capacity and 60 GWh in daily energy), with however the difficulty of managing some peak days. For individuals, intelligent charging (slow charging during off-peak times) will have to be preferred, with boost charging used only in exceptional circumstances.
- Pricing for these two types of charge will therefore have to take this into account.

An extensive program to support the development of electric transport in France

The government provides strong and ongoing backing for the development of electric transport modes, as borne out by the Grenelle Environment Round Table and more particularly the Grenelle 1 Law passed in July 2009, the Electric Vehicle plan announced by the President of the Republic at the French Motor Show in autumn 2008, the national strategy for deployment of charging infrastructures for electric and hybrid vehicles launched in February 2009, together with the automobile sector recovery plan.

Within the framework of the Grenelle 1 law, France has set itself some ambitious targets for the development of electric transport. For rail transport, it is planned to practically double the proportion of rail freight, to double the network of high-speed lines and inter-city traffic, and to increase exclusive-way public transport infrastructures by 25% in the Paris region and six-fold in the provinces.

For electric vehicles, an extensive support program has been put in place by the French government. As part of this program, the automobile sector recovery plan, which is an extension of the "carbon-free" vehicle plan presented by the President of the Republic at the last Paris Motor Show, includes provision for loans of up to a total of €250 million to contribute to financing cooperative research and development programs on electric vehicles. One of the major objectives of the plan is to create a French sector specializing in batteries and drive trains.

In addition, in order to support the increasing numbers of industrial initiatives in these areas, the amount of the ADEME demonstration fund dedicated to electric and hybrid research projects has just been increased by €50 million. Eleven projects are already underway, with a grant amounting to €57 million. The national strategy for the deployment of charging infrastructures for electric and rechargeable hybrid vehicles aims for 100,000 vehicles by 2015 (objective divided between public fleets and those of leading French groups) in order to launch the market.

The development of electric transport should make it possible to reduce urban pollution and noise, and in some cases, CO_2 emissions from the transport sector. Although they have their own specific constraints, these transport modes should be judiciously incorporated into the supply-demand balance of the power generation system to achieve the best environmental footprint with as few as possible technical constraints for the power supply grid.

A development to be integrated into a relatively fixed power generation fleet in 2020

The assessments made within the framework of the 2009 French multi-year investment plan (Planification Pluriannuelle d'Investissements - PPI) provide indicators on changes to the power generation structure that will enable consumption requirements to be met by 2020. These estimates take into account implementation of the measures included in the Grenelle 1 law in terms of energy efficiency for the central Grenelle scenario. The deferred Grenelle scenario corresponds to the hypothesis of a delay in meeting the Grenelle objectives and in application of the planned measures *(diagram 1)*.

Diagram 1: Final electricity consumption in TWh in 2020 based on trend, Grenelle and deferred Grenelle scenarios

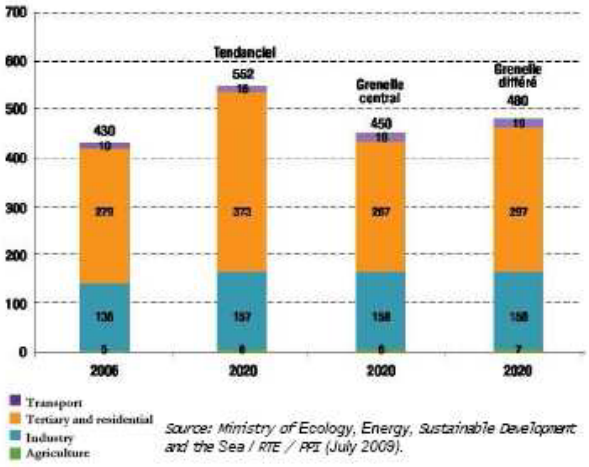

Source: Ministry of Ecology, Energy, Sustainable Development and the Sea / RTE / PPI (July 2009).

For instance, the modeling studies produced by MEEDDAT (sustainable development ministry) with the RTE (national power supply network) identify a predictable 18% decline in consumption in 2020 in relation to trends, representing savings of the equivalent of some 100 TWh. In parallel, power generated by renewable energies should increase by 30%, which would partly compensate for the planned decrease in generation by thermal resources[2], and therefore reduce CO_2 emissions resulting from power generation. These figures however only partly take account of the increased demand for power by

the transport sector (a million electric vehicles in 2020) and do not take any dynamic elements into account, particularly after 2020. It is unlikely that the power generation fleet will be systematically adapted to the demand. As far as electric vehicles are concerned, the constraint does not appear to concern the volume of this new demand, but rather the demand itself. The autonomy of electric vehicles could mean that certain users require frequent recharging facilities, especially in peak periods.

The development of rail transport: an undeniable comparative environmental advantage

In order to measure the real advantages, as well as the possible constraints on the electrical power system supply-demand balance that would be created by the development of electric transport, we estimated the maximum impact of such a development in terms of the quantity of electricity to be produced and the power to be mobilized. This estimate has been produced firstly for rail transport, and secondly for electric vehicles.

The consumption by rail transport (high-speed train, exclusive-way public transport, freight, inter-city travellers) has been assessed on the basis of the development assumptions included in the Grenelle 1 bill. The current energy consumption ratios have been projected in an identical manner (based on the underlying hypothesis of stability of occupation and load ratios and similar levels of rolling stock consumption). The additional electricity consumption is estimated at 12.5 TWh in 2020 *(cf. table 1)*.

The impact in terms of maximum demand may be significant and lead to consumption peaks in rail transport of over 3.5 GW, compared with 1.7 GW at present.
The CO2 content per kWh for rail transport is currently low, since it is considered at base load (40 g CO2/kWh).[3]
For 2020, it has been assumed (in order to avoid favouring rail modes) that additional capacity requirements could be covered by thermal resources, which would probably be the case for some of this peak period consumption, but in all probability not for most consumption, and particularly not for freight which circulates mainly at night using electricity at base load.

Table 1: Maximum power consumption forecasts for rail transport

Electricity consumption (TWh)							
Fret		TCSP*		LGV*		Autres circulations ferrées	
2007	2020/ 2030	2007	2020/ 2030	2007	2020/ 2030	2007	2020/ 2030
2	4,2	2,5	9	3,4	7	2,5	2,7

*Electricity consumption: operators and RTE for 2007, and ADEME for forecasts. * TCSP: exclusive-way public transport; LGV: high-speed line.*

Nevertheless, even assuming that all new consumption can be covered by combined cycle gas plants (i.e. the most highly developed power capacities at present) or coal-fired power plants (unlikely in respect of the projects in progress but possibly corresponding to peak demand or to power imports), the efficiency of rail transport in terms of CO_2 emissions per passenger-km or tonne-km, by comparison with other modes, remains undeniable (*cf. diagrams 2, 3, 4*).

Diagram 2: CO_2 emissions "well to wheel"[4] – Inter-city passenger transport

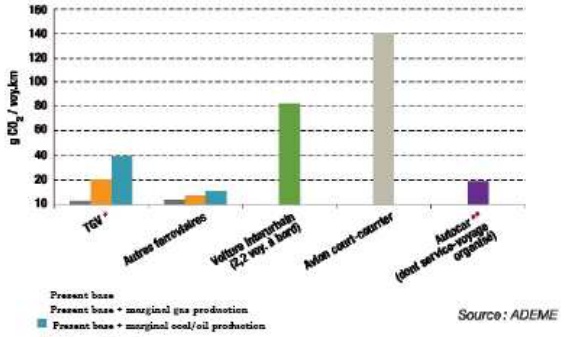

Source: ADEME

* High-speed train.
** Organized travel services have load factors close to 100%. Their efficiency is as good as or better than that of the TGV. By contrast, bus connection services are less efficient than electric rail modes.

Diagram 3: "Well to wheel" CO_2 emissions – Inter-urban and peri-urban passenger transport

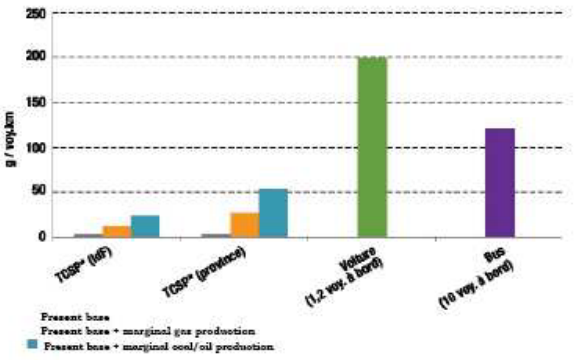

* TCSP: Exclusive-way public transport.

Source: ADEME

Diagram 4: "Well to wheel" CO_2 emissions – Freight transport

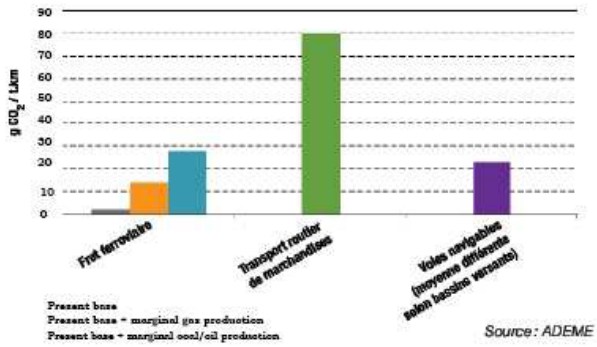

Source : ADEME

Rail modes therefore have considerable advantages in terms of energy consumption and CO_2 emissions. Their significant development should therefore be encouraged. However, attention must be paid in the longer term to ensuring that full advantage is taken of their intrinsic efficiency (reduced energy consumption, load factor, service, etc.) and to verifying that the increase in the power demand does not pose major problems for the power supply grid or cause any excessive deviation from the CO_2 content per kWh.

The electric vehicle: a environmental advantage in urban and peri-urban use

Electric motorization presents a certain environmental advantage for urban and peri-urban use:
- much better energy performance than the internal combustion engine: (maximum torque on start-up and possible recovery of energy on braking);
- silent operation;
- the absence of pollutant emissions at vehicle level.

The power capacity at base load available in 2020 allows for 4M vehicles

The conditions for generating the electricity required for traction of electric vehicles, and therefore their autonomy, are crucial points for ensuring a comparative advantage in terms of CO_2 emissions of electric vehicles over their internal combustion engine equivalents. In terms of CO_2 emissions, private electric vehicles, unlike rail modes, do not present a "well to wheel" overall footprint that is systematically to their advantage by comparison with other transport modes, especially in relation to internal combustion Effectively, while the electric vehicle is clearly more efficient than its internal combustion engine equivalent and therefore produces less CO_2 in use, it calls on an energy production-distribution chain that is less energy efficient: the CO_2 factor of power production is the significant element.
As soon as vehicles are charged using an electricity mix emitting average levels of CO2 (400 g/kWh, i.e. approximately the current European average, which should however be improved on if the energy and climate package objectives[5], among others, are met), the footprint of a vehicle in CO_2/km is close to that of a class B car at present (126 g CO_2/km "well to wheel" compared with 161 g/km for the average car sold in 2008)
(cf. diagram 5).

Diagram 5: CO2 emissions: "well to wheel" of electric and internal combustion engine vehicles

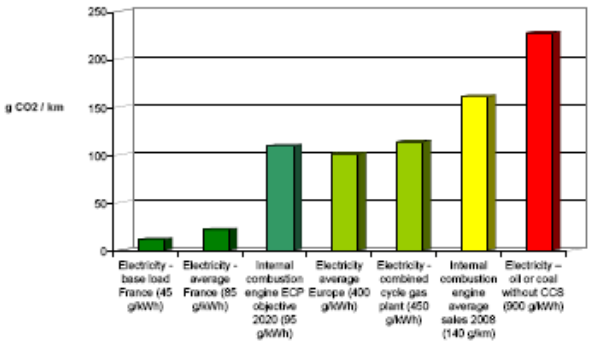

The mass development of electric and rechargeable hybrid vehicles therefore raises two important questions:
- What power capacity at base load (low CO_2 content) would be available at night, once other uses have been taken into account?
- When the constraints of vehicle fleet use call for charging outside these specific periods, how can a comparative advantage be maintained over internal combustion engine vehicles?

The current inertia of the French vehicle fleet (2 million new vehicles sold per year, out of over 30 million light vehicles) makes it seem unlikely that there will be a huge influx of electric vehicles by 2020. If the development options mentioned in the different studies under way materialize, we could envisage just over a million electric vehicles by 2020, or approximately 3% of the fleet.

To answer the question of night-time charging capacity, we assessed the average non-carbon power capacities available for recharging electric vehicles.
Although limited to a reduced time slot (midnight to 7 am), current capacities represent up to 4 GW (cf. *diagram 6)*. A fleet of a million vehicles (corresponding to a demand set up of 3 GW with slow night-time charging), already supported by considerable development of the sector, can be managed intelligently with the resources in place

Diagram 6: Non-carbon power generation - consumption in 2007

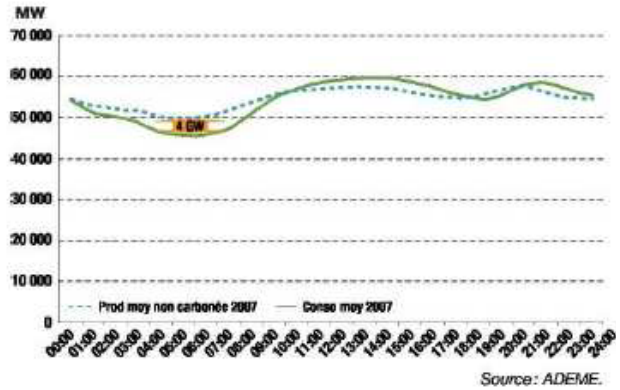

Source: ADEME.

In the medium term, in a dynamic approach covering the period until 2020, considering the overall consumption increase of renewable energies, mainly wind turbines (25 GW installed capacity), should give additional non-carbon capacities at night time of up to 8 GW[9]. Since the energy efficiency of rail transport is much higher than that of other modes, non-carbon power capacities are "allocated" in priority to these transport modes rather than to electric vehicles.

Nevertheless, the night-time non-carbon capacities, for an average day[10], would only be slightly affected by the development of rail transport (reduction from 9 GW to 8 GW available capacity, i.e. approximately 60 GWh – *cf. diagram 7*). The charging capacities, spread over the period between midnight and 7 am are equivalent to over 4 million vehicles, a fleet size that will not be reached by 2020 even in the most optimistic development scenarios**.** The CO_2 savings associated with 4 million vehicles, with the most favorable assumptions– non-carbon production mix – could be approximately 6 Mt per annum.

Diagram 7: Non-carbon power generation - forecast consumption by 2020

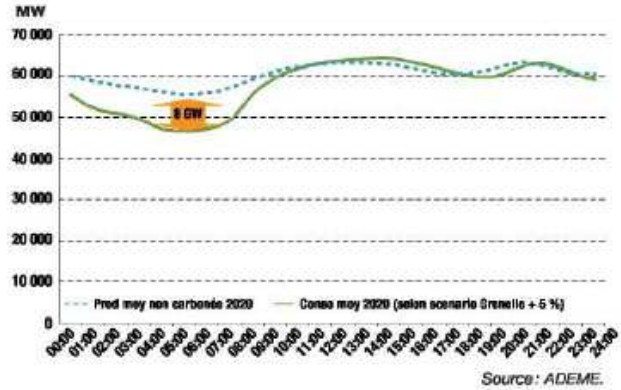

Source: ADEME.

Systematic intelligent charging and low consumption levels are key factors for electric vehicles

"Flash" charging sessions lasting ten minutes or more must be avoided, since they cause a high demand for capacity, very probably during the day, creating a considerable additional constraint on the power supply grid.
For instance, if 50,000 electric vehicles were to simultaneously require a boost charge (40 kW capacities), the equivalent of 2 GW would be on demand, with a reactivity that could only be achieved by fossil fuel power plants (or hydraulic power plants, whose capacities are already fully used at present).
In periods of very cold weather, these consumption peaks would make management of the supply grid even more complex. This would result in significant CO_2 emissions, either resulting from fossil fuel power plant production on French territory, or calling on imported carbon power.
Secondly, if electric vehicles are to be developed, this will only be possible *at least* on a European scale (where the production mix is significantly higher-carbon at approximately 400 g CO2/kWh).
It is therefore essential to take action by increasing the intrinsic performance of electric vehicles, by reaching the lowest possible consumption levels (cf. Focus inset) and by acquiring the resources for intelligent management

of electric vehicle charging. In view of its energy and environmental performance, urban and inter-urban public transport by rail must be given priority in terms of transport development.

ADEME has made two recommendations on the national strategy for deployment of charging infrastructures
for electric and rechargeable hybrid vehicles launched in February 2009, and in particular the "Economic models" sub-group.
Firstly on a European scale with
the electric mix planned for 2020 (approximately 400 g CO_2/kWh), the **performance thresholds**
of electric vehicles must be complied with in order to ensure that these vehicles do not emit more greenhouse gases than internal combustion vehicles. With a load efficiency of 60%, the vehicle must not consume over 0.16 kWh/km; for 95% efficiency (advanced lithium-ion battery), the vehicle
can consume up to 0.25 kWh/km (consumption level of existing vehicles).
If production methods based on carbon without capture and storage (CCS) were to develop significantly, particularly in response to the new requirements of electric vehicles, the performance thresholds should then be
0.07 kWh/km (at load efficiency 60%) and 0.10 kWh/km (at load efficiency 95%). These more demanding thresholds may therefore be considered as "no regrets" thresholds, in which the electric vehicle is still an improvement on the internal combustion engine vehicle in terms of CO_2 emissions. In addition, going beyond questions of CO_2, energy efficiency makes it possible to reduce the total cost of ownership (TCO) of a vehicle, the cost per tonne of CO_2, charging infrastructure requirements and financing requirements as well as externalities, and therefore be of interest to the different players. Then, in order to avoid placing additional constraints on the power grid , intelligent night-time charging systems with adapted pricing must be preferred.

Then, taking into account the CO2 content/kWh constraints, light electric vehicles, initially via captive fleets and shared car services, could play an important role. For these two uses, it will be no easy matter to organize night-time charging, particularly in the case of shared car services. A battery exchange system could be one solution, but the level of consumption of electric vehicles must be kept low in order to maintain a comparative advantage whatever the charging period for these restricted uses. Small urban vehicles will really become the best choice in urban area.

For private individuals, the third use of electric vehicles requiring development, which must become the norm, is intelligent night-time charging, with boost charging a method to be used only in exceptional circumstances. In addition to the charging infrastructure which will have to be adapted to meet these requirements, pricing for the different types of charge will therefore have to take this into account. The eleven research projects on carbon-free vehicles supported by the ADEME demonstration fund also contribute to these studies.

Electric vehicle and plug-in hybrid energy efficiency and life cycle emissions

H. Helms, M. Pehnt, U. Lambrecht and A. Liebich

Ifeu – Institut für Energie- und Umweltforschung, Wilckensstr. 3, D-69120 Heidelberg (www.ifeu.de)

Introduction

Mobility is an important basis for many economic and private activities and thus a crucial part of our life. In many industrialised countries, the demand for mobility is mostly covered by road traffic. Modern vehicles and a well developed network of roads allow for a high degree of individual mobility. However, this mobility also leads to substantial environmental problems: In Germany, for instance, transport is responsible for over 20% of the energy consumption and CO_2 emissions. The majority of these emissions are due to road traffic, which in turn is dominated by passenger transport (see Figure 1). Though CO_2 emissions from road traffic and especially passenger cars are slightly decreasing in Germany since about 2000, this decrease is still limited. The associated consumption of fossil resources by road traffic not only contributes significantly to climate relevant CO_2 emissions, but also faces limited resources and leads to political dependencies.

Additionally, road traffic is a cause of noise and emits various pollutants with direct negative effects on human health. For pollutants such as carbon monoxide (CO) and hydro carbons (HC), already substantial improvements have been achieved in the past. In respect to other substances such as diesel particles and nitrogen oxides, road traffic - despite a considerable emission decrease in recent years (see Figure 1) - still makes a relevant contribution to current exceedances of air quality limit values for PM10 and NO_2.

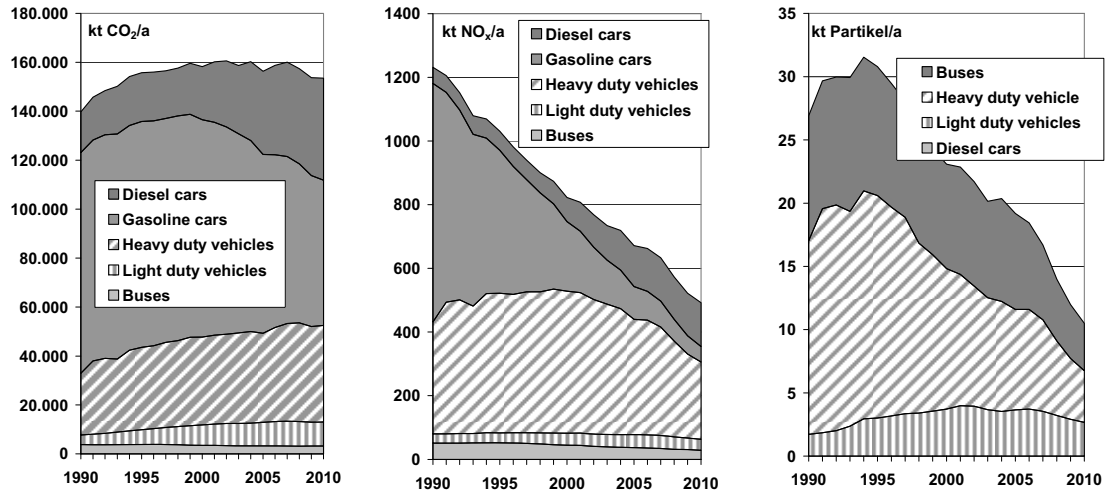

Figure 1: Direct CO_2, NOx and particle emissions of road traffic in Germany (Source : TREMOD (Knörr, 2010))

This calls for an improvement of the environmental profile of road traffic. For vehicles with conventional combustion engines, a further tightening of the emission legislation as well as new limit values for carbon dioxide are already on their way on a European level. These strategies, however, can only partly solve the environmental problems of transport. Another potential pillar of an 'environmental strategy for road traffic' is electric mobility: Electric vehicles have quiet engines, are locally emission free and allow for the use of many (also renewable) energy sources in road traffic - which so far could not be used.

Electric mobility has always been the first choice whereever electricity has been available: For long distances in trains, for short distances in trams or subways and even within buildings in elevators and escalators. In Germany, electric local and long distance trains have consumed about 9 TWh of electricity in 2007 - 1.5% of the gross electricity consumption. For road traffic,

however, there has been the problem of mobile storage of electricity. Batteries have been heavy and had a low energy density, electric vehicles thus had a very short driving range. Now, new technological developments, triggered also by consumer electronics such as laptops and mobile phones, have lead to a considerable improvement of the performance of batteries. Electric vehicles are therefore considered as a serious alternative for conventional vehicles.

In order to improve the environmental profile of road traffic, advantages and disadvantages of electric vehicles have to be identified and addressed at an early stage. This calls for a thorough environmental assessment of electric vehicles, which covers the full life cycle, from vehicle production via vehicle use and electricity generation to disposal and/or recycling. A previous screening LCA by IFEU (Pehnt et al., 2009) showed that the highest contribution to life-cycle emissions comes from the use phase. These emissions are mainly influenced by the energy efficiency of electric vehicles and the electricity generation. Both aspects are now therefore analysed in more detail in this paper.

First, a realistic assessment of electric vehicle energy consumption is presented, which is based on realistic speed profiles and also considers auxiliary consumers. Afterwards, electricity generation for charging of electric vehicles is analysed, taking into account that the mix of power plants for charging is a function of economic framework conditions in the energy sector. Finally, life cycle results are presented and discussed.

The results published in this paper are based on various IFEU research activities, including the environmental assessment of various electric mobility pilot projects, and will be further refined in the future. In particular, a more detailed balance of the production process, empirical data on electricity consumption patterns, as well as an energy economic modelling of the interactions with the electricity sector will be included.

Electric vehicle energy efficiency

The specific energy consumption of electric vehicles is an important parameter in the assessment of life-cycle emissions. Energy efficiency not only influences the absolute energy consumption vehicles and thus the life cycle balance. Energy efficiency also has a considerable impact on the electric driving range or the required battery capacity which in turn influences vehicle weight and costs. Furthermore, conventional vehicles are expected to improve their environmental performance in the future and electric vehicles will need to further enhance their energy efficiency to keep up with this development. This calls for a thorough analysis of the energy consumption of electric vehicles under realistic conditions.

So far, only few measured data are available of which some are only measured in standardised cycles (e.g. NEDC) and thus do not represent the energy consumption in realistic use profiles or take into account auxiliary consumers such air conditioning or heating. Furthermore, only few electric vehicles are yet available and test vehicles or prototypes do not reflect vehicles in mass production. Therefore a consistent modelling of the energy consumption of electric vehicles is undertaken, which allows for the variation of vehicle parameters and the consideration of different framework conditions. This approach – in contrast to the direct use of measurement data from different vehicles and drivers – also allows for good comparability of results, which is of special significance in a comparative LCA. Also scenarios for the further development of electric vehicles can be defined.

Methodology

The calculation of the energy demand for vehicle propulsion is based on a second-by-second speed profile. The physical energy demand at the wheel can be calculated for such a speed profile with defined vehicle parameters such as vehicle weight, front area as well as rolling resistance and air drag coefficients. However, despite the high energy efficiency of electric vehicles compared to conventional combustion engines, further energy losses in the drive train and at the engine have to be taken into account.

The “Tank-to-Wheel-Efficiency” (TtW-efficiency) is of special importance in a comparative analysis of the energy consumption of vehicles with different engine concepts. The TtW-efficiency is largely constant for electric vehicles, while considerable differences occur for combustion engines, depending on the speed profile. In urban areas, combustion engines often operate in partial load and thus with low efficiency. The fuel consumption of conventional

vehicles is therefore mostly higher in urban areas compared to extra urban roads and motorways.

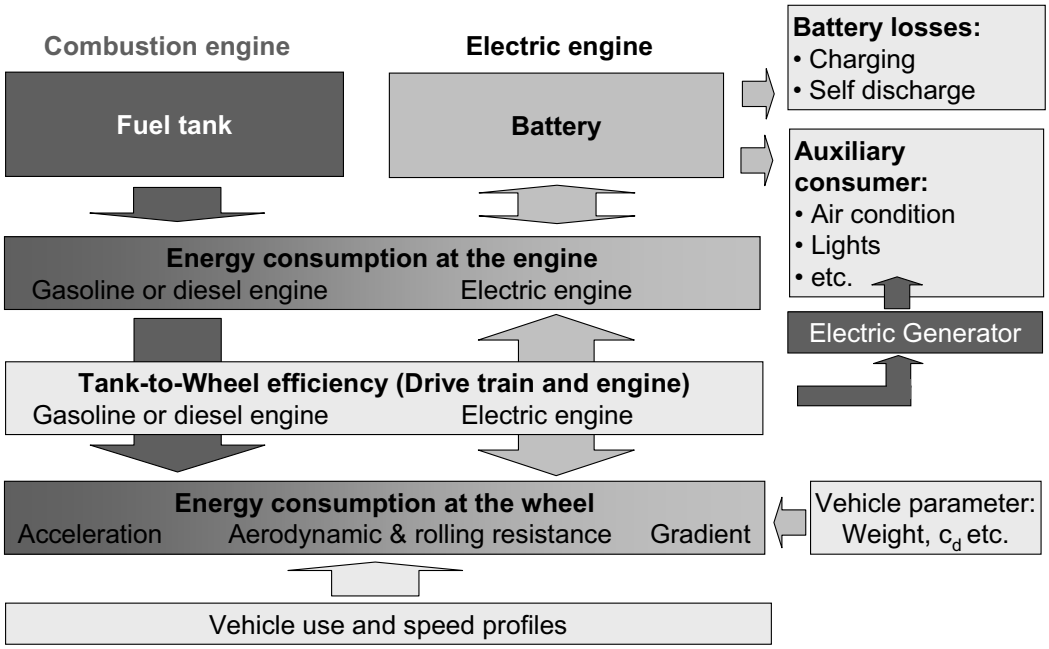

Figure 2: Energy flow in differentdrive train concepts

Battery Electric Vehicles (BEVs)

The vehicle parameters and TtW-efficiencies (Table), which are used for the electric vehicles in this paper, are largely based on the available literature and expert judgment. They are defined in order to represent an average compact car (e.g. Volkswagen Golf). Vehicle weights are based on (Öko-Institut, 2009), but rounded to a lower value to represent state of the art vehicles. Accordingly, a Plug-In Vehicle with 50 km electric range is assumed with a weight of 1500 kg and the full electric vehicle with a weight of 1600 kg. Similarly, front area and air drag coefficient are based on (Hausberger et al., 2009). The efficiencies of the electric energy chain are based on the available literature (Engel, 2007; Mazza and Hammerschlag, 2005; Weiss et al., 2000; Raskin and Shah, 2006; Kendall, 2008; Gielen and Simbolotti, 2005; Edwards et al., 2006; Garche, 2007).

The recuperation of braking power is calculated based on the energy loss in phases of negative acceleration, from which the natural breaking by rolling resistance and air drag have been subtracted. Additionally, it is assumed that 30% (see e.g. Guttenberg, 2004) of the kinetic energy is lost due to mechanical breaking. Afterwards, the same individual efficiencies as for propulsion (Table) are applied to the energy flow from the wheel to the battery and back to the wheel.

Table 1: Vehicle parameters and energy efficiency

Vehicle parameter	**Weight**	**Front area**	**Air drag coefficient**	**Rolling resistance coefficient**
PHEV-50	1500kg	$2m^2$	0,28	0,01
BEV	1600kg			
Efficiencies	**Charging**	**Battery**	**Engine**	**Drive Train**
Combined: 73%	90%	95%	90%	95%

Finally, also an assessment of the energy consumption of auxiliary consumers has been undertaken. It is based on a compilation of the average power demand of the common consumers (mainly Soltic, 2001; Wallentowitz and Reif, 2006 and Fabis, 2006) and estimates on their average use in summer and winter. The analysis resulted in an annual average power demand of about 1'000 Watts. In contrast to vehicles with combustion engines, electric vehicles

will require additional heating in winter and partially also cooling for the batteries. In many cases, the use pattern of different consumers could only be estimated since no hard data have been available. The resulting power demand of 1'000 Watts should be regarded as an estimate for the annual average; temporarily, a much higher power demand may occur e.g. on hot summer days or cold winter days, when a lot of cooling or heating is required.

In order to consider a realistic driving profile, the traffic situations of the 'Handbook Emission Factors' (HBEFA) (INFRAS, 2010) are used. The different traffic situations are weighted according to the average traffic in Germany in urban areas, extra-urban areas and on motorways according to TREMOD (Knörr, 2010). 28 different traffic situations are taken into account, which have been recorded as part of extensive measurement programmes in real world traffic. The speed profiles of four selected driving cycles are presented in Figure 3. Using the driving cycles of the 'Handbook Emission Factors', the calculated values can also be compared to and complemented by the emission factors for conventional vehicles in TREMOD and HBEFA. This allows for the use of fuel consumption and pollutant emission factors from TREMOD and HBEFA for the reference vehicles.

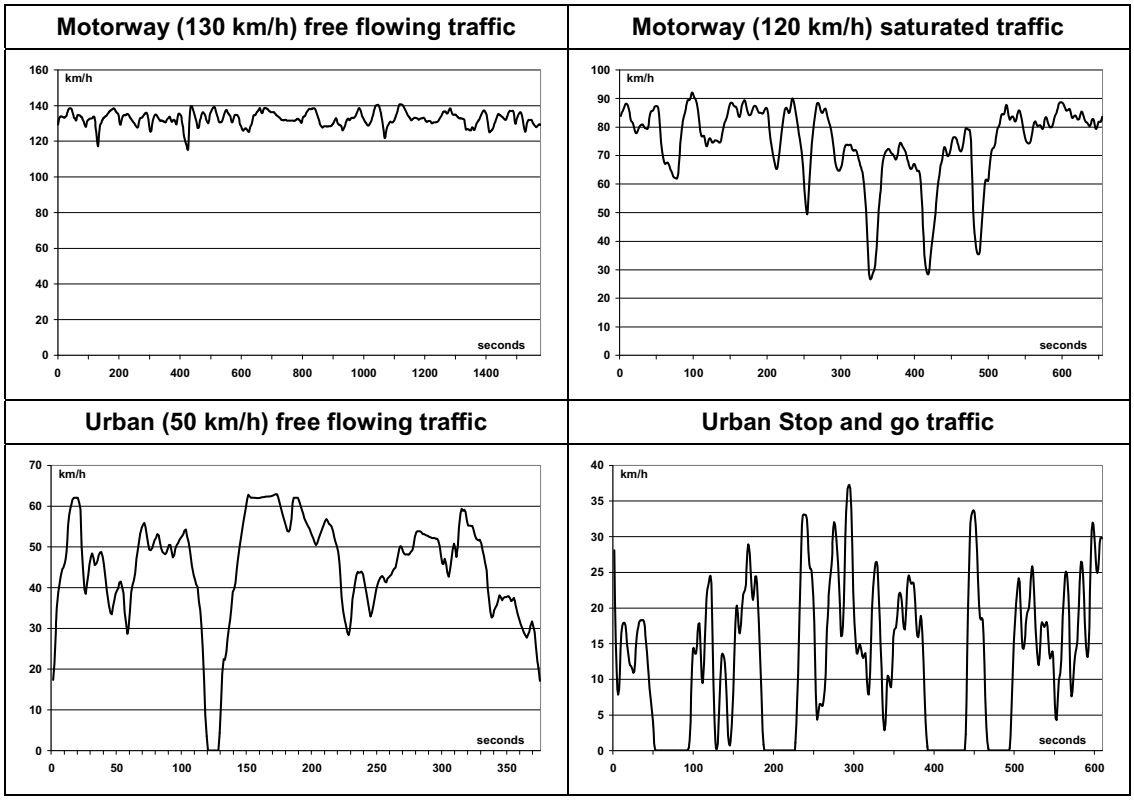

Figure 3: Speed profiles of selected traffic situations of the Handbook Emission Factors

Plug-In Hybrid Vehicles (PHEVs)

Due to the comparatively low energy density of batteries and thus limited driving range of 'Battery Electric Vehicles' (BEVs), also a 'Plug-in Hybrid Electric Vehicle' (PHEV) will be analysed. These vehicles combine the advantages of electric vehicles (high energy efficiency, regenerative breaking, charging from the grid) with the advantages of conventional vehicles, mainly the large driving range and possibility for fast refuelling. PHEVs are therefore regarded as an important short- to mid-term concept to open up the market for BEVs. PHEVs can be further distinguished by their electric driving range, which requires different battery capacities. In this paper, a PHEV -50 is considered which has a 50 km electric driving range.

Since PHEVs have two different engines they can either be operated in a dedicated mode (using only either the electric or the combustion engine) or a blended mode (using both engines at the same time either for reasons of power demand or energy efficiency). Not many data or information are yet available on the preferred driving mode for PHEVs as well as fuel consumption and pollutant emissions in blended mode. Different fleet tests are currently conducted which will allow a further insight into this complex topic. At this time, a pragmatic

approach for an environmental assessment of plug-in hybrids is the assumption of dedicated operation only.

The 50 km electric driving range will cover most of the everyday trips which are assumed to be mostly in an urban area. The combustion engine in turn is assumed to be mainly used for longer distances, especially on motorways. Hence, the share of electric operation is assumed to be 90% in urban areas, 50% in extra urban areas and 10% on motorways. The differentiation of the electric mileage by road category is important due to the different efficiencies of electric and combustion engines in these traffic situations. Other vehicle parameters - except for the weight (see Table) - are assumed to be the same as for the BEV.

Electricity consumption in different traffic situations

Differentiated results for the specific electricity consumption of the defined BEV and PHEV-50 are presented in Figure . It can be seen, that the realistic energy consumption of a current electric compact car is in the range between 20 and 25 kWh/100km. In contrast to vehicles with combustion engines, energy consumption of the defined vehicle is lowest in urban areas (about 20 kWh/100km). This is due to the constantly high efficiency of electric engines, while the high fuel consumption of vehicles with combustion engines in urban areas is mainly due to the low engine efficiency in partial load. For electric vehicles in turn, the highest energy consumption occurs on a motorway.

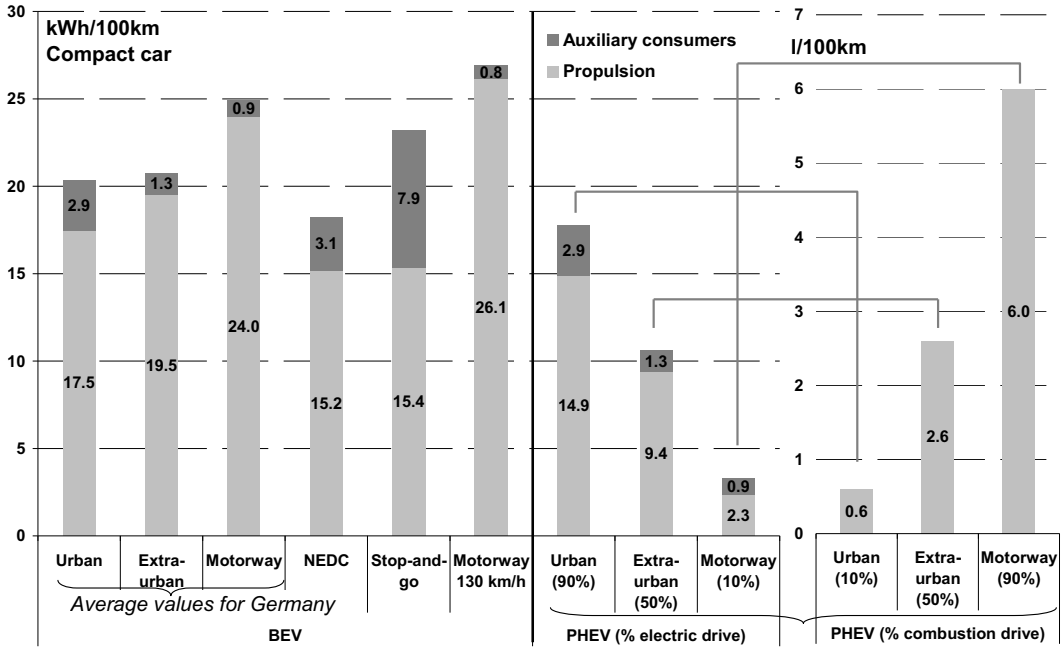

Figure 4: Electricity consumption of BEVs and PHEVs for different road categories

In addition to the average traffic situations in Germany, also the NEDC energy consumption has been analysed and is comparably low (about 18 kWh/100km) due to the less dynamic speed profile. The flexible modelling approach also allows for the analysis of defined traffic situations which can afterwards be grouped to specific use profiles if necessary. In stop-and-go traffic for instance (see Figure), energy consumption is about 15% higher compared to the urban average. Likewise on motorways, energy consumption in free flowing traffic with a 130 km/h speed limit is about 8% higher compared to the average motorway driving (which includes shares with lower speed limits).

The share of auxiliary consumers on total energy consumption differs significantly by road category. Auxiliary consumer energy consumption mostly depends on the duration of use, irrespective of the mileage driven during this time. The ‘per 100km’ average energy consumption is thus much higher in urban areas (14% of total energy consumption) compared to the motorway (4% of total energy consumption). Again it has to be noted, that the presented results are average figures and that the share of auxiliary consumers can be much higher temporarily, e.g. on hot summer days.

The presented electricity consumption of the PHEV is mainly influenced by the assumptions made for the share of electric drive and is complemented by an additional fuel consumption for the remaining share of combustion engine drive. Except for the slightly lower weight of the PHEV, all vehicle parameters are assumed to be the same for reasons of comparability. The energy consumption of auxiliary consumers is assumed to be taken directly from the battery.

Electricity generation for electric vehicles

Electricity for the operation of electric vehicles has to be supplied by a portfolio of power plants, whose composition is of major importance for the life cycle balance of electric vehicles. Though electric vehicles are counted as emission free in the framework of the EU legislation on CO_2 from passenger cars, this naturally does not correspond with the real situation in the energy sector.

The mix of power plants actually used for charging the vehicles is a function of economic framework conditions in the energy sector. Of relevance are the “merit order” of the power plants, the charging strategy (incentives for temporal flexibility), but also the possible consideration of an additional consumer segment “electric vehicles” in emissions trading.

Electric vehicles, as an additional electricity consumer, lead to the use of power plants which other wise would not have been used. As long as the diffusion of electric vehicles is limited, this concerns the load factor of existing power plants. In other words: already existing plants will increase their electricity production. The expected absolute electricity demand in a midterm perspective is limited: 1 million electric cars in Germany in 2020 would be an optimistic scenario and would lead to an electricity consumption of about 2 TWh – about 0.3% of today’s gross electricity consumption in Germany. In the long-run, however, also new capacities have to be built to meet the additional energy and - especially - capacity demands.

The plant actually used in a specific situation is determined by the so called merit order, which classifies the electricity production capacities according to operating costs. Several economic framework conditions determine the merit order, especially the price of fuels and certificates. Also the temporal distribution of the additional demand is of importance: Electricity demand is generally low at night, therefore marginal power plants will be those with lower variable costs (e.g. fuel costs) compared to marginal power plants during the day. At the same time, a smart charging strategy for electric vehicles (e.g. charging at night) leads to a better capacity utilisation. This can be an advantage for power plants with high capital costs, such as coal-fired power plants.

Not only the limited capacity of regional grids, but also the power requirement for electric vehicle charging calls for an intelligent charging strategy beyond conventional “plug-and-play” solutions. If one million electric vehicles would be charged at standard outlets at the same time, four large scale power plants would be necessary to meet this peak demand. Therefore flexible charging schemes are currently being developed, guided by variable electricity rates and so called ‘smart meters’. This way, electric mobility could support the integration of renewable energies into the power system with its combined battery capacity and a communication link to transmission grid and/or distribution network operators. The use of fluctuating energies (e.g. wind or solar power) can be significantly improved. In a long term perspective, the batteries of electric vehicles could also feed electricity back into the grid (‘vehicle-to-grid’ or ‘V2G’). Therefore, also the temporal distribution of vehicle charging has an influence on the mix of power plants to be considered for charging electric vehicles.

IFEU, in cooperation with other research institutes, currently undertakes a detailed modelling approach to analyse the interactions between mobility and electricity sector, including effects such as grid restrictions, emission trading, energy price elasticities and political constraints. Various scenarios will be investigated: a scenario without any constraints, i. e. no further restrictions with respect to charging time or electricity supply, a scneario including a smart charging strategy, where the daily charging tariff depends on the residual load (difference between fluctuating renewable electricity and grid load), and a scenario where additional renewable power plants are built as a consequence of the growth of electric vehicles. First results show that under the reference scenario, the electricity for charging vehicles is likely to be a mix of coal and gas fired power plants if no political initiatives are considered.

At this point, however, only a variation of possible power plant technologies can be presented:

- **Charging with the average electricity in Germany**: This applies if the additional electricity consumption of electric vehicles is considered to be too small to lead to any changes in the average electricity split.

- **Charging with old coal fired power plants (37% efficiency)**: Analyses show that such plants in many situations will be the marginal power plants.

- **Charging with a modern coal-fired or gas fired power plant**: Such plants could be built in the future to meet the additional demand from electric vehicles. They could also be the marginal power plants, if older plants already have been closed.

- **Charging with 100% renewable energies**: It is assumed that these are additional systems, i.e. that they would not have been built without the market penetration of electric vehicles. In this case, their low impacts can be credited to electric vehicles.

Electric vehicle life cycle emissions

First results of a comparative LCA are presented which are based on the discussed data. This means that the life cycle emissions of the defined BEV and PHEV will be compared to conventional gasoline and diesel reference vehicles. For this purpose, IFEU is currently developing an LCA model for electric vehicles called eLCAr (Electric Car LCA), using the software UMBERTO[1]. The following presentation of preliminary results will focus on greenhouse gases (CO_2-equivalents) and acidification (SO_2-euqivalents). The geographical reference is Germany and the results refer to the current or short term future situation. Functional unit is the life-time of a passenger car with different use patterns.

While BEVs are often assumed to be more suitable for urban areas due to their limited driving range, PHEVs can cover longer distances and are thus more suitable to replace passenger cars with mixed use. Results are therefore first presented for a BEV and PHEV with predominant use in urban areas (70% of the total mileage), with only a small share of extra urban (20%) and very little motorway driving (10%). These urban vehicles are assumed to have a limited life-time mileage of 120'000 km. Additionally a PHEV is analysed with the average use pattern of medium gasoline cars in Germany as considered in TREMOD (Knörr, 2010). This means 29% of the life-time mileage on urban roads, 39% on extra urban roads and 32% on motorways. As mentioned above, the PHEV in both cases is assumed to be mostly used in an electric mode (90%) in urban areas, on extra urban roads using both engines with equal shares (50% electric drive) and on motorways predominantly using the combustion engine (10% electric drive). The overall share of electric drive is thus different for the use patterns: While the average mixed use leads to share of 49% electric drive due to more extra urban and motorway driving, the urban use allows for a share of 74% electric drive.

An assessment is made for the vehicle production which is based on data for the Golf 4 in (Ecoinvent, 2008). For electric vehicles, the battery production is of special importance and thus considered in more detail. The assumed battery capacity is 25 kWh for the BEV and 12.5 kWh for the PHEV-50. The current mass balance of lithium ion batteries is based on (Ecoinvent, 2008). The energy demand stated therein, however, appears to be overestimated. Latest data (e.g. Sanyo, 2008) suggest a much lower energy consumption of battery production and is thus used as a reference for the results in this paper. Environmental impacts – especially from battery production – are expected to decrease in the future due to large scale production and increasing recycling rates. Data for this development are currently gathered as part of several IFEU research projects and will be integrated into eLCAr for future LCAs.

As reference vehicles, state of the art Euro 5 gasoline and diesel compact cars are defined. The fuel consumption is assumed in between the 2010 fuel consumption of small and medium car new registrations in TREMOD (Knörr, 2010). The PHEV is assumed to be equipped with a gasoline engine having the same fuel consumption as the reference car on extra urban roads and on motorways. Fuel consumption of the PHEV combustion engine on urban roads is - despite the higher weight - assumed to be 20% lower compared to the conventional vehicle, due to advantages such as recuperation and the avoidance of partial load.

[1] http://ifeu.de/index.php?bereich=oek&seite=umberto

For NO_x emissions, the factors for Euro 5 vehicles from the latest version of the Handbook Emission Factors (INFRAS, 2010) are used. The difference in NO_x emissions between a conventional and a hybrid car can not be clearly determined. Available data show a lot of variability which can not easily be attributed to hybrid vehicle advantages. NO_x emissions are therefore assumed to be the same as for the conventional vehicles (see also (Schwingshackl, 2009)). Field tests currently being conducted will probably allow for a more differentiated and robust consideration of pollutant emissions from PHEVs.

Table 2: Fuel and electricity consumption values used in LCA

Vehicle	Urban areas	Extra urban areas	Motorway
Vehicle use (Urban)	70%	20%	10%
Vehicle use (Average)	29%	39%	32%
Gasoline car	7.5 l/100km	5.2 l/100km	6.7 l/100km
Diesel car	5.6 l/100km	4.0 l/100km	5.3 l/100km
BEV	20.4 kWh/100km	20.8 kWh/100km	24.9 kWh/100km
E-drive PHEV	90%	50%	10%
PHEV (Electricity)	17.8 kWh/100km	10.6 kWh/100km	3.3 kWh/100km
PHEV (Fuel)	0.6 l/100km*	2.6 l/100km	6.0 l/100km

* PHEV in urban area assumed to have 20% lower fuel cosumption than conventional vehicle

Results for life cycle greenhouse gas emissions based on the data and assumptions described in this paper are presented in Figure 5 and Figure 6. With predominant urban use and a limited life-time mileage (Figure 5), the BEV and PHEV using average German electricity lead to greenhouse gas emissions which are lower than for the gasoline car and slightly higher than for the diesel car. As expected, the highest contribution comes from the use phase, though especially for electric vehicles, also vehicle production (including the battery) is of relevance. This share of vehicle production is slightly lower for the PHEV due to the smaller battery. It has to be noted, however, that data for vehicle and battery production are considered to be more uncertain compared to the other values. Considering these uncertainties, life cycle emissions for a BEV and a PHEV using average German electricity in the described urban use profile are about comparable.

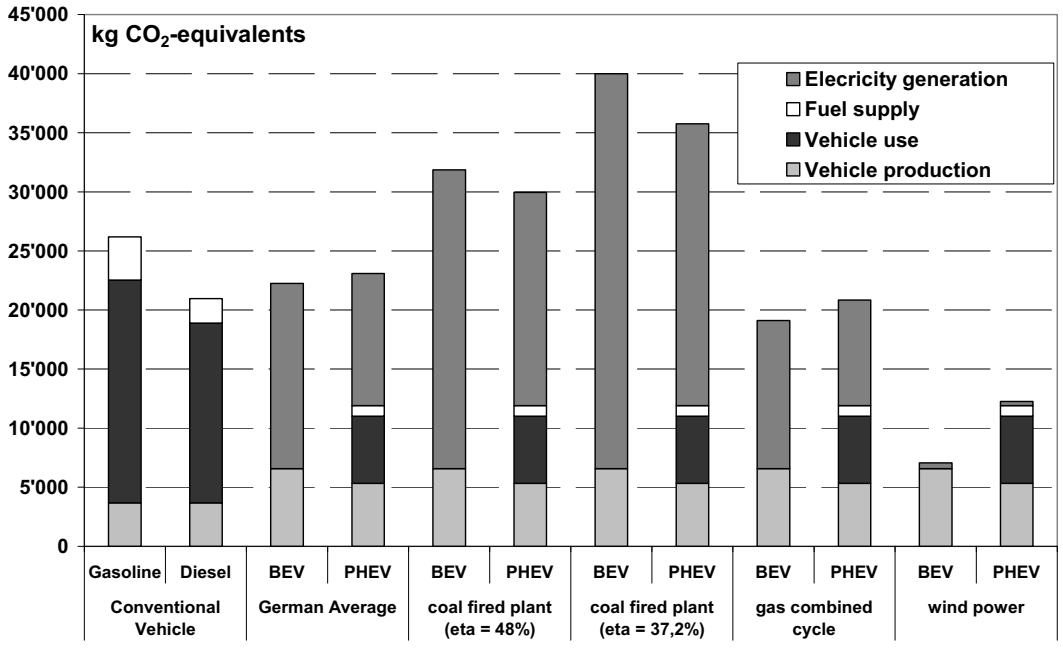

Figure 5: Life cycle greenhouse gas emissions of a compact car with different drive trains (120'000km ; 70% urban driving)

Greenhouse gas emissions increase significantly if coal fired power plants are used for charging the vehicles. The increase is less significant for the PHEV since they only partly use electricity. With coal fired power plants, life cycle emissions of BEVs and PHEVs are higher than for their conventional reference. Though also charging with a modern gas combined cycle plant may lead to a slight advantage over conventional vehicles, only the use of renewable energies - such as wind power - results in a significant reduction of life cycle greenhouse gas emissions.

Results for the PHEV with average mixed use and a life-time mileage of 150'000km are presented in Figure . The share of vehicle production is slightly lower due to the higher mileage. Greenhouse gas emissions are therefore slightly lower with average German electricity than for both conventional reference vehicles. Again emissions increase and are higher than for gasoline and diesel vehicles if coal fired power plants are used for charging. The benefits due to the use of renewable electricity are limited due to the lower share of electric drive, but still considerable.

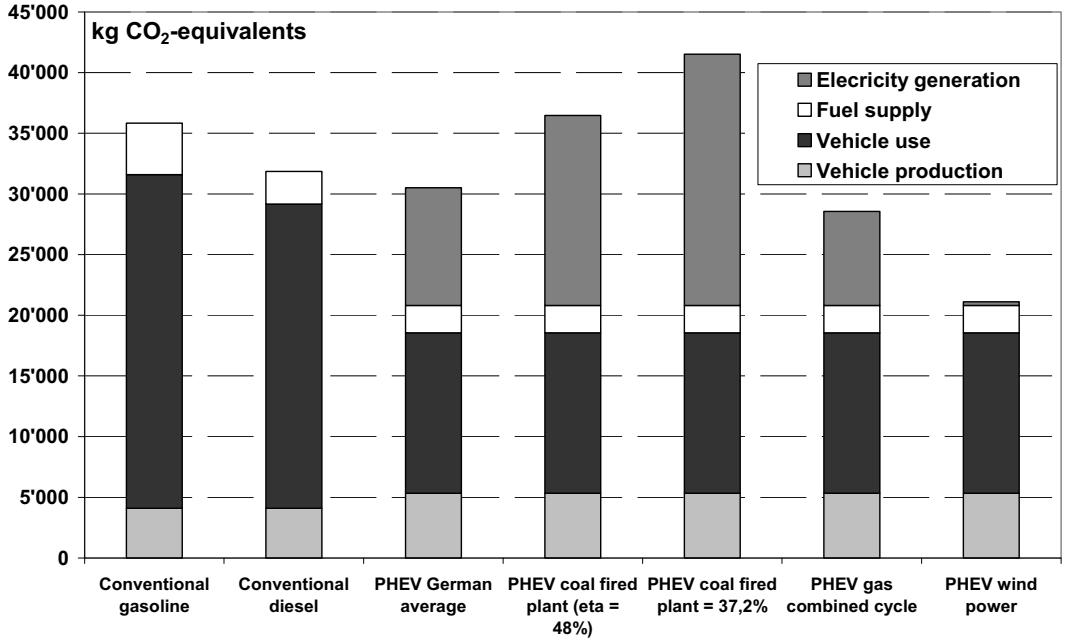

Figure 6: Life cycle greenhouse gas emissions of a conventional and plug-in hybrid compact car (150'000km; average mixed use)

Life cycle results for acidification (see Figure 7 and Figure 8) mostly show a similar pattern with the exception of conventional diesel vehicles. The fuel efficiency of these vehicles is contrasted by high NO_x pollutant emissions. However, future emission regulations (Euro 6) are expected to improve the NO_x balance of diesel cars.

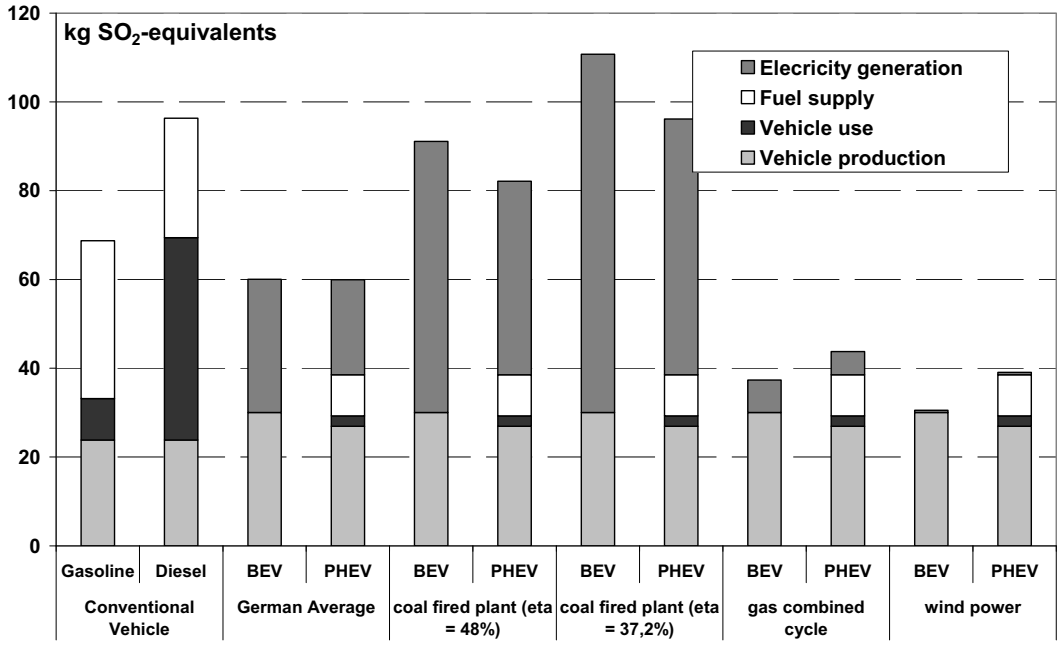

Figure 7: Life cycle acidification of a compact car with different drive trains (120.000km ; 70% urban driving)

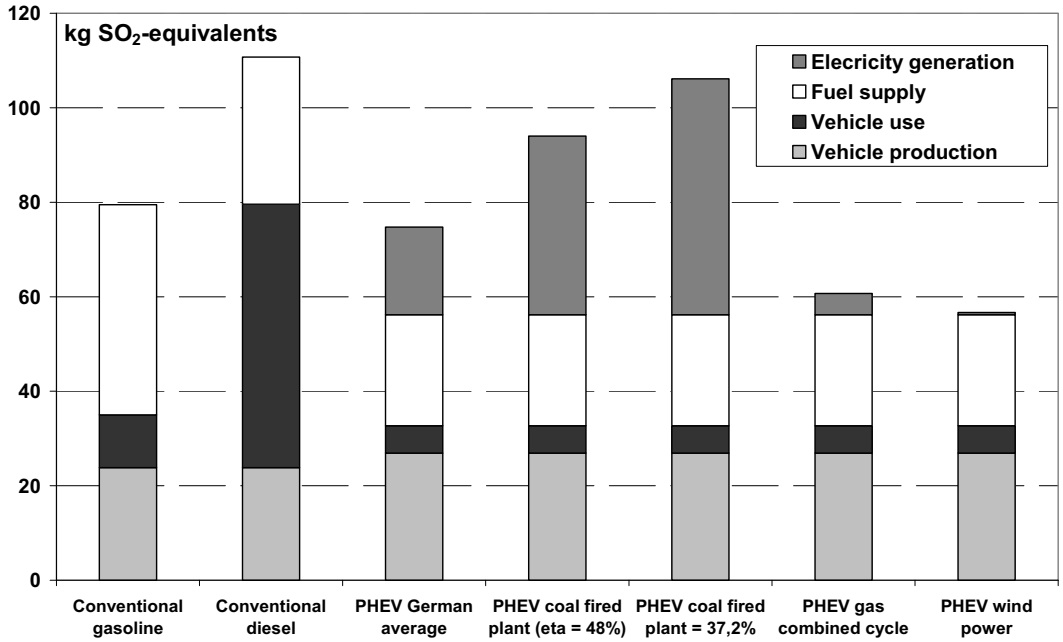

Figure 8: Life cycle acidification of a conventional and plug-in hybrid compact car (150'000km; average mixed use)

Conclusions

The presented results show, that electric vehicles charged with additional renewable energies lead to a significant improvement in the greenhouse gas balance, whereas other electricity sources lead to no substantial improvement or even higher life cycle emissions. Regarding acidification, the gasoline vehicle is comparable to electric vehicles using the German average electricity mix, whereas BEVs charged with coal fired plants lead to higher emissions. From an environmental point of view, it is therefore necessary that the market penetration of electric vehicles is based on the use of renewable sources.

In the discussion of GHG reductions with electric vehicles using renewable electricity, the question of additionality needs to be addressed. In countries with support schemes such as feed-in tariffs, many of the renewable power plants would be built anyway. Renewable energy systems should therefore only be credited to electric vehicles, if they are truly additional to the systems which are built based on the already existing legislation.

Hence, the question arises how renewable electricity systems can be solely allocated to electric vehicles. A real additionality of renewables requires further policital measures which need to be discussed. This may include not counting renewable electricity for electric mobility towards the renewable electricity and final energy targets as defined by the European Renewables Directive (EC, 2009) and national governments. Another approach securing more additionality of renewable electricity for electric mobility involves giving financial incentives (e. g. time-resolved tariffs) for load shifting based on the amount of fluctuating renewable energy (wind and solar) in the grid as well as based on grid restrictions due to wind feed-in. Thus, the use of the electric vehicle battery could enhance the capability of a system to integrate renewable electricity and thus contribute to additional renewable electricity. It is, however, essential, that such a smart charging strategy does not substantially increase the contribution of mid load power plants such as hard coal. A strong link of the tariff to renewable feed-in is necessary.

The methodological discussion also shows that life cycle emissions depend on a range of factors other than the electricity split, especially energy efficiency. Conventional vehicles are expected to further improve their environmental performance, also due to the EU CO_2 and pollutant emission legislation. Electric vehicles will therefore also have to further improve - not only for reasons of life cycle emissions, but in short term perspective also in order to achieve the highest possible driving range.

Besides the required propulsion energy, also the consumption of auxiliary consumers is significant. This applies even more to operation in urban areas, which is assumed to be preferable for electric vehicles due to the limited driving range. Thus also the energy consumption of auxiliary consumers will have to be paid further attention to. This includes energy efficient air conditions and possibly alternative (e.g. fuel based) heating system.

The methodology and data base will be further developed in order to improve and further differentiate the results. Such an in depth analysis of electric mobility is important in order to address advantages and disadvantages at an early stage and thus realise the full environmental potential of electric mobility. Overall, electric vehicles offer some promising mid- to long-term perspective in reducing environmental impacts of road transport.

References

EC (2009), Directive 2009/28/EC of the European Parliament and of the Council of 23 April 2009 on the promotion of the use of energy from renewable sources and amending and subsequently repealing Directives 2001/77/EC and 2003/30/EC.

Ecoinvent (2008), Ecoinvent Database Version 2.1, Zurich 2008.

Edwards R., J-F. Larivé, V. Mahieu and P. Rouveirolles (2006), Well-to-Wheels Analysis of future automotive fuels and powertrains in the European context. Tank-to-Wheels Report Version 2b, CONCAWE/JRC/EUCAR.

Engel, T.: Plug-in Hybrids - Abschätzung des Potentials zur Reduktion der CO2-Emissionen im Pkw-Verkehr bei verstärkter Nutzung von elektrischen Antrieben im Zusammenhang mit Plug-in Hybrid Fahrzeugen. Deutsche Gesellschaft für Sonnenenergie (DGS), Munich 2007.

Fabis R. M. (2006), Beitrag zum Energiemanagement in Kfz-Bordnetzen, Dissertation at the ‚Technische Universität Berlin'.

Garche J. (2007), Forschung und Entwicklung für die nächste Generation von Lithium-Batterien, Presentation at the Workshop ‚Electric Mobility' for the German Federal Ministry for the Environment, Berlin 2007.

Gielen D. and G. Simbolotti (2005), Prospects for hydrogen and fuel cells, International Energy Agency (IEA), Paris 2005.

Guttenberg P. (2004), Der Autarke Hybrid am Prüfstand – Funktion, Kraftstoffverbrauch und energetische Analyse. Dissertation at the ‚Technische Universität München'.

Hausberger S., M. Rexeis, M. Zallinger and R. Luz (2009), Emission Factors from the Model PHEM for the HBEFA Version 3, Graz 2009.

INFRAS (2010), Handbook of Emission Factors for Road Transport (HBEFA), Version 3.1, Zurich 2010.

Kendall G. (2005), Plugged in – the end of the oil age, World Wide Fund for Nature (WWF), Brussel 2008.

Knörr W. (2010), Transport Emission Model (TREMOD), Version 4.17 with internal updates 2010, Institute for Energy and Environmental Research (IFEU), Heidelberg 2010.

Mazza P. and R. Hammerschlag (2005), Wind-to-Wheel Energy Assessment. Institute for Lifecycle Environmental Assessment (ILEA), Seattle 2005.

Öko-Institut (2009), RENEWBILITY - Stoffstromanalyse nachhaltige Mobilität im Kontext erneuerbarer Energien bis 2030, Final report for the German Federal Ministry for the Environment (BMU), Institute for applied ecology (Öko-Institut), Freiburg 2009.

Pehnt M., H. Helms, U. Lambrecht, C. Lauwigi and A. Liebich (2009), Umweltbewertung von Elektrofahrzeugen, Environmental Assessment of Electric Vehicles, *VDI-Bericht* Nr. 2075, 21 – 39.

Raskin A. and Shah, S. (2006), The emergence of hybrid vehicles, AllianceBernstein, New York 2006.

Sanyo (2008), Sustainability Report 2008, Sanyo Electric Co. Ltd., Osaka 2008.

Schwingshackl M. (2009), Simulation von elektrischen Fahrzeugkonzepten für PKW, Diploma Thesis at the ‚Technische Universität Graz'.

Soltic P. (2001), Nachführung der Emissionsgrundlagen Strassenverkehr – Ergänzung der Messdaten auf das Bezugsjahr 2000, Teilbericht: Einfluss elektrischer Verbraucher auf die Emissionen, Dübendorf 2001.

Wallentowitz H. and K. Reif K. (2006), Handbuch Kraftfahrzeugelektronik: Grundlagen, Komponenten, Systeme, Anwendungen, Wiesbaden 2006.

Weiss M. A., J. B. Heywood, E. M. Drake, A. Schafer and F. AuYeung (2000), On the road in 2020. A life-cycle analysis of new automobile technologies. Massachusetts Institute of Technology (MIT), Energy Laboratory, Cambridge MA 2000.

Life Cycle Assessment of Battery Electric and Internal Combustion Engine Drivetrains for a Small Passenger Car

A. Simons and C. Bauer*

PSI, Paul Scherrer Institute, CH-5232 Villigen-PSI, Switzerland, andrew.simons@psi.ch

Abstract

Using life cycle assessment methodologies the paper compares the use of a passenger electric vehicle (EV) with the use of the same vehicle but with a conventional internal combustion engine (ICE). A range of electricity supply scenarios for charging the Na-$NiCl_2$ (ZEBRA) battery are contrasted to petrol and diesel as engine fuel. Operating an equal transport performance within an urban environment showed that for the EV the electricity supply source is critical in terms of greenhouse gas (GHG) emissions. The demand on mineral resources increases for the physical components of the EV but further analysis of the reference system is required in this respect. The second part of the assessment concentrated on air pollution as both a direct and indirect result of driving. Non-exhaust emissions from tyre and brake wear play a significant role on human health factors within the urban environment and although final quantification of actual potential damage factors could not yet be integrated the research was able to compare on relative terms the possible reductions from using the EV.

Introduction

The research and results described in this paper are an extension of research commissioned by the Elektrizitätswerke des Kantons Zürich (Simons and Bauer, 2010). It addresses the potential environmental and human health impacts of electric passenger vehicles (EV) and compares these with the results of conventional passenger vehicles using an internal combustion engine (ICE). The scenario analysis included petrol and diesel versions of ICE and a range of actual and hypothetical electricity mix scenarios for operation of the EV. In order to gain a comprehensive perspective of the impacts and to allow comparisons to be made it is essential to look at the complete life cycle, not only of the vehicle production and disposal but also at the energy chains which supply the motive power. The exchange of an ICE for an electric drivetrain alters the relationship between exploitation of the stored energy (fossil fuel or electric charge) and the location of emissions to the environment. By using a life cycle assessment (LCA) approach emissions over time are accumulated which highlights the potential impacts resulting from this change. The comparison concerns vehicles used within the urban environment and so in terms of potential impacts on human health it was therefore of interest to analyse this relationship between direct and indirect emissions. The process of determining representative potential human health impacts from EV use was commenced by making an initial differentiation between the generic urban environment within which the vehicle operates and the non-urban environment within which all other processes occur. Of particular interest here are the emissions from the upstream processes of the operation related energy chains so that changes within the urban environment resulting from a switch to electricity as the energy carrier can be contrasted against the petrol and diesel fuel chains. Although the environments containing the various energy chains will differ widely this basic differentiation is sufficient to gain initial insights.

Methodology

The Life Cycle Inventory (LCI) stage includes analysis of the extraction, processing and distribution of energy carriers (electricity mixes for EV; petrol and diesel for the ICE vehicle) as well as production, operation, maintenance and disposal of the vehicles and other infrastructures. All inventory modelling was conducted using the ecoinvent database and its methodology (Frischknecht et al, 2007a). For the construction of the inventories and for calculation of the impact assessment the SimaPro v7.1.8 software was used. Inventory modelling of the electric drivetrain and the incorporation of performance characteristics was to a large extent possible using the product documentation and production process descriptions

published by the battery manufacturer[2] and EV retailer[3]. Additional data was found in Dustmann (2004), Manzoni et al. (2003), MES-DEA (2004) and gained through individual correspondence[4]. For the operation (driving) phase the direct fuel use, fuel related emissions as well as non-fuel related emissions from tyre, brake and road surface wear per vehicle km (vkm) are accounted for. During this phase an EV will have a direct use of electricity and cause only the non-fuel related emissions. These emissions are assumed to be directly related to vehicle weight. Use of a passenger car also incurs maintenance and eventual disposal. It also requires the construction, maintenance and disposal of the road network infrastructure and a fraction of these must also be allocated to each vkm. The average number of people per journey in Switzerland is approximately 1.6 whilst for purely commuting travel this falls to around 1.1 (BfS, 2007). In this study these factors, together with the small size of the vehicle and its confinement to urban driving conditions, encouraged a transport of 1 person per vehicle to be used as reference unit and so 1 vkm therefore equals 1 passenger km (pkm). In Switzerland, of those having a car and living in urban regions the average daily distances driven in the largest cities has been determined as around 31km, rising to 39km in less compact urban areas (BfS, 2007). The EV in question can achieve more than 100km on a single charge and is therefore assumed to fulfil the daily transport demands with no loss of utility to the users.

Vehicle characterisations

The EV in question integrates an electric drivetrain into the rolling chassis of a Renault Twingo (Generation 1). It was therefore natural for the assessment to aim to compare this version of an EV with the conventional Renault Twingo with ICE. Both the ICE Twingo and the components surrounding the electric drivetrain of the Twingo EV are based on the ecoinvent inventory of a VW Golf (Spielmann et al., 2007) which reflects modern vehicle production as of the year 2000. This vehicle is more than 200kg heavier than the ICE Twingo and it was necessary to apply a reduction factor of 0.807 to all processes of the vehicle production. Subtracting the ICE and its associated components from the inventory of the smaller vehicle then allowed integration of the electric drivetrain inventory to give the complete EV, which is 80kg heavier than the ICE version. Due to waste streams the total material use is greater than the finished weight by a calculated factor of 1.21 and this relationship was also considered to be the same for the smaller vehicle.

The main feature of the electric drivetrain is a Na-$NiCl_2$ battery. The salt electrolyte within the cells requires heat to become liquid and the actual operating temperature of the cells is between 270 and 350°C. Achieving the operating temperature from cold requires a heating period of up to 24 hours and so when not in use the cell temperature must be maintained by constant heating (Dustmann, 2004; MES-DEA, 2004; Galloway and Dustmann, 2003). The production stages of the ZEBRA battery are described by Manzoni et al. (2008). According to the manufacturer the battery should achieve 1500 charging cycles at full depth of discharge and be in operation for 10 years (MES_DEA, 2004). Calculation of an overall energy demand of 22.3kWh/100km was achieved using the cell and battery characteristics. This figure was validated by an analysis of the real-life performance of the electric Twingo with ZEBRA battery conducted by Domeniconi et al. (2005). It was assumed that the battery and surrounding vehicle will have equal lifetimes (10 years) and there will therefore be an equal demand for all components per km. The ICE vehicle is assumed to achieve the same driving performance as the EV. To achieve a fair comparison of the results both the petrol and diesel versions of the ICE vehicle were modelled with EURO5 standard engines. Values for urban fuel consumption were taken from Renault's used car portal[5]. The ICE uses 0.06kg of petrol and 0.0437kg of diesel per km (7.5l/100km and 5.2l/100km, respectively).

Electricity mix scenarios

In the consideration of scenarios for the charging of the battery the study used the European electricity mix of the EU27 countries and the Swiss supply mix as relevant references. Both mixes are representative of 2004 and their main generation sources are given in Table .

[2] MES-DEA are since 1 Feb. 2010 a commercial part of FZ SONICK S.A., Stabio, Tessin, CH.
[3] Kamoo AG Electrocars, Wagistr. 23, CH-8952 Schlieren.
[4] Dr. C-H Dustmann, Battery Consult sagl, CH-6839 Sagno. In response to a questionnaire.

[5] Accessed 15 Feb. 2010: http://www.renault.de/gebrauchtwagen/gebrauchtwagen-suche/

Table 1: 2004 Electricity supply mixes for Europe and Switzerland (Frischknecht et al., 2007b)

	Fossil	Nuclear	Hydro	Other
EU27 mix	50.7%	29.2%	14.4%	5.7%
CH supply mix	8.1%	49.3%	35.4%	7.2%

To give an impression of the impacts of various generation technologies the assessment also included electricity from single centralised sources of fossil (average coal and natural gas CC plants in Germany), nuclear (Swiss PWR and BWR mix) and hydro (Swiss reservoir and run-of-river mix) as well as decentralised solar (solar photovoltaic) according to the ecoinvent LCA database (ecoinvent, 2007). Battery charging uses low-voltage electricity from the domestic electricity supply network and it was assumed that the mixes would remain the same whether charging at night or during the day as well as at the home or other possible place i.e. at work.

Impact assessment: Cumulative life cycle impact indicators

The methodology of life cycle assessment functions on the basis that all quantifiable potential burdens or impacts to the environment and human health are the result of emissions (to the atmosphere, the ground or to water systems) or the use of naturally existing resources. Within the context of this paper the quantification of GHG emissions, measured in terms of their equivalent global warming potential to CO_2 (IPCC, 2007) also provides an indication of fossil fuel use as a resource. Other important aspects of natural resource depletion are then the non-combustible mineral resources (abiotic resources) invested in infrastructures and measured in equivalent values to the abundance of antimony (Sb) after (Guinée et al. 2001).

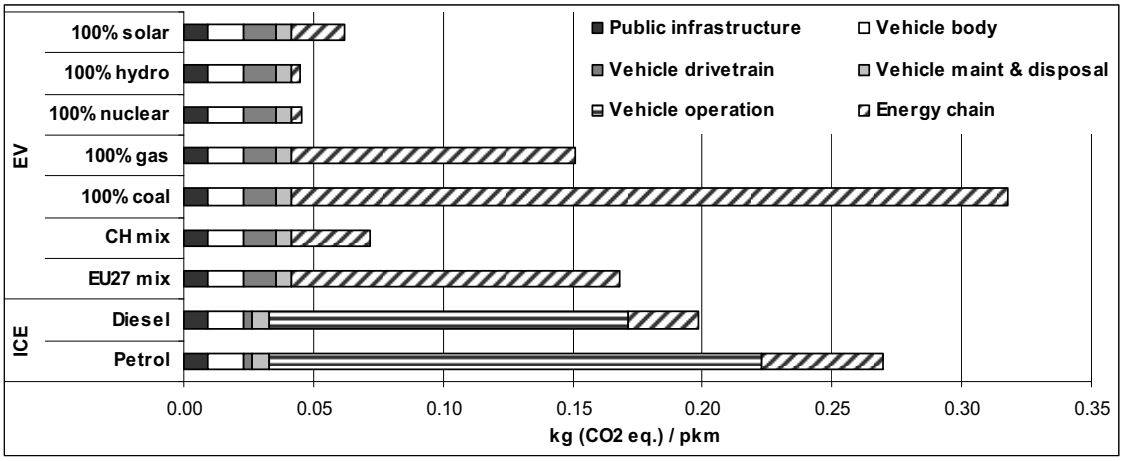

Figure 1: Life cycle greenhouse gas emissions.

In Figure 1 the GHG emissions from the different life cycle aspects of all scenarios are shown. The emissions from the EV drivetrain manufacture are larger than the ICE drivetrain but remain within the ranges for other infrastructures. It can be seen that exchanging an ICE for an electric drivetrain and using electricity from the European mix does not reduce overall GHG emissions significantly beyond the efficiency gained by using a diesel engine. The largely hydro and nuclear based Swiss electricity mix provides a large reduction potential and to a level where emissions from charging the battery become similar to the total of all other life cycle aspects. The other scenarios demonstrate the influence that an electricity generation source can have on the overall results and that going electric does not automatically mean lower GHG emissions.

In Figure 2, showing the consumption of abiotic resources, a closer examination of the factors contributing to construction of the EV showed that the higher value is in large due part to the rare minerals used in the electronics of the battery management and battery charging units. The VW Golf based inventory of the Twingo with ICE represents a modern passenger car which would also be expected to contain a quantity of ICE related electronics, which are, however, not included in the inventories. The results therefore indicate the need for a re-assessment of the inventory in order to determine the amount of electronic components in the reference vehicle.

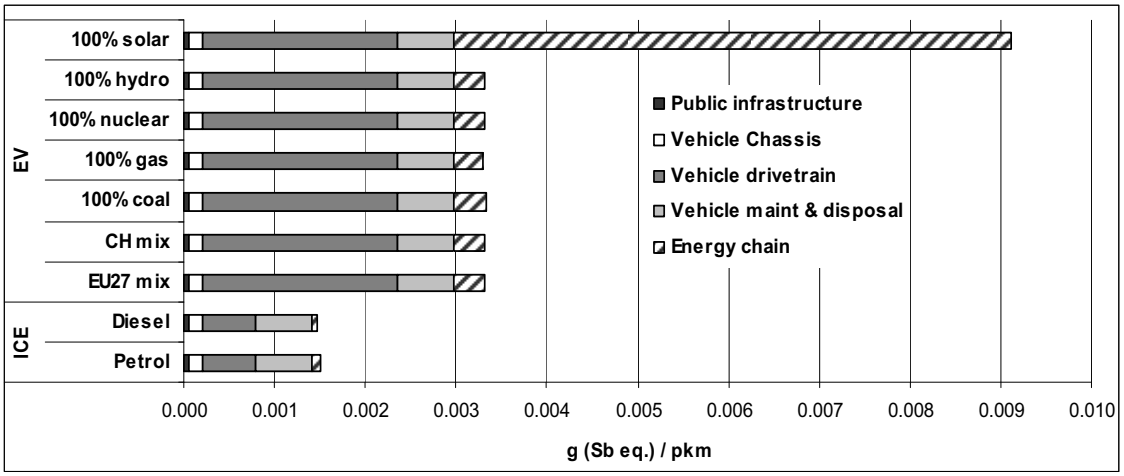

Figure 2 : Life cycle abiotic resource use

The infrastructures of the electricity mixes and the centralised sources have a higher relative depletion of resources compared with the petrol and diesel fuel chains although relatively little variation between them. The very much higher value for photovoltaic (PV) is largely due to the silver and tellurium in the anodes of the individual cells.

Impact assessment: Preliminary indications of ICE and EV related air pollution

This section of the paper looks at the changes and differences at the location of airborne emissions if the car is electric instead of petrol/diesel fuelled. The direct emissions from vehicle operation occur entirely within the urban environment and so it is preferential to understand these in terms of their potential damage to human health. Although the EV is slightly heavier than the ICE resulting in higher non-exhaust emissions, the absence of exhaust emissions leads to a large reduction in direct airborne emissions (Figure 3).

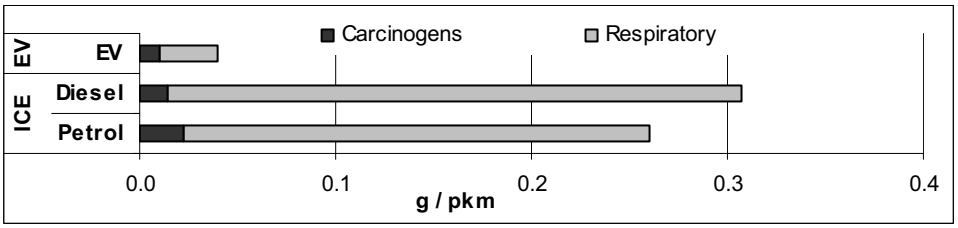

Figure 3 : Mass of direct emissions from vehicle operation with potential carcinogenic and respiratory damage effects.

The emissions shown in figures 3 and 4 are categorised in the form of their aggravation to human health and do not yet determine levels of human exposure to them and emissions occurring in the upstream energy chain stages will be in significantly less densely populated areas than the urban environment. Whilst emissions which attack the respiratory system are significantly reduced the level of carcinogenic substances (both expressed in terms of grams per km) emitted is only marginally lower for the EV than for the diesel fuelled vehicle, and the energy chains have the potential to increase the overall total (

Figure4). Carcinogenic emissions from the EU27 mix exceed those of electricity entirely from coal. This is largely due to fine particulates emitted from lignite power plants and less well filtered coal plants than the German reference plant used for 100% coal.

By changing to an EV the quantities of emissions which damage the respiratory system are almost completely reduced in the urban environment but depending on the mix, electricity as an energy carrier can lead to both significant reductions or equal or greater emissions. For the purposes of comparison between the ICE reference systems and the EV scenarios the results can be viewed in a purely relative manor. In the urban environment, where direct exposure to the emissions will be high, it is reasonable to assume that the application of damage factors

according to population density to provide quantification will not change the relative relationship between ICE and EV. The relationship of ICE to EV can therefore be gauged with the application of existing damage factors incorporated into the Eco-Indicator 99 impact assessment method (Goedkoop and Spriensma, 2001).

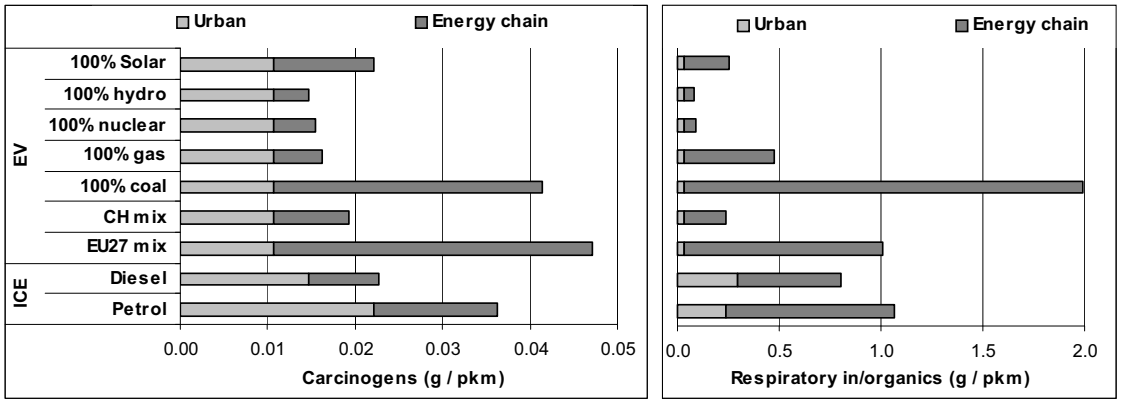

Figure 4 : Direct and indirect airborne emissions from vehicle operation and all energy chains

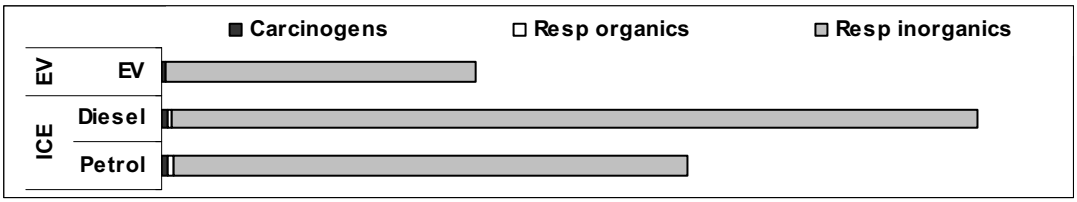

Figure 5: Relative human health impact potentials from direct driving emissions.

The release of respiratory in-organics is shown to pose the largest risk to human health with carcinogens and respiratory organics playing only a relatively minor role (Figure5). In terms of the respective damage areas changing to the EV will reduce the potential health impacts within the urban area by around one-third those of the petrol ICE and by more than half those of the diesel ICE. The non-exhaust emissions therefore prove to be a significant aspect and the tendency for EV's to be heavier than their ICE counterparts maintains this significance. These results would also indicate the need for future research to model regenerative braking which may reduce the use and therefore the emissions from conventional disc brakes.

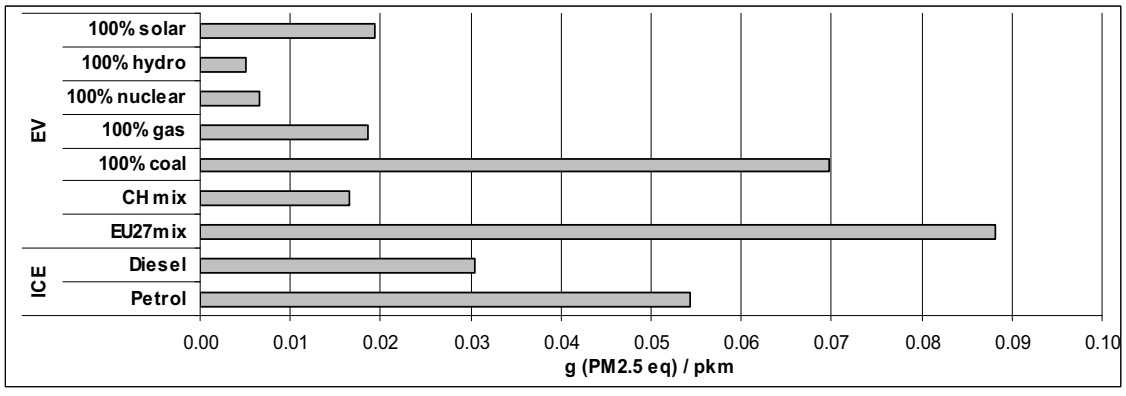

Figure 6: Emissions of respiratory in-organics from the energy chains

Although the energy chain emissions cannot be so easily compared without knowledge of the varying exposure levels it is possible to characterise the emissions at a mid way stage by determining them equivalent to a reference substance. Figure5 showed that the most significant category of emissions is respiratory in-organics and so using Jolliet et al. (2003) Figure6 focuses on just this one category in order to form a comparison.

Conclusions

Operating an equal transport performance within an urban environment showed that within an LCA of EV the electricity supply source is the central factor in terms of greenhouse gas (GHG) emissions and that use of hydro and nuclear power allows a reduction of around 80%, while a large percentage of electricity from fossil sources, particularly coal, may not lead to overall reductions compared to gasoline or diesel cars. The demand on mineral resources increases for the EV due to rare metals used in electronics but analysis highlighted the need to re-assess the inventory of the conventional vehicle for similar components not currently included. The second part of the assessment concentrated on air pollution both directly resulting from driving and occurring outside of the urban environment due to the fossil and electric energy chains. Although representative human health impact factors could not yet be integrated the research was able to compare on relative terms the possible reductions from using the EV (Figure5). At this stage this is, however, limited to direct driving emissions and does not account for energy chain emissions also impacting on the urban population. Here, the non-exhaust emissions from tyre and brake wear play a significant role and although potential impacts are reduced by the EV they continue be around two-thirds of the petrol vehicle per passenger km. Respiratory system damaging emissions in the fuel chains were seen to show a similar alternation between scenarios as did GHG emissions, where the coal chains and coal use within the chains have the potential to cause large quantities of fine particulates. It can be concluded that the EV can reduce hazardous urban related emissions but the non-exhaust emissions remain to be significant. The aspect of regenerative braking should be analysed to show its influence on this. If an electricity mix with low shares of coal is used for EV then large reductions of harmful emissions can also be achieved in the energy chains.

References

BfS (2007), Mobilität in der Schweiz: Ergebnisse des Mikrozensus 2005 zum Verkehrsverhalten, Bundesamt für Statistik, Neuchâtel.

Domeniconi R., N. Mona, C.-H. Dustmann, R. Manzoni and M. Pulfer (2005), Mendrisio Operating Results using NiCd and ZEBRA Batteries, *Proc. EVS-21*, Monaco.

Dustmann C.-H. (2004) Advances in ZEBRA batteries, *Journal of Power Sources,* 127, 85-93.

ecoinvent (2007) The ecoinvent LCA database, v2.0. online: www.ecoinvent.org

Frischknecht R., Jungbluth N., Althaus H.-J., Doka G., Heck T., Hellweg S., Hischier R., Nemecek T., Rebitzer G., Spielmann M., Wernet G. (2007a), Overview and Methodology: ecoinvent report No. 1, *Swiss Centre for Life Cycle Inventories*, Dübendorf, Switzerland.

Frischknecht R., Tuchschmid M., Faist Emmeneger M., Bauer C., Dones R. (2007b), Strommix und Stromnetz, ecoinvent report No. 6-XVI, v2.0., *Paul Scherrer Institute*, Villigen, Switzerland.

Galloway R.C., C.-H. Dustmann (2003), ZEBRA Battery – Material Cost and Recycling. *Proc. EVS-20*, Long Beach, California.

Goedkoop M., R. Spriensma (2001), The eco-indicator 99; A damage orientated method for life cycle impact assessment: Methodology Report, Third edition, *PRé Consultants B.V*, Amersfoort.

Guinée J.B., M. Gorrée, R. Heijungs, G. Huppes, R. Kleijn, A. de Koning, L. van Oers, A. Wegener Sleeswijk, S. Suh, H.A. Udo de Haes, H. de Bruin, R. van Duin, M.A.J. Huijbregts (2001), Life cycle assessment; an operational guide to the ISO standards - Part 2b: Operational annex. *Centre of Environmental Science*, Leiden University (CML).

IPCC (2007) Intergovernmental Panel on Climate Change, 2007, Climate Change 2007: The Physical Science Basis, Cambridge University Press, Cambridge, UK.

Jolliet O., M. Margni, R. Charles, S. Humbert, J. Payet, G. Rebitzer, R. Rosenbaum (2003), IMPACT 2002+: A New Life Cycle Impact Assessment Methodology, *International Journal of LCA*, 8, 324-330.

Manzoni R., M. Metzger, G. Crugnola (2008), ZEBRA Electric Energy Storage System: From R&D to Market. *Proc. HTE hi.tech.expo*, Milan.

MES-DEA (2004) ZEBRA: Electric Energy Storage. *MES-DEA SA*, Stabio, Switzerland.

Simons A., C. Bauer (2010), Life cycle assessment of electric vehicles: the analysis of a passenger car with Na-$NiCl_2$ battery, *Paul Scherrer Institute*, Villigen, Switzerland.

Spielmann M., C. Bauer, R. Dones, M. Tuchschmid (2007), Transport Services: ecoinvent report No. 14, *Swiss Centre for Life Cycle Inventories*, Dübendorf, Switzerland.

Effect of Battery Performance on Determining CO_2 Emissions of Hybrid Electric Vehicles under Real-World Conditions

Robert Alvarez1, Peter Schlienger1, Martin Weilenmann1*

[1] Empa, Swiss Federal Laboratories for Materials Testing and Research, Laboratory for Internal Combustion Engines, Ueberlandstrasse 129, CH-8600 Duebendorf, Switzerland, robert.alvarez@empa.ch

Abstract

Hybrid electric vehicles (HEVs) can potentially reduce vehicle CO_2 emissions by further using recuperated kinetic vehicle energy stored as electric energy. This ability mainly depends on the type and layout of the electric storage device, its manufacturing deviation and in-use deterioration. The resulting performance affects net HEV CO_2 emissions in a certain driving pattern, described as equivalent to unchanged net energy content of that storage device. This energy content cannot be measured externally, demanding a correction procedure to determine net HEV CO_2 emissions from their raw CO_2 emissions. The present study investigates such effects on HEV CO_2 emissions based on chassis dynamometer test results with three identical in-use examples of a conventional HEV model featuring different mileages. Statutory and real-world driving cycles together with full electric vehicle operation modes have therefore been considered. It is shown that the individual drive battery performance of the single HEVs affects both their raw CO_2 emissions and the outcomes of the statutory correction procedure. The corrected CO_2 emissions of a HEV in any driving pattern resulting from this statutory procedure clearly underestimate their true level which can be only reproduced when account is taken on the individual HEV drive battery performance.

Introduction

Hybrid electric vehicles (HEVs) represent a promising approach to reducing vehicle exhaust emissions of CO_2. An additional electric powertrain including an energy storage device, typically a rechargeable drive battery or supercapacitors, is combined with a combustion engine to provide the desired overall vehicle power output. This configuration makes it possible both to design and employ the single powertrains in their most efficient operating conditions and to recuperate kinetic vehicle energy during deceleration for further use, leading to reduced overall CO_2 vehicle emissions (Sundström, 2009, Sundström et al., 2009, 2008). HEVs are categorized according to their capability for full electric driving (full hybrid) or not (mild hybrid) and whether they are externally rechargeable (plug-in hybrid) or not (conventional hybrid). However, such types of vehicles are expected to attain a considerable market share in the near future (Christidis et al., 2005, Duleep et al., 2004), also because of specific CO_2 vehicle emission reduction policies (An, 2007) and legislation such as in Europe (Regulation EC 443/2009) (Fontaras and Samaras, 2010), and first studies have already been carried out to determine their real-world pollutant emission performance (Fontaras et al., 2008). Furthermore, HEVs are assumed to open up the way towards electricity-based powertrain solutions such as electric or fuel cell vehicles (Van Mierlo et al., 2006).

A crucial feature of HEVs is the ability of their electric storage device to further use stored electric energy, because the latter then needs not be provided by the combustion engine and facilitates most savings in CO_2 emissions. When drive battery is employed, this battery performance generally depends on the battery technology used and its layout, but is also device-specific due to manufacturing deviation and in-use deterioration. However, net CO_2 emissions of a HEV in any driving pattern are affected because they are described as equivalent to the unchanged net energy content or state of charge (SOC) of its battery. Therefore, an adequate procedure for correcting the recorded raw CO_2 emissions of individual HEVs needs to be applied that reflects its true respective emission level, because battery SOC cannot be measured externally.

In order to study the effect of battery performance on determining net CO_2 emissions of HEVs under real-world conditions, an experimental investigation with three identical in-use examples of a conventional HEV model featuring different mileages has been conducted on a chassis dynamometer. Test runs with the statutory cycle for Europe NEDC and the real-world Common Artemis Driving Cycle (CADC) including urban, rural and motorway driving patterns have been performed together with constant-speed full electric driving and vehicle traction mode. The test

results obtained are discussed in detail, highlighting the importance of including the individual HEV drive battery performance when determining true net CO_2 emissions in any driving pattern in contrast to the statutory correction procedure.

Methodology

Vehicle sample

The main characteristics of the three identical in-use examples of a particular HEV model selected for the test series with different mileages are summarized in Table 1. This HEV is categorized as a 'conventional full hybrid', i.e. the drive battery employed is not externally rechargeable but allows full electric vehicle operation in certain driving situations as well as assisting the combustion engine and recuperating kinetic vehicle energy during deceleration (Danisch and Goppelt, 2004). Therefore, a certain range of drive battery SOC is made available by this HEV, whereas when it reaches its lower limit recharging up to a higher level via the combustion engine is carried out. Under normal operating conditions, however, the overall HEV control system attempts to operate around a defined battery SOC level where the latter situation does not occur. Note that no particular servicing was carried out before the test runs except a general vehicle function check.

Table 1: Main characteristics of the considered vehicle sample; IC: internal combustion

characteristic			HEV A	HEV B	HEV C
vehicle	make & model	[-]		Toyota Prius II	
	inertia setting[a]	[kg]		1425	
	gearbox	[-]		CVT	
	certification class	[-]		Euro-4	
	1st certification	[-]	Feb 06	Aug 06	Jun 05
	mileage	[km]	32768	60761	104266
IC engine	displacement	[cm^3]		1497	
	rated power	[kW]		57	
electric motor	rated power	[kW]		50	
drive battery	type	[-]		NiMH	
	nominal voltage	[V]		201.6	
	number of cells	[-]		168	

[a] empty mass plus 100kg

Experimental Program

Several driving cycles were employed in the test series in order to determine the effect of battery performance on the CO_2 emissions of the selected HEVs. The statutory cold-start driving cycle for Europe (Council Directive 70/220/EEC) was included, as well as the real-world Common Artemis Driving Cycle (CADC). The warm-start CADC was derived from car driving behavior studies within the ARTEMIS research program, and its cycle sections represent European real-world urban, rural and motorway driving behavior for cars (André, 2004). Additionally, test runs with full electric driving and vehicle traction mode, simulating coasting conditions, were executed at a constant speed of 25 km h-1 to determine the resulting net battery charge flow when maximally discharging and charging the drive battery over its whole available SOC range.

The single cycle sections of the CADC were started with different initial battery SOC to investigate the sensitivity with regard to CO_2 emissions of each driving pattern on actual battery SOC and to further apply a correction method to determine net CO_2 emissions of the single HEVs as presented below. There, maximum and minimum initial battery SOC level have been considered that are defined by either having no more charge leading to the drive battery in vehicle traction mode or having the combustion engine started in full electric vehicle driving to ensure the minimum permitted SOC level, respectively. A medium initial battery SOC level

between these two initial SOC levels has also been included, set identically for all tests using the respective information on the instrument panel of the individual vehicles. However, this initial SOC condition was not strictly adjustable. The test runs with the statutory cycle NEDC were all started with maximum battery SOC.

Experimental Setup

Figure 1 shows the overall experimental setup employed for the test series. The exhaust was sampled with a Constant Volume Sampling (CVS) system. Exhaust emissions of CO_2 were measured time-resolved and according to the statutory procedure specified in Council Directive 70/220/EEC of storing a sample of diluted exhaust in a tedlar gas sampling bag and analyzing its content offline after completion of the test run. In both cases an adequate exhaust gas analyzer (HORIBA AIA-110S) as specified by Council Directive 70/220/EEC was employed. The time-resolved drive battery wire current was measured with a clamp-on ammeter (LeCroy CP500) fulfilling the criteria specified in Regulation ECE R-101 of Council Directive 70/220/EEC together with the terminal voltage of the battery using differential probe analyzers (LeCroy ADP305), both recorded via a digital sampling oscilloscope (LeCroy WaveRunner 44Xi).

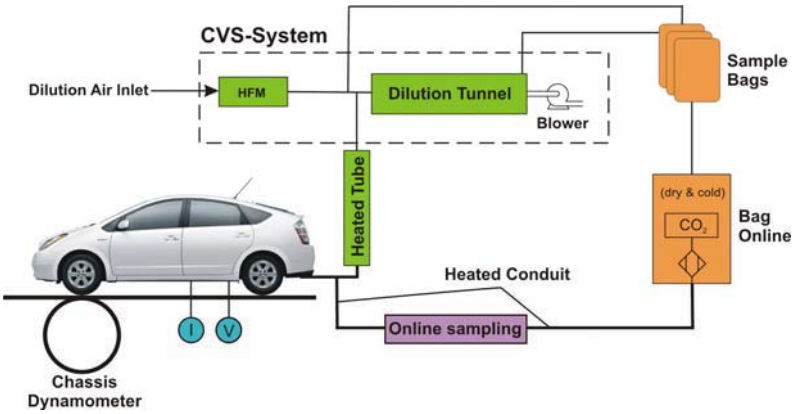

Figure 1 Schematic diagram of the test setup; HFM: hot-film air-mass flow meter; V: measurement of battery terminal voltage; I: measurement of battery wire current.

The chassis dynamometer and its settings were applied according to the provisions of Council Directive 70/220/EEC. The driving resistance of the vehicle was simulated using the respective coast-down data provided by the manufacturer, and the inertia settings were set at empty vehicle mass plus 100 kg payload. The ambient conditions of the test cell were set to 23°C temperature and 50% relative air humidity. All HEVs were operated with the same standard fuel with low sulfur content.

Correction of raw CO_2 emissions

Net emissions of CO_2 of a HEV in any driving pattern need to be described as equivalent to unchanged net energy content or state of charge (SOC) of the drive battery within the driving pattern in order to avoid any under- or overestimation. However, a driving pattern with unchanged net battery SOC is unlikely to be performed, and the resulting raw CO_2 emissions thus need to be adjusted. Because battery SOC cannot be measured externally, an adequate correction procedure has to be derived to achieve this aim.

The statutory procedure for correcting CO_2 emissions of conventional HEVs is described in Regulation ECE R-101 of Council Directive 70/220/EEC. The change in electric energy of the battery ΔE_{batt} is defined to be equivalent to the nominal battery energy content E_{TEbatt} weighted with the change in battery SOC and expressed by the product of the net charge flow Q recorded on the battery wire in a driving pattern and the battery nominal voltage:

$$\Delta E_{batt} = \Delta \mathrm{SOC}[-] \times E_{TEbatt} = Q \times V_{batt} \quad (1)$$

The measured charge balance Q is therefore the only indicator used to reflect changes in battery SOC. Given this, a number of n measurements in a certain driving pattern are executed with a particular HEV in order to obtain a data set of different raw CO_2 emissions M_i together

with respective Q_i, whereas at least one of the latter should be negative in order to be able to derive a correction factor for CO_2 applying a linear regression on this data set:

$$K_{CO_2} = \frac{n \cdot \sum Q_i \times M_i - \sum Q_i \times \sum M_i}{n \cdot \sum Q_i^2 - \left(\sum Q_i\right)^2} \quad (2)$$

This correction factor has to be provided by the manufacturer for certification purposes. The resulting net emissions of CO_2 M_0 from the raw emissions M of a particular HEV obtained in this certain driving pattern are then defined as:

$$M_0 = M - K_{CO_2} \times Q \quad (3)$$

For this statutory procedure of describing battery ΔE_{batt} via ΔSOC and correcting HEV CO_2 emissions, two assumptions are made: first, it is assumed that the battery terminal voltage remains constant and equal to the battery nominal voltage. Secondly, no irreversibility during storage and further usage of the charge provided to the battery is implicitly assumed.

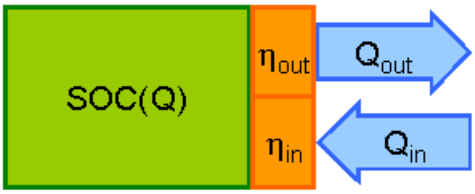

Figure 2: Schematic flow diagram of the charge flows of a HEV drive battery.

In real operation, however, neither of the two assumptions is likely to occur, in particular the charge provided to the battery Q_{in} and further used Q_{out} are to be efficiency-delimited as depicted in Figure 2. The single efficiencies η_{in} and η_{out} generally depend on actual SOC, current, voltage, temperature and state of deterioration of the battery. The resulting charge balance equivalent to battery ΔSOC in a driving pattern is then:

$$Q = \int \eta_{in}(t) \times \frac{dQ_{in}}{dt} \partial t - \int \frac{1}{\eta_{out}(t)} \times \frac{dQ_{out}}{dt} \partial t \quad (4)$$

And when η_{in} and η_{out} are assumed to be constant, the relation between the charge flows provided to and further used from the battery per unit battery SOC can be expressed as:

$$Q_{out} = \eta_{in} \times \eta_{out} \times Q_{in} \quad (5)$$

Therefore only the fraction $\eta_{in} \times \eta_{out}$ of the charge provided to the battery is further used, a characteristic that indicates the battery performance in terms of its individual ability to store and further use charge provided to the battery. This performance needs to be considered when using charge balance to describe battery SOC and subsequently to derive adequate correction factors to determine net CO_2 emissions of HEVs.

Results

Maximum battery charging and discharging

Several repetitions of test runs have been performed operating the single vehicles in full electric driving and vehicle traction mode at constant speed of 25 km h^{-1} utilizing their whole permitted battery SOC range. The resulting net charge flows when maximally charging and further discharging the same SOC range of the single vehicle drive batteries are presented in Figure 3. It can be seen there that the maximum amount of charge available from the single drive batteries decreases significantly with increasing vehicle mileage, indicating a possible deterioration effect caused by in-use ageing. The respective maximum amount of charge

needed to be provided to the single batteries is also always substantially higher than the charge further available. This observation does not comply with vehicle mileage, leading to ratios of charge further used from and provided to the battery in this driving regime of 78%, 67% and 72% for HEV A, B and C, respectively, for the given driving pattern.

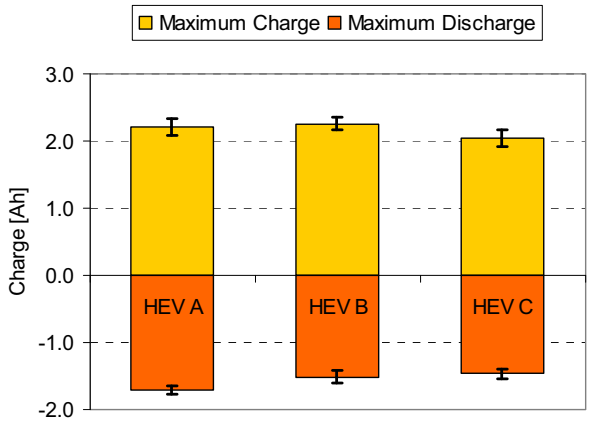

Figure 3: Maximum net charge flows provided to and further used from the individual batteries of the single HEVs in full electric driving and vehicle traction mode at 25 km h^{-1}.

As the battery demand was almost constant during full electric constant-speed operation of the vehicles, these ratios may represent the characteristic $\eta_{in} \times \eta_{out}$ of the single batteries and thus reflect the individual battery performance with respect to further using stored charge provided to the battery. These levels of performance are more likely to be affected by the number and depth of in-use battery charge and discharge cycles occurred than by battery ageing due to absolute vehicle mileage. The excess electric energy provided to the battery is assumed to be finally dissipated as heat via the air cooling system of the single vehicle's drive batteries.

Statutory emission performance

Figure 4 shows the single HEV emission performance in the driving cycle NEDC of raw and corrected CO_2 emissions according to the statutory correction procedure, employing the same correction factors for CO_2 provided by the HEV manufacturer for that cycle. No particular trends for the single HEVs can be detected from the raw CO_2 emissions, indicating that the low driving dynamics of the NEDC does not make great demands on their hybrid powertrains. All three vehicles exhibit final CO_2 emissions similar to the official value of 104 g km^{-1} CO_2 stated for this HEV model (Danisch and Goppelt, 2004) even though the chosen inertia settings exceed the respective certification specification by 65 kg.

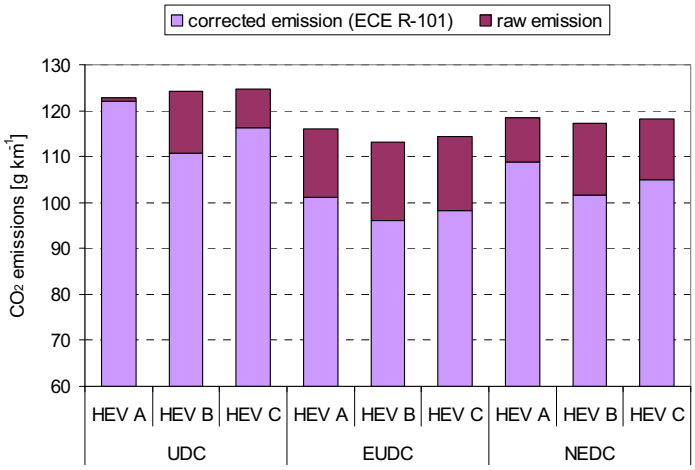

Figure 4: Raw and corrected CO_2 emissions according to the statutory correction procedure of the single HEVs in the statutory driving cycle NEDC started with maximum drive battery SOC.

But it can be seen that although these test runs have been started with a maximally charged drive battery, a correction towards lower CO_2 emissions already has to be applied in the first cycle section of the NEDC, named the Urban Driving Cycle (UDC). According to the correction methodology used, described above, this observation would imply an increase in battery SOC in the first cycle section UDC, which, however, cannot have occurred, as also indicated by the respective information on the instrument panel of the single vehicles.

This observation can be explained by the findings summarized in Figure 3. More charge than can be further used per unit SOC always has to be provided there to the drive batteries of the single HEVs, i.e. whenever these vehicles attempt to maintain a certain SOC level in regular driving conditions, as in the UDC, more charge will have to be provided to the battery than is effectively used. This circumstance distorts the outcomes of the statutory correction procedure, which does not consider any irreversibility in battery charge flow, resulting in the misleading indication that all the excess charge provided to the battery will be further available to save vehicle CO_2 emissions. Therefore, the single drive battery performance levels with regard to the ability to further use provided charge presented above are also reflected here: the lower the stated ratio is, the greater the resultant absolute statutory CO_2 correction.

Real-world emission performance

The test results for raw CO_2 emissions obtained for the different cycle sections of the CADC representing real-world urban, rural and motorway driving pattern, and started with minimum, medium and maximum battery SOC, are summarized in Figure 5. Strong influence of initial battery SOC on the resulting raw CO_2 emissions of the single HEVs can be stated in real-world urban driving in a range of around 30% to 40% of the average. This effect is less pronounced for rural driving and almost non-existent for motorway driving, indicating that hybrid electric driving of the HEVs considered is most effective in real-world urban driving patterns.

There also, raw HEV CO_2 emissions tend to increase with vehicle mileage for the different initial battery SOC conditions. The lower absolute amount of charge that the single drive batteries can facilitate with increased vehicle mileage, see Figure 3, is mainly responsible here, leading to more extensive demand on the combustion engine when performing this driving pattern.

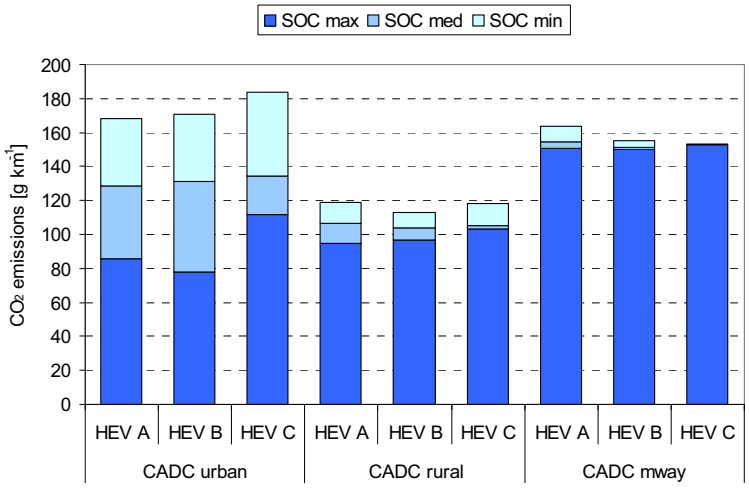

Figure 5: Raw CO_2 emissions of the single HEVs in the real-world driving cycle CADC started with maximum, medium and minimum drive battery SOC.

Given the data set for the CADC, the statutory procedure for deriving CO_2 correction factors according to Equation 2 is applied and the outcomes for the single HEVs are summarized in Figure 6 together with the respective range of measured raw CO_2 emissions shown in Figure 5. Again, HEV B features the largest correction in CO_2 emissions, especially for the urban section of the CADC, which is also assumed to be caused by its lowest drive battery performance of further using charge provided to the battery, see Figure 3. All the corrected CO_2 emissions tend to lie in the lower third of the total range of raw CO_2 emissions.

Additionally, corrected CO_2 emissions of the HEVs were calculated when applying the same correction procedure but weighting the measured charge flow with the ratios presented in Figure 3 to include the individual HEV drive battery performance, see Figure 6. These corrected emissions are up to around 25% higher than the outcomes of the statutory correction procedure and typically lie closer to the average of the range of their raw CO_2 emissions. The corrected emissions from the weighted method are therefore assumed to represent much better the true net CO_2 emissions of these HEVs. However they are not equivalent as they exceed the range of their measured raw CO_2 emissions in some cases. The cause for this circumstance is due to the fact that the individual HEV drive battery performance depends on the driving pattern, which determines the theoretically possible battery usage of an HEV. The ratio applied here stated in Figure 3 is thus most probably excessive because it has been derived from full electric vehicle operation that represents a more pronounced demand to the drive battery than in the driving patterns of the CADC.

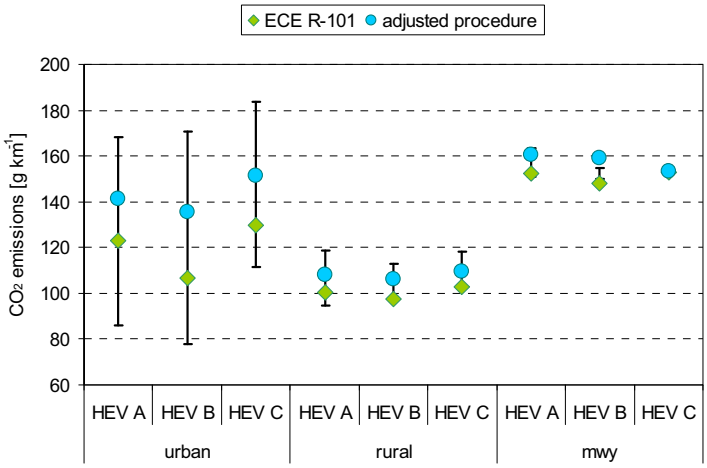

Figure 6 Corrected CO_2 emissions of the single HEVs in the real-world driving cycle CADC derived from the statutory correction method and an adjusted procedure with weighted charge flows; error bars represent the range of their raw measured CO_2 emissions.

Summary and Conclusions

The present experimental investigation with three examples of a conventional HEV offers varied insight into the effect of drive battery performance on determining CO_2 emissions of HEVs under real-world conditions. It is shown that the individual drive batteries of the single HEVs perform differently under equivalent driving conditions. First, the total charge output of the batteries is lower with increasing mileage and therefore most probably caused by in-use deterioration. Secondly, it is observed that only a fraction of the charge provided to the single drive batteries can always be further used per unit battery SOC, which also varies considerably for each battery. The latter circumstance is presumably to be attributed to the number and depth of in-use charge and discharge cycles performed by each battery.

These findings influence both the raw CO_2 emission performance of HEVs and particularly the outcomes of the statutory procedure for correcting HEV CO_2 emissions with respect to unchanged net battery energy content in a driving pattern. Because this procedure bases upon the measured charge flow but does not consider any irreversibility in further using the charge provided to the battery, the resulting corrected CO_2 emissions may considerably underestimate the true CO_2 emission level of a HEV in any driving cycle, as indicated by the present test results. The measured net battery charge flow within a driving pattern for itself does therefore not correctly indicate the effective change in energy content of the HEV drive battery.

It can be concluded that the individual HEV drive battery performance needs to be taken into account when determining true CO_2 emissions of a conventional HEV in any driving pattern. The most appropriate approach for it appears to be to have direct access to the battery SOC information of the HEV powertrain control system to apply to the respective correction procedure. Alternatively, subsequently repeating this pattern until stabilized CO_2 emissions are reached would also be feasible because the energy content of the drive battery of a conventional HEV is self-sustaining.

Acknowledgements

The authors thank the Swiss Federal Office for the Environment (FOEN) for principally funding the study and Toyota Motor Europe for providing valuable technical information.

References

An F. (2007), International Comparison of Policies to Reduce Greenhouse Gas Emissions from Passenger Vehicles, in: Sperling, D., Cannon, J.S. (Eds.), *Driving Climate Change - Cutting Carbon from Transportation*, Academic Press, Amsterdam, pp. 143-164

André M. (2004), The ARTEMIS European driving cycles for measuring car pollutant emissions, *Science of the Total Environment*, 334-335, 73-84

ARTEMIS: Assessment and Reliability of Transport Emission Models and Inventory Systems. http://www.trl.co.uk/ARTEMIS

Council Directive 70/220/EEC of 20 March 1970 on the approximation of the laws of the Member States relating to measures to be taken against air pollution by gases from positive-ignition engines of motor vehicles, http://eur-lex.europa.eu/LexUriServ/LexUriServ.do?uri=CONSLEG:1970L0220:20070101:en:PDF

Christidis P., Hernandez H., Georgakaki A., Peteves S.D. (2005), Hybrids for road transport: status and prospects of hybrid technology and the regeneration of energy in road vehicles, European Commission Joint Research Centre Technical Report EUR21743EN. ftp://ftp.jrc.es/pub/EURdoc/eur21743en.pdf

Danisch R., Goppelt G. (2004), Der neue Toyota Prius, *Auto Technology*, 3, 186-189

Duleep K.G., Greene D.L., McManus W. (2004), Future potential of hybrid and diesel powertrains in the U.S. lightduty vehicle market, *Report No. ORNL/TM-2004/181,* http://www-cta.ornl.gov/cta/Publications/Reports/ORNL_TM_2004_181_HybridDiesel.pdf

Fontaras G., Samaras Z. (2010), On the way to 130 g CO_2/km - Estimating the future characteristics of the average European passenger car, *Energy Policy*, 38, 1826-1833

Fontaras G., Pistikopoulos P., Samaras Z. (2008), Experimental evaluation of hybrid vehicle fuel economy and pollutant emissions over real-world simulation driving cycles, *Atmospheric Environment*, 42, 4023-4035

Regulation EC 443/2009 of the European Parliament and of the Council of 23 April 2009 setting emission performance standards for new passenger cars as part of the Community's integrated approach to reduce CO2 emissions from light-duty vehicles, *Official Register of the European Union*, http://eur-lex.europa.eu/Notice.do?val=496639:cs&lang=en&list=496639:cs,&pos=1&page=1&nbl=1&pgs=10&hwords=443/2009~

Sundström O., Guzzella L., Soltic P. (2008), Optimal Hybridization in Two Parallel Hybrid Electric Vehicles using Dynamic Programming, *Proceedings of the 17th IFAC World Congress*, July 2008, Seoul, Korea

Sundstrom O., Guzzella L., Soltic P. (2009), Torque-Assist Hybrid Electric Powertrain Sizing: From Optimal Control Towards a Sizing Law, *IEEE Transactions on Control Systems Technology*, Article in press

Sundström O. (2009), Optimal Control and Design of Hybrid Electric Vehicles, *Dissertation Swiss Federal Institute of Technology*, No. 18543, Switzerland, pp. 154

Van Mierlo J., Maggetto G., Lataire Ph. (2006), Which energy source for road transport in the future? A comparison of battery, hybrid and fuel cell vehicles, *Energy Conversion & Management*, 47, 2748-2760

Session 3: Secondary Pollutants and Exposure

Long-term trend of direct NO_2 emissions from urban road traffic in Zurich, Switzerland

Ch. Hueglin[1], Juerg Brunner[2], B. Buchmann[1]

[1] Empa, Swiss Federal Laboratories for Materials Testing and Research, CH-8600 Duebendorf, Switzerland, christoph.hueglin@empa.ch
[2] UGZ, Walchestr 31, CH-8021 Zurich, Switzerland

Abstract

Long-term measurements of NO, NO_2 and O_3 from an urban roadside site and a nearby urban background site in Zurich (Switzerland) have been analysed for the trend of the NO_2/NO_x emissions ratio (f-NO_2) of urban road traffic. It was found that f-NO_2 has increased from about 7% in the 1990's to about 13% in 2008, a result that is in line with findings from other European cities. In spite of the observed increase, directly emitted NO_2 from road traffic account for a relatively small fraction of the average total NO_2 at urban roadside sites. Our analysis showed for the urban roadside site in Zurich that direct NO_2 emissions from road traffic account on annual average for 16% of total NO_2. At this site, the ambient NO_2 is mainly determined by the urban NO_2 background (63%) and NO_2 that is produced from reaction of locally emitted NO with ozone (local secondary NO_2, 21%). Consequently, a reduction of f-NO_2 would only have a small effect on the average NO_2 concentration at urban roadside sites. For an efficient reduction of NO_2 levels at urban sites, further reductions of total NO_x emissions from road traffic and from other important sources are necessary.

During meteorological situations where high NO_2 levels are prevailing (e.g. in winter during stationary temperature inversions), local production of secondary NO_2 is often low. At urban roadside sites, the fraction of directly emitted NO_2 from road traffic can be well above average during these situations. Therefore, a reduction of f-NO_2 has a larger effect on peak NO_2 concentrations than on annual mean NO_2 levels.

Introduction

The emissions of nitrogen oxides (NO_x=NO+NO_2) from road traffic is continuously decreasing in Switzerland and other European countries since the beginning of the 1990's. However, it is known from several studies at different European sites that the percentage of NO_x emitted from road traffic as NO_2 (f-NO_2) is increasing (e.g. Grice et al., 2009). The reason for this increase of f-NO_2 is the rising fraction of diesel vehicles in the road traffic fleet and implementation of new exhaust treatment technologies for diesel vehicles. Increasing fractions of NO_2 in the exhaust of vehicles can have implications for compliance with the existing ambient air quality standards for NO_2, mainly at urban locations that are strongly influenced by road traffic emissions.

In this study, long-term measurements of NO, NO_2 and O_3 from an urban roadside site and a nearby urban background site in Zurich (Switzerland) have been analysed for the trend of f-NO_2 and the trend of the contribution of directly emitted NO_2 to the total concentration of nitrogen dioxide at the urban roadside site.

Measurement Sites

Hourly mean concentrations of NO, NO_2 and O_3 from 01.01.1989 to 31.12.2008 measured at two nearby sites in the city centre of Zurich (Switzerland) have been analysed: One of the sites is an urban background site (Zurich Kaserne) that belongs to the Swiss National Air Pollution Monitoring Network (NABEL). The second site (Zurich Schimmelstrasse) is an urban roadside site located at a main urban transit road (27000 vehicles per day). The Zurich Schimmelstrasse measurement site is operated by the Environment and Health Department of the city of Zurich (Umwelt und Gesundheit Zürich).

Method

The hourly air quality data from the two measurement sites were analysed using the method described in detail by Abbott (2005). The approach described by Abbott (2005) is based on a mass balance for NO_2 and consideration of the two most important reactions, i.e. the reaction of nitrate monoxide and ozone to form (secondary) NO_2

$$NO + O_3 \rightarrow NO_2 + O_2 \quad (1)$$

and photodissociation of NO_2 in the presence of sunlight

$$NO_2 + h\nu\ (+O_2) \rightarrow NO + O_3. \quad (2)$$

It is shown in Abbott (2005) that at an urban roadside site the average f-NO_2 in the exhaust of the local traffic fleet can be derived from

$$[O_x]_1\text{-}[O_x]_0 = \text{f-}NO_2 \cdot ([NO_x]_1\text{-}[NO_x]_0) + \beta, \quad (3)$$

where $[O_x]_1$ is the sum of the concentrations of the oxidants NO_2 and O_3 ($O_x = NO_2 + O_3$) as measured at the roadside site, $[O_x]_0$ is the corresponding sum of simultaneously measured concentrations at the urban background site. Similarly, $[NO_x]_1$ and $[NO_x]_0$ are the measured NO_x concentrations at the urban roadside site and the urban background site, respectively. The constant β represents a remaining NO_2 fraction that accounts for reactions other than (1) and (2) and for processes such as deposition. The average f-NO_2 and the constant β can be estimated from regression of $[O_x]_1\text{-}[O_x]_0$ against $[NO_x]_1\text{-}[NO_x]_0$.

Equation (3) can be rearranged to

$$[NO_2]_1 = [NO_2]_0 + ([O3]_0\text{-}[O3]_1) + \text{f-}NO_2 \cdot ([NO_x]_1\text{-}[NO_x]_0) + \beta, \quad (4)$$

meaning that the total NO_2 concentration at the urban roadside site is subdivided into an urban background concentration $[NO_2]_0$, a contribution from locally formed secondary NO_2 ($[O3]_0$-$[O3]_1$) and a contribution from primary NO_2 emitted by the local traffic at the measurement site (f-$NO_2 \cdot ([NO_x]_1\text{-}[NO_x]_0)$).

Results

Figure 1 shows the development of the monthly average NO_2/NO_x emissions ratio (f-NO_2) of the local traffic nearby the Zurich Schimmelstrasse site for the period from 1989 to 2008. The shown f-NO_2 were estimated by linear regression of hourly values measured during each month of the considered time period (see equation 3). The f-NO_2 in the exhaust of urban road traffic was roughly constant and about 5 to 7% during the 1990's, since 2002 the percentage of NO_x emitted as NO_2 has been increasing and reached about 13% in 2008. The observed increase in f-NO_2 is in agreement with findings in other studies for European cities (e.g. Grice et al, 2008) and can be explained by an increasing fraction of diesel vehicles in the fleet and the introduction of new exhaust treatment technologies for diesel vehicles.

The estimated f-NO_2 values are used in equation 4 to calculate the average monthly contributions of the urban NO_2 background, locally produced secondary NO_2, and locally emitted primary NO_2 to total NO_2 at the urban roadside site Zurich Schimmelstrasse (Figure 2). It was found that primary NO_2 from local road traffic account only for a relatively small fraction of the total NO_2. Our analysis showed for the urban roadside site in Zurich that direct NO_2 emissions from road traffic account on annual average for about 16% of total NO_2. At this site, the ambient NO_2 is mainly determined by the urban NO_2 background (63%) and NO_2 that is produced from reaction of locally emitted NO with ozone (local secondary NO_2, 21%). The fact that these findings are in good agreement with other studies (e.g. Grice et al, 2008) indicate that they can be considered as representative for other similar urban environments in Switzerland. Consequently, a reduction of f-NO_2 in the exhaust of road traffic vehicles would have only a small effect on the average NO_2 concentration at urban roadside sites. For an efficient reduction of NO_2 levels at urban sites, further reductions of NO_x emissions from road traffic and from other important sources are necessary.

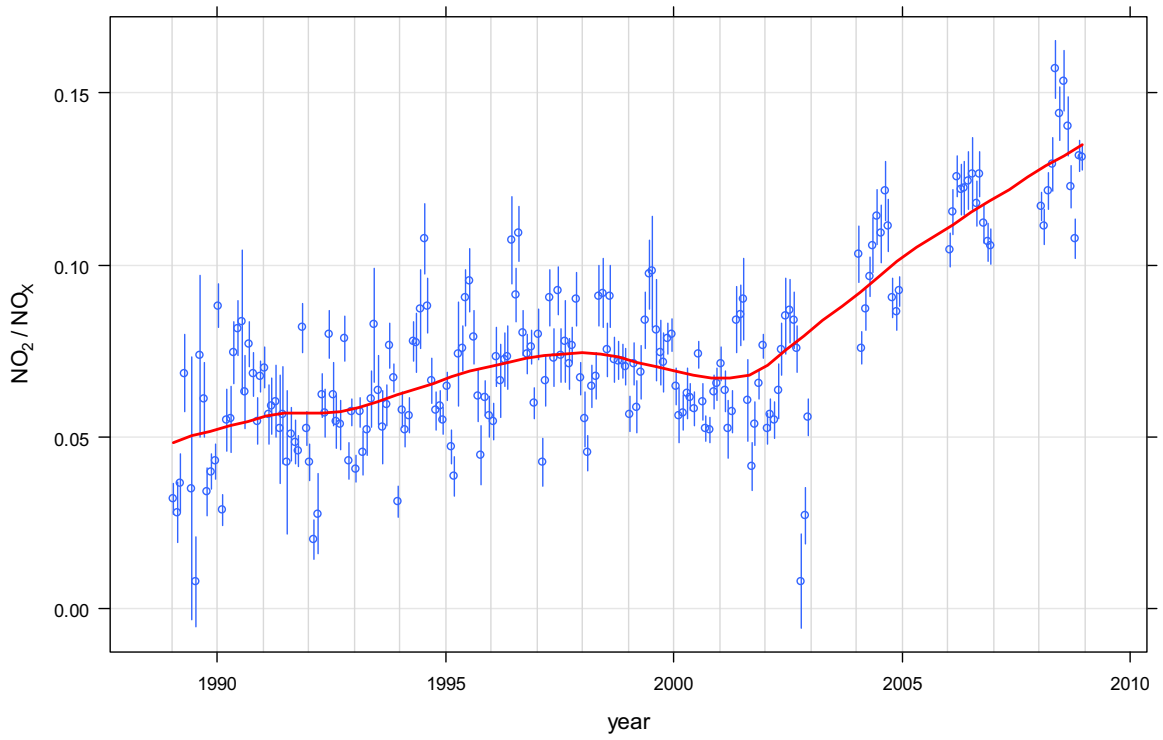

Figure 1: Trend of the monthly NO_2/NO_x emissions ratio (f-NO_2) of the urban traffic nearby the site at Zurich Schimmelstrasse for the 1989 to 2008 time period (blue circles, the vertical blue lines indicate 95% confidence intervals). The red line is a smooth trend line fitted to the monthly f-NO_2 estimates. Since 2002, the Zurich Schimmelstrasse site is operated only every second year, the values for 2003, 2005 and 2007 are therefore missing.

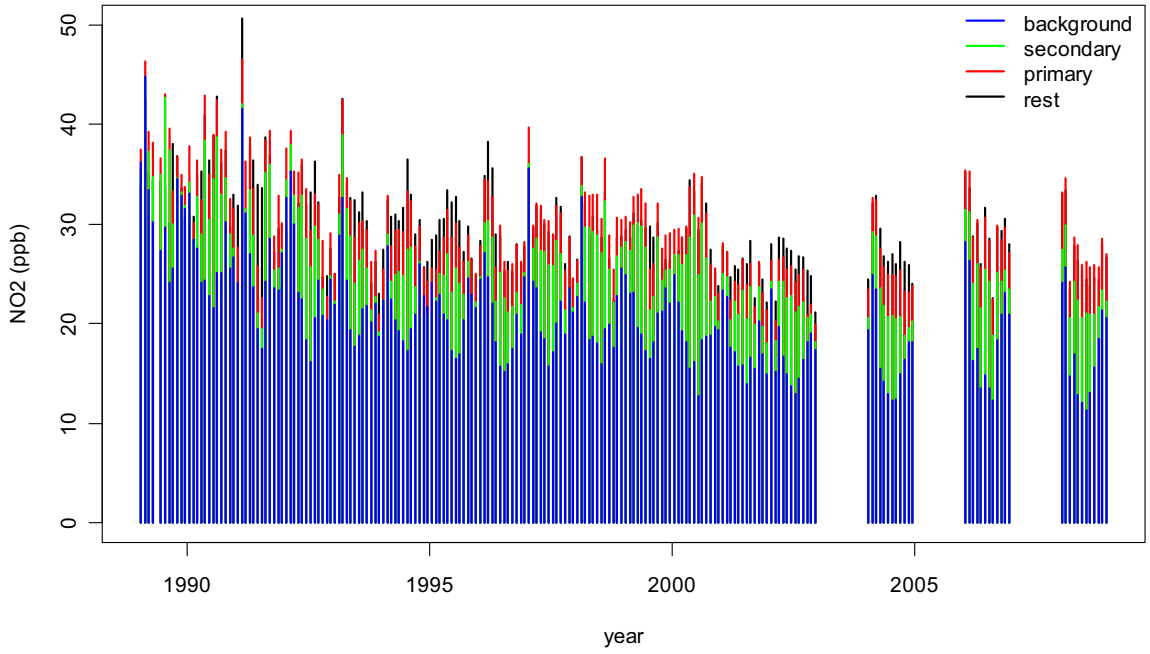

Figure 2: Average contribution of urban background NO_2, locally produced secondary NO_2, and primary NO_2 from local traffic to the total monthly NO_2 level at the urban kerbside site Zurich Schimmelstrasse (see equation 4).

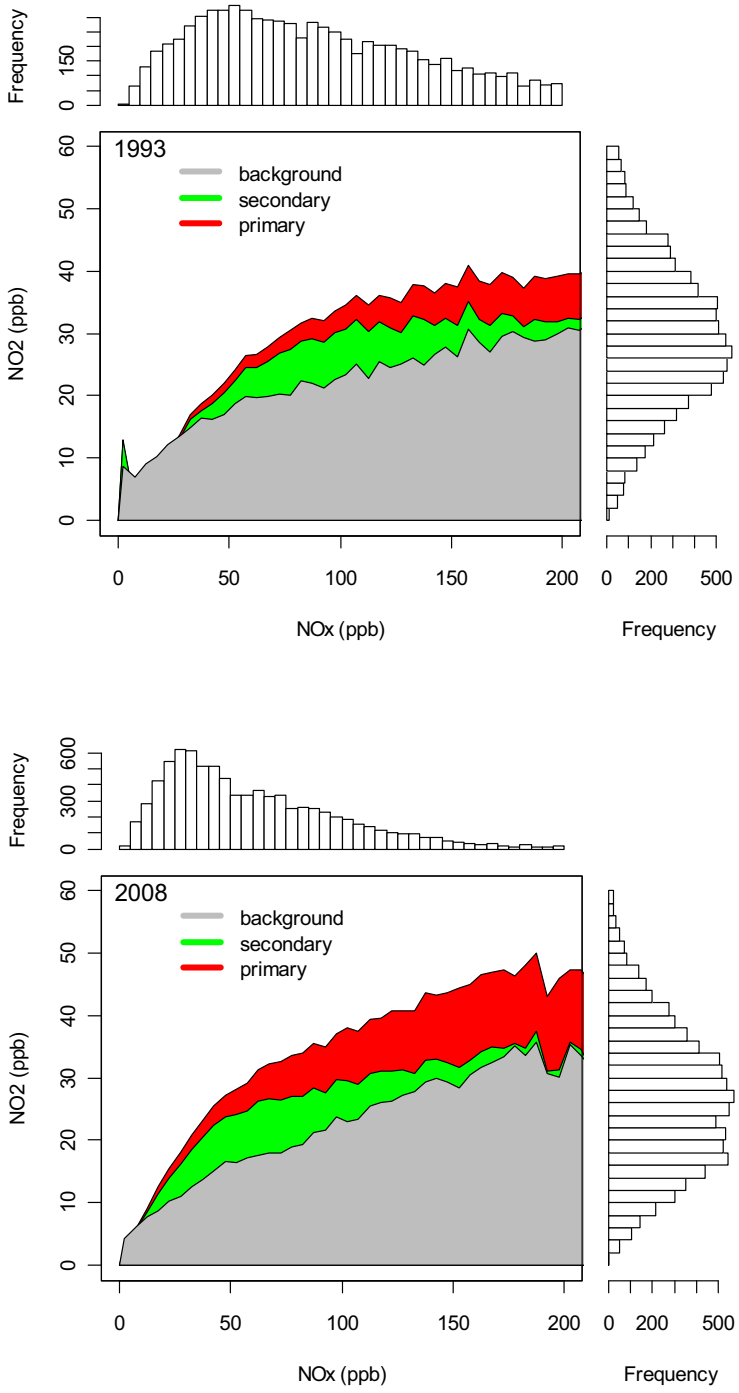

Figure 3: Dependence of NO_2 on NO_x at the urban roadside site Zurich Schimmelstrasse for the years 1993 (upper panel) and 2008 (lower panel). Total NO_2 is split into estimated contributions from the urban background as well as locally produced secondary and locally emitted primary NO_2. The average NO_2 concentrations were calculated from hourly values that were combined in 5ppb NO_x intervals. The frequency distributions of measured hourly NO_x (histogram above x-axis) and NO_2 averages (histogram right from the y-axis) are also shown.

The average contributions of urban background, locally produced secondary and locally emitted primary NO_2 was analysed in dependence of NO_x at the urban roadside site Zurich Schimmelstrasse for the years 1993 and 2008 (Figure 3). During situations where high NO_2 levels are

prevailing (e.g. in winter during stationary temperature inversions), local production of secondary NO_2 is often low and the fraction of directly emitted NO_2 from local road traffic can then be well above average. This indicates that increasing f-NO_2 has a larger effect on peak NO_2 concentrations than on annual mean NO_2.

At high NO_x levels, a clear increase of the contribution of primary NO_2 from local road traffic at Zurich Schimmelstrasse can be found for 2008 compared to 1993. This is due to the observed increase in f-NO_2. However, the frequency of NO_x peak concentrations has declined as a result of decreasing NO_x emissions during the past years.

Acknowledgement

We thank the Swiss Federal Office for the Environment (FOEN) for discussions and support.

References

Abbott, J. (2005). Primary nitrogen dioxide emissions from road traffic: analysis of monitoring data. AEA Technology, National Environmental Technology Centre, *Report AEAT-1925*. http://www.airquality.co.uk/reports/cat05/0703151041_primno2v3.pdf.

Grice S., Stedmann J., Kent A., Hobson M., Norris J., Abbott J., Cooke S. (2009). Recent trends and projections of primary NO_2 emissions in Europe. *Atmospheric Environment*, 43, 2154-2167.

City-dwellers exposure to atmospheric pollutants when commuting in Paris urban area

*H. Ravelomanantsoa[1], Y. Le Moullec[1], C. Delaunay[2],G. Goupil[2], S. Mazoué[3]**

[1] Laboratoire d'Hygiène de la Ville de Paris, 11 rue George Eastman, 75013 Paris, France, hanitriniala.ravelomanantsoa@paris.fr, yvon.le-moullec@paris.fr
[2] Laboratoire central de la Préfecture de Police, 39 bis rue de Dantzig, 75015 Paris, France, claudie.delaunay@interieur.gouv.fr, ghislaine.goupil@interieur.gouv.fr
[3] Régie Autonome des Transports Parisiens, 54 quai de la Râpée, 75599 Paris cedex 12, France, sophie.mazoue@ratp.fr

Context

Several studies in the bibliography deal with the citizen exposure in transport environments. Most of them focus on one or two most preoccupying pollutants in a few main modes of transportation. Thus, fine particulate matter exposure is the subject of many studies because of its health effects (Adams et al., 2001; Chan et al., 2002; Gulliver et al., 2004; Aarnio et al., 2005). Other studies document also specifically pollutants like carbon monoxide (Chan and Liu, 2001; Duci et al., 2003), nitrogen dioxide (Farrar et al., 2001), aldehyde (Jo and Lee, 2002) and volatil organic compounds (Lau and Chan, 2003). On the other hand, some studies focus on a particular mode of transport. Subway systems are among the best documented (Coparly, 2002; Johansson and Johansson, 2003; Seaton et al., 2005; Airparif and RATP, 2009). Exposition in the car and on the bike has also been studied for few pollutants in the Ile-de-France area (Airparif, 2008; Airparif, 2009).

This study aims at providing more complete information about the exposure levels of the Ile-de-France inhabitants when they commute in Paris area between their dwelling and their workplace, during morning and afternoon rush hour periods. The six major modes of transport used was studied for five pollutants with known sanitary interests. It has been conducted by two Parisian laboratories (LHVP[1]and LCPP[2]) and the Parisian public transport company (RATP[3]).

Methods

A significant number of contrasted situations were retained. Twenty routes were chosen implementing the main modes of transport: car, bus, subway, tramway, cycle and walking. The majority of them were in Paris; only three routes went toward the suburbs. Each route has been reproduced thirty times (fifteen round trips). Each trip lasted one hour.

The measurement campaign took place during the winter period of 2007 and 2008, a previous study (Le Moullec et al., 1998) showed that the highest levels of pollutants were observed during this period.

The selected pollutants were those coming from road traffic and public transport emissions:

- carbon monoxide,
- nitrogen dioxide,
- monocyclic aromatic hydrocarbons,
- aldehydes and acetone, which is rather a human presence indicator
- two indicators for fine particulate matter of aerodynamic diameter lower than 2.5 µm (PM2,5): weight concentration and absorption coefficient which is an indicator of black carbon level).

In addition, a specific program was implemented to characterize the grading distribution of the numerical concentration of particles having optical diameter over 0,3 µm.

Continuous measurements and active sampling methods were chosen for the samplings. Table 1 presents an overview of sampling and analytical methods used for each pollutant.

Table 1: Sampling and analytical methods

Pollutants	Samping method	Analytical method
Carbon monoxide	Continuous	Electrochemical detection
Nitrogen dioxide	Active sampling	Griess Saltzman method
Aldehydes	Active sampling	HPLC & UV spectrophotometry
Monocyclic aromatic hydrocarbons	Active sampling	Mass spectrometry
Fine particles $PM_{2,5}$	Active sampling	Gravimetry and reflectometry

Results

A total of 4209 results were validated during this study. The results of NO_2, benzene, formaldehyde and $PM_{2,5}$ are presented in the figure 1 below. Carbon monoxide results was not presented because of its low level, which was significantly detected only in the car and in the bus were median concentrations were respectively of 2,2 and 1,2 ppm.

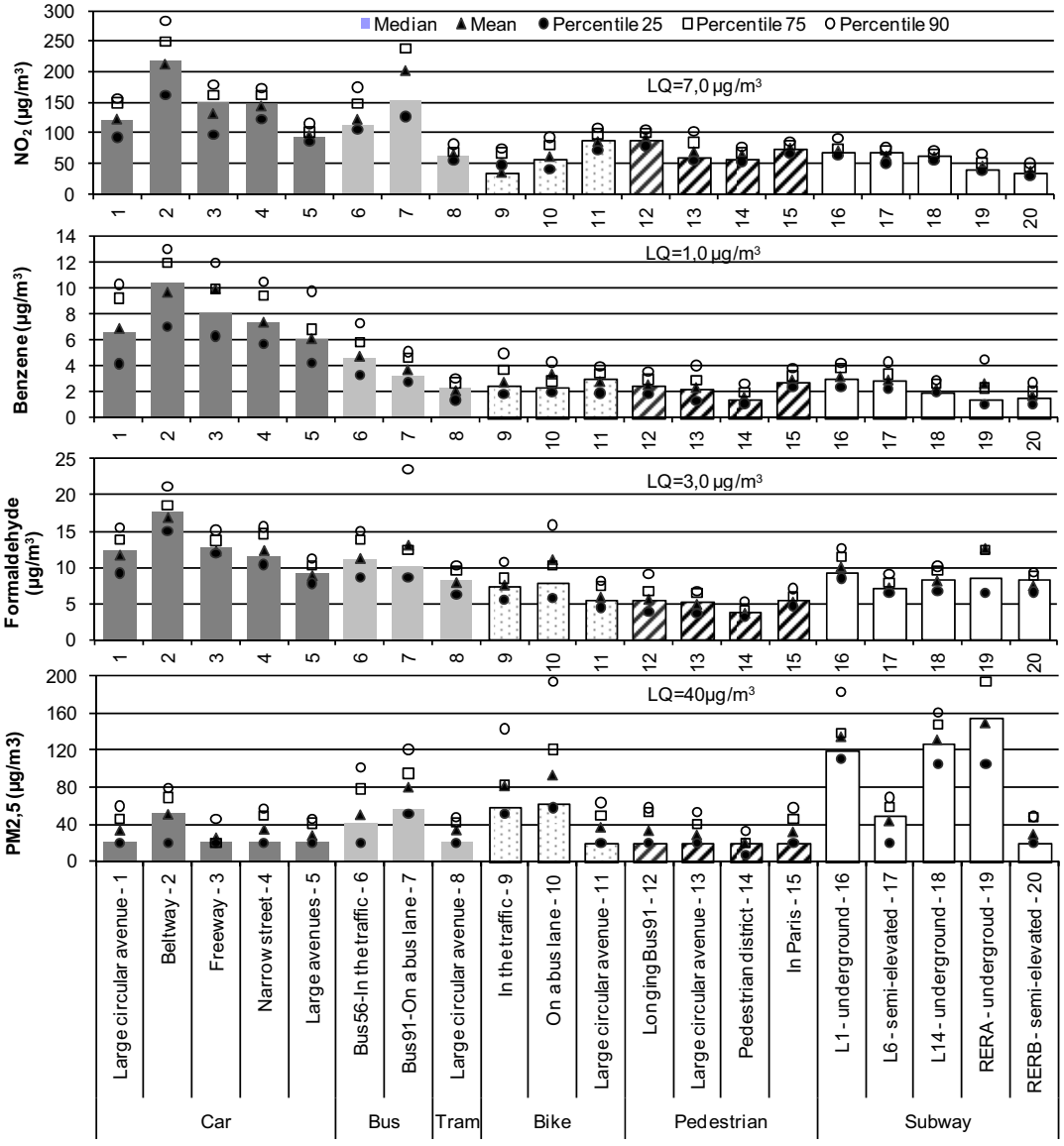

Figure 1: Distribution of NO_2, benzene, formaldehyde and $PM_{2,5}$ concentrations according to the route and the mean of transportation

Discussion

Three comparisons are carried out to discuss the results:

- comparison of exposure levels between modes of transport used during rush hours (figure 2)
- comparison of measured exposure levels with data obtained in a similar study led 10 years ago
- comparison of exposure levels with air quality standards.

1- Exposure levels for each mode of transport

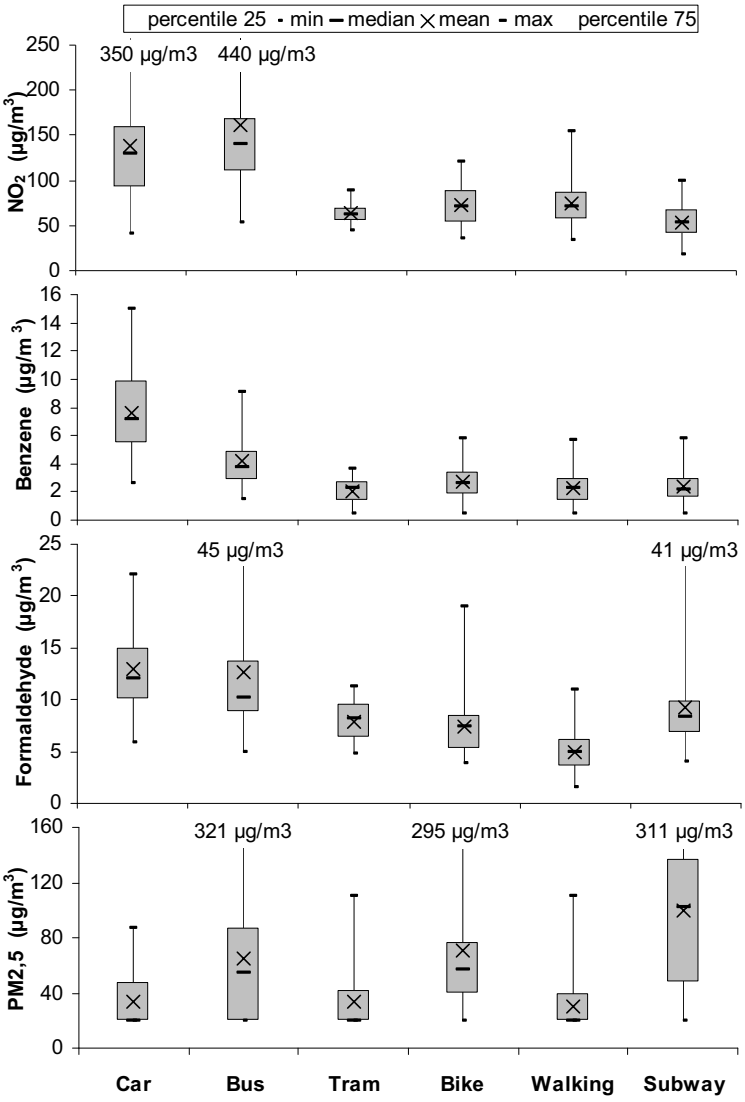

Figure 2: NO_2, benzene, formaldehyde and $PM_{2.5}$ levels according to the means of transportation used

Different levels of NO_2, benzene, formaldehyde and $PM_{2.5}$ concentrations are measured according to the main modes of transport (figure 2).

- Car users are the most exposed to the three studied gaseous atmospheric pollutants from car exhausts. Median concentrations are: 130 µg/m3 for NO_2, 7,2 µg/m^3 for benzene, 12 µg/m^3 for formaldehyde. This last pollutant is probably emitted by two sources: car exhausts and the various coatings existing inside the car. The beltway around Paris is the most polluted route with median level of NO_2 and benzene respectively at 218 and 10 µg/m^3. Median concentration of $PM_{2,5}$ in the car (< 40 µg/m^3) is not quantified by the analytical method used, except on the beltway route where median level is 52 µg/m^3 .
- Bus passengers are exposed to a pollution level close to that of car users, excluding the beltway, for NO_2, $PM_{2,5}$ and formaldehyde. Median concentrations are respectively: 140 µg/m^3,

54 µg/m3 and 10 µg/m3. Benzene level is much lower with a median concentration of 3,7 µg/m3. Moreover, aromatic monocyclic hydrocarbon concentrations are generally lower in the bus passing on bus lane than when circulating on car lane.

- Cyclists, running alongside the road, are the third most exposed to atmospheric pollution. Despite its proximity to car traffic, the "open air" situation of the cyclist exposes him to a much lower level of pollutants than the two first modes of transport. Median levels are 71 µg/m^3 for NO_2, 2,6 µg/m^3 for benzene, 7,4 µg/m^3 for formaldehyde. However, fine particulate matter concentrations are close to that of the bus, 57 µg/m^3 for $PM_{2,5}$, maybe because of resuspension phenomenon.
- Users of the Parisian subway lines are exposed to a specific fine particles emission from the rolling stocks during braking. $PM_{2,5}$ median level reaches 102 µg/m^3. Particulate matter levels are higher inside underground lines trains than in semi-elevated one (128 µg/m^3 vs <40 µg/m^3 in median). Formaldehyde concentration, 8,3 µg/m^3, is at the same level as found in other public transportation. NO_2 and benzene median levels measured in the subway are among the lowest of the study, with 54 µg/m^3 and 2,2 µg/m^3 respectively.
- Tram passenger is one of the least exposed to atmospheric pollution. Formaldehyde is the only pollutant which concentration in the tram, 8,2 µg/m^3, is comparable to these measured in other modes of transportation. Other pollutants concentrations are relatively low: 61 µg/m^3 for NO_2; 2,3 µg/m3 for benzene and inferior to 40 µg/m^3 for $PM_{2,5}$.
- Pedestrians are globally the least exposed to atmospheric pollution, taking into account the four pollutants. However, levels may vary sensibly according to the distance to car traffic. Thus, people walking in the pedestrian district of Paris, where car traffic is forbidden, are exposed to a level of pollution much lower than those going along the road. In this last situation, median levels are 79 µg/m^3 for NO_2, 2,5 µg/m^3 for benzene, 5,6 µg/m^3 for formaldehyde. In the pedestrian district, levels decrease at 56 µg/m^3 for NO_2, 1,4 µg/m^3 for benzene and 3,8 µg/m^3 for formaldehyde. Level of $PM_{2,5}$ could not be quantified for both situations.

In addition, the highest level of acetone, a human presence indicator, is of course observed in public transport. Median levels are very close, around 22 µg/m^3 in the bus, the tramway and the subway. They are lower in other modes of transportation, the lowest level corresponding to the pedestrian mode with a median concentration of 2,5 µg/m^3.

2- Evolution of levels in ten years (1998-2008)

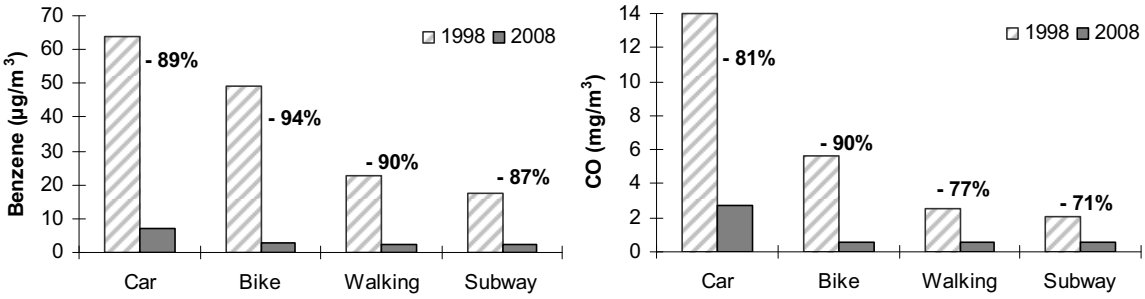

Figure 3: CO and benzene levels evolution over ten years according to the mode of transport

The results of this study are also compared with those obtained during a previous measurements campaign led in similar conditions ten years ago (Le Moullec et al., 1998) (figure 3). Carbon monoxide, benzene, toluene and black smoke indicator were followed on eleven strictly identical routes (black smoke indicator being deducted from the reflectance measurements).

A significant decrease of benzene and carbon monoxide levels is observed in ten years between the studies of 1998 and 2008 on the same routes. The CO levels have decreased by 80% whereas those in benzene fell of 90% on average. This result can be explained by the global improvement of air quality in Parisian area during the same period.

3 – Comparison of exposure levels with standards:

Measurements results are compared to recommendations of the World Health Organization guidelines (WHO, 2000), to the national air quality criteria and European directives.

NO_2 threshold is exceeded in different cases. In the passenger compartment of cars circulating on the beltway and inside the bus line 91, respectively 57% and 38% of the values exceed the hourly threshold of 200 µg/m^3 recommended by the WHO.

Concerning $PM_{2.5}$, WHO recommendations are fixed for exposures integrated on 24 hours (25 µg/m^3) at least. It is difficult to compare them to the measurements data. Particles levels measured in the Parisian underground are higher than 25 µg/m^3 during the sampling hour (mean values respectively of 135 µg/m^3, 132 µg/m^3, 150 µg/m^3 on lines 1 and 14 of the subway and line A of the regional express network).

Conclusion

This quasi-exhaustive study enables to improve the knowledge on Ile-de-France inhabitants exposure to pollution during their daily trip between their place of residence and their workplace.

A first study carried out in 1998 allowed to benefit from methodological teachings concerning the sampling strategy, by choosing the optimal measurements period, as well as the analytical methods. .

Globally, it is the car user, in particular when driving on the beltway, which is the most exposed (CO, benzene, toluene, NO_2, formaldehyde, acetaldehyde, $PM_{2,5}$ absorption coefficient) except for fine particles $PM_{2,5}$ and acetone. For these two indicators, public transport users are the most exposed, in particular subway underground lines users for $PM_{2,5}$ and buses, tramway, and subways users for acetone.

The pedestrian walking in the pedestrian area is the least exposed whatever the pollutant. The tramway user is also among the least exposed, except for acetone and formaldehyde. Other pedestrians and cyclists undergo intermediate exposure levels.

All the presented data will contribute to quantify the part of transport in the evaluation of the global exposure of the Ile-de-France inhabitants in one day. Considering the health impact of particles, it would be interesting to conduct new investigations to study the chemical composition of the $PM_{2.5}$ for each route.

Acknowledgements

This work has been co-financed by ADEME (French Environment and Energy Management Agency) – PRIMEQUAL 2 / PREDIT program.

References

Aarnio P. et al. (2005), The concentrations and composition of and exposure to fine particles (PM2,5) in the Helsinki subway system.

Adams HS, Nieuwenhuijsen MJ, Colvile RN, McMullen MAS, Khandelwal P (2001), Fine particle (PM2,5) personal exposure levels in transport microenvironments, London, UK.

Airparif (2008), Influence des aménagements de voirie sur l'exposition des cyclistes à la pollution atmosphérique, *http://www.airparif.asso.fr/airparif/pdf/Rvelo_20090217.pdf*

Airparif, Ratp (2009), Campagne de mesures à la station de métro Faidherbe-Chaligny, *http://www.airparif.asso.fr/airparif/pdf/Rratp_20090701.pdf*

Airparif (2009), Exposition des automobilistes franciliens à la pollution atmosphérique liée au trafic routier, *http://www.airparif.asso.fr/airparif/pdf/Rexpovoituredomtra.pdf*

Chan L.Y., Lau W.L., Lee S.C., Chan C.Y. (2002b), Commuter exposure to particulate matter in public transportation modes in Hong Kong, Atmospheric Environment, 36, 3363-3373.

Chan L.Y, Lau W.L., Zou S.C., Cao Z.X., Lai S.C. (2002a), Exposure level of carbon monoxide and respirable suspended particulate in public transportation modes while commuting in urban area of Guangzhou, China. *Atmospheric Environment*, 36, 5831-5840.

Chan L.Y., Liu Y.M. (2001), Carbon monoxide levels in popular passenger commuting modes traversing major commuting routes in Hong Kong. *Atmospheric Environment,* 35, 2637-2646.

Coparly (2002), Etude préliminaire de la qualité de l'air dans le métro lyonnais.

Duci A., Chaloulakou A., Spyrellis N. (2003), Exposure to carbon monoxide in the Athens urban area during commuting, The Science of the total Environment, 309, 47-58.

Farrar D., Dingle P., Tan R. (2001). Exposure to nitrogen dioxide in buses, taxis, and bicycles in Perth, Western Australia. Bull. Environ. Contam. Toxicol,66, 433-438.

Gulliver J., Briggs D.J. (2004), Personal exposure to particulate air pollution in transport microenvironments, Atmospheric environment, 38, 1-8.

Jo W-K, Lee J-W (2002), In-vehicle exposure to aldehydes while commuting on real commuter routes in a Korean urban area, Environmental research, 88, 44-52.

Johansson C., Johansson P.A. (2003), Particulate matter in the underground of Stockholm, Atmospheric Environment, 37, 3-9.

Lau WL, Chan LY (2003), Commuter exposure to aromatic VOCs in public transportation modes in Hong-Kong, *Science of the total environment*, 308 (1-3), 143-155.

Le Moullec Y, Alary R, Laurent AM, Person A, Coursimault A, Delaunay C (1998), City-dwellers exposure to atmospheric pollutants originated by cars when commuting in Paris urban area, *Proceeding of the 11th World Clean Air and Environmental Congress,* Durban South Africa.

Oramip (2008), A pied, en vélo, en métro, en bus, en voiture : quel air respirons-nous ?, *ORAMIP Infos,* n°92.

Seaton A., Cherrie J., Dennekamp M., Donaldson K., Hurley JF, Tran CL (2005), The London underground : dust and hazards to health, *Occupational and environmental medicine*, 62 (6),355-362.

WHO (2000). Air quality Guidelines for Europe, second edition, Who Regional Publications, European Series, n°91

Modeling of Exposure to Highway Traffic Exhaust in Alpine Valleys in Switzerland

R. Ducret-Stich[1,2], HC. Phuleria[1,2], M. Ragettli[1,2], A. Ineichen[1,2], C. Schindler[1,2], L.-J. S. Liu[1,2,3]*

[1] Swiss TPH, Department of Epidemiology and Public Health, CH-4002 Basel, Switzerland, regina.ducret@unibas.ch
[2] University of Basel, CH-4003 Basel, Switzerland
[3] University of Washington, [3]Department of Environmental and Occupational Health Sciences, Seattle, Washington, USA

Abstract

From November 2007 to June 2009 13 children (ages 7–13) with asthma participated in monthly monitoring of respiratory health indicators including exhaled NO and oxidative stress markers in exhaled breath condensate. Monthly indoor and outdoor NO_2 as well as outdoor PM_{10} and $PM_{2.5}$ measurements in three seasons were taken at the children's homes. During the whole study period NO_2 was measured at 13 locations spread over the community. In addition, concurrent measurements of PM_{10}, PM_1, particle number concentrations (PN), and NO_x were taken at two fixed and four mobile locations. These air pollution measurements together with selected GIS parameters are used in LUR models to estimate the home outdoor exposure. Model predictions are validated with the home outdoor measurements. PM_{10} filters are analyzed for elemental (EC) and organic carbon (OC), 48 trace elements, the diesel marker 1-nitropyrene and the wood smoke marker levoglucosan. Using receptor models such as Positive Matrix Factorization, these data are utilized to quantify contributions of trucks, gasoline cars, biomass burning and urban background sources. Model estimates and source apportionment results are then used to assess the impact of general air pollution and diesel truck exhaust on respiratory health.

Introduction

Traffic exhaust is a significant source of residential air pollution and was shown to have an impact on human health all over the world (HEI report). Especially respiratory symptoms and asthma in adults (Bayer-Oglesby et al., 2006; Künzli et al., 2009) and children (Salam et al., 2008) are associated with traffic air pollution. A previous questionnaire study with schoolchildren in Kanton Uri, Switzerland, found significant associations between dispersion estimates for PM_{10} from trucks and wheezing in the chest (OR=1.24, 95%CI: 1.01-1.52) and hay fever (OR=1.26, 95%CI: 1.05-1.52). Significant associations were also found between PM_{10} from cars and wheezing (OR=1.30, 95% CI: 1.02-1.67) (results not published).

This panel study uses a subset of 13 children with asthma living in the community of Erstfeld in Canton Uri. These children undergo comprehensive respiratory assessment including measurements of inflammation and oxidative stress makers via exhaled NO and exhaled breath condensate as well as air pollution exposure assessment.

To assess the health measurements with accurate air pollution exposures, measured or modeled air pollution concentrations are needed on a refined spatial scale. The NO_2 dispersion model used in the SAPALDIA study showed unsatisfactory performance in the Alpine regions (Liu, 2007). This paper, thus, focuses on developing land-use regression models for characterizing spatial air pollution exposures.

Methods

Study Design

This work is part of an asthma panel study done in Erstfeld, Switzerland. This Alpine community is located in a narrow valley (about 1km wide) crossed by a major highway. From November 2007 to June 2009 13 children (ages 7–13) with asthma participated in monthly monitoring of respiratory health indicators including exhaled NO and oxidative stress markers in exhaled breath condensate.

Prior to each health monitoring 14-day passive NO_2 was measured indoors and outdoors of the children's homes with Passam tubes (www.passam.ag). During the last year of the study three PM_{10} and $PM_{2.5}$ measurements spread over different seasons were taken outside of 9 homes and the highway site. We measured 14-day averages of PM_{10} and $PM_{2.5}$ collected on Teflon filters using Harvard Impactors (Air Diagnostics and Engineering, Inc., Naples, ME) with a flow rate of 4L/min by running the pump for 10 minutes per hour for 14 days.

During the whole study period 14-day passive NO_2 was measured with Passam tubes at one highway and one background station in addition to seven mobile and 9 fixed sites spread over the community. Continuous NO_2, NO_x, particle number concentrations (PN) and meteorological parameters such as wind speed and direction, relative humidity and temperature were measured at the fixed highway and background sites as well as the mobile site, which was moved every four weeks to a new location covering all four seasons per site. At the highway and mobile sites daily PM_{10} was collected on quartz filters with a high volume sampler (Digitel KHA-80) with a flow rate of 500 L/min and analyzed for elemental (EC) and organic carbon (OC) with the EUSAAR2 protocol (Cavalli et al., 2010). At the mobile station daily PM_{10} was also collected on Teflon filters using a partisol sampler (Thermo Partisol Low Volume Sampler) with a flow rate of 16.7 L/min and analyzed for 48 trace elements, the diesel marker 1-Nitropyrene and the wood smoke marker levoglucosan.

Analysis

Box plots were used to visualize the changes of passive NO_2 concentrations with the distance to the highway. Continuous measurements were averaged over the day and summary statistics were calculated for all pollutants at the highway, background and mobile sites. A land-use regression model for daily NO_2 was built using the measurements at the highway and mobile sites. We used stepwise linear regression with a significance level chosen for a covariate entering or staying in the model. Variables put into the model consisted of pollutant concentrations (NO_2 and NO_x at the background site, ozone at highway site), traffic variables (distance weighted traffic counts for light and heavy duty vehicles at the highway), geographic variables (land-use, elevation, minimal distance to the highway, main road and railway), time variables to account for weekly cycles (sin(t) and cos(t), with $t=2\pi$*date/7) and meteorological variables (relative humidity, temperature, air pressure, wind speed and direction). Daily wind speed and direction was calculated with the vector sum of hourly wind speed and directions. Variables were kept in the model if the parameter estimates were not contradicting physical laws and no collinearity between the variables was present. The model was then used to predict daily NO_2 at all fixed and home sites. Passive NO_2 measurements at all sites were then compared with matched 14-day averages of the predicted daily concentrations. All statistical analyses were performed with SAS9.2 (SAS Institute Inc., Cary, NC).

Results

NO_2 concentrations from passive measurements are plotted by distance to the highway in Figure 1. They drop from 33.4µg/m^3 at the highway site to background levels (around 22µg/m^3) within 100 meters from the highway. The mobile site at 49m distance shows lower concentrations because the highway runs through a tunnel at this location. The very low concentrations at 250m and 979m were measured at the homes of the child who lives outside the village at higher elevation.

Not only NO_2, but other pollutants too show a spatial gradient. EC and PN measurements were higher at the highway site than the mobile and background sites, whereas PM_{10} and OC were more homogeneously distributed (Table 1). All pollutants showed seasonal patterns with higher concentrations in winter than in summer (Table 1).

The land-use regression for daily NO_2 estimates had a model R^2 of 0.91. The main part was explained by NO_2 concentrations at the background site (part. R^2=0.77) together with distance weighted traffic counts for heavy duty (partial R^2=0.11) and light duty vehicles (partial R^2=0.02). Other variables staying in the model were temperature, wind speed, background NO_x, elevation, air pressure, wind direction and a weekly time term (sin). This model was then used to predict daily NO_2 concentrations for all sites. To evaluate the model estimates matched 14-day averages were compared with the passive measurements at each site. This comparison

showed R^{2}'s between 0.66 and 0.97 for the different sites. Only the two homes which are located above the village had R^{2}'s of 0.25 and 0.

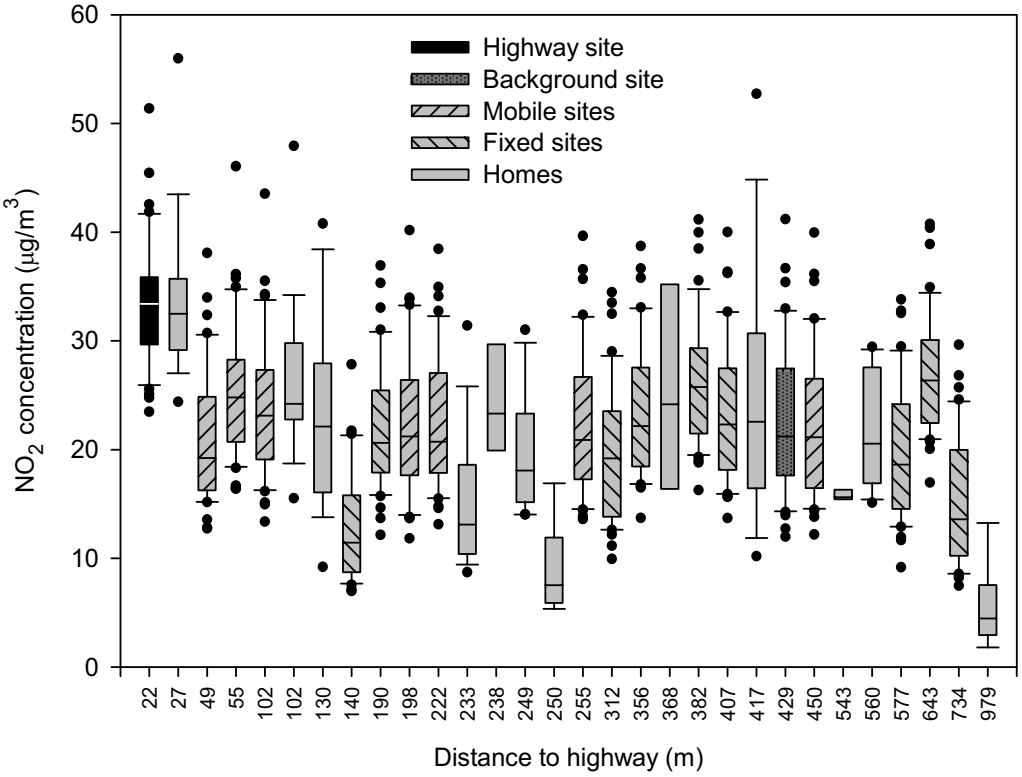

Figure 1: NO_2 concentrations from passive measurements at all sites.

Table 1: Mean pollutant concentrations at highway, mobile and background sites by season and over the whole study period.

Pollutant		**Highway** Mean (SD)	**Mobile** Mean (SD)	**Background** Mean (SD)
NO_2 (µg/m^3)	Summer	27.1 (6.7)	18.5 (5.6)	16.2 (6.0)
	Winter	39.8 (15.1)	31.5 (13.9)	30.8 (13.7)
	Overall	32.7 (12.6)	23.4 (11.5)	22.6 (11.8)
PM_{10} (µg/m^3)	Summer	14.0 (6.2)	12.6 (5.9)	N/A
	Winter	21.8 (12.6)	20.5 (12.5)	N/A
	Overall	17.7 (10.6)	16.6 (10.8)	N/A
EC (µg/m^3)	Summer	1.50 (0.49)	1.02 (0.43)	N/A
	Winter	1.93 (1.01)	1.50 (0.87)	N/A
	Overall	1.59 (0.81)	1.16 (0.71)	N/A
OC (µg/m^3)	Summer	3.10 (1.09)	3.49 (1.19)	N/A
	Winter	4.25 (2.16)	4.21 (2.01)	N/A
	Overall	3.39 (1.65)	3.52 (1.58)	N/A
PN (#/cm^3)	Summer	14,470 (6,964)	8,799 (2,758)	7,805 (2,570)
	Winter	19,236 (9,849)	10,634 (6,319)	9,441 (5,116)
	Overall	16,094 (8,192)	9,091 (4,495)	8,187 (4,014)

We also did a sensitivity analysis to see if the highway measurements had a too big influence on the model. For this purpose we removed the highway measurements form the training data. The resulting model was only slightly different form the model described above and had also a model R^2 of 0.91. Main predictor was again background NO_2 (partial R^2=0.89). Compared with the passive measurements at all the sites, this model performed slightly worse than the model above.

Discussion

We found gradients in concentrations with the distance to the highway for NO_2, EC and PN, which mainly represent the traffic sources. NO_2 concentrations decreased within about 100m to background levels. Similar results were reported before for NO_2, black carbon and ultrafine particle counts (Gilbert et al., 2003; Zhou and Levy, 2007; Beckerman et al., 2008). PM_{10} and OC showed a more homogeneous distribution. These pollutants are likely influenced by additional local sources *e.g.* dust from the work at the NEAT site or wood smoke from the heating in winter. All pollutants showed a seasonal pattern with higher concentrations in winter than in summer. In addition to residential heating in winter, trapping of the air pollutants in the valley due to inversions, lead to higher concentration levels.

Land-use regression models are widely used to predict air pollution exposure in residential areas (Ryan and LeMasters; 2007). Our daily NO_2 model was mainly influenced by the background levels and the traffic counts from the highway pointing to the importance of the highway traffic in this narrow valley. Although we had only eight sites to built the model, performance at the 13 fixed and other 12 home sites was very good. Exceptions were the two home locations at higher elevations, for which predictions were not satisfactory. Because we did not have measurements at higher elevations in our training data, the model could not capture these special cases.

Models for the other pollutants are currently being developed. Receptor models such as Positive Matrix Factorisation will be applied to quantify contributions of different local and regional sources e.g. trucks, gasoline cars, biomass burning and urban background sources. These results together with the model estimates will then be used to assess the impact of total air pollution as well as source specific (e.g. diesel truck exhaust) exposures on children's respiratory health.

References

Bayer-Oglesby L., Schindler C., Hazenkamp-von Arx M.E., Braun-Fahrländer C., Keidel D., Rapp R., Künzli N., Braendli O., Burdet L., Liu S.L.-J., Leuenberger P., Ackermann-Liebrich U., (2006), Living near main streets and respiratory symptoms in adults: The swiss cohort study on air pollution and lung diseases in adults, *Am J Epidemiol* 164:1190–1198.

Beckerman B., Jerrett M., Brook J.R., Verma D.K., Arain M.A., Finkelstein M.M., (2008), Correlation of nitrogen dioxide with other traffic pollutants near a major expressway, *Atmos Environ*, 42:275–290.

Cavalli F., Viana M., Yttri K. E., Genberg J., and Putaud J.-P., (2010), Toward a standardised thermal-optical protocol for measuring atmospheric organic and elemental carbon: the EUSAAR protocol, *Atmos Meas Tech*, 3: 79–89.

Gilbert N.L., Woodhouse S., Stieb D.M., Brook J.R. (2003), Ambient nitrogen dioxide and distance from a major highway, *Sci Total Environ,* 312:43–46.

HEI Panel on the Health Effects of Traffic-Related Air Pollution, (2010), Traffic-Related Air Pollution: A Critical Review of the Literature on Emissions, Exposure, and Health Effects, *HEI Special Report 17*, Health Effects Institute, Boston, MA.

Künzli N., Bridevaux P.-O., Liu S.L.-J., Garcia-Esteban R., Schindler C., Gerbase M.W.,Sunjer J., Keidel D., Rochat –T., (2009), Traffic-related air pollution correlates with adult-onset asthma among never-smokers, *Thorax*, 64:664-670.

Liu L.J., Curjuric I., Keidel D., Heldstab J., Kunzli N., Bayer-Oglesby L., Ackermann-Liebrich U., Schindler C., (2007), Characterization of source-specific air pollution exposure for a large population-based Swiss cohort (SAPALDIA), *Environ Health Perspect* 115(11):1638-1645.

Ryan P.H., LeMasters G.K., (2007), A Review of Land-use Regression Models for Characterizing Intraurban Air Pollution Exposure, *Inhalation Toxicology*, 19(1 supp 1):127 - 133.

Salam M.T., Islam T., Gilliland F.D, (2008), Recent evidence for adverse effects of residential proximity to traffic sources on asthma, *Curr Opin Pulm Med,* 14:3-8.

Zhou Y., Levy J.I., (2007), Factors influencing the spatial extent of mobile source air pollution impacts: A meta-analysis, *BMC Public Health*, 7:89.

Session 4: New Technologies

Performance of Clean City Bus Technologies in Real World Traffic

S. Hausberger[1], W. Stadlhofer[1] , J. Blassnegger[1], M. Rexeis[1], A. Flanschger[2]*

[1] University of Technology Graz, Institute for Internal Combustion Engines and Thermodynamics; Inffeldgasse 21a, A 8010 Graz; hausberger@ivt.tugraz.at

[2] *University of Technology Graz, Institute of Business Economics and Industrial Sociology; Kopernikusgasse 21, A 8010 Graz; andreas.flanschger@tugraz.at*

Abstract

More stringent emission limits for heavy duty vehicles as well as tightened air quality limits have stimulated the development of advanced technologies for emission reduction of trucks and buses. An assessment of the behaviour of the various technologies in real world bus driving is hardly possible by the actual type approval procedure since the actual type approval cycle does not represent urban driving very well. However, sound information on the performance in real world service operation is needed to select a suitable solution for the local bus fleet from the numerous technological options.

In the project ICUT (Innovative Clean Urban Transport, an A3plus project funded by the Austrian BMVIT and FFG), different clean bus technologies were analysed, tested and developed. The project partners were Shell, Haberkorn Ulmer, Ceram, RTA, FVT, GrazAg, Watzke, the University of Klagenfurt and the Kf University of Graz. The following topics were covered in the project:

- Expectations of customers for clean bus technologies
- Emission levels of OEM EURO II up to EEV buses with diesel and CNG engines in real bus cycles
- Retrofitting of particle filters and SCR systems, low ash lube oils and alternative fuels

An important result of the project was that type approval procedures for retrofit systems should also assess the minimum exhaust gas temperature level for the durable operation of the systems. This temperature range has to be a criterion in the selection of the proper retrofit system. The low exhaust gas temperatures in typical city bus operation can lead to incomplete regeneration of particle filters and to low NO_x-conversion levels of SCR systems. Insufficient DPF regeneration can cause an overloading and consequently can damage the filters during the next regeneration. In the project ICUT, a SCR retrofit system was also developed. This system was implemented in a city bus in Graz and tested on the chassis dynamometer and in real world service operation.

Expectations of customers for clean bus technologies

An extensive opinion poll was conducted by TU Graz, and the Institute of Business Economics and Industrial Sociology. More than 1000 people where surveyed on their suggestions for improvement in the city bus system, on their awareness level and on their ranking of existing clean bus technologies and on their satisfaction with the existing bus system (Flanschger et al., 2010).

The main reason why passengers chose the bus was environmental protection (Figure). Concerning the question on which measure would cause a person to take the bus more frequently, lower fares were rated as the most attractive measure followed by higher frequencies of the buses and by more environmentally friendly buses in third place.

It was concluded from this survey that people regard the bus systems as an option for environmentally friendly city transport, although most of the buses in Graz are rather old EURO III diesel buses without efficient exhaust gas after treatment. Obviously, investments in clean city bus technologies can be an incentive for citizens to use public transport more frequently.

However, the analysis of the answers concerning the rating of environmentally friendly technologies showed that only diesel particle filters (DPF) are really commonly known and have a very positive image. Hydrogen was second in the rating on environmental friendliness followed by DeNOx catalysts. However, only 25% have ever heard about DeNOx catalysts. Even the fuel cell was better known with 45% of persons stating that they had heard about this technology while 95% have heard about DPF.

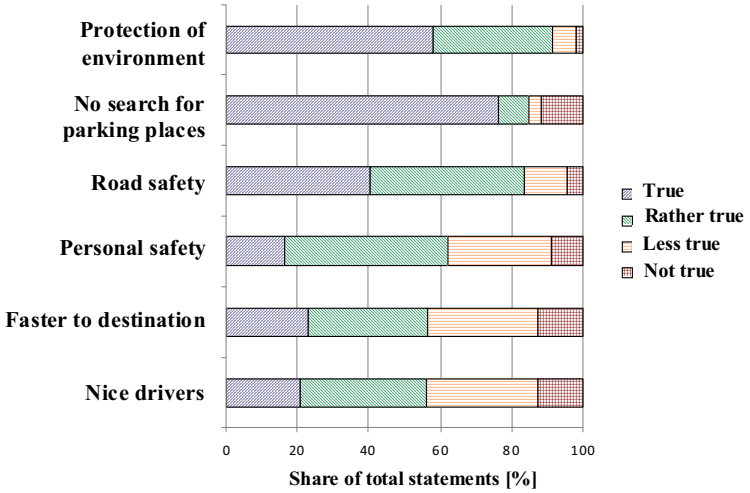

Figure 1: Result of the poll on which measures would lead to more frequent usage of the city bus system.

Exhaust gas legislation

The limit values for exhaust gases from heavy duty vehicles (HDV) have been reduced for EURO V for NO_x by 60% and for PM by 80% compared to EURO III legislation. HC and CO from HDV proved to already be at a very low level for EURO III engines. Thus, EURO V and EEV buses – which have to fulfil lower PM limits than EURO V – are expected to be quite clean technologies.

However, the type approval cycles – in which the particular emission limit values have to be fulfilled - focus only on particular operation patterns of heavy duty engines (HDE). In these cycles, the engines are driven in defined engine power and engine speed curves and the emissions are then related to the positive engine work during the test cycle [g/kWh]. From EURO I up to EURO V, the test cycles changed from the R49 cycle to the ESC to ESC&ETC. All of these test cycles reflect quite well the share of the engine load distribution of European HDV driving which is dominated by highway driving. As a result, the test cycles are located most of the time in the engine speeds typical for 80 to 88 km/h vehicle speed with varying engine power demand (Figure). Furthermore, the ETC is started after full load pre conditioning, i.e. with hot exhaust gas after treatment systems.

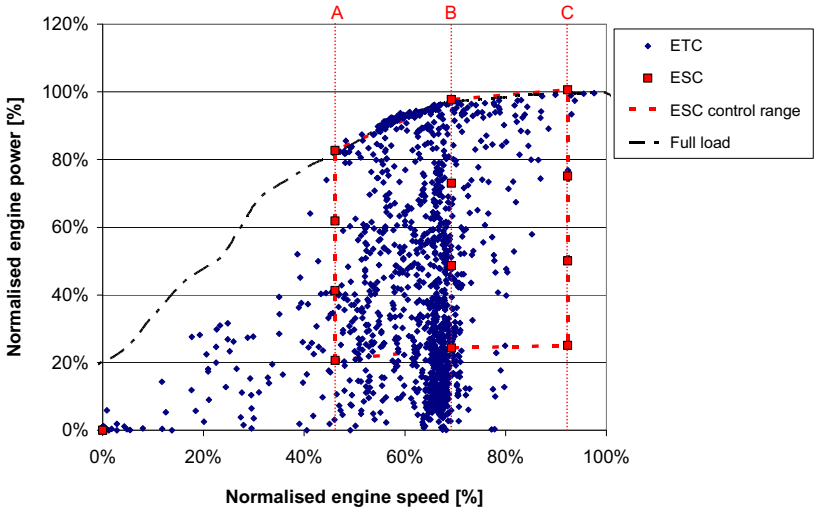

Figure 2: Test points in the ESC and in the ETC, where each point in the ETC represents one second in the test cycle.

A disadvantage is that driving conditions, as they typically occur in city buses with automatic gear boxes, are not covered very well by the ESC and by the ETC. Modern engines can be operated quite differently in individual regions of the engine map due to the fact that all relevant systems are electronically controlled. As a consequence, the emission levels achieved in the ETC are not necessarily representative of the emissions in real world bus operation.

Real world emission levels of city buses

At TU Graz, 10 city buses with EURO IV, EURO V and EEV type approval were measured on the chassis dynamometer for HDV in the Braunschweig cycle and in the HBEFA 9040 cycle, which are real world bus cycles (Hausberger et al., 2010). Additionally, data on more than 100 HDV and HDE from the ARTEMIS project were used to simulate the emission levels of city buses from EURO I to EURO III in city bus cycles (Rexeis et al., 2005). The comparison of all city bus concepts showed a clear trend towards lower emission levels of PM, HC and CO from EURO I to EURO V. For PM in particular, the introduction of a wall flow DPF led to emission levels even below the emissions of CNG buses (Figure). For NO_x, a trend towards lower emissions was visible. EURO V had on average approximately 50% less NO_x emissions than EURO III. However, single EURO V models showed a similar NO_x level to EURO III in the 9040 cycle, which is a rather low engine load city bus cycle. The variation of the performance of DPF and Selective Catalytic Reduction (SCR) systems is discussed in the next chapter.

CNG buses had lower PM and NO_x emissions compared to diesel buses up to EURO III. EEV buses showed similar low emissions as CNG and diesel. Thus, the advantage of CNG was reduced due to the introduction of DPF and SCR after treatment systems in diesel buses. However, the bus with the lowest NO_x emissions tested was an EEV CNG vehicle.

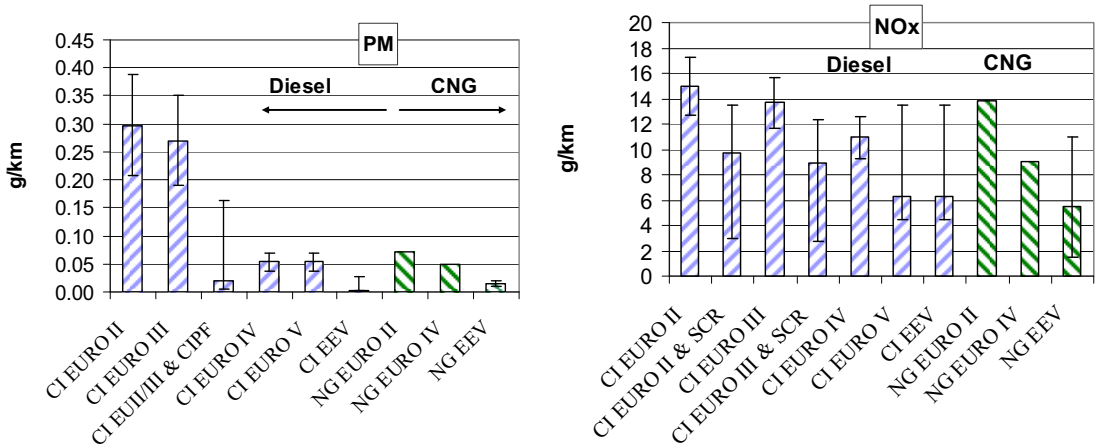

Figure 3: Average emission levels of city buses in the HBEFA 9040 cycle (bars show the scattering between highest and lowest emitting make and model)

Using FAME as fuel for diesel buses resulted in lower PM but increased NO_x. GTL was found to reduce all exhaust gas components. The low ash Shell Rimula R6 LME 5W-30 tested in the field tests proved to reduce fuel consumption by approximately 1% compared to standard oil qualities and enlarged the periods between ash removals from the DPF. More details can be found in (Hausberger, 2010).

For EURO VI, the emission limits for both PM and NO_x will be reduced by approx. 70% and 80% respectively compared to EURO V. Additionally, new type approval cycles will be introduced (WHTC and WHSC), which cover low engine loads much better than the ETC and which include a cold start, too. Thus, we can expect much lower emission levels for EURO VI vehicles than for EURO V vehicles in real world bus cycles as well (Rexeis, 2009).

Real world operation of SCR and DPF

The efficiency of SCR systems in NO_x reduction depends on the exhaust gas temperature. Starting from approximately 180°C, the efficiency reaches its maximum at approximately 300°C. Additionally, the SCR needs NH_3 as a reductant for NO_x. The NH_3 is gained from an aqueous dilution of urea (AdBlue) via hydrolysis and thermolysis. When the AdBlue is injected into the exhaust stream without additional measures, exhaust gas temperatures of more than 200° are typically necessary to prevent accumulations of depositions of by products in the exhaust line. SCR activity at low temperatures can be improved by means of hydrolysis catalysts (for the improvement of NH_3 generation from AdBlue) and the application of a diesel oxidation catalyst (to increase the share of NO_2 in the exhaust gas to improve the DeNOx in the SCR catalyst). However, these measures to improve SCR efficiency at low exhaust gas temperatures add costs to the SCR system and thus are not generally used.

The efficiency of wall flow DPFs is not directly influenced by the exhaust gas temperature level. To regenerate the soot trapped in the DPF, exhaust gas temperatures of more than approx. 280°C are typically necessary if NO_2 is used to oxidise the soot and more than 500°C are necessary to oxidise the carbon with oxygen. Due to the much lower NO_2 concentration in the exhaust gas compared to the O_2 concentration, O_2 leads to much faster soot oxidation. Even with O_2, the threshold temperature has to be exceeded for longer periods to initiate oxidation. Without sufficient oxidation, the soot accumulates in the DPF and leads to increased exhaust gas backpressure. This leads to higher fuel consumption and can harm the engine. The most probable negative impact, however, seems to be an overloading with soot which leads, in the case of uncontrolled regeneration, to local temperature peaks and thermal stress which can cause damage to the filter. Cordierite, in particular, is sensitive to these events.

Due to the high thermal efficiency of the diesel engines, the exhaust gas temperature levels are generally low in urban driving. Figure shows the measured exhaust temperature course of a city bus line in Graz (left graph) and the distribution of the temperature within this trip (right graph). It can be seen that the exhaust gas only had sufficient temperature to have an SCR system active approx. 50% of the time, if no hydrolysis catalyst was used. For active regeneration of a DPF, the temperature distribution of this city bus line was not sufficient, even at rather hot ambient temperatures. Newer engine concepts show rather lower exhaust gas temperatures due to their higher thermal efficiency. Thus, the exhaust gas temperature is a very demanding boundary condition for after treatment systems in OEM buses as well as for retrofit systems.

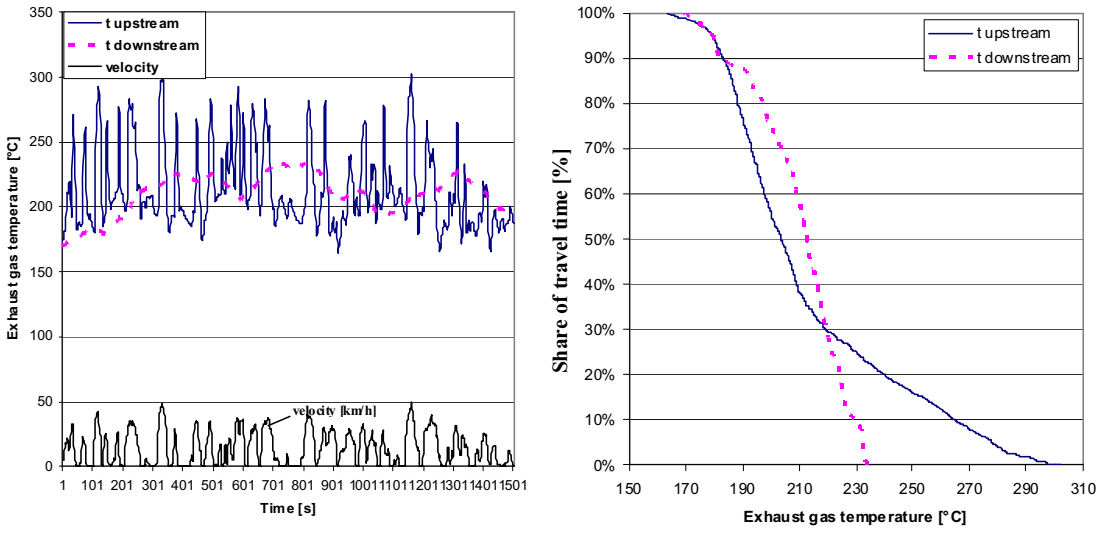

Figure 4: Exhaust gas temperature upstream and downstream of a retrofit SCR for a EURO II city bus measured on a bus line in Graz at 25°C ambient temperature

As a result of the low temperature levels, some of the DPF tested in field operation in the ICUT project showed cracking, most likely due to thermal stress after phases with insufficient regeneration. These defects reduced the filtration efficiency on average by 50% (Figure). Partial flow filters showed no malfunctions during the two years of field tests. However, after

insufficient regeneration, the increased pressure drop in the filter medium in the system reduced the share of exhaust gas volume flow through the filter medium. As a result, the efficiency was also found to be reduced by approximately 50% after long periods with insufficient exhaust gas temperature.

In the ICUT project, a retrofit SCR system was developed, which uses a Bosch AdBlue injection system, a CERAM catalyst, a canning from RTA, one or two NO_x Sensors, a mass flow sensor, temperature sensors and a micro controller board. A feed forward control strategy based on one NO_x sensor and the exhaust temperature signal was developed as well as a closed loop control algorithm using two NO_x sensors. The system was tested on the engine test bed and retrofitted in a EURO II city bus. This set up was measured on the chassis dynamometer and in the regular service line in Graz. In the basic configuration, no oxidation catalyst and no hydrolysis catalyst upstream of the AdBlue dosing were used. The control strategy of the SCR system was set to 70% conversion ratio in the ETC, defined by the function for the target feed ratio ($\alpha = \dot{n}_{NH3} / \dot{n}_{NOx}$).

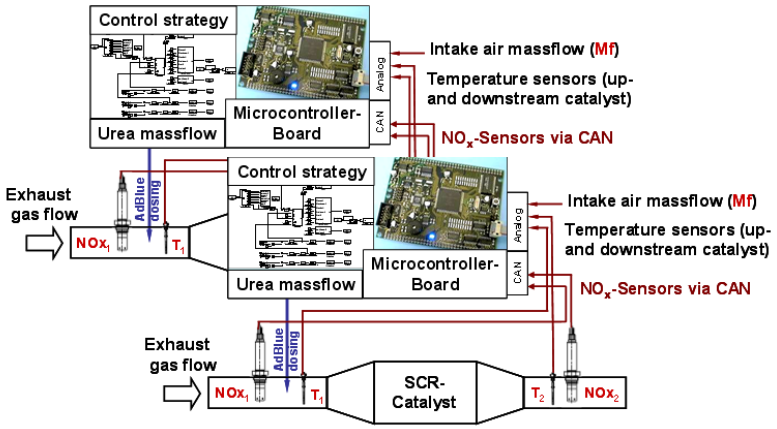

Figure 5: Schematic diagram of the ICUT SCR retrofit system

Due to the high exhaust gas temperature in the ETC, the ICUT SCR system was in favorable operating conditions during the entire test. Mounted in the city bus, the exhaust gas temperature dropped in the Graz bus line on average by 25% compared to the ETC test. As a result, the AdBlue dosing was reduced by the control algorithm in many phases of the cycle and the SCR conversion efficiency dropped by approx. 50% compared to the ETC results. In winter and on some low load lines, even lower temperature levels can occur. This would result in further reduced NO_x conversion efficiencies.

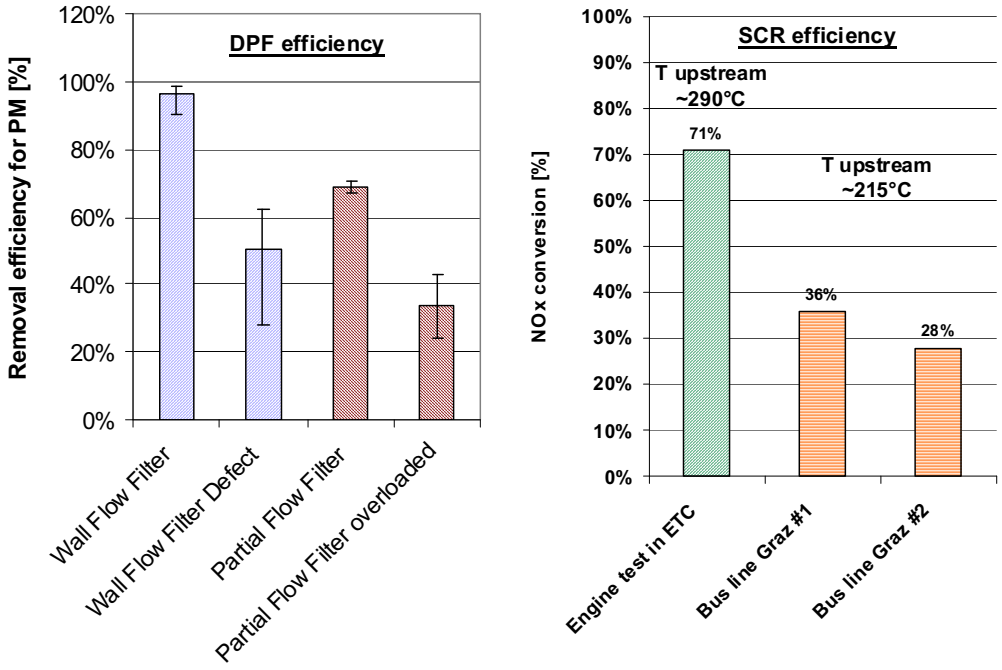

Figure 6: Efficiencies of DPF and SCR systems measured in city bus cycles in Graz

Similar effects were also found during the tests on OEM diesel buses equipped with SCR systems. In low load conditions, SCR efficiency can be worse due to the low exhaust gas temperature. This effect explains the rather high NO_x emission levels of some of the tested city buses in Figure . Kleinenbrahm (2010) reported similar results for PEMS measurements on board of city buses in German cities. In this case, the NO_x emissions varied greatly on different bus lines depending on the exhaust gas temperatures.

Summary and conclusions

The type approval cycle for EURO III to EURO V HD engines focuses on rather high engine load and high exhaust gas temperature levels and does not represent real world bus operating conditions very well. As a result, the efficiency of SCR systems can be much lower in real world city bus cycles than measured in the ETC cycle on the engine test bed. Measures to increase SCR efficiency at low exhaust gas temperatures add costs and are not needed in today's type approval. Thus, several systems are not optimised for typical bus operating conditions. Since low pollutant emissions are expected for new city bus fleets, this situation makes tests with PEMS or on the chassis dynamometer necessary to evaluate the real world performance of the different makes and models under consideration. The EURO VI legislation is expected to improve this situation very much and should lead to low emission levels in almost every city cycle.

For DPF and SCR retrofit systems, the typical driving conditions for city buses are even more challenging than for the OEM systems. Retrofit DPF without equipment for active filter regeneration can be damaged if the exhaust gas temperature is not sufficient for passive regeneration in all bus lines during every season of the year. All retrofit SCR systems will show high efficiencies in the ETC test cycle while performance can be completely different in typical city bus cycles. This influence of the exhaust gas temperature has to be taken into consideration when selecting appropriate systems for a city. Temperature profiles should be measured on the bus lines during the cold season and the best options for these conditions have to be discussed with manufacturers.

For type approval tests of retrofit systems, changing to low load cycles as soon as possible (e.g. the WHTC from EURO VI) and mandating a test for the lower temperature treshold for proper operation should be considered. Otherwise, we may find systems on the road, which are a quite expensive ballast without reasonable functionality in buses.

References

Flanschger A., Pfleger P. (2010) Saubere Stadtbustechnologien Nachrüstlösungen und Neufahrzeuge, Endbericht aus dem Projekt ICUT, Teil Kundenakzeptanz und innovatives Marketing, TU Graz, Institut für Betriebswirtschaftslehre und Betriebssoziologie

Hausberger S., Stadlhofer W., Blassnegger J., Rexeis M., et.al. (2010) Saubere Stadtbustechnologien Nachrüstlösungen und Neufahrzeuge, Broschüre aus dem Projekt ICUT, TU Graz, Institut für Verbrennungskraftmaschinen und Thermodynamik

Kleinebrahm M. (2010) Messergebnisse aus Untersuchungen unterschiedlicher Fahrzeugkonzepte im realen Linienbetrieb, presentation from TÜV NORD Mobilität GmbH & Co. KG, *NO_2 Conference Heidelberg*

Rexeis M. (2009) Ascertainment of Real World Emissions of Heavy Duty Vehicles. Dissertation, Institute for Internal Combustion Engines and Thermodynamics, Graz University of Technology

Rexeis M, .Hausberger S, Riemersma I., et.al. (2005) Heavy duty vehicle emissions, Final Report of WP 400 in ARTEMIS (Assessment and Reliability of Transport Emission Models and Inventory Systems), DGTREN Contract 1999-RD.10429, University of Technology, Graz, report no. : I 02/2005/Hb 20/2000 I680

Emissions Control Systems and Climate Change Emissions

J. May, D. Bosteels and C. Favre*

Association for Emissions Control by Catalyst (AECC), Boulevard Auguste Reyers 80, B-1030 Brussels, Belgium, info@aecc.eu

Introduction:

The effectiveness of emissions control technologies for reducing emissions of key air pollutants, especially oxides of nitrogen and particulate matter, is well known and is demonstrated by the overwhelming use of such systems to control emissions from cars, vans, trucks, buses, and motorcycles, and increasingly on construction machinery, tractors, ships, recreational boats, and railway locomotives and railcars.

The effect of engines, vehicles and machinery on emissions classed as relevant to climate change is now a significant element in their design. In Europe only CO_2 emissions have been considered in this respect, although the US is now looking at emissions of other climate-relevant emissions. Emissions control systems can have an effect on CO_2 emissions, depending on the engine, emissions system and calibration used – experience with cars shows that the average effect of an efficient diesel particulate filter on a new car is near-neutral, and experience with heavy-duty vehicles shows that use of SCR systems allows more fuel-efficient engine calibration with a consequent reduction in both CO_2 emissions and operating costs.

The effect of emissions control systems on other climate-relevant gases has not, so far, been fully considered. Measurements undertaken by AECC indicate that the potential for reduction of Black Carbon emissions may be particularly significant.

The Positive Impact of Emissions Control on Air Quality

Combustion engines emit reactive hydrocarbons, carbon monoxide (CO), oxides of nitrogen (NOx), and particulate matter (PM) including ultrafine particles. They are a key contributor to local air pollutants. Toxic emissions from transport adversely affect air quality both in the immediate vicinity ('at the kerbside'), in the local area and regionally. Modelling studies indicate that in many areas urban air quality will not meet standards for PM and NO2 in the 2010-2015 timeframe, and this is borne out both by the numerous requests submitted to the European Commission for time extensions to meet the Air Quality Standards and by the European Environment Agency's NEC Directive Status Report (European Environment Agency, 2009), which indicates that 12 Member States currently do not expect to meet their 2010 NOx target.

Emissions control systems produce major reductions in pollutants affecting air quality. Three-way catalysts are used to control CO, hydrocarbon (HC) and NOx emissions from petrol-engined vehicles. Oxidation catalysts control CO and HC from diesel engines. Selective Catalytic Reduction (SCR) is now widely used on new heavy-duty (truck/bus) diesel engines to control NOx emissions whilst allowing a benefit on fuel consumption and CO_2 emissions, and this technology is now starting to appear on cars. An alternative system (Lean NOx traps – LNT) is also in use on diesel and direct-injection petrol cars. Finally, new light-duty diesel vehicles are now fitted with particulate filters which very efficiently remove sooty particulate matter, including the ultrafine particles. Some buses are already using this technology, and it is expected that from 2014 all heavy-duty vehicles will need to use diesel particulate filters.

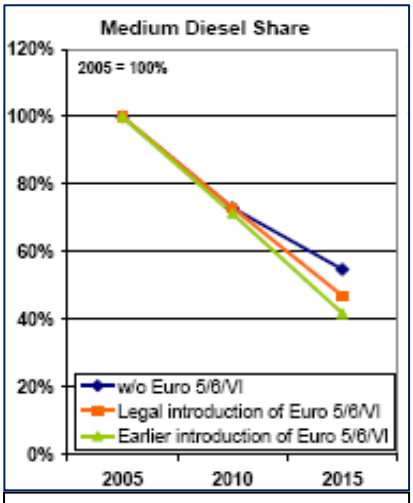

Figure 1: Future NOx emissions compared to 2005: Source: Lambrecht (IFEU) 2007

Effective legislation stimulates the use of emissions control technologies and so improves local air quality. Early implementation of these technologies, through incentives or implementation of Low Emission Zones, can

assist in improving urban air quality to meet legislative targets for ambient air quality. Modelling by IFEU (Lambrecht, 2007) indicates that early implementation of the technologies needed to meet the future light-duty and heavy-duty emissions limits can give a significant boost to the rate of reduction in emissions (see Figure 1).

The Impact of Emissions Control on Climate Change Emissions

The United Nations Intergovernmental Panel on Climate Change (IPCC) says that global warming can be related to atmospheric levels of various emissions (Pachauri, 2007) of which CO_2, one of the main products of combustion, is the most prevalent. Engine and vehicle development trends are continually decreasing CO_2 emissions and this will be driven further through the new EU legislation setting CO_2 targets for cars (Official Journal of the European Union, 2009) and that proposed for light commercial vehicles (European Commission, 2009).

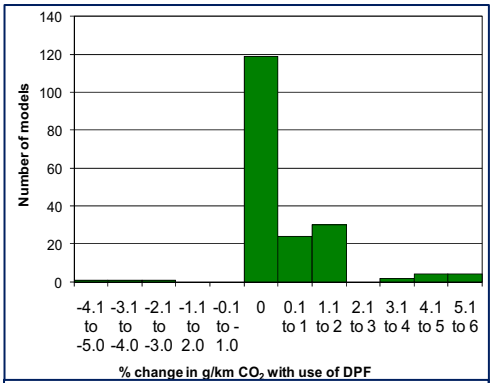

Figure 2: Change in CO_2 emissions with DPFs
184 Models paired in description, engine size, power, V_{max} manufacturer's engine code and Euro emissions standards.
Source: AECC analysis from KBA 2007 database.

For some types of emissions control systems, there may be a small CO_2 penalty due to, for instance, regeneration of particulate traps, but the system as a whole provides major benefits to improve local air quality as discussed above. Using German Type Approval data for 2007 (Kraftfahrt-Bundesamt, 2007) a comparison, shown in Figure 2, of the same cars that were available both with and without an optional Diesel Particulate Filter (DPF), shows an average CO2 increase of only 0.6% for fitment of a DPF. The modal value was 0.0% (119 models).

Other systems such as SCR allow the optimisation of the vehicle to provide improved fuel efficiency. Most European manufacturers of heavy-duty vehicles have selected SCR as their preferred technology to control NOx emissions for Euro IV, V and beyond. The European automobile manufacturers' association said (ACEA, 2003) that SCR technology would enable their members to comply with the Euro IV and V emission standards and, at the same time, achieve fuel consumption levels 5 to 6% lower than those of equivalent EU III engines. Diesel engines used in Non-Road Mobile Machinery such as construction equipment, tractors, railway locomotives and railcars should also benefit from this optimisation.

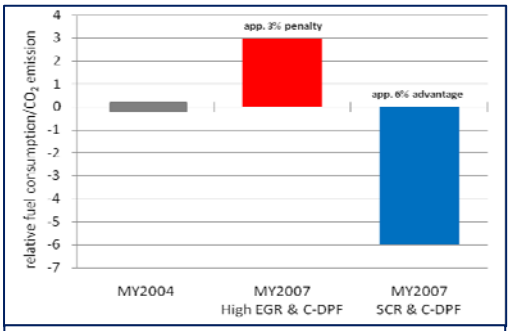

Figure 3: Fuel consumption and CO_2 emission of MY 07 emission strategies. *Source: (Schittler, 2003) DaimlerChrysler Powertrain; 9th Diesel Engine Emission Reduction Conference 2003.*

The contribution of motor vehicles to Global Warming is reported to be not only through CO_2 emissions but also (to a much lesser extent) emissions of N_2O (trace levels) and methane (typically ~10% of total HC). Both the emissions rate and the reported global warming potential of that emission over various timeframes need to be considered to understand the overall effect. These are shown in Table 1. Both methane and N_2O are classed as having a higher global warming potential than CO_2 but the net effect of their emissions from gasoline and diesel-fuelled engines, even taking into account their global warming potential, remains small. For a range of light-duty petrol and diesel vehicles tested by AECC in 2008, for instance, the global warming potential of their methane emissions

Greenhouse Gas	Time Horizon	
	20 years	100 years
Carbon dioxide	1	1
Methane	72	25
Nitrous oxide	289	298
Black Carbon	2000 §	350 – 1500*

Table 1: Global Warming potentials
CO_2, methane and N_2O data from IPCC, 2007
§ Bond (2007)
* Jacobson (2007) reports 1500 - 2240

ranged from 0.06% of that of the emitted CO_2 to 0.25% (measured on the European Driving Cycle, NEDC).

It is now also recognised that particulate matter plays a significant short-term role in climate change, but the effect of vehicle particulate matter is only just starting to be considered. Black Carbon (equivalent to the Elemental Carbon content of vehicle particulate emissions (Bahner, 2007) can be transported over very long distances. It has a direct effect on the scattering and absorption of radiation but also its deposition on snow can change the melting properties of snow. The UK's Meteorological Office Hadley Centre reports (Reddy, 2007) that the indirect GWP due to the BC effect on snow albedo is estimated to be largest for Europe (possibly as large as 1200), suggesting that BC emission reductions from this region are more efficient to mitigate climate change. Black Carbon is considered to have a high 100-year GWP figures by reputable authorities. Table 1 shows figures for the 20-year and 100-year global warming potential (GWP) of species found in vehicle exhaust emissions.

According to estimates by Prof. Mark Jacobson of Stanford University's (Jacobson, 2007), Black Carbon accounts for 16% of global warming, making it second only to CO_2 as a climate change emission. Estimates by the UN's Intergovernmental Panel on Climate Change (IPCC) in its 4th Assessment Report appear to corroborate this assumption.

Whilst transport is not the only source of Black Carbon, it is a significant one, especially in Europe and the US, where it forms a high proportion of the emitted Black Carbon (Streets, 2004), as shown in Figure 4. The authors of this assessment comment that Black Carbon emissions from the transport sector are expected to increase under most scenarios. They anticipate that the BC/OC (Black Carbon/Organic Carbon) emission ratio for energy sources would rise from 0.5 to as much as 0.8, signifying a shift toward net warming of the climate system due to carbonaceous aerosols. Measured Elemental Carbon (EC) is typically used as equivalent to Black Carbon for combustion engines. The US Environmental Protection Agency estimates (Somers, 2004) that EC accounts for some 50 to 80% of diesel particulate.

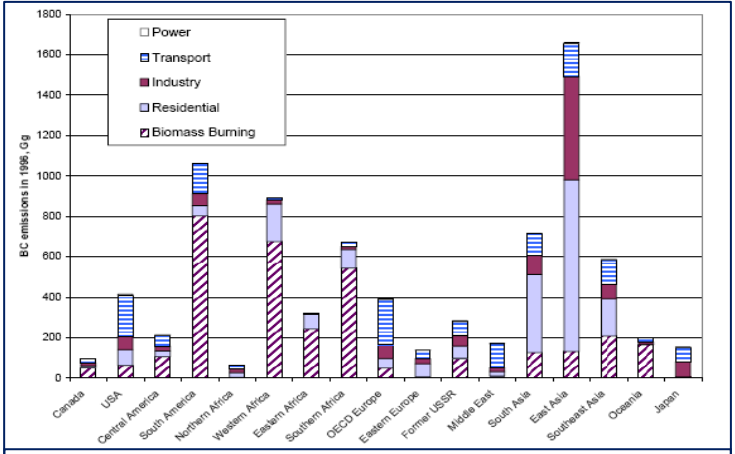

Figure 4: Worldwide BC emissions estimates (from Streets, 2004).

Figures 5, 6 and 7 show the Elemental Carbon content of particulate matter (PM) and the effects of Diesel Particulate Filters on both total particulate and Elemental Carbon. Figure 5 (Andersson, 2002) shows analyses of PM from a Euro III heavy-duty diesel engine fitted with an integrated emissions control system (ECS) of oxidation catalyst, particulate filter and SCR system. Samples were taken 'engine-out' (before the particulate filter) and at tailpipe, after the full ECS. Not only were the total particulate mass emissions substantially reduced, but the carbonaceous content of the remaining total particulate was also minimal.

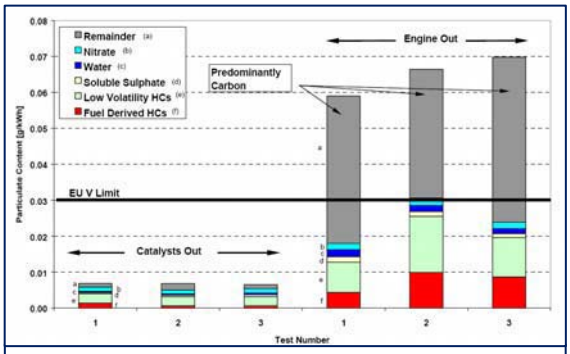

Figure 5: Particulate analyses from a Euro III engine with Integrated ECS, *Source: Ricardo/AEEC*

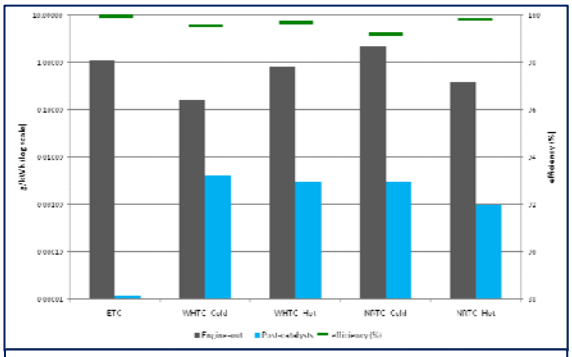

Figure 6: Elemental Carbon missions from Euro VI demonstration engine. *Source: AECC/Ricardo.*

A similar exercise in 2006 demonstrated the potential to meet the (then) proposed Euro VI emissions levels using a heavy-duty engine originally designed to meet the US 2007 emissions standards (May, 2007). The engine was again fitted with an integrated emissions control system including a diesel oxidation catalyst (DOC), wall-flow particulate filter and SCR system. Figure 6 shows the engine-out and tailpipe (post-ECS) emissions of Elemental Carbon and the related filtration efficiency for Elemental Carbon over three transient cycles – European (ETC), cold- and hot-start world-harmonised heavy-duty cycle (WHTC) and cold- and hot-start world-harmonised non-road cycle (NRTC).

The third graph, Figure 7 shows a comparison of the emissions over the NEDC (New European Driving Cycle) test from four cars; one petrol-engined, two different diesel-engined vehicles without particulate filters; and one diesel-engined vehicle with an original-equipment diesel particulate filter (DPF). The Elemental Carbon and Organic Carbon content of particulate matter from each vehicle was analysed by thermo-gravimetric analysis (Bosteels, 2006). The graph shows the near-elimination of Elemental Carbon on the vehicle with particulate filter, in addition to the substantial reduction in particulate matter, resulting in both particulate mass emissions and Elemental Carbon emissions comparable to those of the gasoline engine. Further tests confirmed that the low Elemental Carbon content of the particulate matter from the diesel with particulate filter was maintained over other duty cycles (The Artemis Suite of Urban, Extra-Urban and Highway cycles).

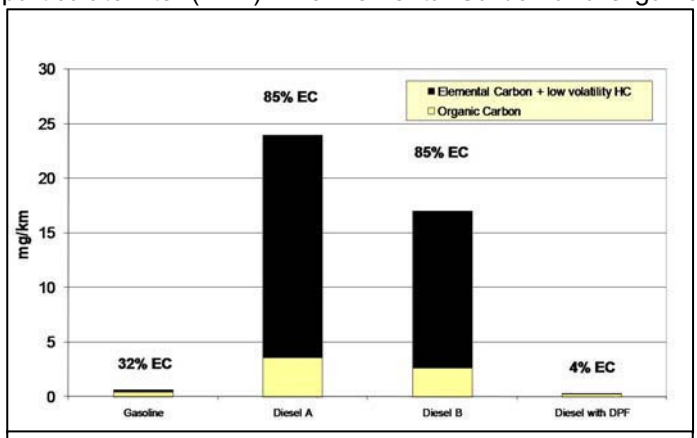

Figure 7: Elemental and Organic Carbon emissions of four cars
Source: AECC / AVL-MTC

To date, European legislation is only considering CO_2 in control tailpipe emissions of substances considered important for global warming. To consider the total effect of an emissions control system on such emissions, it is necessary to consider the mass emissions together with their respective global warming potentials (GWP) as discussed earlier. Total CO_2-equivalent emissions could thus obtained by multiplying the emissions of each climate change-relevant material by its Global Warming Potential for the given time horizon and then summing the CO_2-equivalent emissions of each gas. The Intergovernmental Panel on Climate Change (IPCC) uses the 100-year GWP figures, so the following calculations have been made using the 100-year figures shown in Table 1. There is still considerable debate on the appropriate GWP for Black Carbon. In testimony to the US EPA Hearing on Greenhouse Gases in May 2009 the 20-year Global Warming potential of Black Carbon was quoted as about 4500 and the 100-year figure as about 1500-2200 (Jacobson, 2009). Other sources quote figures as low as 350 for the 100-year GWP. Reddy & Boucher quote figures of 374 to 677, depending on region, but comment that the indirect GWP due to Black Carbon's albedo effect on snow may be as much as 1200. The following calculations, using measured emissions over cold-start and hot-start WHTC (World Harmonized Test Procedure) tests from AECC's heavy-duty Euro VI

demonstration programme, use a typical figure of 1500 for the GWP but also show the effect of using the low figure of 350.

Table 2: CO_2-equivalent emissions (g/kWh); heavy-duty engine over hot-start WHTC test.

	CO_2 GWP = 1	CH_4* GWP = 25	N_2O GWP 298	Φ = BC (GWP 1500)	† = Total (GWP 1500)	= BC (GWP 350)	= Total (GWP 350)) =
Cold-start WHTC test							
Without emissions control system (ECS)	834.0	1.6	2.6	782.3	1620.5	182.5	1020.7
With emissions control system (ECS)	834.0	0.5	16.0	0.078	850.6	0.035	850.5
Difference	0	-1.1	13.4	-782.2	-769.9	-182.5	-170.2
Hot-start WHTC test							
Without emissions control system (ECS)	840.4	0.385	0.567	1006.9	1848.3	234.9	1076.3
With emissions control system (ECS)	840.4	0.792	14.9	0.077	856.2	0.018	856.1
Difference	0	0.407	14.3	-1006.8	-992.1	-234.9	-220.2

* methane emissions calculated from FTIR continuous measurements; 9.9% of THC without ECS, 13.8% with ECS.
Φ N_2O emissions calculated from FTIR continuous measurements.
† measured EC was 87.8% of 0.594 g/kWh PM without ECS, 2.4% of 0.002 g/kWh PM with ECS.

Overall, the figures indicate that the global warming potential of the Black Carbon emissions removed by the Particulate Filter system amount to at least 22% of the engine's CO_2 emissions. Using the higher GWP for Black Carbon, the reduction in total Global Warming Potential could

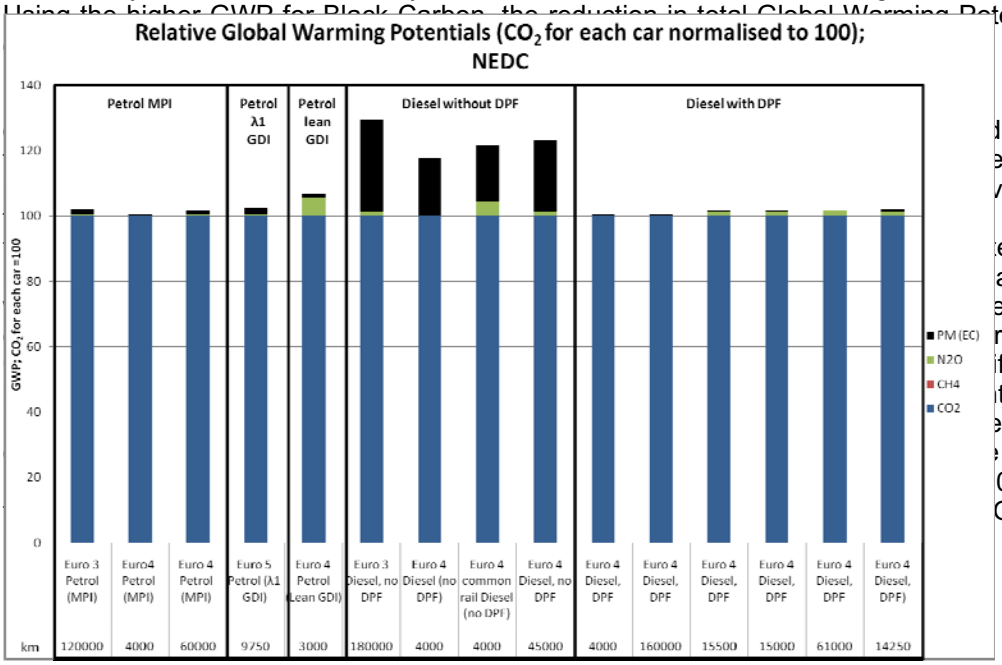

petrol- and
been used
tests have
ve, in which
DPF) were
er durability
asurements
e total CO_2-
r Elemental
fferences in
t emissions
ex of 100 for
to this.
0.005 g/km,
O2 figure is

Figure 8: CO_2-equivalent emissions, light-duty vehicles over the NEDC test.

The significant effect on total emissions of materials reported to be relevant to climate change, including diesel particulate emissions and the effectiveness of the use of Diesel Particulate Filters on diesel engines can be seen.

Conclusions

There are increasing numbers of papers suggesting that emissions of Black Carbon have a significant short-term global warming potential, especially in Western Europe. There is debate over a figure for the Global Warming Potential (GWP) of Black Carbon, but the consensus appears to be that the 100-year figure is in the range of 350 to 1500 times that of CO_2.

Soot and particulate matter are measured in a number of ways. It is generally accepted that the Elemental Carbon (EC) content of engine and vehicle particulate matter (PM) emissions equates to Black Carbon. This Elemental Carbon can be measured by thermogravimetric analysis of collected PM.

Analysis of tests on light-duty vehicles and heavy-duty engines conducted by AECC shows that the use of particulate filters removes the majority of both the particulate matter and the Elemental Carbon emitted from engines. This indicates that the use of particulate filters could provide a substantial benefit in the overall reduction in emissions from motor vehicle of substances now considered to be of concern for climate change, in addition to the benefits to ambient air quality and health.

References

ACEA (2003), Statement on the Adoption of SCR Technology to Reduce Emissions Levels of Heavy-Duty Vehicles. ACEA Position Paper, 15 July 2003, ACEA European Automobile Manufacturers' Association, Brussels, Belgium.

Andersson, J.D., Jemma C.A., Bosteels, D., and Searles, R.A. (2002), Partikelemission eines EU 3 Heavy-duty Dieselmotors mit katalytischem Partikelfilter und selektiver katalytischer Reduktion: Größe, Anzahl, Masse & Chemie ; 11. Aachener Kolloquium 2002.

Bahner, Weitz, Zapata and DeAngelo (2007), Use of Black carbon and Organic carbon Inventories for Projections and Mitigation Analysis; US EPA 16th Annual International Emission Inventory Conference, 14-17 May 2007, *www.epa.gov/ttn/chief/conference/ei16/session3/k.weitz.pdf*.

Bond, T.C. (2007), Testimony for the Hearing on Black Carbon and Global Warming; House Committee on Oversight and Government Reform, United States House of Representatives, 18 October 2007, *http://oversight.house.gov/images/stories/documents/20071018110647.pdf*.

Bosteels, D, May, J.H., Karlsson H., and de Serves, C. (2006) 'Regulated' and 'Non-regulated' Emissions from Modern European Passenger Cars; SAE 2006-01-1516.

European Commission (2009), COM(2009) 593 final; Proposal for a Regulation of the European Parliament and of the Council setting emission performance standards for new light commercial vehicles as part of the Community's integrated approach to reduce CO_2 emissions from light-duty vehicles, *http://eur-lex.europa.eu/LexUriServ/LexUriServ.do?uri=COM:2009:0593:FIN:En:PDF*,
European Commission, Brussels, Belgium

European Environment Agency Technical report No. 11/2009 (2009), NEC Directive Status Report 2008, *www.eea.europa.eu/publications/nec-directive-status-report-2008*, EEA, Copenhagen, Denmark,

Jacobson, M.Z. (2007) Testimony for the Hearing on Black Carbon and Global Warming; House Committee on Oversight and Government Reform, United States House of Representatives, 18 October 2007, *http://oversight.house.gov/images/stories/documents/20071018110606.pdf*.

Jacobson, M.Z. (2009), Testimony for U.S. Environmental Protection Agency Public Hearing on the Proposed Endangerment and Cause or Contribute Findings for Greenhouse Gases Under the Clean Air Act, 18 May 2009, Arlington, Virginia USA,
http://www.stanford.edu/group/efmh/jacobson/PDF%20files/EPAEndang0509.pdf

Kraftfahrt-Bundesamt (2007), Systematisches *Verzeichnis, Kraftstoffverbrauchs- und Emissions-Typprüfwerte von Kraftfahrzeugen mit Allgemeiner Betriebserlaubnis oder EG-Typgenehmigung, SV 2*, Stand: 1. März 2007, Kraftfahrt-Bundesamt (Federal Motor Transport Authority), Flensburg, Germany.

Lambrecht U. (2007), Effects of planned legislation on transport emissions in Germany, IFEU contribution to the AECC Technical seminar on Heavy-duty Engine Emissions,
www.aecc.be/content/HD%20Seminar/6 D%20IFEU Lambrecht.pdf, AECC, Brussels. Belgium

May, J.H., Bosteels, D., Nicol, A.J., Andersson, J.D., & Such, C. (2007), Die Anwendung von Technologien zur Emissionsreduzierung an einem Niedrigemissionsmotor zur Potenzialbeurteilung zukűnftiger Systeme fűr Europäische und weltweit harmonisierte Richtlinien; 16. Aachener Kolloquium Fahrzeug- und Motortechnik 2007.

Official Journal of the European Union (2009), Regulation (EC) No.443/2009 setting emission performance standards for new passenger cars as part of the Community's integrated approach to reduce CO_2 emissions from light-duty vehicles, *Official Journal L140 (2009), pp. 1 – 15*.

Pachauri, R.K. and Reisinger, A. (eds.) (2007) *Climate Change 2007: Synthesis Report. Contribution of Working Groups I, II and III to the Fourth Assessment Report of the Intergovernmental Panel on Climate Change*, IPCC, Geneva, Switzerland.

Reddy, M.K. and Boucher, O. (2007), Climate Impact of Black Carbon emitted from Energy Consumption in the World's Regions; *Geophysical Research Letters, 34, L11802. doi:10.1029/2006GL028904*.

Schittler, M. (2003), State-of-the-art and emerging truck engine technologies, DaimlerChrysler presentation at 9th Diesel Engine Emission Reduction Conference (DEER*),* 24-28 August 2003, Rhode Island, USA, *www1.eere.energy.gov/vehiclesandfuels/pdfs/deer_2003/session8/2003_deer_schittler.pdf*, United States Department of Energy.

Somers, J. (2004), Mobile Source Black Carbon Emissions; Black Carbon Emissions and Climate Change: A Technical Workshop, 13-15 October 2004, San Diego, California.
www.nrel.gov/vehiclesandfuels/nfti/pdfs/bc12_j_somers.pdf.

Streets, D.G., Bond, T.C., Lee, T., and Jang C. (2004), On the future of carbonaceous aerosol emissions; *Journal of Geophysical Research, 109, D24212, doi:10.1029/2004JD004902*

Investigation of guanidinium formate as novel ammonia precursor compound for selective catalytic reduction of NO_x

*D. Peitz*1, O. Kröcher1, M. Elsener1*

[1]Paul Scherrer Institut, 5232 Villigen PSI, Switzerland, daniel.peitz@psi.ch

Introduction

Steadily tightening emission standards have been limiting the amount of pollutants in internal-combustion engine exhaust gas for more than four decades by now. Even more stringent guidelines will be employed in the next few years. Nitrous oxides (NO_x) in particular have been moving into the focus of legislature (EC, 2007; EPA, 2000). As the imposed reductions in NO_x-emissions are immense, only additional exhaust aftertreatment systems are able to cope with this challenge.

Selective catalytic reduction (SCR) is a very efficient process for NO_x reduction, which is already used in diesel vehicles since 2005 (Jacob, 2006). Aqueous urea solution (AdBlue®) is used as an ammonia precursor compound in automotive applications to safely transport the necessary ammonia for the SCR process (Jacob, 1992). However, there is a number of drawbacks associated with this solution, especially the poor temperature stability. The optimum operating and storage conditions of AdBlue® are in the relatively small range of -11 to 30°C (Kröcher et al., 2008). Moreover, the amount of ammonia which can be released from a given volume of solution is not satisfying for many mobile applications. Therefore, guanidinium formate has been proposed as a novel ammonia precursor compound, which exhibits as mixture with urea a temperature window of -30 to 60°C and releases almost 1.5 times as much ammonia by weight and volume (Kröcher et al., 2009; Hammer et al., 2008).

Table 1: Comparison of the characteristics of AdBlue® and guanidinium formate

Ammonia precursor compound		Melting point [°C]	Boiling point [°C]	Composition [wt.-%]			NH_3 content	
				Urea	GF	H_2O	Per weight [kg/kg]	Per volume [kg/L]
Urea (AdBlue®)	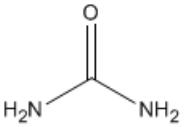	**- 11**	**≈ 108**	**32.5**	**0**	**67.5**	**0.20**	**0.22**
Guanidinium formate (GF) 41/16	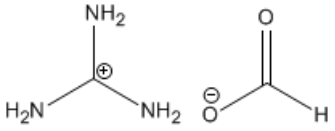	**≈ - 30**	**≈ 100**	**16**	**41**	**43**	**0.29**	**0.32**

Due to the more complex structure of the compound in comparison to urea, detailed investigations are necessary to ensure the quantitative decomposition of guanidinium formate to yield all contained nitrogen atoms as ammonia. Side reactions resulting in higher molecular compounds should be suppressed to prevent deposits in the exhaust gas system. These issues are being addressed by our experiments on a novel laboratory scale SCR test system, featuring injection of authentic liquid reducing agent solutions and a sophisticated analytical combination of FTIR-spectroscopy and HPLC-analysis.

While the decomposition is investigated on laboratory scale at the Paul Scherrer Institute, the results are used for a real scale system operated at the Chair for Thermodynamics of the TU Munich. This system is then implemented as a separate ammonia generator on an engine test bench at the TU Munich's Chair for Internal Combustion Engines (Krämer, 2008).

Experimental setup

As already mentioned, a novel laboratory scale SCR system was used for the investigations. Being set in a chemical laboratory, all exhaust gas components are mixed from gas bottles instead of being taken from an operating engine. For the dosing of water vapor, a platinum catalyst is used to oxidize hydrogen in an excess of oxygen, giving the advantage of pulsation-free water vapor dosing unlike all other available techniques. The gas composition is regulated by computer controlled mass flow controllers to allow fast and easy changes. All gases are mixed and heated to the desired temperature to model the exhaust gas composition of any operating condition of a real engine. A tubular glass reactor is used as exhaust gas aftertreatment housing for either ceramic or metallic catalyst supports. The reactor is well insulated and temperature controlled by various heating systems. Liquid reducing agents are injected into the reactor using a combination of an HPLC pump and an ICP nebulizer, the liquid flow is monitored gravimetrically. A part of the gas flow exiting the reactor is transferred to an FTIR spectrometer for analysis of gaseous low molecular weight compounds, while another part of the gas flow can be inserted into an absorber in order to wash aerosols out of the gas and dissolve higher molecular weight compounds by an HPLC eluent.

The following operating conditions were used in our experiments: An overall gas flow of 500 L_N/h was sent through the reactor, into which 50 µL/min reducing agent were injected via the nebulizer. The gases were preheated to the catalyst temperature before entering the reactor. Upon leaving the reactor, the gases were transferred in trace heated tubes to prevent condensation of gaseous components. A gas flow of 330 L_N/min was pumped by a heated membrane pump to the FTIR spectrometer (Thermo Nicolet Antaris IGS Analyzer) in a 180°C heated gas-measuring cell with a volume of 200 mL and 2 m path length. A multi-component method for the correction of non-linear responses and cross-sensitivities was then used to measure the gas component concentrations. The method allowed the quantification of the gas components NO, NO_2, N_2O, NH_3, H_2O, CO, CO_2, isocyanic acid (HNCO), nitric acid (HNO_3), formic acid (HCOOH), formaldehyde (H_2CO), methanamide ($HCONH_2$) and hydrocyanic acid (HCN) with an accuracy of ± 1% and a detection limit of 1-3 ppm.

For the SCR-based validation experiments, a 2.5% V_2O_5-containing extruded catalyst (300 cpsi) was employed, with a space velocity of 16800 h^{-1} at a temperature of 225°C. In these experiments, a 500 L_N/h feed gas mixture of 1000 ppm NO, 5% H_2O and 10% O_2 in N_2 was used. If NH_3 was added as a gas, the N_2 flow was adjusted in order to keep an overall flow of 500 L_N/h.

In the hydrolysis experiments, either a ceramic cordierite monolith (400 cpsi, GHSV = 8350 h^{-1}) coated with TiO_2 (anatase) (38 g/L) or a metallic support (200 cpsi, GHSV = 9650 h^{-1}) coated with a commercial TiO_2 (anatase)-based washcoat (101 g/L) was used.

Results and discussion

In order to evaluate the homogeneous distribution of the reducing agent spray on the catalyst, an experiment with AdBlue® was performed. First, gaseous NH_3 and NO were mixed in the gas flow, later the gaseous NH_3 dosing was stopped and, instead, AdBlue® was sprayed on the catalyst to release NH_3 which could be consumed in the SCR reaction. The ammonia slip at different levels of SCR activity was measured, as the NH_3 slip constituted a clear indication of an inhomogeneous distribution of reducing agent in the catalyst channels.

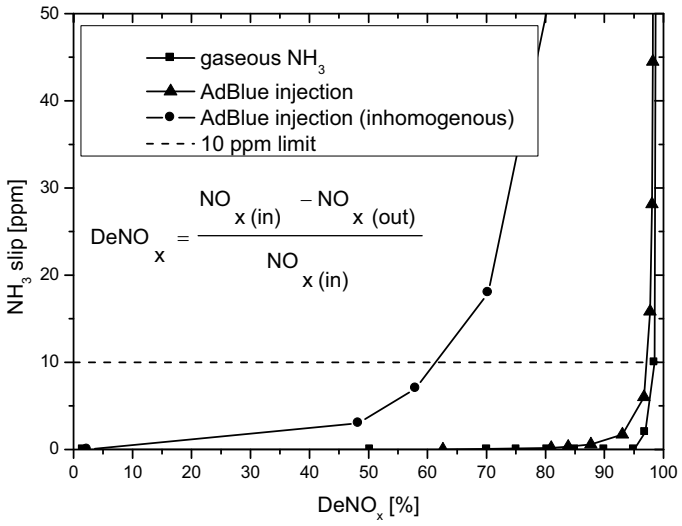

Figure 1: SCR comparison of gaseous NH_3 and liquid AdBlue® solution sprayed on catalyst.

When adding gaseous NH_3 to the NO containing feed gas, the product gas contained less than 10 ppm of NH_3 up until a $DeNO_x$ value of 98.5%. In case of spraying AdBlue® onto the catalyst, an NH_3 slip of 10 ppm was already reached at a $DeNO_x$ value of 97.4%. The difference, however, is very small – thus indicating a relatively homogeneous distribution of reducing agent and NO in all the catalyst channels. In a comparative experiment, the catalyst was placed closer to the reducing agent injection, causing an inhomogeneous distribution of the reducing agent in the catalyst channels. Therefore, a $DeNO_x$ value of only 64% could be reached at 10 ppm NH_3 slip. By the experiments it could be shown that the experimental setup is suited for liquid reducing agent investigations on a laboratory scale. Also, by utilizing AdBlue® injection, its decomposition and direct coupling with SCR as a reference the performance of guanidinium formate solutions could be evaluated in the future.

The decomposition of guanidinium formate was initially separately investigated, instead of combining it directly with SCR. A solution of 10% guanidinium formate (by mass) was sprayed on a TiO_2-coated cordierite monolith. The product gases were analyzed by FTIR spectroscopy.

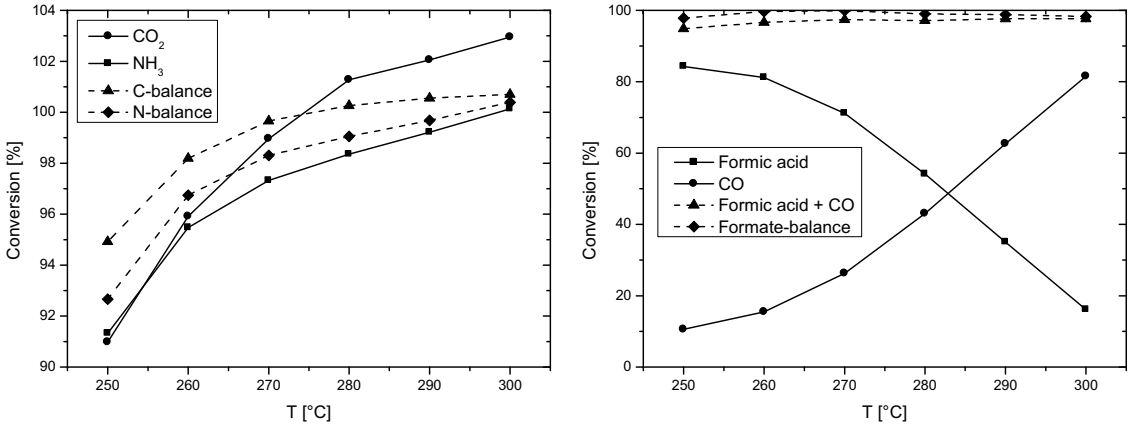

Figure 2: Catalytic decomposition of an aqueous 10% guanidinium formate solution on a cordierite monolith coated with TiO_2 (anatase).

CO_2 = conversion of guanidinium-C atoms to CO_2
NH_3 = conversion of guanidinium-N atoms to NH_3
C-balance = sum of all measured C-compounds relative to the number of all inserted C-atoms
N-balance = sum of all measured N-compounds relative to the number of all inserted

Formic acid = conversion of formate-ions to formic acid
CO = conversion of formate-ions to CO
Formic acid + CO = sum of formic acid and CO conversion
Formate-balance = sum of all compounds from formate-ion

N-atoms	decomposition relative to the inserted number of formate-ions

As the temperature is raised from 250°C to 300°C, the degree of decomposition of guanidinium formate steadily increases. However, there is a steep increase in conversion as the temperature is raised from 250 to 260°C while from 260°C up to 300°C the increase of conversion is much slower. The proportion of NH_3, the most desired N-containing product, grows with higher temperatures, as less isocyanic acid and methanamide is formed. Methanamide is thought to be a condensation product of formic acid and ammonia, whereas isocyanic acid is a possible intermediate in the decomposition of guanidine.

The decomposition of the formate anion seems to take place independently of the guanidinium decomposition, it therefore is regarded in an isolated graph (Figure 2b). The decomposition of formic acid is strongly dependent on the temperature, as there seems to be a chemical equilibrium between free formic acid and its decomposition product CO. These two compounds actually represent almost all of the inserted formate anions, as can be seen by comparison of the "formic acid + CO" balance with the formate-balance. At low temperatures more formic acid is emitted, causing an increased condensation with NH_3 to form methanamide. At around 285°C equal amounts of formic acid and CO are present in the product gas mixture.

The same aqueous solution of 10% guanidinium formate was also sprayed on a commercial TiO_2 (anatase) based hydrolysis catalyst coating on a metallic catalyst support.

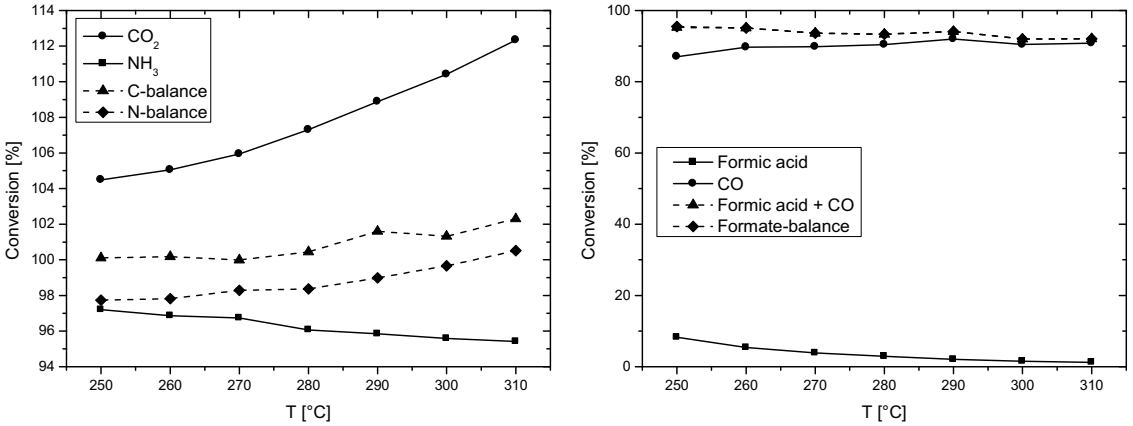

Figure 3: Catalytic decomposition of an aqueous 10% guanidinium formate solution on a metallic support coated with a commercial TiO_2 (anatase)-based hydrolysis catalyst.

The catalyst showed a strong correlation of temperature and CO_2 formation, but only a slight increase in emission of C-compounds with raising temperatures. The decomposition to NH_3 dropped as the temperature was increased, but N-compounds were quantified to ascend with temperature. Also, the formic acid concentration constantly decreased with increasing temperature as expected, but the CO concentration did not increase at a similar rate – it actually remained at a constant level. The sum of all formate anion decomposition products was decreasing at the same time, as there were virtually no side products formed.
The combination of a CO_2 conversion surpassing 100% significantly and a declining formate-balance pointed towards a connection of these two balances. If all C compounds of the decomposition were put into one balance, it remained almost constant, therefore indicating an oxidation of released CO to CO_2. The oxidation of CO was more pronounced at elevated temperatures, at which also a decrease in NH_3 emission but increased formation of NO and N_2O could be monitored. Therefore, also an oxidation of NH_3 to N_2 could not be excluded, which would consequently lead to reduced values for the N-balance due to the invisibility of N_2 in the FTIR analysis.
In additional control-experiments the catalyst proved to oxidize gaseous CO and NH_3, thus, supporting the presented explanations for the high values of CO_2 and low values of NH_3 conversion at high temperatures. Possibly as a result of the CO oxidation, the ratio of CO to formic acid at a given temperature was much higher than in the previous experiment with a cordierite catalyst support and pure TiO_2 (anatase) coating. This effect is appreciated very much though, as high formic acid emissions are undesired due to their condensation in the automotive exhaust gas aftertreatment system at low ambient temperatures which gives rise to corrosion.

The amount of CO from formic acid decomposition which will be released instead amounts to around 0.04 g/km for an engine producing 0.16 g/km NO_x and 0.25 g/km CO, therefore, causing no violation of the EURO 6 limit of 0.50 g/km CO.

Besides the investigations with diluted solutions of guanidinium formate, there were also experiments with an aqueous 38% guanidinium formate / 15% urea mixture. The decomposition properties, however, should not differ significantly because of this minor deviation in composition.

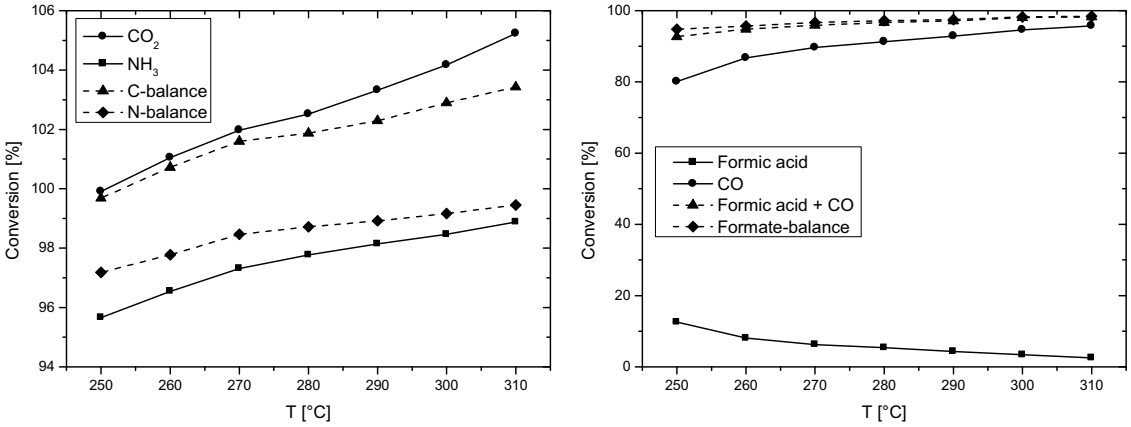

The commercial hydrolysis catalyst was again used for the decomposition of the reducing agent solution. The obtained conversion of this application-oriented reducing agent solution did not turn out to be worse than that of the laboratory solution with just 10% guanidinium formate, even though the latter was explicitly mixed in order to guarantee a complete decomposition. The 38/15 mixture was decomposed better at elevated temperatures. However, above 270°C almost no change in the degree of conversion occurred even if the temperature was further increased. The C-compounds summed up to values approaching 104%, which on the one hand could be due to the inaccurate preparation of the reducing agent solution, and on the other due to the inevitable error in quantitative FTIR spectroscopy, which, however, should be rather around 1%. The N-balance exhibits values ranging from 97 to 99%, however, as previously described, molecular N_2 is not included in these values so they should in fact be larger. Interestingly, the amount of NH_3 increased with elevated temperatures, even though at these temperatures more NH_3 was oxidized to NO and N_2O. The increase in temperature also caused a decline in HCN formation, which peaked at 270°C with a concentration of 18 ppm (0.7% of the N-content). The most probable mechanism of HCN formation is a further dehydration of methanamide which was actually exhibiting a peak concentration at temperatures lower than 270°C, but might not easily release water at these temperatures to form HCN. Besides these compounds, also traces of HNCO could be reliably detected, indicating an incomplete hydrolysis possibly due to an imperfect homogeneous distribution of the reducing agent spray in the catalyst channels. The decomposition of the formate anion proceeded similar to the previously recorded decomposition of the low concentrated solution. The equilibrium-concentrations differed for the two concentrations. A possible explanation could be that the equilibrium is adjusted by the catalyzed decomposition of formic acid on the catalyst. A saturation of active sites might be caused by the (slow) reaction as there is more reducing agent applied to the catalyst surface and a high concentration of reactants. Still, by far the major part of the formate anion is decomposed to CO – the described differences are actually quite small. Thus, decomposition of the 38/15-mixture in automotive applications is feasible if a temperature of 270 to 300°C can be maintained.

Conclusion

A novel reducing agent solution based on a mixture of guanidinium formate and urea was investigated, which overcomes the shortcomings of the conventional AdBlue® solution. The major issue of a quantitative decomposition of the components on a hydrolysis catalyst was addressed in a specially constructed laboratory-scale SCR test stand. A solution of 38% guanidinium formate and 15% urea could be decomposed on a commercial catalyst without critical side-product formation. Most of the contained carbon and nitrogen left the system as

CO_2 or CO and NH_3, respectively. Side products included NO, N_2O and N_2 from NH_3 oxidation, undecomposed gaseous formic acid, traces of HNCO and methanamide of the condensation of formic acid and NH_3. Further catalyst screening targets resolving the emission of undesired compounds in the future. The presented results influenced the construction of a prototype NH_3 generator at the TU Munich, which is to be tested on a running engine in various driving cycles.

Aknowledgement

We cordially thank C. Gerhart for valuable contributions in our discussions. Financial support of the project granted by the *Bayerische Forschungsstiftung* and *Alzchem Trostberg GmbH (Germany)* is gratefully acknowledged.

References

EC (2007), Regulation (EC) No 715/2007: Euro 5 and Euro 6 standards, *Official Journal of the European Union.*

EPA (2000), TIER II bin 5 Federal Register: 65, 6851.

B. Hammer, H. Krimmer, B. Schulz, E. Jacob (2008), *Use of aqueous guanidinium formate solution, optionally with urea and-or ammonia or ammonium salt, for the selective catalytic reduction of nitrogen oxides with ammonia in motor vehicle exhaust gas*, WO2008077587-A1; WO2008077588-A1.

E. Jacob (1992), *Selective catalytic denitrification of exhaust gas contg. oxygen - with ammonia generated by spraying aq. urea soln. in hydrolysis catalyst in vaporizer*, EP487886-A1; EP487886-B1.

E. Jacob (2006), Perspektiven der mobilen SCR-Technik, *15. Aachener Kolloquium Fahrzeug- und Motorentechnik*, Vol. 2, 1303-1336.

L. Krämer (2008), Assessment of 3rd Generation SCR Systems for Potential Future Applications, *Proc. of 2nd Conference "MinNO_x – Minimization of NO_x-Emissions Through Exhaust Aftertreatment"*, IAV.

O. Kröcher, M. Elsener, E. Jacob (2009), A model gas study of ammonium formate, methanamide and guanidinium formate as alternative ammonia precursor compounds for the selective catalytic reduction of nitrogen oxides in diesel exhaust gas, *Appl. Catal. B*, 88, 66-82

O. Kröcher, M. Elsener, E. Jacob (2008), New reducing agents for the low-NO_x SCR technology, *5th International Exhaust Gas and Particulate Emissions Forum, Ludwigsburg (Germany).*

Combustion of mineral diesel and alternative fuels in a heavy duty on-road engine with combined NO_x and particle exhaust gas treatment

P. Soltic, D. Edenhauser, T. Thurnheer, D. Schreiber, A. Sankowski*

Empa, Swiss Federal Laboratories for Materials Testing and Research, CH-8600 Dübendorf, Switzerland, patrik.soltic@empa.ch

Abstract

Because of several reasons, there is a need to use alternatives to mineral diesel fuel for internal combustion engines in on- and off-road applications. Unfortunately, most alternative fuels have different chemical and physical properties than mineral diesel which leads to some practical problems. Until a few years ago, heavy duty diesel engines were comparably simple and did not have any exhaust gas after treatments systems. Starting with Euro-IV, which came into force 2005, heavy duty on-road engines for the European market started to be equipped with exhaust gas after treatment systems. The next large challenge for the industry is to meet the Euro-VI standards (2013) which will demand clean combustion combined with complex exhaust gas treatment. The off-road engines will have to follow similar stringent emissions limits with the introduction of Tier-4 (2014). In order to achieve these low levels of pollutant emissions, the engines will have to use flexible injection systems, cooled EGR, oxidation catalysis, selective catalytic reduction and particle filtering. All these systems will have be precisely designed and calibrated to operate with standard diesel fuel. One important question is how these complex system will perform when an alternative fuel is used. The work presented here investigates systematically the influence of some alternative fuels regarding pollutant emissions and efficiency when they are used in an engine with Euro-VI layout.

Goals and Setup of the Experiments

There are four important types of alternative fuels used in compression ignition engines:

1. Fuels synthesised from fossil or biogenic gas (gas-to-liquid GTL or biomass-to-liquid BTL).
2. FAME (Fatty Acid Methyl Ester), often called "bio diesel", made from different vegetable oils. A US stan-dard (ASTM D 6751) exists since 2001; a European standard (EN 14214) exists since 2004.
3. Neat vegetable oil. A German pre-standard exists for rapeseed oil fuel (DIN V 51605).
4. Recycled waste-oil from fossil or biogenic sources.

This paper focuses on fuels 1-3, Table 1 shows the most important properties of the fuels used.

Table 1: Properties of the fuels used for the experiments

	Unit	Diesel market fuel	GTL	RME	Neat rapeseed oil	Neat soy-bean oil
Density at 15°C	kg/m^3	835	778	881	920	924
Viscosity at 40°C	mm^2/s	2.65	2.56	4.40	35.0	30.9
Flash point	°C	62	87	93	245	260
LHV per mass	MJ/kg	43.05	44.3	37.9	36.8	36.9
H_2O/S/N content	mg/kg	60/10.1/-	39/<1/-	690/2.5/7	850/3.6/2	547/2.1/8
Cetane index	-	52	79	52	39	36
C/H/O mass fraction	% kg/kg	85.2/14.8/0.0	83.6/16.4/0.0	77.3/11.7/11.0	77.9/13.2/8.9	77.1/12.9/10.0
H/C (molar)	-	2.07	2.34	1.81	2.03	1.99

The experiments were performed on an engine with main parameters as listed in Table 2. The engine was equipped with a diesel oxidation catalyst (DOC), a wall-flow diesel particle filter

(DPF) and a selective catalytic reduction system (SCR). The SCR process was performed using ammonia (NH_3) which was hydrolysed prior to the SCR catalyst from an aqueous urea solution. This automotive urea solution used is known under the market name AdBlue; it has a urea content of 32.5 mass-% and is standardised (ISO 22241).

Table 2: Main engine specifications

Cylinders / Bore / Stroke	6 / 128 mm / 166 mm	**Rated power / torque**	335 kW / 2240 Nm
Injection system	pump-line-nozzle (adjustable injection pressure)	**EGR**	water cooled

The following questions were addressed:

Case A. How do the different fuels affect engine torque, efficiency and pollutant emissions if the injection timing and duration do not differ from diesel calibration?

Case B. How do the different fuels affect efficiency and exhaust emissions if the injection duration is adapted to maintain the same engine torque for all fuels while keeping all other calibration parameters constant?

Case C. How is the engine efficiency affected if the injection pressure, start of delivery, injection duration and the EGR rate are adapted to each fuel to keep NO_x raw emissions and engine torque on the level achieved with the EN 590 diesel?

Oxygen-containing fuels such as FAME and neat vegetable oils normally increase NO_x emissions and reduce soot emissions compared to mineral diesel due to an enhanced local availability of oxygen in the diffusion controlled flame (Mueller et al., 2003; Szybist et al., 2005). Other authors (Rakopoulos et al., 2006) report on contrary effects which indicates, that the effect of the fuels on NO_x emissions depends on the combustion system (chamber geometry and size, injection system) and its calibration. It is known that GTL fuel leads to less NO_x if the engine is not being re-calibrated (Szybist et al., 2005; Abu-Jrai et al., 2006). Since the fuels used have also different physical properties, they induce differencies in the engine's injection system which can lead to different injection rates (Kegl, 2006) with all the consequences for the engine's efficiency and pollutant emissions. For the work discussed here, experiments were performed using a modern heavy-duty diesel engine equipped with a combined exhaust gas aftertreatment system. The aim of the work was to quantify the effects of the different fuels on the engine and on the aftertreatment system according to the cases A, B, C mentioned above.

A typical full load operating point was chosen for the experiments: 2000 rpm engine speed and a brake mean effective pressure of 20.6 bar (which corresponds to a brake torque of 2100 Nm and a brake Power of 286 kW).

The engine was operated on an engine test bench equipped with a double-line standard emission bench to measure CO, CO_2, NO_x, O_2, and total hydrocarbons (THC). NH_3 emissions were measured with a laser diode spectrometer. A part of the engine's raw emissions was sampled and diluted with a heated partial flow dilution tunnel. After additional dilution, the soot mass was measured with a photo acoustic sensor. The particles were counted with a condensation particle counter with a cut-off size of 7 nm behind an evaporation tube operating at 300 °C which could be bypassed. The exhaust gas flow was fed to a full-flow constant volume sampling (CVS) system for the particle mass measurement. Fiberfilm filters were used and weighted after the tests in a low-vibration, temperature and humidity conditioned room. A second condensation particle counter wit a cut-off size of 7 nm sampled from the CVS tunnel behind an additional dilution step and an evaporation tube operating at 300 °C. Fresh air flowing to the engine was conditioned to a temperature of 25 °C and a dew point of 13.8 °C (i.e. 50 % relative humidity). A crank-angle based data acquisition system recorded the combustion pressure of one cylinder.

The urea dosing was kept constant and it was monitored, that the ammonia concentration at tailpipe position did not exceed 10 ppmV. The test bench was operated in speed-control mode, i.e. it kept the engine speed constant at 1300 min^{-1} and the torque was set by the calibration parameters injection pressure, start of injection, injection duration and EGR rate.

Results

Figure 1 depicts the injection and combustion peak pressures, and the brake torques.

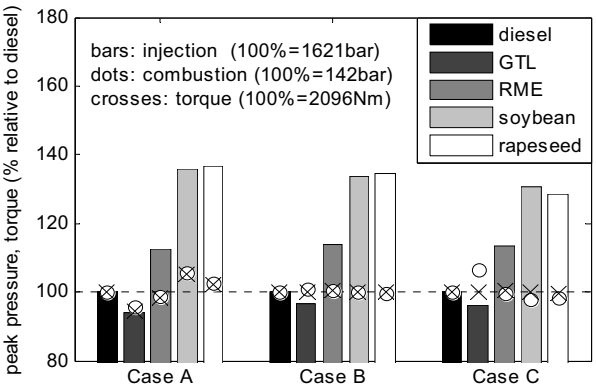

Figure 1: Injection pressures, combustion peak pressures, brake torques.

Unlike with common-rail systems, pump-line-nozzle systems as used here do not measure and control the injection pressure. It can clearly be seen that the injection peak pressure is quite considerably increased for the neat vegetable oils. This behaviour was also observed by other authors (Kegl, 2006; Czerwinsky et al., 2007; Lapuerta et al., 2008) and explained by lower fuel losses in the fuel pump due to the higher viscosity of these fuels. Differences in density, bulk modulus and sound velocity may also play a roll. Such an increase in injection pressure can be problematic regarding the life-time of the injection system. The injection peak pressure not only was increased by the neat vegetable oils but also, to a smaller extent, by RME.

Looking at case A where all calibration parameters were kept constant it can be seen that the torque and the combustion peak pressures change along the different fuels. It is important to notice that, although the volume-specific heating values of RME and the vegetable oils were 5-6% lower than for diesel, the brake torque did not decrease but increase for the vegetable oils. The reason for this behaviour being that the higher injection pressure led to higher fuel flow rates which (over-) compensated the lower volumetric energy densities. GTL fuel led to a lower output due to its lower energy density and the reduced injection pressure compared to diesel. Burning such pure neat vegetable oils in unmodified engines with pump-line-nozzle technology will most likely yield higher engine power at the cost of a diminished lifetime of the fuel system.

In case B where the injection duration was adapted to meet the desired brake torque, the picture of the injection peak pressures remains the same. The resulting combustion peak pressures are comparable for all fuels.

In case C where start of delivery, injection pressure and EGR rate were adjusted to meet the NO_x values of the diesel case, the combustion peak pressure was elevated for GTL fuel and reduced for the neat vegetable oils. The peak injection pressure for the neat vegetable oils was reduced as far as the pump-line-nozzle system allowed. Figure 2 depicts the resulting brake efficiencies with their confidence intervals for the three cases.

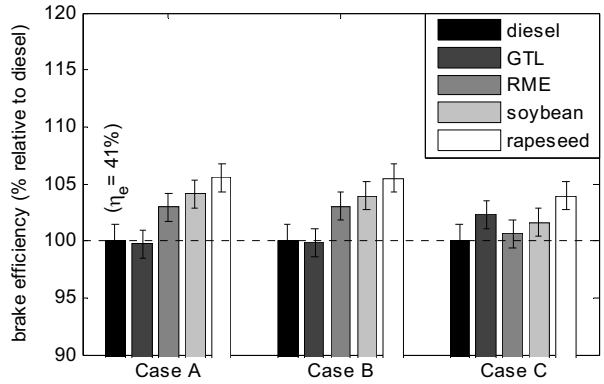

Figure 2: Brake efficiencies relative to diesel fuel.

In cases A and B, increases of the efficiencies can be seen for the RME and the vegetable oils. According to (Lapuerta et al., 2008), most studies do not report on changes in efficiency using FAME or vegetable oils. But other authors (Babu and Devaradjane, 2003) also report on this effect. After calibration to meet the NO_x targets (case C), some of the efficiency advantages of RME and the vegetable oils disappear because combustion has to be retarded. Efficiency using GTL fuel can be increased by earlier injection without exceeding the NO_x targets.

The left plot of Figure 3 depict the pressure traces and the right plots depict the resulting heat release rates for case C. Injection could be advanced for GTL in order to reach the NO_x level of diesel fuel. For RME, rapeseed and soybean oil, the injection had to be slightly retarded. The heat release rates show almost no premixed combustion for all fuels in both cases. This behaviour can be expected for this comparably large engine running at low speed and with late fuel injection timing. Other authors (Kitano et al., 2005) reported on common rail passenger car engine results using GTL at higher engine speeds. They saw decreasing premixed combustion and decreasing injection delay of GTL compared to diesel and attributed this observation to its large cetane number. This behaviour cannot be seen using the combustion system described here. Even the neat vegetable oils with very low cetane numbers did not show distinct differences to the other fuels. (Ejim et al., 2007) report on increasing droplet sizes for neat vegetable oils. It is therefore possible that this lack of increasing premixed combustion with decreasing cetane numbers is caused by increasing droplet sizes.

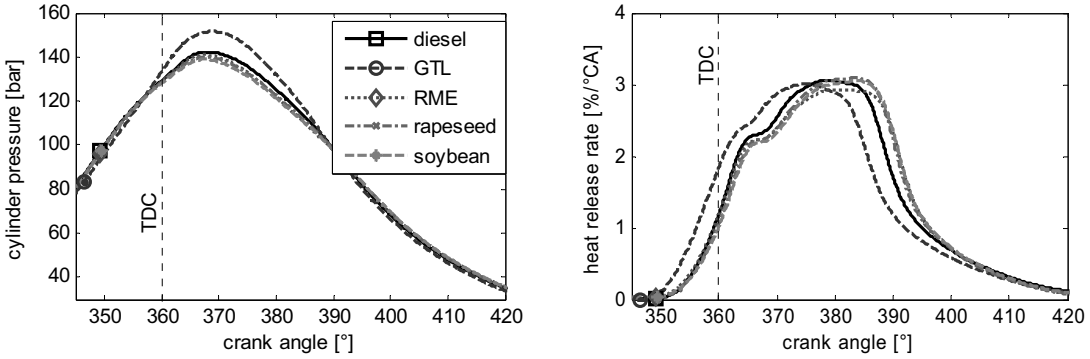

Figure 3: Cylinder pressure and heat release rates for case C (markers indicate start of injection).

Engine-out and tailpipe NO_x emissions are shown in Figure 4. It can be seen that GTL lowered NO_x emissions if no re-calibration was performed. The use of oxygenated fuels RME and the neat vegetable oils resulted in quite considerably increased NO_x emissions. This observations are in line with many other studies. This is not only true for case A where the engine output was increased but also for case B where the amount of fuel was adjusted to meet the output of the diesel fuel case. For case C, it was not possible to re-calibrate the engine for the neat vegetable oils exactly to the envisaged NO_x target of 3.6 g/kWh but only to 3.8 g/kWh because the injection would have been so late, that the fuel spray could have reached the cylinder walls. Figure 4 shows that the SCR system used was capable to reduce NO_x by about 1.5 g/kWh for all the cases and fuels. Larger NO_x reductions could have been reached but the ammonia slip would then exceed the envisaged maximum slip of 10 ppm.

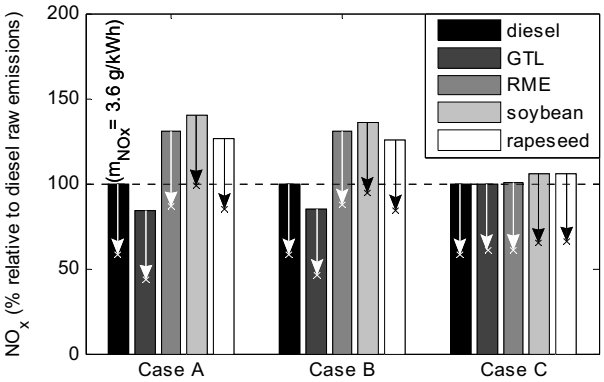

Figure 4: NO_x emissions (the bars represent engine-out emissions, the arrows show the emission reduction from the aftertreatment system).

For particle counting, the diluted exhaust gas was fed through an evaporation tube to reduce the amount of volatile particles measured by the downstream condensation particle counters. In case of the particles measurements in the raw exhaust gases (i.e. prior to any exhaust gas aftertreatment system), the evaporation tube was first used and then bypassed to measure the amount of evaporable particles. The soot mass was measured using a photo acoustic sensor (AVL Micro Soot Sensor). The measurement results before any exhaust gas aftertreatment are shown in Figure 5 (only for case A).

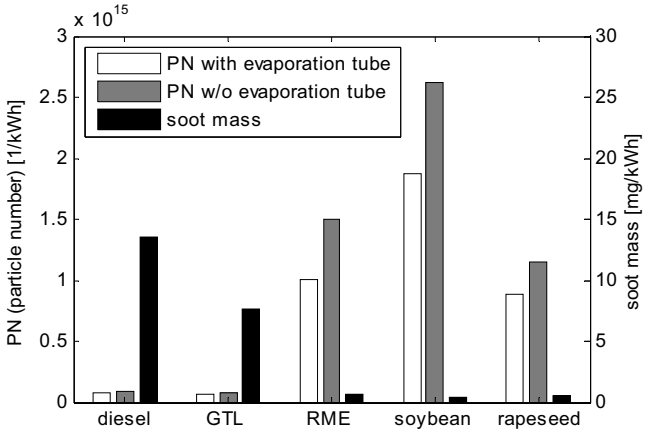

Figure 5: Particle counting and soot mass prior to exhaust gas treatment (for case A).

A large difference in particle number emissions between diesel/GTL and the oxygenated fuels is visible. About 10% of the counted particles could be evaporated at 300°C for diesel and GTL fuel. Up to 30% of the counted particles could be evaporated for the oxygenated fuels. The soot measurements show also a large difference between diesel/GTL and the oxygenated fuels. Particle emissions of Diesel and GTL consist mostly of soot; those from the oxygenated fuels contain very little soot. Consequently, a major fraction of the particle emissions from the oxygenated fuels have to be organic condensates that are not evaporated at 300°C. This interpretation corresponds well with the elemantary carbon/organic carbon (EC/OC) results shown in (Czerwinsky et al., 2007).

Particle number emissions measured after exhaust gas aftertreatment, relative to the engine's raw emissions for the diesel case, are depicted in Figure 6. The DPF faced an inlet gas temperature of about 500 °C which was sufficient for a continuous regeneration. Figure 6 shows that the DPF was able to reduce a large amount of the soot and the organic condensates. The GTL's lower amount of soot compared to diesel also becomes apparent in lower particle number emissions after DPF. The DPF seems to reduce the condensates with similar efficiency for all tested oxygenated fuels so that the DPF does not change their ranking. It has to be pointed out that the DPF used for the measurements described here showed a particle number filtration efficiency between 87.0% and 98.6% which is not an excellent value. Best available technology DPF systems show better particle number filtration efficiencies.

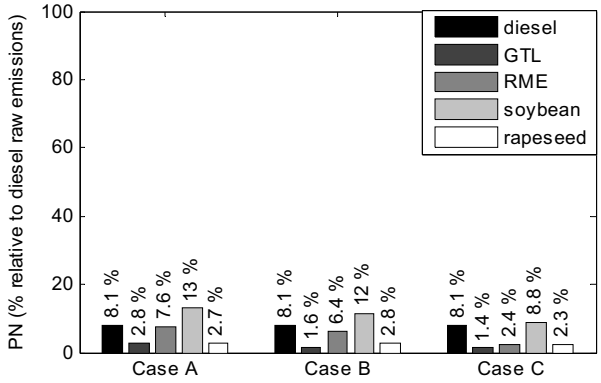

Figure 6: Particle numbers (with an evaporation tube) after exhaust gas treatment.

Conclusions

The experiments showed that the studied engine allowed stable combustion of diesel fuel, GTL fuel, RME, neat soybean and neat rapeseed oil at nearly full load operation. As all fuels had different chemical and physical properties, the engine torque, the peak injection pressure and the peak combustion pressure varied as the engine calibration (i.e start of injection, injection duration, EGR rate) remained unchanged. The oxygenated fuels RME, neat soybean and rapeseed oil increased the engine efficiency quite considerably by up to 5% while the NO_x emissions were increased. After re-calibration of the engine for each fuel in order to set the NO_x raw emissions on an equal level around 3.6 g/kWh, only neat soybean oil and GTL led to higher engine efficiencies than diesel.

Looking at particle emissions, the situation is more complex. The engine raw emissions contained far more soot for mineral diesel and GTL fuel than for the oxygenated fuels RME, neat soybean and rapeseed oil. The oxygenated fuels produced a much higher number of organic condensates and volatile particles. Looking at particle number and mass measurements it can be seen that the wall-flow DPF was able to reduce the particle emissions from all fuels to a similar extent.

It has to be pointed out that the long-term behaviour of the exhaust gas aftertreatment systems for the different fuels was not studied in this work. It is very likely that the alternative fuels generate different accumulation/regeneration behaviours of the DPF in transient operation compared to standard diesel fuel (Tschoeke et al, 2002). This could result in different system efficiencies but also in reduced lifetime of the exhaust gas aftertreatment systems. The experiments have shown that the different physical properties of the fuels have a keen influence on the injection system which can also impose lifetime problems using neat vegetable oils or RME with pump-line-nozzle injection systems. The extended results of this work are presented in (Soltic et al, 2009).

References

Abu-Jrai et al. (2006), Effect of gas-to-liquid diesel fuels on combustion characteristics, engine emissions, and exhaust gas fuel reforming, *Energy & Fuels*, 20, 2377-2384.

Babu A. K., Devaradjane G (2003), Vegetable oils and their derivatives as fuels for CI engines: An overview, *SAE paper*, 2003-01-0767.

Czerwinsky J. et. al. (2007), Injection, combustion and (nano) particle emissions of a modern HD-diesel engine with GTL, RME & ROR, *SAE paper*, 2007-01-2015.

Ejim C. E., Fleck B. A., Amirfazli A. (2007), Analytical study for atomization of biodiesels and their blends in a typi-cal injector: Surface tension and viscosity effects, *Fuel,* 86, 1534-1544.

Kegl B. (2006), Numerical analysis of injection characteristics using biodiesel fuel. *Fuel,* 85, 2377-87.

Kitano K., Dakata I., Clark R. (2005), Effects of GTL fuel properties on DI diesel combustion, *SAE paper*, 2005-01-3763.

Lapuerta M., Armas O., Rodríguez-Fernández J. (2008), Effect of biodiesel fuels on diesel engine emissions, *Progress Energy Combustion Sci*, 34, 198-223.

Mueller C. J. et al. (2003), Effects of oxygenates on soot processes in DI diesel engines: experiments and numerical simulations, *SAE paper* 2003-01-1791.

Rakopoulos C. D. et al. (2006), Comparative performance and emissions study of a direct injection diesel engine using blends of diesel fuel with vegetable oils or bio-diesels of various origins, *Energy Conversion and Management*, 47, 3272-3287.

Soltic P. et al. (2009), Experimental investigation of mineral diesel fuel, GTL fuel, RME and neat soybean and rapeseed oil combustion in a heavy duty on-road engine with exhaust gas aftertreatment, *Fuel*, 88, 1-8.

Szybist J. P., Kirby S. R., Boehmann A. L. (2005), NOx emissions of alternative diesel fuels: a comparative analysis of biodiesel an FT diesel, *Energy and Fuels*, 19, 1484-1492.

Tschoeke H. et al. (2002), Motoruntersuchungen mit Abgasnachbehandlungssystemen, project report of the Otto-von-Guericke University Magdeburg, Universitätsplatz 2, 39106 Magdeburg, Germany.

Session 4: Emission Policies

Effects of GHG-certificate trade on transport demand in Austria

C. Link, J. Stark*, R. Hoessinger*, G. Sammer*, G. Maier**, J. Lechner**, A. Sonntag***

* University of Natural Resources and Applied Life Sciences Vienna (BOKU), Institute for Transport Studies, A-1190 Vienna, Austria, attn. Christoph.Link@boku.ac.at
** Vienna University of Economics and Business (WU), Institute for Regional Development and Environment, A-1090 Vienna, Austria, attn. Julia.Lechner@ruw.ac.at

Abstract

Road traffic is a dominant source of air pollution. One possibility to limit traffic induced greenhouse gas (GHG) emissions could be its inclusion in the European Union Emissions Trading Scheme (EU ETS). The research project MACZE (Emissions Trading on the Road: Potential Design Options and their Impact on Traffic Volume and Fleet Efficiency in Austria) examines this thought. Its main objective is the development of a quantitative two-component-model combining an econometric travel demand model and an econometric GHG-certificate market model. The model expresses the relationship between travel demand, fuel consumption, fuel costs and the availability resp. price of GHG-emission certificates.

Keywords: CO_2, emissions, emissions trading scheme, road traffic, discrete choice-model

1 Introduction

The Kyoto Protocol, entered into force in 2005, sets the binding target for European Union member states to reduce GHG-emissions in the period of 2008-2012 of 8,0 % on average compared to 1990 level. In addition, Austria has imposed itself to lower GHG-emissions about 13 % in the same period. In the efforts to design a post-2012 proceeding European Union has committed itself to a further reduction of at least 20 % until 2020 compared to 1990 level. According to Austrian Federal Environmental Agency It is uncertain if Austria will be able to fulfil its obligations. While GHG-emissions of several sectors like room heating or agriculture have decreased since 1990 other ones cross this development: The past decade revealed a sharp increase in industry and traffic induced GHG-emissions in Austria. At present, GHG-emissions caused by road transport have a share of 28 % of Austria`s total greenhouse gas emission (Umweltbundesamt 2009). In future, one can expect a further increase of both traffic volume and CO_2 emissions.

A key tool of climate protection within European Union is the Emission Trading Scheme (EU ETS) which was introduced in 2005. Certificates traded allow their owner to emit a certain amount of GHG. Every participant has to hold allowances to fully cover up for his GHG-emission. To assure ongoing climate protection measures the number of allowances is reduced from 2013 yearly for 1,74 %. Up to now the trading scheme is limited on facilities of energy supply and industry, the largest GHG emitting source both in Austria as well as in the EU. Road transport is not included yet. The EU ETS guarantees, opposite to other measures of climate protection, GHG-reductions at optimal costs. If the individual costs of GHG-saving for a market participant are below the market price of emission allowances he should aim for a reduction of emissions. Saved allowances can be sold.

One promising strategy to limit GHG-emissions from road traffic is its inclusion into EU ETS. This suggestion is treated in the research project MACZE “Emissions Trading on the Road: Potential Design Options and their Impact on Traffic Volume and Fleet Efficiency in Austria” (Möglichkeiten und Auswirkungen eines EU-weiten CO_2-Zertifikathandels für den Straßenverkehr in Österreich). Its main objective is the development of a quantitative model to estimate the effects of the inclusion of road transport in the Emissions Trading Scheme. This concerns the development of emission certificate price and its impacts towards transport demand and car ownership. The project is funded by the Climate and Energy Fund of the Austrian federal government. The interdisciplinary project consortium consists of the University of Natural Resources and Applied Life Sciences – Department for Spatial, Landscape and

Infrastructure Science, Institute for Transport Studies (IVe) – and the Vienna University of Economics and Business – Department of Social Sciences, Institute for Regional Development and Environment (RUW).

This paper is meant as a status report of the research project MACZE. The following section provides basic information on options for the design of an Emissions Trading Scheme for road transport. Section 3 outlines the MACZE model, the underlying methodology and the survey concept. Preliminary simulation results of this research project are shown afterwards.

2 Emissions Trading Scheme

In order to estimate and analyse the consequences of an emissions trading scheme for road traffic, the scheme must be clearly defined. There are different basic design options. This concerns both the trading model with a decision between trading scheme per sector of the economy or trans-sectoral and the certification approaches. This determines which economic agents are obliged to obtain a certificate. There is an upstream, midstream and downstream approach. Also are the emission objectives (absolute or relative values), the initial allocation of allowances and the reporting, control and sanctioning system important.

Trans-sectoral vs. sectoral trading

The trade with certificates of carbon offset can either be trans-sectoral (open trade model) or limited to individual sectors of the economy (closed trade model). An open trade model means a full integration to the existing EU ETS. In this case certificates of carbon offset are freely transferable between the sectors energy, industry, and (road) traffic. In a closed trade model several schemes run in parallel and no trans-sectoral trade is permitted. Another option would be a semi open trade model. In this case certificates transfer in one direction is inhibited or only feasible with a price overhead.

The economic advantage of a trade with certificates of carbon offset is based on the fact that the desired reductions of emissions are achieved by those pollution sources whose marginal abatement cost is the lowest. The more heterogeneous the cost structure, the bigger is the efficiency potential of emission trading. From this can be derived that as many sectors as possible should be involved in an open trade model. With respect to technological progress in the road transport sector a closed trade model may be more advantageous. The closed trade model approach is usually based on the assumption that the marginal abatement costs in the road transport sector are considerably higher than in the sectors industry and energy. This fact would cause a permanent net surplus of transferred certificates of carbon offset to the transport sector. Because of that there will only be low pressure to innovate.

Various certification approaches

The certification approach determines who would be obliged to obtain a certificate. This should be based on the polluter pays principle. Therefore in the traffic sector both vehicle users (downstream approach) and vehicle manufacturers (midstream approach) might be included in the emissions trading scheme. Moreover, there is the possibility to oblige both producers and importers of fossil fuels to obtain a certificate (upstream approach).

The downstream approach addresses the problem at the level where the "decision to pollute" is made. As far as road traffic is concerned, this is the individual vehicle user. If this approach is used every vehicle user must have a sufficient number of certificates to compensate for his traffic-related pollutant emission. Raux and Marlot (2005) recommend an annual fuel or certificate quota. If more than the allocated amount of fuel is needed, additional certificates must be bought. Fuel savings mean that unused certificates can be sold. Given the high number of vehicle users, this approach is connected with a high monitoring and administration effort.

The midstream approach is based on relative emission objectives. This means that a baseline-and-credit scheme would be used with a fleet emission standard for vehicle manufacturers and importers. It is assumed that a midstream approach causes comparatively low measure and monitoring costs (Ewringmann et al. 2005). The advantage of the midstream approach is the generation of direct incentives to innovate. Its disadvantage is the fact that the mobility or driving behaviour will not be influenced and that the emission capping is limited to new cars, i.e. the emissions of pre-existing cars are not taken into account.

At present most discussions focus on an upstream approach in the form of a traditional cap-and-trade scheme. In this case individual fuel producers would need to obtain a number of certificates in accordance with the amount of fuel they sell. The upstream approach is in line with the polluter-pays-principle since there is a direct correlation between fossil fuels and pollutant emission. Moreover the cost caused by the obligation to obtain certificates is passed on to the vehicle users via the price. Compared to the downstream approach an upstream approach causes lower measure and monitoring costs.

Because of the weaknesses of each approach integrated concepts are gaining in importance. In order to create direct incentives for car users within the midstream approach, one might adjust the monthly taxes and/or the variable operating costs accordingly. On the other hand, the emission standards for new cars which will be implemented from 2012 onward, would be a meaningful addition to an upstream approach, to offer manufacturers incentives to invest (Kampman, Davidson & Faber 2008).

3 Macze-model and car user survey

Within the framework of MACZE an EU-wide (partly) open emissions trading scheme for the road transport sector is analysed. A comparison of the advantages and disadvantages of the various certification approaches shows that the downstream approach can be ruled out, because it does not seem to be manageable. Moreover, the discussion points to the fact that neither a midstream nor an upstream approach is obvious favourite. Therefore the quantitative analysis looks at the effects of both midstream and upstream approaches. This is done to allow comparisons on the basis of quantitative models and fill a current gap in scientific knowledge.

As main part of the research project an individual travel demand model and an econometric market model are developed and combined to show the connection between travel demand, fuel consumption, fuel costs, and the availability or price of GHG-certificates (Figure 1).

The travel demand model for the transport of passengers and goods describes – depending on selected influential factors – the relationship between travel demand and fuel prices from 'the users' point of view. The model is based on a discrete-choice model and the theory of individual utility maximization, which has proved useful to describe travel behaviour. While data for private vehicle road transport are surveyed, transport of goods is a result of literature research.

The GHG-emission certificate market model is used to show the connection between fuel consumption, fuel price and the availability or price of GHG-emission certificates. The parameters of the model are based on an econometric analysis of the European market for certificates since the start of the EU ETS in 2005. The output of the model, the price of GHG-emission certificates, is mainly driven by the demand of the competing economic sectors and the available overall quantity of emission allowances.

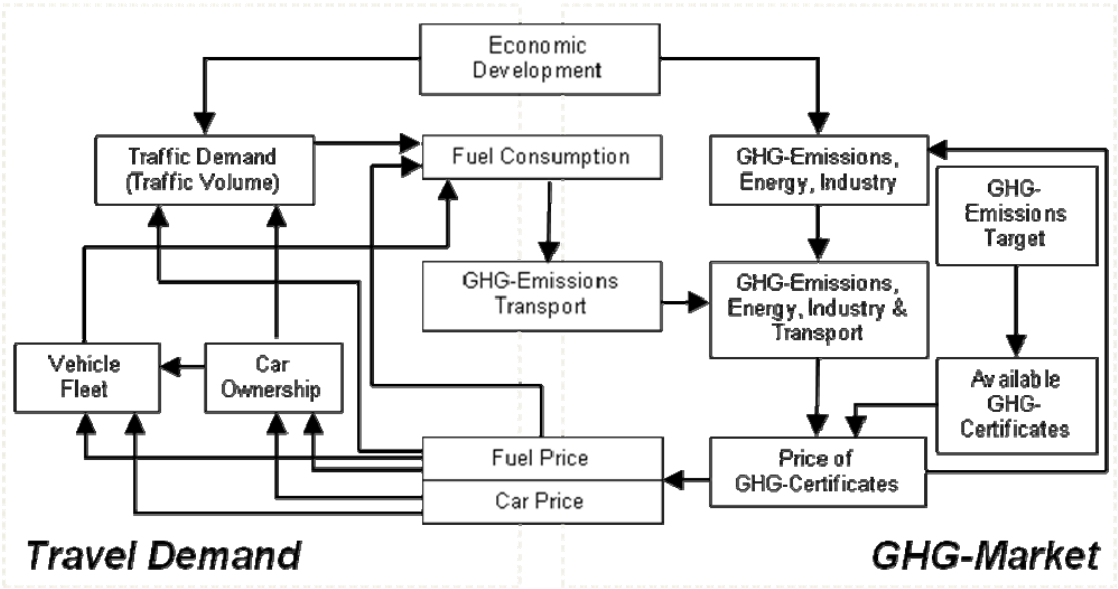

Figure 1: MACZE-model (developed by the authors)

Data for the econometric travel demand model were delivered by a multi-stage stated response survey. Main feature of this technique is the quantification of interdependencies which cannot be determined by other qualitative and quantitative methods. The technique provides good estimations of reactions to hypothetical scenarios (FGSV 1995; Axhausen & SAMMER 2001).

Our population refers to car drivers with periodic car use, specified as car driver trips at least at one of three specific reference days. Target persons who were willing to participate in the survey were identified by a telephone interview. Up to four car driver trips that had been realized on the latest Saturday, Sunday or working day were surveyed. If possible, all household members got surveyed. Secondly, in-depth household interviews were conducted. In these interviews persons were faced with various hypothetical fuel and car price scenarios based on the actual travel behaviour describing the impacts of obligatory emissions allowance – that in the case of a midstream model affects vehicle costs and in an upstream model fuel price; the respondents had to decide how they would react in the hypothetical situations (discrete-choice process).

In several steps, respondents were asked for mode choice with changing circumstances. In scenario 1 respondents were faced with increasing travel expenses. That were calculated by fuel consumption of the chosen car, trip distance and the price categories 1,50, 2,00, 3,00 or 4,00 Euro per liter fuel considering the price of emission allowances. In scenario 2 respondents got additionally cleared up on trips` alternatives using public transport with information on stops, duration and travel costs. This corresponds to an information scenario. In the third scenario respondents were exposed with changing fuel costs calculated for an entire year. To get also information about long-distance car trips also the last holiday trip by car was surveyed. However, only one scenario with changing travel expenses – scenario 4 – was conducted.

Car ownership was focused in scenario 5. For every car it was asked if it would get sold, replaced or kept under given circumstances. As influencing variable yearly running costs were given in the scenario. Besides the actual cost level another one was calculated including a higher fuel price level. In the case of car exchange respondents had to declare a preferred vehicle category differing small, medium and high. This answer was picked up in scenario 5a – car transaction – that was conducted for every car of the household that would be changed. For the chosen category four vehicles were drafted with differing types of power (gas, hybrid and electric), fuel consumption and purchasing price. Concrete appointment of values was chosen randomly by an amount of given characteristics. Fuel consumption of electric-powered cars was defined as zero, of hybrid-powered cars half as much as a gas-powered car on average.

In the discrete-choice-model besides alternative-specific variables characteristics of choice situation as trips or cars, characteristics of the choice maker as age or gender and textual factors as household and settlement are included. Characteristics of the alternative are:

- Travel-demand-model: trip expenses, trip duration and the quotient of duration and trip distance. Last one was chosen, because the correlation of single trip distance and both expenses and duration were nearby the value one.
- Holiday-trip-model: trip expenses
- Car ownership-model: potential asking price, average fuel consumption, yearly fuel consumption, willingness to pay for a new car
- Car transaction-model: mode of drive, fuel consumption, purchasing price.

Outcomes of discrete-choice-models will be used as input parameters to develop the econometric model in an upstream or a midstream approach. Giving a starting amount of emission allowances their development of prices can be calculated. Calculated prices of emission allowances affect car ownership, vehicle fleet mixture and travel demand. Changing car ownership and vehicles` fuel consumption determine in turn fuel consumption demand and therefore emission allowances prices. By pass through an iterative procedure emission allowances price should converge to a final price.

4 First results

The survey was conducted between July 2009 and January 2010. The sample consists of 232 persons out of 188 households with 313 cars. The number or valid car driver trips amounts to 499. In the following descriptive results are shown. Focus lies on the different scenarios of mode choice and car ownership.

Results of scenarios 1-3 are given in Table 1. Evident is a tendency to maintain car use and to avoid use of public transport in case of behaviour change. In scenario 1 all 499 trips were included. 6 % of trips are taken by public transport, whereas in almost 20 % of the trips the answer “others” meaning e.g. the abandonment of the trip or use of bicycle was chosen. Elucidation of trip alternatives by use of public transport (scenario 2) was meant as an information scenario. In fact mode choice is affected clearly: Public transport is going to be used in 10 % of trips within these circumstances. Changes of mode choice in favour of public transport aren’t at the expenses of car use. In fact it is a zero-sum situation of public transport and “others”. Information about yearly costs affects mode choice of respondents (scenario 3). Nearly each third of the answers is “Others”.

Table 1: Results of scenarios 1-3 (Travel behaviour)

	Status quo (1,00 Euro)	Scenario 1	Scenario 2	Scenario 3
Sample size [trips]	499	499	331	161
Average fuel price	-	2,56 Euro	2,60 Euro	2,54 Euro
Car use	100 %	75 %	75 %	61 %
Use of public transport	-	6 %	10 %	9 %
Others	-	19 %	15 %	30 %

Table 2 shows the change of mode choice depending on the price level per liter fuel in scenario 1. There is no linear tendency. Up to a fuel price level of 3,00 Euro per liter fuel, car use decreases and other behaviour to avoid costs increase. However, exposed with a fuel price level of 4,00 Euro, car use is chosen more often and “Others” rarely. This may be a random or a reactance effect. Allocation of use of public transport has a relative minimum of mentions at a price level of 3,00 Euro. Altogether there is a relative distinctive stability in car use. That supports supposition of low price elasticity of travel demand (Graham and Glaister 2002, Goodwin, Dargay and Hanley 2004). It can be shown that willingness to use public transport decreases with an increasing number of cars per household. This fact demonstrates a clear vehicle affinity. Surprisingly the share of car use is more constant in urban areas.

Table 2: Results of scenario 1 (Travel behaviour)

Price per liter fuel	Status quo (1,00 Euro)	1,50 Euro	2,00 Euro	3,00 Euro	4,00 Euro	All (2,56 Euro)
Sample size [trips]	499	89	181	118	100	499
Car use	100 %	85 %	82 %	63 %	68 %	75 %
Use of public transport	-	4 %	6 %	4 %	9 %	6 %
Others	-	11 %	12 %	33 %	23 %	19 %

117 holiday trips were examined in scenario 4. Altogether 70 % of trips would be repeated in the same way unaffected by an increase of fuel prices. Compared to scenarios 1-3 car use is taken less into consideration. This is up to higher trip costs compared to daily trips depending on higher trip length. Behaviour as result of different fuel price levels is shown in Table 3. Car use decreases with increasing fuel price level. One third of respondents chooses other destinations or changes the mode of travelling when fuel price reaches the 3,00 Euro level. Less than one of two holiday trips is unaffected by a fuel price level of 4,00 Euro.

Table 3: Results of scenario 4 (Holiday trips)

Price per liter fuel	Status quo (1,00 Euro)	1,50 Euro	2,00 Euro	3,00 Euro	4,00 Euro	All (2,60 Euro)
Sample size [trips]	117	21	46	28	22	117
Car use	100 %	91 %	77 %	62 %	44 %	70 %
Others	-	9 %	23 %	38 %	56 %	30 %

Table 4 shows the results of scenario 5. A continuous decrease of number of cars is obviously with higher fuel price level. Preferred alternative to keep the car is `replace`. Respondents are rather willing to replace their car with another one with lower consumption than to pass on a car. This affects households` mobility moderately, travel behaviour can be maintained. Willingness to change the car is quite higher in households living in central areas (47 % willingness to replace a car). The answer `selling` is chosen more often with increasing number of vehicles per household. There is no difference between a fuel price of 3,00 Euro and of 4,00 Euro. Obviously there is a critical price value for car ownership. Its exceeding doesn't affect car ownership anymore – due to missing alternatives or due to missing willingness to abandon.

Table 4: Results of scenario 5 (Car ownership)

Price per liter fuel	Status quo (1,00 Euro)	1,50 Euro	2,00 Euro	3,00 Euro	4,00 Euro	All (2,43 Euro)
Sample size [cars]	306	59	129	75	43	306
Keeping the car	-	86 %	77 %	63 %	63 %	73 %
Replacing the car	-	10 %	21 %	29 %	30 %	23 %
Selling the car	-	4 %	2 %	8 %	7 %	4 %

Respondents who change their car had to choose a new type of car out of four. Results concerning type of power are given in Table 5. Although only one of four cars is hybrid-powered, it was chosen in more than every third case. Less than expected people decided in spite of low consumption costs as a result of both high purchasing prices and doubt in technical reliability for electric-powered vehicles.

Table 5: Results of scenario 5 (Car transaction: Choice of type of power)

Price per liter fuel Mode of drive	Status quo (1,00 Euro)	1,50 Euro	2,00 Euro	3,00 Euro	4,00 Euro	All (2,60 Euro)
Sample size [cars]	67	6	27	22	12	67
Gas-powered	-	67 %	33 %	52 %	42 %	45 %
Hybrid-powered	-	33 %	30 %	48 %	33 %	36 %
Electric-powered	-	-	37 %	-	25 %	19 %

Preview

While descriptive interpretations have progressed considerably, discrete choice analyses are just getting started. Results are expected within next two months (until end of May 2010). Their inclusion enables the development of the travel demand model. So far results ensure that a sharp increase of fuel price clearly affects both travel behaviour and car ownership. This is particularly valid for holiday trips.

References

Axhausen K.W. & G. Sammer (2001), Stated responses: Überblick, Grenzen, Möglichkeiten, *Internationales Verkehrswesen*, vol. 53 (6), pp. 274-278, Hamburg.

Ewringmann D., H. Bergmann, R. Bertenrath, R. Betz, F. Dünnebeil, U. Lambrecht, L. Liebig, K. Rogge & W. Schade (2005), ‚Emissionshandel im Verkehr: Ansätze für einen möglichen Up-Stream-Handel im Verkehr, In Studie im Auftrag des Umweltbundesamtes, Dessau.

FGSV – Forschungsgesellschaft für Straßen- und Verkehrswesen (1995), Hinweise zur Messung von Preferenzstrukturen mit Methoden der Stated Preferences, FGSV, Köln.

Goodwin P., J. Dargay and M. Hanley (2004): Elasticities of Road Traffic and Fuel Consumption with Respect to Price and Income: A Review. Transport Reviews, 24 (3), pp. 275-292.

Graham D.J. & S. Glaister (2002): The Demand for Automobile Fuel: A Survey of Elasticities. *Journal of Transport Economics and Policy*, 36 (1), pp. 1-25.

Kampman B., M.D. Davidson & J. Faber (2008): Emissions trading and fuel efficiency in road transport. Swedish Environmental Protection Agency. Delft.

Raux C. & G. Marlot (2005), A scheme of tradable CO_2 permits applied to fuel consumption by motorists, Transport Policy, vol. 12, pp. 255-265.

Umweltbundesamt - Federal Environment Agency (2007), Treibhausgasemissionen in Österreich 1990–2005, Datenstand 2007, Homepage des Umweltbundesamtes Österreich, viewed 22. July 2009, <http://www.umweltbundesamt.at/fileadmin/ site/presse/news2007/ Treibhausgasemissionen_1990_2005.pdf/>.

Umweltbundesamt - Federal Environment Agency (2009), Klimaschutzbericht 2009, Homepage des Umweltbundesamtes Österreich, viewed 22. July 2009, <http://www.umweltbundesamt.at/ fileadmin/site/publikationen/REP0226.pdf />.

Air Quality Impact Assessment of the Environmental Zone in Copenhagen

*S.S. Jensen*1, M. Ketzel1, J.K. Nøjgaard1, P. Wåhlin1*

[1] National Environmental Research Institute (NERI), Department of Atmospheric Environment, Aarhus University, Denmark. * ssj@dmu.dk

ABSTRACT

In this study we assess the expected effects on emissions and air quality from the implementation of the environmental zone in Copenhagen in two stages in 2008 and in 2010 that requires particle filters on heavy-duty vehicles. The evaluation is based on street canyon and urban background air quality models and includes 138 busy street canyons in Copenhagen. Compared to a reference scenario the environmental zone reduces total NO_x emissions by 17% in 2010 and it reduces the number of exceedances of the NO_2 limit value in 2010 from 65 to 35. Total PM_{10} emissions are reduced by 9% and total $PM_{2.5}$ emissions by 16% in 2010. On average PM_{10} concentrations in the 138 streets are reduced by 0.7 µg/m^3 (2.5%) and $PM_{2.5}$ concentrations by 0.7 µg/m^3 (3.5%).

1. INTRODUCTION

Environmental zones have been implemented in a number of European cities in recent years (www.lowemissionzones.eu). The purpose of environmental zones is to reduce urban air pollution and associated health risks, and to reduce exceedances of EU air quality limit values for especially PM_{10} and NO_2. The Danish law about environmental zones allows the five largest urban municipalities to define zones and to require particle filters on heavy-duty vehicles with emission standard Euro 2 or older by September 1, 2008 and with emission standard Euro 3 or older by July 1, 2010. The main purpose of the Danish law is to reduce particle emissions from heavy-duty vehicles. A number of pre-assessment studies of the expected impacts of the Danish environmental zones have been carried out. These studies have focused on air quality, population exposure and social costs based on air quality models for urban background and street canyons, emission modelling, detailed traffic counts, and cost-benefit methods.

Furthermore, simultaneous air quality measurements of PM_{10}, $PM_{2.5}$ and particle number concentrations (ToN) in urban background and streets in combination with receptor modelling have been used for source apportionment. Although, particle filters on heavy-duty vehicles are assumed to reduce particle exhaust emissions by 80%, the reduction in concentrations is modest in urban background, and even in busy streets. Modelled PM_{10}, $PM_{2.5}$ and ToN concentrations in a busy street in Copenhagen are expected to decrease by 4%, 6%, and 13-20%, respectively (Palmgren et al. 2005a,b). The reason why the reduction is modest for PM_{10} and $PM_{2.5}$ is that the regional contribution is large and that particle filters do not reduce non-exhaust (re-suspension, road, tire and brake wear) that is an important contributor to total PM as mass. The reduction in ToN concentrations is substantial since street concentrations are less influenced by the regional contribution and non-exhaust. Cost-benefit analyses based on reduction of population exposure to $PM_{2.5}$ have also shown positive results despite modest reductions in $PM_{2.5}$ concentrations (Palmgren et al. 2005a). Before the legislation was passed different requirements have been discussed for the environmental zones and the above mentioned pre-assessment studies do not fully reflect the final requirements.

A recent study includes an assessment of the impact of the environmental zone legislation with focus on the air quality of NO_2, PM_{10} and $PM_{2.5}$ (Jensen et al., 2010). In this study we assess the expected effects on emissions and air quality from the implementation of the environmental zone in Copenhagen in 2008-2010 that requires particle filters on heavy-duty vehicles. The evaluation is based on urban background and street canyon air quality models and gives detailed results for 138 busy street canyons in Copenhagen. The study also included an analysis of before and after measurements of air pollutants in a busy street related to the first stage implementation of the environmental zone regulations. Air pollutants measured before and after implementation of first stage of the environmental zone requirements include NO_x, NO_2, CO, PM_{10}, $PM_{2.5}$ and particle number size distribution. The study also included an evaluation of the applied street air quality model comparing measurements and model results.

This paper presents the methodology and findings of this study with focus on the assessment for the 138 streets.

2. METHODOLOGY

The environmental zone is here defined as the geographical extent of the municipalities of Copenhagen and Frederiksberg to ease emission estimation although it is slightly larger than the legal extent of the original environmental zone (www.miljozone.dk). However, the municipalities decided later to extend the boundaries of the environmental zone to match the geographical extent of the municipalities which came into force on November 1, 2009.

The reference scenario includes the predicted development in traffic on the road network. It is assumed that traffic increases 24% from 2010 to 2020 on the main arterials and no increase on other roads is expected. The environmental zone scenario corresponds to the legal requirements in 2010 of the environmental zone legislation. Heavy-duty vehicles that comply with emission standard Euro 3 or older have to be equipped with particle filters. These requirements have been implemented in the following way. Euro 3 heavy-duty vehicles have been equipped with particle filters whereas Euro 0-2 are assumed to be replaced with new Euro 5 vehicles. For buses, it is assumed that Euro 0-1 and 50% of Euro 2 are replaced with Euro 5, 50% of Euro 2 and all Euro 3 buses are equipped with particle filters.

The AirGIS system was used to calculate air quality levels at selected streets in Copenhagen. AirGIS is a deterministic location-based model system for air pollution and human exposure estimation in urban areas based on the OSPM and UBM models together with digital maps including road links with traffic data and building footprints with building heights, and a Geographic Information System (GIS) (Jensen et al., 2001) (airgis.dmu.dk).

Air quality calculations have been carried out in a two stage process. Firstly, urban background concentrations have been calculated to represent the general air pollution levels in Copenhagen using the Urban Background Model (UBM) (Berkowicz, 2000a). The urban background concentrations form a part of the input for calculations of street concentrations. Secondly, air quality calculations are carried out for 138 busy streets in the municipalities of Copenhagen and Frederiksberg using the Operational Street Pollution Model (OSPM) (2000b). These streets represent street canyon conditions with Average Daily Traffic of 15,000 - 60,000 where potential NO_2 compliance problems may occur.

Air pollutants modelled include NO_x, NO_2, PM_{10}, $PM_{2.5}$, CO as well as CO_2 emissions. Calculations were carried out for the reference year of 2005, and for the scenario years 2010, 2015 and 2020. This paper reports on NO_2, PM_{10} and $PM_{2.5}$ that potentially may be close to or exceed limit values.

Emissions were estimated with the OSPM emission module that is based on the EU COPERT 4 emission model (EEA 2007). This methodology includes information about the car fleet and its distribution on vehicle categories, fuel types and emission standards (Euro classes), and associated emission factors. The distribution of emission classes, fuel type (petrol and diesel) have been updated as part of the study.

Years ago the diesel share of passenger cars was about 5% and 80% for vans. The diesel share has increased in recent years and it is assumed that the diesel share will gradually increase to reach 55% for passenger cars and 88% for vans in 2020.

A decade ago, the directly emitted NO_2 fraction of NO_x (NO_2 and NO) emission from vehicles was about 5-10%. This fraction has increased in recent years and is expected to be about 15-20% in 2010. This is one of the main reasons why NO_2 concentrations have not decreased in urban street despite substantial NO_x emission reductions. The increase in directly emitted NO_2 is due to the increase in the number of mainly diesel-powered passenger cars, but also of diesel-powered vans, that are equipped with oxidative catalysts that oxidise NO to NO_2. Furthermore, certain particle filters also increase the directly emitted NO_2. Most buses in central Copenhagen are equipped with particle filters, and more heavy-duty vehicles are expected to become equipped with particle filters to meet the emission requirements of the environmental zone in Copenhagen. The direct NO_2 fraction is estimated to be 18% in 2010, increasing to 25% in 2015, and then decreasing slightly to 24% in 2020. Direct NO_2 fractions are implemented in the OSPM emission module with separate values for each vehicle category and emission class.

The particle emission module includes exhaust and non-exhaust of $PM_{2.5}$ and PM_{10}. Particle filters are assumed to reduce particle exhaust emissions in average by 80% accounting for potential filter failure in some vehicles.

3. RESULTS AND DISCUSSION

NO_x source apportionment for selected busy streets (H.C. Andersens Boulevard and Jagtvej) in Copenhagen in 2010 show that heavy-duty vehicles (trucks and buses) account for about 30-35% of NO_x emissions but only 3-4% of traffic, taxis for about 7% of NO_x emissions and about 8-9% of traffic, vans for 14-18% of NO_x emissions and 10-12% of traffic, and passenger cars for about 48-54% of NO_x emissions and 77% of traffic. In total, diesel-powered vehicles contribute about 80-85% of NO_x emissions.

In the reference scenario (without environmental zone) the number of exceedances of the NO_2 limit value in 2010 is about 65 in busy streets in Copenhagen, 22 in 2015 and 3 in 2020 (Table 1). These calculations indicate that the problem of NO_2 exceedances will be solved within a decade due to the continuous introduction of more stringent Euro emission standards in the car fleet. The NO_2 limit value in 2010 for annual mean is 40 $\mu g/m^3$.

The environmental zone reduces the number of exceedances of the NO_2 limit value in 2010 from 65 to 35 (Figure 1). Although the emission requirements of the environmental zone are directed towards particle filters on heavy-duty vehicles (Euro 3 or older) the impact on NO_x emissions and NO_2 concentrations are profound due to the expected implementation of the requirements. It is assumed that Euro 0-2 trucks are replaced with new Euro 5 vehicles and Euro 0-1 buses and 50% of Euro 2 buses are also replaced with Euro 5. Since NO_x emissions are significantly lower for Euro 5 compared to Euro 0-2 it has a profound impact on emissions and concentrations.

Model calculations show that NO_x emissions decrease in the reference scenario from 2010 to 2020 due to introduction of vehicles that comply with more and more stringent emissions standards (Table 2). On the other hand, the total amount of directly emitted NO_2 in the reference scenarios increases from 2005 to a maximum in 2015 and then decreases towards 2020. The NO_2 fraction shows a similar pattern. The environmental zone reduces total NO_x emissions by 17% and the directly emitted NO_2 by 16% in 2010.

Table 1. Modelled average annual NO_2 levels at 138 streets in Copenhagen and at two selected streets with air quality monitoring. Street concentrations and urban background concentrations are shown.

Scenario	Street levels at 138 streets ($\mu g/m^3$)	Background levels at 138 streets ($\mu g/m^3$)	No. of exceedances of NO_2 limit value (over 40 $\mu g/m^3$)	Street level at H.C. Andersens Boulevard ($\mu g/m^3$)	Background level at H.C. Andersens Boulevard ($\mu g/m^3$)	Street level at Jagtvej ($\mu g/m^3$)	Background level at Jagtvej ($\mu g/m^3$)
2010	39.9	18	65	53.3	20.7	45.2	19.6
2015	34.9	16.4	22	47.3	18.6	39.2	17.7
2020	27.3	14.6	3	37.1	16.1	30.4	15.5
2010	36.5	17.0	35	48.4	19.3	41.6	18.3
2015	33.5	16.0	15	44.2	18.0	37.0	17.1
2020	27.1	14.5	2	35.1	15.9	29.1	15.3

Table 2. Total NO_x emissions for vehicle categories in reference scenario and with environmental zone requirements. Index for reference scenario is 100 in 2010. Direct NO_2 fractions are also shown.

Year	Scenario	Passenger cars (Index)	Vans (Index)	Trucks <= 32t (Index)	Trucks > 32t (Index)	Buses (Index)	Total (Index)	Direct NO_2 fraction (%)	NO_2 emissions (Index)
2005	Reference	137	107	104	106	115	119	7.4	49
2010	Reference	100	100	100	100	100	100	18.0	100
2015	Reference	74	75	77	76	78	75	25.0	105
2020	Reference	52	49	48	46	50	50	24.5	68
2010	EnvZone	100	100	62	65	71	83	18.4	84
2015	EnvZone	74	75	60	62	66	68	25.4	96
2020	EnvZone	53	49	43	43	47	48	24.6	66

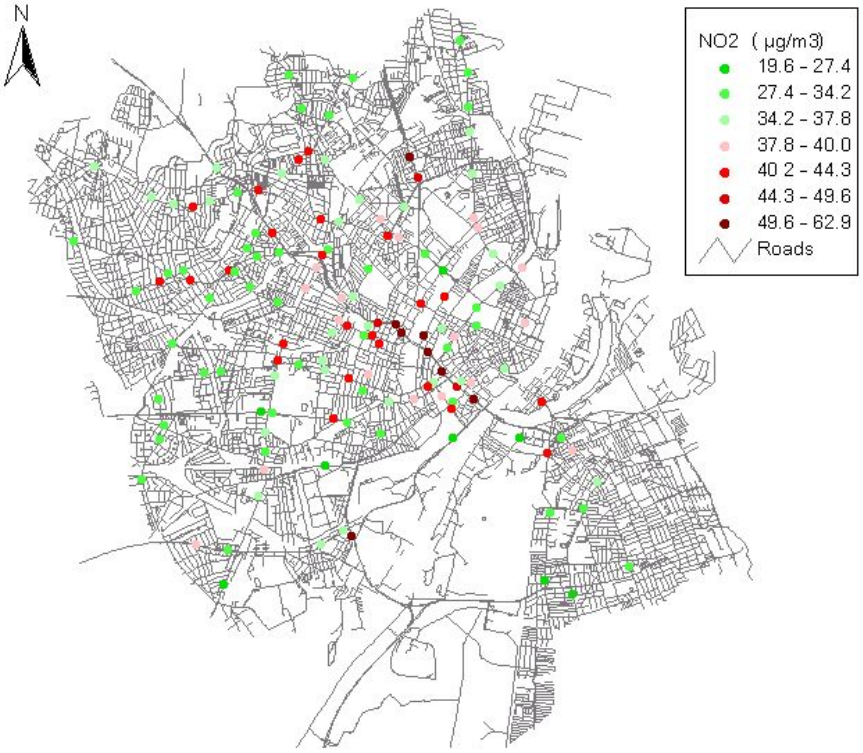

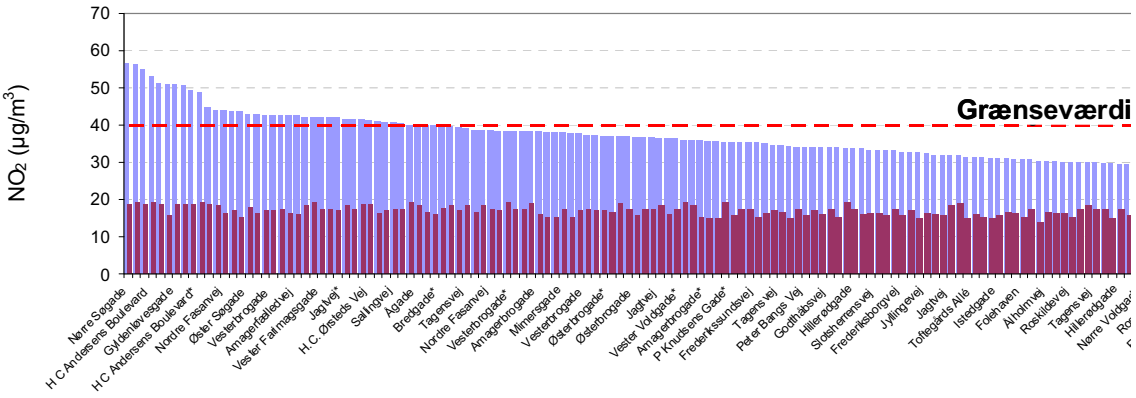

Figure 1. Upper: Location of the 138 busy streets in the Municipality of Copenhagen and the Municipality of Frederiksberg with the annual modelled NO2 street concentrations in 2010 (incl. environmental zone). Lower: Histogram of the same streets. Blue bars show street concentrations and purple bars show urban background concentrations. Not all of the 138 street names are shown. The limit value of 40 µg/m3 is shown as a dashed red line.

Heavy-duty vehicles (trucks and buses) contribute to about 26% of particle exhaust, and 15% and 14% of PM_{10} non-exhaust and $PM_{2.5}$ non-exhaust, respectively. Heavy-duty vehicles contribute 19% and 22% to total PM_{10} emissions (exhaust and non-exhaust) and to total $PM_{2.5}$ emission (exhaust and non-exhaust), respectively (Table 3).

Table 3 Source apportionment for particle emission at H.C. Andersens Boulevard in 2010 (excl. environmental zone)

	Passenger cars	Taxis	Vans	Trucks <=32t	Trucks > 32t	Buses	*Heavy-duty vehicles*	Total
	(%)	(%)	(%)	(%)	(%)	(%)	*(%)*	(%)
PM_{10} non-exhaust	63	10	12	9	2	5	*15*	100
$PM_{2.5}$ non-exhaust	64	10	11	8	2	5	*14*	100
PM exhaust	42	12	20	13	3	10	*26*	100
PM_{10} (exhaust and non-exhaust)	56	11	15	10	2	7	*19*	100
$PM_{2.5}$ (exhaust and non-exhaust)	50	11	17	11	3	8	*22*	100

Average modelled PM_{10} and $PM_{2.5}$ concentrations at the 138 streets are summarized in Table 4 and particle emissions in Table 5. There is only a very modest reduction of about 1 µg/m^3 in PM_{10} and $PM_{2.5}$ concentrations in the streets in the reference scenario from 2010 to 2020. The urban background concentrations, that are dominated by the regional concentrations, play a much larger role for PM_{10} and $PM_{2.5}$ compared to NO_2. Hence, the street contribution for PM_{10} and $PM_{2.5}$ is smaller than for NO_2. Furthermore, the street contribution includes exhaust emissions and non-exhaust emissions (re-suspension, road, tire and brake wear). In the reference scenarios from 2005-2020, the non-exhaust emissions increase proportional to the expected increase in traffic whereas PM exhaust decreases due to more stringent emission standards. Total PM_{10} emissions (exhaust and non-exhaust) are expected to decrease by 5% and $PM_{2.5}$ by 23% from 2010 to 2020 in the reference scenario. The impact of the environmental zone in 2010 is a reduction of 9% in total PM_{10} emissions and 16% in total $PM_{2.5}$ emissions due to reduced exhaust emissions caused by particle filters and a shift to newer Euro emission standards for heavy-duty vehicles. The emission reduction is less for PM_{10} compared to $PM_{2.5}$ since exhaust emissions play a less significant part of total emissions for PM_{10}. On average

PM_{10} concentrations in the 138 streets are reduced by 0.7 μg/m^3 (2.5%) and $PM_{2.5}$ concentrations by 0.7 μg/m^3 (3.5%).

Table 4. Modelled average annual street and urban background concentrations of PM_{10} and $PM_{2.5}$ at 138 streets in Copenhagen.

Year	Scenario	PM_{10} street levels at 138 streets (μg/m^3)	PM_{10} background levels at 138 streets (μg/m^3)	$PM_{2.5}$ street levels at 138 streets (μg/m^3)	$PM_{2.5}$ background levels at 138 streets (μg/m^3)
2010	Reference	29.1	23.1	20.0	16.7
2015	Reference	28.6	23.0	19.3	16.7
2020	Reference	28.3	23.0	18.9	16.6
2010	EnvZone	28.4	23.0	19.3	16.7
2015	EnvZone	28.2	23.0	19.0	16.6
2020	EnvZone	28.2	23.0	18.8	16.6

Table 5. Total emissions of PM_{10} NonExhaust, $PM_{2.5}$ NonExhaust, PM Exhaust emissions, PM_{10} and $PM_{2.5}$ in reference scenario and with environmental zone requirements. Index for reference scenario is 100 in 2010.

Year	Scenario	PM_{10} NonExh (Index)	$PM_{2.5}$ NonExh (Index)	PMExh (Index)	PM_{10} (Index)	$PM_{2.5}$ (Index)
2005	Reference	84	85	110	93	101
2010	Reference	100	100	100	100	100
2015	Reference	108	107	72	96	85
2020	Reference	116	116	54	95	77
2010	EnvZone	100	100	74	91	84
2015	EnvZone	108	107	60	92	77
2020	EnvZone	116	116	49	94	73

None of the 138 streets are expected to exceed the annual limit value for PM_{10} of 40 μg/m^3 in 2010-2020. Additionally, the limit value for $PM_{2.5}$ of 25 μg/m^3 in urban background in 2015 is not expected to be violated.

4. CONCLUSIONS

An impact assessment based on dispersion models was carried out for 138 busy street canyons of the expected effects on emissions and air quality of the environmental zone implemented in Copenhagen in two stages in 2008 and in 2010 that requires particle filters on heavy-duty vehicles (Euro 3 or older). Compared to a reference scenario the environmental zone reduces total NO_x emissions by 17% in 2010 and it reduces the number of exceedances of the NO_2 limit value in 2010 from 65 to 35. The reduction is due to a partly shift towards Euro 5 vehicles instead of equipping all heavy-duty vehicles with Euro 3 or older emission standard with particle filters. The impact of the environmental zone in 2010 is a reduction of 9% in total PM_{10} emissions (exhaust and non-exhaust) and 16% in total $PM_{2.5}$ emissions due to reduced exhaust emissions caused by particle filters and a shift to newer Euro emission standards for heavy-duty vehicles. The emission reduction is less for PM_{10} compared to $PM_{2.5}$ since exhaust emissions play a less significant part of total emissions for PM_{10}. On average PM_{10} concentrations in the 138 streets are reduced by 0.7 μg/m^3 (2.5%) and $PM_{2.5}$ concentrations by 0.7 μg/m^3 (3.5%). The modest reduction in PM concentrations in streets is due to the large contribution from the urban background concentrations dominated by the regional background and that particle filters and

more stringent Euro emission standards only reduce exhaust emissions and not non-exhaust emissions.

References

Berkowicz, R. (2000a), A Simple Model for Urban Background Pollution, *Environmental Monitoring and Assessment* Vol. 65, Issue 1/2, pp. 259-267.

Berkowicz, R. (2000b), OSPM - A parameterised street pollution model, *Environmental Monitoring and Assessment*, Volume 65, Issue 1/2, pp. 323-331.

EEA (2007), EMEP/CORINAIR Atmospheric Emissions Inventory Guidebook 2007, Methodology for the calculation of exhaust emissions, COPERT 4, European Environmental Agency. 105 p.

Jensen, S. S., Berkowicz, R., Hansen, H. S. and Hertel, O. (2001), A Danish decision-support GIS tool for management of urban air quality and human exposures, *Transportation Research Part D-Transport and Environment* 6, 229-241.

Jensen, S.S., Ketzel, M. (2009), Catalogue of abatement measures to reduce exceedances of the NO_2 air quality limit value in larger Danish cities, (In Danish with English summary), Danish Environmental Protection Agency. Environmental Project No. 1268, 2009. 84 p. http://www2.mst.dk/udgiv/publikationer/2009/978-87-7052-918-1/pdf/978-87-7052-919-8.pdf

Jensen, S.S., Ketzel, M., Nøjgaard, J. K., Wåhlin, P. (2009), Air Quality Assessment of Environmental Zones in Denmark, Midterm Report, NERI report No. 748. ISBN: 978-87-7073-136-2, ISSN (electronic): 1600-0048, In Danish with English summary.

Palmgren, F., Glasius, M., Wåhlin, P., Ketzel, M., Berkowicz, R., Jensen, S.S., Winther, M., Illerup, J.B., Andersen, M.S., Hertel, O., Vinzents, P.S., Møller, P., Sørensen, M., Knudsen, L.E., Schibye, B., Andersen, Z.J., Hermansen, M., Scheike, T., Stage, M., Bisgaard, H., Loft, S., Lohse, C., Jensen, K.A., Kofoed-Sørensen, V. & Clausen, P.A. (2005a), Particulate Air Pollution in Denmark. Danish Environmental Protection Agency, Report 1021, 84 p. (In Danish with English summary) http://www.mst.dk/udgiv/Publikationer/2005/87-7614 ... -7614-721-5.pdf

Palmgren, F., Berkowicz, R., Fogh, C.L. (2005b), Assessment of the impact of different types of environmental zones in Copenhagen, NERI report, nr. 222, 23 p. (In Danish with English summary) http://www2.dmu.dk/1_viden/2_Publikationer/3_arbrapporter/rapporter/AR222.pdf

Acknowledgement

The study is part of an evaluation of environmental zones in Denmark funded by the Danish Environmental Protection Agency and carried out by NERI.

CO_2 Emissions and Daily Mobility: Factors for Change The Case of the Lyon Urban Area

Authors: Louafi Bouzouina [a], Jean-Pierre Nicolas [a], Florian Vanco [b]
[a] LET, ENTPE, 2 Rue Maurice Audin – 69518 Vaulx-en-Velin Cedex – France
[b] CERTU, 9 Rue Juliette Récamier, 69006 Lyon – France

Introduction

Recent discussions regarding the environment and sustainable development show that most European cities encourage alternative modes of transport such as cycling, reinvesting in public transport networks. They also seek more coordinated and better controlled forms of urban development. Furthermore, the global economic crisis in general, and the pressure on energy prices in particular, create an additional economic constraint with regard to car use. In this context, a number of local travel surveys show that motor vehicle mobility in large cities in France tends to fall in favour of sustainable transport modes and public transport (Hubert, 2009). However, what is the reality of the situation, and is this trend reflected in a reduction in greenhouse-gas emissions related to urban mobility (Dupont et al., 2009)? We shall try to answer this question in this article by examining the case of the Lyon urban area, where this trend has been observed. We have therefore used as part of our analysis the last two household travel surveys (HTSs) carried out in the Lyon area, in 1995 and 2006, in order to estimate the CO_2 emissions generated by its inhabitants. We have then tried to identify the most important factors behind the trends observed, that are linked to the changing characteristics and composition of the population, the mobility-related behaviour of different socio-economic groups, and the technological characteristics of the motor vehicle fleet as a whole.

First, we shall present the methodology that was adopted to ensure the comparability of data from the two surveys, calculate greenhouse-gas emissions (which shall here be assimilated to CO_2 emissions), and then identify the different factors that have an impact on daily mobility and the emissions they generate. The second part of our article is dedicated to the results of our analyses, and will first outline the general trends, before highlighting the groups for which the margins for manoeuvre are greatest. This shall enable us to discuss, in the conclusion, the most efficient measures for reducing CO_2 emissions related to daily travel.

Measuring and comparing CO_2 emissions related to daily mobility using French household travel surveys

The Lyon urban area and household travel surveys carried out between 1995 and 2006

Lyon, capital of the Rhône-Alpes region, has a population of 620,000 in the urban core formed by the municipalities of Lyon and Villeurbanne, and a total of 1.2 million inhabitants in the wider urban area (which shall here be considered to be coextensive with the Greater Lyon urban community). It is a dynamic city which historically has benefited from a strong manufacturing base, and which is today recognised as a major higher education and research centre. The urban core is very densely populated, and is therefore well suited to modes of transport other than the car, as well as to an efficient public transport network. The urban area extends further to the east (across plains) than it does to the west (where development is constrained by the Monts du Lyonnais); nonetheless, the urban area presents clearly a monocentric structure.
Our analysis of changes in daily mobility and CO_2 emissions is based on the last two household travel surveys carried out in Lyon, in 1995 and 2006. These surveys were organised according to a standard procedure, which was monitored by a national organisation, CERTU (*Centre d'études sur les réseaux, les transports, l'urbanisme et les constructions publiques* – Centre for the Study of Urban Planning, Transport and Public Facilities). This homogeneity at national level means that comparisons can be made between different urban areas in France, as well as between several successive surveys. These surveys are carried out at roughly 10-year intervals in all the major urban areas in France. The observation unit used for statistical purposes is the household. All persons aged five years and over that belong to a given household are asked questions about the journeys they made the day before the survey. All surveys are carried out between Tuesday and Saturday, and do not take account of any weekend travel. The data collected concerns the key socio-economic characteristics of the household and its members,

as well as information about each journey, such as start and end points, the reason for the journey, the transport modes used, and travel times.

The survey carried out in Lyon in 1995 resulted in the collection of data for 6,001 households, representing a total of 13,997 people aged five and over and 53,213 journeys. This sample was selected from a slightly wider area than that covered by Greater Lyon. In 1995, this area had a total of 536,000 households and 1,280,000 inhabitants (including children under five years of age). The 2006 survey involved a larger sample: 11,229 households, representing a total of 25,656 people aged five and over and 96,250 journeys. The geographical area used for the 2006 survey was also much larger (see Figure 1), covering a total of 832,618 households and a population of 1,975,260 (including children under five years of age).

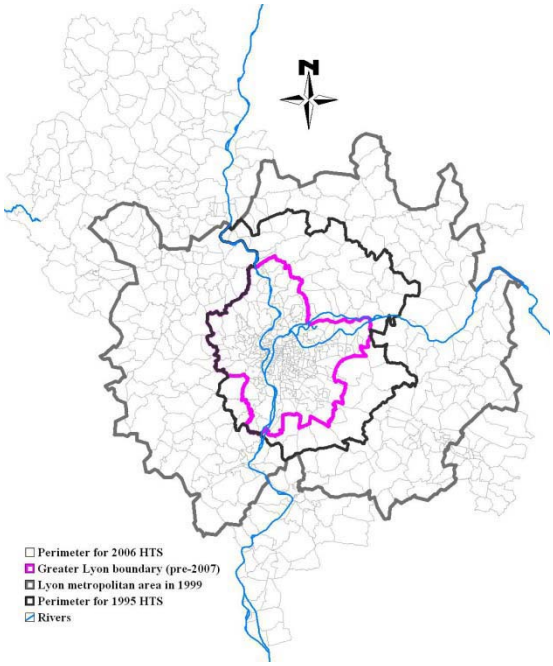

Figure 1: Urban area, metropolitan area and household travel survey area boundaries

In order to ensure comparability from a geographical standpoint, we have analysed the changes in CO_2 emissions related to the daily mobility of inhabitants within the 1995 HTS perimeter only (see Figure 1). However, this method has one significant limitation: urban growth necessarily results in the permanent enlargement of a city's sphere of influence. The perimeter within which most daily activities take place is therefore not stable over time. It must therefore be remembered that trends for a certain proportion of CO_2 emissions related to daily mobility have not been taken into consideration. The perimeter imposed by the 1995 survey had 1,301,076 inhabitants in 2006, which represents three quarters of the population of the Lyon metropolitan area. Of all the journeys made by inhabitants within this reduced perimeter, 97% started and ended within the same perimeter – a percentage that has remained relatively stable compared to 1995 (96%). However, the remaining 3% of journeys that extended beyond this perimeter in 2006, but which remained within the metropolitan area, were responsible for 20% of CO_2 emissions related to the daily mobility of inhabitants within the 1995 perimeter. This illustrates the environmental stakes associated with journeys in peripheral areas, the growth of which we cannot analyse, as no data is available for 1995.

Calculating traffic-related CO_2 emissions

The methodology for calculating and analysing emissions using household travel survey data is now well established (Gallez & Hivert, 1998; Nicolas et al., 2001; Bouzouina & Nicolas, 2009), and combines characteristics relating both to individuals (socio-economic status, geographical location) and to the journeys they make (modes and types of vehicles used, estimated distances). This methodology has been adapted in accordance with the work of Nicolas et al. (2001), by evaluating the conditions for comparability between the two household travel survey periods, using emissions graphs in the context of the European MEET (Methodologies for Estimating Air Pollutant Emissions from Transport) programme (Hickman et al., 1999).

As far as cars and motorised two-wheelers are concerned, MEET provides graphs showing emissions as a function of average travel speed, cylinder capacity, and the vehicle's age and type of carburation. These last two characteristics can be obtained directly from household travel surveys, while information on cylinder capacity can be inferred from the vehicle's taxable horse power and from the vehicle's age and carburation type. Furthermore, the distances and speeds of local journeys are recalculated using a traffic model. As the departure and arrival times are known, it is also possible to deduce whether the vehicle was started with a cold engine, taking account of the previous journey. If a cold engine start is involved, an overemission coefficient is calculated. Finally, given that the household travel survey provides no information on the number of passengers in the vehicle, all CO_2 emissions are attributed to the driver; journeys made as a car passenger are considered to emit no CO_2.

For public transport, we have used the total annual distances travelled by each mode (bus, trolleybus, tram, metro), supplied by the Lyon public transport authority (SYTRAL) for inclusion in the Urban Transport Database managed by CERTU. The average speed of buses across the network – 17 km/h – has been used here to calculate bus emissions on the basis of graphs provided by MEET. Emissions from electrically powered modes are considered to be nil, given that electricity in the Lyon area is essentially generated by nuclear power and, to a lesser extent, hydroelectric power (Nicolas et al., 2001). Furthermore, since we know the annual number of journeys made using the Lyon public transport network (from the Urban Transport Database, CERTU, 2009) and the average distance travelled per journey (from the household travel survey), we have been able to estimate the average emission per passenger-kilometre, which is subsequently applied to all journeys made using public transport. This method gives acceptable results overall, even if it masks variations between individual journeys resulting from the combination of public transport modes involved. As the 1995 survey does not supply the information necessary to estimate the distances travelled using each sub-mode during a public transport journey, we have simply used this average coefficient per passenger-kilometre.

Analysing the factors behind changes in emissions levels:

Once calculated, these CO_2 emissions can be attributed to the individual who made the journey concerned. From this point on, our analysis concentrates on these individuals and aims to explain changes in the emissions they generate through their daily mobility. The overall volume of emissions (E_t) for an average day in a given year *t* corresponds to the average distance travelled per person per day (d_t, in km/person/day), multiplied first by the average emissions level per unit of distance (eu_t, in g/km) and secondly by the total population (p_t, the number of inhabitants), i.e. $E_t = p_t \times d_t \times eu_t$. This means that the overall emissions level E_{t+1} for day *t+1* can be deduced from E_t and from population growth rates, the average distance travelled per person, and unitary emissions (respectively r_p, r_d and r_{eu}):
$E_{t+1} = E_t \times (1 + r_E) = E_t \times [(1 + r_p) \times (1 + r_d) \times (1 + r_{eu})]$.

These equations can then be made more complex, in order to more effectively take account of detailed behaviours and modal splits, but the decomposition principle remains the same. A typology of individuals was therefore established that sought to minimise the explained variance within classes while retaining a consistent explanation for mobility patterns. This means that changes within each of the groups can be observed. The total daily distance has also been detailed between the number of journeys per day and the average distance per journey. Finally, a distinction between seven different modes was made, in order to more effectively take account of variations in CO_2 emissions. These modes are: car journeys as a driver, car journeys as a passenger, journeys made using public transport, journeys that combine car travel and public transport use, bicycle journeys, journeys made on foot, and journeys made by other means. The initial formula can therefore be extended in the following way: $\mathrm{E}_t = \sum_i \mathrm{pop}i . \sum_{j/i} (\mathrm{dep}_i^j . \mathrm{dist}_i^j . \mathrm{eu}_i^j)$, where: E_t and E_{t+1} are the CO_2 emissions volumes for *t* and *t+1* respectively; $\mathrm{pop}i$ is the total population of group *i* on day *t*; dep_i^j is the average daily number of journeys made by people in group *i* using mode *j*; dist_i^j is the average distance of a journey made using mode *j* by people in group *i*; and eu_i^j represents the average unitary emissions for mode *j* for people in group *i*.

The rates of change of these four key factors, which can be designated respectively $\mathrm{rpop}i$, rdep_i^j, rdist_i^j and reu_i^j reflect the different dynamics within each group, and make it possible to recreate the overall changes, while keeping in mind those groups responsible for trends that are to be promoted – or discouraged.

CO_2 emissions related to the daily mobility of Lyon area residents: an apparent stability that masks major behavioural changes

An apparent stability in CO_2 emissions related to the daily mobility of Lyon area residents

The total volume of CO_2 emitted increased only slightly between 1995 and 2006 (+3%). However, initial aggregate analysis shows that this is, to some extent, the result of contrasting trends counterbalancing one another. First, there was a slight increase in the population over the period concerned (+1.6%), mainly due to a positive rate of natural increase (INSEE Rhône-Alpes, 2007). However, the population travelled less as a whole, with the average number of journeys per person per day falling from 3.7 to 3.5. This reduction concerned car journeys in particular, while the number of journeys made using sustainable transport modes and public transport increased. Above all, it is residents in the central area who are travelling less. Mobility figures fell overall, but less so in peripheral areas, where – in contrast to central areas – the distances covered per journey rose sharply (see Table 1): the average distance of a journey has increased from 3.7 km to 4.3 km, with a modal share for cars that has remained stable (73.9% of distances travelled were covered as a motorist or car passenger in 1995, compared with 73.6% in 2006). Consequently, the overall volume of distances travelled each day continued to rise, with recorded growth of +9%.

Unitary emissions for an average journey fell by 5%, from 136 g/km to 129 g/km. A major factor behind this decrease was the reduction in the average unitary emissions of cars, from 209 g/km to 201 g/km (-3%). The number of passengers in vehicles has remained constant, however, and has not contributed to this reduction. Rather, we are seeing a minor impact due to intrinsic changes in the overall motor vehicle fleet, which was more diesel-based and less fuel-hungry in 2006 than in 1995. Public transport represents a second factor that has contributed to lower average unitary emissions. On the one hand, there has been extensive electrification of public transport with the introduction of new-generation trolleybuses, the arrival of the tramway and the extension of the metro; on the other hand, demand has increased considerably, rising from 210 million to 367 million journeys per year between 1995 and 2006 (figures taken from the Urban Transport Database, CERTU, 2009).

Divergent changes in different socio-economic groups

However, beyond this initial general observation, we feel that it is important to analyse trends within different social groups, by examining both demographics and mobility-related behaviour. To this end, a typology of the population was established that sought to maximise the variance between the different groups using the average distance travelled per person per day in 1995 (Nicolas et al., 2003). In all, 22 types were identified; these types reflect possible explanatory factors, notably status (schoolchildren, students, employed persons, unemployed persons, homemakers, retired persons) and location (divided here into three concentric zones: the dense urban core formed by Lyon and Villeurbanne; "first-ring" suburbs adjoining this urban core; and "second-ring" suburbs on the edge of the urban area). Two additional factors are also taken into consideration: access to a car for adults, and gender for employed persons. Certain variables have not been included, such as household revenue, the effects of which seem less clear, and which to some extent are already implicit in categories concerning status and access to a motor vehicle.

A considerable disparity in emissions between groups can be highlighted (see Table 1): primary-school pupils emitted just 0.04 kg each per day on average in 1995, compared with 4.84 kg for employed males with car access in second-ring suburbs. The 12 groups whose behaviour generated the least emissions (in kg/person/day) represent 50% of the population and just 14% of emissions. By contrast, the 3 groups with the highest emissions represent 12% of the population and 29% of emissions. Furthermore, the trends observed tend to reinforce these contrasts:

1) First, the number of journeys per day is down in almost all groups (-7%). This overall reduction is more marked for groups with imposed daily journeys, such as people in employment and schoolchildren, compared with homemakers or retired people. It would therefore appear that the optimisation of daily travel is still continuing, with fewer people returning home for lunch.
2) Distance travelled per journey is the factor that has increased most (+16%). Consequently, this has the effect of increasing overall emissions, as growth in distance is essentially due to car use. Distance per journey is higher among residents of second-ring suburbs than

residents of the urban core, regardless of status. It is also higher for people in employment than for other groups. We can therefore observe an urban sprawl phenomenon, largely due to the fact that people are tending to live further from their workplace.

3) Finally, the 5% drop in unitary emissions is less marked for car users – particularly among people in employment, for whom car use is more intensive than for other groups.

Table 1: growth coefficients for the CO_2 emissions of different population groups

	Population in 1995	Emissions (kg/pers./ day)	*1995–2006 growth coefficient*				
			Pop.	Journeys/ pers.	Dist./ journey	Unitary emissions	**Total emissions**
In full-time education							
Primary – core & 1st ring	58,845	0.04	1.04	0.92	1.00	0.47	**0.45**
Primary – 2nd ring	36,993	0.04	0.82	0.89	1.07	0.78	**0.61**
Sec'dary – core & 1st ring	86,929	0.31	1.04	0.91	1.07	0.74	**0.75**
Secondary – 2nd ring	55,938	0.45	0.87	0.95	1.26	0.85	**0.89**
Students – core	52,018	1.06	0.83	0.89	1.08	0.72	**0.57**
Students – 1st & 2nd rings	28,193	2.52	0.83	0.89	1.26	0.89	**0.83**
Employed persons							
Female – core with car	93,596	2.09	1.10	0.92	1.17	0.93	**1.10**
Female – 1st ring with car	37,941	2.83	1.21	0.98	1.14	0.99	**1.35**
Female – 2nd ring w/ car	67,030	4.01	1.10	0.95	1.21	0.97	**1.21**
Male – core with car	110,696	3.33	1.07	0.87	1.20	0.90	**1.01**
Male – 1st ring with car	50,507	4.11	1.04	0.92	1.14	0.94	**1.02**
Male – 2nd ring with car	90,668	4.84	0.90	0.93	1.30	0.90	**0.98**
Employed with no car	73,704	0.73	0.81	0.94	1.03	0.47	**0.37**
Unemployed persons							
Core & 1st ring with car	26,438	2.25	0.83	0.86	1.08	0.78	**0.60**
2nd ring with car	11,122	3.79	0.75	0.84	1.17	0.92	**0.68**
No car access	20,613	0.35	0.90	0.94	0.93	0.74	**0.58**
Homemakers							
Core & 1st ring with car	26,278	1.84	1.04	0.96	0.87	0.96	**0.84**
2nd ring with car	19,211	2.70	0.67	0.99	1.14	0.91	**0.68**
No car access	32,161	0.13	0.60	1.03	1.20	0.95	**0.70**
Retired persons							
Core with car access	62,317	1.21	1.21	0.95	1.10	0.98	**1.23**
1st & 2nd rings with car	63,520	2.09	1.72	0.98	1.16	0.89	**1.74**
No car access	90,287	0.17	0.94	0.98	0.88	0.58	**0.48**
Total	**1,195,004**	**1.89**	**1.01**	**0.93**	**1.16**	**0.95**	**1.03**

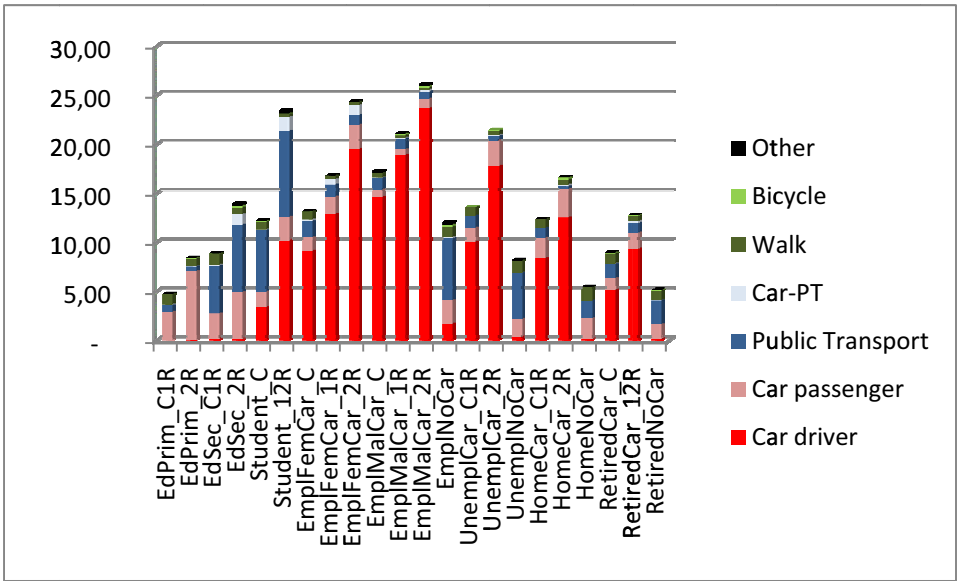

Figure 2: Distances travelled per person per day by mode in 2006 (in km)

Two groups in particular raise the average emissions level: retired people and women in employment. First, the number of retired people with access to a motor vehicle has risen sharply (by up to +72% in peripheral areas); this can be explained by a demographic effect – an ageing population – combined with a generational effect – newly retired people have greater car access than their elders. However, if we compare groups with equivalent characteristics (in terms of location and car access), we can see that behavioural changes among groups of retired people are consistent with the average for the population as a whole. Women in employment also contribute to the growth in emissions. First, the number of women in employment has increased considerably, while the number of people staying at home has fallen. And secondly, this demographic growth has gone hand in hand with a marked increase in distances travelled, which explains the rise in emissions for this group.

Conclusion

Three main phenomena counterbalance the observed trend of falling daily mobility, and the concomitant reduction in CO_2 emissions that might reasonably be expected. First, while the number of journeys made has indeed fallen, this is compensated by the increased distances travelled in peripheral areas. Here, it may be judicious to question the relevance of our study perimeter, determined by the 1995 HTS. Might our conclusions on the stability of CO_2 emissions have been different if we had been able to carry out our study across the whole metropolitan area? Second, distances between home and work continue to increase; this phenomenon is linked to urban sprawl. As a consequence, those groups comprising women in employment are particularly responsible for raising emissions levels, as they combine demographic growth – the increasing proportion of women in employment – with an overall increase in distances travelled (by car) for all persons in employment. Finally, the effects of an ageing population can be clearly observed, with new generations of older people that have greater access to motor vehicles than ever. At the scale of the areas concerned by daily mobility, the dynamics behind the increase in emissions therefore appear to be structurally linked to spatial aspects, most notably the fact that people are having to travel further to work. Measures that aim to reduce CO_2 emissions by directly targeting journey-related aspects, such as carbon taxes, will only be accepted with considerable reluctance, as no alternative is available. Furthermore, such measures seem intrinsically unfair, as less well-off households already dedicate a significant proportion of their budget to daily mobility, particularly in peripheral areas (Polachinni, Orfeuil, 1998; Nicolas et al., 2003; Vanco, Verry, 2009). In view of this situation, it might therefore be better to implement measures that, on the hand, concern the renewal of the overall motor vehicle fleet, as unitary emissions for cars have fallen very little (feebates systems, as the French "bonus–malus" example, could be used as a model) and which, on the other hand, seek to control urban development more effectively, by minimising urban sprawl and favouring densely populated centres with a wide variety of functions.

References

Bouzouina L., Nicolas J.-P., 2009, Harmoniser politiques sociale et environnementale : évaluation de l'impact d'une réhabilitation de quartiers défavorisés sur les émissions de CO2 liées aux déplacements. VertigO, Vol. 9, n°2. en ligne : http://www.vertigo.revues.org./index8771.html .

Dupont A., Kolli Z., Krakutovski Z., Hivert L., 2009, Travel Behavior regarding demographical changes and GHG emissions in the Parisian Region. 12th International Conference on Travel Behaviour Research, Jaipur, India, December 13-18, 2009.

Gallez C., Hivert L., 1998. BEED: mode d'emploi. Synthèse méthodologique pour les études "budget énergie environnement des déplacements". Arcueil, Ademe-Inrets report.

Hickman J., D. Hassel, R. Joumard, Z. Samaras, S. Sorenson, 1999. MEET – Methodology for calculating transport emissions and energy consumption. European Commission, DG VII, Luxembourg. http://www.inrets.fr/infos/cost319/M22.pdf

Hubert J.-P., 2009, Dans les grandes agglomérations, la mobilité quotidienne des habitants diminue, et elle augmente ailleurs. Insee première 1252.

Nicolas J.-P., P. Pochet, and H. Poimboeuf, 2001, Indicateurs de mobilité durable. Application à l'agglomération de Lyon. Lyon, LET, Coll. Etudes & Recherches. 127 p.

Nicolas J.-P., P. Pochet, and H. Poimboeuf, 2003, Towards sustainable mobility indicators: application to the Lyons conurbation, Transport Policy, 10, 197-208.

Orfeuil J.-P., Polacchini A., 1998, Dépenses pour le logement et pour les transports en Île-de-France, Arcueil, INRETS report. 91 p.

Vanco F., Verry D., 2009, Rising fuel price and household vulnerability: a French comparison, 2nd EuroCities-DATTA Workshop Urban mobility in Europe, Namur, January 8-9 2009.

Development and Evaluation of a Generalised Model for Traffic Induced Road Dust

J. Berger[1] and B. Denby[1]*

[1] Norwegian Institute for Air Research, P.O. Box 100, N-2027 Kjeller, Norway, janne.berger@nilu.no

Abstract

We have tested and evaluated a generalised road dust emission model on two datasets in and just outside Oslo in Norway during the studded tyre season. The model performs excellent for temperatures above 0 ºC and less well during colder periods. Since the model does not yet include salting as an additional mass source, underestimations are evident under dry periods with temperatures around 0 ºC, under which salting occur. Furthermore, the model overestimates the measured PM_{10} (particulate matter less than 10 µm in diameter) concentrations under heavy precipitation events since the model does not take the amount of precipitation into account. In spite of the current limitation, we have indeed developed a generalised road dust emission model that does not rely on local measurements. Moreover, the model presents a generalised conceptual framework for further development. Given more monitoring data and refinement of specific parameterisations, the model will in the future be used for more effective air quality planning.

Introduction

Traffic related exhaust emissions of particulate matter (PM) have become significantly reduced over the last decades e.g. by introducing particle filters in diesel engines. Road dust emissions, defined as emission of PM generated from the road surface due to road surface wear and resuspension of particles deposited onto the road surface and shoulders, are not affected by these efforts, and have therefore become increasingly important (Lenschow et al., 2001; Luhana et al., 2004). However, while legislations exist for reducing exhaust emissions, the sources of road dust emissions are unregulated in spite of the health related responses of airborne PM (respiratory and cardiovascular morbidity and mortality, and cancer (Laden et al., 2000)). With this motivation, we analyse and evaluate a generalised road dust emission model when applied onto two datasets from measurement campaigns in and just outside Oslo, Norway.

Description of the generalised model

In this section we summarize the most important features in the model; a more detailed description of the model as well as of the parameterisations can be found in Berger and Denby (2010). The basis of the model is as follows:

(i) The PM road dust emissions are separated into direct and resuspended emissions and the road surface and road shoulder are treated as two different sources:

$$E(PM_x) = E_{direct}(PM_x) + E_{turb-road}(PM_x) + E_{mech-road}(PM_x) + E_{turb-shoulder}(PM_x) \quad (1)$$

where $E_{direct}(PM_x)$ is direct emission through road surface, tyre and brake wear, and $E_{turb\text{-}road}(PM_x)$, $E_{mech\text{-}road}(PM_x)$ and $E_{turb\text{-}shoulder}(PM_x)$ are resuspension through turbulence on the road (turb-road), through the mechanical emission of particles due to the direct contact of the tyre with the road (mech-road) and through turbulence on the road shoulder (turb-shoulder), respectively. PM_x is some pre-defined size interval.

(ii) Road, tyre and brake wear measurements, $W_{i,j,k}$, are used as the basis for the emission factors of direct emissions:

$$E_{direct}(PM_x) = \sum_{i=1}^{3}\sum_{j=1}^{3}\sum_{k=1}^{C}\sum_{m=1}^{F} N_{j,k} \cdot W_{i,j,k}(V, T_s, w) \cdot f_{direct,i,j,k}(V, T_s, w) \cdot h_{m,i} \quad (2)$$

where $N_{j,k}$ (veh s^{-1}) is the number of vehicles with tyre type j (j=1: studded tyres, j=2: winter (friction) tyres, j=3: summer tyres), vehicle category k (k=1: two-wheelers,…, k=C: large trucks); $W_{i,j,k}$ (g veh^{-1} m^{-1}) is the wear due to wear source i (i=1: road wear, i=2: tyre wear, i=3: brake wear), tyre type j and vehicle category k; the function $f_{direct,i,j,k}(V,T_s,w)$ represents the fraction of wear particles from the i'th source due to the use of the j'th tyre type that becomes directly emitted due to the passage of one vehicle of category k and $h_{m,i}$ is the proportion of the directly emitted particles from wear source i in the size interval m (e.g. m=1: <10-20 µm, m=2: 2.5-10 µm, m=3: <2.5 µm).

The function $f_{direct,i,j,k}(V,T_s,w)$ is expressed as

$$f_{direct,i,j,k}(V,T_s,w) = f_{0,direct} \cdot \left(f_{1,direct}(V) \cdot f_{2,direct}(T_s) \cdot f_{3,direct}(w)\right) \quad (3)$$

where $f_{0,direct}$ is the fraction of road wear mass that is emitted as TSP deduced from a range of laboratory and field measurements and f_1, f_2 and f_3 are functions related to vehicle speed, V, surface temperature, T_s, and road wetness, w, that inhibit or enhance the emission of road wear particles. Note that V is divided with a reference speed, V_{ref}, which is the mean trip speed on the particular site.

(iii) Road dust is accumulated on the road surface and road shoulder through the mass balance concept:

$$\frac{\partial M_{road}}{\partial t} = P_{road} - S_{road} \quad (4)$$

$$\frac{\partial M_{shoulder}}{\partial t} = P_{shoulder} - S_{shoulder} \quad (5)$$

where M_{road} (g m^{-1}) and $M_{shoulder}$ (g m^{-1}) are the dust load available for resuspension on the road surface and road shoulder, respectively, P_{road} (g m^{-1} s^{-1}) and $P_{shoulder}$ (g m^{-1} s^{-1}) are the production of dust load on the road surface and the road shoulder, respectively, due to road surface, tyre and brake wear, and deposition from other sources, and S_{road} and $S_{shoulder}$ are the sinks related to the dust load on the road surface and road shoulder, respectively. P_{road} and $P_{shoulder}$ are expressed as

$$P_{road} = \sum_{i=1}^{3}\sum_{j=1}^{3}\sum_{k=1}^{C}\sum_{m=1}^{F} N_{j,k} \cdot W_{i,j,k}(V,T_s,w) \cdot \left(1 - f_{direct,i,j,k}(V,T_s,w)\right)\left(1 - f_{shoulder,i,j,k}\right) + N_{j,k} \cdot f_{sandpaper,j,k}(M_{road}) + Deposition \quad (6)$$

$$P_{shoulder} = \sum_{i=1}^{3}\sum_{j=1}^{3}\sum_{k=1}^{C}\sum_{m=1}^{F} N_{j,k} \cdot W_{i,j,k}(V,T_s,w) \cdot (1 - f_{direct,i,j,k}).f_{shoulder,i,j,k} + Deposition + Runoff + Ploughing \quad (7)$$

The first term in eq. 6 is related to road, tyre and brake wear, the second term represents the additional production of dust load due to the increased road wear resulting from the tyre-sand-road interaction and the third term is any deposition from external sources such as exhaust, wind blown dust and addition of sand or salt. We have not included the second term in this study due to lack of sufficient information to deduce this function. The function $f_{shoulder,i,j,k}$ represents the fraction of road dust particles from the i'th source due to the use of the j'th tyre type becoming deposited onto the road shoulder due to the passage of one vehicle of category k.

S_{road} and $S_{shoulder}$ are expressed as

$$S_{road} = M_{road} \cdot \sum_{k=1}^{C}\sum_{m=1}^{F} N_k \cdot \left(g_{turb-road,k}(V,T_s,w) \cdot h_{m,turb-road} + g_{mech-road,k}(V,T_s,w) \cdot h_{m,mech-road}\right) \quad (8)$$

$$S_{shoulder} = M_{shoulder} \cdot \sum_{m=1}^{F} N_{HDV} \cdot g_{turb-shoulder,HDV}(V,T_s,w) \cdot h_{m,turb-shoulder} \quad (9)$$

The functions $g_{turb-road,k}(V,T_s,w)$, $g_{mech-road,k}(V,T_s,w)$ and $g_{turb-shoulder,k}(V,T_s,w)$ represent the fraction of particles on the road surface and road shoulder becoming resuspended due to vehicle induced turbulence at the road surface, mechanical emission of road dust particles and vehicle induced turbulence on the road shoulder, respectively, expressed as

$$g_{p,k}(V,T_s,w) = g_{0,p} \cdot \left(g_{1,p,k}(V) \cdot g_{2,p,k}(T_s) \cdot g_{1,p,k}(w)\right) \quad (10)$$

p=turb-road,mech-road,turb-shoulder and g_1, g_2 and g_3 are analogous to f_1, f_2 and f_3 in eq. 3, but related to resuspension.

The solution to eq. 4 is (the same applies to eq. 5):

$$M_{road}(t) = M_{road,0}\left(\frac{P_{road}}{S_{road,0}} - \left(1 - \frac{P_{road}}{S_{road,0}}\right) \cdot \exp\left(-g_{road} \cdot t\right)\right) \quad (11)$$

where $M_{road,0}$ and $S_{road,0}$ are the mass load and sink of the road surface at the previous time step. g_{road} is expressed as

$$g_{road} = \sum_{k=1}^{C}\sum_{m=1}^{F} N_k \cdot \left(g_{turb-road,k}(V,T_s,w) \cdot h_{m,turb-road} + g_{mech-road,k}(V,T_s,w) \cdot h_{m,mech-road}\right) \quad (12)$$

The time scale for M_{road}, τ_{road} (s), is expressed as

$$\tau_{road} = \frac{M_{road}}{P_{road}} = \frac{M_{road}}{S_{road}} = \frac{1}{g_{road}} \quad (13)$$

If the time t is large enough, i.e. $t >> \tau_{road}$, then

$$M_{road} = \frac{P_{road}}{g_{road}} = \frac{S_{road}}{g_{road}} \quad (14)$$

which is the steady state solution to eq. 4, i.e. there is balance between the production, P_{road}, and sink, S_{road}, of M_{road}. A more detailed description of the model concept is presented in Berger and Denby, 2010)

In the following, due to lack of sufficient information we let $g_{road,k}(V,T_s,w)=g_{turb-road,k}(V,T_s,w)=g_{mech-road,k}(V,T_s,w)$ and $g_{shoulder,k}(V,T_s,w)= g_{turb-shoulder,k}(V,T_s,w)$.

Measurement sites and handling of data

In order to validate the model, we have applied the model on two datasets from measurement campaigns at two major roads/highways in Oslo, Norway; Nordbysletta, about 20 km north of Oslo, and RV4 near Aker Hospital in Oslo. At both sites the traffic density is ~35 000 veh day^{-1} and the speed limit is 90 km h^{-1}. Measurements of PM_{10} and NO_x were conducted in the period 1 January 2002 – 15 April 2002 at Nordbysletta and 15 January – 30 April 2004 at Aker Hospital. In addition, meteorological parameters such as precipitation, temperature, wind speed, wind direction and relative humidity were measured on an hourly basis. On both sites, emissions of NO_x were calculated using the AirQUIS emission module at the Norwegian Institute for Air Research (NILU) (Laupsa, 2004). These emissions, together with the PM_{10} and NO_x measurements, were used to test and evaluate the generalised model.

To estimate the concentration of modelled PM_{10}, $C_{PM10,mod}$, we use the net concentration and emission of NO_x, $C_{NOx,net}$ and $E(NO_x)$, respectively. We obtain the net concentration of a pollutant by subtracting the background concentration of the pollutant from the near-road measurements, thereby obtaining only the contribution from the road traffic. Hence, we assume that

$$C_{PM_{10},\mathrm{mod}} = \frac{C_{NO_x,net}}{E(NO_x)} \cdot E(PM_{10}) \quad (15)$$

where $E(PM_{10})$ is emission of road dust PM_{10}. Note that we in this study have included parameterisations of road cleaning, salting and ploughing since data concerning these activities were not available.

Results and discussion

Fig. 1 presents time series of daily averaged measured and modelled PM_{10} concentrations at Aker Hospital (left) and Nordbysletta (right). Fig. 2 presents the daily averaged temperature and precipitation for the same periods at both sites. In general, when comparing the model results with measurements, the model performs better for temperatures well above 0 ºC, e.g. from 8-30 April 2004 at Aker Hospital and 19 March – 15 April 2002 at Nordbysletta. However, for temperatures close to 0 ºC, the model fails to reproduce the net observed PM_{10} levels; during the period ~23 February – 1 April 2004 at Aker Hospital, the model underestimates the peak values at Aker Hospital. However, in this period Hagen et al. (2005) showed that roughly 50% of the measured PM was due to road salting. As the model currently does not include salting as an additional mass source, the road dust distribution, that we are modelling, is actually around half of the measured PM concentration. However, at Nordbysletta (right) the model significantly overestimates the net observations at the beginning of the period (1 January – 22 January 2002). Though no precipitation occurred during this period, the low temperatures may have inhibited the road dust emissions, due to less efficient drying of the road surface for low temperatures. Clearly, the model does not capture this effect in this period. However, with regard to the rest of the period, the overall overestimate most likely occurs due to more and heavier precipitation events at Nordbysletta compared with Aker Hospital, as seen on the right panel of fig. 2, since the model does not take the amount of precipitation into account. Overall, this also illustrates the sensitivity of road dust emissions to the combination of precipitation and temperature close to or below 0 ºC.

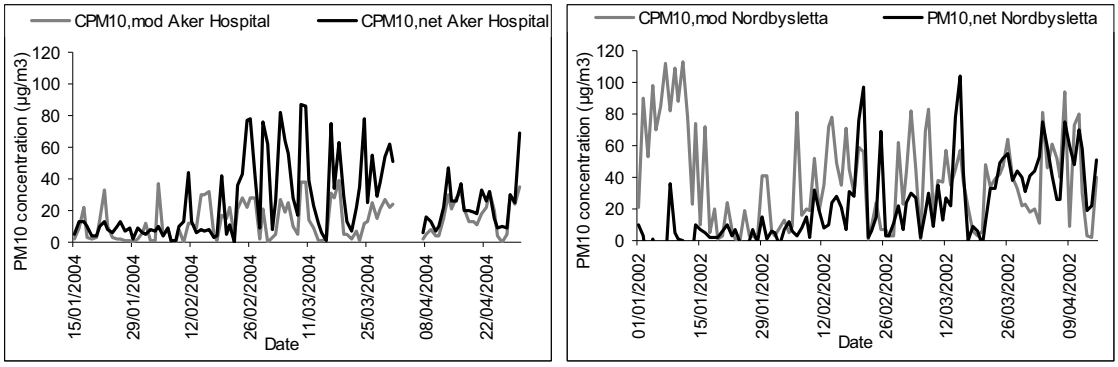

Figure 1: Daily averaged net observed (black line) and modelled (grey line) PM_{10} concentrations (µg m^{-3}) for Aker Hospital (left) and Nordbysletta (right).

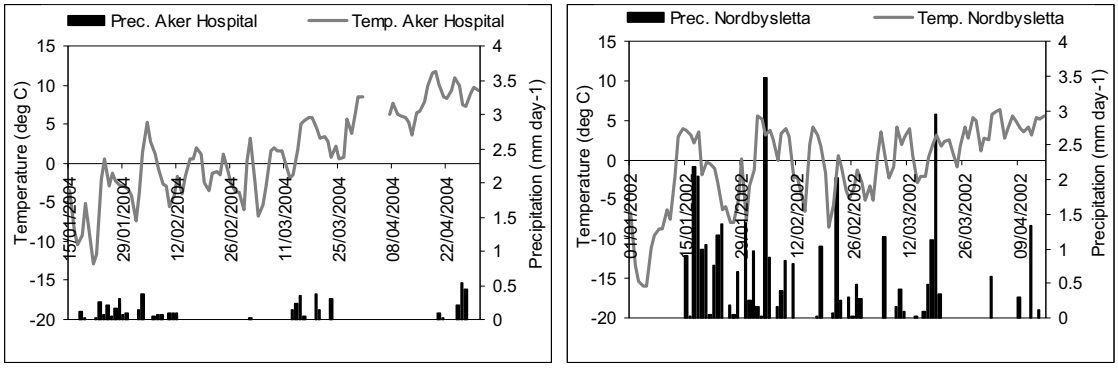

Figure 2: Daily averaged precipitation (mm $hour^{-1}$) (black bars) and temperature (ºC) (grey line) at Aker Hospital (left) and Nordbysletta (right).

Table 1 presents statistical analysis of the modelled and measured daily averaged PM_{10} concentrations at the two sites where we have applied means of the modelled and observed PM_{10} concentrations, Pearson's coefficient of determination (R^2) and relative bias (RB). Letting C_{obs} and C_{mod} be the modelled and observed concentrations, respectively, and n be the number of data points, these are defined as

$$R^2 = \frac{\sum_{i=1}^{n}\left(C_{obs} - \overline{C_{obs}}\right)\left(C_{\mathrm{mod}} - \overline{C_{\mathrm{mod}}}\right)}{\sigma_{obs}\sigma_{\mathrm{mod}}}$$

where σ_{obs} and σ_{mod} are the standard deviations of the measured and modelled concentrations, respectively.

$$RB = \frac{\overline{C_{\mathrm{mod}}} - \overline{C_{obs}}}{\overline{C_{obs}}}$$

As far as the coefficient of determination is concerned, the agreement between the daily averaged model estimates and observations is absent at Nordbysletta, while some correlation is evident for the Aker Hospital data. This is mainly due to inadequate parameterisation of the effect of road surface conditions related to precipitation, surface temperature and surface drying. Furthermore, the *RB* values clearly reflect the overall trend in fig. 1, i.e. underestimate of the Aker Hospital data and overestimate of the Nordbysletta data due to the points mentioned previously in this section.

Table 1: Statistical analysis of modelled and measured daily averaged PM_{10} concentrations at Aker Hospital and Nordbysletta.

	Aker Hospital	Nordbysletta
Mean net observed daily averaged PM_{10} concentrations (μg m^{-3})	25.1	21.4
Mean modelled daily averaged PM_{10} concentrations (μg m^{-3})	13.8	38.1
R^2	0.38	0.03
RB	-0.45	0.78

Conclusion

We have tested and evaluated a new and generalised road dust emission model in which the mass balance concept is used to describe the variation of dust load on the road surface and shoulders, and road, tyre and brake wear factors are used as the basis for the emission factors of direct emissions. We have applied the model onto two datasets in and outside Oslo, Norway, during the studded tyre season. On a daily basis, analysis of the results showed that the model gave excellent results under warm conditions, and needs refinement of the road surface condition parameterisations under other conditions. One of the reasons for the underestimation of observed PM_{10} during periods around 0 ºC was the significant salt contribution in the measured PM_{10} concentrations. The model currently does not include salting as an additional mass source. Furthermore, at Nordbysletta, the precipitation events were heavier and more frequent compared with Aker Hospital and overestimation of the measured concentrations at Nordbysletta was evident under precipitation events. Since the model does not take the amount of precipitation into account, it underestimated the effect of precipitation at Nordbysletta.

Clearly, further development of the generalised model is still needed. For example, the comparison with PM_{10} measurements showed the strong sensitivity of the modelled emissions to the road surface conditions. In addition, the model does not yet include algorithms related to salting or sanding, nor does it include the impact of snow ploughing or cleaning activities.

In spite of the current limitations of the model, the model reflects a number of processes that no other model has ever done before, e.g. with regard to the particle redistribution rates (*f*- and *g*-functions), the treatment the road shoulder as an individual source and giving as output the time scales for build up of road dust on the road surface and shoulders. Overall, the model presents a generalised conceptual framework for further development and can lay the course for future measurement campaigns. As more monitoring data is obtained and specific parameterisations are refined, the model will in the future enable improved estimates of road dust emissions and provide the potential for good air quality planning and management.

References

Berger J., B. Denby, 2010. A generalised model for traffic induced road dust emissions. Part 1: concept and model description. Submitted to *Atmospheric Environment.*

Hagen L.O., S. Larssen, J. Schaug, 2005. Speed limit in Oslo. Effect on air quality of reduced speed on RV4. NILU OR 41/2005, Norwegian Institute for Air Research, Kjeller, Norway (in Norwegian).

Laden F., L.M. Neas, D.W. Dockery, J. Schwartz, 2000. Association of Fine Particulate Matter from Different Sources with Daily Mortality in Six U.S. Cities. *Environmental Health Perspectives* 108, 941-947.

Laupsa H., 2004. AirQUIS emission inventory module. User's guide. NILU TR 04/2004. Norwegian Institute for Air Research, Kjeller, Norway.

Lenschow P., H.J. Abraham, K. Kutzner, M. Lutz, J.D. Preuss, W. Reichenbächer, 2001. Some ideas about the sources of PM10. *Atmospheric Environment* 35 Supplement No. 1, S23-S33.

Luhana L., R. Sokhi, W. Lynne, H. Mao, P. Boulter, I. McCrae, J. Wright, D. Osborn, 2004. Measurement of non-exhaust particulate matter. Deliverable 8 from EU Project PARTICULATES – Characterization of Exhaust Particulate Emissions from Road Vehicles, *European Commision 5th Framework Programme.* 96 pp.

Potentials and Costs for GHG Mitigation in the Transport Sector

J. Borken-Kleefeld, J. Cofala, P. Rafaj, F. Wagner and M. Amann*

IIASA – International Institute for Applied Systems Analysis, Atmospheric Pollution and Economic Development Programme (APD), AT-2361 Laxenburg, Austria; borken@iiasa.ac.at

Mitigation pledge of the European Union

Mitigating dangerous climate change requires that industrialised countries (Annex-I) reduce their combined greenhouse gas (GHG) emissions by 25% to 40% by 2020 compared to 1990, according to scientific analysis. A reduction by 80% to 95% is required until 2050. This target was endorsed by the G8 at their L'Aquila Summit. Prior to the UN-Summit on Climate Change in Copenhagen, the European Union offered to reduce its GHG emissions by 20% to 30% in 2020 relative to 1990, all sectors combined.

What would such a reduction target imply for the transport sector in the EU? What additional measures would be needed in the transport sector? How much would its realisation costs extra? To answer such questions the GAINS model was adapted to determine cost-efficient reduction potentials for greenhouse gases and air pollutants covering all emission sectors (Amann et al. 2009). The projection of the World Energy Outlook 2009 including the implications of the economic crisis is taken as reference baseline (IEA WEO 2009). In this baseline, total CO_2-eq emissions in EU27 would reduce already by 15% until 2020 and 2030 from 5468 Mt CO2-eq emitted in 1990 (Figure 1). To fulfil the pledge, additional reductions of 5% to 15% below this baseline projection would be needed by 2020.

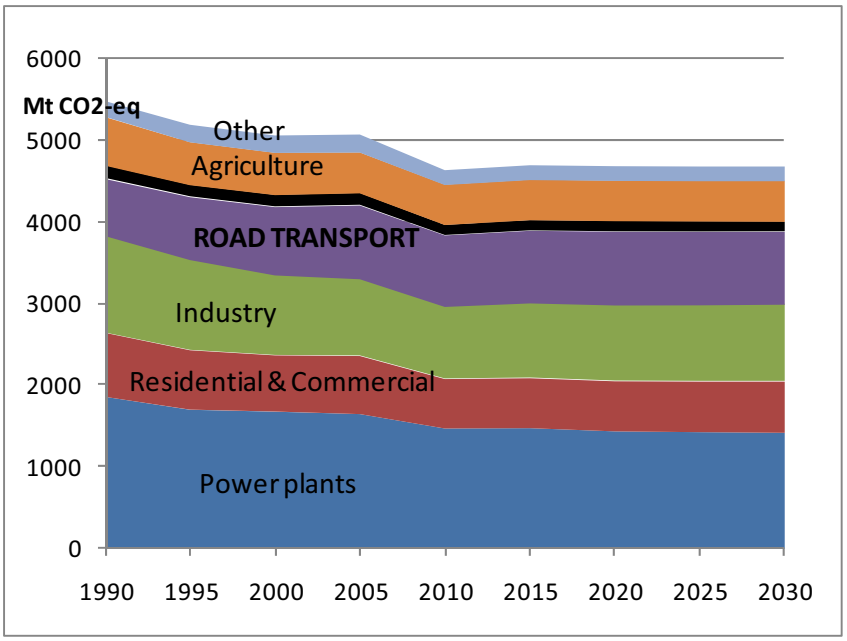

Figure 1: Development of greenhouse gas emissions from major sectors in EU27 from 1990 to 2030. EU reduction proposal: 20% to 30% lower emissions in 2020 than in 1990, i.e. between 3800 and 4375 Mt CO2-eq. [IIASA GAINS, following IEA WEO 2009 for baseline].

This paper focuses on the technical mitigation potential for the road transport sector and the related abatement costs in EU27; results for other sectors have been reported by Amann et al. (2009). The fuel efficiency of new vehicles, the turn-over of the fleet and the carbon intensity of the fuel determine the resulting CO2 emissions, once travel demand and driving behaviour are taken for granted. New vehicles with better efficiency usually have higher investment costs. Higher vehicle efficiency however also results in fuel savings. The value of these fuel savings depends on the fuel price and a potential carbon charge. Extra costs are discounted over the lifetime of the technology. When extra costs are less than fuel savings, then the technology is considered economical. Here we determine the technical portfolio with least overall economic costs as a function of the carbon price (or the marginal abatement costs). For details on the

approach, cf. Amann et al. (2009) and Borken-Kleefeld et al. (2009); all input data can be accessed under http://gains.iiasa.ac.at/index.php/gains-annex-1.

Mitigation through technical efficiency

Compared to other sectors, transportation has higher marginal abatement costs (Figure 2). The biggest extra mitigation potentials for a given carbon price (in percent change relative to the baseline development) are in the domestic & commercial and the power plant sectors. Extra mitigation measures in the agricultural, industrial and transport sectors are below average. Nonetheless, sizeable potentials for efficiency improvements and emission reductions exist also for the transport sector. This is analysed in detail in the following.

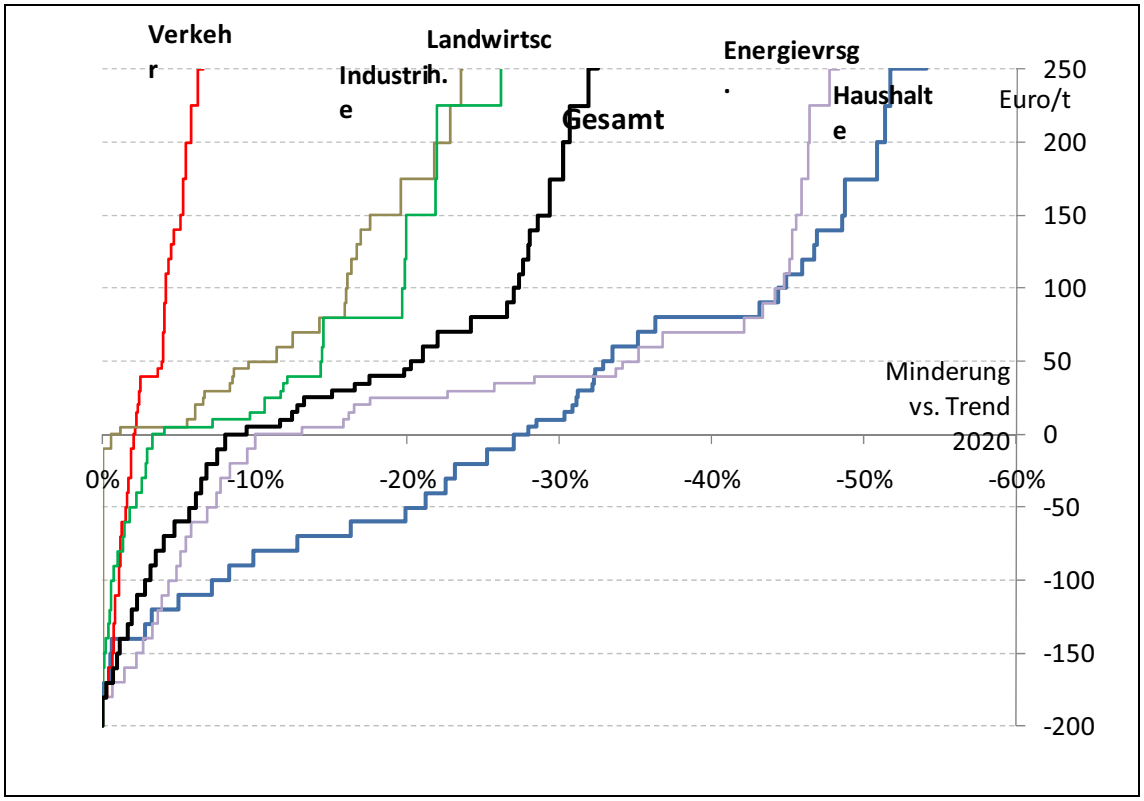

Figure 2: Marginal GHG abatement potential vs. costs for all major sectors relative to baseline emission in 2020 in EU27. [Baseline: IEA WEO2009, lifetime cost accounting].

In the trend scenario (IEA WEO 2009) the emissions of the long-lived greenhouse gases from all sectors except transport would go down by more than 20% until 2020 and 2030 relative to 1990 levels (Table 1). By contrast, emissions from road transportation in EU27 would stagnate at about 900 Mt CO2-eq in 2020 to 2030, almost 30% higher than in 1990. Their growth has been driven by strongly increased emissions from trucks (+60% in 2005 vs. 1990) that more than offset efficiency improvements from cars. In the same period transport volumes from cars are projected to increase by 70% and from trucks by 90% in EU27 combined.

Mt CO2-eq	1990	1995	2000	2005	2010	2020	2030
Road transport	700	772	838	903	878	905	894
Non-road transport (domestic)	155	140	140	143	123	124	117
All other sectors	4614	4270	4072	4017	3632	3651	3665
TOTAL EU27	**5468**	**5181**	**5051**	**5063**	**4632**	**4680**	**4676**
Road in total	*13%*	*15%*	*17%*	*18%*	*19%*	*19%*	*19%*
Domestic transport in total	*16%*	*18%*	*19%*	*21%*	*22%*	*22%*	*22%*

Table 1 Greenhouse gas emissions in EU27 [1990 to 2005] and trend projection until 2030, accounting already for economic crisis, for road transport and other sectors (IIASA GAINS, following IEA WEO 2009 for baseline).

Assuming no change in transport demand or consumer behavior, a quicker introduction of more efficient vehicles and a higher use of biofuels can moderately bring down emissions below these baseline developments. Extra savings of 3% by 2020 and of 4.5% by 2030 could be achieved at no extra costs. Extra emission reductions of 5% and 6% by 2020 and 2030 respectively could become economical for marginal abatement costs of 50 € per ton CO2-eq abated. Only few additional measures become economical at 100 € per ton CO2-eq abated. The maximal technically feasible reduction potential is estimated at 8% and 10% below baseline by 2020 and 2030 respectively. The economic mitigation potential becomes larger with time as additional measures starting in 2010 have more time to penetrate the fleet.

The economic reduction potential is lowest for cars with 1% and 3% at marginal abatement costs of 0 and 50 € per ton CO2-eq abated in 2020. These reflect the fact that many efficiency measures have already been introduced and are part of the baseline development. Trucks have a technical reduction potential with 4% and 6% emission reduction below baseline at marginal abatement costs of 0 and 50 € per ton CO2-eq abated in 2020. That cost-efficient abatement measures exist for trucks may surprise at first sight. However, truck holders decide on investments based on a requested payback period of about 18 months. This effectively allows only cheap investments and precludes major efficiency gains that are economical over the lifetime of the vehicle. This difference between private and social investment perspectives is an important example where markets do not deliver possible efficiency improvements.

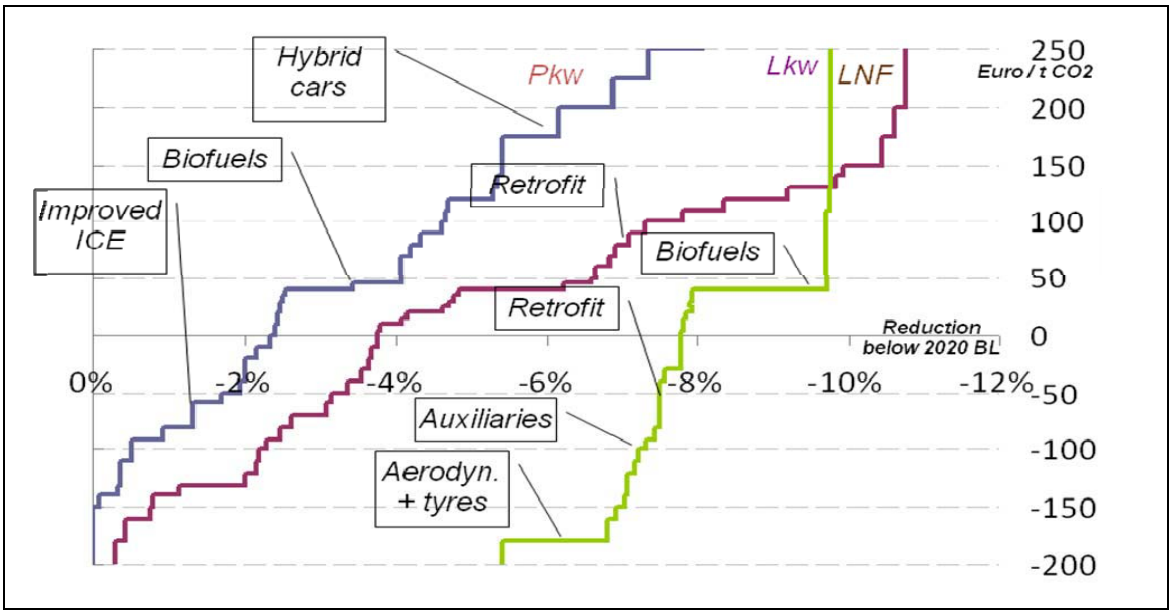

Figure 3: Marginal GHG abatement potential vs. costs for road vehicles in EU27 by 2020. Each step represents one additional technology becoming cost-effective at the respective carbon abatement costs in one of the European Member States. Indicated are major technology packages. [Baseline development: IEA WEO2009, lifetime cost accounting].

Most important in terms of their potential as well as cheapest are improvements of the conventional combustion engine and the power train for cars and light duty vehicles. Better aerodynamics and low-friction tyres are important and cheap measures for trucks. A higher use of biofuels (above mandatory requirements) becomes economical at about 45 € per ton CO2-eq abated. Hybrid and electric cars would certainly provide a sizeable extra reduction potential. However, with projected high costs notably of the battery their marginal abatement costs are above 200 € per ton CO2-eq. abated.

Mitigation costs

Here we calculated how much greenhouse gases could be abated by 2020 and 2030 in industrialised countries, if more efficient technology would be introduced earlier or more widespread than in the baseline development. Leaving transport demand, travel, driving and purchase behaviour unchanged, this means purchase of more efficient vehicles (than in the baseline). These vehicles would require an initial extra investment of about 40 billion Euro in EU27 combined by the year 2020, about 500 Euro extra per car, about 1200 Euro extra per light truck and about 9000 Euros extra per truck (Table). However, through fuel savings over the lifetime of the vehicle, the initial extra capital investment would pay back. Indeed, most investments would already be cost-efficient at standard fuel prices; the higher the fuel price becomes, e.g. as a consequence of a carbon charge, the more or the earlier an investment in more efficient vehicles will pay back. For instance marginal abatement costs of 60 Euro per ton CO2-eq. abated would equate to a carbon charge of 0.15 Euro per litre gasoline. However, mitigation through vehicle technology is also limited by the turnover-time of the fleet. In any case abatement by vehicle technology that pays off itself through fuel savings is quite limited; further abatement becomes costlier than in other sectors with marginal abatement costs above 200 Euros per ton CO2-eq abated. Abatement costs are lower in 2030 than in 2020 as costs for more advanced components, notably the battery for hybrid vehicles, are assumed to fall.

	2020				2030			
	Marginal abatement costs [€ per ton CO2eq]				Marginal abatement costs [€ per ton CO2eq]			
	0	50	100	Max	0	50	100	Max
Greenhouse gas emissions from transportation [Mt CO2eq / % reduction below baseline]								
	1000/ -2%	982/ -4%	980/ -4%	955/ -7%	998/ -4%	953/ -8%	944/ -9%	879/ -15%
Number of vehicles that could be improved beyond baseline [mio. veh.]								
Cars	28.3	31.1	31.4	67.7	49.8	49.8	49.8	90.7
LDT	5.9	6.0	6.9	12.5	22	26.1	26.6	26.9
HDT	2.2	2.2	2.2	2.3	4.4	4.4	4.4	4.4
Extra investments for mitigation [bio. Euro]								
Cars	12.4	14.8	15.6	114	2	5	14	100
LDT	7.0	7.3	9.1	21.5	4.1	5.7	6.75	9
HDT	19.1	19.1	19.1	19.2	45	46	46	46
Extra investment per vehicle [Euro]								
Cars	438	476	497	1684	40	100	281	1103
LDT	1186	1217	1319	1720	186	218	254	335
HDT	8682	8682	8682	8348	10230	10455	10455	10455

Table 2 GHG emissions, number of vehicles that could be improved, the required capital investment as a function of the marginal abatement costs in EU27 in years 2020 and 2030. [baseline development: IEA WEO2009, lifetime cost accounting].

Discussion

These results are robust for a wide range of future fuel prices and investment costs. However, the cost break-even point critically depends on the payback period required for the initial investment. If payback is required within months to few years, as private investors often calculate, then less than half the economic reduction potential would be realised.

Important differences exist between countries and vehicle categories. For instance, the relative reduction potential is larger for the USA and Australia, where light duty vehicles have not been so efficient, than for the EU or Japan. Furthermore, efficiency gains for light duty vehicles appear less costly than for heavy duty vehicles.

Compared to other sectors transportation has higher costs per unit reduction. But given the size of the transport sector, reductions in total national emissions in the order of 20% or more can only be achieved with reductions in the transport sector. Technical measures have in EU27 an extra mitigation potential of 4% by 2020 and 8% by 2030 at marginal abatement costs of up to 100 Euros per ton CO2-eq abated. Further abatement needs to address travel demand, purchase decisions (notably car weight and engine power) and mode choice.

References

Access to all input data presented here: http://gains.iiasa.ac.at/index.php/gains-annex-1

Amann, M., I. Bertok, et al. (July 2009 (version 2)). GAINS – Potentials and Costs for Greenhouse Gas Mitigation in Annex-1 Countries – Initial Results. Laxenburg/Austria, IIASA - International Institute for Applied Systems Analysis.

Borken-Kleefeld, J., J. Cofala, et al. (2008). GHG mitigation potentials and costs in the transport sector of Annex 1 countries - Methodology. Laxenburg, Austria, International Institute for Applied Systems Analysis (IIASA).

IEA (2009). *World Energy Outlook 2009*. Paris/France, International Energy Agency (IEA).

Session 5: Biofuels 1

Experimental evaluation of straight vegetable oil-diesel blends application on vehicle regulated and non-regulated exhaust emissions over legislated and real world driving cycles

Georgios Fontaras[1], Marina Kousoulidou[1], Georgios Karavalakis[2], Stamoulis Stournas[2†] and Zissis Samaras[1]

[1] Laboratory of Applied Thermodynamics, Aristotle University Thessaloniki P.O. Box 458, GR 54124 Thessaloniki, Greece, Corresponding author: Prof. Zissis Samaras :zisis@auth.gr

[2] Laboratory of Fuels Technology and Lubricants, National Technical University of Athens 9 Iroon Polytechniou Str., Zografou Campus, 15780 Athens, Greece

Abstract

This paper attempts an experimental evaluation of various straight vegetable oil-diesel blends as automotive fuels for passenger cars. Straight vegetable oil (SVO) application as diesel-engine fuel has been considered as a possible alternative to fossil fuel since the development of diesel engines. During the first phase of the biofuels introduction in the European market, SVO's achieved a small but important market share reaching up to 4%. In addition several non-European countries are reported to use SVOs in various applications such as off road vehicles. This study attempts to identify the impact of SVO application on emissions, regulated and non regulated, on a common rail diesel passenger car. For this purpose three different vegetable oils (cottonseed, sunflower, rapeseed) were blended with diesel fuel, on a 10-90% v/v ratio each, and were applied on a Euro 3 common rail vehicle. Chassis dynamometer measurements were conducted including both regulated gaseous pollutants and non regulated pollutants. In the case of rapeseed oil-diesel blend, carbonyl compounds (13 aldehydes and ketones) were identified and investigated. In addition to the legislated procedure, the Artemis driving cycles were used in the experiments for quantifying the fuels' impact over realistic driving conditions. Results indicate that all blends presented good operating characteristics and have limited effects on gaseous pollutants and vehicle performance. Reductions were observed on PM emissions, while NOx remained at baseline levels. Comparison with the emission levels measured when using esterified fuels of the same feedstock indicates that SVO does not affect engine exhaust in the same way as biodiesel. It is concluded that SVO application at low concentrations may be performed without significant impact on vehicle emissions.

Keywords: vegetable oils, exhaust emissions, non regulated pollutants, Artemis cycles

Introduction

Biofuels application in transportation is promoted for both environmental and energy security reasons. Measures to achieve this have been adopted by European Union (EU) and other states in the world. In 2008, biofuel contribution in EU fuels market stood for a 3.3% of the total transport fuels consumption with their market share presenting continuously increasing trends. Straight vegetable oils (SVO) represented the 4% of the total biofuels consumption (Eurobserver, 2009). In less developed countries where the costs for developing transesterification infrastructure, or other post processing of straight vegetable oils for biofuels production and distribution, might be a constraining factor SVO application might be an interesting alternative for promoting biofuels.

There are several studies on the application of pure vegetable oils and their blends with diesel as automotive fuels. Several of these studies can be traced back to the mid-nineties. Nevertheless, since then diesel engines and their fuelling systems have evolved significantly initially moving from indirect injection to direct injection and then to high-pressure direct fuel injection (common rail) systems. Consequently part of the conclusions derived from past research activities need to be re-validated. In addition, developments led to fuelling systems that are much more precise regarding fuel delivery timing and quantity but also highly sensitive

to changes in fuel properties. More recently a number of vegetable oils have been studied for direct application as diesel engine fuels such as rapeseed oil (Grau, et al., 2010), jatropha oil (Forson, et al., 2004), coconut oil (Semrisi, et al.), rubber oil , cottonseed oil (Fontaras, et al., 2007), cooked vegetable oils and even tomato seed oil . These studies reveal the potential vegetable oils have as fuels either directly or through transesterification. However these studies are usually limited to the investigation of the physical properties of the oils and fuels, in comparison to various fuel standards, without examining their effect on the vehicle operation and environmental performance.

This paper attempts an experimental evaluation of three straight vegetable oils-diesel blends as automotive fuels for passenger cars under various conditions with respect to their potential environmental impacts. In this context both aspects (vehicle performance and fuel compatibility) were addressed. Initially three different SVO were chosen and investigated with respect to their physical properties while in a second step 10% v/v blends were employed on a common rail diesel passenger car used for chassis dynamometer tests.

Experimental

Test vehicle and fuels

A Euro 3 emission standard compliant, Renault Laguna 1.9 dCi passenger car, was employed for the measurements. The vehicle was equipped with a common-rail diesel engine with exhaust gas recirculation (EGR) .The exhaust aftertreatment system of the vehicle comprised a closed-coupled pre-catalyst and an underfloor main oxidation catalyst.

Three different straight vegetable oil-diesel blends (10%v/v vegetable oil concentration) were tested, cottonseed oil (CSO), sunflower oil (SFO) and rapeseed oil (RSO). It should be noted that the cottonseed oil used in the blends had undergone a refining process while the other two oils were used crude having subjected only to filtration and drying. The blends were produced by splash-mixing refined oils with the reference diesel fuel. The reference fuel was a typical automotive, low sulphur diesel (<50ppm S) complying with EN 590 (Directive 2003/17/EC).

Testing facility

The vehicle was tested on a transient vehicle dynamometer, simulating drag, inertia and rolling resistances, as specified by EU regulations. The exhaust was primarily diluted and conditioned by means of Constant Volume Sampling (CVS). A 6 m long corrugated stainless steel tube transferred the exhaust from the tailpipe to the CVS tunnel inlet. The tube was insulated to minimize heat losses and was clamped onto the vehicle exhaust pipe with a metal-to-metal connection to avoid exposing the hot exhaust gas to any synthetic material connectors. A flowrate of 500 Nm3/h (Normal cubic meters per hour) was maintained in the CVS tunnel by a positive displacement pump. The dilution air was filtered through a HEPA class H13/EN1822 filter at the inlet of the dilution tunnel. All gas analyzers employed were in line with European regulations.

Particle emissions measurements were also extended to non legislated particle properties, such as number concentration and size distribution. Samples were taken from the constant volume sampler (CVS) with a Dekati Fine Particle Sampler (FPS- 4000) operating at a nominal dilution ratio of 12:1. Additionally, two calibrated ejector-type diluters were employed in order to bring the particle emissions levels within the measuring limits of the instruments. A Condensation Particle Counter (TSI's 3010 CPC) was employed to monitor the total particle number concentration. A Dekati's Electrical Low Pressure Impactor (ELPI) provided the aerodynamic size distribution in real time. The ELPI operated with wet (oil-soaked) sintered plates and a filter stage that extended the lower cutpoint to ~7 nm (Marjamaki, et al., 2002). ELPI was sampling aerosol through a Thermodenuder, operating at 250°C, which removed volatile and semivolatile exhaust components. Over steady–state tests (120 km/h), a scanning mobility particle sizer (Model 3936 SMPS) was used instead of CPC, monitoring the number weighted size distribution.

Test cycles and protocol

The daily measurement protocol started with the New European Driving Cycle (NEDC), which is a cold-start driving cycle, used for passenger car certification in Europe. NEDC was followed by three more transient driving cycles, developed in the framework of the ARTEMIS project. The three Artemis driving cycles are respectively considered representative of city (Urban), rural (Road), and highway (Motorway) driving conditions in Europe. The daily sequence was concluded with a 120 km/h steady state mode conducted for the total particle size distribution measurement. Three EUDC cycles were performed for vehicle conditioning prior to each measurement day.

Each fuel was tested twice based on the aforementioned protocol. Prior to the testing of each fuel the vehicle was conditioned for at least 1000km. The measurement sequence started with the reference fuel. The test blends were then employed in the following series, The testing was finalised with a second pair of measurements with the reference fuel. Comparison of the initial and final baseline measurements indicated that the effect of increasing mileage on carbonyl emissions was marginal.

Carbonyl compound sampling and analysis

For the determination of the carbonyl compounds (CBCs) in the exhaust gas, diluted exhaust gas was drawn from the CVS through cartridges at a rate of 150 ml min-1 using a pump. These cartridges contained 2,4-dinitrophenylhydazine (Chromafix-DNPH, Macherey-Nagel) supported on a silica substrate. A total volume of 3 l was pumped through the DNPH cartridge. The DNPH reacts in-situ with the carbonyl compounds in the gas phase to yield derivative compounds, which are more stable than their reactive counterparts. The carbonyl-DNPH derivatives were analyzed according to ISO 16000-3 using an Integral 4000 HPLC system (Perkin Elmer) with an ultraviolet-visible detector (λ=360 nm). For the separation of the CBCs a C18 column (3 μm in film thickness, 4.6 mm i.d., and 150 mm in length) was used (Waters, USA). A mixture of CH3CN/H2O was used as mobile phase with gradient elution from 50:50 to 75:25. The flow rate was maintained at 1.5 ml min-1 and the injection volume was 20 μl. The limits of detection of the CBCs were ranged from 0.067 to 2.89 ng. The limit of detection was defined using the standard method: 3.3*SD, where SD is the standard deviation calculated from reproducible experiments. The recovery efficiency of CBCs varied from 65% to 105% and it was calculated using spiked cartridges. The mean relative standard deviation in recovery efficiencies was below 15%. In total, ten carbonyls (aldehydes and ketones) were identified and quantified in the exhaust, including formaldehyde, acetaldehyde, acrolein, acetone, propionaldehyde, crotonaldehyde, methacrolein, 2-butanone, butyraldehyde, benzaldehyde, valeraldehyde, p-tolualdehyde, and hexanaldehyde.

Results

Vehicle emissions

Figure summarizes the results of the exhaust emission measurements. Results are presented normalized by the average baseline emission values over each cycle (see average values in Table). Error bars in each case indicate the maximum and minim values recorded.

Table 1 Average baseline (diesel) emission measurement results over the various cycles

	NEDC	Ar. Urban	Ar. Road	Ar. Mt/way	Euro 3 limit (NEDC)
CO2	151.0	219.9	133.2	153.2	-
CO	0.23	0.06	0.02	0.01	0.64
HC	0.02	0.02	0.01	0.005	(HC+NOx=0.56)
NO x	0.44	0.96	0.48	0.62	0.5

PM	0.04	0.07	0.04	0.05	0.05
PN	1.6.E+14	2.0.E+14	1.8.E+14	1.6.E+14	-

Starting with CO_2 emissions (subfigure a) it appears that the differentiations were limited, laying in a ±1% range from the baseline values and within the accuracy limit of the test method. The overall impact of SVO application appears to be neutral with respect to CO_2 emission levels with a possible increasing trend over NEDC of about +1.5%. Over the Artemis Urban cycle CSO and SFO blends application resulted in a more prominent increase and decrease respectively but the overall trend seems to validate the neutral effect of SVO application on CO_2.

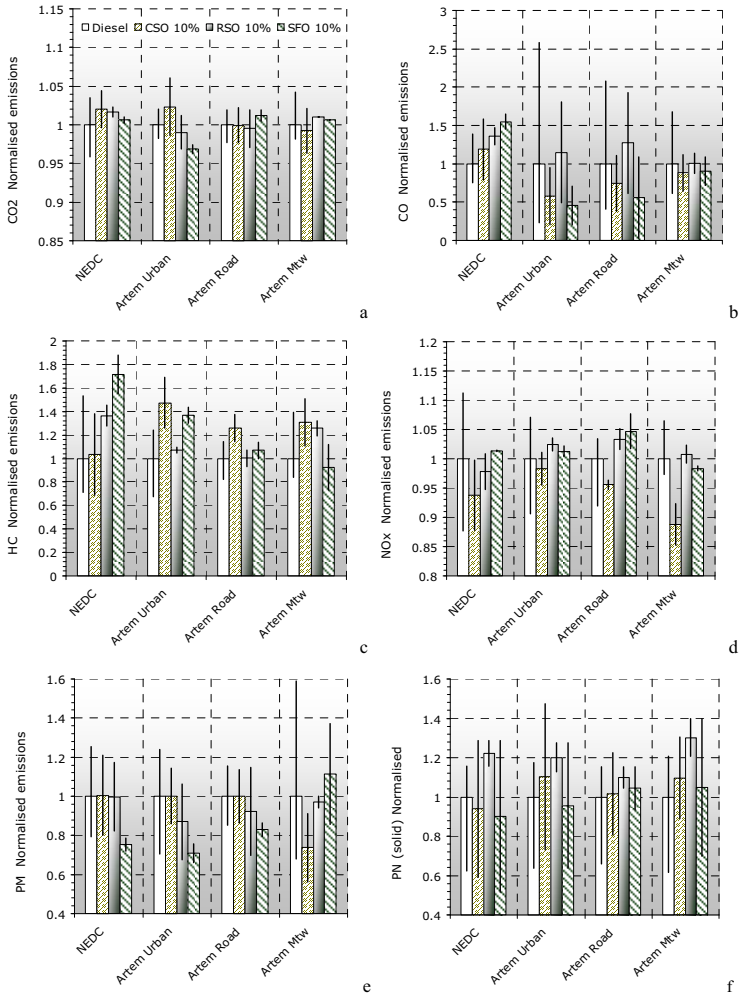

Figure 1: Normalised measurement results for CO_2 (a), CO (b), HC (c), NOx (d), PM (e) and Particle Number (f) over the various driving cycles (Baseline diesel emissions=1). Error bars reflect the maximum and minimum values recorded with each fuel.

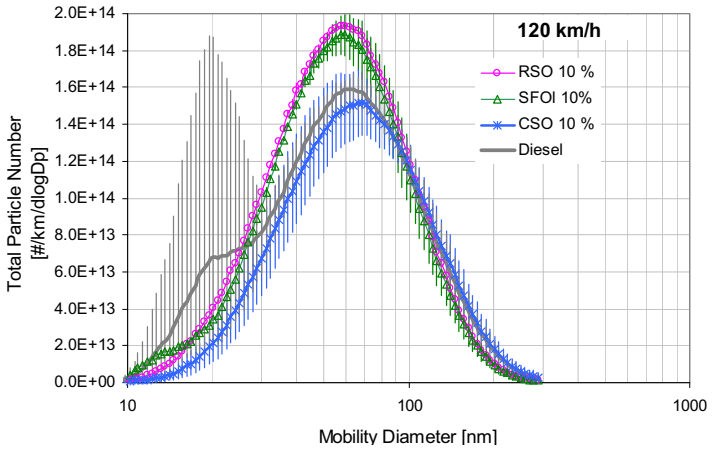

Figure 2: Number weighted size distributions at 120 (b) km/h steady speed cruising

Regarding CO (b) and HC (c) emissions, a different picture was obtained between NEDC and the Artemis cycles. In both cases SVO application appears to increase emissions over NEDC and cause a non uniform effect over Artemis. Over NEDC CO was increased by 20, 35 and 55% and HC emissions increased by 5, 35 and 71% with the presence of CSO, RSO and SFO respectively. Over Artemis Urban and Road CSO and SFO presence led to reductions in CO in the order of 30-55% while over the same cycles their application resulted in HC increases of about 40% (A. Urban) and 10-20% (A. Road). RSO effect is rather neutral considering also the scatter of the results. Under Motorway conditions CO emissions appeared unaffected while certain increases in HC were recorded for CSO and RSO. It should be noted that emissions levels over Artemis are significantly lower than those of NEDC, which is a cold start cycle. The consistent increases observed over NEDC are possibly related to the vehicle's oxidation catalyst operation and efficiency.

With regard to NOx emissions the three different blends appear to have a non uniform effect. CSO tends to lead to lower NOx of about -6, -2, -4 and -10% over NEDC and the three Artemis respectively. RSO and SFO blends had a neutral effect with differentiations laying in a ±5% range over the various cycles, a usual uncertainty for this kind of measurements. Since CSO was a refined oil possible association of NOx emissions with the physical properties of the fuel should be further investigated in order to reach a solid conclusion.

Regarding PM emissions a neutral effect was experienced for CSO and RSO over NEDC, Artemis Urban and Road while over the same cycles SFO led to significant decreases in the order of 20-30%. Under Motorway conditions RSO remains neutral but CSO causes an important reduction while the SFO effect is reversed leading to increases in the order of 10%. Regarding particle number the differentiations observed in PM emissions are not reflected in the number of solid particles emitted. Considering the scatter of the PN measurements a neutral effect on PN is extracted with a possible increasing trend for RSO blends. However the increased variability of particle number measurements makes it difficult to draw solid conclusions regarding this pollutant.

Regarding particle characterisation Figure summarizes the results of particle size distribution measurements. The distribution in the case of SVO blends presents a single mode while for diesel both single and bi-modal distributions were observed suggesting the formation of nucleation mode particles under certain circumstances. It is possible that the presence of the vegetable oil molecule suppresses the formation of nucleation particles. In addition in two out of the three occasions (SFO and RSO) the presence of the vegetable oil led to an increase in the total particles and a slight decrease of the mean particle mobility diameter (59nm vs 63). On the contrary the presence of CSO led to reductions in the total particle number and an increase in the mean diameter (69 vs 63nm). Since CSO was the only vegetable oil undergone a refining process it is possible that the origins of these differentiations could be traced down to certain vegetable oil properties affected by refining.

Table :2 Carbonyl emissions for the base diesel fuel and RSO blend over the NEDC and the Artemis driving cycles

Carbonyls (mg/kg)	Diesel				RSO 10%			
	NEDC	Art. Urban	Art. Road	Art. Motorway	NEDC	Art. Urban	Art. Road	Art. Motorway
Formaldehyde	0.28	0.23	0.15	0.27	0.48	0.53	0.43	0.48
Acetaldehyde	0.28	0.17	0.22	0.21	0.40	0.30	0.44	0.45
Acrolein/acetone	0.26	0.29	0.19	0.21	0.42	1.16	1.27	0.62
Propionaldehyde	0.11	0.10	0.06	0.05	0.10	0.13	0.07	0.04
Crotonaldehyde	0.17	0.15	0.11	0.09	0.15	0.20	0.24	0.11
Methacrolein	0.11	0.10	0.09	0.07	0.16	0.15	0.14	0.15
2-Butanone	0.11	0.09	0.08	0.06	-	-	-	-
Butyraldehyde	0.09	-*	-	-	0.10	0.20	0.19	0.16
Benzaldehyde	0.05	0.06	-	-	-	-	-	-
p-Tolualdehyde	0.07	0.08	-	-	0.08	0.13	0.10	0.09

[a] Below the limit of the UV detector.

Carbonyl compounds

Ten carbonyl compounds (aldehydes and ketones) were identified and quantified in the exhaust for the baseline fuel and the RSO blends. Their concentrations measured over the various driving cycles are given in Table . In general, the addition of RSO led towards higher carbonyl emissions over all driving conditions. Consistent with previous studies, low molecular weight compounds such as formaldehyde, acetaldehyde, acrolein, and propionaldehyde were found to be the most abundant carbonyls emitted (Correa and Arbilla, 2008; Karavalakis, et al., 2009). Heavier carbonyls were found in lesser amounts, whereas aromatic aldehydes were almost undetectable with both fuels. It is worthy of note that butyraldehyde was consistently present in the exhaust only with the vegetable oil blend while 2-Butanone only appeared with the reference fuel.

Conclusions

Regulated pollutant emissions remained in most cases close to baseline levels. Minor fluctuations were observed for CO_2 and consumption. CO and HC were influenced more by the presence of the vegetable oil particularly over the cold start cycle where exhaust aftertreatment system performance plays an important role. The overall picture, however, does not raise important concerns considering also the very low emission levels of these pollutants. Regarding NOx and PM certain reductions were observed with CSO and SFO respectively but the general impression is neutral for both pollutants. The NOx/PM tradeoff observed for biodiesel did not appear in the case of straight vegetable oils. Solid particle number differentiations were not in accordance with those of PM and presented a high variability. Particle characterization suggested that SVOs may suppress the formation of lower size, nucleation particles. The size distribution however was different in the case of the refined and non refined vegetable oils, implying an impact of oil quality on particle characteristics. Overall, most differentiations remained within the regular uncertainty levels for such measurements. RSO application led to important increases in carbonyl compound emissions over all cycles tested. Overall it appears that SVO application may be performed without important impact on vehicular emissions provided that the resulting blends remain in accordance with the existing diesel fuel quality

standard. Nevertheless certain issues such as the effect on carbonyl emissions should be further examined in order to obtain a clearer picture regarding the mechanisms causing these effects.

Acknowledgements

Authors would like to acknowledge the valuable help of Dr. Panayotis Pistikopoulos and Mr. Theodoros Tzamkiozis in the experimental activity.

References

Correa, S.M., Arbilla, G., 2008. Carbonyl emissions in diesel and biodiesel exhaust. Atmospheric Environment 42, 769-775.

Eurobserver, 2009. Biofuels Barometer - Barometer Biocarburant, p. 18.

Fontaras, G., Tzamkiozis, T., Hatziemmanouil, S., Z., S., 2007. Experimental Study on the Potential Application of Cottonseed Oil-Diesel Blends as Fuels for Automotive Diesel Engines. Process Safety and Environmental Protection Official journal of the European Federation of Chemical Engineering: Part B 85, 396–403.

Forson, F., Oduro, E., Donkoh, E., 2004. Performance of jatropha oil blends in a diesel engine. Renewable Energy 29, 1135-1145.

Grau, B., Bernat, E., Antoni, R., Jordi-Roger, R., Rita, P., 2010. Small-scale production of straight vegetable oil from rapeseed and its use as biofuel in the Spanish territory. Energy Policy 38, 189-196.

Karavalakis, G., Stournas, S., Bakeas, E., 2009. Effects of diesel/biodiesel blends on regulated and unregulated pollutants from a passenger vehicle operated over the European and the Athens driving cycles. Atmospheric Environment 43, 1745-1752.

Marjamaki, M., Ntziachristos, L., Virtanen, A., Ristimaki, J., Keskinen, J., Moiso, M., Palonen, M., Lappi, M., 2002. Electrical filter stage for the ELPI. SAE paper 2002-01-0055.

Semrisi, A., Charooenphonphanich, C., Kammool, P., Study of Injector Nozzle of DI Diesel Engine for Blended Coconut Oils. Department of Mechanical Engineering, Faculty of Engineering King Mongkut s Institute of Technology Ladkrabang.

The Impact of Biodiesel Blends on Emissions

*Curt Robbins1, S. Kent Hoekman1, Amber Broch1, Mani Natarajan2, and Alan Gertler1**

[1] Desert Research Institute, Division of Atmospheric Sciences, Reno, Nevada 89509, United States, Alan.Gertler@dri.edu
[2] Marathon Petroleum Company LLC, 539 South Main St, Findlay, OH 45840, United States

INTRODUCTION AND BACKGROUND

The results presented in this paper are part of a larger study, with the overall objective of assessing the state of knowledge regarding biofuels as blending materials for ultra-low sulfur diesel (ULSD) fuel in transportation applications. Besides emissions impacts, the entire study dealt with policy drivers, feedstocks, fuel production technologies, fuel properties and specifications, in-use handling and performance, and life-cycle impacts (Hoekman et al., 2009).

An earlier review of the impact of B20 on dynamometer-based emissions conducted by EPA (2002) reported substantial decreases in HC, CO, and PM emissions, and slight increases in NOx emissions (see Figure 1 and Table 1). These findings raised serious questions as to the potential impact on NO_x emissions following the introduction of biodistillate fuels. More recently, McCormick et al. (2006) performed an analysis using updated information and concluded that, on average, there was no net increase in NO_x emissions when using B20. (Table I). Both studies reported significant reductions in CO, HC, and PM emissions.

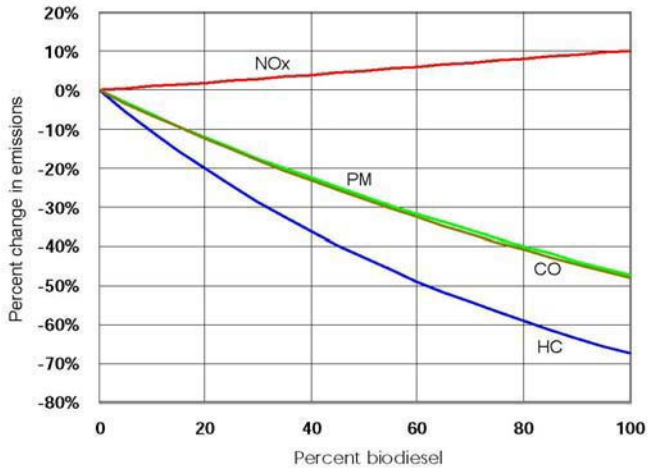

Figure 1: Average emissions impacts of biodiesel used in heavy-duty (HD) highway engines (EPA, 2002).

Table 1: Average percent change in emissions from use of B20 in HD dynamometer tests

Pollutant	EPA (2002)	McCormick et al. (2006)
NOx	+2.0	+0.6*
CO	-11.0	-17.1
HC	-21.1	-11.6
PM	-10.1	-16.4**

*Reported as statistically insignificant
**Excludes engines equipped with DPF.

This discrepancy in NO_x emissions results between these previous studies is a critical issue that needs to be resolved, since any potential increase in NO_x could limit the use of biodistillate fuels. Using the extensive literature review compiled as part of the broader study (Hoekman et al., 2009), this paper investigates the range of reported biodistillate emissions results to develop a better understanding of the true impacts of these fuels.

ANALYSIS METHODOLOGIES

Approximately 1000 literature papers and reports compiled as part of the overall study were reviewed for emissions data. This literature review focused on the years 2000 to 2008. The references containing emissions data are contained in Hoekman et al (2009), with the most relevant emissions data have been published within the past five years.

A total of 94 references were identified, which reported 346 distinct emissions test results for different engine types [heavy-duty (HD), light-duty (LD), and single-cylinder test engines (TE)], blend levels (B20, B50, B100, etc.), biodistillate sources (soy oil, rapeseed oil, etc.), and test conditions (steady-state and transient). The few cases using medium duty (MD) engines were lumped with the HD cases.

Absolute emissions rates vary greatly from one test to another, due to large influences of engine type, test cycle, control technology, and other factors. Therefore, the percentage change in emissions when using a biodistillate vs. a reference diesel fuel was the metric chosen for analysis, rather than absolute emission rates. This approach more clearly identified the impacts of specific biodistillate blends on emissions. Publications that did not include a reference diesel fuel for comparison were not used in this evaluation.

Significant advancements in engine and emissions control technology have occurred over time. However, there is not a direct correlation between model year and publication date. Many studies did not report the model year as a characteristic of the test engine. (In some cases, old technology systems may be used, even though the publication is very recent.) This lack of information about technology of the test engines also introduced variability into the analysis.

RESULTS AND DISCUSSION

The process of sorting the data and eliminating outliers left a data set of the percentage change in emissions from a biodistillate fuel test compared to a reference diesel fuel test for 4 pollutants (CO, HC, PM and NO_x) and 3 classes of engines, (HD, LD and TE.) [PM results included only gravimetric-based measurements (TPM or PM_{10}), not opacity or smoke measurements.] These data were analyzed and displayed in two basic ways to explore: (1) the influence of biodistillate blend level upon criteria emissions and (2) the influence of engine model year upon criteria emissions.

Influence of Biodistillate Blend Level

To display the influence of biodistillate blend level upon emissions, the data were plotted in a series of three graphs for each engine type, as follows:

1. Data points are shown for averages of each reported test in a given study at a given biodistillate level. This assessment is designed to illustrate variability in the reported emissions test results.

2. Data points are shown for averages of all tests from all studies at a given biodistillate level, with error bars representing the minimum and maximum percent change. This simplifies the previous representation by collapsing several test results to a single point for each blend level.

3. Using the average dataset from above, a best-fit logarithmic trend line was developed for each emissions species as a function of biodistillate level. This representation is similar to what was used in the 2002 EPA document.

The series of graphs developed from this approach are displayed in Figure 2 for the HD case (the graphs for the LD and TE engines are contained in Hoekman et al., 2009). The top panel shows a single data point for the average test result at a given biodistillate level, and is color coded by pollutant (NO_x, CO, PM and HC). To display the full range of observations, the y-axis spans a percent change of +/- 100%. A linear trend line for each of the species is included, which provides an assessment of the overall change in emissions with increasing levels of biodistillate.

The middle panel collapses the data from the top panel by displaying the average of all test results at a given blend level vs. blend level. Error bars represent the minimum and maximum percent change from a reference diesel fuel for all test results at a specific biodistillate blend level. (These data points and error bars are offset slightly along the x-axis to provide better graphical clarity.) Again, they are color coded based on the four pollutants, and a linear trend line is displayed for each of the species.

The bottom panel uses the same dataset as the middle panel, but displays a logarithmic trend line based on the average of all emissions for a given biodistillate level. (Note that for this case, the range in the y-axis is from +20% to -40%) This is the simplest way of showing the trend in emissions for each pollutant as a function of biodistillate level, and allows for better comparison with the trends reported in previous reviews.

For all three approaches, trend lines were extrapolated beyond the data set to a B5 level, but were not force fit through zero (i.e., 0 % change for 0 % biodistillate). The location of the trend line at the lowest biodistillate levels should be treated with caution. This is especially true for the logarithmic results, where both the magnitude and direction of the trend line are primarily determined by the lowest % biodistillate data points. A thorough statistical analysis of these data was beyond the scope of our study.

A number of observations regarding the potential impacts of biodistillate blend levels on emissions can be made, with the caveat that this approach does not allow for the assessment of the impacts of specific biodistillate sources, test cycles, control technologies, operating conditions, or model years. A further limitation of this approach is that by not evaluating specific biodistillate sources, a linkage between biodistillate fuel properties and emissions cannot be determined. Given these limitations, we made the following observations regarding the trends in emissions effects across the range of engines, fuels, and test cycles used:

Heavy-Duty Engines (including medium-duty):

- NO_x emissions differ very little from reference diesel fuel. The effects at B20 and below are indistinguishable from zero. A slight NO_x increase (2-3%) may occur with B100.
- CO, HC, and PM are decreased for all B levels, and decrease further with increasing % B.
- There is a greater impact of % B on HC and PM than on NO_x and CO.

Light-Duty Engines:

- NO_x emissions are elevated for all B levels, and increase slightly with increasing % B.
- The magnitude of the NO_x increase is greater than for the HD case.
- CO, HC, and PM decrease for all B levels, but there is less of an impact of % B on emissions than for HD engines.
- There is a greater impact of %B on HC and PM than on CO.

Single Cylinder Test Engines:

- All emission species decrease with use of biodistillate at all blend levels.
- NO_x emissions increase slightly with increasing % B.
- CO and HC emissions are relatively flat and do not appear to be greatly influenced by % B.
- PM emissions decrease with increasing % B.

Overall NO_x emissions appear to have increased and CO, HC, and PM emissions decreased with increasing biodistillate content. However, the magnitude of the effects varied somewhat from one engine type to the next. In most cases, the PM effect appeared to be strongest, while the NO_x effect was weakest.

To compare the results of these analyses with the findings of other reported studies, the regression equations derived from the logarithmic trend lines were used to predict the % change in emissions of a given pollutant for a specified % B. These regression equations were determined for two different data sets:

1. Full data set: included results from both biodiesel and renewable diesel fuels.

2. Partial data set: included only results from biodiesel fuels. This data set was slightly smaller, with 0-3 data points eliminated, depending upon the engine type and pollutant species investigated.

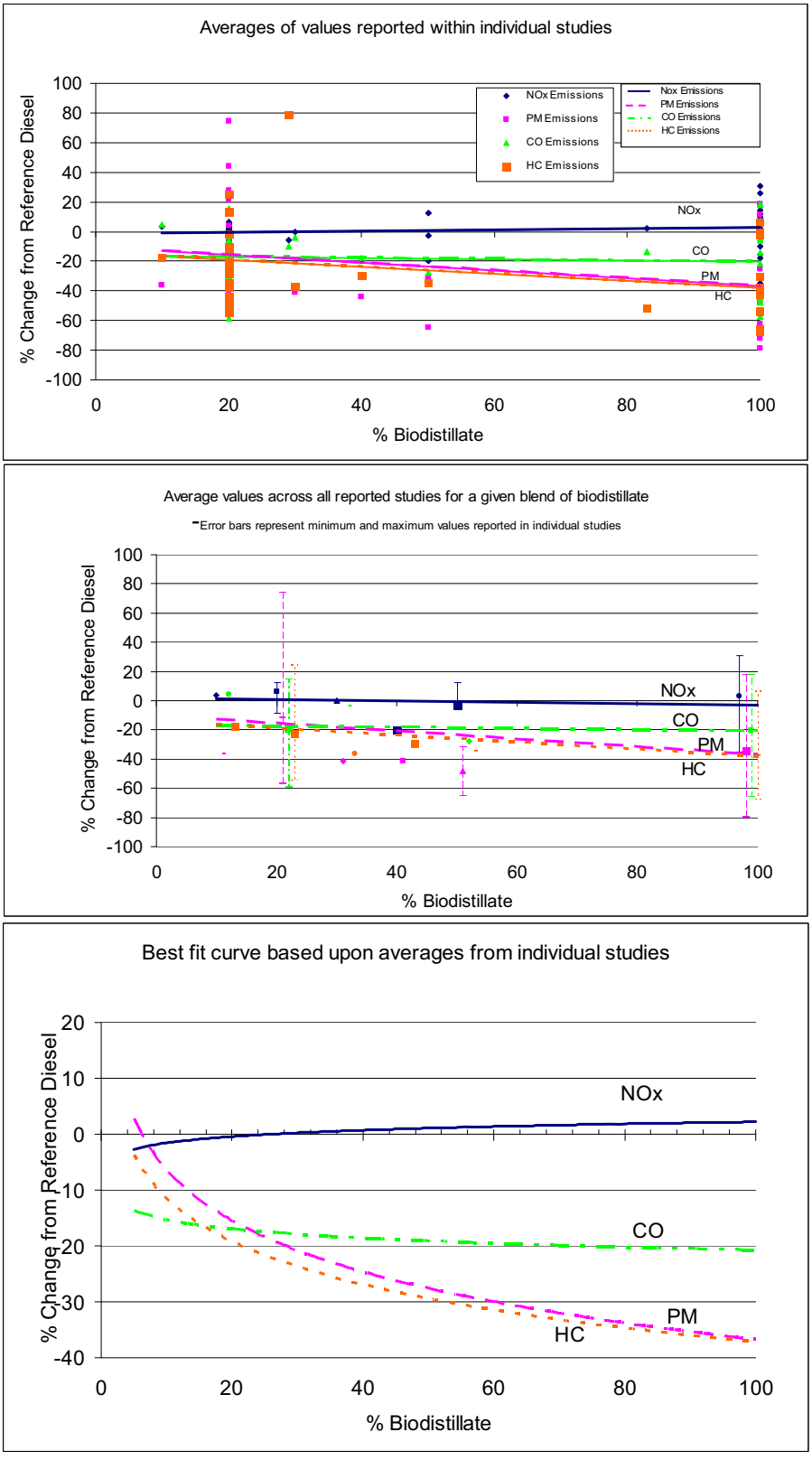

Figure 2. Effects of Biodistillate Blends on Exhaust Emissions from HD Engines

The emissions impacts of biodistillates at the 20% and 100% blend levels are shown in Table 2. Results from the two different data sets are similar. This is to be expected, since very few data points were eliminated in the "biodiesel only" data set. (In fact, the two data sets are identical for the single cylinder test engines.) With HD engines, the "biodiesel only" data set gave slightly

larger emissions reduction benefits for CO, HC, and PM. However, the differences are small, and more sophisticated statistical analyses would be required to determine whether they are significant.

Table 2: Predicted percent changes in emissions using B20 and B100

	Pollutant	Full Data Set			Biodiesel Only Data Set		
		HD	LD	TE	HD	LD	TE
B20	NOx	-0.3	+10.8	-8.1	-0.6	+10.8	-8.1
	CO	-16.6	-10.1	-13.4	-18.7	-10.4	-13.4
	HC	-19.2	-16.6	-15.4	-21.2	-17.4	-15.4
	PM	-15.5	-14.6	-12.9	-24.1	-13.9	-12.9
B100	NOx	+2.5	+15.3	-1.7	+3.0	+15.3	-1.7
	CO	-20.2	-12.3	-16.2	-23.2	-12.2	-16.2
	HC	-37.2	-22.9	-16.3	-40.4	-22.5	-16.3
	PM	-36.8	-31.7	-26.8	-42.2	-32.1	-26.8

Notes: HD = heavy-duty and medium-duty CI engines

LD = light-duty CI engines

TE = single cylinder CI test engines

Going from B20 to B100 reduced emissions of CO, HC, and PM for all three engine types. NOx results are less clear. This assessment of HD NOx results suggests that biodistillates have no effect at low levels (B20), but increase NOx slightly (2-3%) at B100 levels. LD results suggest a more consistent NOx increase of 10-15% for B20 and B100, respectively, though the high variability in the emissions results makes these conclusions questionable. For the single cylinder TE cases, NOx emissions appear to be reduced slightly at a B20 level, but not at a B100 level. More sophisticated statistical analyses are required to assess the significance of these small effects.

The HD results for all blend levels reported in this study can also be compared with the EPA (2002) findings that were shown in Fig. 1. Overlaying the data from Fig. 2 (bottom panel) with those of Fig. 1 yields the chart shown in Fig. 3. The solid lines represent findings from this work, while the dashed lines present the EPA (2002) findings. It is important to remember these data represent a wide collection of engines and control technologies, model years, biodistillate sources, and test cycles, with the EPA (2002) observations reflecting an older set of experiments and engines. Given this caveat, the findings from the two data sets are quite similar, with NO_x emissions increasing and CO, HC, and PM emissions decreasing as the biodistillate level increases.

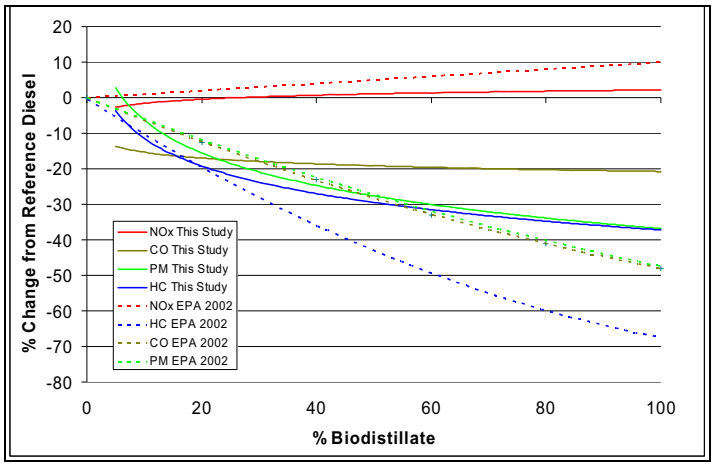

Figure 3: Comparison of HD Engine Results from this Study with EPA (2002).

Figure 3 also shows that the percent changes in emissions for all pollutants are lower from this study than in the previous report, i.e. the overall fuel effects are smaller in this study compared

to the EPA report. One possible explanation is that emissions from newer engines (and more advanced control technologies) included as part of the current study are lower overall, leading to a reduced impact from the introduction of biodistillate blends.

As a final point of reference, the B20 HD results from this study can also be compared with those determined by EPA (2000) and McCormick et al. (2006). The comparisons are shown in Table 3. Overall, the predictions for all species are quite similar. Based upon these findings, it is concluded that use of biodistillate blends at a 20% level has a positive impact on diesel CO, HC, and PM emissions, with little impact on NO_x emissions. Perhaps the most valid conclusion regarding NO_x is that offered in a recent NREL report, "…examination of the NO_x results shows that the effects of biodiesel can vary with engine design, calibration, and test cycle. At this time, the data are insufficient for users to conclude anything about the average effects of B20 on NOx, other than it is likely very close to zero." (McCormick et al., 2002).

Table 3: Comparison of average percent change in emissions from HD dynamometer tests using B20.

Pollutant	**EPA, 2002**	**McCormick et al., 2006**	**This Study**	
			Full Data	Biodiesel Only
NO_x	+2.0	+0.6*	-0.3	-0.6
CO	-11.0	-17.1	-16.6	-18.7
HC	-21.1	-11.6	-19.2	-21.2
PM	-10.1	-16.4**	-15.5	-24.1

*Reported as statistically insignificant.

** Excludes engines equipped with DPF.

CONCLUSIONS

Reduction of exhaust emissions has been one of the drivers for biodiesel fuels for many years. Compared to conventional petroleum-derived diesel fuel, most literature reports indicate 10-20% reductions in CO, HC, and PM emissions when using B20 blends, with larger benefits at higher blend levels. Similar benefits were observed with both LD and HD engines/vehicles, though individual results varied widely from one study to the next. Although data are much more limited for renewable diesel cases, it appears that similar benefits in reduction of CO, HC, and PM were observed with these hydroprocessed fuels.

The fuel effects upon NOx emissions were much smaller, and difficult to discern. This review of HD NOx results suggests that biodistillates have no effect at low levels (B20) but increase NOx slightly (2-3%) at B100 levels. LD results suggest a more consistent NOx increase of 10-15% for B20 and B100, respectively, though the high variability in these emissions results makes such conclusions somewhat questionable. Based upon the small amount of available information, it appears that the NOx emissions effects of renewable diesel are not greatly different from the effects of biodiesel. More work is needed in this area to assess whether significant differences exist.

Acknowledgments

This work was conducted under sponsorship and funding of the Coordinating Research Council (CRC), as Project AVFL-17. The authors gratefully acknowledge the CRC AVFL-17 Panel for their helpful discussions and suggestions. We also acknowledge the efforts of Mr. John Ford of

DRI in helping to identify and obtain copies of technical papers and reports. We are also appreciative of Ms. Vicki Hall's efforts in preparing this complex document.

References

Hoekman SK, Gertler A, Broch A, and Robbins C (2009). Investigation of Biodistillates as Potential Blendstocks for Transportation Fuels, CRC Project AVFL-17, Desert Research Institute Final Report to the Coordinating Research Council, June 2009. http://www.crcao.com/reports/recentstudies2009/AVFL-17/CRC%20Report%20No%20AVFL-17%20June%202009_f.pdf.

McCormick RL, Williams A, Ireland J, Brimhall M, and Hayes RR (2006). Effects of Biodiesel Blends on Vehicle Emissions, NREL/MP-540-40554, October 2006.

USEPA (2002). A Comprehensive Analysis of Biodiesel Impacts on Exhaust Emissions, EPA 420-P-02-001, US Environmental Protection Agency.

Session 6: Emission Modelling 2

Uncertainty and Sensitivity Analysis of COPERT 4

L. Ntziachristos[1], I. Kioutsioukis[2], C. Kouridis[2], D. Gkatzoflias[2], Z. Samaras[1], P. Dilara[3]

[1] Laboratory of Applied Thermodynamics, Dept. of Mechanical Engineering, Aristotle University of Thessaloniki, Greece, email: zisis@auth.gr

[2] EMISIA S.A., Thessaloniki, Greece

[3] Institute for Environment and Sustainability, Transport and Air Quality Unit, EC-Joint Research Centre, Ispra, Italy

Introduction

Road transport is a significant source of air pollution, especially in urban areas. According to a review of the LRTAP data by the European Environment Agency (EEA, 2008), road transport is the most significant source of NOx, CO, and Non-Methane Volatile Organic Components (NMVOCs), and the second most important source of PM emissions in Europe. In 2006, road transport was responsible for 39,4% of total NO_x and 17,8% of total $PM_{2.5}$ in the 27 European Union countries (EU27). Because of this large contribution, the accuracy of road transport emission inventories has measurable repercussions to the attainment of national targets (e.g. Emissions Ceilings) and to how the impact of various policies is reflected in the total emissions.

This paper presents the results of a study on the calculation of the uncertainty of road transport inventories compiled with COPERT 4. COPERT is the most popular road transport emission model in Europe, with 22 out of the EU27 member states using it for their CLRTAP official submissions. COPERT is also part of the EMEP/EEA air pollutant emission inventory guidebook while greenhouse gas emission factors based on the model are used in the IPCC 2006 revised guidelines. Its development has been coordinated by the Lab of Applied Thermodynamics in the Aristotle University of Thessaloniki and has been funded by the European Environment Agency, through the European Topic Centre on Air and Climate Change and by the Joint Research Centre of the European Commission.

The calculation of total emissions in COPERT is based on emission factors, which are functions of speed and are implemented in the model, and activity data introduced by the user. The most important input data include the stock of vehicles distinguished into different categories (passenger cars, heavy duty vehicles, and two-wheelers) and emission standards (Euro-classes), the annual mileage of vehicles and mean travelling speeds, distinguished into urban, rural and highway patterns, and finally the ambient conditions.

The uncertainty in the calculation originates from uncertainties both in the model formulation (e.g. emission factors parameterization) and in the uncertainty of the input data. The uncertainty in the emission factors originates from the experimental data, i.e. the variance in the emission level of different vehicles and engines. The uncertainty in the input data originates from the stock characteristics and the activity pattern in a country. It is impossible to know with accuracy the real operation of all vehicles in a country, while the quality of the statistics of the operational vehicle stock varies from country to country. Other parameters that contribute to the input data uncertainty include the meteorological conditions, the fuel characteristics, etc.

This paper quantifies the uncertainty of the Italian road transport emissions in 2005, calculated with COPERT 4. The probability distribution of the factors contributing to the input uncertainty is built via direct data (as in the case of emission factors, total fleet, meteorological conditions, etc) or expert judgement (as in the case of mean trip length, driving shares, etc). The output uncertainty is quantified in a probabilistic framework through a series of Monte Carlo simulations. In addition, the model sensitivity to the different (uncertain) input variables and parameters is quantified.

Method

Global sensitivity analysis (GSA) has been selected as the approach to estimate the uncertainty of the model and prioritize the importance of the uncertain items. Its advantage is that it considers the full range of variation of the modelling items along with their joint distribution. In this respect, an "item" is either an input variable (e.g. number of vehicles) or an internal parameter (e.g. an emission factor). Moreover, it allows decomposing the total output variance into the individual contributions from each item. Hence, the importance of any item can be measured via the so-called sensitivity index, which is defined as the fractional contribution of the uncertainty of each item to the model output variance. GSA involves Monte-Carlo (MC) sampling of the different modelling items according to specific sampling strategies. The GSA approach implemented in this study has been applied in the past by Kioutsioukis et al. (2004). In principle, the analysis was performed in two steps: First, a screening analysis, according to Morris (1991) identified the most influential items. Then, a variance based sensitivity analysis technique (FAST – Saltelli et al 1999) quantified the uncertainty of total emissions.

COPERT uses a large number of items to perform the calculations. Table 1 shows the input variables and the model parameters for which the uncertainty was quantified, following an initial screening analysis. Some of these items are multi-dimensional. For example, the hot emission factor appears as one item on Table 1 but it has several dimensions (pollutant, vehicle type, engine size, technology class, speed class). Similarly, the N_{cat} value has one dimension (vector) with six entries, i.e. as many as the vehicle categories in COPERT, while others are scalar (e.g.mean trip length).

Table 1: COPERT 4 input variables and model parameters ("modelling items") for which uncertainty has been assessed

Item	Description	Item	Description
Ncat	Vehicle population at category level	LFHDV	Load Factor
Nsub	Vehicle population at sub-category level	Tmin	Average min monthly temperature
Ntech	Vehicle population at technology level	Tmax	Average max monthly temperature
Mtech	Annual mileage	Mm,tech	Mean fleet mileage
UStech	Urban share	RVP	Fuel reid vapour pressure
Hstech	Highway share	H:C	Hydrogen-to-carbon ratio
RStech	Rural share	O:C	Oxygen-to-carbon ratio
USPtech	Urban speed	S	Sulfur level in fuel
HSPtech	Highway speed	ehot, tech	Hot emission factor
RSPtech	Rural speed	ecold/ehot,tech	Cold-start emission factor
Ltrip	Mean trip length	b	Cold-trip distance

The uncertainty of the stock data (N_{cat}, N_{sub}, N_{tech}) was estimated for Italy 2005 on the basis of the available sources (Table 2). The mean value and the standard deviation of the stock is also quoted on Table 2. This shows that the Italian stock is known with very good confidence, with the exception of mopeds. The high share of two wheelers (mopeds and motorcycles) is also an particular characteristic of the Italian stock. The distinction to the different sub-categories (N_{sub}) has been done using data from ACI (2009). The numbers of unidentified vehicles that are included in that database were distributed to the different sub-categories and the variance this produces was taken as a measure of the N_{sub} uncertainty. The technology allocation (N_{tech}) was considered exact because Italian records contain the emission standard as part of the registration.

The mileage driven per vehicle category is an important input variable to estimate emissions. In our simulations, mileage was estimated as a function of vehicle age. Data for the annual mileage of vehicles in Italy originated from Caserini et al. (2007) and are shown in Figure 1a for gasoline and diesel passenger cars. These were approached mathematically as the product of the annual mileage for zero vehicle age (*M0*) and a Weibull function of age – $\varphi(age)$. The

mathematical expression of the approach is given in eq.1. The uncertainty in the *M0* value was considered zero, while the uncertainty of the φ–function was estimated using limit curves corresponding to the extent of the data provided by different European countries. For the modelling, all pairs of (b_m,T_m) values in Eq.1 that provided φ–functions within the two limits were selected (Figure 1b).

Table 2: Italian stock (N_{cat}) in the year 2005 according to different sources, together with the mean and standard deviation values used in the calculations.

Values In thousand units	ANFAC (2009)	ACEM (2009)	ACI (2009)	Eurostat (2009)	μ	σ
Passenger Cars	34 667		34 667	34 636	34 657	17.9
Light Duty Vehicles	3 257			3 633	3 445	266
Heavy Duty Vehicles	1 070			958	1 014	79
Buses	94,4		94,4	94,1	94,3	0,195
Mopeds		5 325	4 560		4 943	540
Motorcycles		4 938	4 938	4 933	4 937	2,75

The uncertainty of the hot emission factors was assessed by exploring the experimental data used to develop them. The speed range 0-120 km/h was distinguished into 10-km/h intervals. The variance of all individual tests in driving cycles with mean speed within these intervals contributed to estimating the uncertainty of emission factors. This is shown in Figure 2 with the example of NOx from diesel Euro 3 passenger cars. The uncertainty per speed interval has been simulated with lognormal distributions which have been fitted to the experimental data. The lognormal distribution was deemed appropriate to simulate the uncertainty of the experimental data for two reasons. First, it can receive no negative value (similar to the emission values). Second, it is highly skewed, thus centres around the majority of experimental data but also representatively includes the contribution of high emitters. Developing the uncertainty of emission factors was a tedious procedure, as it involved 241 vehicle types in Copert 4, 12 speed intervals, and six pollutants (CO, HC, NOx, PM, N_2O, NH_3) and fuel consumption. The parameters for the lognormal functions in each case are contained in the report of Kouridis et al. (2009). In the absence of detailed data, the hot emission factor uncertainty range was also used for cold-start factors, normalized to the e_{hot} over e_{cold}/e_{hot} ratio.

$$M_{tech}(age) = \phi(age) \cdot M0 \qquad \text{Eq.1}$$

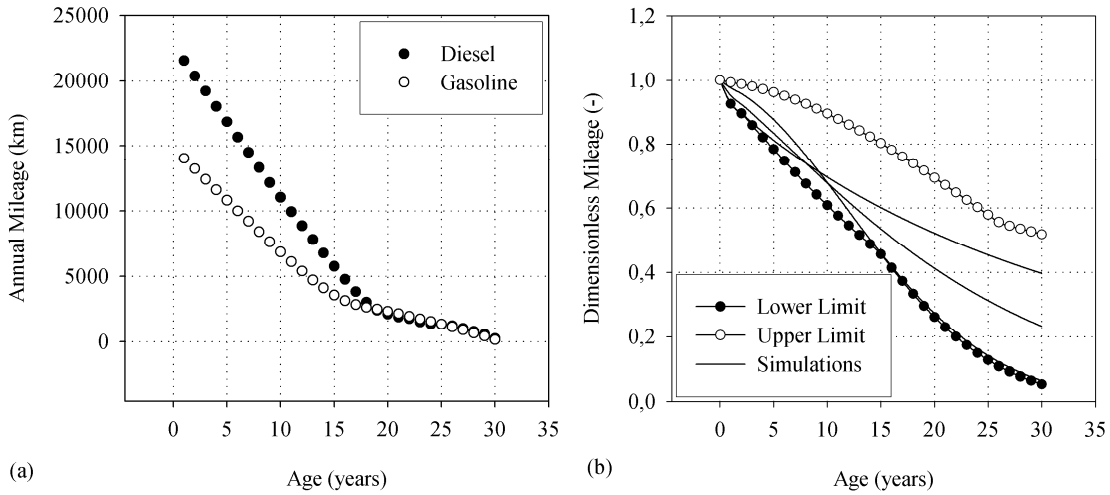

Figure 1: (a) Mileage as a function of age for different passenger car categories, (b) Uncertainty of mileage as a function of age.

The uncertainty of non-exhaust PM (tyre and break wear) was estimated based on the ranges included in the corresponding guidebook chapter (Ntziachristos and Boulter, 2009). The uncertainty of all other parameters was estimated on the basis of any available data. For example, the uncertainty in speeds and shares in urban, rural, and highway driving as well as the *Ltrip* uncertainty were taken from Duboudin et al. (2002). Fuel properties were taken to range within typical limits for RVP, sulphur content, oxygen to carbon and hydrogen to carbon ratio, while a model based on actual recordings for Italy was built for the temperature variation. More details are given in Kouridis et al. (2009).

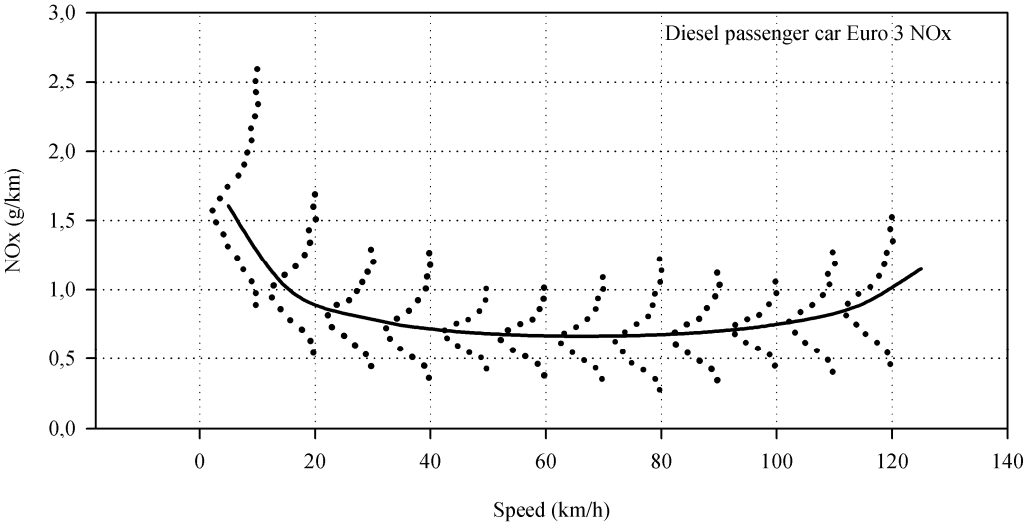

Figure 2: Example of uncertainty of emission factor. The dotted line lognormal distributions correspond to the uncertainty of the emission factor per 10-km/h speed intervals.

Results

Figure 3 shows the results of the Morris method for selected pollutants. A general order of importance for the different items can be established considering the Euclidean distance from the origin in the (MU, SIGMA) space. According to this distance, the most influential items are the emission factor (*eEF*) practically for all pollutants and, depending on the pollutant, the HDV mileage (*milHDV*), the urban share of passenger cars (*UPC*), the l_{trip} value, the cold-start ratio (*eEFratio*). Some other items, like the mileage of passenger cars, the oxygen-to-carbon ratio, and the stock of HDVs, are important for some pollutants only. Moreover, motorcycles mileage and the mopeds stock were found important for VOC emissions. The Morris method identified 16 items in total that drive most of the model output uncertainty for all pollutants.

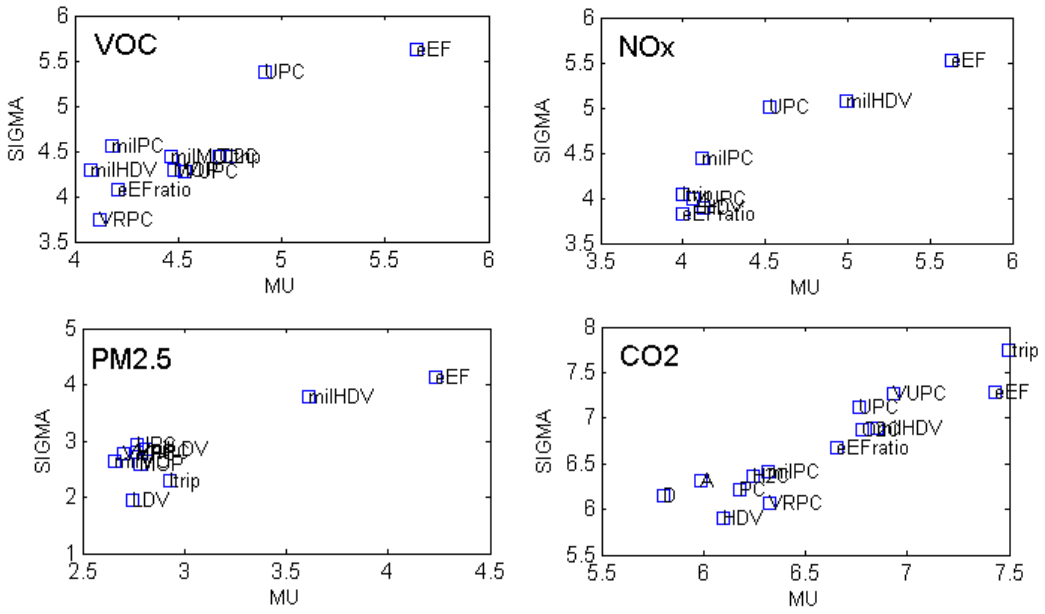

Figure 3: Morris results for selected pollutants. The influence of each item for each pollutant increases with distance from the axes origin.

The 16 most influential items identified from the screening analysis were next used in a quantitative sensitivity analysis. For this purpose, a sample was built by selecting 5904 design points over a particular space-filling curve in the 16th dimensional input space, so as to explore each factor with a different frequency (Cukier et al., 1978). The results of this procedure are shown in a graphical form in Figure 4 for selected pollutants. Descriptive statistics for distributions of all pollutants are shown in Table 3 (case "w/o fuel consumption limitation"). The coefficient of variation (CoV) ranges from 7% for CO_2 to 44% for CH_4, with values for most pollutants ranging from 10-20%. The calculation of sensitivity indices has shown that most of this uncertainty originates from the emission factors. Input variables are known with rather good confidence in the case of Italy and do not contribute much to the output uncertainty. Comparison of the CO_2 and CO_{2e} (equivalent CO_2 including the equivalent global warming potential of CH_4 and N_2O) shows that despite the much larger uncertainty and global warming potential of non-CO_2 gases, the greenhouse gas uncertainty is dominated by CO_2, because its emissions are thousand of times larger than the other gases.

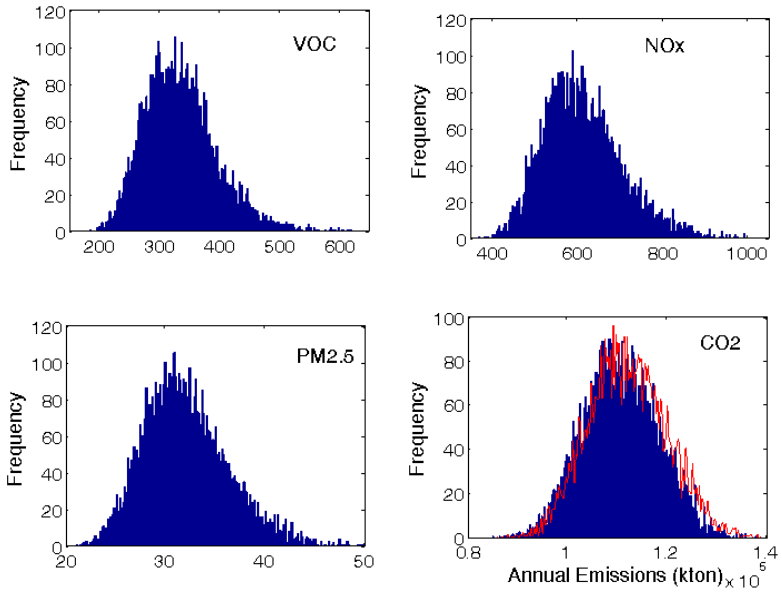

Figure 4: Uncertainty analysis of annual emissions of selected pollutants. Red curve corresponds to CO2–equivalent of all greenhouse gases.

Table 3: Descriptive statistics of uncertainty analysis per pollutant. Values in kt.

Case	Statistic	CO	VOC	CH_4	NO_X	N_2O	$PM_{2.5}$	PM_{10}	PM_{exh}	CO_2	CO_{2e}
W/O Fuel Consumption Limitation	Mean	1,215	335	21	613	3.2	32	36	27	110,570	111,999
	St. Dev.	371	60	9	92	1.1	4	5	4	7,596	7,902
	Coef. Var. (%)	30	18	44	15	33	13	13	14	7	7
With Fuel Consumption Limitation	Mean	1,134	325	19	614	3.1	32	37	27	110,735	112,094
	St. Dev.	218	38	7	59	0.8	3	3	3	4,079	4,203
	Coef. Var. (%)	19	12	34	10	26	9	8	9	4	4

Table 3 also includes descriptive statistics when a “fuel consumption limitation is applied”. When this limitation was applied, the Monte Carlo simulations that led to fuel consumption differing by more than ±10% of the fuel sold were filtered out. This was based on the limitation that a Copert calculation which would result to a fuel consumption much different than the fuel actually sold would not be accepted by the inventory compiler and would have to be corrected. This is a realistic limitation when performing any road transport inventory, while this control is also requested by the 2009 EMEP reporting guidelines (EMEP, 2009).The uncertainty of the calculation drops significantly when applying the fuel consumption limitation. CO_2, NO_x and PM emissions are calculated with CoV values less than 10%, VOC with 12%, CO with 19%, and only CH_4 and N_2O are still quite uncertain (CoVs of 34% and 26% correspondingly). This shows that the fuel consumption limitation is a very useful condition that removes the ‘non-realistic’ simulations, reflecting the real output uncertainty.

Conclusions

The uncertainty of the road transport emissions of Italy in 2005 were studied using COPERT 4. Italy is a country characterised by very good knowledge of the stock and stock activity (mileage) and a high share of mopeds and motorcycles.

Sixteen out of the 51 items studied were found important using a qualitative framework for sensitivity analysis. Then, using variance-based sensitivity analysis, the most important items (with different relative importance depending on the pollutant) identified were the hot and cold emission factors, the ltrip value, the mileage of heavy-duty vehicles, passenger cars and motorcycles, and the urban speed and share.

Without respecting fuel consumption, the total uncertainty ranges from 7% of the mean for CO_2, to 44% for CH_4. Most of the pollutants are calculated with a coefficient of variance in the range 10-20%. By introducing the limitation that the calculated fuel consumption cannot differ by more than 10% of the fuel sold, the uncertainty drops to 4% for CO_2, less than 10% for NO_x and PM, 12% for VOC and 19% for CO. The high CO uncertainty is mainly due to the large stock of power two wheelers.

The uncertainty in the calculation of greenhouse gases is dominated by CO_2, despite of the much higher uncertainty in the calculation of CH_4 and N_2O and their relatively high global warming potential. This is because CO_2 emissions are thousand times higher.

References

ACEM (2009), Circulating park, Available online at www.acem.eu.

ACI (2009), Automobile Club d’Italia – Dati e statistiche, Available online at www.aci.it.

ANFAC (2009), European motor vehicle parc 2007, Available online at www.acea.be.

Caserini S., C. Pastorello and S. Tugnoli (2007), Relationship between car mileage and length of service: influence on atmospheric emission assessment. TFEIP Expert Panel on Transport. Milan, Italy.

Cukier R., H. Levine H. and K. Shuler (1978), Nonlinear sensitivity analysis of multiparameter model systems, *Journal of Computational Physics*, 26, 1-42.

Duboudin C., C. Crozat and T. Fauret (2002), Analyse de la méthodologie COPERT III. Analyse d'incertitude et de sensibilité, Rapport d'activité remis à l'ADEME par la Société de Calcul Mathématique, SA. En application du contrat n° 01 03 021, Paris, France, p.262.

EEA (2008), *Annual European Community LRTAP Convention emission inventory report 1990–2006*, European Environment Agency Technical Report No 7/2008, Copenhagen, Denmark, p.82.

EMEP (2009), Guidelines for reporting emission data under the convention on long-range transboundary air pollution, United Nation Economic Commission for Europe, ECE/EB.AIR/97, p.21.

Eurostat (2009), Transport statistics – Road transport equipment – Stock of vehicles, Available online at http://epp.eurostat.ec.europa.eu/portal/page/portal/transport/data/database.

Kioutsioukis I., S. Tarantola, A. Saltelli and D. Gatelli (2004), Uncertainty and global sensitivity analysis of road transport emission estimates, *Atmospheric Environment*, 38, 6609-6620.

Kouridis Ch., D. Gkatzoflias, I. Kioutsioukis and L. Ntziachristos (2009), Uncertainty estimates and guidance for road transport emission calculations. Emisia Report No. 09.RE.014.V2, Thessaloniki, Greece, p.179.

Morris M. (1991), Factorial sampling plans for preliminary computational experiments, *Technometrics*, 33, 161-174.

Ntziachristos L. and P. Boulter (2009), Road vehicle tyre and brake wear, road surface wear. EMEP/EEA air pollutant emission inventory guidebook – 2009, Copenhagen, Denmark.

Saltelli A., S. Tarantola and K.P.S.Chan (1999), A quantitative model-independent method for global sensitivity analysis of model output, *Technometrics*, 41, 39-56.

Coupling of microscale traffic and emission models to minimize emissions by traffic control systems

Authors, M. Zallinger[1], R.Luz[1], S. Hausberger[1], K. Hirschmann[2] and M. Fellendorf[2]*

[1] IVT, Institute for Internal Combustion Engines and Thermodynamics, Graz University of Technology A-8010 Graz, Austria, Zallinger@ivt.tugraz.at
[2] ISV, Institute for Highway Engineering and Transport Planning, University of Technology Graz, A-8010 Graz, Austria

Introduction

Statistical methods as well as physical models are being used to estimate vehicle emissions and fuel consumption. The variety of models is determined by the variety of applications which greatly differ in terms of the purpose of the study. When modelling traffic flow and traffic induced emissions, three levels of detail exist:

- Microscopic traffic flow simulation and instantaneous emission models
- Traffic network and emission models (mesoscopic)
- Inventory models (macroscopic)

Macro- and mesoscopic emission models like COPERT or HBEFA are used for general considerations like national emission inventories or large road networks where the analysis of individual vehicles is usually not required. Instantaneous emission models are used to calculate the emissions from the speed course of individual vehicles. They provide a high level of detail, but need speed curves as model input and are thus not applicable to large road networks.

To make use of the advantages of all model categories the instantaneous emission model PHEM was used to provide basic emission factors for defined traffic situations. These emission factors are used by the more aggregated emission model HBEFA V3.1. For this task, PHEM was updated and calibrated by a huge data base on measured emissions to provide representative fleet emission factors for passenger cars (PC), light commercial vehicles (LCV) and heavy duty vehicles (HDV).

Microscopic traffic flow models simulate individual vehicle movements stochastically within well-defined road networks. Since microscopic traffic simulation models simulate the time/space trajectories of all vehicles through a network, this vehicle speed data was used as the input for PHEM. This combination makes it possible to evaluate and optimise the effects of measures influencing the traffic flow and the driving behaviour on the fuel consumption and emissions in a road network. While the PHEM model has been validated in several projects, the coupling with microscopic traffic flow simulation models has not been tested before. In the Austrian research project GAVE (Hirschmann et.al, 2009), the application and the uncertainties of such a coupled simulation were tested.

PHEM Emission Model

PHEM (Passenger Car and Heavy Duty Emission Model) is an emission map based instantaneous emission model, which has been developed by the IVT since the late 1990's. It calculates the fuel consumption and emissions of road vehicles in 1Hz for a given driving cycle based on the vehicle longitudinal dynamics and emission maps. The model has already been presented in several papers, e.g. Hausberger, 2003 and Zallinger et. al., 2008.

For the latest version of the *Handbook Emission Factors for Road Traffic* (HBEFA V3.1), a new concept has been elaborated for the traffic situations, resulting in 272 totally new driving cycles (Steven, 2009). To elaborate emission factors for these new cycles from the existing measurements, the PHEM model was used to calculate the emission factors for:

- **Heavy Duty Vehicles:** 19 vehicle categories, 3 vehicle loadings, 9 emission concepts (Pre-Euro to Euro VI, EGR and SCR[6])

[6] EGR and SCR only available for EURO IV and V

- **Passenger Cars:** 2 engine types (gasoline and diesel), 8 emission concepts (Pre-Euro to EURO 6, w/ DPF and w/o DPF[7]),
- **Light Commercial Vehicles:** 2 engine types (gasoline or diesel), 8 emission concepts (Pre-Euro to EURO 6, w/ DPF and w/o DPF), 3 reference mass classes (N1-I, N1-II, N1-III)

All these vehicle combinations were used to calculate the emission factors for all traffic situations with 7 road gradients for CO_2, NO_x, NO_2, HC, CO, PM, PN. This leads to a total of more than 8 million emission factors.

For simulating the emission factors for the HBEFA V3.1, the data base for the engine emission maps and for the vehicle data in PHEM was enlarged and calibrated against a huge number of bag measurements. This calibration work is described later in this paper.

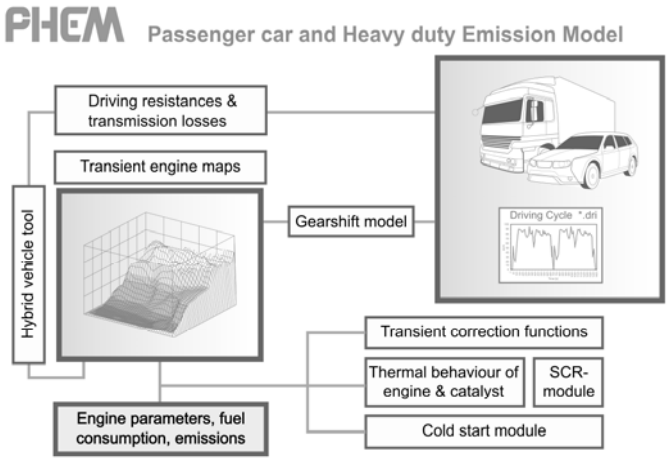

Figure 1: Scheme of the PHEM model

For the simulation of fleet emissions, PHEM offers a predefined data base for PC, LCV and HDV from EURO 0 to EURO 6 and for diesel and gasoline. When coupled with traffic models, the user can define the share of these vehicle layers over the entire vehicle mileage. PHEM then automatically allocates the vehicle data during the simulation process.

Calibration of the Simulation Vehicle Database

The current version of PHEM uses instantaneous emission measurements in 1 Hz resolution in transient cycles on the roller test bed or from engine tests to set up the engine emission maps. For this procedure, proper correction of the measured emissions for time delays and smoothening effects in the exhaust line is a prerequisite. At the moment, this type of correction is only available for the PC roller test beds at EMPA and TU Graz. Thus, the basic engine emission maps for passenger cars were set up using all measured vehicles from these two labs, which resulted in 41 gasoline and 37 diesel cars. From the other labs within the working group on the HBEFA, a much larger number of measurements are available as bag values (g/km for the entire cycle). This data was collected in the ARTEMIS 300 data base (A300db)[8]. All vehicles available in the A300db were used for the calibration of the engine emission maps of PHEM to be representative of the European PC fleet. The driving cycles used from the A300db mainly consist of real world cycles like the CADC (Andre, 2001) and HBEFA (Steven, 2009) cycles. Legislative cycles such as the FTP were only used if no others were available.

Each of the cycles was simulated for all segments of the passenger cars (i.e. all combinations of Euro classes and propulsion systems). Then the model results were compared to the average emission values measured for the corresponding vehicle segment.

[7] DPF concepts only available for EURO 4

[8] Data base started in the FP5 project ARTEMIS, work package 300, including all available measurements on passenger cars and LCV from former projects and also from the most recent national and international measurement campaigns.

For the calibration, the weighted absolute deviation between measurement and simulation was tuned towards a minimum. The weighting factor takes into consideration that different numbers of vehicles have been measured in the different test cycles. If, for example, only one EURO 1 car of the sample in A300db was measured in the CADC, but 19 EURO 1 cars were measured in HBEFA cycles, then the weighting factor of the emission level of CADC was 1/20 and the one of HBEFA cycles 19/20.

The model calibration was performed for each vehicle segment and for each exhaust gas component according to the following system:

1. If the modelled fuel consumption showed deviations larger than 5% and the deviations were different at different average speed levels, the vehicle specifications were slightly adapted within logical boundaries. Then all emissions were recalculated using the adapted vehicle data.
2. The deviation between simulated and measured emissions was then calculated and the absolute level of the emissions stored in the PHEM emission maps were calibrated to result in the same absolute emission level as the average of the measured vehicles.
3. The emission levels simulated and measured were plotted over average cycle power and average cycle speed (each calculated by PHEM) and a weighted polynomial trend line was drawn for measured and simulated emissions. If the two trend lines showed a pronounced difference, the emissions in the engine map were adapted simply by the ratio of the two trend lines. This proved to be necessary for some of those segments in which less than 10 vehicles were available for setting up the engine maps.

Figure 2 shows as an example the final result of the calibration of the NO_x emissions of EURO 0 diesel cars. For this segment, 34 cars in BAB and 2 cars in the CADC sub cycles were measured. Thus, the BAB has a high weighting factor. For EURO 0 diesel cars, no instantaneous emission data with sufficient quality was available to set up the emission maps by PHEM. Thus, the EURO 2 map was used as a base. The calibration of the absolute NO_x level and the adaptation of the engine map shape were performed as described above. The result shows a very good correlation with the measured data.

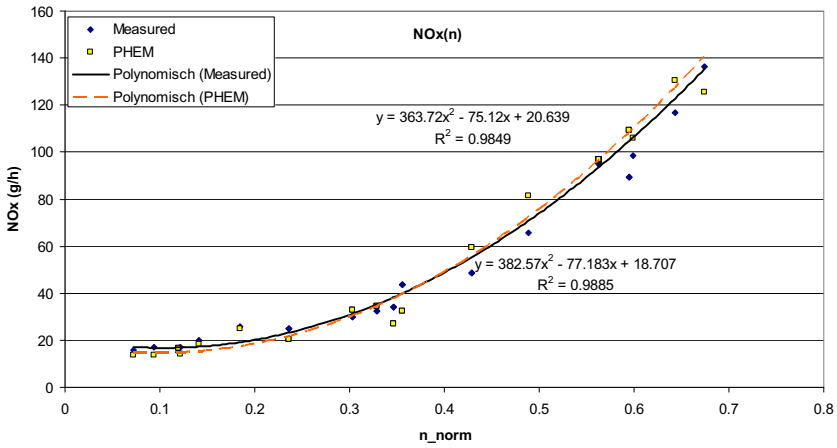

Figure 2: Final result of the calibration of the NO_x emissions of EURO 0 diesel cars (34 cars measured in BAB and 2 cars in the CADC sub cycles)

In total, more than 3000 vehicles were available from the A300 db (Table). In total, approx. 1000 of these vehicles were tested in cycles useful for the determination of calibration factors. This is a sufficient number to assess the average emission levels. Especially for vehicle segments older than EURO 3, a large number of vehicles were measured quite often in only one or two cycles (e.g. EURO 0 diesel in Figure). The model calibration for the trends over engine power and engine speed is thus not very reliable for these old vehicle segments. However, the approach seemed to be the best option for transferring old measured data into emission factors for the huge set of new driving cycles in the HBEFA. Since PHEM can also provide emissions for various road gradients, all emission factors are now simulated in a consistent way. This shall make future updates easier and adding new traffic situations or exchanging the speed curves representing the traffic situations can be handled in a straight forward way by simply running PHEM using the new speed curves.

Table 1: Number of vehicles in the A300 db measured in at least one cycle

Fuel type	Total	pre-EURO	EURO-1	EURO-2	EURO-3	EURO-4
	[number of vehicles measured in ≥1 cycle]					
diesel	543	207	48	54	135	99
gasoline	2597	878	1191	164	156	208

The updated version of PHEM is also used to simulate emissions in combination with traffic flow simulators such as VISSIM and AIMSUN.

Coupling of PHEM with traffic flow simulators

The target of coupling these models is to set up a system capable of evaluating the effects of measures influencing the traffic flow and driving conditions. These influences generally cannot be depicted by mesoscopic or macroscopic models. When two complex models are coupled, extensive validation is necessary to get an understanding of the behaviour of the model and to assess and improve the accuracy of the model.

In the Austrian research project GAVe (Hirschmann et.al, 2009), a street network was selected for the simulation and for tests on the road. The light signals of the network are controlled by the software MOTION version 4.0 (Mück, 2005), which controls the traffic lights based on detector signals on the traffic volume. In GAVe, the first step was to couple the models VISSIM and PHEM using a common interface to load the results from VISSIM into the PHEM model. Then the VISSIM model was used to optimise the traffic light control strategies together with the MOTION system. For the optimisation, the results from PHEM were used (Figure).

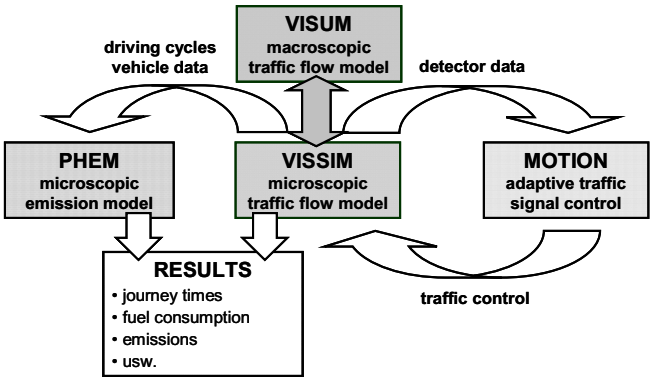

Figure 3: Schematic overview of the coupled simulation models and the interfaces

The result data delivered by VISSIM contain time, speed and type of every single vehicle. If information about the simulated road network is available (i.e. geo-coded street networks), PHEM can assign the calculated emissions to road segments as input for emission dispersion models. The vehicle and engine data required from PHEM for the simulation is taken from the data base on the average vehicles, as described above. The classification into vehicle categories (cars, LCV, HDV, buses etc.) is taken from the result file of the traffic model. The classification into compression ignition (CI) or spark ignition (SI) engines and EURO classes is chosen automatically from PHEM for each individual vehicle according to the user defined fleet composition.

When coupling traffic and emission models, additional important impacts like gear shift behavior or cold start effects have to be considered. In GAVe, the gear-shift model and the simulation of cold-start trips were used as embedded within PHEM.

The user of the traffic model should carefully define the traffic flow parameters of VISSIM to obtain speed trajectories that lead to realistic emissions. The acceleration data, in particular,

shall be adapted to default settings which provide quite high vehicle acceleration levels. The time resolution in the VISSIM simulation should be at least 3 Hz to achieve realistic speed profiles.

Case study and validation of the coupling

For the validation, measurements of the speed trajectories in the field and of vehicle emissions on the roller test bed were compared with the results of the simulation (Figure).

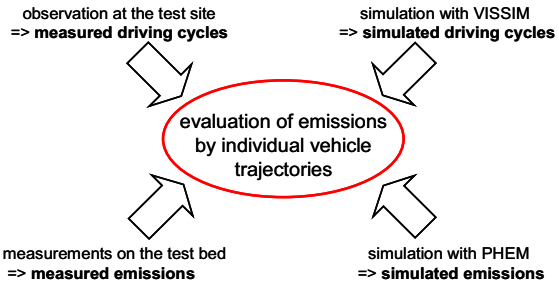

Figure 4: Evaluation structure for the results of the measurement and simulation with the two microscopic models

This methodology provides the possibility of evaluating the accuracy of the whole simulation chain by the following steps:

- Observations of the driving behaviour were made by instrumented cars. Representative test cycles for the roller test bed were extracted from the measured speed trajectories for the base situation and for the optimised traffic light situations.
- The VISSIM traffic simulation model was set up and calibrated for the test site. Representative driving cycles were selected from the VISSIM simulation for the base situation and the optimised traffic light situations.
- Emissions and fuel consumption were measured on a chassis dynamometer on a EURO 4 diesel car for observed and simulated driving cycles for both traffic light situations.
- Emissions were simulated by PHEM for all selected driving cycles.

Afterwards, the results of the simulation and of the measurements were compared.

Table shows the validation results of the whole simulation sequence for both directions of the test route. The values of “measured basic versions” are the results of the observed driving cycles of the base traffic control case and the emissions were measured on the chassis dynamometer. The values of the “measured optimized version” present the driving cycles which where recorded on the test route during the 1-day operation of optimized traffic control and measured afterwards on the chassis dynamometer. On the other hand, the driving cycles were simulated by the VISSIM traffic simulator for both cases and the emissions were also simulated by the PHEM emission model.

Table 2: Validation results of the measured and simulated emissions

		fuel consumption [g/km]	NO_x [g/km]	CO [g/km]	HC [g/km]	PM [g/km]	PN [g/km]	NO [g/km]
Direction North	measured basic version	72.24	0.509	0.014	0.035	0.045	7.97E+13	0.355
	measured optimised version	63.68	0.497	0.013	0.025	0.039	6.94E+13	0.364
	Changing	***-12%***	***-2%***	***-4%***	***-29%***	***-12%***	***-13%***	***3%***
	simulated basic version	81.31	0.827	0.073	0.040	0.058	8.81E+13	0.496
	simulated optimised version	69.98	0.666	0.073	0.033	0.048	7.37E+13	0.374
	Changing	***-14%***	***-19%***	***-1%***	***-18%***	***-17%***	***-16%***	***-25%***
Direction South	measured basic version	68.45	0.528	0.020	0.035	0.045	7.84E+13	0.352
	measured optimised version	67.40	0.576	0.042	0.033	0.047	7.63E+13	0.379
	Changing	***-2%***	***9%***	***108%***	***-4%***	***4%***	***-3%***	***8%***
	simulated basic version	79.28	0.876	0.097	0.039	0.052	8.04E+13	0.490
	simulated optimised version	78.87	0.814	0.086	0.038	0.054	8.26E+13	0.471
	Changing	***-1%***	***-7%***	***-11%***	***-2%***	***5%***	***3%***	***-4%***

For the fuel consumption, the measurement showed a reduction potential of 12% northbound and 2% southbound due to the optimised traffic control case. The main focus was to optimise the signal control site northbound. The simulation yielded the same tendencies with a 14% reduction of fuel consumption northbound and 1% southbound. For the other exhaust gas components, the simulation also showed correct trends, excluding the case of nitrogen oxide (NO_x) in all directions and carbon monoxide (CO) southbound.

The simulated NO_x reduction was not evident in the measurement. There are two reasons for the difference between measurement and simulation. The first is that only a few test drives could be performed on the 2 cars during the observation and therefore it was hard to obtain the average driving behavior at the test site. The second reason is an improvable calibration regarding the acceleration of the vehicles within the testing area. For a more detailed validation of both reasons, it is necessary to make more test drives within the testing area or in urban areas.

The reason for the CO divergence is mainly the poorer repeatability of the very low CO emissions from modern vehicles in the tests on the chassis dynamometer. Driving cycles with low engine loads show high variations in the CO emissions caused by cool down effects of the catalytic converter, the exhaust gas recirculation system and the turbocharger. Therefore, CO peaks can sometimes occur during the measurement. These emission peaks cannot be simulated in an accurate way by PHEM yet.

Summary and Conclusion

The PHEM instantaneous vehicle emission model was used to update the emission factors for the new set of traffic situations in the HBEFA V3.1 for passenger cars, LCV and HDV. The emission levels of the passenger cars were calibrated by a large data base (A300 db) which includes the measurement of more than 1000 passenger cars in real world driving cycles. For HDV, PHEM is based on more than 120 tested HDV and heavy duty engines (HDE). With this updated data, PHEM shall deliver representative emissions for the entire vehicle fleet in European countries.

Beside the simulation of emission factors, PHEM is also applied to calculate emissions based on speed curves simulated by microscopic traffic flow models. The coupling of PHEM with the VISSIM model was successfully performed in the GAVe project and options to optimise the traffic light control strategy in a road network in Graz have been elaborated by the coupled model.

A first validation showed reliable results for fuel consumption, CO_2, PM and HC while the vehicle speed profiles simulated by VISSIM led to rather high deviations for NO_x and CO. Thus, further work will be performed at the TU Graz to elaborate better settings of the model parameters. However, the prototype of the coupled model showed a high potential for simulating the complex effects in the interaction of engines, vehicles, drivers and traffic control systems.

The simulation of an urban test site in Graz with 12 signalized junctions has shown potential to reduce emissions by improving the traffic light coordination. The level of coordination available and the requirements of public transport priority certainly will be case dependent. However, the coupled model also offers new options to optimise traffic control strategies for low exhaust gas emissions and to quantify this potential. Without proper simulation it seems to be very unlikely that complex systems will run at their optimum.

References

Andrè M., (2001), Driving cycles derived from real-world in vehicle measurements for passenger cars and light duty vehicles, Principles, database and main results – Particular case of the ARTEMIS driving cycles, Bron

Hausberger, S., (2003), Simulation of Real World Vehicle Exhaust Emissions, *VKM-THD Mitteilungen Heft/Vol 82*, Verlag der Technischen Universität Graz, ISBN 3-901351-74-4

Hirschmann K., Zallinger M., Fellendorf M., Hausberger S., Mück J., (2009), GAVe – Grazer adaptive Verkehrssteuerung, I2 – Intelligente Infrastruktur, Projekt 812719, Endbericht

Mück J., (2005) Recent developments in Adaptive Control Systems in Germany, Proceedings 12th World Congress on Intelligent Transport Systems, San Francisco

Steven H., (2009), Driving Cycles for the HBEFA 3, TÜV Nord Mobilität, Report in preparation

Zallinger M., Tate J., Hausberger S. (2008), An Instantaneous Emission Model for the Passenger Car Fleet, 16th International Conference „Transport and Air Pollution", VKM Mitteilungen Band 91 ISBN: 987-3-85125-016-9, Graz

Speed-time profiles as a basis for emission modelling of road traffic – the example of Munich

R. Gerike and F. Hülsmann[1*]

[1] mobil.TUM, Technische Universität München, 80333 Munich, Germany, regine.gerike@mobil-tum.de, friederike.huelsmann@mobil-tum.de

Introduction

Existing urban air quality problems cause negative external effects including the impact on human health and the environment. One of the major driving forces is road traffic. The emissions per distance travelled differ significantly with respect to driving speed, acceleration and stop duration as well as vehicle characteristics such as fuel type (André and Rapone, 2009). The focus of this paper is to develop typical real-world driving patterns that represent traffic situations ranging from congestion to free traffic flow as a prerequisite of detailed emission modelling. In addition, such driving patterns are linked to a transport simulation tool to assess environmental effects for a whole urban transport network. The advantage of such a direct linkage between transport and emission modelling is the impact assessment of transport policies with respect to the external effects of road traffic and distribution effects. The analysis is twofold. At first, a method that is suitable for the construction of typical driving patterns is developed and applied to actual speed-time profiles using empirics. Secondly, the transport simulation tool, MATSim, is presented to carry this microscopic analysis over to a region-wide emission modelling. The methodology including driving cycle construction and an interface with MATSim is described in the subsequent sections. An empirical analysis follows applying the methodology to determine typical driving patterns.

Methodology - Driving cycle development

The literature on the construction of real-world driving cycles shows a variety of methodologies applied. A common basis for the development of driving cycles are speed-time profiles which are mostly used to calculate speed and acceleration distributions to find classes of similar travel behaviour (André, 2004; Hung et al., 2007). However, the studies use different data on kinematic characteristics, differ in the statistical method applied and in the spatial dimension. With respect to the methods, for example, a correspondence analysis combined with a cluster analysis (André, 2004) and a principal component analysis followed by a Markov-chain based cycle construction approach (Niemeier et al., 2008) are applied. Whereas Esteves-Booth et al. (2001) develop an average driving cycle for Edinburgh, Niemeier et al. (2008) and André (2009) develop approximate driving cycles for different traffic situations based on data from different urban regions.

Against the background of the literature review, the methodology of this paper must be suitable for the development of driving patterns for different road types, but should cover an entire urban region simultaneously. Therefore, driving patterns with respect to road type beyond the three typical types, urban, rural, highway, are investigated. The number of lanes, the traffic signal system and the speed limit may lead to different driving patterns. With respect to each road type, driving patterns are distinguished by the traffic situation which can range from *stop and go* to *free flow*. A classification of traffic situations is defined in HBEFA 3.1

(Handbook Emission Factors for Road Transport)[9] referring to the definitions used for the ARTEMIS European driving cycles (André, 2004).

Considering the existing concepts of driving cycle construction such as the ARTEMIS European driving cycles, the methodology is developed also using speed-time profiles which are collected from on-board measurements on Munich's roads. The first step is to find similarities between the speed-time profiles to identify groups of similar driving patterns. In order to be comparable, speed-time profiles of the same road type are portioned into segments of the same distance. However, the length of the segments differs by the main road types, urban, rural and motorway. Only urban roads and motorways are analysed. Rural roads are not considered due to the focus on the city of Munich. Urban segments have a shorter length than motorways as crossings and traffic lights frequently occur and, thus, provide interesting information about driving patterns already after some hundred meters or a few kilometres. In contrast, longer segments are needed for motorways to determine representative driving patterns. With regards to the statistical analysis, two segmentation approaches are conducted having both advantages and disadvantages. First, the urban speed time profiles are portioned into segments containing several crossings with traffic signals. Second, they are portioned into smaller segments between two traffic signals. They are bounded by idling time in the case of red traffic signals. The first attempt includes the variety in driving patterns induced by switching signal phases, whereas the second approach reduces the heterogeneity of speed-time profiles. Therefore, more distinct traffic situations may be determined as the speed-time profiles cannot be affected by more than two traffic signals.

For each segment, speed and acceleration are calculated per second resulting in a distribution of instantaneous speed and acceleration. In addition, the kinematic characteristics of each segment are determined. A contingency table per segment is calculated describing the frequency a certain speed and acceleration level occurs. In addition, the mean driving speed and the mean stop duration per km is appended to the vector of speed and acceleration frequencies of each segment. Statistical tools are applied to find driving patterns for each road type. Several multivariate statistics such as principal component analysis, factorial analysis and correspondence analysis have been considered and tested. The latter provided some visual support to distinguish between road types.

With respect to the analysis of driving patterns for a specific road type, a two-stage clustering approach and some graphical representation are applied (Götze et al., 2002). Agglomerative hierarchical clustering is combined with the partitioning of single segments into groups of particular driving patterns. During the first stage, the number of clusters is identified. In order to find dissimilarities between clusters, the Euclidian distance between two clusters is measured. By creating dendrograms of single, complete and average linkage based on the inter-cluster dissimilarities, an idea of the number of clusters is obtained.[10] In addition to dendrograms, a graphic visualisation known as the "elbow criterion" is applied. A stepwise integration of clusters shows the decrease in homogeneity of the partitions. Indices of heterogeneity are calculated and displayed in dependence of the cluster number. The resulting

[9] HBEFA provides emission factors for air pollutants and climate gases differing by traffic situations.
[10] See Götze et al. (2002) and Everitt and Hothorn (2009) for further information on agglomerative hierarchical clustering.

figure shows a line with elbows. The sharpest elbow indicates a possible number of clusters. Having identified the number of clusters, i.e. driving patterns, also considering existing findings and experience, the next stage, the partitioning of the segments into such clusters is conducted. The k-means algorithm is applied. First, the centroid of each cluster is determined, followed by the calculation of the Euclidian distances of the segments to the centroid. Then, the segments are rearranged in case another centroid is closer. Finally, the centroids of the clusters are calculated again and the whole procedure is repeated until minimal distances are determined. Consequently, each segment is assigned to a cluster (Götze et al., 2002).

In order to identify the most representative segment of each cluster of a specific road type, the median of the kinematic characteristics is determined for each cluster. The information obtained from kinematic characteristics and further influencing variables can explain the different driving patterns. The parameters shown in table 1 reveal important information about driving patterns, in regard to emission modelling. They are a selective choice of parameters that have been used in the literature (Hung et al., 2007; André and Rapone, 2009) and some additions. Mean driving speed gives an approximation about the traffic situation of the driving pattern such as *congestion* or *free flow*. The additional variables as stop duration, the time spent in acceleration, deceleration and cruising provide more information about the steadiness of a pattern. A high stop duration and relatively high relative positive acceleration indicate unsteady flows, whereas less stops and time spent in the acceleration mode reveal steady flows if the driving speed is similar in both cases. Additionally, a low share of cruising in the total travel time indicates unsteady flows. Using the variables, mean driving speed and relative positive acceleration, the different patterns are displayed graphically as a scatterplot which is shown in the empirical analysis.

Table 1: Kinematic characteristics and influencing variables

Parameter	Unit
Stop duration	s
Mean driving speed	km/h
Relative positive acceleration	m/s²
Time spent in acceleration	s
Time spent in deceleration	s
Time spent in cruising	s
Traffic signal system	Dummy (0: Non progressive signal system, 1: Progressive signal system)
Time period	Hourly (rush hours, midday, etc)

Methodology - Interface with the transport simulation tool MATSim

MATSim stands for *Multi-agent transport simulation* which provides a toolbox for large-scale transport projects on a microscopic level. With this transport simulation tool, individual and time-dependent traffic behaviour can be simulated for every agent, e.g. the road user (Balmer et al., 2008). MATSim is an open source simulation tool developed by the Technische Universität Berlin and the ETH Zurich. The traffic flow simulation used in MATSim relates to the

queue simulation[11] (Cetin et al., 2003). A region-wide transport simulation as for the European metropolitan region of Munich is possible. MATSim is considered a micro-simulation because individual demand is modelled by giving each agent a plan or several plans which exhibit different activities (Balmer et al., 2008). The explicit modelling of individual decisions of each agent showing every movement from one link to another makes an identification of the driving pattern per vehicle and, thus, per agent possible. In this paper only the driving behaviour related to *hot* emissions is regarded.[12] The link and agent specific linkage of the transport model with driving patterns and, thus, environmental effects is the reason why MATSim is applied.

As a result of the traffic flow simulation in MATSim event files are created. They show the movement of each vehicle through the network over the day. This feature is the major link to assign the driving cycles. The parameters in table 2 are obtained from the event files and from the attributes of the road network. Using the time entering and leaving a link as well as the distance of the link, the mean speed per vehicle and of all vehicles per link can be calculated. Driving patterns can be assigned using the type of the road, the mean speed, the speed limit, the time period, the traffic signal system as well as the traffic load in relation to the capacity of the link. The latter is needed to further differentiate the traffic situation at the time of driving. The traffic signal system can be used to determine the difference in driving patterns related to progressive and non-progressive signal systems. The attributes that are linked with a vehicle ID provide socioeconomic information of the owner and technical information about the vehicle in use. Such vehicle attributes are especially important for the emission calculation of consecutive studies. The driving pattern describes the level of emissions by giving the number of stops, the acceleration and deceleration behaviour at a certain speed level. However, the emission level depends highly on the vehicle characteristics. Every vehicle characteristic that is considered as relevant can be linked to the vehicle ID and, consequently, to a driving pattern.

Table 2: Parameters as a result of the traffic simulation

Parameter	Details and Units
Time entering a link	s
Time leaving a link	s
Link length	m
Speed limit	km/h
Vehicle ID	Characteristics: fuel type, vehicle age, kW etc.
Traffic signal system	Dummy (0: Non progressive signal system, 1: progressive signal system)
Traffic load	Actual number of vehicles on a link for a time period
Capacity	Maximal number of vehicles on a link for a time period

[11] A queue simulation means that each link is represented as a FIFO (first-in first-out) queue.
[12] Hot emissions are the emissions occurring during driving when the engine is warm. The implementation of a module in MATSim calculating cold start and evaporative emissions is essential, but will be conducted in consecutive studies.

Empirical analysis - Measurement of speed-time profiles, databasis

The data used for the development of typical driving cycles is obtained from on-board measurements installed in passenger cars driving along several different roads in Munich. The city of Munich is characterized by a monocentric structure. Apart from the city, the suburban area of the European metropolitan region of Munich shows a high level of economic activity leading to a high commuting demand that even encloses *sub-centres* like Augsburg (Thierstein et al., 2007). With respect to road traffic, major connections throughout the city such as the *Mittlerer Ring*, *Frankfurter Ring* and *Landsberger Allee* carry major traffic loads. They show a high capacity which is continuously increased by infrastructure projects, traffic management and information. Beyond urban and commuting road traffic, Munich faces long-distance travellers that either take the motorway leading through the suburban area or the Mittlerer Ring which goes right through the city. From field experiments along the Frankfurter Ring it has been observed that there is also a high traffic demand in off-peak periods. Driving patterns in Munich should, therefore, be analyzed carefully as the traffic demand is multifaceted.

In 2005, 2006 and 2009 field experiments were carried out for roads ranging from one lane to four lanes including the Mittlerer Ring as well as urban motorways. Additionally, the measurements differ by speed limit, traffic signal system and the number of traffic signals per km. Over a certain distance, speed and distance per second is measured by a GPS device. Approximately 2500 speed-time profiles ranging from a distance of a few to more than 10 km are measured resulting in more than 20,000 km travelled. They are collected on different weekdays from early in the morning until the evening covering both road directions. Further on-board measurements are planned which will be used for further improvements of the driving patterns.

Empirical analysis - Determination of representative driving cycles

The driving patterns are determined by using the statistic software R and its packages on multivariate statistics. An example of the empirical analysis is given by assessing driving patterns along urban roads with three lanes, a speed limit of 60 km/h and frequently occurring traffic lights. Four different driving patterns shown in figure 1 are identified by clustering tools described above. There is a distinct difference between the first driving pattern which shows a dense traffic flow with frequently occurring stops, and the other driving patterns. The fourth driving pattern with the highest mean driving speed also exhibits some time spent in the idling mode. This is most likely due to several traffic signals occurring along the travel distance. With respect to the driving patterns two and three an explanation is difficult as it is not known if and which stops are caused by high traffic loads or red traffic signals. However, the effect on travel behaviour and, consequently, on emissions is similar. As relative positive acceleration is higher for driving pattern three than for two, it is regarded as relatively unsteadier compared to the second pattern.

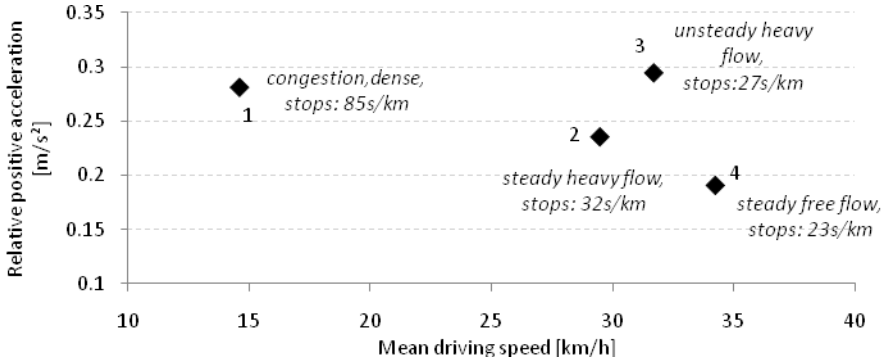

Figure 1: Driving patterns for an urban road with three lanes and a speed limit of 60km/h.

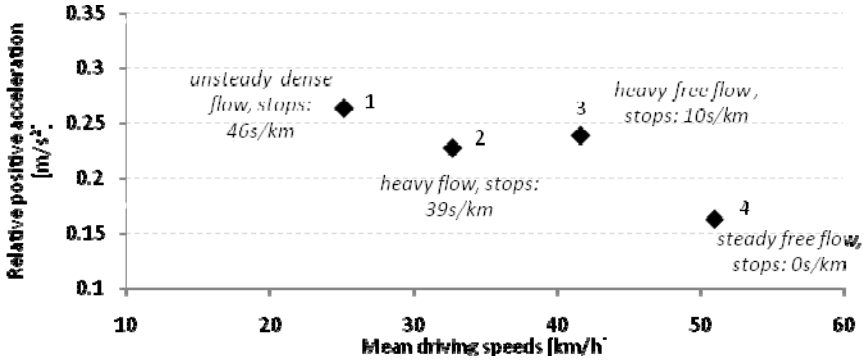

Figure 2: Driving patterns using segments bounded by traffic signals for an urban road with three lanes and a speed limit of 60km/h.

Figure 2 shows driving patterns developed from the analysis on short segments bounded by traffic signals. The linking of several segments to a driving cycle is not conducted yet. The driving patterns are clearly different with respect to the mean driving speed and relative positive acceleration. Especially the fourth driving pattern shows a high mean driving speed and a low relative positive acceleration. In contrast to the first driving pattern shown in figure 1, the comparable driving pattern in figure 2 shows a higher mean driving speed. This may be explained by fewer traffic signals per km for the driving patterns in figure 2.

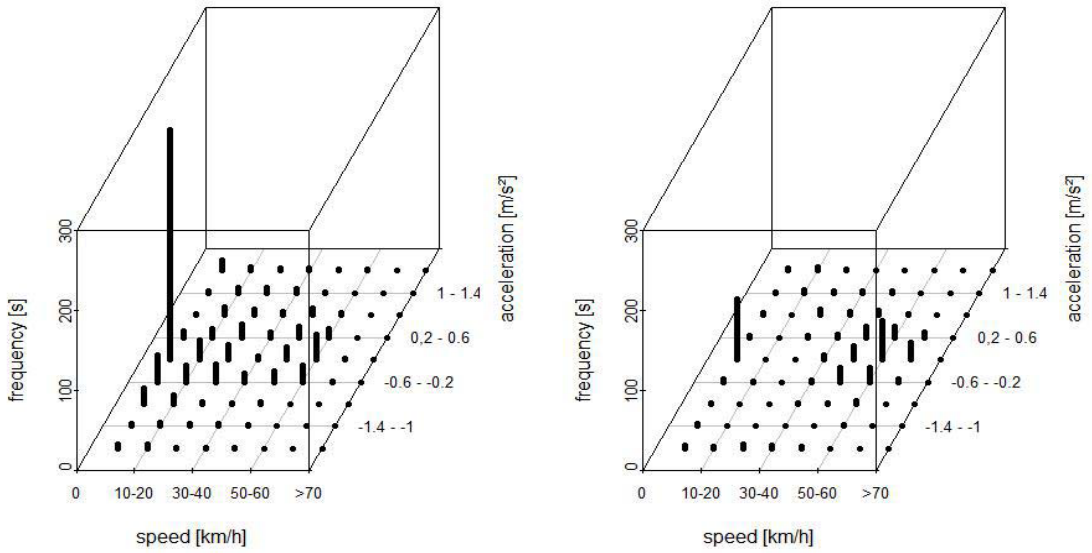

Figure 3: Instantaneous speed and acceleration distribution of driving pattern one (left) and four (right) from figure 1.

The difference in instantaneous speed and acceleration distribution between driving pattern one and four is shown in figure 3. Acceleration and deceleration modes appear more often in the left than in the right driving pattern leading to different emission factors that will be applied in the emission modelling. Figure 4 shows speed-time profiles for driving pattern one and four. The unsteady flow is characterized by an enormous fluctuation between high and low speeds. In contrast, the driving cycle on the right side shows much less fluctuation with only four major deceleration and acceleration phases.

With respect to the time period, a similar correlation between the driving pattern and the time of measurement are found. The driving cycles of the first driving pattern were measured in the peak hours, whereas the free flow driving patterns were predominantly found during midday and in the evening. All other driving patterns cannot be directly assigned to peak or off-peak time periods because they were measured during the whole day.

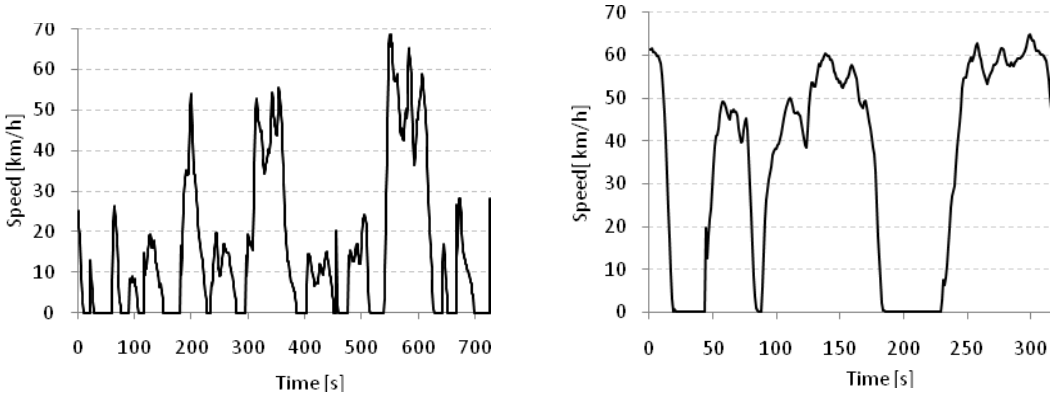

Figure 4: Driving cycle of driving pattern one (left) and four (right).

References

André M., M. Rapone (2009), Analysis and modelling of the pollutant emissions from European cars regarding the driving characteristics and test cycles, *Atmospheric Environment,* 43, 986-995.
André M. (2004), The ARTEMIS European driving cycles for measuring car pollutant emissions, *Science of the Total Environment*, 334-335, 73-84.
Balmer M., M. Rieser, K. Meister, D. Charypar, N. Lefebvre, K. Nagel and K.W. Axhausen (2008), *MATSim-T: Architecture and Simulation Times,* submitted to book edited by Ana Bazzan.

Cetin N., A. Burri and K. Nagel (2003), *A large-scale multi-agent traffic microsimulation based on queue model,* Paper presented at the 3rd Swiss Transport Research Conference.
Esteves-Booth A., T. Muneer, H. Kirby, J. Kubie and J. Hunter (2001), The measurement of vehicular driving cycle within the city of Edinburgh*, Transportation Research Part D*, 6, 209-220.
Everitt B.S., T. Hothorn (2009), *A Handbook of Statistical Analysis using R*, Chapman & Hall/CRC.
Götze W., C. Deutschmann and H. Link (2002), *Statistik*, Oldenbourg Wissenschaftsverlag GmbH.
Hung W.T., H.Y. Tong, C.P. Lee, K. Ha and L.Y. Pao (2007), Development of a practical driving cycle construction methodology: A case study in Hong Kong, *Transportation Research Part D*, 12, 115-128.
Niemeier D., Z. Dai and D. Eisinger (2008), Driving cycles: a new cycle-building method that better represents real-world emissions, *The U.C. Davis-Caltrans Air Quality Project*.
Thierstein A., V. Goebel and S. Lüthi (2007), *Functional polycentricity in the Mega-City Region of Munich*, Paper presented at the AESOP conference.

Session 6: Biofuels 2

Carbonyl compounds in exhaust from alternative fuels used in modern engines and from two stroke mopeds

C. Astorga, M. Clairotte, T. Adam, A. Farfaletti, G. Martini*

[1] EC Joint Research Centre Ispra, Institute for Environment and Sustainability, Transport and Air Quality Unit, 21027 Ispra (VA), Italy

* corresponding author: covadonga.astorga-llorens@jrc.ec.europa.eu

Introduction

Carbonyl compounds are also major constituents in urban atmospheres and they are supposed to play an important role in the tropospherric ozone formation. In city areas, they often initiate photochemical smog and keep up reactions leading to ozone formation by an oxidation process involving OH radicals, ozone, and nitrogen oxides in a cyclic mechanism (Hallquist, M. et al,2009) In particular formaldehyde, acetaldehyde and acetone, constitutes the most abundant group of oxygenated organic compounds ubiquitously present in the troposphere and some of them are known to be carcinogenic (U.S. Dep. of Health and Human Services Report on Carcinogens, U.S. 11th Edition. 2005).

Regardless of the important role of these compounds in the atmospheric processes in Europe and, even if motor vehicle exhaust is one of the main outdoor sources of carbonyls, these compounds are not included in any monitoring protocol at the exhaust stage and their concentration is not measured on a regular basis.

We have address this problem together with other non regulated compounds in vehicle exaust, like PAH and VOCs, in order to give a better assesment to new energy and transport strategies that affect fuel composition or engine technology. All these new approaches will have different impact on the exhaust, and may reduce emissions of some pollutants while increasing or having no effect on others.

The growing worry about the stable and secure energy supplies, as well as the important increase in the fuel prices, have been the main reasons for the promotion of biofuels in transport, but together with the search for new sources of alternative energies, we must be aware that new challenges may arise when refering to the exhaust composition. Before blends of alternative fuels will be available in the market it is necessary to know if the emissions from such fuels, specially the toxic pollutants, will be lower, or at least the same as the fuel before its implementation. We should also consider that the positive or negative effect on PM and gaseous emissions varies significantly among vehicles, fuel origin and load.

In this work we have quantified carbonyl compounds in the emissions from biodiesel/diesel blends in a Euro 4 common rail system car, Ethanol/gasoline blends in a Euro 4 flexi fuel vehicle, GLP fuelled vehicles as well as three mopeds with two-stroke engines.

Experimental Section

Experimental work was carried out in the Vehicle Emissions Laboratory (VELA) of the Institute for Environment and Sustainability (IES) at the EC-JRC Ispra, Italy. Vehicle testing was carried out on a 48” chassis dynamometer (Maha GmbH, Germany) equipped with a conventional constant volume sampling (CVS) system with a critical flow Venturi (Horiba, Germany).

The vehicle fleet varied from various Euro 4 light duty vehicles powered by gasoline, diesel, biodiesel, ethanol and liquefied petroleum gas (LPG) as well as two-stroke scooters. All emission tests were performed following the European legislative procedure for vehicle certification: official driving cycle for the LD vehicles (NEDC) and ECE 47 cycle for two- stroke mopeds, in accordance with the related legislative regulation (EU Directive 98/77/EC). Three replicates were taken for each test. The regulated exhaust constituents THC, NOx, and CO were measured according to the legislative procedures for vehicle emissions (EU Directive 70/220/EEC) and following amendments. For technical reasons, VOC and carbonyls were sampled and investigated over the sum of both phases, whereas all other target compounds were analyzed separately (Fig. 1).

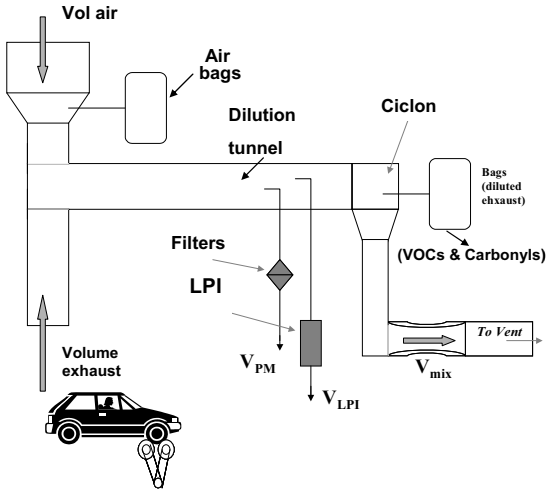

Figure 1: Typical layout for the emission test facility and sampling points.

Sampling of carbonyls from the CVS-diluted exhaust was done according to the standard of the European Monitoring network, EMEP (Rembges D. et al. 1999) The air sample (flow 0.9-1 l/min up to a total of 9-10 liters of exhaust after the dilution tunnel) was drawn through the 2,4-dinitrophenylhydrazine (DNPH) coated C18 cartridges (Waters Sep-Pak DNPH-cartridges). The analytical method has been developed on the basis of the "Compendium of Methods for the Determination of Toxic Organic Compounds in Ambient Air" (Compendium Method TP-11A [EPA/625/R-96/-1-b]). DNPH-cartridges were eluted in the laboratory with 2.5 ml of acetonitrile, diluted with 2.5 ml of H_2O and stored at 5°C until analysis. The samples were analysed by HPLC-UV (High Performance Liquid Chromatography diode array detection 360 nm) with a thermostated (20°C). The quantification of the carbonyls compound was done using an HPLC-UV. Separation was done using a Discovery Supelco C18 15 cm*2,1mm 5u reversed phase column. Eluents were H_2O (A-eluent) and acetonitrile (B-eluent). The gradient was programmed from 50% B to 90% B in 42 min. Detection limit for this method was in the range of 5-20 ng for formaldehyde hydrazone (S/N=3).

Results and Discussion

Values of formaldehyde, acetaldehyde, acrolein and acetone as well as propionaldehyde have been quantified in the exhaust samples. It has not been possible to separate chromatographically the two peaks corresponding to acrolein and acetone. By means of the chromatographic method used these two compounds are coming together as already reported by other authors (Martins, E.M and Arbilla 2003; Correa and Arbilla, 2008). Eventually we also found and quantified a larger group of compounds in the exhaust samples coming from two-stroke vehicles, namely acrolein, acetone, propionaldehyde, crotonaldehyde, methacrolein, 2-butanone, butyraldehyde, benzaldehyde, valeraldehyde, p-tolualdehyde and hexanaldehyde.

Total carbonyl content, represented graphically was calculated by adding-up all the individual carbonyl emission factors.

Biodiesel fuel. Beyond the positive effects on greenhouse gas emissions and secure of energy stores, biodiesel significantly influences pollutant emissions as well. One of the most important characteristics of biodiesel is the presence of oxygen in its molecules; biodiesel contains about 10.8% w/w of oxygen and that affects the combustion process to a large extent.

In the present study we have accomplished an experimental program on emissions from a LD-common rail diesel engine passenger car complying with EURO 4 emission standard and 6 different biodiesel-diesels blends. A broad analysis of the chemical composition of particle and gaseous emissions was carried out. All results were consistent with data already available for older technologies showing that effects on emissions clearly depend on the biodiesel content.

Mean values and standard deviations of formaldehyde, acetaldehyde, acetone/acrolein and propionaldehayde are shown in Figure 2, both for the reference fuel (commercial fossil diesel) and rape seed methyl ester, RME (B10, B20 and neat RME or B100). Other carbonyl derivatives (C4-C6) were also identified but not quantified (under detection limit). For technical reasons, the emission factors correspond to the overall NEDC. Both phases, urban and extra urban, were collected in the same cartridge.

Mean values of formaldehyde emission factors ranged from a minimum value of 4.2 mg/km (RME B10) to 5.54 mg/km (RME B100). The trend was the same for acetalaldehyde, 1.30mg/km (B10) and 1.81 mg/km (B100) and Propionaldehyde 0.6 mg/km (RME B10) and 0.1 mg/km (RME B100). Emission factors of RME B10 for HCHO and CH_3CHO have been found to be lower than emission factors in the gasoline reference fuel (4.87 mg/km and 1.60 mg/km respectively). Total values for emission factors of carbonyls corresponding to the overall NEDC, reached yields from 5.67mg/km (RME B10) to 7.55 mg/km (RME B100).

The lowest mean emission factor of carbonyls was observed with RME B20. The effect is opposite with neat biodiesel. These results suggest that due to the very different properties of biodiesel (i.e. density) compared to standard diesel means, that the engine is not operating within its optimum conditions and certain pollutants may increase significantly.

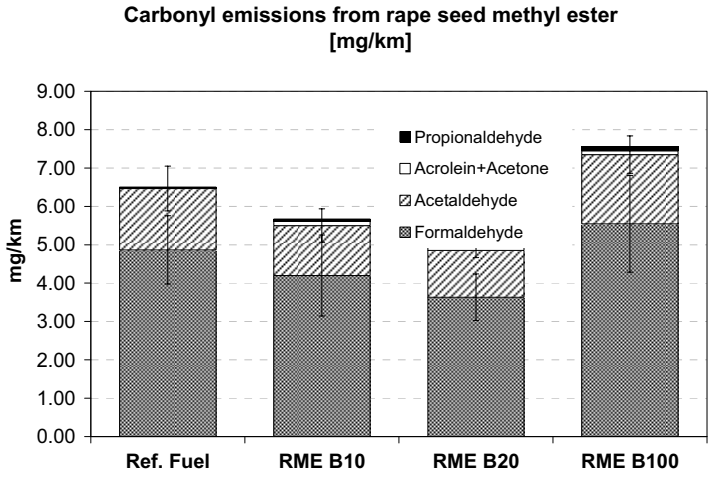

Figure 2. *Mean of emission factors for carbonyl compounds (mean of three tests with standard deviation) quantified in the exhaust from a light duty vehicle powered with reference fuel (commercial Diesel) and RME (B10, B20, B100).*

Due to the particular concern for a possible modification of the EN 590 diesel standard to allow the inclusion of 10% biodiesel, we illustrate the results regarding the addition of 10% of different biodiesel fuels to the reference fuel. The main aspect of this research is the impact of the origin of the biofuel on the emissions. Figure 3 shows the mean values for all biodiesel blends tested containing 10% biofuel (B10).

Differences of emission factors corresponding to B10 blends over the NEDC were found to be small (variations between 7-14% depending of the origin of the biodiesel blended). Total emission factors for B10 blends were lower than those found for the gasoline reference fuel. HCHO reached its lower yield at 4.20 mg/km (RME B10) and it maximum at 4.59 mg/km (Palm B10). CH_3CHO varied between 1.3 mg/km (RME B10) and 1.50 mg/km (Palm B10) and Propionaldehyde showed values between 0.02 mg/km (Mix3 B10) and 0.1 mg/km (Mix 1 B10). Total mean values for emission factors of carbonyls reached yields from 5.44mg/km (Mix3 B10) to 6.21 mg/km (Palm B10), always below the reference value 6.5mg/km (commercial diesel). We can conclude that the origin of biodiesel or, in other words, the vegetable oil used to produce the methyl ester, seems to have a very limited effect on emissions if blended at a low percentage.

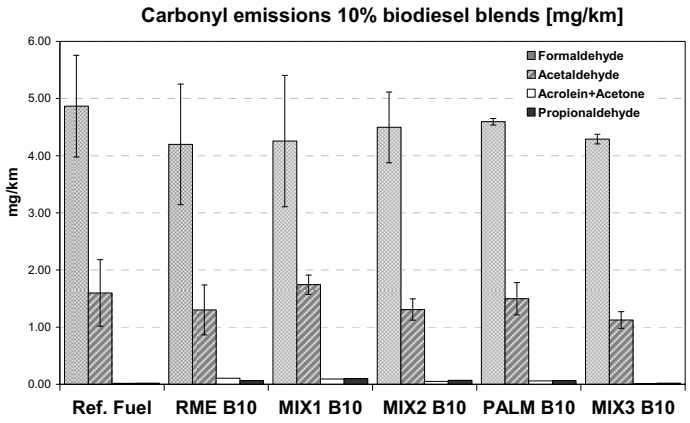

Figure 3. *Mean of emission factors with standard deviation for carbonyls quantified in the exhaust from a light duty vehicle when 10 % of biodiesel is added to a reference fuel. (RME: rapeseed oil methyl ester; MIX 1 blend containing 70% RME, 20% soy oil methyl ester and 10% palmolein methyl ester; MIX 2: blend containing 70% RME, 15% hoso and 15% sunflower oil methyl ester; PALM: palmolein methyl ester ; MIX 3: blend containing 50% soy oil methyl ester and 50% sunflower oil methyl ester.*

EtOH and Flexi fuel vehicle: Clean air criteria encouraged, more than 30 years ago, the promotion of oxygenated fuels in areas where ambient carbon monoxide (CO) exceeded the mandatory standards. New additives (MTBE and TBE) were used to increase the oxygen content of the gasoline. Later on, EtOH largely produced from vegetable crops, was thought to be blended with standard gasoline.

The vehicle selected for this program was a Euro 4 emission standard flexible fuel vehicle fuelled with gasoline or gasoline - EthOH blends: commercial gasoline complying with the EN228 specifications and blends containing respectively 10% (E10) and 85% (E85) ethanol in volume. The emission tests were carried out following the European legislative procedure for vehicle certification (NEDC cycle) as mentioned in the experimental part. Eventually, for this particular program and due to the stricter legislation on evaporative emissions in the United States, a U.S. driving cycle (US 06) was driven as well.

Mean values and standard deviations of formaldehyde, acetaldehyde, acetone + acrolein, and propionaldehayde are shown in fig 4 both for the gasoline reference fuel and EtOH blends E10

and E85. Other carbonyl derivatives, (C4-C6) could be also separated for some tests but not quantified (under the detection limit). We observed very low yields of HCHO for E10 (0.23 mg/km) and even for E85 (0.6 mg/km). Indeed, the main effect of EtOH is the clear change of emissions factors profile by increasing the acetaldehyde values: 0.63 mg/km (E10) and 4.0 mg/km (E85). These values are higher than the rate found for the gasoline reference fuel (0.12 mg/km). The acetaldehyde increase in the emissions with the higher content of ethanol in the fuel is statistically significant. The HCHO / CH_3CHO (usually > 1) is upturned when increasing the amount of EtOH in the blend. Formaldehyde was slightly more abundant only in the exhaust from the reference fuel (HCHO / CH_3CHO=1.43) while in both blends E10 and E85 the ratio HCHO / CH_3CHO is <1 (0.37 and 0.14 respectively).

The high amount of CH_3CHO found over the NEDC was even higher for the American cycle (US06). Very possibly, the more realistic nature of this cycle leads to a much higher content of CH_3CHO in the exhaust. The US6 ratio HCHO / CH_3CHO (0.03) is almost 6 times lower that the value we found for the NEDC cycle. The absolute value of CH_3CHO produced during the US06 cycle (11.0mg/km) is more than twice the amount emitted when the vehicle is running under the European cycle. The measurements were only taken at the hot phase of the test cycle US 06 and we may anticipate from these results that higher emissions of acetaldehyde ma be correlated with acceleration events.

This level of emissions may have consequences in air quality. Studies performed in Brazilian cities (Martins, E.M and Arbilla, G, 2003) have found that formaldehyde/acetaldehyde ratios were always below one. The same results are found in tunnels where only light-duty vehicles fueled mainly with gasohol (a mixture containing 78-80% (v/v) gasoline and 20-25% ethanol) are circulating. This is an even situation which contrasts with European cities.

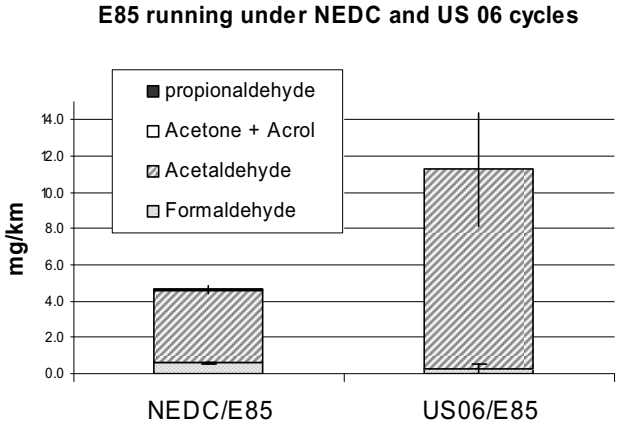

***Figure 4**. Mean of emission factors with standard deviation for carbonyls quantified in the exhaust from a light duty vehicle powered with E85.*

LPG fueled vehicles. In some European countries liquefied petroleum gas (LPG) is used as fuel for light duty vehicles as an alternative to gasoline but often the coverage of service stations providing LPG is insufficient. Therefore, these types of vehicles are usually available as dual fuel vehicles i.e. running on LPG and gasoline, whereby the driver can choose between the fuels.

Carbonyls content of the exhaust of two cars from different manufacturers, running on either gasoline or LPG (dual fuel cars) have been characterized. Absolute values of emission factors for reference gasoline were, as expected, very low. Results showed that differences of the carbonyls composition between both fuels were very small. This was mainly due to the fact that

all dual fuel cars tested started on gasoline and did not switch to LPG before a certain operating temperature was reached.

Vehicle	**car 1**				**car 2**			
Fuel	**gasoline**		**LPG**		**gasoline**		**LPG**	
EMISSION FACTOR	Mean	Stdev	Mean	Stdev	Mean	Stdev	Mean	Stdev
Formaldehyde	0.331	0.016	0.385	0.037	0.313	0.026	0.244	0.013
Acetaldehyde	0.251	0.011	0.253	0.025	0.163	0.003	0.156	0.006
Acetone+Acrolein	0.178	0.010	0.162	0.013	0.127	0.000	0.137	0.007
Propionaldehyde	0.052	0.002	0.061	0.007	0.027	0.006	0.023	0.011
Total	**0.812**	0.015	**0.861**	0.076	**0.630**	0.028	**0.559**	0.001

Table 1. Mean of emission factors with standard deviation for carbonyls quantified in the exhaust from light duty vehicles powered with gasoline or LPG.

MOPEDS. With the entry into force of the latest LD and HD emission standards (Euro 5/6 and Euro VI respectively) the contribution of two wheelers to overall road transport emissions and therefore to air pollution must be taken into account and the share of this vehicle type is expected to be increasing in the next few years. In view of the preparation of a new amendment to the European directive 97/24/EC we have carried out a comprehensive study in order to evaluate unregulated emissions of mopeds complying with the present legislation EURO-2 and analysis of carbonyls have been included in this assesment.

The test fleet consisted of three new mopeds from different manufacturers with two-stroke engines, displacements of 50 cm^3, and oxidation catalysts. All three complied with the latest European emission legislative standard for mopeds, EURO-2, but had three different engine technologies. In particular, one moped (moped-CA) was equipped with an ordinary carburettor, second moped (moped-DI) had direct injection technology, and the third moped (moped-CAec) was equipped with an electronic carburetion system (ECS). The latter one consists of an engine control unit (ECU) and an electro-actuated carburettor, whereby the air/fuel (A/F) ratio and the oil dosing are electronically-controlled according to several engine operating conditions. The moped provided with ECS (Electronic Carburetion System) has been tested twice, once after the optimization of of the settings of the electronic carburattor. All tests have been conducted following the ECE 47 driving cycle.

Together with formaldehyde and acetaldehyde, another 11 carbonyls have been identifed and quantified for this type of vehicles (acrolein, acetone, propionaldehyde, crotonaldehyde, methacrolein, 2-butanone, butyraldehyde, benzaldehyde, valeraldehyde*, p*-tolualdehyde and hexanaldehyde). It is worth mentioning that all these compounds have been found to be always under the detection limit in the previous analysis for LD vehicles. The sum of these eleven compounds ranges from the 12% of the total amount of carbonyls in the moped with ECS (CA ec2) optimized up to 26% of the total for the moped with carburettor (CA). It is acknowledged that particles from 2-stroke mopeds are mainly unburned fuel and oil droplet and this is the most possible reason for the high and varied presence of carbonyls in the exhaust of this type of vehicle if we compare it with LD vehicles discussed before.

Results from four different types of mopeds indicate that a number of carbonyls are present in the engine exhaust from 2-stroke motorcycles. The highest amount of this class of compounds was found for the moped provided with a DI system (38 mg/km emitted for the ECE 47 cycle)

Results show that the three mopeds without the ECS behave generally the same and the differences on the overall carbonyls emissions are variable (up to 26%). The DI moped is the one with the highest emissions, followed by carburattor and ECS. In the following table the emissions measured before and after the re-programming of moped ECS are shown. This new system with the new configuration is also capable of electronic lubrication control.

There is a clear effect of the ECS optimization over its emissions (CA ec2). The effect of the new settings for this moped is evident. The results revealed a significant (P=0.03) reduction in carbonyls in the range of 49% with the application of new settings of the moped with the ECS.

Formaldehyde and acetaldehyde together build up between 67% and 83% of all the carbonyls emissions, where formaldehyde is the carbonyl emitted in a higher quantity, up to 20 mg/Km. Formaldehyde amounted to 50 % to 65 % of all carbonyls throughout all tests.

ECE47 cycle	moped-CA		Moped DI		Moped CA ec1		Moped CA ec2	
Carbonyls [mg/km];	CP+HP		CP+HP		CP+HP		CP+HP	
Emission Factor	Mean	Stdev	Mean	Stdev	Mean	Stdev	Mean	Stdev
Formaldehyde	19.56	2.14	20.43	0.82	18.42	2.62	11.03	0.49
Acetaldehyde	7.63	0.61	8.92	0.43	5.40	0.80	3.11	0.16
Acetone+Acrolein	0.08	0.01	0.13	0.07	0.11	0.11	0.11	0.07
Propionaldehyde	1.47	0.11	1.77	0.11	0.82	0.15	0.37	0.20
Crotonaldehyde	0.83	0.05	0.97	0.06	0.74	0.06	1.00	0.03
Methacrolein	0.67	0.08	0.91	0.06	0.53	0.09	0.33	0.03
2-Butanone+Butyraldehyde	4.58	0.18	3.13	0.38	3.87	0.17	0.07	0.06
Benzaldehyde	0.57	0.17	0.81	0.09	0.47	0.06	0.01	0.02
Valeraldehyde	0.32	0.42	0.59	0.06	0.65	0.04	0.47	0.14
p-Tolualdehyde	0.69	0.05	0.50	0.20	0.50	0.10	0.30	0.03
Hexaldehyde	0.35	0.01	0.20	0.13	0.36	0.02	0.22	0.10
Total carbonyls	**36.75**	3.41	**38.35**	1.28	**31.85**	2.63	**17.00**	0.24

Table. 2 Mean values and standard deviation (mean of thee tests) for carbonyl compounds quantified in tow stroke motorcycles (Adam, T. et al, 2010)

Once the carbonyls were quantified the concept of maximum increment reactivity (MIR) of ozone formation was applied to estimate ozone formation potential (OFP) of the emissions of the mopeds. In general, the MIR method is based on a scenario in which optimum conditions of precursor/NOx ratios yield in a maximum ozone formation. For all sorts of individual ozone

precursors, MIR factors have been derived, whose product with the compound's emission factor gives the potential amount of ozone formed (Carter, W. P. L., 1994). The OFP of a mixture is calculated by summing up the contributions of all individual emission constituents. It has to be stressed that difficulties in chromatographic separation between acetone and acrolein as well as between 2-butanone and butanal were experienced, which has also been described by others (Martins, E.M and Arbilla, 2003). As a consequence, their yields are reported as the sum of both and no OFP was calculated because their MIR factors differ. OFP of the residual carbonyls and CO were in the same range for the three mopeds. In addition OFP of VOC was determined according to directive 2002/3/EC for ambient air and also the OFP of CO was included. Even if the values for total emission of carbonyls in the mopeds exhaust are considerably high, still the share of carbonyls and CO to the total OFP ranged between 7% (moped CA) and 20% (moped DI). (Adam, T. et al, 2010)

On line measurements, FT IR. Regardless this study may provide valuable data to adjust future emission standards, they are off-line average data calculated over the whole cycle and they cannot provide enough information about the origin and possible causes of formation of carbonyls during the combustion process. Taking advantage of new online real time measurement techniques, we may be able to asses more accurately sources and origin of this class of compounds. Formaldehyde and Acetaldehyde have been monitored by a High Resolution Fourier Transforms Infrared spectrometer (HR-FTIR - MKS Multigas analyzer 2030, Wilmington, MA). This system is a semi-quantitative technique based on a PLS model which allows the prediction of the concentration of 20 exhaust compounds from gasoline engines. Results will be provided for different cycles and driving conditions.

Conclusions

Even if the solution to the energy security and supply is a long term issue most probably based on completely new means of propulsion like hydrogen, other alternatives must be undertaken including biofuels like biodiesel, EtOH-gasoline blends, liquefied petroleum gas (LPG), compressed natural gas (CNG). Before any alternative fuel will be available in the market or technologies improvement is set up, it is necessary to know if the emissions from such fuels, specially the toxic pollutants, will be lower, or at least same as the diesel fuel before its implementation

Formaldehyde was the most abundant carbonyl derivative in the exhaust from biodiesel blends, GPL fuelled vehicles and mopeds while there is a clear effect of the increasing fuel content of ethanol on the emissions of acetaldehyde, which is statistically significant and considerably high when E85 is used. Consequences of this effect have been found in the atmospheres from Brazil where the formaldehyde/acetaldehyde ratios vary if compared with other cities in Europe. By having a better knowledge of the potential emitters for ozone precursors we are trying to prevent the formation of smog episodes and to extend the availability of data to be used in the chemical models in order to strength their capability to thereby anticipate the smog episodes. One part of this work was related to the assesesment for the use of alternative fuels and for the revision of the motorcycles legislation (2010) to the commision and policy makers.

References

Adam, T., Farfaletti, A. Montero, L. Martini, G., Manfredi, U. Larsen, B. De Santi, G., Krasenbrink, A. and Astorga C.. (2009) Chemical Characterization of Emissions from Modern Two-Stroke Mopeds Complying with Legislative Regulation in Europe (EURO-2). Environmental Science & Technology 2010, 44(1): 505-512.

Carter, W. P. L. Development of ozone reactivity scales for volatile organic compounds. *J. Air Waste Manage. Assoc.* 1994, *44*, 881-899.

European Commission. Directive 98/77/EC of 2 October 1998 adapting to technical progress Council Directive 70/220/EEC on the approximation of the laws of the Member States relating to measures to be taken against air pollution by emissions from motor vehicles Official Journal of the European Communities L 286 1998, 34 - 52.

European Commission. Directive 70/220/EEC of 20 March 1970 on the approximation of the laws of the Member States relating to measures to be taken against air pollution by gases from positive-ignition engines of motor vehicles Official Journal of the European Communities OJ L76 1970.

Hallquist, M. *et al,* The formation, properties and impact of secondary organic aerosol: current ad emerging issues, Atmos. Chem. and Phys., 2009, 5155-5236.

Martins, E.M and Arbilla, G. " Computer modeling study of ethanol and aldehyde reactivities in Rio de Janeiro urban air" *Atmospheric environment*, 2003, 37, 1715-1722. Machado Correa, S. and Arbilla G. "Carbonyl emissions in diesel and biodiesel exhaust" *Atmospheric environment,* 2008, 42, 769-775.

Rembges, D., Fantecchi G., Dutaur L., Brum C., 1999, "Airmon Annual Report, EC, EUR 19665 EN

U.S. Department of Health and Human Services. Report on Carcinogens, 11th Edition. 2005. Available at http://ntp.niehs.nih.gov/ntp/roc/toc11.html

U.S. Environmental Protection Agency. Compendium of methods for the determination of toxic organic compounds in ambient air. EPA/625/R-96/010b. Washington, DC, 1999. U.S. Environmental Protection Agency. Determination of formaldehyde in ambient air using adsorbent cartridge followed by high performance liquid chromatogrophy (HPLC). EPA TO-11A. Washington, DC, 1999.

Determination of VOC components in the exhaust of light vehicles fuelled with different biofuels

F. Cazier [1,4], A. Delbende [1,4], H. Nouali [1,4,5], B. Hanoune [2,4], D. Pillot [3], R.Vidon [3], P. Perret [3] and P. Tassel [3]*

[1] Centre Commun de Mesures, Université du Littoral Côte d'Opale, MREI, F- 59140 Dunkerque, France, cazier@univ-littoral.fr

[2] Physicochimie des Processus de Combustion et de l'Atmosphère, UMR CNRS 8522 – Université des Sciences et Technologies de Lille, F-59655 Villeneuve d'Ascq, France

[3] Laboratoire Transport & Environnement, INRETS, F- 69675 Bron, France

[4] Université Lille Nord de France, F-59000 Lille, France

[5] Laboratoire Matériaux à Porosité Contrôlée, LRC CNRS 7228 – Institut de Science des Matériaux – Ecole nationale Supérieure de Chimie Université de Haute Alsace, F-68093 Mulhouse, France (New affiliation)

Abstract

The speciated exhaust emissions of VOCs in the C_2-C_{19} range were measured on 4 Euro-4 certified vehicles (3 diesel and 1 gasoline) equipped with a catalytic converter, according to 5 real-world driving cycles. To determine the effects of blended fuels on the emission factors, several test fuels were used: gasoline, E10 (10% of ethanol, by volume), diesel, B5, B30 (5% and 30% of biodiesel or FAME) and HVO (pure Hydrotreated or Hydrogenated Vegetable Oil). These tests were performed on a chassis dynamometer with constant volume sampling (CVS). The sampling of compounds was made using dedicated Carbotrap and Tenax cartridges, analysed by GC-FID and GC-MS respectively. Carbonyl compounds were sampled on DNPH-coated cartridges and analysed by UV-HPLC. The emission factors of individual pollutants were determined, especially of 1,3-butadiene, benzene, and formaldehyde, which are recognized as genotoxic carcinogens. Detailed speciation of the emissions shows changes with the composition of the biofuel in the levels of hydrocarbons, aromatic compounds and carbonyls present in diesel and gasoline engine exhaust gases. This evolution of the emission factors for the different compound families is compared to the results obtained in previous studies, where the influence of driving cycles, technology and type of fuels were evaluated (Caplain et al., 2006). In the framework of this study, the first results show that an addition of ethanol in the unleaded gasoline leads to a decrease of the emissions of aromatics especially of benzene and an increase of the 1,3-butadiene emission. An increase of aromatics emissions but no specific trend for carbonyl compounds emission factors was observed when partially substituting biodiesel to diesel. Pure HVO leads to higher carbonyl emissions than pure or substituted diesel fuel.

Introduction

Volatile organic compounds (VOCs) play a major role in urban atmospheric chemistry. They are important precursors of photochemically formed secondary pollutants, such as ozone, which poses a serious air pollution problem. They are also compounds that adversely affect the human health due to their high toxicity (e.g. benzene, 1,3-butadiene). Vehicular traffic highly contributes to these VOCs emissions and, to reduce these emissions, biofuels are introduced in EU, partially substituting petroleum diesel by fatty acid methyl esters (FAMEs), commonly known as biodiesel, and gasoline by ethanol. Biodiesel blends up to 30% by volume can be used for diesel engine without modification because of their properties similar to those of diesel. It is recognized that there is a substantial reduction in regulated emissions such as HC, CO, PM with the exception of NOx emissions when diesel vehicles are fuelled with biodiesel. With the increasing percentage of biofuels in the petroleum based fuels supplied at gas stations and the development of the synthetic biofuels, it is relevant to assess the pollutants in car exhaust with these alternative fuels, under various traffic conditions. In this work, we report the emission factors (EF) of the speciated gas

phase hydrocarbons and carbonyls collected from recent technology (Euro 4) light vehicles fuelled with conventional fuel or biofuel, to determine the effect of biofuel on the unregulated exhaust emissions, with a special interest in toxic and carcinogenic compounds. The blends selected in this study were a blend of 10% ethanol in gasoline (E10) and blend of 5 % and 30 % of biodiesel (FAMEs) in the diesel fuel (called B5 and B30). A 100% pure HVO was also tested. The emission factors of unregulated pollutants emission were measured using real-world test driving cycles performed on a chassis dynamometer with constant volume sampling (CVS) at INRETS facility. The tailpipe emissions were sampled for light hydrocarbons (C_2-C_6), semi-volatile hydrocarbons (C_7-C_{19}) and carbonyl compounds. The results obtained in this work are compared to the data obtained in the previous Artemis Project study (Caplain et al., 2006), which investigated the emissions of cars complying to less restrictive standards (Euro 3 and before).

1. Materials and methods

1.1 Vehicles, fuels and driving cycles

The unregulated pollutants (VOCs) were sampled and analysed for gasoline (GDI) and diesel (D1, DPF, LDD) vehicles, all Euro-4 certified, using real-world test driving cycles. The gasoline car is equipped with a direct injection and turbocharged engine. This type of spark ignition engine is an emergent and promising technology to reach better performances and decrease pollutant emissions. For diesel engines, the first one (D1) has direct and common rail injection. The second one (DPF) is equipped with a fuel-borne catalyst (FBC) type particulate filter on the exhaust. The third vehicle (LDD) is a 3.5 t gross weight light-duty diesel van. All three Diesel vehicles have turbocharged engines.
The GDI car was fuelled with the reference gasoline and with E10. The three diesel vehicles were run successively on the 4 following fuels: reference diesel fuel, B5, B30 and HVO. When shifting fuels, the vehicle was run dry and the fuel pipes “rinsed” with the new fuel. The vehicle was then driven along dozens of kilometres till the tank was empty again. The gasoline and diesel reference fuels are used as bases for comparisons. They are both neat petroleum based fuels, and are used currently in Europe for vehicle certification. The driving cycles were the Artemis cycles (urban, rural and motorway) analysed separately and an INRETS specific short urban cycle (IRSUC) (André et al., 2006) whose aim is to assess the effect of "cold start" and “hot start” in urban traffic.

1.2 Sampling and analysis

The vehicle exhaust gas is diluted with filtered ambient air using a constant volume sampler (CVS). This method of sampling reflects the natural dilution and cooling of the exhaust gas as it leaves the tailpipe and eliminates the problem of water condensation during the sampling. VOCs are sampled in the dilution tunnel using sorbent tubes: Carbotrap B and C, Carbosieve III for “light” hydrocarbons (C_2-C_6), Tenax for semi-volatile hydrocarbons (C_7-C_{19}), and DNPH-coated silica cartridges for carbonyl compounds. Before each set of sampling of exhaust gas the background contribution of the dilution air was measured. The procedure for the sampling and the analytical methods used for the analysis of the light and semi-volatile hydrocarbons were already applied for the Primequal – Predit Research Programs (Caplain et al., 2006) and improved in this work the Carbotrap and Tenax samples were analysed by a thermal desorption preconcentration method, followed by quantification by high resolution gas chromatography with a flame ionisation detector (GC/FID) for compounds from C_2 to C_6 and with a mass spectrometer detector (GC/MS) for the compounds from C_7 to C_{19}. DNPH cartridges were analysed by the standard UV-HPLC method.

2. Results and Discussion

2.1 Compound families characterised in the exhaust gas

The different compound families characterised by GC are alkanes (C_2 to C_{19}), alkenes (C_2 to C_6) and aromatics compounds (BTEX, propylbenzene and butylbenzene (linear or branched – chain alkyl). For the GDI vehicle fueled with E10, depending on the driving cycle, the aromatics mass proportion in the total hydrocarbon species (except carbonyls) varies from 31 to 66%, the alkanes

proportion from 33 to 59%, and the alkenes proportion from 1 to 11%. The same car fuelled with the reference gasoline emits from 19 to 78% aromatics species, 2 to 72% alkanes and 2 to 10% alkenes. The fraction of alkanes and olefins decreases from Artemis- urban to Artemis-motorway while the proportion of aromatics increases when the GDI vehicle is fuelled with the reference gasoline. The trend is reversed with E10.

For the emission factors of the different compound families emitted by diesel engines, no trends were observed with respect to the four fuels under test. As for gasoline engine, the major VOC groups emitted by the diesel vehicles fuelled with different biodiesel blends are alkanes and aromatic compounds. For example with the LDD vehicle, the emission of aromatics decreases from B5 to HVO (e.g. cold cycle 65% - 19% - 16%) and the emission of alkanes increases from B5 to HVO (e.g. cold cycle 18 - 82%).

The carbonyl emissions are dominated by formaldehyde, acetaldehyde, butyraldehyde and acroleine, as previously observed (Corrêa and Arbilla, 2008). Propionaldehyde, crotonaldehyde and methacroleine were also present in the exhaust gases. The other carbonyl compounds (benzaldehyde, valeraldehyde, tolualdehyde, hexaldehyde) are negligible. The emission factors of all the aldehydes are strongly correlated.

2.2 Influence of cold and hot starts on the emissions

The influence of cold or hot starts on the VOCs composition was determined by the difference of the emissions obtained during the IRSUC cold and IRSUC hot cycles. The measured emission factors of the VOCs grouped in different substance classes are given in Table 1. The total VOCs emission factor is larger for the hot IRSUC whatever the technology of diesel vehicle and the type of blended diesel fuel, but for carbonyls the situation is reversed with an overproduction in the cold cycle. For the diesel vehicle D1 fuelled with blended fuels B5 and B30, the amount of total emitted VOCs is twice more important in a hot start than a cold one while for the DPF diesel car fuelled with blended fuel B5, the amount of emitted VOCs is 11 times more important. A six-fold increase of VOCs emission is also observed with the LDD diesel vehicle when it is fuelled with blended biodiesel B5. For these two latter vehicles and the two other blended fuels, the variation of the emission factor is not marked. We can also notice that for the two IRSUC cycles the emission factors of the diesel vehicles fuelled with biodiesel blends are higher than those obtained with regular diesel fuel, except in the case of B5 tested in cold start condition, where the use of biofuel decreases the emissions. The emission factor obtained with the IRSUC cold driving cycle also increases from the diesel vehicle D1 to LDD with B30 and HVO fuel, showing an influence of the vehicle technology (engine, particulate filter) on the emissions. In the case of LDD the emission of aromatics compounds decreases from cold to hot driving cycle (e.g. B5: 65 % - 15%) and the emission of alkanes increases from cold to hot driving cycle (e.g. B5: 18% - 79%). For carbonyl compounds, the emission factor decreases when increasing the content of biofuel in the blends, though the use of pure HVO leads to higher emissions.

The gasoline engine VOCs emissions (Table 2) are not influenced by fuel blend (E10) in the case of cold and hot IRSUC cycles (EF ≈ 110 mg.km^{-1}). Nevertheless, an addition of ethanol increases the emission of alkanes (3 to 74 mg.km^{-1}) and reduces the emission of aromatics (86 to 39 mg.km^{-1}), especially for the IRSUC cold cycle, and of carbonyl compounds. For the IRSUC hot cycle, the difference between E10 and gasoline is reversed (alkanes decrease from 66 to 35 mg.km^{-1}, while aromatics increase from 50 to 69 mg.km^{-1}. A higher emission of aromatics is observed with the reference gasoline fuel in cold start conditions, and in hot start conditions with E10. Whatever the fuel used, alkenes emissions are 10 to 20 times larger for IRSUC cold than for IRSUC hot.

2.3 Influence of driving cycle on the emissions

The use of B5 and B30 blends leads to a reduction of total VOCs emission factor for Artemis-urban driving cycle (DPF B5 21.48 mg.km^{-1}, B30 5.85 mg.km^{-1}) while the use of HVO increases the emissions (D1 76.27 mg.km^{-1}, DPF 53.7 mg.km^{-1}) compared to reference diesel (D1 16.1 mg.km^{-1}, DPF 36.72 mg.km^{-1}) (Table 3). For all the vehicles under test, the highest emissions of every

pollutant analysed in this study are observed during the Artemis urban driving cycle. The pollutants with the highest emission factors are ethane, propane, toluene, ethylbenzene, C_3 benzene and saturated alkanes C_{10} to C_{14}. The reduction observed with B5 and B30 may be due to the intrinsic oxygen contained in the methyl ester (Sureshkumaret al., 2008).

Table 1*: IRSUC cold and IRSUC hot Diesel vehicles emission factors (mg.km-1)*

	IRSUC cold				IRSUC hot			
	Ref.	B5	B30	HVO	Ref.	B5	B30	HVO
Vehicle D1								
Alkenes	1.77	4.55	2.07	0.54	13.19	10.19	0.65	2.25
Alkanes	1.61	5.54	5.40	17.95	8.86	9.07	18.61	33.79
Aromatics	3.81	4.82	8.81	22.29	5.87	8.85	20.24	13.58
Carbonyls	4.87	3.29	3.17	1.29	3.67	1.40	1.08	3.29
1,3-butadiene*	26.8	378.5	126.6	N.D.	155.7	765.9	362.9	1098.3
Benzene*	13.5	130.6	54.1	11.9	14.4	16.0	34.9	43.9
Formaldehyde*	836.1	698.9	482.2	296.4	710.9	335.1	283.3	591.0
Vehicle DPF								
Alkenes	2.21	3.02	0.73	1.68	0.73	2.38	1.75	0.47
Alkanes	26.36	1.59	26.55	25.19	8.13	61.78	21.21	14.68
Aromatics	35.73	2.88	10.35	23.71	8.98	22.44	22.95	17.33
Carbonyls	1.97	No data	1.40	3.98	8.74	1.41	2.17	7.72
1,3-butadiene*	9.6	16.6	103.4	N.D.	5.5	N.D.	N.D.	17.3
Benzene*	15.8	41.1	12.3	7.6	18.2	7.2	11.9	9.7
Formaldehyde*	613.3	No data	347.4	723.6	298.3	337.3	579.3	1015.0
Vehicle LDD								
Alkenes	1.27	2.10	1.92	0.76	0.73	3.89	0.74	1.20
Alkanes	19.95	2.36	37.44	56.09	19.47	60.82	29.86	57.29
Aromatics	12.69	8.55	9.27	11.02	15.63	11.83	6.94	5.11
Carbonyls	7.81	7.10	3.29	3.74	1.52	3.91	1.24	4.40
1,3-butadiene *	5.8	N.D.	N.D.	0.4	N.D.	N.D.	N.D.	2.4
Benzene*	68.8	29.8	71.0	42.1	26.9	60.6	38.4	37.8
Formaldehyde*	898.4	934.5	428.2	338.9	283.0	1050.8	333.9	366.7

*except benzene, formaldehyde and 1,3- butadiene in µg.km^{-1}.

The results obtained with the reference diesel (16, 37, 41 mg.km^{-1} respectively for D1, DPF and LDD) may be compared with the data on Euro-3 diesel vehicles (Caplain et al., 2006). Compared to Euro-3 vehicles the emission factors of Euro-4 vehicles are divided by a factor 10 to 100 for IRSUC cold, 15 to 30 for IRSUC hot, 30 to 100 for the Artemis-urban and motorway driving cycles. Whatever the Artemis cycle and type of fuel, for gasoline vehicle the total VOCs emissions

decrease in the following order: Artemis-urban > Artemis-rural > Artemis-motorway, and especially the light saturated and unsaturated COV ($C_2 – C_6$) (Table 2). Compared to diesel car real-world test driving cycles, VOCs emission levels are higher (e.g. IRSUC cold GDI E10 126 mg.km^{-1}, D1 B5 14.9 mg.km^{-1}). The same observation holds for the carbonyl compounds.

For all the vehicles, driving cycles and fuels used in this study, the emission factor observed for 1,3-butadiene, benzene and formaldehyde is quite low compared to emission factors obtained in previous studies (Aakko et al., 2006).

*Table 2: Artemis and IRSUC driving cycles gasoline vehicle emission factors (mg.km^{-1}) **

	IRSUC cold		IRSUC hot		ARTEMIS-urban		ARTEMIS-rural		ARTEMIS-motorway	
	Ref.	E10	Ref.	E10	Ref.	E10	Ref.	E10	Ref.	E10
Vehicle GDI										
Alkenes	21.29	12.93	N.D.	0.24	18.07	0.52	1.00	0.47	0.20	0.91
Alkanes	3.07	73.73	66.91	35.19	138.16	20.38	9.15	15.62	5.75	3.62
Aromatics	86.30	39.38	50.19	68.74	36.51	26.64	6.23	15.46	4.71	3.68
Total VOC	110.66	126.03	117.10	104.16	192.74	47.55	16.39	31.55	10.66	8.22
1,3-butadiene *	N.D.	483.05	N.D.	N.D.	N.D.	27.48	14.87	35.39	N.D.	N.D.
Benzene*	N.D.	37.5	N.D.	16.0	118.8	N.D.	7.4	N.D.	182.7	N.D.
Formaldehyde*[a]	990	850	570	350	2790	1320	430	220	170	210

[a] only formaldehyde has been quantified for the GDI vehicle

*Table 3: Artemis driving cycle Diesel vehicle emission factors (mg.km^{-1}) **

	ARTEMIS-urban				ARTEMIS-rural				ARTEMIS-motorway			
	Ref.	B5	B30	HVO	Ref.	B5	B30	HVO	Ref.	B5	B30	HVO
Vehicle D1												
Alkenes	0.36	2.82	0.46	2.05	0.35	0.98	0.24	0.31	0.72	0.08	0.21	0.16
Alkanes	6.22	4.98	2.31	53.88	0.88	3.81	3.97	11.61	5.76	0.85	1.83	5.91
Aromatics	9.48	7.51	3.70	20.34	2.10	0.52	6.01	3.48	3.73	1.09	4.66	2.91
Carbonyls	11.09	9.95	3.03	9.73	1.62	3.28	1.24	1.39	2.06	1.11	2.40	0.92
1,3-butadiene*	N.D.	N.D.	N.D.	343.3	20.6	71.9	N.D.	28.9	41.4	N.D.	N.D.	N.D.
Benzene*	N.D.	N.D.	N.D.	31.2	1.4	0.4	11.2	12.1	1.2	N.D.	9.4	7.5
Formaldehyde*	1463.2	1423.5	659.6	1248.6	352.7	499.5	288.1	115.1	551.6	168.1	331.4	123.7
Vehicle DPF												
Alkenes	0.50	0.24	N.D.	0.05	0.20	0.18	0.18	N.D.	0.33	0.01	0.03	0.44
Alkanes	25.27	8.32	2.19	39.73	0.74	1.80	2.00	3.46	1.45	2.45	1.90	1.00
Aromatics	10.96	12.93	3.66	13.93	1.87	3.15	0.01	4.83	1.90	3.51	1.11	2.14
Carbonyls	6.61	12.62	Nodata	15.23	0.89	0.96	1.97	3.76	1.46	0.83	1.31	3.59

1,3-butadiene*	N.D.	N.D.	N.D.	4.7	N.D.	N.D.	N.D.	4.9	5.8	9.5	N.D.	0.1
Benzene*	22.2	19.8	15.5	20.5	N.D.	9.5	5.1	3.7	N.D.	2.4	5.5	0.2
Formaldehyde*	1965.6	1687.1	Nodata	3532.9	226.7	267.9	362.6	656.2	377.4	214.7	228.9	357.7
Vehicle LDD												
Alkenes	0.63	1.61	N.D.	0.75	0.77	0.14	0.23	0.19	0.73			
Alkanes	30.47	39.26	6.26	21.33	3.04	0.15	4.05	0.06	0.38			
Aromatics	9.93	9.40	N.D.	4.21	1.25	2.44	1.27	N.D.	5.94	No data		
Carbonyls	4.20	7.82	7.69	13.89	0.92	1.91	0.81	3.22	1.07			
1,3-butadiene*	N.D.	2.9	N.D.	1.5	N.D.	N.D.	N.D.	N.D.	N.D.			
Benzene*	N.D.	20.1	N.D.	30.7	N.D.	7.2	15.1	N.D.	4.9			
Formaldehyde*	930.1	2301.5	1624.6	3445.7	163.7	485.3	161.8	826.0	164.8			

2.4 Influence of biofuels

An addition of ethanol to the reference fuel seems to reduce the emissions of volatile organic compounds in the exhaust gas, especially for the Artemis-urban driving cycle (from 192 to 47 $mg.km^{-1}$). Formaldehyde and acetaldehyde emissions also decrease when switching from reference gasoline to E10.
Changes are observed in the aromatics and alkanes emissions when fuelling diesel engines with biodiesel blends instead of reference diesel. For D1 under IRSUC cold and hot cycles, the amount of aromatics and alkanes emitted increases significantly when the percentage of biodiesel increases in the fuel (Ref < B5 < B30 < HVO). The trend is less pronounced for the other driving cycles. For this vehicle, the biodiesel content seems to have a positive influence on the emission factors. The results obtained for the two others diesel vehicles (DPF, LDD) are not so clear, and a weak increase of the emission factors from reference diesel to HVO is noted. The use of biofuel decreases slightly the production of carbonyls compared to reference gasoil, except for the Artemis urban cycle, but pure HVO leads also to high emissions of carbonyls.

Conclusions

The analysis presented in this study shows that the use of biofuel pure or in blends at different concentration (E10, B5, B30, HVO) in gasoline or diesel engines and under different driving cycle conditions, has an impact on the tailpipe emissions. Non-regulated pollutants mainly emitted are alkanes and aromatics compounds whatever the type of engine. On the whole, the addition of ethanol to gasoline reduces the aromatics emissions but does not affect the total VOCs emissions as regards IRSUC cold and IRSUC hot cycles, where the emissions levels stay almost similar. With biodiesel blends, the emission factors are higher with the hot start driving cycle than with the cold start one. For the Artemis driving cycles, the emission factors of the gasoline vehicle are reduced when going from urban to rural to motorway driving cycle, but no clear trend is noted with the diesel vehicles. The emission factors obtained during this study are significantly reduced compared to the ones obtained with Euro-3 compliant diesel and gasoline vehicles.

Acknowledgements

This study was supported by ADEME, the French environment agency.

References

Aakko P., Laurikko J., Weilenmann M., Joumard R., André J.M., Prati M.V., Castagliola M.A., Merétei T., Cazier F., Mercier A., Nouali H., Paturel L., Combet E., Devos O., Dechaux J.C., Caplain I., Nollet V., (2006), Emission factors of unregulated atmospheric pollutants for passengers cars , *Task 322 of EU Artemis Project*

André M., Joumard R., Vidon R., tassel P., Perret P., (2006), Real-world European driving cycles, for measuring pollutant emisions from high and low-powered cars, *Atmospheric Environment*, 40, Issue 31, 5944-5953

Caplain I., Cazier F., Nouali H., Mercier A., Déchaux J.C., Nollet V., Joumard R., André J.M., Vidon R. (2006), Emissions of unregulated pollutants from European gasoline and diesel passenger cars, *Atmospheric Environment,* 40, 5954 – 5966.

Corrêa S.M., Arbilla G., (2008), Carbonyl emissions in diesel and biodiesel exhaust, *Atmospheric Environment*, 42, 769-775

Sureshkumar K., Velraj R., Ganesan R., (2008), Performance and exhaust emission characteristics of a CI engine fuelled with PPME and its blends with diesel, *Renewable Energy*, 33, 2294-2302

Emissions and fuel consumption of modern flexifuel and gasoline vehicles on various ethanol blends

L. Pelkmans, G. Lenaers, J. Bruyninx, I. De Vlieger*

VITO, Flemish Institute for Technological Research, Boeretang 200 BE-2400 Mol, Belgium,
luc.pelkmans@vito.be

Introduction

Biofuels are today one of the only direct substitutes for oil in road transport, available on a significant scale. They can be used today, in existing vehicle engines, unmodified for low blends, or with cheap modifications to accept high blends. Biofuels are expected to represent a substantial part of the 10% target for renewable energy in transport by 2020, set by the European Commission in the Renewable Energy Directive 2009/28/EC.

When looking at gasoline vehicle models, bio-ethanol is the main biofuel candidate. In low blending rates up to 10% with gasoline, bio-ethanol works as oxygenate. This generally has a positive effect on emissions, but also on thermal efficiency. The use of higher ethanol blends is also possible, but this requires an adaptation of the vehicle. More and more car manufacturers offer flexifuel models (FFVs), which are adapted to drive on any gasoline-ethanol blend. The most common high ethanol blend is E85, which contains 85% ethanol and 15% gasoline. Important for high ethanol blends is that ethanol only has two thirds of the energy content of regular gasoline, so an increase of the ethanol blending percentage will lead to higher volumetric fuel consumption.

Within the Belgian research project 'BIOSES' a roadmap is being developed for the introduction of biofuels in Belgium. Timeframe for the roadmap is 2010-2030. The project develops ten scenarios for the introduction of biofuels, based on the technological evolution in vehicle models, the likely biofuel blends on the European markets, and the possible interest of certain end user groups. Bio-ethanol as a fuel can play an important role in the roll-out of biofuels in the gasoline car segment. Indeed, bio-ethanol can be produced from ligno-cellulose feedstock using so-called 2nd generation production technologies, so it can be considered a long-term option as a transport fuel. For impact analyses of the different scenarios it is important to have good data on the effect ethanol blends will have on vehicle emissions and fuel consumption. Within BIOSES a number of dedicated emission tests were performed on modern vehicles. The results of these tests will be discussed in this paper.

Emission tests

Next to collecting public data in literature on the effect of bio-ethanol blends on emissions, we selected two current flexifuel vehicle models, a Saab 9.5 BioPower and a Volvo V50 flexifuel, and one modern direct injection gasoline model, a VW Golf Plus 1.4 TSI, to be tested on various ethanol blends for regulated emissions and fuel consumption. The vehicle specifications are shown in Annex.

The tests were performed with VITO's on-board emission measurement system (VOEMLow), on proving ground in Lommel, Belgium. The VOEMLow system is the second generation of a dedicated system for on-road measurements [Lenaers, 2003]. The system consists of a sampling system for the exhaust gas, laboratory grade analyzers, measuring equipment for fuel consumption, vehicle speed, engine speed and lambda value, a power supply and a data-acquisition and -processing system. It measures fuel consumption and emission concentrations (CO2, CO, THC, NO_x and PM), combined with the total mass flow of the exhaust gases, so the results are expressed in gram pollutant per second. This new system has a drastically increased sensitivity to measure low emission levels from vehicles complying with future emission levels. VOEMLow measurements are performed at 1 Hz allowing investigating the influence of several vehicle and engine parameters on the fuel consumption and emissions.

We tested these vehicles on the NEDC (New European Driving Cycle, start with hot engine) and a test cycle based on real traffic (MOL30 cycle, with part city traffic, part rural and part motorway). All tests were performed at least three times per fuel/vehicle combination.

Test results

All detailed test results are mentioned in Annex 2. In this chapter we will discuss the overall trends of the three test vehicles.

Fuel and energy consumption

In terms of fuel consumption it is expected that higher ethanol blends will have higher volumetric fuel consumption as the calorific value of ethanol is only two third of gasoline. In literature we found a number of test results with various ethanol blends, e.g. [Westerholm, 2008], [van Rooijen, 2008], [de Serves, 2005], [West, 2007] and [Shockey, 2007]. The low blends E5 and E10 mostly have comparable fuel consumption to regular gasoline. E85 will on average increase fuel consumption by 30 to 35%. Nevertheless there are variations between 20 and 40%, depending on vehicle type and test cycle. If these results are transformed into energy consumption per km, we see an average reduction of 5% compared to gasoline operation.

In our measurements we found for the Saab BioPower an average fuel consumption increase on E85 compared to gasoline of around 25%, meaning that energy consumption is actually reduced by 10%. Surprising for this vehicle was that the fuel consumption test results on the NEDC cycle were fully in line with the figures on the real traffic based cycle MOL30. This was very different for the other two vehicles, which systematically had 20 to 25% higher fuel consumption in the real traffic based cycle. What was striking for the Volvo V50 is that for higher ethanol content, the difference between NEDC and MOL30 became much smaller (only 5% for E85).

To really be able to derive conclusions, we need to convert fuel consumption figures into energy consumption, based on calorific value.

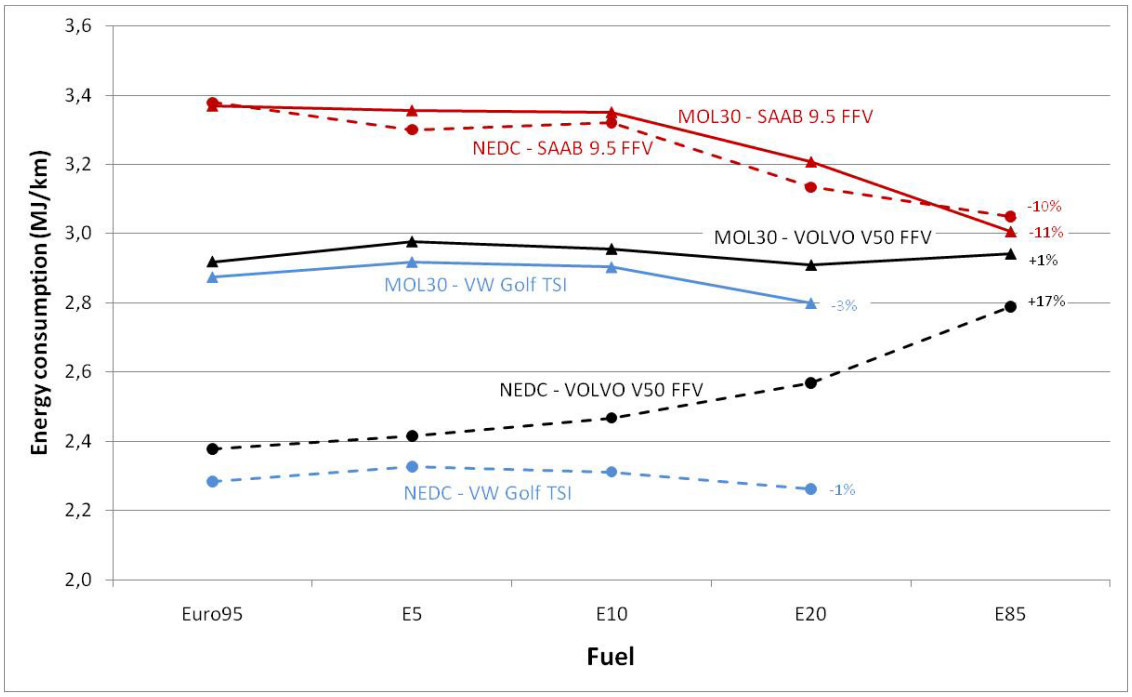

Figure 1: Comparison of energy consumption of the three test vehicles.

For the MOL30 cycle, the energy consumption for the Volvo (as well as for the VW Golf) is fairly constant with variations lower than 2%. On the other hand for the NEDC cycle energy consumption clearly rises with increasing ethanol content, up to 17% higher for E85. So it seems that in this case the vehicle has lower average efficiency than on gasoline. This trend is not seen for the other two vehicles.

When looking deeper into the Volvo test results, we noticed that the difference is highest in the parts of the cycles with lowest speed and demand and high fractions of stand-still (especially in

the city part ECE in the European Drive Cycle). In cycle parts with higher demand and higher speeds, energy use and efficiency seem comparable for most ethanol blends and gasoline.

Table 1: extra energy consumption of E10 and E85 per cycle part, in comparison with RON95 gasoline

	E10	E85
MOL-city	+ 5%	+ 12%
MOL-rural	- 1%	+ 1%
MOL-highway	+ 1%	- 3%
ECE	+ 7%	+ 34%
EUDC	+ 2%	+ 6%

In any case it seems that the Volvo V50 flexifuel is most optimized for gasoline operation, while the Saab 9.5 BioPower is more optimized for E85 operation.

Impact on emissions

CO_2 tailpipe emissions are related to the carbon content of the fuel and the fuel consumption. Ethanol has somewhat lower specific CO_2 emissions in comparison to gasoline. So as a result, we measured a 15% reduction of CO2 emissions for the Saab FFV on E85 in comparison with gasoline operation. For the Volvo FFV we saw a big variation, related to the trends in fuel consumption, with a reduction of 5% for the MOL30 cycle, while CO2 tailpipe emissions increased by 10%. Of course CO_2 and other greenhouse gas emissions need to be considered on a well-to-wheel basis, in which tailpipe emissions are only one part of the chain.

When looking at the measurements of **NO_x emissions**, there are also clear differences between the test vehicles. The Saab FFV has extremely low NO_x emissions, and this is hardly changed by increasing the ethanol concentration in the fuel. NO_x emissions of the other vehicles were somewhat higher, although still below 0.08g/km, which is the Euro 4 limit for gasoline vehicles in the European test cycle - although full comparison should not be done, as test circumstances and vehicle weight in the homologation test are different from our test circumstances. Nevertheless we see a decreasing trend in NO_x emissions for the Volvo FFV in the real traffic based cycle with higher ethanol blends. For the VW there is a slight increasing trend, although limited.

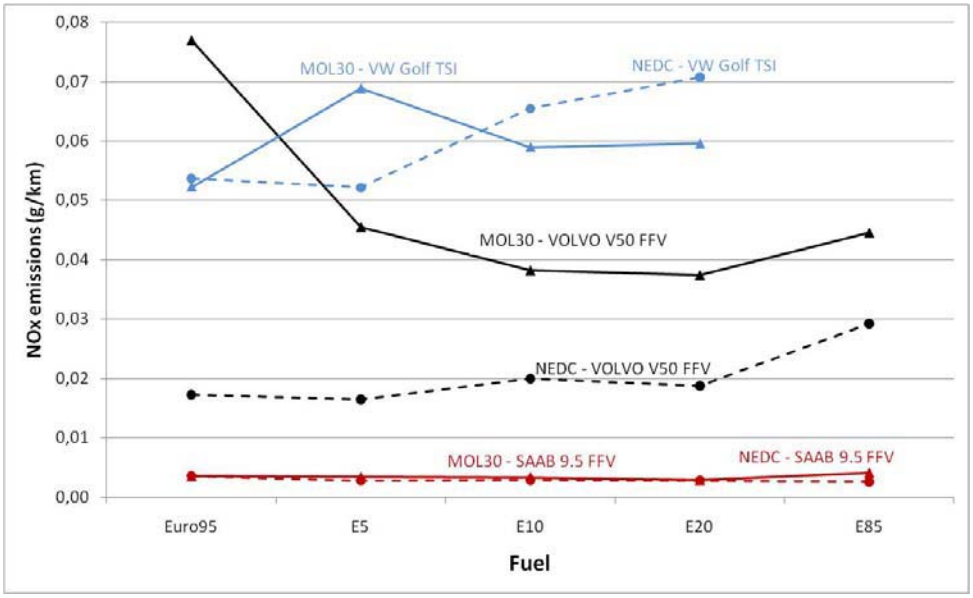

Figure 2: Comparison of NO_x emissions of the three test vehicles.

CO emissions are at much higher level, and there is also a clear difference between the NEDC cycle and the real traffic based MOL30 cycle, for all three test vehicles. When looking the Saab FFV, Levels on the NEDC (gasoline operation) were around 0.3 g/km, while CO emissions on the MOL30 cycle were between 1 and 2 g/km, which is four to five times higher. We also noticed high variation in the results. Most of the CO is produced in peaks during accelerations and CO peaks tend to vary in size, resulting in high variations of the results. This is especially true for the MOL30 cycle; in the NEDC cycle, accelerations are much smoother and CO peaks are less pronounced. Mind that the Euro 5 limit for CO emissions is 1 g/km.

For the Volvo FFV and the VW Golf we also measured big differences between the two cycles, although the absolute values are lower than for the Saab.

Looking to the evolution as a function of ethanol content, in most cases we see a clear decreasing trend with higher ethanol content. For E85 we even measured CO decreases up to 80% compared to gasoline operation.

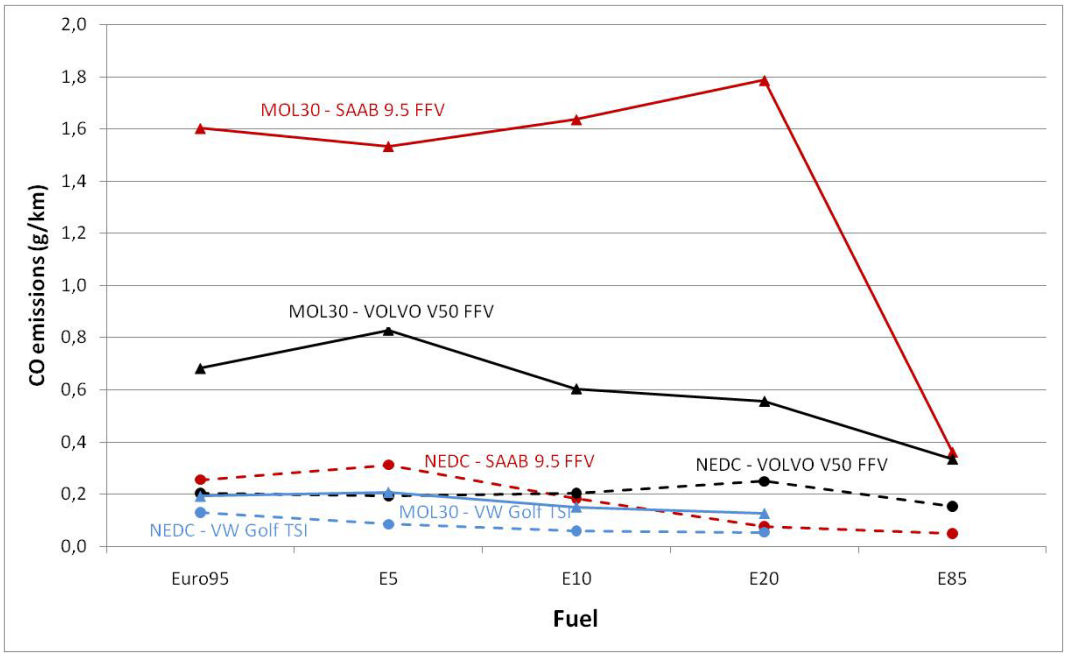

Figure 3: Comparison of CO emissions of the three test vehicles.

For total hydrocarbon (THC) emissions we also see a decreasing trend with higher ethanol content. Figures are, however, in all cases much lower than the Euro 5 limit of 0.1 g/km, as can be seen in Annex 2.

Conclusions

When we look at the overall results we can conclude that overall results are quite positive for ethanol blends, although we should keep in mind that car technologies can have important impact. In terms of **exhaust gas emissions**, base levels on gasoline operation are usually very low, and these emissions are kept at very low level with increasing ethanol blends. For CO and THC emissions there is a clear decreasing trend. **Fuel consumption** (litre/100km) generally increases with higher ethanol blends, more or less following the energy content of the fuel. When expressing the results in energy consumption (MJ/km), the results are neutral to positive, with up to 10% lower energy consumption for one flexifuel vehicle on E85. One exception was energy consumption of the Volvo flexifuel model on the NEDC cycle, which showed a clear increasing trend with higher ethanol blends. This however cannot be generalized, as on the real traffic based test cycle, energy consumption did not increase at all.

Apart from the traditional 'New European Test Cycle' (NEDC), which is known to underestimate real traffic fuel consumption and emissions, there is clearly a need to also perform tests on other test cycles which are more related to real traffic driving. Trends on the NEDC are not necessarily the same in real traffic based cycles, and customers are entitled to know what they can expect from these vehicles and fuel combinations in real traffic circumstances.

References

Lenaers G., L. Pelkmans and P. Debal (2003): The Realisation of an On-board Emission Measuring System Serving as a R&D Tool for Ultra Low Emitting Vehicles. *Int. J. Veh. Design*, Vol.31, No. 3, pp 253-268.

Pelkmans L. et al. (2008): Introduction of biofuels in Belgium - Scenarios for 2010 - 2020 – 2030, BIOSES report for task 1, March 2008.

van Rooijen T. et al. (2008): Car performance with different an-hydrous and hydrous ethanol blends, TNO, BEST deliverable No 3.11, April 2008.

de Serves C. (2005): Emissions from Flexible Fuel Vehicles with different ethanol blends, REPORT No AVL MTC 5509MTC, October 2005.

Shockey R. et al. (2007): Optimal ethanol blend-level investigation, final report. Energy & Environmental Research Center. Report 2007-EERC-11-02, November 2007.

West B.H., et al. (2007): Fuel Economy and Emissions of the Ethanol-Optimized Saab 9-5 Biopower, Oak Ridge National Laboratory, *SAE 2007-01-3994*.

Westerholm R., P. Ahlvik, H.L. Karlsson (2008): An exhaust characterisation study based on regulated and unregulated tailpipe and evaporative emissions from bi-fuel and flexi-fuel light duty passenger cars fuelled by petrol (E5), bio-ethanol (E70, E85) and biogas tested at ambient temperatures of +22°C and -7°C, March 2008.

Annex 1: vehicle specifications

Table 2: Specifications of the test vehicles

VEHICLE			
Make	Saab	Volvo	Volkswagen
Model	9.5 Sedan	V50	Golf Plus
Vehicle empty weight	1580 kg	1420 kg	1380 kg
Max. vehicle weight	2050 kg	1890 kg	n.a.
In use since	2008	2008	2008
ENGINE			
Engine type	2.3t, 4 cyl. 'BioPower'	1.8f, 4 cyl. flexifuel	1.4 TSI, 4 cyl.
Cylinder vol.	2290 cm^3	1798 cm^3	1390 cm^3
Compr. ratio	9.3	10.8	10
Fuel injection system	Multi-point indirect injection	Multi-point indirect injection	turbocharged direct injection
Max. power	154kW @ 5500 rpm	92 kW @ 6000 rpm	90 kW @ 5600 rpm
Max. torque	310 Nm @ 2000 rpm	165 Nm @ 4000 rpm	220 Nm @ 3500 rpm
Transmission	5-speed manual	5-speed manual	6-speed manual
TEST DATA			
Test period	27/03 – 06/04/2009	03 – 09/10/2008	08 – 11/12/2008
Mileage	11900 km	3900 km	7900 km
Vehicle test weight	1950 kg	1740 kg	1640 kg
Test fuels	RON95, E5, E10, E20, E85	RON95, E5, E10, E20, E85	RON95, E5, E10, E20
Test cycles	NEDC, MOL30	NEDC, MOL30	NEDC, MOL30

Annex 2: detailed test results

Table 3: test results of the Saab 9.5 2.3t BioPower (average of 3 runs)

	Test \ Fuel	RON95	E5	E10	E20	E85
Fuel (l/100km)	NEDC	10.49	10.43	10.67	10.44	13.30
	MOL30	10.46	10.60	10.77	10.69	13.11
Energy (MJ/km)	NEDC	3.38	3.30	3.32	3.13	3.05
	MOL30	3.37	3.36	3.35	3.21	3.01
CO_2 (g/km)	NEDC	247.7	240.8	239.7	222.1	213.0
	MOL30	244.8	242.8	239.5	224.6	209.5
CO (g/km)	NEDC	0.26	0.31	0.18	0.08	0.05
	MOL30	1.60	1.53	1.64	1.79	0.36
NO_x (g/km)	NEDC	0.0037	0.0028	0.0029	0.0028	0.0026
	MOL30	0.0035	0.0034	0.0034	0.0029	0.0041
THC (g/km)	NEDC	0.0054	0.0054	0.0045	0.0023	0.0022
	MOL30	0.0188	0.0197	0.0193	0.0164	0.0121

Table 4: test results of the Volvo V50 1.8f (average of 3 runs)

	Test \ Fuel	RON95	E5	E10	E20	E85
Fuel (l/100km)	NEDC	7.39	7.63	7.93	8.56	12.16
	MOL30	9.07	9.40	9.50	9.69	12.82
Energy (MJ/km)	NEDC	2.38	2.42	2.47	2.57	2.79
	MOL30	2.92	2.98	2.96	2.91	2.94
CO2 (g/km)	NEDC	175.6	176.3	178.1	181.7	192.9
	MOL30	214.8	216.3	212.7	205.3	203.1
CO (g/km)	NEDC	0.205	0.194	0.205	0.250	0.153
	MOL30	0.683	0.829	0.605	0.557	0.336
NOx (g/km)	NEDC	0.017	0.017	0.020	0.019	0.029
	MOL30	0.077	0.046	0.038	0.037	0.045
THC (g/km)	NEDC	0.0008	0.0007	0.0009	0.0010	0.0010
	MOL30	0.0038	0.0040	0.0039	0.0041	0.0048

Table 5: test results of the Volkswagen Golf Plus 1.4 TSI (average of 3 runs)

	Test \ Fuel	RON95	E5	E10	E20	E85*
Fuel (l/100km)	NEDC	7.09	7.35	7.43	7.54	n.a.
	MOL30	8.93	9.22	9.33	9.33	n.a.
Energy (MJ/km)	NEDC	2.28	2.33	2.31	2.26	n.a.
	MOL30	2.88	2.92	2.90	2.80	n.a.
CO2 (g/km)	NEDC	168.7	170.0	167.0	160.3	n.a.
	MOL30	212.3	213.0	209.7	198.3	n.a.
CO (g/km)	NEDC	0.131	0.085	0.060	0.054	n.a.
	MOL30	0.192	0.207	0.152	0.127	n.a.
NOx (g/km)	NEDC	0.054	0.052	0.065	0.071	n.a.
	MOL30	0.052	0.069	0.059	0.060	n.a.
THC (g/km)	NEDC	0.0055	0.0044	0.0035	0.0022	n.a.
	MOL30	0.0065	0.0067	0.0047	0.0034	n.a.

* E85 *was not measured for the VW Golf Plus, as this model was not flexifuel.*

Reduction of GHG Emissions from Road Transport in the Major Economies of the World and in the European Union: Patterns of Research and Policy Output and Priorities

E. Vouitsis and Z. Samaras

Laboratory of Applied Thermodynamics, Aristotle University of Thessaloniki, GR – 541 24 Thessaloniki, Greece, zisis@auth.gr

Introduction

The publication pattern of a country is an indicator of its capacity and commitment to perform mainstream research in certain specific areas. The research output is the cumulative effect of resources allocation and policy decisions in the past for different areas/sub-areas of science, whether explicitly or implicitly (Braun, et al., 1995). The main objective of this paper is to assess the research priorities in areas/subjects relative to GHG emissions reduction (focusing in transportation) and to reveal trends, gaps, similarities and differences of research and policy efforts using some bibliometric measures based on the corresponding literature. Subjects of high activity and subjects of low activity were identified for the time period 2000 -2009.

Data and Methodology

The data on publication output were compiled from Elsevier's scientific database ScienceDirect. The database was scanned through "Abstract, Title, Keywords" and "Affiliation" fields to compile the data using several keywords ("Abstract, Title, Keywords" field) and the name of each country ("Affiliation" field). Countries evaluated included those of EU 16 (Austria, Belgium, Denmark, France, Finland, Germany, Greece, Ireland, Italy, Luxembourg, Malta, Netherlands, Portugal, Spain, Sweden and United Kingdom (UK)), those of EU-27 (the aforementioned plus Bulgaria, Cyprus, Czech, Estonia, Hungary, Latvia, Lithuania, Poland, Romania, Slovakia and Slovenia), those of G-8 (Canada, France, Germany, Italy, Japan, Russia, UK and United States (USA)), those of G-20 (the G-8 plus Argentina, Australia, Brazil, China, India, Indonesia, Mexico, Korea, Saudi Arabia, South Africa, and Turkey) and Switzerland, Norway and Israel. In total, 45 countries. The results are classified according to the number of publications of each country, that number adjusted for the population and the GDP (nominal, in year 2000 US dollars) of each country (both averaged over the decade) and according to the so-called research Priority Index (PI) (Bhattacharya, 1997) of each group of countries, an index appropriate for cross-national comparisons. The PI is computed as: $PI= (n_{ij}/n_{io})/(n_{oj}/n_{oo}) \times 100$, where n_{ij}= the number of papers of country i in subject j, n_{io}= the number of papers of country i in all subjects, n_{oj}= the number of papers of all countries in subject j, n_{oo}= the number of papers of all countries in all subjects. Here 'all' refers to the comparison set (i.e. the set of 45 countries and the set of subject - keywords examined). We selected the following 10 keywords – subjects for the examination: air pollution, air quality, automobiles, emissions, energy consumption, energy efficiency policy, environment, fuel consumption, greenhouse gas emissions, and transportation.

The value of PI=100 indicates that research priority of a country for a given subject corresponds precisely to the average of all countries, i.e. average priority. PI>100 indicates higher than average priority and PI<100; lower than average priority. From the values of PI; we can compare:

- The priorities of a given country to different subjects in a given time-span.
- The priorities of different countries to a given subject in a given time-span.
- The priorities of a country to a given subject in different time-spans.

We have used the following five-point scale for fixing the bench-marks (Bhattacharya, 1997):

PI≤70	70<PI≤90	90<PI≤110	110<PI≤130	PI>130
low	below average	average	above average	high

Results

General overview of the publication output

Table 1summarizes the output, the share as well as the change (second quinquennium of the decade relative to the first one) of publications (in all scientific fields) of the countries consist the four groups examined (plus Switzerland, Norway and Israel). Countries are ranked according to the publication counts. Also, the number of publications adjusted for the population and the GDP of each country are shown. The ten countries at the top of the table (USA, Japan, France, China, Germany, Italy, Canada, Spain, Australia, and India) account for 71.51% of the total output for the decade. China and UK have nearly tripled their outputs in the second quinquennium of the decade, Spain, Turkey Luxembourg and Cyprus over double it (although in the latter cases the small number effect – i.e., a small change in a small number reflects as a high percentage change- is significant.) Switzerland was by far the more productive country in terms of per capita number of publications (more than 3 times the average value that is 699 publications per 100000 persons vs. 226 publications per 100000 persons). Yet nineteen countries are above the average value: Israel, Sweden, Denmark, Finland, Netherlands, Norway, Australia, Belgium, Ireland, Canada, France, Slovenia, Austria, Spain, Greece, Germany, USA, Italy and Portugal. In terms of number of publications per GDP, Israel was the more productive country (about three times the average value, that is 274 publications per ($) billion vs. 100 publications per ($) billion). Yet twenty-one countries are above the average value: Slovenia, Hungary, Czech, Sweden, Poland, Switzerland, Australia, Finland, Bulgaria, Netherlands, Portugal, Greece, Belgium, Spain, Canada, Denmark, France, Estonia, India, Austria and China. For the countries groups (Table 2), G-20 was the more productive one in absolute terms. However, when the number of publications was adjusted for group's entire population it presented as the less productive group. On the other side, the 8 richest countries represent the less productive group in terms of number of publications adjusted for the GDP. In these terms, european countries are the more productive (EU-16 when the number of publications adjusted for population and EU-27 when the number of publications adjusted for GDP).

Table 1: General publication output and world share (Countries)

No.	Country	NoP	% share	% change*	NoP (1)**	NoP (2)***
1	USA	732723	23.99	11	251	62
2	Japan	232852	7.62	8	201	53
3	France	226047	7.40	43	368	117
4	China	224888	7.36	197	19	100
5	Germany	207430	6.79	19	251	80
6	Italy	140078	4.59	40	241	88
7	Canada	126696	4.15	48	389	124
8	Spain	125124	4.10	111	306	127
9	Australia	87616	2.87	56	436	145
10	India	80335	2.63	88	7	105
11	Netherlands	78103	2.56	35	478	137
12	Korea	74241	2.43	86	153	99
13	Brazil	56166	1.84	72	31	65
14	Switzerland	52117	1.71	35	699	149
15	Sweden	51697	1.69	19	575	155
16	UK	48179	1.58	182	80	24
17	Belgium	44165	1.45	43	426	99
18	Turkey	42518	1.39	101	62	131

Table 1: Cont.

No.	Country	NoP	% share	% change*	NoP (1)**	NoP (2)***
19	Poland	41734	1.37	29	108	274
21	Russia	37352	1.22	9	26	51
22	Greece	28721	0.94	75	268	134
23	Denmark	28635	0.94	25	528	124
24	Austria	28003	0.92	34	342	101
25	Mexico	27099	0.89	43	26	34
26	Finland	25605	0.84	26	490	143
27	Portugal	22476	0.74	88	237	136
28	Norway	20143	0.66	51	438	73
29	Argentina	18719	0.61	44	48	87
30	Czech	18325	0.60	52	178	165
31	Ireland	16959	0.56	58	422	98
32	Hungary	16280	0.53	22	162	177
33	South Africa	15016	0.49	66	34	75
34	Romania	8156	0.27	64	37	47
35	Slovenia	6945	0.23	59	350	214
36	Bulgaria	6046	0.20	19	80	139
37	Saudi Arabia	4969	0.16	44	20	18
38	Slovakia	3313	0.11	79	61	42
39	Lithuania	2530	0.08	69	70	62
40	Estonia	2459	0.08	61	180	115
41	Indonesia	1854	0.06	64	1	6
42	Cyprus	1433	0.05	101	184	76
43	Latvia	1025	0.03	7	44	33
44	Luxembourg	960	0.03	116	207	29
45	Malta	292	0.01	78	73	42

* Second quinquennium relative to the first one
** Adjusted for the population (number of publications per 100000 persons)
*** Adjusted for the GDP (number of publications per ($) billion of GDP)

Table 2: General publication output and world share (Groups)

Group	NoP	% share	% change	NoP (1)	NoP (2)
EU-16	1072474	16.8	46.4	280	92
EU-27	1180720	18.5	45.6	242	94
G-8	1751357	27.4	21.9	207	67
G-20	2384778	37.3	39.5	61	71

Publication output in different subjects

The total output of publications of the 45 countries for the selected subject-keywords is given in Table 3 (for the two time periods of the decade). It is obvious that “environment” and “emissions” are the landslides of the output, accounting together for 86% (2000-2004) and for 83% (2005-2009) of the total. In all cases, the output increase for the second five years period is significant.

Table 3: Publication output for the ten subjects – keywords examined

Subject keyword	2000 2004	2005 2009	%	Top 3 countries (in NoP)*	Top 3 countries (in NoP (1))**	Top 3 countries (in NoP (1))***
air pollution	1880	3048	62	USA (993) China(398) France(316)	Denmark (2.306) Norway (1.893) Finland (1.436)	Czech (0.809) Estonia (0.656) Bulgaria (0.644)
air quality	2062	3779	83	USA (1355) China (513) France (355)	Finland (1.877) Ireland (1.666) Denmark (1.605)	Greece (0.745) Finland (0.548) Portugal (0.464)
Automobiles	818	1194	46	USA (466) Japan (205) Canada (186)	Luxemb. (0.645) Canada (0.571) Cyprus (0.514)	Korea (0.215) Cyprus (0.213) Canada (0.183)
Emissions	26810	40573	51	USA (10123) China (9012) Japan (6108)	Sweden (16.027) Switz. (15.390) Finland (14.554)	Estonia (6.652) Czech (5.062) Poland (4.930)
energy consumption	2181	4681	115	USA (1118) China (740) Japan (371)	Cyprus (2.315) Finland (1.992) Switz. (1.919)	Cyprus (0.957) Greece (0.838) Slovenia (0.678)
energy efficiency policy	216	558	158	USA (147) China (67) Netherl. (52)	Sweden (0.545) Norway (0.305) Switz. (0.255)	Lithuania (0.195) Sweden (0.147) Greece (0.070)
Environment	36762	59208	61	USA (22627) France (6972) Germany (6358)	Switz. (25.131) Sweden (23.128) Finland (21.659)	Slovenia (10.564) Israel (7.381) Australia (6.785)
Fuel consumption	518	1405	171	USA (350) China (141) Turkey (110)	Sweden (0.935) Cyprus (0.772) Greece (0.597)	Cyprus (0.319) Greece (0.298) Lithuania (0.268)
greenhouse gas emissions	721	1849	156	USA (525) Canada (209) Germany (174)	Norway (1.197) Netherl. (1.023) Denmark (0.996)	Netherl. (0.292) Finland (0.285) Australia (0.284)
Transportation	2264	4331	91	USA (1661) China (701) Japan (498)	Sweden (2.070) Denmark (1.420) Netherl. (1.396)	Greece (0.564) Sweden (0.557) Israel (0.493)

* Number in parentheses refer to the total publication count

** Number in parentheses refer to the total publication count adjusted for the population (number of publications per 100000 persons)

*** Number in parentheses refer to the total publication count adjusted for the GDP (number of publications per ($) billion of GDP)

Priority indexes in different subjects

Table 4: Priority indexes of the countries groups for the ten subjects – keywords examined

	Air Pollution			Air Quality		
Group	2000-04	2005-09	2000-2009	2000-04	2005-09	2000-2009
EU-16	119	97	105	102	128	118
EU-27	149	121	131	93	107	101
G-8	84	85	85	74	85	82
G-20	98	96	96	102	86	92

Table 4: Cont.

	Automobiles			Emissions		
Group	2000-04	2005-09	2000-2009	2000-04	2005-09	2000-2009
EU-16	116	69	86	90	89	89
EU-27	86	63	69	100	101	100
G-8	81	109	101	106	100	103
G-20	93	97	97	97	97	97

Table 4: Cont.

	Energy consumption			Energy Efficiency Policy		
Group	2000-04	2005-09	2000-2009	2000-04	2005-09	2000-2009
EU-16	134	118	126	111	121	120
EU-27	142	103	117	129	116	123
G-8	85	78	81	55	78	74
G-20	126	112	117	141	121	129

Table 4: Cont.

	Environment			Fuel Consumption		
Group	2000-04	2005-09	2000-2009	2000-04	2005-09	2000-2009
EU-16	105	103	104	106	111	112
EU-27	98	98	98	104	129	125
G-8	101	104	102	78	73	76
G-20	101	102	101	106	123	124

Table 4: Cont.

	Greenhouse gas emissions			Transportation		
Group	2000-04	2005-09	2000-2009	2000-04	2005-09	2000-2009
EU-16	105	119	117	86	118	103
EU-27	84	106	100	74	96	85
G-8	70	96	90	93	96	95
G-20	93	104	103	88	99	96

Table 4 summarizes the PIs achieved by the groups of countries examined in each subject – keyword for the two time periods of the decade as well as for the whole decade. Research priorities of a given group to the different subjects and of different groups to a given subject can be easily identified. Table 5 shows the average PIs achieved by each country.

Table 5: Average Priority Index for each country examined

Lithuania (197)	Netherlands (121)	Korea (106)	Italy (94)	Argentina (76)
Turkey (189)	Denmark (119)	Latvia (106)	Malta (93)	Estonia (76)
Cyprus (173)	China (116)	South Africa (106)	Czech (91)	Romania (77)
Indonesia (152)	Ireland (116)	Luxembourg (104)	Germany (89)	Israel (73)
S. Arabia (150)	Finland (114)	Mexico (102)	Japan (89)	Slovenia (68)
Greece (145)	Portugal (109)	Belgium (101)	Spain (88)	Bulgaria (66)
Austria (137)	Brazil (108)	Switzerland (101)	France (85)	Canada (66)
Norway (133)	Slovakia (107)	USA (100)	UK (81)	Poland (66)
Sweden (130)	India (107)	Australia (96)	Hungary (79)	Russia (57)

Table 6: Average Priority Index of the 10 subjects – keywords

No.		**Priority Index**
1	Energy Efficiency Policy	128
2	Fuel Consumption	127
3	Energy consumption	120
4	Air Pollution	119
5	Greenhouse gas emissions	105
6	Environment	100
7	Air Quality	98
8	Emissions	98
9	Transportation	90
10	Automobiles	80

If all the subjects are concentrated in the middle of the five-point scale, i.e. average PI=100 or near (for example, USA, Switzerland and Belgium), the profile can be considered more or less homogeneous, that is research effort is diffused and there are no clear-cut priorities. On the other hand, if the average PI is higher or lower from this value the profile is differentiated, i.e. there are clear-cut priorities. In the case of subjects, greenhouse gas emissions, environment, emissions and air quality have the most homogeneous profile (Table 6).

Conclusions

A comparative analysis of the research priorities has important implications for strategic planning in science, especially the allocation of resources to different areas and identification of research areas and countries for translational cooperation in research. Tracking of trends and priorities in time can provide important insights into the impact of decisions taken in the past. The results of this study indicate that environmental issues have become a common place in the scientific research. However, as far concern the greenhouse gases emissions, it seems that despite the average priority status calculated according to present methodology and the significant increase of the relevant publication output in the course of the decade, much more scientific work is needed to achieve, not the wanted, but the optimal minimum at the least.

References

Braun, T., G. Wolfgang, and G. Harald (1995), The scientometric weight f 50 nations in 27 science areas, 1989–1993. Scientometrics 33 (3), 263–293.

Bhattacharya, S. (1997). Cross-national comparison of frontier areas of research ın physics using bibliometric indicators, Scientometrics 40 (3), 385-405.

Simultaneous study of gas phase and secondary organic aerosols' chemical composition

S. Rossignol[1], L. Chiappini[1], E. Perraudin[2], J.F. Doussin[2]*

[1]Institut National de l'Environnement industriel et des Risques (INERIS), Parc Technologique ALATA, 60 550 Verneuil-en-Halatte, France, stephanie.rossignol@ineris.fr

[2]Laboratoire Interuniversitaire des Systèmes Atmosphériques (LISA), 61 Avenue du Général de Gaulle, 94 010 Créteil, France

Introduction

Secondary Organic Aerosols (SOAs) are formed in the atmosphere by gas-to-particle conversion of organic gases. Processes involve gas phase reaction of anthropogenic or biogenic Volatile Organic Compounds (VOCs) with atmospheric oxidants (OH, O3, NO3) leading to the formation of oxygenated Semi-Volatile Organic Compounds (SVOCs). SVOCs partition between gas and particulate phases is achieved either by condensation on pre-existing aerosols, or by nucleation (new particles formation). SOAs take part to the atmospheric physic-chemistry and influence :

- Climate regulation by reflecting and diffusing solar radiations and acting as Cloud Condensation Nuclei (CCN)
- Human health because of their submicron size allowing them to cross respiratory barriers.

However, if global processes are well known, due to excessive complexity of atmospheric chemistry and chemical composition of secondary organic matter, the community currently lacks of data to fully describe these multiphase phenomena, characterise SOAs formations pathways and accurately assess their climate and health impacts.

This analytical work intends to improve our understanding of SOAs life cycles providing access to chemical speciation of gaseous and particulate phases simultaneously and allowing :

- Characterization of secondary compounds partitioning according to environmental parameters, age of air mass, reactivity in both phases, etc, and confrontation with theoretical data
- Exploration of chemical processes in both phases leading to SOAs formation and evolution
- Evaluation of potential SOAs toxicity using chemical speciation data in structure-toxicity relationship models.

This original study is based on the development of a low-volume simultaneous sampling of gaseous and particulate phases and an analysis by a unique sensitive and fast analytical technique coupling thermal-desorption, gas chromatography and mass spectrometry (TD-GC-MS). The awkward point of this work is the necessary adaptation of derivatization techniques of polar secondary organic compounds, in gaseous and particulate phases, to the powerful TD-GC-MS analytical method. Here are presented the method development and validation by the use of complementary tools : dynamic atmospheric simulation chamber (INERIS), static atmospheric simulation chamber especially designed for multiphase chemistry (CESAM, LISA), and real atmospheres sampling. Same ways, simulated and real multiphase atmosphere sampling, are taken for first applications of the method.

Sampling and analytical methods

Exploration of chemical speciation of secondary atmospheric organic matter requires the use of an analytical technique meeting three principal characteristics : high sensitivity to detect trace compounds, powerful chromatographic separation to resolve very complex matrices and a detection system allowing structural identification of unknown compounds.

Thermal extraction of sampling material of gas and particulate phases enables high sensitivity minimizing manipulations and limiting losses and contaminations, in opposition to solvent extraction protocols. GC and MS techniques fulfill the sensitivity and identification requirements.

To fit with this analytical method, the gas phase is collected on Tenax TA sorbent tubes and particulate phase on quartz fiber filters, two sampling material which resist to the high temperatures required by thermal extraction (around 300°C).

Both phases are collected simultaneously, during five hours for relevant atmospheric concentrations. For field campaign, the functional commercial sampling system Partisol Speciation (Figure 1) was adapted. It has four mass flow regulator and nine sampling lines, allowing to simultaneously collect two sets of gas/particules samples. Aerosols are collected on 47 mm quartz fibers filter using ChemComb system at a flow rate of 16,7 $mL.min^{-1}$. ChemComb integrates an impaction plate (PM 10, PM 2,5 or PM 1), a filters pack and the possibility to place ozone or VOCs denuder before filter (Figure 1). Gases are collected at around 100 $mL.min^{-1}$ on Tenax TA stainless steel tubes (from Perkin Elmer) or on other sorbents if needed. Flow rate can be adjusted as necessary for gaseous phase. To avoid unwanted aerosols collection on sorbent, Teflon filter, material limiting gas adsorption in comparison with quartz, is placed upstream the sorbent tube. For simulation chamber experiments, analog sampling systems are used.

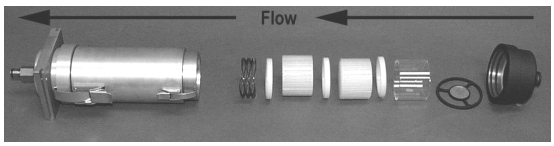

Figure 1 : Partisol Speciation (Model 2300, Thermo Scientific) and ChemComb system

If TD-GC-MS method is commonly used for a large range of primary compounds in gas phase, its application on secondary organic compounds, oxygenated and polar, requires analytical developments. Indeed, polar organic compounds are generally lost in the injection system and/or are not properly eluted in the chromatographic column leading to poor sensitivity. The use of reactive and oxygenated compounds derivatization, reduces polarity and so improves thermal extraction, chromatographic separation and also identification by characteristic fragmentations in mass spectrometry. Derivatization technique is commonly used in SOAs chemical speciation studies when using solvent extraction. However, its adaptation to thermal extraction, involving derivatization on solid support, represents an important challenge.

Derivatization of secondary organic compounds

One of the aims of this work is to adapt derivatization techniques of secondary oxygenated compounds on solid derivatization while maintaining the advantages of thermal extraction, as the minimization of samples manipulations.

Two derivatization reagents have been selected to react with two family compounds :

- O-2,3,4,5,6-(PentaFluoroBenzyl)HydroxylAmine (PFBHA) for carbonyl compounds (ketones, aldehydes). It is largely used by SOAs community when using solvent extraction (e.g. Jang and Kamens 2001; Reisen et al., 2003; Carrasco et al., 2007)The reaction of carbonyl with PFBHA proceeds in two step (Figure 2). As a consequence gas and aerosols samples need a 5-6 days storage before analysis to achieve complete derivatization. The reaction is normally achieved in aqueous solution. Besides, atmospheric ozone can potentially generate negative artifacts by reaction with derivatized coumpounds.

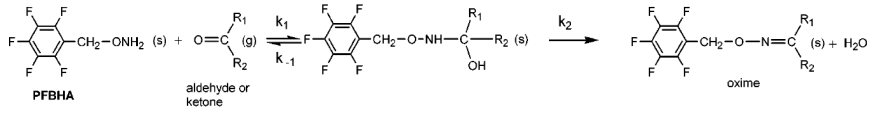

Figure 2 : PFBHA derivatization reaction of carbonyl compounds (Ho and Yu 2002)

- N-Methyl-N-(Tert-ButyldiméthylSilyl)TriFluoro-Acétamide (MTBSTFA) for hydroxyls coumponds (alcohols, carboxylic acids) (Figure 3). It is less sensitive to hydrolysis than BSTFA, and is usually used by community (e.g. Spaulding et al., 1999; Jones and Ham 2008). Giving good responses in GC-MS (Schummer et al., 2009), this agent and its derivatised compounds is still influence by humidity and easily hydrolysed.

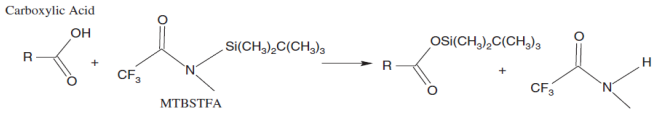

Figure 3: MTBSTFA derivatization reaction or hydroxyl compounds (Buch et al., 2006)

For gas phase collection, Tenax TA is coated with derivatization agent before sampling, which allows to couple sampling to derivatization in order to minimize manipulations, losses and contaminations. On-sorbent deposition is achieved by PFBHA sublimation under nitrogen stream at around 110°C during 20 min. MTBSTFA deposition is carried out by thermal evaporation of pure reagent under nitrogen stream allowing Tenax TA coating.

For particulate phase sampling on quartz fiber filters, derivatization is performed after sampling by filter exposure to derivatization reagent vapors to prevent gas collection from reacting with the coated agent. Humidity influence on derivatization efficiency is expected to be similar to on-sorbent gas phase derivatization. Derivatization of sample filter is performed in a 1,5 L glass vessel where reagent and sample(s) have been introduced for 2 hours. After complete procedure, filter is roll-on and introduce in an empty stainless steel tube suitable for thermal extraction system.

Special attention is drawn to humidity effects on derivatization processes regarding foreseeable behaviour of both reagents.

INERIS exposure chamber experiments

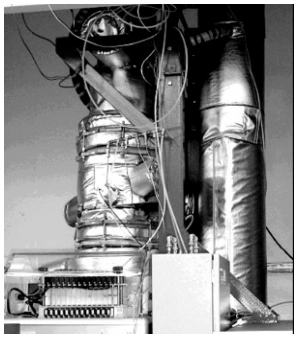

Figure 4 : INERIS exposure chamber

The INERIS continuous flow chamber is a cylindrical glass vessel with a usable volume of 150 L where samplings are performed. Temperature and humidity are continuously controlled and monitored. Gas phase pollutants atmosphere can be created by a generation system providing continuous control of dilution parameters from gas bottles. As a result, the INERIS exposure chamber is a very interesting tool for humidity influence study on gas collection and derivatization.
Indeed, humidity is expected to improve carbonyls derivatization with PFBHA, reaction being widely performed in aqueous solution. On the contrary, it is expected to penalize hydroxyls derivatization by MTBSTFA and derivatives hydrolysis. However these dependences have to be confirmed and characterised.

A preliminary test on the humidity influence on gaseous carbonyls collection was thus realised by generating a simulated atmosphere of simple aldehydes at relative humidities of 0 % and 50 %. Sampling was performed during five hours at 100 mL.min^{-1} on Tenax TA coated with PFBHA on five sampling tubes simultaneously.

Results comparison of dry and wet sampling tests (Figure 5) show significant improvement of the collection efficiencies on one hand (around 3,5 times for benzaldehyde and around 2 times for

others compounds better at 50 %HR than in dry situation) and of reproductibility on the other hand (10 to 20 % error in dry situation, 8 to 12 % error at 50 % HR). Moreover, pentanal quantification by sampling results comparison with derivatization of pure compound in acetonitrile/water solution showed good agreement between theoretical generated concentration and sampling at 50 % HR (theoretical concentration : 14,3 µg.m^{-3}, quantification : 13,9 µg.m^{-3}).

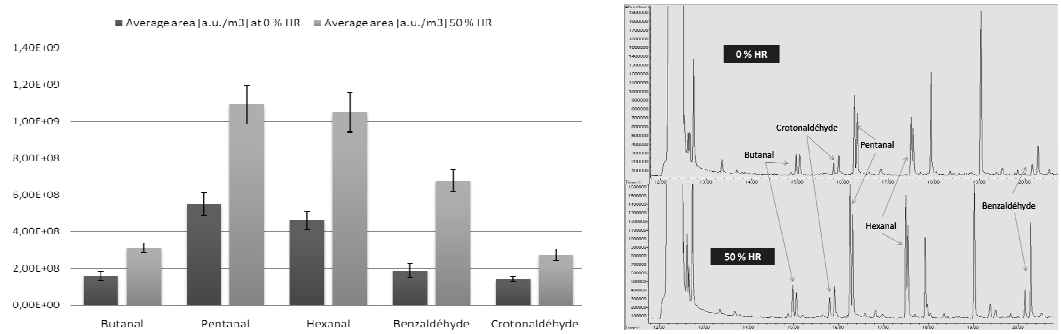

Figure 5 : Comparison of average area (in area units per cubic meter sampling) for five replicates of aldehydes sampling in a dry atmosphere and in a 50 % HR atmosphere. Examples of chromatograms.

These first results confirm the positive influence of relative humidity on carbonyl collection with PFBHA derivatization. Nevertheless, since the method is dedicated to relevant atmospheric conditions (i.e. rarely under 30 % HR or above 80 % HR), further characterization of humidity dependence is required. The aim is to evaluate if a minimum of 30 % HR is enough to achieve complete (or maximum) collection of carbonyls compounds or if a gas stream humidifier is required to achieve suitable results in all relevant atmospheric humidity conditions.

Thus, additional experiments were performed in the INERIS exposure chamber at 30, 50 and 80 % HR. In order to get closer to relevant secondary atmospheric compounds, an alternative series of 10 carbonyls is generated including unsaturated aldehydes (e.g. methacroleine), ketones (e.g. 4-heptanone) and one polyfonctional (hydroxyacetone). Data processing is still ongoing.

Similar experiments will be scheduled for relative humidity influence on hydroxyls collection on MTBSTFA if other experiments (for example CESAM chamber experiments, see below) do not provide complete characterisation.

MEGAPOLI field summer campaign

The European project “Megacities : Emissions, urban, regional and Global Atmospheric PoLlution and climate effects” (MEGAPOLI) has been created in the aim to evaluate present and future impacts of megacities on air quality, atmospheric chemistry and climate at local, regional and global scales. The 2009 summer field campaign took place in the Paris area on several urban and suburban locations, and lumped together a varieties of measurement instruments (IR, PTR-MS, SMPS, TEOM-FDMS, AMS, EC/OC, ...).

This campaign has allowed confronting the method to real conditions, testing coating method and gas sampling parameters as flow rate or denuders suitability, and collecting real aerosols samples for particulate phase derivatization development. The adapted Partisol Speciation was used.

In the case of hydroxyls collection by on-sorbent MTBSTFA derivatization, results have highlighted poor derivatization issue (presence of non-derivatized compounds in samples) and expected relationship between ambient relative humidity and derivatization afficiency variability. Flow rate decrease, tested on a few samplings, seems to be a potential, but not ideal, pathway to fix poor derivatization problem. In order to minimize humidity influence sampling flow dryer system is going to be tested before the method optimization is continued. Nafion membrane appears as an appropriate tool. Indeed, double flux counter-current system seems limiting surface exchanges for potential losses. System has to be tested on known simulated atmosphere in order to quantify analytes losses and evaluate its viability and efficiency.

However, humidity variability during the campaign was not sufficiently significant to obtain suitable conclusions on its influence on carbonyls collection. An important outcome concerns

ozone scrubber influence (Sep-Pack Ozone Scrubber, Whatman®). Indeed, results clearly show quasi-total carbonyls retention by the ozone scrubbers which thus is going to be rejected for further tests.

Concerning particulate phase derivatization, it was evaluated in a first step if humidity adsorbed on quartz fiber filter during a five hours sampling is sufficient for complete (or maximum) carbonyls derivatization, or if additional humidity is required in derivatization protocol. In this aim, a filter obtain after a five hours sampling time (at a flow rate of 16,7 mL.min-1 and at an humidity ration of 35 % on average) was cut in two equal parts. One part was derivatized by vapor PFBHA exposure in a nitrogen purge and dry atmosphere. The other part was derivatized by vapor PFBHA exposure in a purge atmosphere moisturized by a 1 mL liquid water reservoir. Both experiences took place under light nitrogen stream (60 $mL.min^{-1}$) to help reagent and water sublimation/evaporation.

On four compounds clearly identified as PFBHA derivative (but not rigorously identified), gains on peaks area for wet situation in comparison with dry situation vary between 18 and 72 %, clearly showing the needed additional water introduction in derivatization protocol (Figure 6). Such as carbonyls gas phase problematic, it is necessary to determine minimum humidity ratio in vessel atmosphere required to achieve complete (or maximum) derivatization efficiency in order not to saturate TD-GC-MS with an unnecessary amount of water. This work is currently in progress as the MTBSTFA derivatization protocol definition.

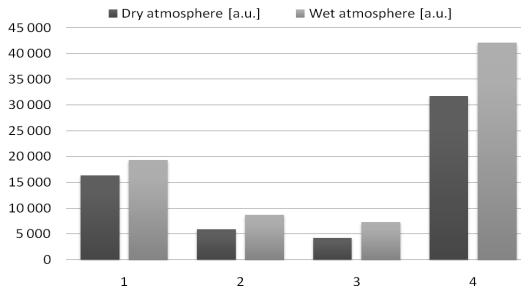

Figure 6 : Improvement of compounds (1 to 4) recovery (in area units) between dry and wet atmosphere aerosols derivatization protocols by PFBHA reagent.

Simulated multiphase atmosphere experiments in CESAM chamber

To refine previous results and apply the method to relevant but simplified atmospheric parameters (range of compounds, multiphase composition, low concentrations, …), three series of experiments are scheduled in the CESAM chamber (Figure 7) in April and May 2010.

Figure 7 : Experimental Chamber for Multiphase Atmosphere Simulation (CESAM, LISA, Créteil, France)

The first experiments specifically concern the gas phase collection : non reactive gaseous atmosphere is generate from about twelve atmospheric relevant carbonyl and hydroxyl pure compounds (e.g. methacroleine, oxalic acid, limonene-1,2-diol) of which concentrations can be precisely monitored by FTIR in the CESAM chamber. These experiments, performed at different concentrations (from 200 to 20 ppb) and relative humidities, will provide more precise information on humidity influence on derivatization performance with both agents. For hydroxyls MTBSTFA derivatization, Nafion membrane to dry the sampling air is to be tested.

In a second step, one or two compounds, of which wall losses have been quantified in the previous experiments, are selected to create a known non reactive multiphase atmosphere by the simultaneous introduction of a gas compound and sulfate seeds in the chamber. Compounds concentration remaining in the gas phase is monitoring by FTIR. The aim is to evaluate the method capacity to give relevant gas/particles partitioning and the potential measurement artifacts (gas adsorption on filter, …).

In a third step, SOAs generation experiments will be performed in order to confront the global method to more complex and atmospheric relevant mixture of compounds in gas and particulate phases. The multiphase atmospheres will be created from, in a first time, well known chemistry system, as the ozonolysis of limonene, biogenic VOC emitted by a large range of plants. This step will enable a complete method performance evaluation, facilitating compounds search and identification in both phases.

Conclusions and perspectives

The experiments carried out in real and simulated atmospheres in the aim to develop the proposed method, allowing simultaneous study of gas phase and secondary organic aerosols' chemical composition, have permitted to validate parts of protocols, as field sampling system or Tenax TA coating protocols, and test and adjust sampling parameters affecting gas phase derivatization, such as sampling flow rate or ambient relative humidity.

Besides, specific laboratory work has allowed characterizing the TD-GC-MS analysis method by the evaluation of thermal extraction efficiency from Tenax TA and quartz fiber filter and the determination of quantification and detection limits.

The original approach of SOA cycle life study providing by this new developed tool going to be applied in different topics as indoor air characterisation, simulated SOA chemistry experiments, and is included in the European project CHARMEX concerning atmospheric chemistry study of the Mediterranean basin. The area is indeed submitted to multiple anthropogenic sources of VOCs, under the marine salts influence and with strong sunshine periods, allowing an important photochemistry development. It is so a privileged zone for studying SOA formation and evolution pathways and taking all advantages and potentialities of the new instrument.

References

Buch, A., Glavin, D.P., Sternberg, R.*, et al.* (2006) A new extraction technique for in situ analyses of amino and carboxylic acids on Mars by gas chromatography mass spectrometry. *Planetary and Space Science*, *54*, 1592-1599.

Carrasco, N., Doussin, J.F., O'Connor, M.*, et al.* (2007) Simulation chamber studies of the atmospheric oxidation of 2-methyl-3-buten-2-ol: Reaction with hydroxyl radicals and ozone under a variety of conditions. *J. Atmos. Chem.*, *56*, 33-55.

Ho, S.S.H., & Yu, J.Z. (2002) Feasibility of collection and analysis of airborne carbonyls by on-sorbent derivatization and thermal desorption. *Anal. Chem.*, *74*, 1232-1240.

Jang, M.S., & Kamens, R.M. (2001) Characterization of secondary aerosol from the photooxidation of toluene in the presence of NOx and 1-propene. *Environmental Science & Technology*, *35*, 3626-3639.

Jones, B.T., & Ham, J.E. (2008) [alpha]-Terpineol reactions with the nitrate radical: Rate constant and gas-phase products. *Atmospheric Environment*, *42*, 6689-6698.

Reisen, F., Aschmann, S.M., Atkinson, R.*, et al.* (2003) Hydroxyaldehyde products from hydroxyl radical reactions of Z-3-hexen-1-ol and 2-methyl-3-buten-2-ol quantified hy SPME and API-MS. *Environmental Science & Technology*, *37*, 4664-4671.

Schummer, C., Delhomme, O., Appenzeller, B.M.R.*, et al.* (2009) Comparison of MTBSTFA and BSTFA in derivatization reactions of polar compounds prior to GC/MS analysis. *Talanta*, *77*, 1473-1482.

Spaulding, R.S., Frazey, P., Rao, X.*, et al.* (1999) Measurement of hydroxy carbonyls and other carbonyls in ambient air using pentafluorobenzyl alcohol as a chemical ionization reagent. *Anal. Chem.*, *71*, 3420-3427.